PERFORMANCE ANALYSIS OF NON-COHERENT IR-UWB COOPERATIVE COMMUNICATION SYSTEM

Ph. D. THESIS

by

RANJAY HAZRA

DEPARTMENT OF ELECTRONICS AND COMMUNICATION ENGINEERING

INDIAN INSTITUTE OF TECHNOLOGY ROORKEE

ROORKEE- 247 667 (INDIA)

JULY, 2015

PERFORMANCE ANALYSIS OF NON-COHERENT IR-UWB COOPERATIVE COMMUNICATION SYSTEM

A THESIS

Submitted in partial fulfilment of the requirements for the award of the degree

of

DOCTOR OF PHILOSOPHY

in

ELECTRONICS AND COMMUNICATION ENGINEERING

by

RANJAY HAZRA

DEPARTMENT OF ELECTRONICS AND COMMUNICATION ENGINEERING

INDIAN INSTITUTE OF TECHNOLOGY ROORKEE

ROORKEE- 247 667 (INDIA)

JULY, 2015

INDIAN INSTITUTE OF TECHNOLOGY ROORKEE
ROORKEE

CANDIDATE'S DECLARATION

I hereby certify that the work which is being presented in this thesis entitled **"PERFORMANCE ANALYSIS OF NON–COHERENT IR–UWB COOPERATIVE COMMUNICATION SYSTEM"** in partial fulfilment of the requirements for the award of the Degree of Doctor of Philosophy and submitted in the Department of **Electronics and Communication Engineering** of the Indian Institute of Technology Roorkee is an authentic record of my own work carried out during a period from **July, 2011** to **July, 2015** under the supervision of Dr. Anshul Tyagi, Assistant Professor, Department of Electronics and Communication Engineering, Indian Institute of Technology Roorkee.

The matter presented in the thesis has not been submitted by me for the award of any other degree of this or any other Institute.

(RANJAY HAZRA)

This is to certify that the above statement made by the candidate is correct to the best of my knowledge.

Dated: 21st July 2015 **(Dr. Anshul Tyagi)**
Supervisor

The Ph. D Viva-Voce Examination of **Mr. RANJAY HAZRA,** Research Scholar, has been held on **3rd March 2016.**

Chairman, SRC **Signature of External Examiner**

This is to certify that the student has made all the corrections in the thesis.

Signature of Supervisor **Head of the Department**

Date: 3rd March 2016

Acknowledgements

First and above all, I would like to thank the almighty who bestowed upon me the blessings and provided me this opportunity and capability, to complete my Ph.D work successfully. This thesis appears in its current form due to the assistance and guidance of several people. It is a pleasure to thank them all who made this thesis possible.

I wish to express my deep sense of gratitude to Dr. Anshul Tyagi for his invaluable supervision, encouragement, constructive criticism, and suggestions during the course of work. He has been generous in undertaking comprehensive discussions and meticulously reviewing of the thesis, without which the work could not have come to its present shape. Throughout my research period, he has provided invaluable inspiration, incessant encouragement and appreciation, sound advice, good teaching, and lots of good ideas.

The working facilities, necessary resources, and friendly environment provided in communication laboratory by Dr. Anshul Tyagi, my supervisor, Prof. Debashis Ghosh, Head of the Department and convener of communication systems Group, IIT Roorkee, helped me to carry out my research work in a lucid manner. My sincere gratitude to all the faculty members of my department for their invaluable support and suggestions. I wish to express my thanks to Mr. Mahendra Singh and Mr. Anand Krishna Yadav, the non−teaching staff members of Communication Lab. I sincerely acknowledge Ministry of Human Resources (MHRD), Government of India, for sponsoring my research program for 4 years.

I would like to express my deep sense of gratitude to my research committee members Prof. D. K. Mehra, Prof. M. J. Nigam, Prof. Dharmendra Singh, Prof. Manoj Mishra, Dr. Madhu Jain, Dr. Vinod Pankajakshan for their continuous support and invaluable suggestions. I would like to thank Dr. Amalendu Patnaik and Dr. Brijesh Kumar for their generous, helping and friendly attitude towards me, and having shared their experiences with me during teaching assistantship.

My heartfelt thanks to my best buddies Dr. A. Sathish Kumar, Shitala Prasad, Anuradha

Ravi, Narayan Roy, Dr. Satish Maheshwaram, Gaurav Singh Baghel, Santosh Kumar Reddy, Shivam Verma, Sunny Bhardwaj, Debanjan Kolay, Praful Ranjan, Snehashish Mukherjee, Ranjan Biswas, Siddharth Datta, Arka Ghosh, Soumyadeep Basu and Ritabrata Bhattacharya, for their invaluable support and encouragement throughout these 4 years. I am extremely thankful to Anuradha Ravi, Ravinder Kumar, Prateek Dolas and Dr. Manju Ashok for their fruitful technical, non-technical discussions and insight into the thesis thereby, improving its quality.

I am extremely thankful to my friends and seniors of my department for their painstaking involvement during the research work and the joyful gatherings during the stay at IIT Roorkee. I thank the support of Prateek Dolas, Niyati Baliyan, Sanchika Gupta, K. Siva Chidambaram, Dinesh Kumar, Sukhwinder Singh, Ajeet Kumar, Himanshu Maurya, Kumar Goodwill, Jagannath Malik, Raja Singh, Dr. Manoj Gupta, Dr. Pankaj Pratap Singh, Manoranjan Rai Bharti, Mayank Awasthi, Ribhu, Shree Garg, Yogita, Dr. Keshavmurthy, Sudarshan Mukherjee, Radhika Gour and Neha Singh for their help during the preparation of the thesis.

Finally, I wish to express my gratitude to my family that never ceased to give me all the support, encouragement and love during the past four years and having faith in me, especially my parents Mrs. Ranjana Hazra and Mr. Rajib Hazra. I am grateful to my sister Mrs. Rajrupa Ghosh and brother-in-law Mr. Arup Ghosh for their constant support and encouragement throughout the research program, which deserves a special mention. With due regards, I wish to thank my grandfather Mr. Ram Kumar Neogi for motivating me during the course of study. I am short of words, to express my loving gratitude to my niece Anushka Ghosh, whose innocent smile inspired me during entire work. Last but not the least, I am thankful to God for helping me find my soulmate Mansi Rastogi, whose love, encouragement and support has inspired me and helped me at hard times of study.

Ranjay Hazra

Abstract

Impulse Radio−Ultra−WideBand (IR−UWB) communication systems of late has attracted strong attention from the researchers, for its high speed and short range applications in the field of wireless communication. According to Federal Communications Commission (FCC), signals that possess a bandwidth larger than $500\ MHz$ or a fractional bandwidth of more than 20% are said to be UWB. IR−UWB is a single band carrierless communication technology, transmitting information onto a sequence of impulse like waveforms (nanosecond duration pulses), thereby occupying the entire bandwidth of $7.5\ GHz$. The enormous bandwidth occupancy of UWB signal, makes it robust to multipath fading and intersymbol-interference (ISI) effects. It also makes the channel frequency selective, resulting in a large number of resolvable multipath components, which offer the potential of multipath energy combining at the receiver end by coherent or non−coherent means. While a coherent Rake receiver gives better bit error rate (BER) performance, it requires accurate channel estimation and synchronization for extracting multipath energy from multipath components that results in high complexity. Hence, simple and less complex non−coherent IR−UWB autocorrelation (AC) systems such as transmitted reference (TR), transmitted reference pulse cluster (TRPC), and differential transmitted reference (DTR) are preferred. But, AC systems require long analog delay lines for performing correlation during detection, thereby leading to hardware complexity issues. Hence, low complexity energy detector (ED) system is preferred, which works by squaring the received signal, followed by integration and detection through decision device.

Owing to the strict guidelines issued by the FCC, UWB systems can operate at a maximum transmit power spectral density (PSD) of -41.3 dBm/MHz, in order to avoid interference with other existing technologies. The low PSD of UWB signals not only limits it from achieving a wide coverage area, but also makes its performance sensitive to distance. So, to overcome such weaknesses, cooperative technology was introduced, which emerged as the perfect scheme to improve quality of service (QoS), coverage area, transmission reliability, and power efficiency.

The two relaying strategies that can be applied to a cooperative domain are regenerative and non−regenerative relaying. In case of Detect and Forward (DTF), a classification of regenerative relaying, the relay node detects the received signal at the relay node in 1^{st} time slot, and then forwards the extracted information to the destination node in the next time slot. However in case of Amplify and Forward (AF), a classification of regenerative relaying, the received signal is forwarded to the destination node after being amplified at the relay node.

The research for cooperative transmission in multipath scenario using non−coherent IR−UWB system is largely unexplored. AC systems such as TR and DTR use long analog delay taps for storing past samples of the received signal that is required for correlation during detection process. This leads to an increase in storage requirement, which increases the hardware complexity and cost of receiver. Due to its less complexity and sensitivity to synchronizing errors, ED system that works by squaring the received signal followed by integration and detection through decision device, is preferred. If complexity is preferred over performance in the trade−off between complexity and performance, then ED receiver acts as the best choice because of its simplicity and less hardware complexity.

Taking inference from the existing study and knowing the research gaps, we firstly present an analytical approach to determine the BER performance of non−coherent IR−UWB system namely AC and ED, in single−link scenario, over IEEE 802.15.4a UWB environment. The analytical approach for evaluating the BER of AC systems such as TR and DTR, is based on autocorrelation principle while, ED systems such as ED−OOK, ED−PPM, use energy detection principle for performance analysis. The analytical results are also validated with simulations for ($N_f = 1, 2$), where N_f signifies the number of frames. Furthermore, computer simulations are used to compare the BER performance of various non−coherent IR−UWB systems namely, TR, DTR, ATR, RTR, RATR, ED−OOK and ED−PPM, in single−link environment.

We then analyse the BER performance of non−coherent IR−UWB AC (TR,DTR) systems using cooperative dual−hop AF and DTF relay strategy for various diversity combining schemes namely, linear combining, selective combining and optimum linear combining, over 802.15.4a UWB environment. The analytical approach used for BER evaluation is based on autocorrelation principle and is validated with the simulation results.

In the 1^{st} time slot, UWB signal modulated by the information bit is transmitted from the source node to relay as well as destination node. The received signal at relay node is either amplified or detected, depending on the relay strategy used, and then forwarded to the destination

node in the next time slot. The decision statistics obtained at the destination node in the two time slots are combined using various combining techniques to form the final decision statistic, which is compared to the decision threshold to recover the original bit.

A novel analytical representation of BER performance of non−coherent IR−UWB ED−OOK and ED−PPM systems using cooperative dual−hop AF and DTF relay strategy for various combining techniques, over IEEE 802.15.4a environment, is illustrated. In particular, the approximate expression based on energy detection principle are derived for various diversity combining schemes namely, linear combining, selective combining and optimal linear combining. The analytical BER expressions are also validated with the simulations for $N_f = 1, 2$.

Computer simulations are also used to compare the BER performance of non−coherent IR−UWB systems based on increase in number of relay paths L, decrease in number of frames N_f, channel used (CM1,CM2), relaying strategies, diversity combining schemes and type of system used.

Table of Contents

Abstract **ix**

List of Abbreviations **xxi**

1 Introduction **1**

1.1 A Brief Introduction to UWB Technology 1

1.1.1 History of UWB 1

1.1.2 Basics of IR−UWB 3

1.1.3 Properties of UWB 3

1.1.4 Applications of UWB 4

1.2 IR−UWB System Model 5

1.2.1 Pulse Shape 5

1.2.2 Signal Model 5

1.2.3 UWB Channel Model 6

1.2.4 Receiver Architecture 7

1.3 Dual−Hop Cooperative System Model 9

1.4 Relay Strategies 9

1.4.1 Amplify and Forward (AF) 10

1.4.2 Detect and Forward (DTF) 10

1.4.3 Decode and Forward (DF) 10

1.5 Motivation 11

1.6 Research objectives and Contribution 11

1.7 Organization of the thesis 12

2 Preliminaries and Review **15**

2.1 Introduction 15

2.2 Coherent UWB System 16
2.2.1 Single-Link Approach 16
2.2.2 Cooperative Approach 18
2.3 Non−Coherent UWB System 22
2.3.1 Single−Link Approach 22
2.3.2 Cooperative Approach 27

3 Performance Analysis of Non−Coherent UWB Single−Link System 31
3.1 Introduction 31
3.2 UWB Signal Model 32
3.2.1 TR system 33
3.2.2 DTR system 33
3.2.3 ED−OOK system 33
3.2.4 ED−PPM system 34
3.3 UWB Channel Model 34
3.4 Receiver Model 34
3.4.1 TR Receiver 36
3.4.2 ATR Receiver 36
3.4.3 RTR Receiver 37
3.4.4 RATR Receiver 39
3.4.5 DTR Receiver 39
3.4.6 ED−OOK Receiver 39
3.4.7 ED−PPM Receiver 40
3.5 Performance Analysis 40
3.5.1 TR System 41
3.5.2 DTR System 44
3.5.3 ED−OOK System 47
3.5.4 ED−PPM System 49
3.6 Simulation Results 53
3.7 Concluding Remarks 57

4 Performance Analysis of Non-Coherent UWB Cooperative AC System 59
4.1 Introduction 59

4.2 Cooperative System Model 60
4.2.1 UWB Signal Model 60
4.2.2 UWB Channel Model 62
4.2.3 TR Receiver Model 63
4.3 Performance Analysis of a Cooperative AF AC System 65
4.3.1 TR System 65
4.3.2 DTR System 78
4.4 Performance Analysis of a Cooperative DTF AC System 91
4.4.1 TR System 91
4.4.2 DTR System 106
4.5 Simulation Results 122
4.6 Concluding Remarks 141

5 Performance Analysis of Non-Coherent UWB Cooperative ED−OOK System 143
5.1 Introduction 143
5.2 System Model 144
5.2.1 Signal Model 145
5.2.2 Channel Model 145
5.2.3 ED Receiver 146
5.3 Performance Analysis of a Cooperative AF ED-OOK system 147
5.3.1 Linear Combining 152
5.3.2 Selective Combining 154
5.3.3 Optimum Linear Combining 154
5.4 Performance Analysis of a Cooperative DTF ED-OOK System 156
5.4.1 Linear Combining 162
5.4.2 Selective Combining 165
5.4.3 Optimum Linear Combining 166
5.5 Simulation Results 167
5.6 Concluding Remarks 184

6 Performance Analysis of Non-Coherent UWB Cooperative ED−PPM System 187
6.1 Introduction 187
6.2 System Model 188

6.2.1 Channel Model 189
6.2.2 Signal Model 189
6.2.3 Receiver Structure 190
6.3 Performance Analysis of a Cooperative AF ED-PPM System 191
6.3.1 Linear Combining 199
6.3.2 Selective Combining 201
6.3.3 Optimum Linear Combining 202
6.4 Performance Analysis of a Cooperative DTF ED-PPM System 203
6.4.1 Linear Combining 210
6.4.2 Selective Combining 212
6.4.3 Optimum Linear Combining 213
6.5 Simulation Results 216
6.6 Concluding Remarks 234

7 Conclusions and Future Work 235
7.1 Concluding Remarks 235
7.2 Future Work 238

A Evaluation of Noise Variance 241

B Evaluation of Expectation of Noise 243

C Linear Optimal Combining Factor 245

D Evaluation of Variance Terms 247

Bibliography 249

List of Publications 269

List of Figures

1.1 (a) DS IR−UWB system having bits $b_1 = 0$, $b_2 = 1$ with DS PN sequence $c = [1, 1, -1, 1, -1, -1]$ (b) TH IR−UWB system having bits $b_1 = 0$, $b_2 = 1$, $N_h = 3$, $N_f = 4$ and ϵ as PPM shift 6

1.2 Coherent IR−UWB RAKE receiver 8

1.3 Cooperative System Model having single link and one relay path 10

3.1 (a) DTR Transmitter (b) DTR Receiver 35

3.2 (a) TR Receiver (b) ATR Receiver 37

3.3 (a) RTR Receiver (b) RATR Receiver 38

3.4 (a) ED−OOK Receiver (b) ED−PPM Receiver 40

3.5 Analytical Vs Simulated BER performance comparison of non−coherent UWB receivers in CM1 channel for $N_f = 1, 2$ namely(a) TR Rxr (b) DTR Rxr (c) ED−OOK Rxr (d) ED−PPM Rxr 54

3.6 BER Performance Comparison of Non−Coherent UWB receivers in (a) CM1 channel for $N_f = 1$ (b) CM1 channel for $N_f = 2$ (c) CM2 channel for $N_f = 1$ (d) CM2 channel for $N_f = 2$ 56

4.1 UWB TR system for Cooperative Communication 62

4.2 UWB DTR system for Cooperative Communication 64

4.3 BER performance of UWB TR system using cooperative AF strategy with various combining schemes in CM1 channel for (a) $N_f = 1$ (b) $N_f = 2$ 124

4.4 BER performance of UWB TR system using cooperative AF strategy with various combining schemes in CM2 channel for (a) $N_f = 1$ (b) $N_f = 2$ 125

4.5 Analytic vs Simulated BER performance comparison of UWB TR system using AF strategy having $N_f = 1, 2$ for various combining schemes namely (a) Optimum Linear Combining (b) Linear Combining and (c) Selective Combining. 127

4.6 BER performance of UWB DTR system using cooperative AF strategy with various combining schemes in CM1 channel for (a) $N_f = 1$ (b) $N_f = 2$ 128
4.7 BER performance of UWB DTR system using cooperative AF strategy with various combining schemes in CM2 channel for (a) $N_f = 1$ (b) $N_f = 2$ 129
4.8 Analytic vs Simulated BER performance comparison of UWB DTR system using AF strategy having $N_f = 1, 2$ for various combining schemes namely (a) Optimum Linear Combining (b) Linear Combining and (c) Selective Combining. 131
4.9 BER performance of UWB TR system using cooperative DTF strategy with various combining schemes in CM1 channel for (a) $N_f = 1$ (b) $N_f = 2$ 132
4.10 BER performance of UWB TR system using cooperative DTF strategy with various combining schemes in CM2 channel for (a) $N_f = 1$ (b) $N_f = 2$ 133
4.11 Analytic vs Simulated BER performance comparison of UWB TR system using DTF strategy having $N_f = 1, 2$ for various combining schemes namely (a) Optimum Linear Combining (b) Linear Combining and (c) Selective Combining. 135
4.12 BER performance of UWB DTR system using cooperative DTF strategy with various combining schemes in CM1 channel for (a) $N_f = 1$ (b) $N_f = 2$ 136
4.13 BER performance of UWB DTR system using cooperative DTF strategy with various combining schemes in CM2 channel for (a) $N_f = 1$ (b) $N_f = 2$ 137
4.14 Analytic vs Simulated BER performance comparison of UWB DTR system using DTF strategy having $N_f = 1, 2$ for various combining schemes namely (a) Optimum Linear Combining (b) Linear Combining and (c) Selective Combining. 139

5.1 UWB ED−OOK Receiver for Cooperative Communication 146
5.2 BER performance of UWB ED−OOK system using cooperative AF strategy with various combining schemes in UWB CM1 channel for (a) $N_f = 1$ (b) $N_f = 2$ 169
5.3 BER performance of UWB ED−OOK system using cooperative AF strategy with various combining schemes in UWB CM2 channel for (a) $N_f = 1$ (b) $N_f = 2$ 170
5.4 Analytic vs Simulated BER performance comparison of UWB ED−OOK system using AF strategy having $N_f = 1, 2$ for various combining schemes namely (a) Optimum Linear Combining (b) Linear Combining and (c) Selective Combining. 172

5.5 Dual−Hop Cooperative System Model with single−link and (a) $L = 5$ relay paths (b) $L = 10$ relay paths 173

5.6 BER performance of UWB ED−OOK system using dual−hop cooperative AF strategy in UWB CM1 channel with (a) Optimum Linear Diversity Combining for $L = 0, 1, 2, 5, 10$ relay paths (b) Linear Diversity Combining for $L = 0, 1, 2, 5, 10$ relay paths and (c) Selective Diversity Combining for $L = 0, 1, 2, 5, 10$ relay paths. 175

5.7 BER performance of UWB ED−OOK system using cooperative DTF strategy with various combining schemes in UWB CM1 channel for (a) $N_f = 1$ (b) $N_f = 2$ 176

5.8 BER performance of UWB ED−OOK system using cooperative DTF strategy with various combining schemes in UWB CM2 channel for (a) $N_f = 1$ (b) $N_f = 2$ 177

5.9 Analytic vs Simulated BER performance comparison of UWB ED−OOK system using DTF strategy in UWB CM1 channel having $N_f = 1, 2$ for (a) Optimum Linear Diversity Combining scheme (b) Linear Diversity Combining scheme and (c) Selective Diversity Combining scheme. 179

5.10 BER performance of UWB ED−OOK system using dual−hop cooperative DTF strategy in UWB CM1 channel with (a) Optimum Linear Diversity Combining for $L = 0, 1, 2, 5, 10$ relay paths (b) Linear Diversity Combining for $L = 0, 1, 2, 5, 10$ relay paths and (c) Selective Diversity Combining for $L = 0, 1, 2, 5, 10$ relay paths. 181

6.1 ED−PPM Receiver for Cooperative Communication 190

6.2 BER performance of UWB ED−PPM system using cooperative AF strategy with various combining schemes in CM1 channel for (a) $N_f = 1$ (b) $N_f = 2$ . . 216

6.3 BER performance of UWB ED−PPM system using cooperative AF strategy with various combining schemes in CM2 channel for (a) $N_f = 1$ (b) $N_f = 2$ . . 217

6.4 Analytic vs Simulated BER performance comparison of UWB ED−PPM system using AF strategy in CM1 channel having $N_f = 1, 2$ for various combining schemes namely (a) Optimum Linear Combining (b) Linear Combining (c) Selective Combining 219

6.5 Dual−Hop Cooperative System Model with single−link and (a) L=5 relay paths (b) L=10 relay paths 220
6.6 BER performance of UWB ED−PPM system using dual-hop cooperative AF strategy in CM1 channel with (a) Optimum Linear Diversity Combining for $L = 0, 1, 2, 5, 10$ relay paths (b) Linear Diversity Combining for $L = 0, 1, 2, 5, 10$ relay paths and (c) Selective Diversity Combining for $L = 0, 1, 2, 5, 10$ relay paths 222
6.7 BER performance of UWB ED−PPM system using cooperative DTF strategy with various combining schemes in CM1 channel for (a) $N_f = 1$ (b) $N_f = 2$ . . 223
6.8 BER performance of UWB ED−PPM system using cooperative DTF strategy with various combining schemes in CM2 channel for (a) $N_f = 1$ (b) $N_f = 2$ . . 224
6.9 Analytic vs Simulated BER performance comparison of UWB ED−PPM system using DTF strategy in CM1 channel having $N_f = 1, 2$ for various combining schemes namely (a) Optimum Linear Combining (b) Linear Combining (c) Selective Combining 226
6.10 BER performance of UWB ED−PPM system using dual−hop Cooperative DTF strategy in CM1 channel with (a) Optimum Linear Diversity Combining for $L = 0, 1, 2, 5, 10$ relay paths (b) Linear Diversity Combining for $L = 0, 1, 2, 5, 10$ relay paths and (c) Selective Diversity Combining for $L = 0, 1, 2, 5, 10$ relay paths 228
6.11 BER performance comparison of non−coherent UWB receivers using dual−hop Cooperative DTF strategy over CM1 environment with (a) Optimum Linear Diversity Combining (b) Linear Diversity Combining and (c) Selective Diversity Combining 230

List of Abbreviations

AC	:	Autocorrelation
ADC	:	Analog to Digital Converter
AF	:	Amplify and Forward
ARAKE	:	All RAKE
ATR	:	Averaged Transmitted Reference
BEP	:	Bit Error Probability
BER	:	Bit Error Rate
BPF	:	Band-Pass Filter
BW	:	Bandwidth
CF	:	Characteristic Function
CIR	:	Channel Impulse Response
CMI	:	Cross Modulation Interference
CSI	:	Channel State Information
D	:	Destination
DF	:	Decode and Forward
DH	:	Delay Hopping
DL	:	Delay Line
DP	:	Dual-Pulse
DPSK	:	Differential Phase Shift Keying
DS	:	Direct Sequence
DTF	:	Detect and Forward
DTR	:	Differential Transmitted Reference
ECC	:	Electronic Communication Commission
ED	:	Energy Detector
EGC	:	Equal Gain Combining

FCC	:	Federal Communication Commission
FR	:	Fixed Relaying
FSR	:	Frequency-Shifted Reference
GA	:	Gaussian Approximation
GDR	:	Group Delay Ripple
GFSK	:	Gaussian frequency shift keying
GLRT	:	Generalised Likelihood Ratio Test
IID	:	Independent and Identically Distributed
IPI	:	Inter Pulse Interference
IR	:	Impulse Radio
ISI	:	Inter Symbol Interference
ITS	:	Intelligent Transportation Systems
LOS	:	Line of Sight
MA	:	Multiple Access
MAI	:	Multiple Access Interference
MB	:	Multi-Band
MD	:	Multiple-Differential
MGF	:	Moment Generating Function
MIMO	:	Multiple Input Multiple Output
ML	:	Maximum Likelihood
MMSE	:	Minimum Mean Squared Error
MRC	:	Maximal Ratio Combining
MSDD	:	Multiple Symbol Differential Detection
MUI	:	Multi-User Interference
NB	:	Narrowband
NLOS	:	Non-Line of Sight
OFDM	:	Orthogonal Frequency Division Multiplexing
OOK	:	On-Off Keying
PAL	:	Precise Location Asset
PAM	:	Pulse Amplitude Modulation
PC	:	Personal Computer
PDF	:	Probability Density Function

PDP	:	Power Delay Profile
PDR	:	Packet Delivery Ratio
PPM	:	Pulse Position Modulation
PRAKE	:	Partial Combining RAKE
PSD	:	Power Spectral Density
QoS	:	Quality of Service
R	:	Relay
RATR	:	Recursive Averaged Transmitted Reference
R-D	:	Relay-Destination
RTR	:	Recursive Transmitted Reference
S	:	Source
SD	:	Single-Differential
S-D	:	Source-Destination
SNR	:	Signal to Noise Ratio
SOVA	:	Soft Output Viterbi decoding algorithm
SR	:	Selective Relaying
S-R	:	Source-Relay
SRAKE	:	Selective Combining RAKE
SV	:	Saleh Valenzuela
TB	:	Training Based
TH	:	Time-Hopping
TR	:	Transmitted Reference
TRPC	:	Transmitted Reference Pulse Cluster
Txr-Rxr	:	Transmitter-Receiver
UAV	:	Unmanned Aerial Vehicles
UCoRS	:	UWB based cooperative retransmission scheme
USB	:	Universal Serial Bus
UWB	:	Ultra-wideband
WED	:	Weighted Energy Detector
WSN	:	Wireless Sensor Networks
WT	:	Time-bandwidth Product

Chapter 1

Introduction

1.1 A Brief Introduction to UWB Technology

Ultra−Wideband (UWB) communication, one of the emerging technologies in the field of wireless communication and spectrum management, finds its base in the form of transmission and reception of extremely short duration pulses (typically subnanosecond) [1, 2, 3, 4]. UWB technology has been approved by Federal Communication Commission (FCC), USA in 2002 and Electronic Communication Committee (ECC), Europe in 2007. According to FCC, signals which possess a bandwidth exceeding $500\ MHz$ or a fractional bandwidth f_b more than 0.2, are said to be UWB [5, 6, 7, 8]. Defined as the ratio of absolute bandwidth to the centre frequency, fractional bandwidth can be expressed as:

$$f_b \ = \ 2\frac{(f_h - f_l)}{(f_h + f_l)} \tag{1.1}$$

where, f_h and f_l represent the upper and lower frequencies at - $10\ dB$ respectively [7, 8]. The UWB systems are allowed unlicensed usage of $7.5\ GHz$ of spectrum in the frequency bands $3.1 - 10.6\ GHz$ [9, 10, 11]. UWB plays a pivotal role in management of spectrum by sharing the already occupied radio spectrum rather than using any new bands, thus obeying the underlay principle.

1.1.1 History of UWB

The earliest prototype of UWB technology can be traced back to 1900, when Marconi transmitted Morse Code using spark gap radio transmitters [12, 13, 14]. However, much attention was not paid to this technology at that time and since then the potential ability to provide large

bandwidth out of that technology was buried for many years. Approximately in 1960s, UWB technology came into light with the pioneering work of Gerald Ross at Sperry Research Center in 1963 [15], Henning Harmuth at Catholic University of America [16] in 1969 and Paul Van Etten at USAF's Rome Air Development Center in Russia [17]. Back then, this technology was referred to as baseband, carrier-free or impulse. Harmauths books and published papers, $1969-1984$, focused on the basic design of UWB transmitters and receivers. At the same time, $1972-1984$, Ross's patents pioneered the use of UWB signals in a number of application areas, including radar, coding schemes and communications while, Etten's empirical testing stressed more on system design and antenna concepts of UWB radar system [17]. The development of sampling oscilloscope in the early 1960s and the corresponding techniques used for generating sub-nanosecond pulses sped up the development of UWB [18].

The basic designs for UWB signal systems were available by 1970s and there remained no major impediment to progress in perfecting such systems. In fact, by 1975, UWB system developed for radar communication was constructed from components purchased from Tektronix. The term $'ultrawideband'$ originated with the Department of Defence of USA around 1989 to describe communication via transmission and reception of impulses; and by that time UWB theory, techniques and hardware approaches had experienced well over $25-30$ years of extensive development. By 1990, around 50 patents had been awarded to Sperry Research Center for their contribution in the field of UWB technology including applications in radar, communications, altimetry, positioning system, automobile collision avoidance, liquid level sensing and positioning systems [18]. By 2000, the attractive features of time-hopping (TH) spread-spectrum multiple-access system employing UWB technology, was outlined by Scholtz [19, 3]. Most of the UWB applications and development occurred in military domain or work funded by the US government. In case of military, accurate radar and low probability of interception was the driving force behind research and development.

The next milestone was however seen in the year 2002, when Report and Order issued by FCC, allowed commercial use of UWB technology due to increasing demand of high data rate service from various organizations. Companies such as Time Domain, Xtreme Spectrum, Intel Corporation and Motorola have built signal generator, amplifier, Precise Location Asset (PAL) system and broadband multimedia [18]. These industries have also taken a positive initiative to not only publish research papers, but also provide pioneer platforms for UWB hardware based research. IEEE has also published its standard for UWB applications namely IEEE 802.15.3a,

IEEE 802.15.4a and IEEE 802.15.6.

1.1.2 Basics of IR−UWB

The most traditional way of emitting a UWB signal is by transmitting ultra−short duration (sub−nanosecond) pulses. Depending on the availability of bandwidth, UWB system is classified as single band and multi−band (MB) UWB. Impulse Radio (IR) UWB, a single band carrierless communication technology transmits information directly onto a sequence of impulse like waveforms, which occupy the entire available spectrum of the order of several GHz ($7.5\ GHz$) of bandwidth whereas, in case of MB−UWB, the total available frequency band is divided into several subbands, where each subbband occupies a bandwidth of atleast $500\ MHz$, in accordance with FCC regulations. Interleaving the information symbols across each subband allows the MB−UWB to maintain the same transmit power, as if the entire bandwidth of GHz order is utilized. In MB−UWB, each subband uses Orthogonal Frequency Division Multiplexing (OFDM) modulation technique to transmit information [20, 21]. The requirement of high performance electronics circuitry for the working of MB−OFDM UWB radio has given rise to its replacement with IR−UWB, which requires, less complexity and low power consumption [22].

In case of IR−UWB, the information symbols (or bits), are represented by pulses which may differ depending on the modulation scheme used. The most commonly used modulation schemes are Pulse Amplitude Modulation (PAM), Pulse Position Modulation (PPM) and On−Off Keying (OOK). In addition to modulation schemes, data symbols sent over the channel are also encoded using pseudorandom or pseudo−noise (PN) sequences, which may be used to spread the impulses in time, in order to avoid co−channel interference. As a result, the encoded data symbols uses either direct sequence (DS) or TH [8] modulation scheme in IR−UWB systems.

1.1.3 Properties of UWB

The UWB technology can be distinctly characterized by its properties, which differentiates it from narrowband technology. The large bandwidth of UWB systems implies extremely high data rate (up to hundreds of Mbit/s) can be achieved. As the UWB pulses are extremely short duration up to the order of sub−nanosecond, they can be distinguished easily from unwanted

multipath reflections, which leads to multipath immunity. UWB signals have superior penetration properties due to the low frequency components in UWB frequency spectrum.

These UWB signals also have a low PSD of $-41.3\ dBm/MHz$, which allows it to share its spectrum with other technologies (narrowband), because of its low interference property (low probability of interception and detection). UWB technology promises low cost, low power consumption, small size, long battery operated devices due to its simple transceiver design. UWB has various advantages over other wireless technologies such as flexibility, reuse of radio spectrum, high immunity to interference, penetration capabilities, large bandwidth, high precision ranging and simple implementation [8].

1.1.4 Applications of UWB

UWB technology has many potential applications supporting high as well as low data rate short range wireless personal and body area networking. For high data rate applications, UWB is considered a replacement for Universal Serial Bus (USB) cable to connect a Personal Computer (PC) and other associated peripherals namely handheld computers, printers, web cams, still cameras and mobile phones [23]. It also plays a vital role in high data rate wireless video and audio streaming from camcorders to computers or TV sets. The low data rate applications of UWB include wireless sensor networks (WSN) [24, 25]. The properties of UWB such as low price, low cost, accurate positioning and ranging capabilities finds its application in medical field such as monitoring of patients, locating equipments [26]. The military applications include network capable low probability of interception and detection radios, data−links for unmanned aerial vehicles (UAVs), wireless intercom systems for secure, untethered communication onboard aircraft, mine detection during warfare, wall imaging for fire−fighters, and precision geo−location systems. The penetrating capability of UWB signals give rise to a whole range of new applications, including wall penetration radars to detect personnel through several intervening walls, ground penetrating radars, intelligent transportation systems (ITS) with vehicle to vehicle and vehicle to roadside communications, collision and obstacle avoidance radars.

1.2 IR−UWB System Model

The various aspects of IR−UWB system model namely Pulse Shape, Signal Model, Channel Model and Receiver Architecture, is described in this section.

1.2.1 Pulse Shape

Pulse shaping is an important aspect of signal transmission as it affects its PSD. The pulse shape used for UWB communication is basically a Gaussian pulse or its derivatives. Gaussian monocycle, first derivative of Gaussian pulse and Gaussian doublet, second derivative of Gaussian pulse are used for UWB communication [27]. As the order of the derivative increases, there is a shift in spectrum, because the centre frequency too shifts in frequency domain [28]. The side lobes of the gaussian spectrum is found to decay, with increase in frequency, but it never reaches zero. So, the signal is said to be infinite in frequency domain. As a signal pulse cannot carry a lot of information, the data is modulated onto a sequence of pulses called pulse train [18].

1.2.2 Signal Model

In a DS IR−UWB system, each information symbol is direct sequence modulated using a spread spectrum PN code, specific to each user [29]. The PN codes are orthogonal and known to the transmitter and receiver. The Fig 1.1(a) represents the DS IR−UWB signal with $b_1 = 0$, $b_2 = 1$ and $c = [1, 1, -1, 1, -1, -1]$. The transmitted DS IR−UWB signal for a single user is represented as:

$$s^{(k)}_{DS-UWB}(t) \;=\; \sqrt{E}\sum_{j=-\infty}^{\infty}(1-2b_j^{(k)})\sum_{i=0}^{N_c} {c_i}^{(k)} p(t - jT_f - iT_c) \tag{1.2}$$

where, PAM modulation scheme is used for transmission. The terms $b_j^{(k)} \in (0, 1)$ denotes the binary information and $c_i^{(k)} \in (-1, 1)$ the DS spread spectrum code for user k.

Similarly, the transmitted TH−PPM signal $s^{(k)}_{TH-PPM}(t)$ for an IR−UWB system can be represented as [3]:

$$s^{(k)}_{TH-PPM}(t) \;=\; \sqrt{E}\sum_{j=-\infty}^{\infty} p(t - jT_f - c_j^{(k)}T_c - \epsilon b^{(k)}_{[j/N_f]}) \tag{1.3}$$

where, T_f represents the frame duration, T_c the chip duration, T_b the bit duration, N_c the number of chips per information bit, $b^{(k)}_{[j/N_f]} \in (0, 1)$ the binary information, E the energy per pulse, $p(t)$

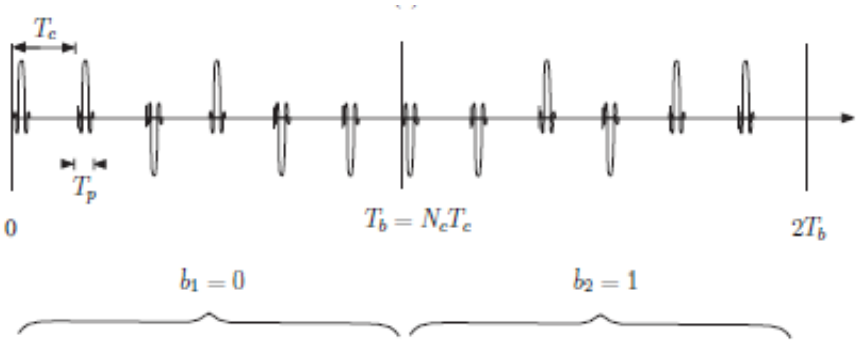

(a)

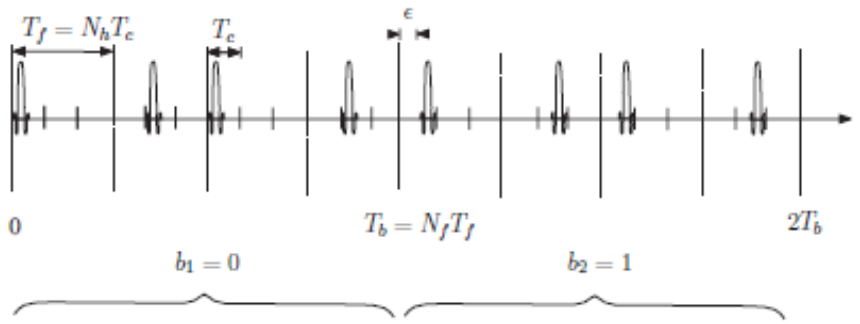

(b)

Figure 1.1: (a) DS IR−UWB system having bits $b_1 = 0$, $b_2 = 1$ with DS PN sequence $c = [1, 1, -1, 1, -1, -1]$ (b) TH IR−UWB system having bits $b_1 = 0$, $b_2 = 1$, $N_h = 3$, $N_f = 4$ and ϵ as PPM shift

denotes the gaussian second order pulse, ϵ the PPM shift, N_h the number of hops and N_f the number of frames. Here, the pseudo−random TH sequence $c_j^{(k)}$ lies in the range $0 \leq c_j^{(k)} \leq N_h$ and bit duration T_b is represented as $T_b = N_c T_c = T_f$. The Fig 1.1(b) represents a TH−UWB signal with $b_0 = 1$, $b_1 = 1$, $N_h = 3$ and $N_f = 4$.

1.2.3 UWB Channel Model

The conventional narrowband channel models are inadequate for UWB communication because of the enormous bandwidth of UWB signals. So, various desirable propagation models have been developed to characterize UWB channels [30, 31, 32, 33], which the most desirable and appropriate is IEEE 802.15.4a, a low data rate wireless UWB channel, based on the modification of Saleh Valenzuela (SV) model [34, 30, 35, 36]. SV model describes the arrival of multipath components as clusters, which are a combination of n number of rays separated from each other in time, due to the reflection and refraction of UWB signals from various surrounding objects.

All the multicluster signals and the multipath signals in a cluster follow log normal fading [37]. The SV model is represented as:

$$h(t) = \sum_{l=0}^{L-1} \sum_{k=0}^{K-1} \alpha_{k,l} \exp(j\phi_{k,l}) \delta(t - T_l - \tau_{k,l}) \tag{1.4}$$

where $\alpha_{k,l}$ represents the tap weight of the k^{th} component in l^{th} cluster, T_l the arrival time of the l^{th} cluster and $\phi_{k,l}$ the phase which is uniformly distributed between 0 to 2π. The modified IEEE 802.15.4a UWB channel is represented by a tap delay line model simplified as:

$$h(t) = \sum_{l=0}^{L-1} \alpha_l \delta(t - \tau_l) \tag{1.5}$$

where $h(t)$ represents the channel model, l the number of multipaths, α_l the amplitude of l^{th} tap, τ_l the delay of l^{th} tap and δ the Dirac Delta function. The number of significant paths considered for simulation are those which have an energy of more than 85% and power within $10\ dB$ of the strongest path [30]. IEEE 802.15.4a UWB model is appropriate for devices operating with data rates between 1 Kb/sec to several Mbit/sec [30]. In order to avoid Inter Pulse Interference (IPI) in IR$-$UWB systems, received pulses should have frame duration, $T_f > (T_{mds} + T_p)$ where T_p is the pulse duration, $T_{mds} = \tau_l - \tau_0$ the multipath delay spread, τ_l and τ_0 are the delay of l^{th} and 0^{th} pulse respectively. IEEE 802.15.4a has eight different channel environments namely CM1$-$CM8, each having different bandwidth, coverage area, environment and usage scenario.

1.2.4 Receiver Architecture

The original transmitted signal gets delayed and attenuated as it passes through a channel, to give rise to a received signal which is intercepted by the antennas present in the receiver. The two types of detectors used for reception of UWB signals are coherent IR$-$UWB Rake receiver and non$-$coherent IR$-$UWB receiver. The coherent and non$-$coherent IR$-$UWB receivers are implemented either in analog or in digital domain. The implementation of the receiver in digital domain requires high computational complexity because of higher data rate, more memory size, higher processing speed and higher sampling frequency due to Analog to Digital Converter (ADC), whereas in analog domain it relies on simplicity and low cost.

(i) *Coherent IR$-$UWB Rake Receiver* Coherent IR$-$UWB RAKE receivers which require exact knowledge of the channel estimation [38]. For evaluating the channel estimation, RAKE receiver must have a copy of the transmitted signal [39]. The coherent IR$-$UWB RAKE re-

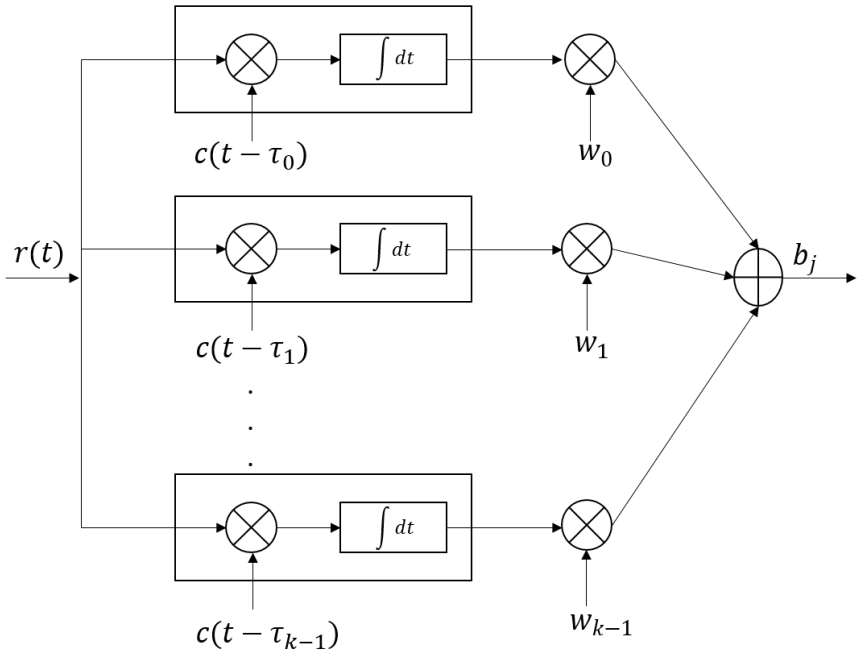

Figure 1.2: Coherent IR−UWB RAKE receiver

ceiver is a combination of matched filters also called correlators, where each correlator is accurately matched to a delayed form of the same transmitted signal. The correlator output then combines the multipath energy from each multipath, using either Maximal Ratio Combining (MRC) or Equal Gain Combining (EGC), thereby making maximum use of multipath diversity [29]. Further, accurate synchronization and timing offset is required for extraction of multipath energy from the multipath components.

As shown in Fig 1.2, coherent IR−UWB RAKE receiver exploits multipath diversity, by correlating the received signal $r(t)$ with k number of delays, providing k replicas of the actual transmitted signal $c(t)$. The combining RAKE weights w_0, w_1,....w_{k-1} multiplied with the various correlator outputs are finally combined using MRC techniques, to extract information symbol. These weights are also determined adaptively by using channel model estimation.

The most commonly used coherent IR−UWB RAKE Receivers are All RAKE (ARAKE), Selective Combining RAKE (SRAKE) and Partial Combining (PRAKE). ARAKE receiver combines information available from all the multipath components, PRAKE receiver combines information from first M arriving multipath components and SRAKE receiver combines information from the strongest multipath components. The Bit Error Rate (BER) performance of

a UWB system is affected by power delay profile (PDP), transmitter−receiver (Txr−Rxr) distance, RAKE combining scheme namely EGC and MRC, number of correlators and the channel used.

(ii) *Non−Coherent IR−UWB Receiver* As the number of multipath components increases, more number of coherent IR−UWB RAKE correlators are required to extract the multipath energy, thereby leading to complexity issues. The problem faced by coherent IR−UWB RAKE receiver is mitigated using a non−coherent IR−UWB receiver, which requires no knowledge of channel estimation or received pulse estimation, yet exploits the rich multipath diversity. Non−Coherent IR−UWB receivers are known to extract good amount of energy despite distortions and multipath propagation. Low complexity applications, less cost and less power consumption give an edge to non−coherent IR−UWB receivers, over its counterpart coherent IR−UWB receivers, though at the cost of poor BER performance. The non−coherent IR−UWB receivers are classified as autocorrelation (AC) receivers and Energy detector (ED) receivers [40, 41].

1.3 Dual−Hop Cooperative System Model

The cooperative network discussed in this section consists of three links, namely, Source−Destination (S−D) (Link-1), Source−Relay (S−R) (Link-2) and Relay−Destination (R−D) (Link-3), as seen in Fig 1.3. A dual−hop cooperative relay strategy consisting of two time slots is considered. In the 1^{st} time slot, UWB signal is transmitted from the source node to relay node as well as destination node. At the relay node, the received signal is either amplified or detected depending on the relay strategy used, and then forwarded to the destination node in the 2^{nd} time slot. The received signals obtained at the destination node in 1^{st} and 2^{nd} time slots are then demodulated using a non−coherent IR−UWB receiver.

1.4 Relay Strategies

In cooperative communication, terminals use relaying to jointly transmit information due to the broadcast nature of wireless medium [42, 43]. The relay protocols are classified as Amplify and Forward (AF), Detect and Forward (DTF) and Decode and Forward (DF) [44, 45, 46].

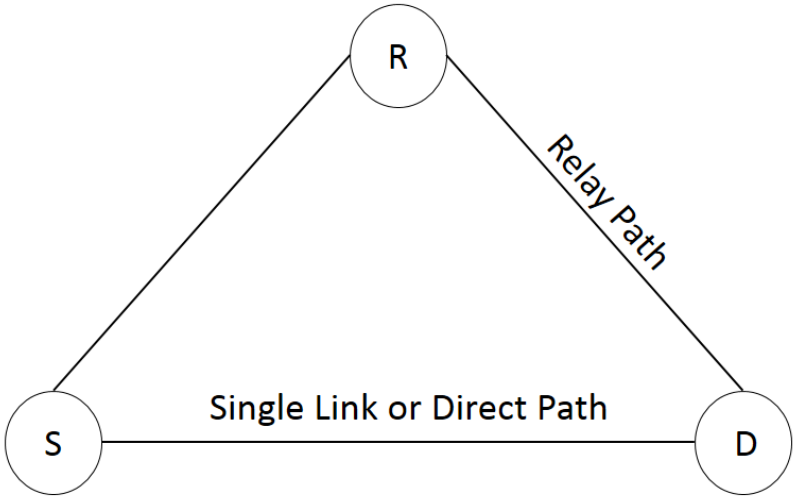

Figure 1.3: Cooperative System Model having single link and one relay path

1.4.1 Amplify and Forward (AF)

AF, which is an analog scheme, works in non regenerative mode. In this scheme, a relay receives the transmitted signal sent by the source node in the first time slot, amplifies it and then retransmits or forwards it to the destination node in the next phase [47]. This is the most preferred method when relay has limited computing time or power available at the time delay. As it is assumed that in AF, the destination knows the channel state information (CSI), it is important to introduce some sort of mechanism to exchange or estimate the information in the implementation. Noise amplification is a major issue for this technique [42, 44].

1.4.2 Detect and Forward (DTF)

In DTF scheme, code repetition is initially applied to the transceiver placed at source and relay node. In the first time slot, the relay node detects or demodulates the transmitted codeword sent by the source node using a hard decision decoding technique. The detected symbols are then forwarded to the destination node, under the same constraint power in the second time slot [48, 49, 50].

1.4.3 Decode and Forward (DF)

DF, which is a digital scheme works in regenerative node. The relay node, situated between the source node and destination node, first decodes the transmitted codeword sent by the source

node using soft output Viterbi decoding algorithm (SOVA), in the first time slot [51, 52, 53, 54, 45, 55]. It then decodes and re−transmits the decoded codeword to the destination node, in the next time slot. As a result, any errors at the relay node can be corrected and avoided from propagating further to the destination node, because of its error correcting capabilities.

1.5 Motivation

IR−UWB communication has emerged as a strong candidate for short range, high bandwidth and low cost applications. One of the challenges associated with UWB systems especially is design of an efficient receiver architecture for WPAN and WSN based applications. It is desirable to use a coherent IR−UWB Rake receiver whose BER performance is much better compared to a non−coherent receiver, but requires accurate channel estimation and synchronization to match the incoming pulse with the template. Coherent receivers are also hard to implement and are power consuming [29]. So, non−coherent IR−UWB receivers such as Transmitted Reference (TR)[56, 57], Differential Transmitted Reference (DTR) [58], Transmitted Reference Pulse Cluster (TRPC) [59, 60, 61, 136, 63, 64] and Energy Detectors (ED) [65, 66, 67], are introduced to overcome the problems faced by a coherent receiver.

In wireless communication channel, fading occurs due to multipath propagation or shadowing from obstacles, affecting the wave propagation. This can be combated using cooperative diversity techniques. Using cooperative communication gives a better BER performance, high data rate and a good coverage area. The motive of our work is to combine the merits of UWB technology with cooperative diversity [68].

1.6 Research objectives and Contribution

The problem statement of the proposed research work is to carry out ”Performance Evaluation of non−coherent IR−UWB system using cooperative and non−cooperative strategies.” The objectives are summarized as given below:

Research objectives:

- To prepare a conceptual background of coherent and non−coherent IR−UWB systems in single−link and cooperative scenario.

- To analytically derive the BER performance of non−coherent IR−UWB system namely AC and ED in single−link environment and validate it with the simulation results. The analytical approach is based on autocorrelation (for AC system) and energy detection principle (for ED system) respectively.

- To derive the BER performance of non−coherent IR−UWB AC system such as TR, DTR and ED system such as ED−OOK, ED−PPM, using cooperative dual−hop AF and DTF relay strategy with various diversity combining strategies namely linear combining, selective combining and optimum linear combining, analytically and validate it with the simulation results. Matlab simulations are used to evaluate the BER performance of non−coherent IR−UWB system in terms of channel used, number of relay paths, number of frames N_f, diversity combining schemes and relay techniques.

Contribution: A typical non−coherent IR−UWB system consists of a signal model, channel model and receiver structure. The research work presented in the thesis focuses primarily on the performance analysis of non−coherent IR−UWB system in cooperative scenario. The receivers used for detection are AC (TR, DTR) and ED (ED−OOK, ED−PPM). A novel analytical approximation in BER evaluation of AC and ED systems using cooperative dual−hop AF and DTF relay strategies with various diversity combining schemes, over IEEE 802.15.4a environment is presented. The theoretical BER approximation for AC and ED systems, based on autocorrelation and energy detection principle respectively, are also compared with the simulation results. The performance comparison is also illustrated in terms of number of frames N_f, relay paths, cooperative relay techniques and combining diversity schemes.

1.7 Organization of the thesis

This thesis aims to evaluate the BER performance of non−coherent IR−UWB system using cooperative and non−cooperative strategies. This thesis explains the theoretical BER performance of non−coherent IR−UWB AC and ED systems using approximation techniques based on autocorrelation and energy detection principle respectively. Simulations have also been carried out to validate its results with the theoretical results. A summary is given at the end of each chapter to highlight the important points given in the chapter. The system model comprising of signal model, channel model and receiver structure are discussed in most of the chapters. The thesis is organized in seven chapters including the present one. The existing research work for

coherent and non−coherent IR−UWB systems in single−link and cooperative scenario, is presented in Chapter two. Chapter three presents an analytical approach to the BER performance of non−coherent IR−UWB system such as TR, DTR, ED−OOK and ED−PPM in single−link scenario. Chapter four discusses the BER Performance of non−coherent IR−UWB AC system using cooperative dual−hop AF and DTF strategy for various diversity combining schemes namely, linear combining, selective combining and optimum linear combining. In chapter five, the BER performance of non−coherent IR−UWB ED−OOK system using cooperative dual−hop AF and DTF strategy with various diversity combining schemes is presented. The sixth chapter presents the performance analysis of non−coherent IR−UWB ED−PPM system using cooperative dual−hop AF and DTF strategy with various diversity combining schemes, over IEEE 802.15.4a environment, in terms of BER. Finally, concluding remarks and future work are presented in chapter seven.

In this chapter, a brief introduction of the thesis is given.

Chapter 2

Preliminaries and Review

In this chapter, the existing research work done by the researchers on coherent and non−coherent IR−UWB system using single−link and cooperative approach, has been discussed in detail, based on their BER performance. The discussion covers a wide range of coherent UWB systems namely ARAKE, PRAKE and SRAKE and non−coherent UWB systems namely TR, DTR and ED.

2.1 Introduction

The history of UWB radar systems manifests its usage mainly in military, because of its nature to penetrate through trees and beneath ground surfaces. With more advancement in the UWB technology, the focus has shifted more towards electronics and communications. Rather than using separate frequencies to broadcast signals, UWB uses wide range of frequencies to spread signals. This makes UWB technology different from its counterpart, narrowband wireless technology. UWB signals are represented by a train of Gaussian pulses transmitted per second having wide bandwidth and consuming less power. This paves way for the UWB signals to appear as background noise.

In single−link scenario, the signal is directly transmitted from the source node to the destination node, resulting in poor BER performance and coverage area. In order to achieve a wide coverage and high data rate, while providing better system performance [69], cooperative diversity technology is introduced [70, 71, 72, 73, 74, 75]. Relay, simplest example of a cooperative network, [76, 77] forms the basis of cooperative diversity. Multiple Input Multiple Output (MIMO) relay communication is one of the most widely used diversity technologies to

improve the BER performance and QoS [53]. Cooperative relay communication handles high data rate, consumes less power, utilizes bandwidth efficiently, improves signal strength intermediately and protects against multipath fading [42, 51, 52, 53, 78, 79, 80]. Furthermore, various diversity combining schemes if incorporated in the cooperative scenario, leads to improvement in BER performance [81, 82]. Many researchers have therefore started working on the combination of UWB technology and cooperative communication, a viable technology for improving the BER performance, QoS and coverage area.

2.2 Coherent UWB System

Coherent UWB RAKE receivers require CSI to extract multipath energy from the various multipaths. This is possible using a collection of correlators, where each correlator is matched to the delayed version of the copy of same transmitted signal. At the destination node, combining strategies such as MRC and EGC are invoked to extract the information symbol [83, 84]. Over a period of time, the various researchers have worked on the improvement of BER performance of UWB RAKE receiver both in single−link and cooperative scenario, which are as described in subsequent sections.

2.2.1 Single-Link Approach

According to Win et al. [85], ARAKE receiver gives the best BER performance among all the coherent UWB receivers. SRAKE receiver gives an acceptable BER performance using moderate number of fingers for a short Txr−Rxr distance, while for larger Txr−Rxr distance, SRAKE receiver requires an additional signal to noise ratio (SNR) of $1.5\ dB$, to achieve the same BER performance. Also, SRAKE receiver shows a better BER performance compared to PRAKE receiver, using MRC and same number of fingers in low data rate UWB channel.

Cassioli [29] stated that, the BER performance of a coherent UWB RAKE receiver can be enhanced by keeping the distance between Txr−Rxr small, using moderate number of fingers and MRC combining. Compared to a non−coherent UWB receiver, coherent UWB RAKE receiver reveals better BER performance, high data rate, less noise and less fading.

It can be observed from the work of Choi and Stark [86], that the performance evaluation of coherent UWB RAKE receiver, is largely improved, using binary block coded PPM and OOK modulation scheme in indoor multipath UWB channels. It can be concluded by saying

that, coherent UWB RAKE receiver with 100 fingers, using PPM modulation scheme, reveals a SNR improvement over OOK scheme. However, with decrease in number of fingers, SNR gain degrades.

Zhang et al. [87], evaluated the BER performance of coherent UWB RAKE receiver in a log−normal fading channel. RAKE reception for UWB signals is very effective, since the radiated power is very low, and there exists many resolvable multipath components. We also infer from the work that, RAKE reception is very effective for UWB signals, and EGC method shows a comparable performance with regard to MRC method. Bose [88] proposed an alternate method to evaluate the BER performance of coherent UWB RAKE receiver in a log−normal channel.

The BER performance of coherent UWB RAKE receiver using TH−PAM and TH−PPM scheme, has been discussed by Amico and Mengali [89], in his research work. It can be inferred from the study that in presence of perfect channel knowledge, coherent UWB RAKE receiver performs much better using TH−PAM modulation scheme, than compared to TH−PPM scheme, in presence of a single user (no multiple access).

As far as BER performance is concerned, ARAKE receiver outperforms the other receivers such as PRAKE and SRAKE. The conclusion obtained from [89] proves that, SRAKE receiver gives a better BER performance compared to PRAKE receiver using MRC combining and with increase in number of correlators, as compared to PRAKE receiver, when its combined with MRC and the number of correlators is increased. Even though SRAKE receiver requires perfect channel estimation to measure path gain, yet it outperforms PRAKE receiver in performance, having less complexity and requiring less accurate channel estimation. It can also be stated from the work of Amico et al [89, 90] that as far as detection of transmitted signal in coherent UWB systems is concerned, PRAKE receiver combined with MRC shows better performance, than when combined with EGC, while for SRAKE receiver, both the combining strategies, EGC and MRC show similar performance.

In single−link scenario, coherent UWB RAKE receivers perform better compared to non−coherent UWB receivers, in terms of less noise, high data rate and less fading [90]. However, the drawback of using a UWB RAKE receiver is its complexity. This complexity is however due to the accurate synchronisation required by the correlators present in the receiver, to extract multipath energy from the multipath components.

It is inferred from [91] that, the BER performance of a S−RAKE receiver degrades in

presence of narrow−band interference, over IEEE 802.15.4a UWB channel. Also, a novel framework is proposed for the performance analysis of coherent UWB systems, based on approximations [92].

2.2.2 Cooperative Approach

Maichalernnukul et al. [93], have introduced a novel cooperative relay scheme in UWB system with a SRAKE receiver for detection of transmitted signal. The relay scheme consists of multiple antennas and uses cooperative DF technique for reception. The UWB signal is transmitted from source to destination, through a relay node using DF scheme. SRAKE receiver with five fingers outperforms SRAKE receiver with one finger by $5\ dB$ at a BER of 10^{-2}, since the former captures more energy compared to the latter, even at the cost of increased complexity. Similarly, using two antennas in a SRAKE system outperform those using single antenna relay by $2\ dB$ at a BER of 10^2. This is due to the spatial diversity gain, obtained using two antennas available at the relay. However under perfect channel estimation, the system consisting of two antennas with five fingers gives a SNR gain of $2\ dB$ at a BER of 10^2, over the system consisting of single antenna with ten fingers. The excellence of a two antenna relay system using more than one finger is because of the decaying PDP characteristic. It is also inferred that increase in number of antennas, gives a better BER improvement than increasing the number of fingers.

A dual−hop DTF multiple relay system for coherent UWB system has been proposed by Maichalernnukul et al. [94]. Each of these relay nodes are equipped with multiple antennas. In the first hop, information is transmitted from the source node to the relay node. At each relay node, detection takes place using a PRAKE receiver, thereby leading to spatial diversity. Similarly in the second hop, detected information is forwarded from the relay to the destination using DTF relay scheme. The increase in number of antennas M at the relay (where $M = 6$,$Q = 1$), produces a superior outage performance gain of 7 dB at a BER of 10^3 in comparison to the increase in number of relays Q (where $M = 1$,$Q = 6$). UWB system with more number of relays ($Q = 4$) and less number of RAKE correlators ($L = 10$), provides a better outage probability than a UWB system with a single relay ($Q = 1$) and having more number of fingers (correlators) ($L = 40$). So, it can be concluded that the use of multiple antennas, saves the number of RAKE fingers and relays required to achieve low outage probability.

Shirazi et al. [95] proposed a novel strategy named UWB based cooperative retransmission scheme (UCoRS). In this scheme, nodes remain static and as a result, information is sent only

once. Also, the process of ranging is performed only once. The scheme achieves multiuser diversity technology for both proactive and reactive settings, by using all the properties of UWB. In proactive setting, decision is made prior to transmission of data, while for reactive environment, decision is made after the relays receive the data. The inference drawn from the research work tells that, the proactive performance is similar to maximum throughput. The reactive and proactive relay schemes produce a much better result than non-cooperative scheme. The packet delivery ratio (PDR) improves with increase in number of relays in UCoRS and is maximum at 0.7 for proactive setting, compared to reactive setting which has a value of 0.6. It is also observed that, throughput improvement in UCoRS is at the expense of minimization in the amount of control packet overhead, thereby eliminating energy cost in coherent UWB.

The throughput of optimal cooperative strategy for proactive and reactive setting, in both static and mobile scenario has been analysed by Shirazi et al. [96]. It can be concluded from the results that, considerable diversity gain is achieved at a low implementation cost. In UCoRS, the exchange of control packets is reduced for both static and mobile cases, thus reducing the control packet exchange cost in UWB receivers.

Abou−Rjeily [43] proposed a non−orthogonal symbol by symbol cooperation strategy, for coherent UWB systems using a single relay PPM constellation. The symbol by symbol cooperation strategy using PPM constellation is achieved within one symbol duration. It can be inferred from the results that, the proposed scheme shows an improved data rate compared to M−ary PPM (M−PPM) system. UWB system using cooperative DF scheme gives a much better BER performance, than cooperative AF and non−cooperative system only at high SNR, not at low SNR. The reason being the decision at relay is with high probability of error.

An optimal DF cooperative scheme for detection of transmitted symbol using a coherent UWB RAKE receiver in CM1 and CM2 environment, has been proposed by Abou−Rjeily et al. [45]. The cooperation strategy used is either coded or space time in nature and is as follows. The performance of a coherent UWB RAKE receiver using selective relaying (SR) strategy shows a much better BER performance than using fixed relaying (FR) strategy. Even in case of errors, UWB RAKE receiver employing SR strategy shows robustness and hence, outperforms UWB receiver using FR strategy.

Yazdi et al. [97], proposed a time reversal technique used for the detection of transmitted symbol using a coherent UWB receiver, that produces a performance equivalent to that of a simple UWB RAKE receiver, without increase in its complexity. In this technique, the trans-

mitting nodes uses pre−diversity filter, in order to filter the UWB signal before transmission. The time reversal signal processing technique at transmitter side exploits the rich multipath scattering, for achieving signal focusing. The proposed method is based on time reversed channel impulse response (CIR), for transmitter side pre−filtering and is applied to the transmitted signals by the source and relay nodes, for reducing the receiver complexity. However, time reversal coherent UWB receiver is more robust to estimation errors compared to the traditional UWB RAKE receiver. It is also noted that the BER performance of time reversal UWB RAKE receiver improves not only with the increase in number of frames, but also with the addition of relay nodes.

The authors, Kwak et al. [98], observed an improvement in BER performance of coherent UWB system using cooperative dual−hop AF scheme, over non−cooperative scheme in multipath fading UWB channel. The location of the relay also plays a major role in improvement of the performance of UWB cooperative relay system.

According to Zu et al. [48, 99], an improvement in performance of UWB system is achieved using cooperative dual−hop cooperative DTF and DF relaying strategies in dense multipath channel. The cooperative DF relaying strategy uses SOVA convolutional coding for decoding of information.

The BER performance of a coherent UWB system using cooperative dual−hop AF strategy in CM3 and CM4 channel respectively, has been compared by Xu et al. [100], in their work. The proposed scheme uses a non−regenerative AF relay scheme instead of a regenerative scheme, so as to avoid system complexity. The authors use Moment Generating Function (MGF) to evaluate average BER performance.

The average Bit Error Probability (BEP) of a coherent UWB system employing TH−PPM scheme is improved using a cooperative DF relay protocol in comparison to a non−cooperative protocol, over IEEE 802.15.4a UWB environment, as stated by Yazdi et al. [101]. The decision variable obtained from the received signal at the destination node helps in evaluating the characteristic function (CF). Once the CF is known, it is easy to evaluate the BEP of the UWB system which depends on SNR, number of frames and the position of relay. The BEP improves with increase in number of frames and SNR. Also, when the relay is situated nearer to the source, BEP further improves.

It can be concluded from the work of Maichalennukul et al. [102] that, UWB systems using dual−hop cooperative AF and DTF strategy and multiple antennas at the relay node, enjoys a

higher SNR advantage over the ones using a single antenna at the relay node[103]. The relay performs hard detection at relay node by estimating the transmitted bit sent by the source node. It is also inferred from the work that using DTF scheme gives a better BER performance than using AF relaying scheme. The BER performance of coherent UWB system using cooperative AF scheme, and having multiple antennas $M > 1$ at the relay node with antenna selection $Q = 1$, improves as M increases and decreases with increase in Q. The outage performance of the UWB system using cooperative AF relay strategy improves with increase in the number of antennas, while with increase in number of relays, the outage performance of the UWB system using cooperative DTF scheme improves.

The authors, Yang et al. [104], proposed a novel AF scheme using cooperative relay selection, based on distance information for detection using UWB receiver. The relay selection depends on the channel conditions between the S$-$R and R$-$D links. The properties of UWB system such as high precision ranging and positioning property, gives the distance information required for the relay system. Coherent UWB RAKE system using cooperative AF scheme gives a much better performance than using all participating opportunistic scheme and non$-$relay scheme.

The authors, Pan et al. [105], analysed the performance of coherent UWB system using AF and DF cooperative relay strategies with TH modulation scheme, in presence of multi$-$user interference (MUI). The performance of UWB system using cooperative AF and DF relay strategies is evaluated in terms of outage probability and average BEP. It is also learnt from the survey that, MUI degrades the SNR of the received signal at the relay and destination node and hence, affects the BER performance and outage probability.

The BER performance of a coherent UWB system using cooperative AF and DF relay scheme with DS and TH scheme, in presence of a single tone narrowband (NB) interferer, both in optimistic scenario and worst case scenario, has been compared by Maichalernnukul et al. [106]. The effect of NB signals on coherent UWB system is significant and in extreme case, these signals jam a UWB receiver completely. In presence of NB interference, coherent UWB system using cooperative relay strategy offers a performance advantage of $5\ dB$ at a BER of 10^{-4}, over non$-$cooperative scenario. Similarly, coherent UWB system using cooperative DTF relay scheme also offers a superior performance gain of 12 dB at a BER of 10^{-4}, over AF relay system, in presence of NB interference. Coherent UWB system using cooperative DF strategy with DS scheme, outperforms DF strategy with TH scheme, AF strategy with DS scheme, AF

strategy with TH scheme, single−link (no relay) UWB system with DS scheme and single link (no relay) UWB system with TH scheme by 0.5, 1, 1.5, 4 and 5 dB, respectively at a BER of 10^{-5}. It can be concluded from the work that UWB system with DS scheme performs better than using TH scheme. Furthermore, coherent UWB system using cooperative AF and DF relay strategy with minimum mean squared error (MMSE) combining scheme, gives similar performance for both optimistic and worst case scenario, but with MRC combining, performance in optimistic scenario is found to be better than worst case scenario.

UWB system takes the advantage of high delay resolution, by using a coherent Rake receiver which uses all its correlators to extract multipath energy from the various multipath components. The use of coherent UWB RAKE receiver leads to complexity issues, since it requires accurate channel estimation, timing synchronization and more number of correlators to extract multipath energy. The problem faced by a coherent UWB RAKE receiver is overcome using a non−coherent UWB receiver [68].

2.3 Non−Coherent UWB System

One of the main advantages of using UWB system for low complexity transmission, is its ability to employ non−coherent receivers even in dense multipath propagation scenario [89]. Non−Coherent UWB receivers do not have any information regarding channel estimation, yet it exploits multipath diversity. Despite distortion and multipath propagation, non−coherent UWB receivers can extract comparable amount of energy from the multipaths [56] and are an advantage over coherent UWB receivers, since it requires less complexity and less cost, but only at the expense of poor BER performance. The non−coherent UWB receivers are classified as TR, DTR and ED [107]. AC receivers [108] such as TR and DTR uses autocorrelation principle, while ED receiver uses energy detection principle for detection [68].

2.3.1 Single−Link Approach

(i) *TR System*: A non−coherent UWB TR system, based on maximum likelihood (ML) criteria, is designed and tested by Giannakis et al. [109, 110] in their research work. It is noted that, UWB TR receiver gives a better BER performance using ML criteria, as compared to conventional one [110, 111]. The authors [112, 111] introduced an optimum receiver for a UWB TR system, whose BER performance is found to be better than the conventional one. The authors,

Franz and Mitra [113], stated that in presence of a single user (no Multi Access Interference (MAI)), the statistics of the received signal obtained from UWB TR system is based on ML and Generalised Likelihood Ratio Test (GLRT). The parameters are assumed known in case of ML while in case of GLRT, the hypothesis' parameters are not completely known. The environment used for analysis is a dense multipath UWB channel, corrupted with AWGN. The conclusion drawn from the study, proved that GLRT and ML based UWB TR system gives a much better BER performance than conventional UWB TR system.

The ML and GLRT based receivers have been discussed and compared with a training based (TB) UWB TR receiver, by Franz and Mitra [114]. For a TB UWB TR receiver, the received training symbol variable is averaged to obtain the channel estimate. The closed form analysis expressed in terms of non−central F−distribution is exact for a TB based receiver and has a lower bound which increases, with increase in SNR for ML and GLRT based receiver. The performance analysis is based purely on Gaussian approximation. It can be concluded from the work that ML and GLRT based UWB TR receiver gives a SNR gain of $2\ dB$ and $2.5\ dB$ over TB based UWB TR receiver, at a BER of 10^4. The improvement in BER performance of GLRT based UWB TR receiver over conventional UWB TR receiver, has also been observed by Amico and Mengali [115].

The performance evaluation of an UWB TR receiver using binary block coded PPM and OOK modulation in multipath UWB and AWGN environment, has been discussed by Choi and Stark [116]. It is also observed that PPM modulation scheme gives a much better BER performance than OOK scheme in UWB environment.

Jia and Kim [117], evaluated the BER performance of balanced UWB TR system in presence of a single user and MAI, over IEEE 802.15.3a environment. The performance of a balanced UWB TR system, is much better in presence of a single user than compared to multiuser scenario. To reduce such effects, M−ary orthogonal modulation is used, which improves the multiple access (MA) capacity in comparison to the conventional TR system, under the constraint that both have the same information rate.

The BER performance of UWB TR system, in conjunction with a simple AC receiver is evaluated by Quek et al. [118], in dense multipath UWB channels using gaussian approximation and sampling expansion approach. A unified approach is introduced by the authors to analyse the BER performance of UWB TR system in presence of narrowband interference [119, 120].

The BER performance of UWB TR system using PPM modulation scheme is evaluated by

Luo [121], and maximum capacity achieved. The BER expression is derived based on a upper bound with a random coding strategy.

Unlike the coherent receiver, non−coherent AC receivers overcome the drawbacks of the conventional Rake receiver through the use of the TR signaling scheme [122, 123].

In a TR system, the specific time delay between the message and the reference signals is realized by using a delay line (DL). In [122, 123], the DL is assumed to be ideal. However, it is infact impossible to design a DL with perfect phase-frequency characteristic. And the unavoidable phase distortion generally leads to a group delay error in signal bandwidth. Therefore, the distortion of DL in the receiver end influence the BER performance of TR system.

In [124, 125, 126], due to the insertion loss fluctuation of transmission line, the designed DLs suffer from stochastic variation of their group delay, the so-called group delay ripple (GDR). The impact of the GDR on some specific non-UWB systems has been researched [127] and more. For UWB system, due to the extremely short time duration of pulse waveforms, even a small timing error between the correct time and the time output by the non-ideal DL degrades system performance dramatically.

The impact of GDR on TR UWB performance is studied in [128]. In this paper, according to the currently designed DL's, a statistical GDR model is proposed for a practical UWB DL, and they investigate the degradation in average BER caused by the GDR for the TR UWB communication systems.

To overcome the problems faced by TR system, weighted AC system is introduced [108, 129, 130]. An improvement in BER performance of weighted AC system is observed, but at the expense of increased complexity.

To address the long DL problem, a frequency multiplexed TR in [131], a frequency shifted reference (FSR) scheme in [132] and a dual-pulse (DP) scheme in [133] and [134] were developed.

Most of the existing research work is focused for single−user until Sadler [135] introduced UWB TR system for detection, in presence of multi−user.

(ii) *TRPC System*: Dong [136] proposed a novel pulse cluster TR (TRPC) system and the integration interval determination methods were further investigated in [137]. The TRPC structure not only provides the best performance among the above mentioned TR signalling schemes but also enables a higher data rate application by allowing IPI in the TRPC structure.

From the implementation point of view, although an analog correlator makes the analog

TRPC receiver a much lower sampling rate of an ADC than other impulse types of UWB, this analog correlator is critical since it handles a very high frequency and large bandwidth signal. Also, for an analog DL, besides the span of its delay time restricted no longer than 10 ns, its delay time error cannot be refrained due to an unavoidable phase distortion in designing the analog DL. Since a digital AC receiver cannot only avoid the above problems but also provide flexibility in its signal processing at the expense of high sampling rate of ADC, digital architectures for the UWB receiver have been investigated in the conventional TR scheme [138, 139, 140]. Jin [141] studies the digital architecture for the recently proposed TRPC scheme, and then propose a reconfigurable digital TRPC receiver and analyzes and compares with that of the original TRPC receiver.

(iii) *DTR System*: Ho et al. [142], evaluated the performance of a DTR system in presence of AWGN and UWB multipath channel. The differential detector or Differential Phase Shift Keying (DPSK) receiver, collects multipath energy from multipath components by mixing signal with the delayed version of itself, and shows better performance at high SNR. DPSK receiver does not require any reference signal, yet its performance is affected by Inter Symbol Interference (ISI) due to the presence of cross products at the output of mixer and hence its overall BER performance is affected. It can be concluded from the work that, that the performance of DPSK receiver is similar to that of coherent UWB RAKE receiver having one finger. This is because coherent RAKE receiver with one finger will extract less multipath energy as compared to the case when it has 10 fingers.

The authors [143] introduced a novel class of algorithm to evaluate the BER performance of a DTR receiver. The analytical approach to evaluate the BER performance is based on CF.

An innovative scheme based on differential detection using an AC receiver has been proposed by Pausini and Janssen [144]. The scheme uses a limiter either in the reference branch or in the signal branch, thereby ignoring the requirement of a complex analog multiplier. The conclusion obtained from the research work claims that, DTR receiver using a non$-$linear limiter device outperforms the one with no limiter (conventional DTR receiver), in terms of BER performance.

It has also been observed by Paussini et al. [145], that the BER performance of AC receivers using differential detection is affected, as interference takes place among the pulses due to multipath propagation. The effects of non$-$linear ISI is combated using a delay hopping (DH) code, which uncorrelates the received signal with its own delayed version, baring the signal

containing the differentially modulated bit. Hence, an improvement in BER performance is observed.

A novel differential detector [146] using GLRT approach, in presence of a single user, is proposed, where symbol by symbol encoding takes place rather than frame by frame encoding. The inference summarized from work proves that DTR receiver using GLRT scheme shows the same complexity, but a double data rate and a power gain of $3\ dB$ over TR system.

A novel multiple symbol differential detector (MSDD) was proposed by Lottici [147] to overcome the problem of channel estimation faced by coherent UWB systems.

(iv) *ED System*: The two most challenging issues faced by ED receiver are estimation of optimal threshold and finding out synchronization and dump points of the integrator [65], which if not solved, leads to BER performance degradation. BER performance is thus improved with the help of parallel integrators, with each of them having different time constants. Further, increase in the time resolution of the receiver due to increase in number of parallel integrator branches, improves the likelihood of obtaining a lower BER, at the expense of hardware complexity.

Cheng et al. [148], stated that cross modulation interference (CMI) affects the BER performance of UWB ED−PPM receivers. So, to alleviate the effect of CMI, orthogonal block coded PPM scheme is proposed for ED receiver. The detection scheme is based on ML criteria using which ED receiver suppresses the effect of CMI and performs well in IEEE 802.15.4a UWB environment, as compared to all the other non−coherent UWB receivers.

A new modulation scheme, Gaussian frequency shift keying (GFSK), based on the different order derivatives of a Gaussian pulse, for extraction of information symbol using energy detection principle in UWB system, has been proposed by Cui [149].

Mengali [150], observed that UWB ED receiver using multiple energy measurements (EDRMM) produce a SNR gain of $2\ dB$ at a BER of 10^3, over conventional ED−OOK receiver.

Among all the non−coherent UWB receivers discussed, ED receiver does not require analogue DL for correlation, hence shows a reduction in implementation complexity. Furthermore, ED receiver requires the lowest power consumption as compared to the other non−coherent UWB receivers, because of simple energy collection procedure, low sampling needs of ADC, low duty cycle and requirement of lower supply power [28].

2.3.2 Cooperative Approach

(i) *TR System*: The combination of UWB communication and cooperative scheme improves the BER performance and reduces the power consumption. In this scheme, the transmitted signal consists of two pulses transmitted per frame, a reference signal followed by a delayed data modulated signal. The cooperation strategy is as follows. The first hop involves the signal being transmitted from the source node to the relay node. The signal is then received at the relay node followed by amplification using AF strategy. The second hop involves the amplified signal obtained at the relay node to be forwarded to the destination node. Along with the signal, evaluated SNR obtained at the relay node is also forwarded to the destination node. The received signal is then detected using a TR receiver at the destination node.

The average BER of a cooperative multi−hop DF relay system is evaluated using UWB TR system over a fading channel, by Kundu and Bose [151]. The BER is solved using Gauss−Hermite Quadrature rule.

Qing [152] inferred from the study that the BER performance of UWB TR system using cooperative AF strategy, is better in LOS environment as compared to NLOS environment.

The BER performance of UWB TR receiver is improved using spatial diversity, employing multiple antenna features in CM2 and CM4 channel, as stated by Feng et al. [153]. The three different kinds of combining strategies such as EGC, MRC and SC are used for evaluating the BER performance. It can be inferred from the study that more the number of antennas used at the relay and destination node, better is the BER performance. This is due to the effect of spatial diversity gain. Also, using EGC combining gives similar performance as that of MRC combining, but better than SC.

(ii) *DTR System*: The performance issues in UWB TR system is greatly improved by the use of a DTR system. A DTR transmitter transmits a data sequence over a frame, by differentially modulating the present data symbol with a previous symbol, thus being more energy efficient and having a higher data rate. A novel cooperative AF strategy with two hop relaying for UWB system is proposed, that exploits both these signals, the one forwarded by the relay node to destination node and the other directly forwarded by the source node to the destination node [154].

Mondelli [154] in his work used a double differential encoding technique at the source node and a single differential demodulation technique at the destination node. The scheme also uses log likelihood ratio criteria based on the decision available at the destination node. The modu-

lation and demodulation scheme used is PAM. UWB DTR system using cooperative AF relay strategy with Jacobi approximation, gives similar BER performance as UWB DTR system using cooperative AF strategy with equal power allocation, and supersedes UWB DTR system using cooperative AF strategy with exact decision rule, UWB DTR system with simple cooperative AF strategy and single−link UWB DTR system. Furthermore, the BER performance of all above mentioned relay strategies used with UWB DTR system degrades, as the relay node moves closer to the destination node.

The BER performance of UWB DTR system using cooperative AF relay protocol with fixed and adaptive amplification factor, has been discussed by Wu and Hou [155]. Since the information symbols are differentially encoded in a UWB DTR system, a previous data carrying pulse acts as a reference to demodulate the incoming pulse. As DF protocol is more complex than AF, AF is preferred. The BER performance analysis and capacity evaluation of the cooperative UWB system is based on CF and non−conventional Gaussian approximation (GA), in presence of multiuser environment. The system capacity improves with increase in number of frames and worsens with increase in number of users. Furthermore, in presence of two users, the system capacity of the cooperative UWB DTR system with adaptive amplification, outperforms the one with constant amplification.

Hamdi et al. [156], proposed a simple two hop cooperative AF relay scheme, for UWB system having a DTR receiver at the relay and destination node. To limit the effects of ISI, a double differential encoding technique is used at the source node, and a single differential decoding technique at the relay and destination node. The proposed UWB system with a DTR receiver at the relay and destination node, using two hop cooperative AF relay scheme with double differential encoding at the source, and a single differential decoding at relay and destination node, gives a much better BER performance than single link UWB DTR system. However, this scheme suffers a marginal loss when AF scheme is replaced by DF scheme.

The authors Hamdi et al. [157] have also proposed a novel multi−hop cooperative AF relaying scheme for the improvement in the system performance and enhancement of coverage area for UWB system, by using a multiple−differential (MD) encoding scheme at the source node, and a single differential decoding at the relay and destination node, thereby limiting ISI at the destination node. In case of DF scheme, the process of demodulation of the transmitted symbol at relay and destination node, is either coded or of uncoded type. The uncoded transmission technique requires a simple slicer for quantizing the detected symbols, while convolutional

coded transmission requires hard or soft Viterbi decoding for detection of symbols. The simulation results prove that, soft input Viterbi decoding outperforms hard input Viterbi decoding, but has a higher complexity, which is a disadvantage for high speed UWB applications. The cooperative scheme uses a recursive formula to find SNR from the received signal available at the destination node. If the relay is located towards the source node, then a much better BER performance is achieved as compared to the relay node being closer to the destination node.

(iii) *ED System*: A novel two way relay network using DF cooperative strategy has been proposed by Wang et al. [158], to boost the throughput of non−coherent UWB system. The relay and destination nodes are provided with a non−coherent UWB ED receiver for detection of UWB transmitted signals. The ED receiver follows the principle of joint demodulation for detection of UWB signals. The signal transmitted from the source is a UWB TR signal. It is concluded from the study that non−coherent UWB ED system using cooperative DF, gives a much better BER performance than non−cooperative UWB ED system.

In this chapter, brief review of the work done by the various researchers on the BER performance of various coherent and non−coherent UWB receivers in single−link and cooperative scenario, is presented. Further, the combination of UWB system with cooperative communication not only improves the system performance but also expands the coverage area of the signals. It is inferred from the study that, ED systems are preferred over the other non−coherent systems because of its less complexity and simplicity. From the review, it can be concluded that not much research work has been done in cooperative scenario using UWB ED systems.

Chapter 3

Performance Analysis of Non−Coherent UWB Single−Link System

Non−Coherent UWB receivers require no CSI, hence are preferred over its coherent counterpart. This chapter discuses the BER performance analysis of non−coherent UWB systems in single−link scenario. The BER performance of AC (TR, DTR) and ED (ED−OOK, ED−PPM) systems have been compared both from analytical and simulation point of view. The organization of the chapter is as follows. A brief introduction is presented in Section 3.1, while Section 3.2 presents the UWB signal model. Section 3.3 describes the channel model, while Section 3.4 illustrates the receiver structure. The detailed theoretical BER performance analysis of single−link non−coherent UWB systems is derived in Section 3.5, while Section 3.6 outlines the simulation results. Finally, Section 3.7 gives the concluding remarks.

3.1 Introduction

The wireless channel frequency is made frequency selective due to the large bandwidth of UWB signals, which results in a large number of resolvable multipath components. This resolvability leads to multipath energy combining, which is solved using a coherent or non−coherent UWB receiver [159]. There are various supporting techniques to solve this multipath resolvability, among which coherent UWB RAKE receiver is the most befitting choice. The multipath energy is extracted from the multipath using correlators of the coherent UWB RAKE receiver, thus exploiting multipath diversity [160, 161]. Though the multipath issue is resolved by the RAKE receivers, they require accurate channel estimation and synchronisation, which results in com-

plexity issues [29, 162]. As far as performance is concerned, coherent UWB RAKE receiver provides a better performance than a non−coherent UWB receiver, but it comes at the cost of increased complexity. So, non−coherent UWB receivers are preferred over coherent UWB receivers, because of less complexity and robustness to synchronization errors [159, 163]. The various non−coherent UWB AC systems discussed in this section are TR, Averaged Transmitted Reference (ATR), Recursive Transmitted Reference (RTR), Recursive Averaged Transmitted Reference (RATR) and DTR.

AC systems work by correlating the received signal with its own delayed version. The resulting correlated signal is then integrated over time interval to retrieve the original transmitted bit. TR system, proposed by Hoctor and Tomilson [164], transmits two pulses per frame i.e. unmodulated reference pulse followed by data modulated pulse. Wastage of energy and power in transmitting a reference pulse is a major drawback of this system. The systems, ATR, RTR and RATR were developed to combat the problems faced by TR system, even though they follow the same transmission procedure as that of TR. The difference however lies in the receiver structure. ATR system averages the reference template over all the frames prior to demodulation, while in RTR system, correlation is performed followed by recursive estimation of reference template to capture multipath energy [165, 166]. RATR system is a combination of ATR and RTR system where, averaging is followed by recursive estimation of reference template before performing demodulation [165, 166]. DTR system transmits differentially modulated information over the frame, by modulating the information bit with previously obtained differential modulated information [58]. The feasibility of AC systems are a point of concern because it requires long analog delay lines for correlating the received signal with its delayed template. Also when the delays exceed few tens of nanoseconds, AC systems cannot be easily integrated and causes attenuation, leading to hardware complexity [56]. ED system, less sensitive to synchronizing errors seeks to be a promising alternative which works by passing the received signal through a square law detector, followed by integration and decision process [167, 40].

3.2 UWB Signal Model

The signal model discussed in this section is applicable for non−coherent UWB AC and ED systems. The modulation scheme used for AC (TR, ATR, RTR, RATR, DTR) system is PAM signalling, while for ED system we use OOK and PPM signalling [168].

3.2.1 TR system

TR system works by transmitting two pulses (doublet) per frame. The first pulse is an unmodulated reference pulse, which is followed by a data modulated pulse, where the former is separated from the latter by a delay of T_d to avoid ISI [169, 170]. For a TR scheme, two pulses represent a frame and N_f number of frames denote a bit or symbol. The transmitted TR signal is expressed as:

$$s_{TR}(t) = \sum_{i=0}^{N_f-1} [p(t - iT_f) + b_i p(t - iT_f - T_d)] \tag{3.1}$$

where $s_{TR}(t)$ represents the transmitted TR signal, $b_i \in (-1, 1)$ the information bit, $p(t)$ the second order gaussian derivative pulse of pulse duration T_p having energy of $\int_0^{T_p} p^2(t)dt = E_p$, T_f the frame duration and $T_d = \frac{T_f}{2}$ the delay between the unmodulated reference and data modulated pulse. Also, each bit is transmitted by N_f successive frames.

ATR, RTR and RATR system follows the same signal model as TR system.

3.2.2 DTR system

DTR system requires less energy to transmit the same information as TR system, because it does not waste energy in sending a reference pulse. In this scheme, differentially modulated data bit (or symbol) is sent over the frame, which is obtained by modulating the binary transmitted bit with the previously obtained differentially modulated bit, thereby saving energy [146, 145]. The transmitted DTR signal is represented as:

$$s_{DTR}(t) = \sum_{i=0}^{\infty} \sum_{j=0}^{N_f-1} b_i p(t - jT_f - iT_s) \tag{3.2}$$

where, N_f refers to the number of frames per symbol. As seen in Fig 3.1(a), b_i represents the differentially modulated bit sent over the frame which is obtained by differentially modulating the information bit $a_i \in (-1, 1)$, with the previously obtained information bit b_{i-1}, by a differential encoding rule $b_i = a_i b_{i-1}$ [171]. The symbol duration is represented as $T_s = N_f T_f$ where, T_f denotes the frame duration.

3.2.3 ED−OOK system

In ED−OOK system, a second order gaussian derivative pulse $p(t)$ is transmitted when information bit $b_i = 1$, whereas no gaussian pulse is transmitted in case of $b_i = 0$. The transmitted

signal for UWB ED−OOK system is represented as:

$$s_{ED-OOK}(t) = \sum_{i=0}^{\infty} \sum_{j=0}^{N_f-1} b_i p(t - jT_f - iT_s) \tag{3.3}$$

where, $s_{ED-OOK}(t)$ represents the transmitted UWB pulse using OOK modulation scheme, $b_i \in \{0, 1\}$ the information bit (or symbol), N_f the number of frames, T_f the frame duration and symbol duration $T_s = N_f T_f$.

3.2.4 ED−PPM system

In ED−PPM system, the gaussian second order derivative pulse $p(t)$ is shifted by Δ units when information bit (or symbol) $b_i = 1$ is transmitted, whereas there is no shift in gaussian second order pulse position in case of $b_i = 0$. The transmitted signal for UWB ED−PPM system is represented as:

$$s_{ED-PPM}(t) = \sum_{i=0}^{\infty} \sum_{j=0}^{N_f-1} p(t - jT_f - iT_s - \Delta b_i) \tag{3.4}$$

where, $s_{ED-PPM}(t)$ represents the transmitted UWB pulse using PPM modulation scheme, $b_i \in \{0, 1\}$ the information bit (or symbol), N_f the number of frames, T_f the frame duration, $T_s = N_f T_f$ the symbol duration and Δ the PPM shift.

3.3 UWB Channel Model

As described in Section 1.2.3, the modified 802.15.4a UWB channel is represented by a tap delay line model of the form:

$$h(t) = \sum_{l=0}^{L-1} \alpha_l \delta(t - \tau_l) \tag{3.5}$$

The channel gains are considered to be non−varying and non−random for better and easier approximation. Also, the squares of the channel gains are normalized, so that their summation $\sum_{l=0}^{L-1} \alpha_l^2 = 1$ becomes 1.

3.4 Receiver Model

Non−Coherent UWB receivers are known to extract enormous amount of energy despite distortions and multipath propagation. Low complexity applications, less cost and less power

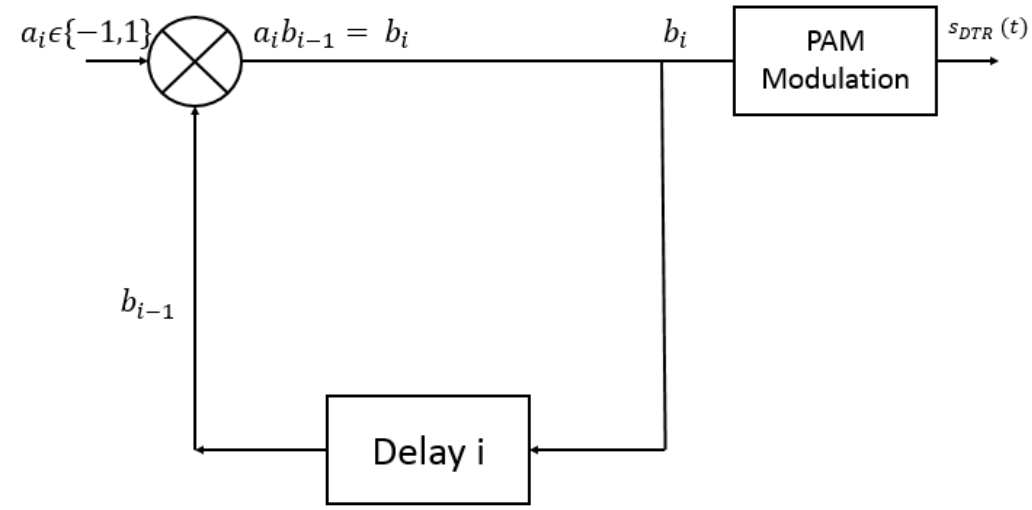

(a)

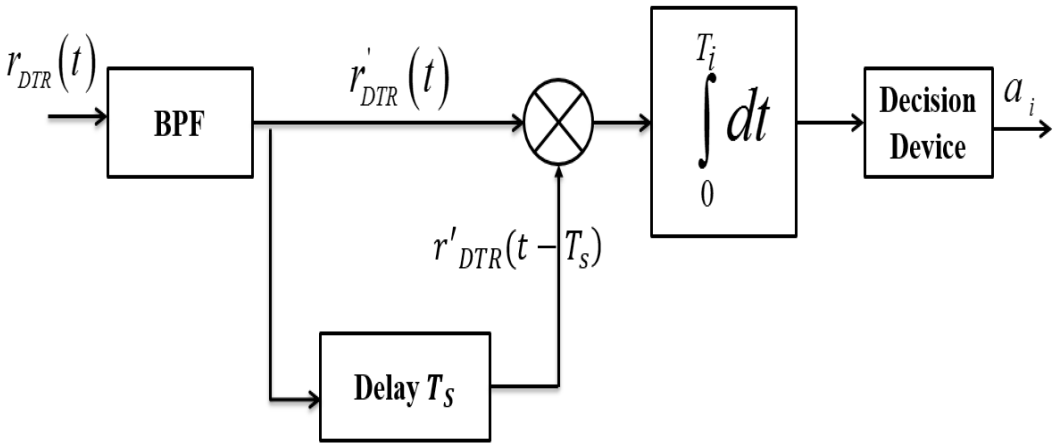

(b)

Figure 3.1: (a) DTR Transmitter (b) DTR Receiver

consumption give an edge to the non−coherent UWB receivers, over its counterpart coherent UWB receivers, though it comes at the cost of poor BER performance. The non−coherent UWB receivers are classified as AC receivers (namely TR, ATR, RTR, RATR, DTR) and ED (namely ED−OOK, ED−PPM) receivers. The received signal obtained at the receiver side is an attenuated and dispersed form of transmitted signal, after it passes through the channel.

3.4.1 TR Receiver

In the receiver, the unmodulated or reference pulse acts as a template during extraction of information bit from the data modulated pulse. The received TR signal is represented as:

$$\begin{aligned} r_{TR}(t) &= s_{TR}(t) * h(t) \\ &= \sum_{i=0}^{N_f-1} [p(t-iT_f) + b_i p(t-iT_f-T_d)] * \sum_{l=0}^{L-1} \alpha_l \delta(t-\tau_l) + n(t) \\ &= \sum_{i=0}^{N_f-1} \sum_{l=0}^{L-1} \alpha_l [p(t-iT_f-\tau_l) + b_i p(t-iT_f-T_d-\tau_l)] + n(t) \\ &= \sum_{i=0}^{N_f-1} [g(t-iT_f) + b_i g(t-iT_f-T_d)] + n(t) \end{aligned} \tag{3.6}$$

where, $n(t)$ denotes the zero mean gaussian process with mean $\frac{N_0}{2}$, $g(t) = \sum_{l=0}^{L-1} \alpha_l p(t-\tau_l) = p(t) * h(t)$ the aggregate signal obtained after convolving the transmitted pulse with the channel impulse. The duration of $g(t)$ is $T_g = T_p + T_{mds}$ where T_p denotes the pulse duration and T_{mds} the multipath delay spread. In order to avoid ISI, $T_g \leq T_d$.

As seen in 3.2(a), the received signal $r_{TR}(t)$ is initially passed through a bandpass filter (BPF) having a bandwidth W and centre frequency f_0. The received filtered signal is represented as:

$$r_{TR}^{'}(t) = \sum_{i=0}^{N_f-1} [g^{'}(t-iT_f) + b_i g^{'}(t-iT_f-T_d)] + n^{'}(t) \tag{3.7}$$

The received filtered signal is then correlated with its delayed version over the integration time interval. Finally using the conventional detection criteria, original information bit b_i is extracted from the correlated product.

3.4.2 ATR Receiver

The problems faced by a TR system is overcome using an ATR system. As observed in Fig 3.2(b), averaging the reference pulse over N_f frames gives rise to an averaged template $g_{ATR}(t)$, which overcomes the problem of using a noisy reference template faced in TR receiver [166]. The averaged template $g_{ATR}(t)$ is represented as:

$$\begin{aligned} g_{ATR}(t) &= 1/N_f \sum_{i=0}^{N_f-1} r^{'}(t + (N_f - i)T_f/2) \\ &= \sqrt{E} g(t) + 1/(N_f \sum_{i=0}^{N_f-1} n^{'}(t + (N_f - i)T_f/2)) \end{aligned} \tag{3.8}$$

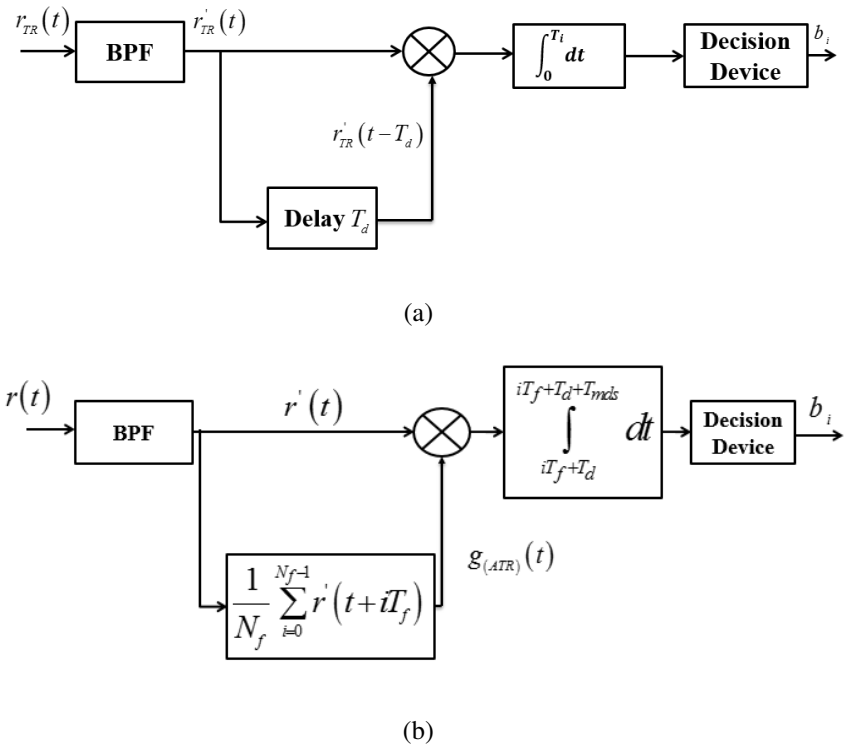

Figure 3.2: (a) TR Receiver (b) ATR Receiver

The received signal $r(t)$ is first filtered by a BPF having a BW of W and center frequency f_0 to obtain $r^{'}(t)$. The filtered signal $r^{'}(t)$ is then correlated with the averaged reference template $g_{ATR}(t)$ and the resultant product is then integrated over the integration time interval. Finally the information bit b_i is extracted using the decision criteria. Here, $r(t)$ is calculated as equation 3.7 where the aggregate signal response is represented as $g(t) = p(t) * h(t)$. ATR, RTR and RATR systems have the same transmitter as that of TR system hence, the received signal $r(t)$ required for correlation in all these systems are the same.

3.4.3 RTR Receiver

In RTR receiver structure, the reference template is estimated recursively to capture multipath energy from the multipath components. As illustrated in Fig 3.3(a), the estimated template obtained in the previous frame $g_{(RTR)_{i-1}}$ is delayed by D units to form previously estimated template $g_{(RTR)_{(i-1)}}(t-D)$. The filtered reference signal and previously estimated template are multiplied by weighting factors β and α, to obtain the updated estimated template $g_{(RTR)_i}(t)$ which is represented as [166]:

$$g_{(RTR)_i}(t) \quad = \quad \beta r^{'}(t) + \alpha g_{(RTR)_{(i-1)}}(t-D) \tag{3.9}$$

where, $\alpha = \beta = 0.5$, delay D is equal to frame duration T_f, T_d signifies the delay between reference and data modulated pulse, $g_{(RTR)_{i-1}}$ represents the previously estimated template at $(i-1)^{\text{th}}$ iteration and $g_{(RTR)_i}(t)$ denotes the updated estimated template at i^{th} iteration. The updated estimated template is then delayed by T_d units to obtain the final template signal $g_{(RTR)_i}(t - T_d)$, which is then correlated with the filtered received signal $r^{'}(t)$. The correlated product is then integrated over the time interval and the resultant is then passed through a decision mechanism to recover the original bit b_i.

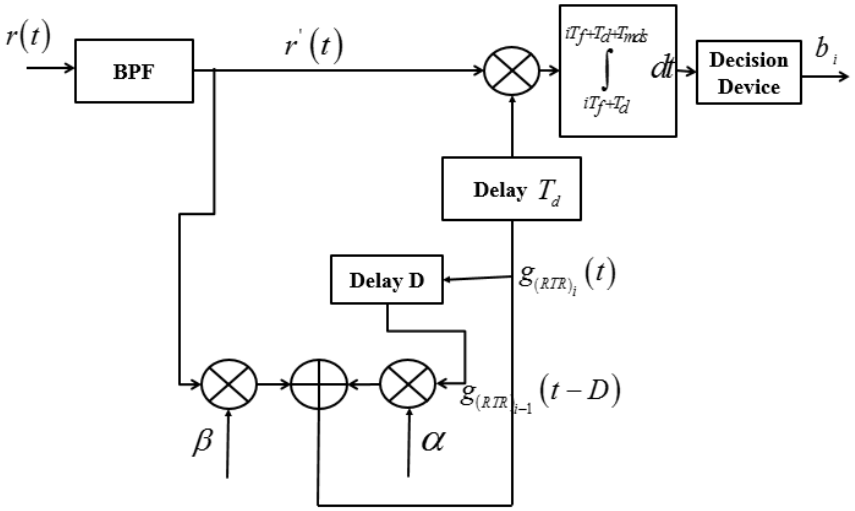

(a)

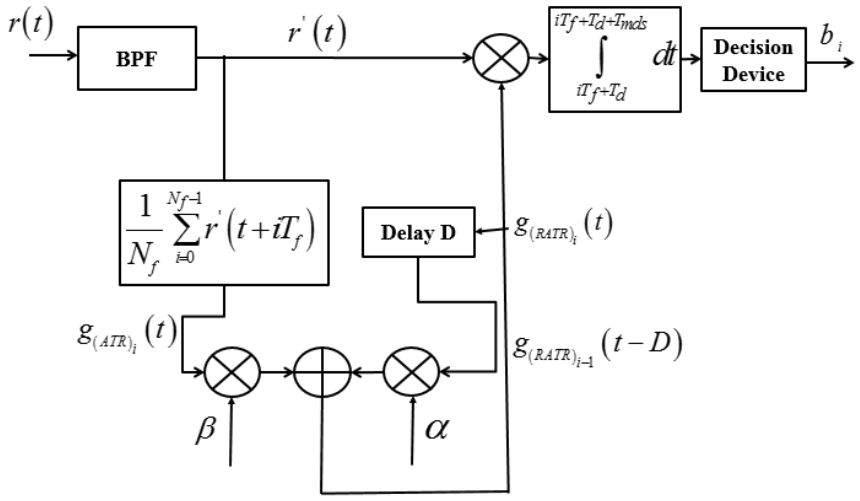

(b)

Figure 3.3: (a) RTR Receiver (b) RATR Receiver

3.4.4 RATR Receiver

RATR is a combination of ATR and RTR system, observed in Fig 3.3(b). The filtered reference template $r^{'}(t)$ is first averaged over N_f frames, to form averaged template $g_{ATR}(t)$. The estimated averaged template obtained in the previous frame $g_{(RATR)_{i-1}}$ is delayed by D units to form previously estimated averaged template $g_{(RATR)_{(i-1)}}(t-D)$. The filtered averaged template signal $g_{ATR}(t)$ and previously estimated averaged templates are multiplied by weighting factors β and α to obtain the updated estimated template $g_{(RATR)_i}(t)$, which is represented as [166]:

$$g_{(RATR)_i}(t) \quad = \quad \beta g_{ATR}(t) + \alpha g_{(RATR)_{(i-1)}}(t-D) \tag{3.10}$$

where, $g_{(RATR)_{i-1}}$ represents the previously averaged estimated template at $(i-1)^{\text{th}}$ iteration and $g_{(RATR)_i}(t)$ denotes the updated estimated averaged template at i^{th} iteration. The updated estimated template is then correlated with the filtered received signal $r^{'}(t)$. The correlated product is then integrated over the time interval to obtain a resultant which is compared to the decision threshold to recover the transmitted bit b_i.

3.4.5 DTR Receiver

Fig 3.2(b) describes a DTR receiver which uses autocorrelation property to extract the original information bit a_i. The filtered received signal $r^{'}_{DTR}(t)$ obtained by passing the received signal $r_{DTR}(t)$ through a BPF, is first correlated with its delayed version of itself $r^{'}_{DTR}(t-T_s)$. The correlated resultant is then integrated over the integration time interval. Finally using decision criteria, the information bit a_i is captured.

3.4.6 ED−OOK Receiver

Energy Detection is a non−coherent methodology used to achieve low complexity, at the expense of some BER performance degradation. ED receiver extracts multipath energy from all the multipath components and is also less sensitive to synchronization errors [172]. The most popular non−coherent modulation technique used for energy detection in UWB system is OOK. As illustrated in Fig 3.4(a), ED receiver comprises of a BPF, square law device, integrator and a decision device. The received UWB signal is initially filtered by passing it through a BPF, to obtain $r^{'}(t)$. The filtered received signal $r^{'}(t)$ is then squared and passed through an integrator having a integration window of T_i. The decision threshold is set to 0.5 since the channel

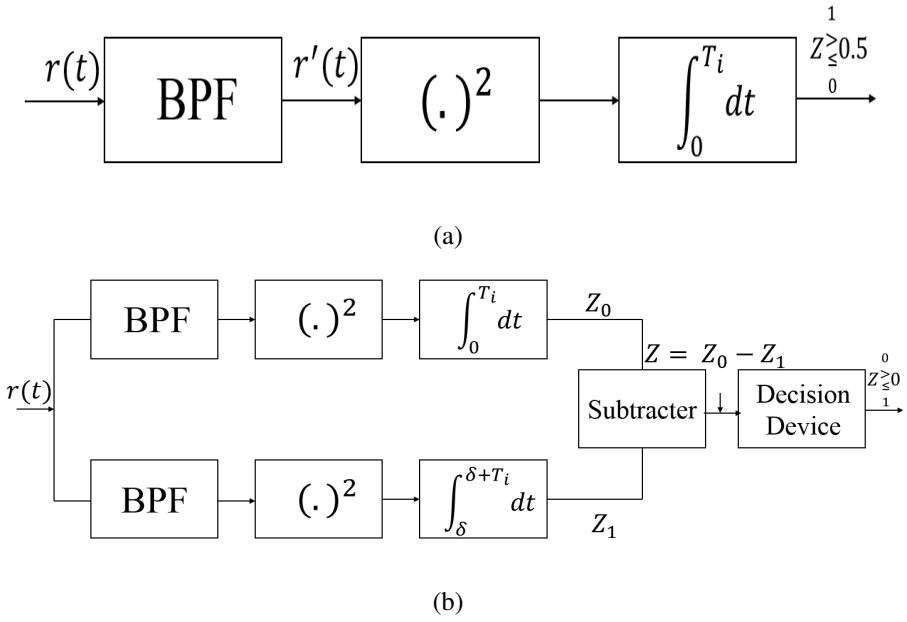

Figure 3.4: (a) ED−OOK Receiver (b) ED−PPM Receiver

gains are set to 1 (constant). So if information bit 1 is transmitted, decision statistic $Z \geq 0.5$ is obtained proving that significant energy was captured during integration interval. In case of information bit 0 being transmitted, $Z \leq 0.5$ proving no energy was captured and hence no pulse was transmitted.

3.4.7 ED−PPM Receiver

The conventional UWB ED−PPM receiver consists of two divisions each consisting of BPF, squarer, integrator, as illustrated in Fig 3.4(b). The upper part works when information bit 0 is transmitted, while the lower section works, in case of information bit 1. The decision statistics obtained from the upper section Z_0 and lower section Z_1 are subtracted to form the final decision statistic $Z = Z_0 - Z_1$. The final decision statistic is then compared to the decision threshold 0, to recover the information bit.

3.5 Performance Analysis

The theoretical performance analysis of AC (TR, DTR) and ED (ED−OOK, ED−PPM) systems are explained vividly in this section [173, 174, 165].

3.5.1 TR System

The transmitted TR signal is represented as:

$$s_{TR}(t) = \sum_{i=0}^{N_f-1} [p(t - iT_f) + b_i p(t - iT_f - T_d)] \tag{3.11}$$

The channel impulse response $h(t)$ is simplified as:

$$h(t) = \sum_{l=0}^{L-1} \alpha_l \delta(t - \tau_l) \tag{3.12}$$

where $h(t)$ represents the impulse response of the channel model, L the number of multipaths, α_l the amplitude of l^{th} tap, τ_l the delay of l^{th} tap and δ the Dirac Delta function. The received TR signal is represented as:

$$\begin{aligned} r_{TR}(t) &= s_{TR}(t) * h(t) \\ &= \sum_{i=0}^{N_f-1} \left[p(t - iT_f) + b_i p(t - iT_f - T_d) * \sum_{l=0}^{L-1} \alpha_l \delta(t - \tau_l) \right] + n(t) \\ &= \sum_{i=0}^{N_f-1} \sum_{l=0}^{L-1} \alpha_l \left[p(t - iT_f - \tau_l) + b_i p(t - iT_f - T_d - \tau_l) \right] + n(t) \end{aligned} \tag{3.13}$$

where, $*$ denotes the convolution operator, N_f the number of frames per symbol, T_f the frame duration, T_d the delay between a reference and data modulated pulse, $p(t)$ the second order derivative gaussian pulse of duration T_p, $b_i \in \{-1, 1\}$ the information bit (or symbol) and $n(t)$ the AWGN noise. The filtered received TR signal is given by:

$$r_{TR}^{'}(t) = \sum_{i=0}^{N_f-1} \sum_{l=0}^{L-1} \alpha_l \left[p^{'}(t - iT_f - \tau_l) + b_i p^{'}(t - iT_f - T_d - \tau_l) \right] + n^{'}(t) \tag{3.14}$$

The filtered received signal $r_{TR}^{'}(t)$ is then correlated with its own delayed version and the resultant is then passed through an integrator to obtain decision statistics Z_{TR} which is expressed as:

$$\begin{aligned} Z_{TR} &= \sum_{i=0}^{N_f-1} \int_{iT_f+T_d}^{iT_f+T_d+T_i} r_{TR}^{'}(t) r_{TR}^{'}(t - T_d) dt \\ &= Y + N_1 + N_2 + N_3 \end{aligned} \tag{3.15}$$

where, Y is the correlator signal output, N_1, N_2 and N_3 are the noise terms. Here, $T_i = T_p + T_{mds}$ refers to the integration time interval and T_{mds} the multipath delay spread. The signal term Y is solved as follows:

$$
\begin{aligned}
Y &= \sum_{i=0}^{N_f-1}\left[\int_{iT_f+T_d}^{iT_f+T_d+T_i} g(t-iT_f)+b_i g(t-iT_f-T_d)dt\right] \\
&= \sum_{i=0}^{N_f-1}\left[\int_{iT_f+T_d}^{iT_f+T_d+T_i}\left\{\sum_{l=0}^{L-1}\alpha_l p(t-iT_f-\tau_l)b_i\sum_{m=0}^{L-1}\alpha_m p(t-iT_f-T_d-\tau_m)\right\}dt\right] \\
&= N_f b_i\left[\int_{iT_f+T_d}^{iT_f+T_d+T_i}\sum_{l=m}\alpha_l^2 p^2(t-iT_f-\tau_l)dt+\underbrace{\sum_{l\neq m}\sum\alpha_l\alpha_m R(\tau_l-\tau_m)}_{value=0}\right] \\
&= N_f b_i\Bigg(\underbrace{\sum_{l=m}\alpha_l^2}_{value=1}\Bigg)E_p \\
&= N_f b_i E_p
\end{aligned}
\tag{3.16}
$$

where, $E_p=\int_{iT_f+T_d}^{iT_f+T_d+T_i}p^2(t-iT_f-\tau_l)dt$ represents the pulse energy and $R(\tau)=\int_{\infty}^{\infty}p(t)p(t-\tau)dt$ the autocorrelation function of signal. If $min\left\{(\tau_l-\tau_m)\right\}>T_p$ for $l\neq m$, then IPI can be avoided. The channel gains are normalized in nature to form, $\sum_l\alpha_l^2=1$.

The filtering of AWGN process having PSD $\frac{N_0}{2}$ with a BPF W, results in noise terms $n(t)$. The autocorrelation function of noise $\theta(\tau)$ is given by [175]:-

$$
\theta(\tau) = \mathbb{E}[n(t)n(t-\tau)]=\frac{N_0}{2}\frac{Sin(\pi W\tau)}{\pi W\tau}cos(2\pi f_c\tau) \tag{3.17}
$$

where, $\mathbb{E}[.]$ denotes the statistical expectation operator and f_c carrier frequency of BPF. Since the Bandwidth is assumed to be sufficiently large, the frequency response of the received signal $g(t)$ at destination node falls inside the PSD $\theta(f)$ of $n(t)$. As PSD $\theta(f)$ is sufficiently flat, the autocorrelation function of noise can be simplified as $\theta(\tau)=\frac{N_0}{2}\delta(\tau)$ [175]. The noise variances are solved as follows.

$$
\begin{aligned}
Var(N_1) &= E[N_1^2]=\sum_{i=0}^{N_f-1}\Bigg[\int_{iT_f+T_d}^{iT_f+T_d+T_i}\int_{iT_f+T_d}^{iT_f+T_d+T_i}\Bigg(\sum_{l=0}^{L-1}\alpha_l b_i p(t-iT_f-\tau_l)\sum_{m=0}^{L-1}\alpha_m \\
&\quad b_i p(\tau-iT_f-\tau_m)\Bigg)\mathbb{E}[n^{'}(t-iT_f-T_d)n^{'}(\tau-iT_f-T_d)]dtd\tau\Bigg] \\
&= \sum_{i=0}^{N_f-1}b_i^2\Bigg[\int_{iT_f+T_d}^{iT_f+T_d+T_i}\int_{iT_f+T_d}^{iT_f+T_d+T_i}\sum_l\alpha_l p(t-iT_f-\tau_l)\sum_m\alpha_m p(\tau-iT_f-\tau_m) \\
&\quad \theta^{'}(t-\tau)dtd\tau\Bigg]
\end{aligned}
$$

$$= \frac{N_f N_0 b_i^2}{2}\Bigg[\int_{iT_f+T_d}^{iT_f+T_d+T_i}\sum_{l=m}\alpha_l^2 p^2(t-iT_f-\tau_l)dt + \underbrace{\sum_{l\neq m}\sum\alpha_l\alpha_m R(\tau_l-\tau_m)}_{value=0}\Bigg]$$

$$= \frac{N_f N_0 b_i^2}{2}\Bigg(\underbrace{\sum_{l=m}\alpha_l^2}_{value=1}\Bigg)E_p$$

$$= \frac{N_f N_0 b_i^2 E_p}{2} \tag{3.18}$$

where, $\int_{iT_f+T_d}^{iT_f+T_d+T_i}\theta^{'}(t-\tau)d\tau = \frac{N_0\delta(t-\tau)}{2} = \frac{N_0}{2}$.

$$Var(N_2) = E[N_2^2] = \sum_{i=0}^{N_f-1}\Bigg[\int_{iT_f+T_d}^{iT_f+T_d+T_i}\int_{iT_f+T_d}^{iT_f+T_d+T_i}\Bigg(\sum_{l=0}^{L-1}\alpha_l p(t-iT_f-T_d-\tau_l)\sum_{m=0}^{L-1}\alpha_m p(\tau-iT_f-T_d-\tau_m)\Bigg)\mathbb{E}[n^{'}(t-iT_f)n^{'}(\tau-iT_f)]dtd\tau\Bigg]$$

$$= \sum_{i=0}^{N_f-1}\Bigg[\int_{iT_f+T_d}^{iT_f+T_d+T_i}\int_{iT_f+T_d}^{iT_f+T_d+T_i}\sum_{l}\alpha_l p(t-iT_f-T_d-\tau_l)\sum_{m}\alpha_m p(\tau-iT_f-T_d-\tau_m)\theta^{'}(t-\tau)dtd\tau\Bigg]$$

$$= \frac{N_f N_0}{2}\Bigg[\int_{iT_f+T_d}^{iT_f+T_d+T_i}\sum_{l=m}\alpha_l^2 p^2(t-iT_f-\tau_l)dt + \underbrace{\sum_{l\neq m}\sum\alpha_l\alpha_m R(\tau_l-\tau_m)}_{value=0}\Bigg]$$

$$= \frac{N_f N_0}{2}\Bigg(\underbrace{\sum_{l=m}\alpha_l^2}_{value=1}\Bigg)E_p$$

$$= \frac{N_f N_0 E_p}{2}. \tag{3.19}$$

$$Var(N_3) = E[N_3^2] = \sum_{i=0}^{N_f-1}\Bigg[\int_{iT_f+T_d}^{iT_f+T_d+T_i}\int_{iT_f+T_d}^{iT_f+T_d+T_i}\mathbb{E}\Bigg[\Big\{n^{'}(t-iT_f)n^{'}(\tau-iT_f-T_d)\Big\}^2\Bigg]dtd\tau$$

$$= \sum_{i=0}^{N_f-1}\Bigg[\int_{iT_f+T_d}^{iT_f+T_d+T_i}\int_{iT_f+T_d}^{iT_f+T_d+T_i}\theta^{'2}(t-\tau)dtd\tau\Bigg]$$

$$= \sum_{i=0}^{N_f-1}\Bigg[\int_{iT_f+T_d}^{iT_f+T_d+T_i}\int_{iT_f+T_d+T_i-t}^{iT_f+T_d+T_i}\theta^{'2}(u)dtdu\Bigg]$$

$$= \sum_{i=0}^{N_f-1}\Bigg[\int_{iT_f+T_d}^{iT_f+T_d+T_i}\frac{N_0^2}{4}2Wdt\Bigg]$$

$$= \frac{N_f N_0^2 W T_i}{2}. \tag{3.20}$$

The variance of $[n^2(t)]$ tends to Dirac-Delta function, hence the integral vanishes outside the range $[-t, T_i - t]$. We then apply Parsevals Theorem to solve equation 3.20. The SNR at the output of the correlator is given by SNR_{TR}:

$$\begin{aligned} SNR_{TR} &= \frac{\sum Y^2}{Var(N_1) + Var(N_2) + Var(N_3)} \\ &= \frac{(N_f b_i E_p)^2}{\frac{N_f N_0 E_p}{2} + \frac{N_f N_0 b_i^2 E_p}{2} + \frac{N_f N_0^2 W T_i}{2}} \\ &= \frac{(N_f E_p)^2}{N_f N_0 E_p + \frac{N_f N_0^2 W T_i}{2}} \\ &= \left(\left(\frac{N_0}{E_p} \right) \frac{1}{N_f} + \left(\frac{N_0}{E_p} \right)^2 \frac{W T_i}{2 N_f} \right)^{-1} \end{aligned} \tag{3.21}$$

Therefore, the BER of UWB TR system is represented as:

$$BER_{TR} = Q\left[\left(2\left(\frac{N_0}{E_b} \right) + \left(\frac{N_0}{E_b} \right)^2 2 N_f T_i W \right)^{-0.5} \right] \tag{3.22}$$

where, $E_b = 2N_f E_p$, represents the energy per bit and Q denotes the Q-function.

3.5.2 DTR System

The received DTR signal is denoted as:

$$\begin{aligned} r_{DTR}(t) &= s_{DTR}(t) * h(t) + n(t) \\ &= \sum_{i=0}^{\infty} \sum_{j=0}^{N_f - 1} \sum_{l=0}^{L-1} \alpha_l \Big[p(t - jT_f - iT_s - \tau_l) \Big] + n(t) \\ &= \sum_{i=0}^{\infty} \sum_{j=0}^{N_f - 1} b_i \Big[g(t - jT_f - iT_s) \Big] + n(t) \end{aligned} \tag{3.23}$$

where, $r_{DTR}(t)$ represents the received DTR signal, b_i the differentially modulated bit sent over the frame, $g(t) = \sum_{l=0}^{L-1} \alpha_l p(t - \tau_l)$ the aggregate signal response and $n(t)$ the AWGN noise. Also, b_i the differentially modulated bit sent over the frame is obtained by modulating the information bit, $a_i \in (-1, 1)$, with the previously obtained differentially modulated bit b_{i-1} using a differential encoding rule $b_i = a_i b_{i-1}$. The received signal $r_{DTR}(t)$ is then passed through a BPF of bandwidth W, to give $r'_{DTR}(t)$ which is expressed as:

$$\begin{aligned} r'_{DTR}(t) &= \sum_{i=0}^{\infty} \sum_{j=0}^{N_f - 1} b_i \Big[g'(t - jT_f - iT_s) \Big] + n'(t) \\ &= \sum_{i=0}^{\infty} \sum_{j=0}^{N_f - 1} \sum_{l=0}^{L-1} \alpha_l \Big[p'(t - jT_f - iT_s - \tau_l) \Big] + n'(t) \end{aligned} \tag{3.24}$$

The filtered received signal is then correlated with its delayed form, and the resultant is then passed through an integrator to obtain the decision statistic Z_{DTR}, which is represented as:

$$\begin{aligned} Z_{DTR} &= \sum_{j=0}^{N_f-1} \int_{jT_f+iT_s}^{jT_f+iT_s+T_i} r^{'}_{DTR}(t) r^{'}_{DTR}(t-T_s)dt \\ &= Y + N_1 + N_2 + N_3 \end{aligned} \tag{3.25}$$

Replacing the value of equation 3.24 in equation 3.25, we obtain the value of Z_{DTR} in equation 3.26.

$$\begin{aligned} &= \sum_{j=0}^{N_f-1} \int_{jT_f+iT_s}^{jT_f+iT_s+T_i} \Big[\sum_l \alpha_l b_i p^{'}(t-jT_f-iT_s) + n^{'}(t) \Big] \Big[\sum_m \alpha_m b_{i-1} p^{'}(t-jT_f-iT_s) \\ &\quad + n^{'}(t-T_s) \Big] \end{aligned} \tag{3.26}$$

where, Y is the correlator signal output, N_1, N_2 and N_3 are the noise terms. Here, $T_i = T_p + T_{mds}$ refers to the integration time interval and T_{mds} the multipath delay spread. The signal term Y is solved as follows:

$$\begin{aligned} Y &= \sum_{j=0}^{N_f-1} \Big[\int_{jT_f+iT_s}^{jT_f+iT_s+T_i} b_i g^{'}(t-jT_f-iT_s) b_{i-1} g^{'}(t-jT_f-iT_s)dt \Big] \\ &= \sum_{i=0}^{N_f-1} \Big[\int_{jT_f+iT_s}^{jT_f+iT_s+T_i} \Big(\sum_{l=0}^{L-1} \alpha_l b_i p^{'}(t-jT_f-iT_s-\tau_l) \sum_{m=0}^{L-1} \alpha_m b_{i-1} p^{'}(t-jT_f-iT_s-\tau_m \\ &\quad) \Big) dt \Big] \\ &= N_f b_i b_{i-1} \Big[\int_{jT_f+iT_s}^{jT_f+iT_s+T_i} \sum_{l=m} \alpha_l^2 p^{'2}(t-jT_f-iT_s-\tau_l)dt + \underbrace{\sum_{l\neq m} \sum \alpha_l \alpha_m R(\tau_l - \tau_m)}_{value=0} \Big] \\ &= N_f b_i b_{i-1} \Big(\underbrace{\sum_{l=m} \alpha_l^2}_{value=1} \Big) E_p \\ &= N_f b_i b_{i-1} E_p \end{aligned} \tag{3.27}$$

where, $E_p = \int_{jT_f+iT_f}^{jT_f+iT_f+T_i} p^{'2}(t-jT_f-iT_s-\tau_l)dt$ represents the energy of the pulse while the autocorrelation function of pulse is defined as $R(\tau) = \int_{\infty}^{\infty} p^{'}(t)p^{'}(t-\tau)dt$. To avoid IPI, $min\{(\tau_l - \tau_m)\} > T_p$ for $l \neq m$. The channel gains are taken to be normalized in nature hence, $\sum_l \alpha_l^2 = 1$. As explained in the section 3.5.1, the autocorrelation of noise can be simplified as $\theta(\tau) = \frac{N_0}{2}\delta(\tau)$ [175]. The noise variances are solved as follows.

$$Var(N_1) = E[N_1^2] = \sum_{j=0}^{N_f-1} \Big[\int_{jT_f+iT_s}^{jT_f+iT_s+T_i} \int_{jT_f+iT_s}^{jT_f+iT_s+T_i} \Big(\sum_{l=0}^{L-1} \alpha_l b_i p^{'}(t-jT_f-iT_s-\tau_l) \sum_{m=0}^{L-1}$$

$$\alpha_m b_i p^{'}(\tau - jT_f - iT_s - \tau_m)\Big)\,\mathbb{E}[n^{'}(t-T_s)n^{'}(\tau-T_s)]dtd\tau\Big]$$

$$= \sum_{j=0}^{N_f-1} b_i^2\Big[\int_{jT_f+iT_s}^{jT_f+iT_s+T_i}\int_{jT_f+iT_s}^{jT_f+iT_s+T_i}\sum_l \alpha_l p^{'}(t-jT_f-iT_s-\tau_l)\sum_m \alpha_m p^{'}(\tau -$$

$$jT_f - iT_s - \tau_m)\theta^{'}(t-\tau)dtd\tau\Big]$$

$$= \frac{N_f N_0 b_i^2}{2}\Big[\int_{jT_f+iT_s}^{jT_f+iT_s+T_i}\sum_{l=m}\alpha_l^2 p^{'2}(t-jT_f-iT_s-\tau_l)dt +$$

$$\underbrace{\sum_{l\neq m}\sum \alpha_l\alpha_m R(\tau_l-\tau_m)}_{value=0}\Big]$$

$$= \frac{N_f N_0 b_i^2}{2}\Big(\underbrace{\sum_{l=m}\alpha_l^2}_{value=1}\Big)E_p$$

$$= \frac{N_f N_0 b_i^2 E_p}{2} \tag{3.28}$$

where, $\int_{jT_f+iT_s}^{jT_f+iT_s+T_i}\theta^{'}(t-\tau)d\tau = \frac{N_0\delta(t-\tau)}{2} = \frac{N_0}{2}$.

$$Var(N_2) = E[N_2^2] = \sum_{j=0}^{N_f-1}\Big[\int_{jT_f+iT_s}^{jT_f+iT_s+T_i}\int_{jT_f+iT_s}^{jT_f+iT_s+T_i}\Big(\sum_{l=0}^{L-1}\alpha_l b_{i-1}p^{'}(t-jT_f-iT_s-\tau_l)$$

$$\sum_{m=0}^{L-1}\alpha_m b_{i-1}p^{'}(\tau-jT_f-iT_s-\tau_m)\Big)\,\mathbb{E}[n^{'}(t)n^{'}(\tau)]dtd\tau\Big]$$

$$= \sum_{j=0}^{N_f-1} b_{i-1}^2\Big[\int_{jT_f+iT_s}^{jT_f+iT_s+T_i}\int_{jT_f+iT_s}^{jT_f+iT_s+T_i}\sum_l \alpha_l p^{'}(t-jT_f-iT_s-\tau_l)\sum_m \alpha_m p(\tau -$$

$$jT_f - iT_s - \tau_m)\theta^{'}(t-\tau)dtd\tau\Big]$$

$$= \frac{N_f N_0 b_{i-1}^2}{2}\Big[\int_{jT_f+iT_s}^{jT_f+iT_s+T_i}\sum_{l=m}\alpha_l^2 p^{'2}(t-jT_f-iT_s-\tau_l)dt +$$

$$\underbrace{\sum_{l\neq m}\sum \alpha_l\alpha_m R(\tau_l-\tau_m)}_{value=0}\Big]$$

$$= \frac{N_f N_0 b_{i-1}^2}{2}\Big(\underbrace{\sum_{l=m}\alpha_l^2}_{value=1}\Big)E_p$$

$$= \frac{N_f N_0 b_{i-1}^2 E_p}{2}. \tag{3.29}$$

$$Var(N_3) = E[N_3^2] = \sum_{j=0}^{N_f-1}\Big[\int_{jT_f+iT_s}^{jT_f+iT_s+T_i}\int_{jT_f+iT_s}^{jT_f+iT_s+T_i}\mathbb{E}\Big[\Big\{n^{'}(t)n^{'}(\tau-T_s)\Big\}^2\Big]$$

$$
\begin{aligned}
& dtd\tau \\
= & \sum_{j=0}^{N_f-1}\left[\int_{jT_f+iT_s}^{jT_f+iT_s+T_i}\int_{jT_f+iT_s}^{jT_f+iT_s+T_i}\theta^{'2}(t-\tau)dtd\tau\right] \\
= & \sum_{j=0}^{N_f-1}\left[\int_{jT_f+iT_s}^{jT_f+iT_s+T_i}\int_{jT_f+iT_s+T_i-t}^{jT_f+iT_s+T_i}\theta^{'2}(u)dtdu\right] \\
= & \sum_{j=0}^{N_f-1}\left[\int_{jT_f+iT_s}^{jT_f+iT_s+T_i}\frac{N_0^2}{4}2Wdt\right] \\
= & \frac{N_fN_0^2WT_i}{2}. \qquad (3.30)
\end{aligned}
$$

The variance of $n^{'2}(t)$ tends to Dirac-Delta function, hence the integral vanishes outside the range $[-t, T_i - t]$. Parsevals Theorem is applied to solve equation 3.30. The SNR at the output of the correlator is given by SNR_{DTR}:

$$
\begin{aligned}
SNR_{DTR} &= \frac{\sum Y^2}{Var(N_1)+Var(N_2)+Var(N_3)} \\
&= \frac{(N_fb_ib_{i-1}E_p)^2}{\frac{N_fN_0b_i^2E_p}{2}+\frac{N_fN_0b_{i-1}^2E_p}{2}+\frac{N_fN_0^2WT_i}{2}} \\
&= \frac{(N_fE_p)^2}{\frac{N_fN_0E_p}{2}+\frac{N_fN_0E_p}{2}+\frac{N_fN_0^2WT_i}{2}} \\
&= \left(\left(\frac{N_0}{N_fE_p}\right)+\left(\frac{N_0}{N_fE_p}\right)^2\frac{N_fWT_{mds}}{2}\right)^{-1} \qquad (3.31)
\end{aligned}
$$

The BER of UWB DTR system is denoted as:

$$
BER_{DTR} = Q\left[\left(\left(\frac{N_0}{E_b}\right)+\left(\frac{N_0}{E_b}\right)^2\frac{N_fWT_{mds}}{2}\right)^{-0.5}\right] \qquad (3.32)
$$

where, $E_b = N_fE_p$ is the energy per bit and is half of that TR scheme because it doesn't transmit a reference pulse. Hence TR system wastes 3dB of energy in transmitting the same information as compared to a DTR system.

3.5.3 ED−OOK System

The received ED−OOK signal is denoted as:

$$
\begin{aligned}
r_{ED-OOK}(t) &= s_{ED-OOK}(t) * h(t) \\
&= \sum_{i=0}^{\infty}\sum_{j=0}^{N_f-1} b_ip(t-jT_f-iT_s) * \sum_{l=0}^{L-1}\alpha_l\delta(t-\tau_l)+n(t) \\
&= \sum_{l=0}^{L-1}\alpha_l g(t-jT_f-iT_s-\tau_l)+n(t) \qquad (3.33)
\end{aligned}
$$

where, $*$ represents the convolution operator, $g(t) = s_{ED-OOK}(t) * \delta(t - \tau_l)$ the aggregate received signal and $n(t)$ the noise term. Here, $T_s = N_f T_f$ denotes the symbol duration, N_f the number of frames per symbol and T_f the frame duration. The received signal $r_{ED-OOK}(t)$ is then passed through a ED$-$OOK receiver, whose decision statistics Z_{ED-OOK} is as follows:

$$\begin{aligned} Z_{ED-OOK} &= \sum_{j=0}^{N_f-1} \int_{iT_s+jT_f}^{iT_s+jT_f+T_i} r^2_{ED-OOK}(t)dt \\ &= \underbrace{A_1}_{signal} + \underbrace{A_2 + A_3}_{\text{noiseterm}} \\ &= \underbrace{sig}_{signal} + \underbrace{Z_{noise}}_{\text{noise}-term} \end{aligned} \tag{3.34}$$

Replacing the value of equation 3.33 in equation 3.34, we obtain the decision statistics of ED$-$OOK system Z_{ED-OOK} in equation 3.35. The equation 3.35 holds good in case of no IPI.

$$\begin{aligned} &= \sum_{j=0}^{N_f-1} \int_{iT_s+jT_f}^{iT_s+jT_f+T_i} \left(\sum_{l=0}^{L-1} \alpha_l g(t - jT_f - iT_s - \tau_l) + n(t) \right)^2 dt \\ &= \sum_{j=0}^{N_f-1} \sum_{l=0}^{L-1} \alpha_l^2 \int_{iT_s+jT_f}^{iT_s+jT_f+T_i} g^2(t - jT_f - iT_s - \tau_l)dt + 2 \sum_{j=0}^{N_f-1} \sum_{l=0}^{L-1} \alpha_l \\ &\int_{iT_s+jT_f}^{iT_s+jT_f+T_i} g(t - jT_f - iT_s - \tau_l)n(t)dt + \sum_{j=0}^{N_f-1} \int_{iT_s+jT_f}^{iT_s+jT_f+T_i} n^2(t)dt \end{aligned} \tag{3.35}$$

where, $T_i = T_{mds} + T_p$ represents the integration time interval. Also, T_p denotes the pulse duration and T_{mds} the multipath delay spread. The signal term obtained from A_1 is represented as:

$$\begin{aligned} A_1 &= \sum_{j=0}^{N_f-1} \sum_{l=0}^{L-1} \alpha_l^2 \int_{iT_s+jT_f}^{iT_s+jT_f+T_i} g^2(t - jT_f - iT_s - \tau_l)dt \\ &= sig = N_f E \end{aligned} \tag{3.36}$$

where, $E = \int_{iT_s+jT_f}^{iT_s+jT_f+T_i} g^2(t - jT_f - iT_s - \tau_l)dt$ denotes the received signal energy due to transmission of information bit $b_i \in \{0, 1\}$. The noise variance is evaluated by solving the decision variables A_2 and A_3. As explained before in Section 3.5.1, the autocorrelation function of noise is approximated as $\theta(\tau) = \frac{N_0}{2}\delta(\tau)$ [175]. The noise variances are evaluated as follows.

$$\begin{aligned} \sigma^2_{N_1} &= \mathbb{E}[A_2^2] = 2 \sum_{j=0}^{N_f-1} \sum_{l=0}^{L-1} \alpha_l^2 \int_{iT_s+jT_f}^{iT_s+jT_f+T_i} \int_{iT_s+jT_f}^{iT_s+jT_f+T_i} g(t - jT_f - iT_s - \tau_l) \\ &\quad g(\tau - jT_f - iT_s - \tau_l)\, \mathbb{E}[n(t)n(\tau)]dtd\tau \end{aligned}$$

$$
\begin{aligned}
&= 2N_f \int_{iT_s+jT_f}^{iT_s+jT_f+T_i} g(t-jT_f-iT_s-\tau_l)g(\tau-jT_f-iT_s-\tau_l) \\
&\quad \theta(t-\tau)dtd\tau \\
&= 2N_f \frac{N_0}{2} \int_{iT_s+jT_f}^{iT_s+jT_f+T_i} g^2(t-jT_f-iT_s-\tau_l)dt \\
&= N_f N_0 E
\end{aligned} \tag{3.37}
$$

where, $\mathbb{E}[n(t)n(\tau)] = \theta(t-\tau) = \frac{N_0}{2}\delta(t-\tau)$ and $\int_{iT_s+jT_f}^{iT_s+jT_f+T_i} \frac{N_0}{2}\delta(t-\tau)d\tau = \frac{N_0}{2}$.

$$
\begin{aligned}
\sigma_{N_2}^2 &= \mathbb{E}[A_3^2] = \sum_{j=0}^{N_f-1} \int_{iT_s+jT_f}^{iT_s+jT_f+T_i} \int_{iT_s+jT_f}^{iT_s+jT_f+T_i} \mathbb{E}\left[\left\{n^2(t)\right\}^2\right] dtd\tau \\
&= N_f \int_0^{T_i} \int_{T_i-t}^{T_i} \frac{N_0^2}{2} d\tau dt = N_f \int_0^{T_i} \frac{N_0^2}{2} 2W dt = N_f N_0^2 W T_i
\end{aligned} \tag{3.38}
$$

where, the value of $\mathbb{E}\left[\left\{n^2(t)\right\}^2\right] = \frac{N_0^2}{2}$ is evaluated in Appendix A. Parseval's theorem is applied to solve equation 3.38.

The SNR obtained is represented as follows:

$$
\begin{aligned}
\rho_{ED-OOK} &= \frac{(sig)^2}{\sigma_{Z_{noise}}^2} \\
&= \frac{(N_f E)^2}{N_f N_0 E + N_f N_0^2 W T_i}
\end{aligned} \tag{3.39}
$$

Therefore, the BER of UWB ED−OOK system is expressed as:

$$
BER_{ED-OOK} = Q\left[\frac{1}{2}\left[\left(\frac{N_0}{N_f E}\right) + \left(\frac{N_0}{N_f E}\right)^2 N_f W T_i\right]^{-0.5}\right] \tag{3.40}
$$

3.5.4 ED−PPM System

The received ED−PPM signal is denoted as:

$$
\begin{aligned}
r_{ED-PPM}(t) &= s_{ED-PPM}(t) * h(t) \\
&= \sum_{i=0}^{\infty} \sum_{j=0}^{N_f-1} p(t-jT_f-iT_s-\Delta b_i) * \sum_{l=0}^{L-1} \alpha_l \delta(t-\tau_l) + n(t) \\
&= \sum_{l=0}^{L-1} \alpha_l g(t-jT_f-iT_s-\Delta b_i-\tau_l) + n(t)
\end{aligned} \tag{3.41}
$$

where, $*$ denotes the convolution operator, $T_s = N_f T_f$ the symbol duration, T_f the frame duration, N_f the number of frames per symbol, $b_i \in \{0,1\}$ the information bit, $p(t)$ the second order gaussian derivative pulse and Δ the PPM shift. The aggregate signal response $g(t)$ is

represented as $g(t-jT_f-iT_s-\Delta b_i-\tau_l) = s_{ED-PPM}(t) * \delta(t-\tau_l)$. The received signal is then passed through a ED−PPM receiver, whose decision statistics Z is represented as $Z = Z_0 - Z_1$ where, Z_0 and Z_1 denote the decision statistics due to transmission of information bit 0 and 1 respectively.

$$\begin{aligned} Z_0 &= \sum_{j=0}^{N_f-1} \int_{iT_s+jT_f}^{iT_s+jT_f+T_i} r^2_{ED-PPM}(t)dt \\ &= \underbrace{B_1}_{signal} + \underbrace{B_2+B_3}_{noise-term} = \underbrace{s_0}_{signal} + \underbrace{Z_{noise-0}}_{noise-term} \end{aligned} \tag{3.42}$$

$$\begin{aligned} Z_1 &= \sum_{j=0}^{N_f-1} \int_{iT_s+jT_f+\Delta}^{iT_s+jT_f+\Delta+T_i} r^2_{ED-PPM}(t)dt \\ &= \underbrace{C_1}_{signal} + \underbrace{C_2+C_3}_{noise-term} = \underbrace{s_1}_{signal} + \underbrace{Z_{noise-1}}_{noise-term} \end{aligned} \tag{3.43}$$

where, $T_i = T_{mds} + T_p$ represents the integration time interval. Replacing the value of equation 3.41 in equation 3.42, we obtain decision statistics Z_0 in equation 3.44, which is shown below. In case of no IPI, equation 3.44 holds true.

$$\begin{aligned} Z_0 &= \sum_{j=0}^{N_f-1} \int_{iT_s+jT_f}^{iT_s+jT_f+T_i} \left(\sum_{l=0}^{L_1-1} \alpha_l g(t-jT_f-iT_s-\Delta b_i-\tau_l) + n(t) \right)^2 \\ &= \sum_{j=0}^{N_f-1} \sum_{l=0}^{L-1} \alpha_l^2 \int_{iT_s+jT_f}^{iT_s+jT_f+T_i} g^2(t-jT_f-iT_s-\Delta b_i-\tau_l)dt + 2 \sum_{j=0}^{N_f-1} \sum_{l=0}^{L-1} \\ &\quad \alpha_l \int_{iT_s+jT_f}^{iT_s+jT_f+T_i} g(t-jT_f-iT_s-\Delta b_i-\tau_l)n(t)dt + \sum_{j=0}^{N_f-1} \int_{iT_s+jT_f}^{iT_s+jT_f+T_i} \\ &\quad n^2(t)dt \end{aligned} \tag{3.44}$$

The signal component B_1 is obtained from decision variable Z_0.

$$\begin{aligned} B_1 &= \sum_{j=0}^{N_f-1} \sum_{l=0}^{L-1} \alpha_l^2 \int_{iT_s+jT_f}^{iT_s+jT_f+T_i} g^2(t-jT_f-iT_s-\Delta b_i-\tau_l)dt \\ &= s_0 = N_f E_0 \end{aligned} \tag{3.45}$$

where, $E_0 = \int_{iT_s+jT_f}^{iT_s+jT_f+T_i} g^2(t-jT_f-iT_s-\Delta b_i-\tau_l)dt$ denotes the received signal energy component in Z_0. The decision variables B_2 and B_3 denote the noise terms, so to solve them, their variance needs to be evaluated. The PSD of noise is sufficiently flat, therefore its autocorrelation function $\theta(\tau)$ can be approximated as $\theta(\tau) = \frac{N_0}{2}\delta(\tau)$ [175], as mentioned in section 3.5.1.

The noise variances are assumed to be independent of the channel under consideration. Hence, the noise variances B_2 and B_3 obtained from Z_1 are as follows:

$$\begin{aligned}\sigma^2_{N_1} &= \mathbb{E}[B2^2] = 2\sum_{j=0}^{N_f-1}\sum_{l=0}^{L-1}\alpha_l^2\int_{iT_s+jT_f}^{iT_s+jT_f+T_i}\int_{iT_s+jT_f}^{iT_s+jT_f+T_i} g(t-jT_f-iT_s-\Delta b_i-\tau_l)\\ &\quad g(\tau-jT_f-iT_s-\Delta b_i-\tau_l)\,\mathbb{E}[n(t)n(\tau)]dtd\tau\\ &= 2N_f\int_{2iT_s+jT_f}^{iT_s+jT_f+T_i}\int_{iT_s+jT_f}^{iT_s+jT_f+T_i} g(t-jT_f-iT_s-\Delta b_i-\tau_l)g(\tau-jT_f\\ &\quad -iT_s-\Delta b_i-\tau_l)\theta(t-\tau)dtd\tau\\ &= 2N_f\frac{N_0}{2}\int_{iT_s+jT_f}^{iT_s+jT_f+T_i} g^2(t-jT_f-iT_s-\Delta b_i-\tau_l)dt = N_fN_0E_0. \end{aligned} \tag{3.46}$$

where, $\mathbb{E}[n(t)n(\tau)] = \theta(t-\tau) = \frac{N_0}{2}\Delta(t-\tau)$ and $\int_{iT_s+jT_f}^{iT_s+jT_f+T_i}\frac{N_0}{2}\Delta(t-\tau)d\tau = \frac{N_0}{2}$.

$$\begin{aligned}\sigma^2_{N_2} &= \mathbb{E}[B_3^2] = \sum_{j=0}^{N_f-1}\int_{iT_s+jT_f}^{iT_s+jT_f+T_i}\int_{iT_s+jT_f}^{iT_s+jT_f+T_i}\mathbb{E}\left[\left\{n^2(t)\right\}^2\right]dtd\tau\\ &= N_f\int_0^{T_i}\int_{T_i-t}^{T_i}\frac{N_0^2}{2}dtd\tau = N_f\int_0^{T_i}\frac{N_0^2}{2}2Wdt = N_fN_0^2WT_i \end{aligned} \tag{3.47}$$

where, the value of $\mathbb{E}\left[\left\{n^2(t)\right\}^2\right] = \frac{N_0^2}{2}$ is derived in equation A.2 of Appendix A. Parseval's theorem is used to solve equation 3.47. The total noise term $Z_{noise-0}$ has a total variance of $\sigma^2_{Z_{noise-0}} = \sigma^2_{N_1} + \sigma^2_{N_2} = N_fN_0E_0 + N_fN_0^2WT_i$.

Similarly, the decision statistics Z_1 is obtained in equation 3.48 by replacing the value of equation 3.41 in equation 3.43. This equation 3.48 holds true, in case of no IPI.

$$\begin{aligned}Z_1 &= \sum_{j=0}^{N_f-1}\int_{iT_s+jT_f+\Delta}^{iT_s+jT_f+\Delta+T_i}\left(\sum_{l=0}^{L-1}\alpha_l g(t-jT_f-iT_s-\Delta b_i-\tau_l)+n(t)\right)^2\\ &= \sum_{j=0}^{N_f-1}\sum_{l=0}^{L-1}\alpha_l^2\int_{iT_s+jT_f+\Delta}^{iT_s+jT_f+\Delta+T_i} g^2(t-jT_f-iT_s-\Delta b_i-\tau_l)dt + 2\sum_{j=0}^{N_f-1}\sum_{l=0}^{L-1}\\ &\quad \alpha_l\int_{iT_s+jT_f+\Delta}^{iT_s+jT_f+\Delta+T_i} g(t-jT_f-iT_s-\Delta b_i-\tau_l)n(t)dt + \sum_{j=0}^{N_f-1}\\ &\quad \int_{iT_s+jT_f+\Delta}^{iT_s+jT_f+\Delta+T_i} n^2(t)dt \end{aligned} \tag{3.48}$$

The signal component C_1 is obtained from decision variable Z_1.

$$\begin{aligned}C_1 &= \sum_{j=0}^{N_f-1}\sum_{l=0}^{L-1}\alpha_l^2\int_{iT_s+jT_f+\Delta}^{iT_s+jT_f+\Delta+T_i} g^2(t-jT_f-iT_s-\Delta b_i-\tau_l)dt\\ &= s_1 = N_fE_1 \end{aligned} \tag{3.49}$$

where, $E_1 = \int_{iT_s+jT_f+\Delta}^{iT_s+jT_f+\Delta+T_i} g^2(t - jT_f - iT_s - \Delta b_i - \tau_l)dt$ denotes the received signal energy component in Z_1.

Similarly, the noise variances C_2 and C_3 obtained from Z_1 are as follows.

$$\begin{aligned}
\sigma^2_{N_1} &= \mathbb{E}[C_2^2] = 2\sum_{j=0}^{N_f-1}\sum_{l=0}^{L-1}\alpha_l^2 \int_{iT_s+jT_f+\Delta}^{iT_s+jT_f+\Delta+T_i}\int_{2iT_s+jT_f+\Delta}^{iT_s+jT_f+\Delta+T_i} g(t - jT_f - iT_s - \Delta b_i \\
&\quad -\tau_l)g(\tau - jT_f - iT_s - \Delta b_i - \tau_l)\,\mathbb{E}[n(t)n(\tau)]dtd\tau \\
&= 2N_f \int_{iT_s+jT_f+\Delta}^{iT_s+jT_f+\Delta+T_i}\int_{iT_s+jT_f+\Delta}^{iT_s+jT_f+\Delta+T_i} g(t - jT_f - iT_s - \Delta b_i - \tau_l)g(\tau - jT_f \\
&\quad -iT_s - \Delta b_i - \tau_l)\theta(t-\tau)dtd\tau \\
&= 2N_f\frac{N_0}{2}\int_{iT_s+jT_f+\Delta}^{iT_s+jT_f+\Delta+T_i} g^2(t - jT_f - iT_s - \Delta b_i - \tau_{l,1})dt \\
&= N_f N_0 E_1
\end{aligned} \tag{3.50}$$

$$\begin{aligned}
\sigma^2_{N_2} &= \mathbb{E}[C_3^2] = \sum_{j=0}^{N_f-1}\int_{iT_s+jT_f+\Delta}^{iT_s+jT_f+\Delta+T_i}\int_{iT_s+jT_f+\Delta}^{iT_s+jT_f+\Delta+T_i}\mathbb{E}\left[\left\{n^2(t)\right\}^2\right]dtd\tau \\
&= N_f\int_0^{T_i}\int_{T_i-t}^{T_i}\frac{N_0^2}{2}d\tau dt = N_f\int_0^{T_i}\frac{N_0^2}{2}2Wdt = N_f N_0^2 W T_i
\end{aligned} \tag{3.51}$$

where, the value of $\mathbb{E}\left[\left\{n^2(t)\right\}^2\right] = \frac{N_0^2}{2}$ is solved in equation A.2 of Appendix A. Parseval's theorem is applied to solve equation 3.51. The noise term $Z_{noise-1}$ has a total variance of $\sigma^2_{Z_{noise-1}} = \sigma^2_{N_1} + \sigma^2_{N_2} = N_f N_0 E_1 + N_f N_0^2 W T_i$. The decision statistics Z is represented as:

$$\begin{aligned}
Z &= Z_0 - Z_1 = \overbrace{(\underbrace{s_0}_{signal} + \underbrace{Z_{noise-0}}_{noise-term})}^{Bit0} - \overbrace{(\underbrace{s_1}_{signal} + \underbrace{Z_{noise-1}}_{noise-term})}^{Bit1} \\
&= \overbrace{(\underbrace{s_0 - s_1}_{sig})}^{TotalSignal} + \overbrace{(\underbrace{Z_{noise-0} - Z_{noise-1}}_{Z_{noise}})}^{TotalNoise}
\end{aligned} \tag{3.52}$$

Therefore, the SNR of UWB ED−PPM system is expressed as:

$$\rho_{ED-PPM} = \left(\frac{sig^2}{\sigma^2_{Z_{noise}}}\right) = \left(\frac{[N_f(E_0 - E_1)]^2}{N_f N_0(E_0 - E_1) + 2N_f N_0^2 W T_i}\right) \tag{3.53}$$

Therefore, the BER of UWB ED−PPM system is expressed as:

$$BER_{ED-PPM} = Q\left[\left(\frac{2}{(\frac{N_0}{N_f(E_0-E_1)}) + (\frac{N_0}{N_f(E_0-E_1)})^2 2N_f W T_i}\right)^{-0.5}\right] \tag{3.54}$$

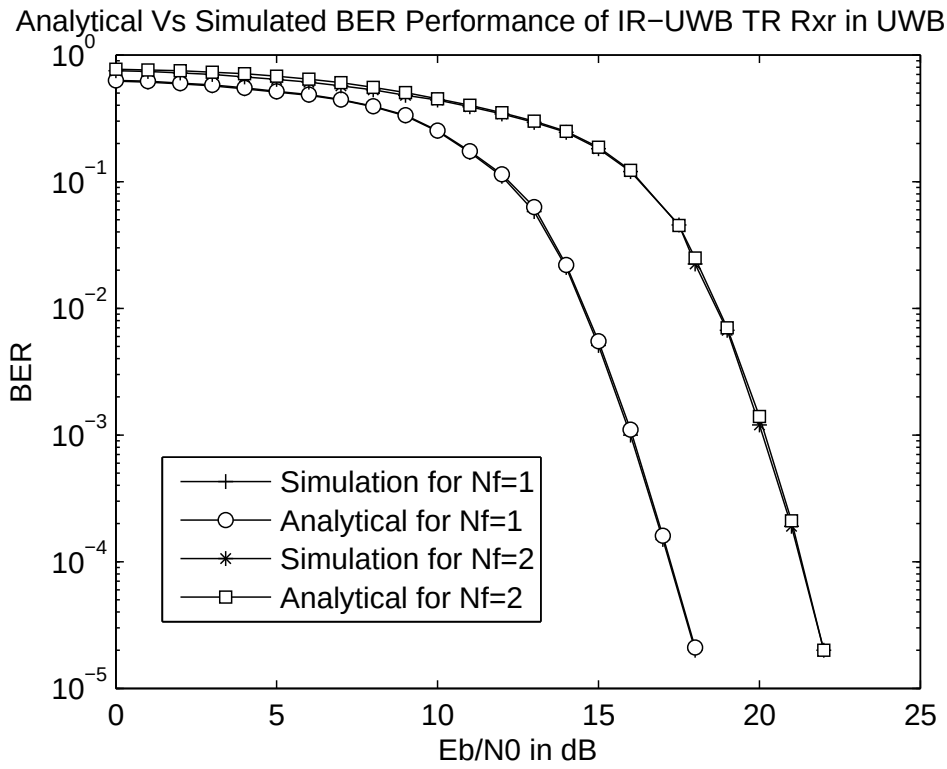

(a)

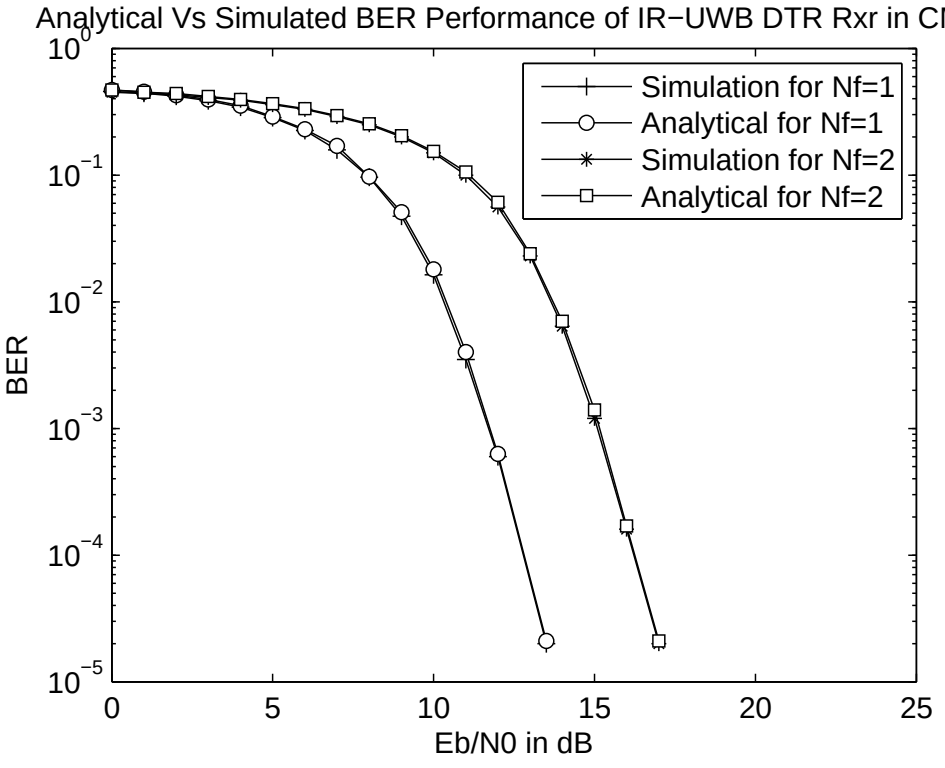

(b)

3.6 Simulation Results

The BER performance of non−coherent UWB systems were simulated in IEEE 802.15.4a UWB environment and compared with the analytical results. The main parameters considered

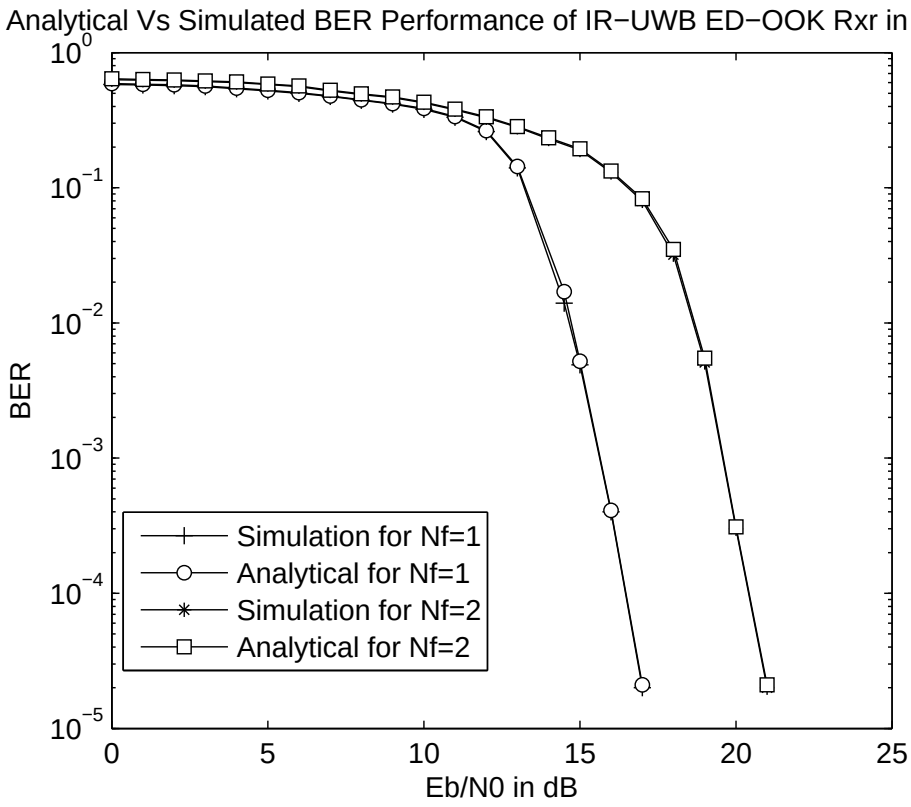

(c)

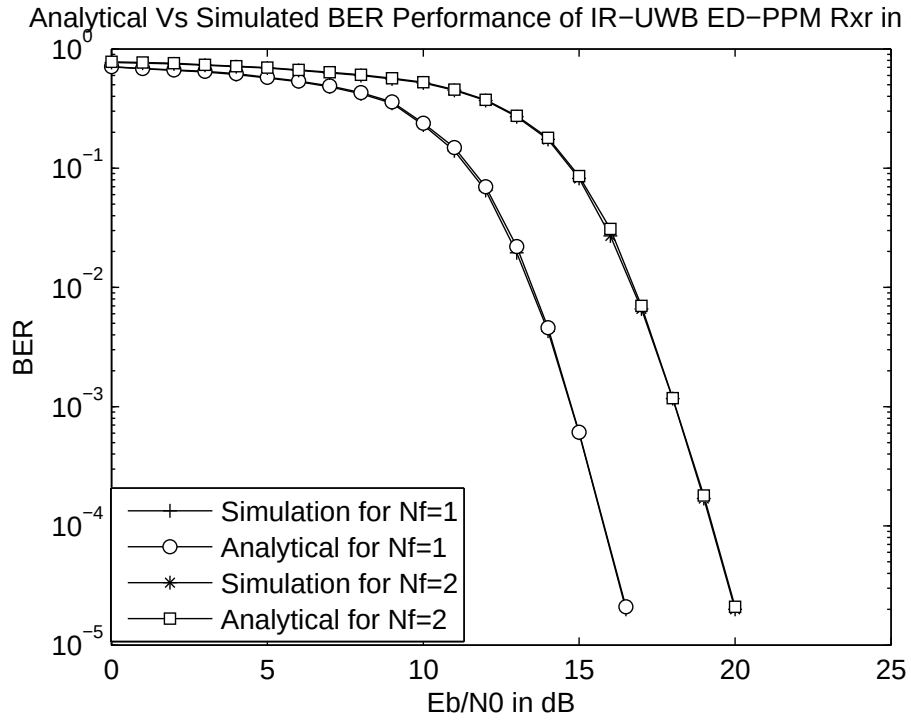

(d)

Figure 3.5: Analytical Vs Simulated BER performance comparison of non−coherent UWB receivers in CM1 channel for $N_f = 1, 2$ namely(a) TR Rxr (b) DTR Rxr (c) ED−OOK Rxr (d) ED−PPM Rxr

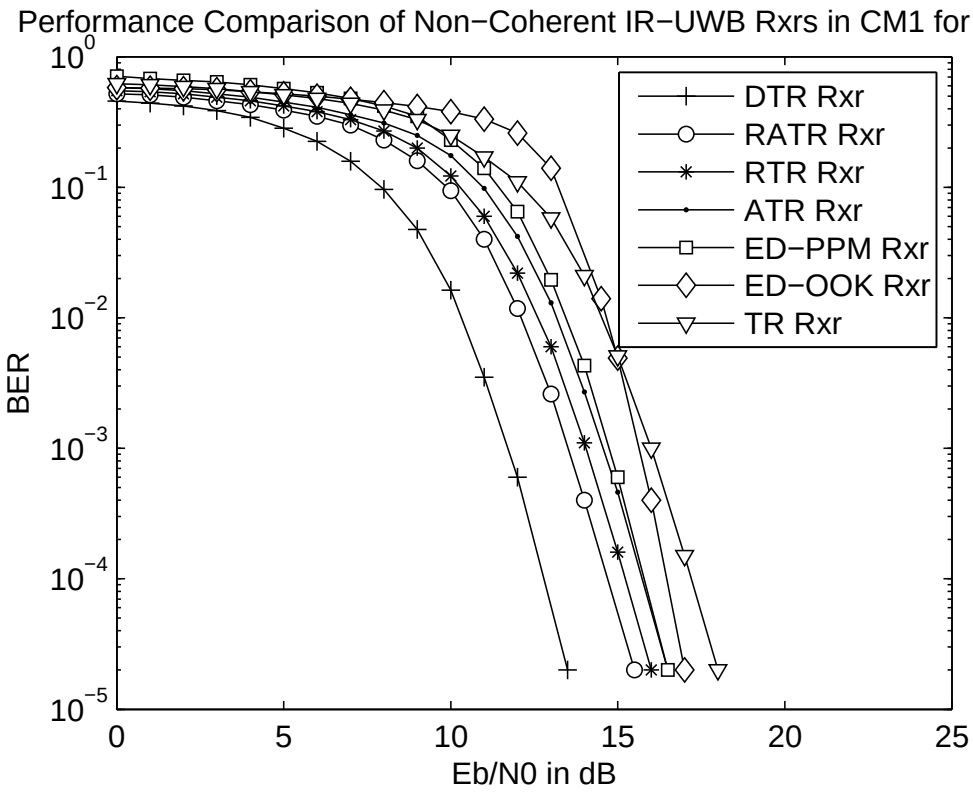
Performance Comparison of Non−Coherent IR−UWB Rxrs in CM1 for Nf=1
BER
Eb/N0 in dB
DTR Rxr
RATR Rxr
RTR Rxr
ATR Rxr
ED−PPM Rxr
ED−OOK Rxr
TR Rxr

(a)

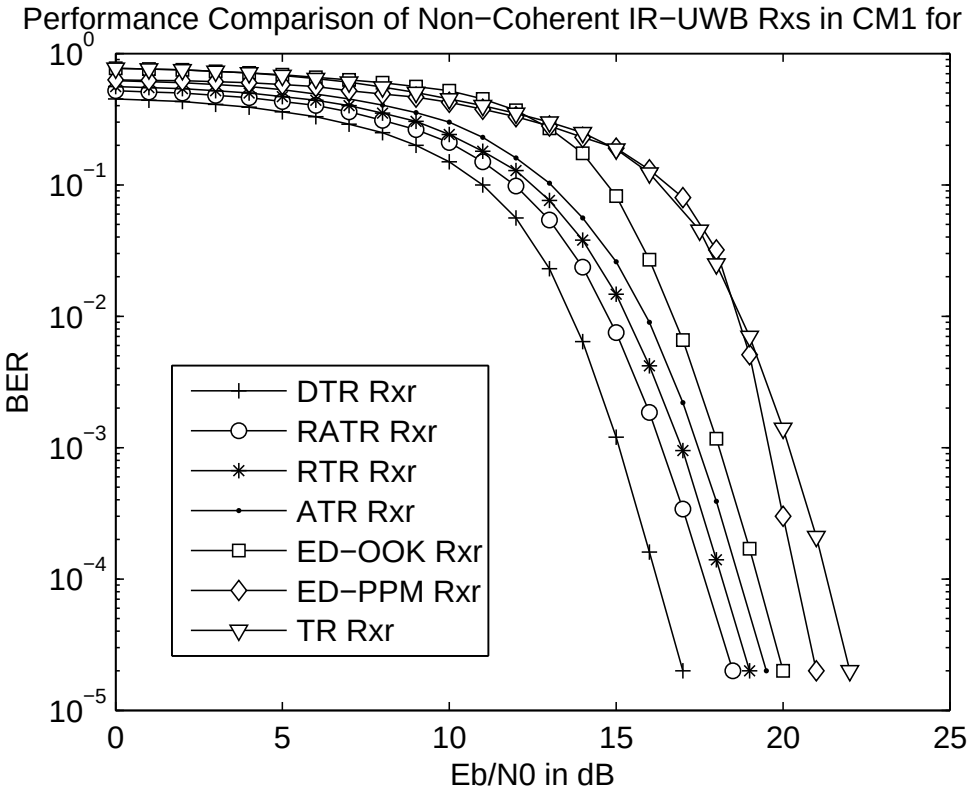
Performance Comparison of Non−Coherent IR−UWB Rxs in CM1 for Nf=2
BER
Eb/N0 in dB
DTR Rxr
RATR Rxr
RTR Rxr
ATR Rxr
ED−OOK Rxr
ED−PPM Rxr
TR Rxr

(b)

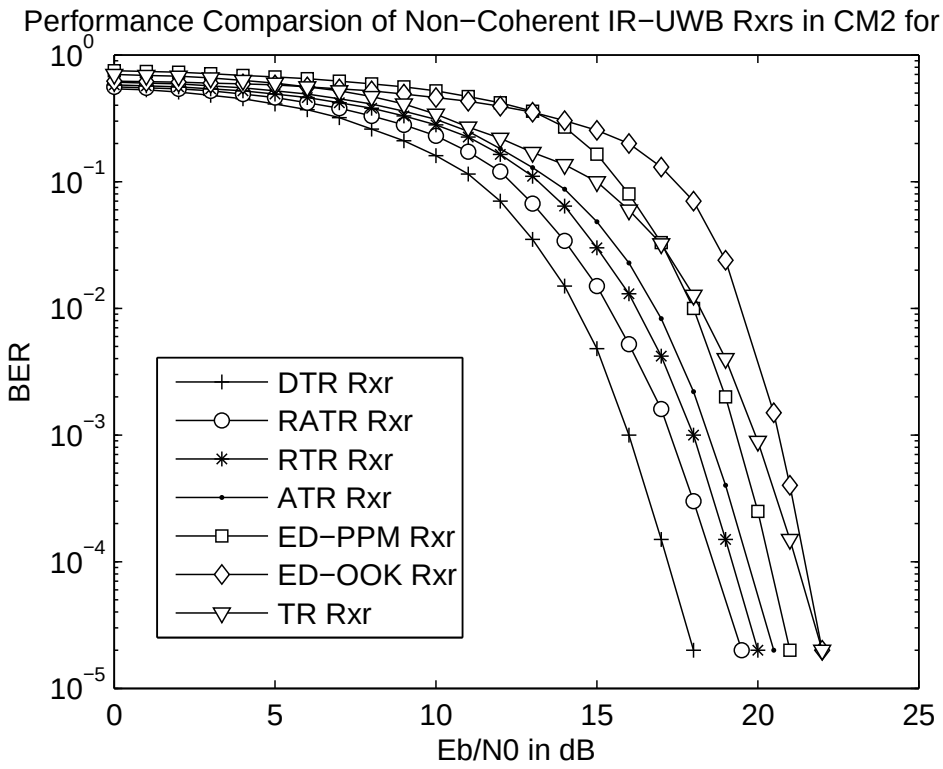

(c)

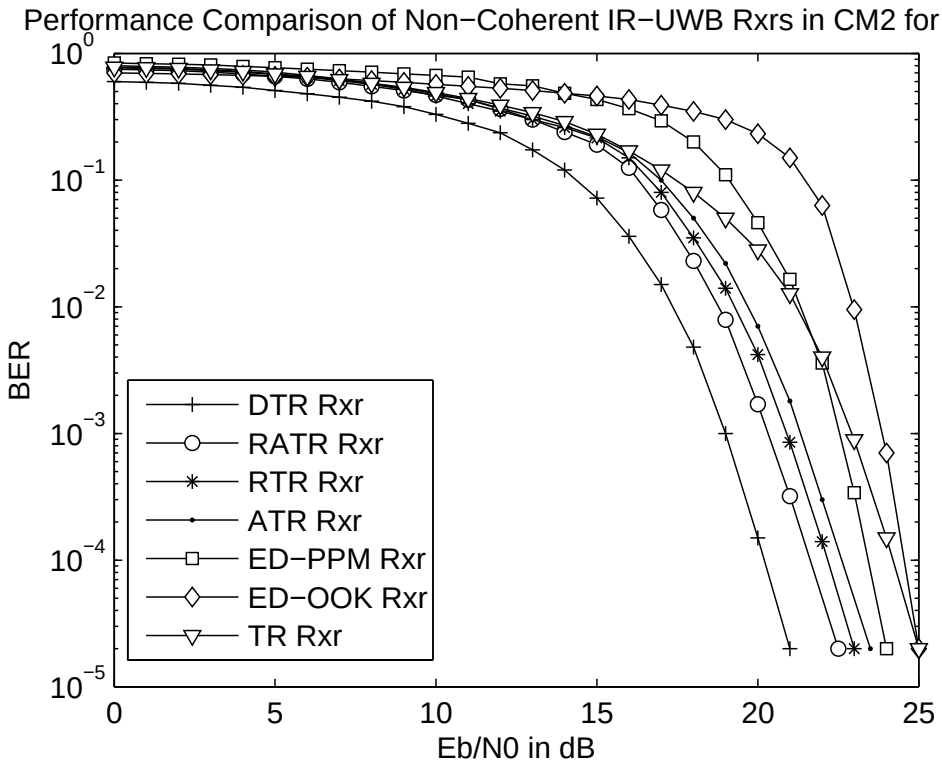

(d)

Figure 3.6: BER Performance Comparison of Non−Coherent UWB receivers in (a) CM1 channel for $N_f = 1$ (b) CM1 channel for $N_f = 2$ (c) CM2 channel for $N_f = 1$ (d) CM2 channel for $N_f = 2$

for simulations are $N_f = 1, 2$, $N = 200000$, $W = 2\,GHz$, $T_i = 4\,ns$ and $F_{samp} = 10\,GHz$, where N_f represents the number of frames in one symbol, N the number of bits, W the bandwidth of bandpass filter, T_i the integration interval and F_{samp} the sampling frequency. A second order Gaussian derivative pulse $p(t) = (1 - 4\pi((t)/T_k)^2)exp(-2\pi((t)/T_k)^2)$ is used for transmission, where t denotes the time interval and $T_k = 0.15$ ns the pulse width control factor. The computer simulations are performed using Matlab tool.

Fig 3.5(a), (b), (c) and (d) illustrates the theoretical BER performance of UWB TR, DTR, ED−OOK and ED−PPM systems respectively, in UWB CM1 environment for $N_f = 1, 2$, and compares it with the simulation results. The conclusion drawn from the Fig 3.5(a), (b), (c) and (d) confirms that the theoretical BER performance of TR, DTR, ED−OOK and ED−PPM systems in CM1 environment respectively, coincides with that of simulation results. It is also inferred that increase in number of frames N_f from 1 to 2, leads to degradation in BER performance.

Fig 3.6 shows the BER performance comparison of non−coherent UWB systems namely TR, ATR, DTR, RTR, RATR, ED−OOK and ED−PPM, over IEEE 802.15.4a (a) UWB CM1 for $N_f = 1$, (b) UWB CM1 for $N_f = 2$, (c) UWB CM2 for $N_f = 1$ and (d) UWB CM2 for $N_f = 2$ environment, respectively. CM2, NLOS channel suffers a SNR loss of $3 - 4\ dB$, compared to CM1, LOS environment, as observed in Fig 3.6(a) and (b) as well as Fig 3.6(c) and (d). It is observed that BER performance degrades as N_f changes from 1 to 2. It can also be concluded from all the figures that as far as BER performance of non−coherent UWB systems are concerned, DTR > RATR > RTR > ATR > ED−PPM > ED−OOK > TR. TR system gives the worst performance among all the non−coherent UWB systems, because it wastes $3\ dB$ of energy in transmitting a reference pulse. The problems faced by TR system is overcome using ATR, RTR, RATR, DTR and ED systems. Among the ED systems considered, ED−PPM system gives a SNR gain of $1\ dB$ over ED−OOK system, at a BER of 10^{-4}. This is because ED−OOK system suffers from noise, as it does not transmit a pulse when information bit 0 is transmitted.

3.7 Concluding Remarks

The analytical BER expression for various non−coherent UWB systems namely TR, DTR, ED−OOK and ED−PPM, has been derived and compared with the simulation results for $N_f =$

$1, 2$. In this chapter, a comparison between the various non−coherent UWB systems in IEEE 802.15.4a low data rate UWB channel, is presented. The non−coherent UWB systems considered for simulation are TR, ATR, RTR, RATR, DTR and ED. It is also observed that with increase in number of frames N_f, the BER performance of the UWB system degrades. Also for UWB simulated channels, CM1 being LOS gives better performance than CM2, NLOS channel. The simulation results prove that among the AC systems discussed, DTR gives the best performance when compared to the other systems namely TR, ATR, RTR and RATR, in UWB environment for $N_f = 1, 2$. DTR system transmits differentially modulated information and wastes no energy in transmitting a reference pulse, thereby saving $3\ dB$ of energy, compared to TR system. DTR system also outperforms RATR system, which uses the combined effect of averaging and recursive estimation, by a SNR margin of $1 - 2\ dB$, at a BER of 10^{-4}. It is also inferred from the simulation results that among the UWB ED systems, ED−PPM outperforms ED−OOK by a SNR margin of $1\ dB$, at a BER of 10^{-4}. This is because OOK scheme wastes energy when bit 0 is transmitted. As a result, no pulse signal is transmitted, thereby inducing noise and leading to performance degradation. It is also observed that even though DTR and RATR system shows performance superiority over ED (ED−PPM,ED−OOK) system in CM1 and CM2 channel for $N_f = 1, 2$, the ED system is preferred over AC system such as DTR and RATR. This is because, AC system requires long analog DL's for performing correlation operation. Furthermore, to correlate the received signal with its delayed version, a storage element is required for storing the previous samples. This leads to hardware complexity. On the contrary, ED system requires less complexity and gives a comparable BER performance in IEEE 802.15.4a CM1 and CM2 environment, for $N_f = 1, 2$.

In this chapter, the BER performance of various non−coherent UWB systems are compared both analytically and by simulation, in single−link scenario. The analytical results are also validated with the simulation results.

Chapter 4

Performance Analysis of Non-Coherent UWB Cooperative AC System

In this chapter, we derive an analytical solution for the BER performance of non−coherent UWB AC system, using cooperative dual−hop AF and DTF relay strategy for various combining schemes. In particular, we obtain the approximate BER expressions for AC systems namely TR and DTR, for various diversity combining cases, such as optimum linear combining, linear combining, and selective combining, based on autocorrelation principle. Section 4.1 presents the basic introduction about UWB AC system using various cooperative dual−hop relay strategies. Section 4.2 describes the system model comprising of signal model, channel model and receiver structure. The detailed theoretical BER performance analysis of UWB AC system is derived using cooperative dual−hop AF and DTF strategy for various diversity combining schemes, in Section 4.3 and Section 4.4 respectively. The simulation results are outlined in Section 4.5 while Section 4.6, concludes the paper.

4.1 Introduction

The low PSD value limits UWB system from achieving a wide coverage and achievable BER performance in single−link scenario [5]. So, we resort to cooperative technology. The main motive of cooperative transmission [70] is that the relay nodes share their antennas to create a virtual MIMO system, thereby helping the source node in transmitting information to the destination node, leading to diversity gain. Relay technology [76, 77] forms the basis of cooperative diversity in UWB communication, and improves QoS, BER performance and transmission re-

liability of the system. Cooperative relay strategies are classified as AF, DF and DTF. The other advantages associated with Cooperative communication are high data rate, less power consumption, effective utilization of bandwidth and improvement in signal strength.

This chapter discusses BER performance of non−coherent UWB TR and DTR system using AF and DTF relay strategy, for a dual−hop cooperative scenario with various diversity combining schemes, both from analytical and simulation point of view.

4.2 Cooperative System Model

The cooperative system model discussed in this section consists of three links, S−D (Link-1), S−R (Link-2) and R−D (Link-3), as shown in Fig 1.3. In the 1^{st} time slot, UWB signal modulated by the information bit, is transmitted from the source node to relay node as well as destination node. In case of AF scheme, the signal received at relay node in 1^{st} time slot is amplified by an amplifying factor and then forwarded to the destination node, in the 2^{nd} time slot. However in case of DTF scheme, the signal received at the relay node in 1^{st} time slot is first demodulated using an AC receiver and forwarded to the destination node, in 2^{nd} time slot. The received signal obtained at the destination node using either of the relaying schemes in the 1^{st} and 2^{nd} time slots, are demodulated using an AC receiver namely TR and DTR. The decision statistics obtained at the destination node due to autocorrelation of received signals in 1^{st} and 2^{nd} time slots, are combined using various combining schemes, namely optimum linear combining, linear combining and selective combining, to form the final decision statistic. The final decision statistic is then compared to a threshold to recover the information bit. The signal model, channel model and receiver model of the cooperative system is described in the subsequent sections.

4.2.1 UWB Signal Model

The cooperative scheme discussed in this section uses a dual−hop AF and DTF relay strategy. PAM modulation scheme is used for transmission in cooperative UWB TR and DTR system [176].

(i) *TR System*: In a TR system, two pulses namely unmodulated reference pulse, followed by data modulated pulse are transmitted per frame, where the former is separated from the latter by a delay of T_d [56]. A number of frames constitute a bit or a symbol. As seen

in Fig 1.3, UWB TR signal is transmitted from the source node to relay node as well as destination node, in 1st time slot. The signal sent from the source node to the relay node is either amplified or detected at the relay node depending on the relay strategy and then forwarded to the destination node, in the next time slot. The UWB TR signal transmitted from the source node to the destination node, in 1st time slot is represented as:

$$s_{TR-SD}(t) = \sum_{i=0}^{\infty} \sum_{j=0}^{N_f-1} \Big[p(t - jT_f - 2iT_s) + b_i p(t - jT_f - 2iT_s - T_d) \Big] \quad (4.1)$$

Similarly in the same time slot, the UWB TR signal transmitted from the source node to relay node is represented as:

$$s_{TR-SR}(t) = \sum_{i=0}^{\infty} \sum_{j=0}^{N_f-1} \Big[p(t - jT_f - 2iT_s) + b_i p(t - jT_f - 2iT_s - T_d) \Big] \quad (4.2)$$

where, $s_{TR-SD}(t)$ and $s_{TR-SR}(t)$ represents the UWB TR signal transmitted from the source node to destination as well as relay node respectively, in 1st time slot. The other terms such as $b_i \in (1, -1)$ represent the information bit, $p(t)$ the gaussian second order pulse, N_f the number of frames per symbol, T_f the frame duration and $T_s = N_f T_f$ the symbol duration. TR signal consists of two pulses wherein, unmodulated reference signal is followed by a data modulated signal, both of which are separated by delay of T_d.

(ii) *DTR System*: In DTR system, instead of transmitting a separate bit, differentially modulated bit is sent over the frame which is obtained by modulating the binary information bit with the previously obtained differentially modulated bit, thereby saving energy. As illustrated in Fig 1.3, UWB DTR signal is transmitted from the source node to relay as well as the destination node, in 1st time slot. The received signal obtained at the relay node is either amplified or detected depending on the relay strategy used and then forwarded to the destination node, in 2nd time slot. The UWB DTR signal transmitted from the source node to the destination node in 1st time slot is represented as:

$$s_{DTR-SD}(t) = \sum_{i=0}^{\infty} \sum_{j=0}^{N_f-1} b_i p(t - jT_f - 2iT_s) \quad (4.3)$$

Similarly in the same time slot, the UWB TR signal transmitted from the source node to relay node is represented as:

$$s_{DTR-SR}(t) = \sum_{i=0}^{\infty} \sum_{j=0}^{N_f-1} b_i p(t - jT_f - 2iT_s) \quad (4.4)$$

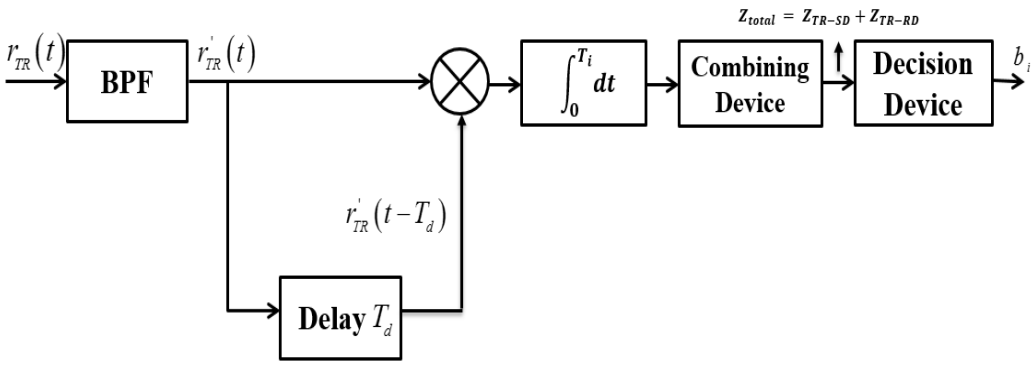

Figure 4.1: UWB TR system for Cooperative Communication

where, $s_{DTR-SD}(t)$ and $s_{DTR-SR}(t)$ represents UWB DTR signal transmitted from the source node to destination node and relay node respectively, in 1^{st} time slot. Here, the differentially modulated bit b_i is transmitted over the frame, which is obtained by differentially modulating the information bit $a_i \in (-1, 1)$ with the previously obtained information bit b_{i-1}, by a differential encoding rule $b_i = a_i b_{i-1}$ [171].

4.2.2 UWB Channel Model

For a signal to cross over from the transmitter to the receiver side, a wireless medium or channel is required. The frequency selective nature of the wireless channel forces delay dispersion in each multipath component of the UWB system. IEEE 802.15.4a, low data rate wireless UWB channel, based on the modification of SV model [34] is represented as:

$$\begin{aligned} h_k(t) &= \sum_{l=0}^{L_k-1} \alpha_{l,k}\delta(t-\tau_{l,k}) \\ &= \sum_{l_k} \alpha_{l_k}\delta(t-\tau_{l_k}) \end{aligned} \tag{4.5}$$

where, $h_k(t)$ represents the impulse response of channel and L_k the number of multipaths. Also, $\alpha_{l,k}$ (α_{l_k}) and $\tau_{l,k}$ (τ_{l_k}) denotes the amplitude response and delay response of l^{th} multipath in k^{th} link, respectively. The indices $k \in \{1, 2, 3\}$ are used to denote S$-$D link, S$-$R link and R$-$D link respectively. The channel gains $\alpha_{l,k}$ follow Nakagami distribution, while δ denotes Delta function. In order to avoid IPI and IFI in UWB TR and DTR system, received pulses must have frame duration $T_f > (T_{mds} + T_p)$, where T_p represents the pulse duration and T_{mds} the multipath delay spread. The UWB channel models, chosen for simulation are CM1$-$CM2, which represent different UWB environments.

4.2.3 TR Receiver Model

The received signal obtained at the receiver side is an attenuated and a dispersed form of the transmitted signal, after it passes through the channel. The non−coherent UWB receivers designed for TR and DTR system follow autocorrelation property, and hence are called AC receivers [162, 177].

(i) *TR Receiver*: As seen in Fig 4.1, the received TR signal $r_{TR}(t)$ is first passed through a BPF having a bandwidth W. The filtered received signal $r_{TR}^{'}(t)$ is then correlated with its delayed version $r_{TR}^{'}(t - T_d)$. The resultant signal is then integrated over time interval followed by decision device, where it is compared to the threshold, in order to recover the information bit b_i [2, 68]. The received TR signal at the destination node in 1^{st} time slot is represented as:

$$\begin{aligned} r_{TR-SD}(t) &= s_{TR-SD}(t) * h_1(t) \\ &= \sum_{i=0}^{\infty}\sum_{j=0}^{N_f-1}\Big[p(t - jT_f - 2iT_s) + b_i p(t - jT_f - 2iT_s - T_d)] \\ &\quad * \sum_{l_1}\alpha_{l_1}\delta(t - \tau_{l_1})\Big] + n_{SD}(t) \\ &= \sum_{i=0}^{\infty}\sum_{j=0}^{N_f-1}\sum_{l_1}\Big[\alpha_{l_1}p(t - jT_f - 2iT_s - \tau_{l_1}) + \alpha_{l_1}b_i p(t - jT_f - 2iT_s - \\ &\quad T_d - \tau_{l_1})\Big] + n_{SD}(t) \\ &= \sum_{i=0}^{\infty}\sum_{j=0}^{N_f-1}\Big[g_{SD}(t - jT_f - 2iT_s) + b_i g_{SD}(t - jT_f - 2iT_s - T_d)\Big] + \\ &\quad n_{SD}(t) \end{aligned} \tag{4.6}$$

where, the aggregate signal response $g_{SD}(t)$ and $g_{SR}(t)$ for S−D and S−R link are expressed as $g_{SD}(t - jT_f - 2iT_s) = s_{TR-SD}(t) * \delta(t - \tau_{l,1})$ and $g_{SR}(t - jT_f - 2iT_s) = s_{TR-SR}(t) * \delta(t - \tau_{l,2})$, respectively. Similarly, the received signal obtained at the relay node in 1^{st} time slot is denoted as:

$$\begin{aligned} r_{TR-SR}(t) &= s_{TR-SR}(t) * h_2(t) \\ &= \sum_{i=0}^{\infty}\sum_{j=0}^{N_f-1}\Big[p(t - jT_f - 2iT_s) + b_i p(t - jT_f - 2iT_s - T_d)] \\ &\quad * \sum_{l_2}\alpha_{l_2}\delta(t - \tau_{l_2})\Big] + n_{SR}(t) \end{aligned}$$

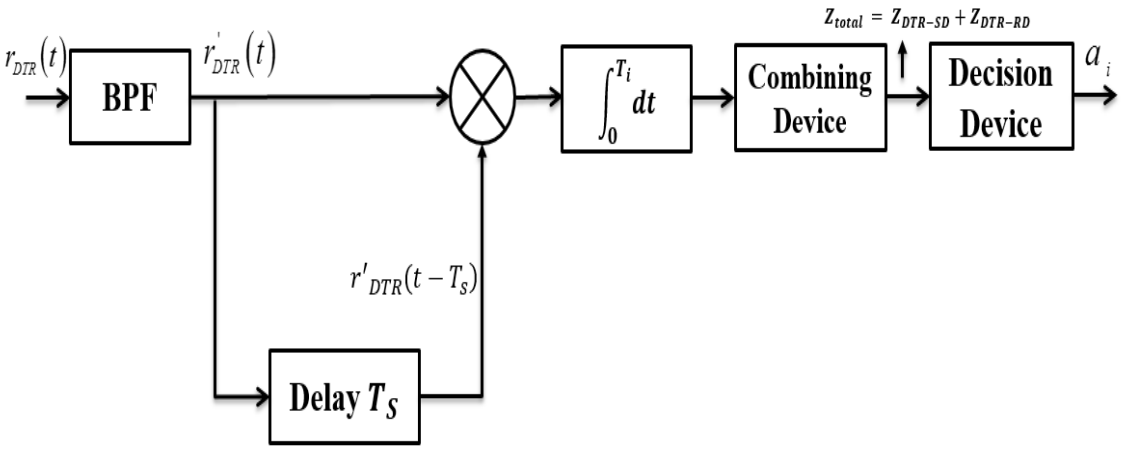

Figure 4.2: UWB DTR system for Cooperative Communication

$$
\begin{aligned}
&= \sum_{i=0}^{\infty}\sum_{j=0}^{N_f-1}\sum_{l_2}\Big[\alpha_{l_2}p(t-jT_f-2iT_s-\tau_{l_2})+\alpha_{l_2}b_i p(t-jT_f-2iT_s- \\
&\quad T_d-\tau_{l_2})\Big]+n_{SR}(t) \\
&= \sum_{i=0}^{\infty}\sum_{j=0}^{N_f-1}\Big[g_{SR}(t-jT_f-2iT_s)+b_i g_{SR}(t-jT_f-2iT_s-T_d)\Big]+ \\
&\quad n_{SR}(t) \qquad (4.7)
\end{aligned}
$$

(ii) *DTR Receiver*: DTR receiver uses autocorrelation property to extract the information bit a_i, as observed in Fig 4.2. The received signal $r_{DTR}(t)$ is first filtered using a BPF to obtain $r'_{DTR}(t)$. The filtered received signal $r'_{DTR}(t)$ is then correlated with its delayed version $r'_{DTR}(t-T_s)$ and the resulting correlated product is integrated over the integration time interval to obtain the decision statistic, which is compared to the threshold, to recover the information bit. The received DTR signal at the destination node in 1st time slot is represented as:

$$
\begin{aligned}
r_{DTR-SD}(t) &= s_{DTR-SD}(t) * h_1(t) \\
&= \sum_{i=0}^{\infty}\sum_{j=0}^{N_f-1}\Big[b_i p(t-jT_f-2iT_s)*\sum_{l_1}\alpha_{l_1}\delta(t-\tau_{l_1})\Big]+n_{SD}(t) \\
&= \sum_{i=0}^{\infty}\sum_{j=0}^{N_f-1}\sum_{l_1}\Big[\alpha_{l_1}b_i p(t-jT_f-2iT_s-\tau_{l_1})\Big]+n_{SD}(t) \\
&= \sum_{i=0}^{\infty}\sum_{j=0}^{N_f-1}\Big[b_i g_{SD}(t-jT_f-2iT_s)\Big]+n_{SD}(t) \qquad (4.8)
\end{aligned}
$$

where, the aggregate signal response $g_{SD}(t)$ and $g_{SR}(t)$ are expressed as $g_{SD}(t - jT_f - 2iT_s) = s_{DTR-SD}(t) * \delta(t - \tau_{l,1})$ and $g_{SR}(t - jT_f - 2iT_s) = s_{DTR-SR}(t) * \delta(t - \tau_{l,2})$ respectively. Similarly, the received signal obtained at the relay node in 1st time slot is denoted as:

$$\begin{aligned} r_{DTR-SR}(t) &= s_{DTR-SR}(t) * h_2(t) \\ &= \sum_{i=0}^{\infty} \sum_{j=0}^{N_f-1} \left[b_i p(t - jT_f - 2iT_s) * \sum_{l_2} \alpha_{l_2} \delta(t - \tau_{l_2}) \right] + n_{SR}(t) \\ &= \sum_{i=0}^{\infty} \sum_{j=0}^{N_f-1} \sum_{l_2} \left[\alpha_{l_2} b_i p(t - jT_f - 2iT_s - \tau_{l_2}) \right] + n_{SR}(t) \\ &= \sum_{i=0}^{\infty} \sum_{j=0}^{N_f-1} \left[b_i g_{SR}(t - jT_f - 2iT_s) \right] + n_{SR}(t) \end{aligned} \tag{4.9}$$

4.3 Performance Analysis of a Cooperative AF AC System

The theoretical BER performance analysis of UWB AC system is explained vividly in this section.

4.3.1 TR System

The theoretical BER performance analysis of UWB TR system using cooperative AF strategy is illustrated in this section [178]. At the end of 1st time slot, the received signal obtained at the destination and relay node is represented by equation 4.6 and 4.7, respectively. This received signal obtained at the destination node in the end of 1st time slot, is detected using a TR receiver, whose decision statistics Z_{TR-SD} is expressed as:

$$\begin{aligned} Z_{TR-SD} &= \sum_{j=0}^{N_f-1} \int_{jT_f+2iT_s+T_d}^{jT_f+2iT_s+T_d+T_i} r_{TR-SD}(t) r_{TR-SD}(t - T_d) dt \\ &= \underbrace{Z_1(k)}_{signal} + \underbrace{Z_2(k) + Z_3(k) + Z_4(k)}_{noise-term} = \underbrace{Z_1(1)}_{signal} + \underbrace{Z_2(1) + Z_3(1) + Z_4(1)}_{noise-term} \end{aligned} \tag{4.10}$$

where, the index $k \in \{1, 2, 3\}$ refers to S$-$D, S$-$R and R$-$D link respectively, as mentioned in equation 4.5 and $T_i = T_p + T_{mds}$ denotes the integration time interval. Also, T_p and T_{mds} denote pulse duration and multipath delay spread respectively. The signal term obtained from S$-$D link is represented as:

$$Z_1(1) = \sum_{j=0}^{N_f-1} \left[\int_{jT_f+2iT_s+T_d}^{jT_f+2iT_s+T_d+T_i} \left(\sum_{l_1} \alpha_{l_1} p(t - jT_f - 2iT_s - \tau_{l_1}) \right) \left(\sum_{m_1} \alpha_{m_1} b_i p(t - jT_f \right.\right.$$

$$
\begin{aligned}
& -2iT_s - T_d - \tau_{m_1})dt\Big)\Big] \\
= \; & N_f b_i \Big[\int_{jT_f+2iT_s+T_d}^{jT_f+2iT_s+T_d+T_i} \sum_{l_1=m_1} \alpha_{l_1}^2 p^2(t - jT_f - 2iT_s - \tau_{l_1})dt \\
& + \underbrace{\sum_{l_1 \neq m_1} \sum \alpha_{l_1}\alpha_{m_1} R(\tau_{l_1} - \tau_{m_1})}_{value=0} \Big] \\
= \; & N_f b_i E_p \underbrace{\left(\sum_{l_1} \alpha_{l_1}^2 \right)}_{value=\gamma_1} \\
= \; & \underbrace{N_f b_i E_p \gamma_1}_{sig_{SD}} \qquad (4.11)
\end{aligned}
$$

where, the pulse energy obtained from S$-$D link is defined as $E_p = \int_{jT_f+2iT_s+T_d}^{jT_f+2iT_s+T_d+T_i} p^2(t - jT_f - 2iT_s - \tau_{l_1})dt$ and autocorrelation function as $R(\tau) = \int_{\infty}^{\infty} p(t)p(t-\tau)dt$. This constraint $min\left\{(\tau_{l_1} - \tau_{m_1})\right\} > T_p$ for $l_1 \neq m_1$ is satisfied, to avoid IPI. Hence, $\sum_{l_1 \neq m_1} \sum \alpha_{l_1}\alpha_{m_1} R(\tau_{l_1} - \tau_{m_1}) = 0$. The channel gains α_{l_k} for IEEE 802.15.4a UWB multipath channels are assumed to be independent and identically distributed (IID) Nakagami. Consequently, their squares will be IID Gamma distributed [179]. Hence, by the use of the Central Limit Theorem, $\sum_{l_k} \alpha_{l_k}^2 = \gamma_k$ may be approximated as Gaussian distributed. In this case, the value is γ_1.

The filtering of AWGN process having PSD $\frac{N_0}{2}$ with a BPF W, results in noise terms $n_k(t)$. The index $k \in \{1, 2, 3\}$ refers to S$-$D, S$-$R and R$-$D link respectively, as discussed in equation 4.5. The autocorrelation function of noise $\theta_k(\tau)$ is given by [175]:-

$$\theta_k(\tau) = \mathbb{E}[n_k(t)n_k(t-\tau)] = \frac{N_0}{2}\frac{Sin(\pi W\tau)}{\pi W\tau} cos(2\pi f_c \tau) \qquad (4.12)$$

where, $\mathbb{E}[.]$ denotes the statistical expectation operator and f_c carrier frequency of BPF. The bandwidth is assumed to be sufficiently large so the frequency response of the received signal $g_k(t)$ at destination node falls inside the PSD $\theta_k(f)$ of $n_k(t)$. As PSD $\theta_k(f)$ is sufficiently flat, the autocorrelation function of noise can be simplified as $\theta_k(\tau) = \frac{N_0}{2}\delta(\tau)$ [175]. Since $Z_2(1)$, $Z_3(1)$ and $Z_4(1)$ denote the noise terms, their variances are solved as shown below.

$$
\begin{aligned}
Var(N_1) = \; & E[Z_2^2(1)] = \sum_{j=0}^{N_f-1} \Big[\int_{jT_f+2iT_s+T_d}^{jT_f+2iT_s+T_d+T_i} \int_{jT_f+2iT_s+T_d}^{jT_f+2iT_s+T_d+T_i} \Big(\sum_{l_1} \alpha_{l_1} p(t - jT_f - \\
& 2iT_s - \tau_{l_1}) \Big) \Big(\sum_{m_1} \alpha_{m_1} p(\tau - jT_f - 2iT_s - \tau_{m_1}) \Big) E[n_{SD}(t - T_d) n_{SD}(\tau - T_d \\
&)]dtd\tau \Big]
\end{aligned}
$$

$$
\begin{aligned}
&= \sum_{j=0}^{N_f-1}\Bigg[\int_{jT_f+2iT_s+T_d}^{jT_f+2iT_s+T_d+T_i}\Bigg(\sum_{l_1}\alpha_{l_1}p(t-jT_f-2iT_s-\tau_{l_1})\Bigg)\Bigg(\sum_{m_1}\alpha_{m_1}p(\tau- \\
&\quad jT_f-2iT_s-\tau_{m_1})\Bigg)\theta_1(t-\tau)dtd\tau\Bigg] \\
&= \frac{N_fN_0}{2}\Bigg[\int_{jT_f+2iT_s+T_d}^{jT_f+2iT_s+T_d+T_i}\sum_{l_1=m_1}\alpha_{l_1}^2p^2(t-jT_f-2iT_s-\tau_{l_1})dt \\
&\quad \underbrace{+\sum_{l_1\neq m_1}\sum\alpha_{l_1}\alpha_{m_1}R(\tau_{l_1}-\tau_{m_1})}_{value=0}\Bigg] \\
&= \frac{N_fN_0E_p}{2}\underbrace{\Bigg(\sum_{l_1}\alpha_{l_1}^2\Bigg)}_{value=\gamma_1} \\
&= \frac{N_fN_0E_p\gamma_1}{2}. \qquad (4.13)
\end{aligned}
$$

where, $\int_{jT_f+2iT_s}^{jT_f+2iT_s+T_i}\theta_1(t-\tau)d\tau=\int_{jT_f+2iT_s}^{jT_f+2iT_s+T_i}\frac{N_0}{2}\delta(t-\tau)d\tau=\frac{N_0}{2}$.

$$
\begin{aligned}
Var(N_2) &= E[Z_3^2(1)]=\sum_{j=0}^{N_f-1}\Bigg[\int_{jT_f+2iT_s+T_d}^{jT_f+2iT_s+T_d+T_i}\int_{jT_f+2iT_s+T_d}^{jT_f+2iT_s+T_d+T_i}\Bigg(\sum_{l_1}\alpha_{l_1}b_ip(t-jT_f \\
&\quad -2iT_s-T_d-\tau_{l_1})\Bigg)\Bigg(\sum_{m_1}\alpha_{m_1}b_ip(\tau-jT_f-2iT_s-T_d-\tau_{m_1})\Bigg)E[n_{SD}(t) \\
&\quad n_{SD}(\tau)]dtd\tau\Bigg] \\
&= \sum_{j=0}^{N_f-1}b_i^2\Bigg[\int_{jT_f+2iT_s+T_d}^{jT_f+2iT_s+T_d+T_i}\int_{jT_f+2iT_s+T_d}^{jT_f+2iT_s+T_d+T_i}\sum_{l_1}\alpha_{l_1}p(t-jT_f-2iT_s-T_d \\
&\quad -\tau_{l_1})\sum_{m_1}\alpha_{m_1}p(\tau-jT_f-2iT_s-T_d-\tau_{m_1})\Bigg)\theta_1(t-\tau)dtd\tau\Bigg] \\
&= \frac{N_fN_0b_i^2}{2}\Bigg[\int_{jT_f+2iT_s+T_d}^{jT_f+2iT_s+T_d+T_i}\sum_{l_1=m_1}\alpha_{l_1}^2p^2(t-jT_f-2iT_s-\tau_{l_1})dt \\
&\quad \underbrace{+\sum_{l_1\neq m_1}\sum\alpha_{l_1}\alpha_{m_1}R(\tau_{l_1}-\tau_{m_1})}_{value=0}\Bigg] \\
&= \frac{N_fN_0b_i^2E_p}{2}\underbrace{\Bigg(\sum_{l_1}\alpha_{l_1}^2\Bigg)}_{value=\gamma_1} \\
&= \frac{N_fN_0b_i^2E_p\gamma_1}{2} \qquad (4.14)
\end{aligned}
$$

$$
\begin{aligned}
Var(N_3) &= E[Z_4^2(1)] = \sum_{j=0}^{N_f-1}\Bigg[\int_{jT_f+2iT_s+T_d}^{jT_f+2iT_s+T_d+T_i}\int_{jT_f+2iT_s+T_d}^{jT_f+2iT_s+T_d+T_i} \\
&\quad \mathbb{E}\left[\{n_{SD}(t)n_{SD}(\tau-T_d)\}^2\right]dtd\tau\Bigg] \\
&= \sum_{j=0}^{N_f-1}\left[\int_{jT_f+2iT_s+T_d}^{jT_f+2iT_s+T_d+T_i}\int_{jT_f+2iT_s+T_d}^{jT_f+2iT_s+T_d+T_i}\theta_1^2(t-\tau)dtd\tau\right] \\
&= \sum_{j=0}^{N_f-1}\left[\int_{jT_f+2iT_s+T_d}^{jT_f+2iT_s+T_d+T_i}\int_{jT_f+2iT_s+T_d+T_i-t}^{jT_f+2iT_s+T_d+T_i}\theta_1^2(u)dtdu\right] \\
&= \sum_{j=0}^{N_f-1}\left[\int_0^{T_i}\frac{N_0^2}{4}2Wdt\right] \\
&= \frac{N_fN_0^2WT_i}{2}. \qquad (4.15)
\end{aligned}
$$

where, $E[n_k^2(t)] = \frac{N_0}{2}$. The value of $E[\{n_k^2(t)\}^2] = \frac{N_0^2}{4}$.

The decision statistic Z_{TR-SD} at destination node in 1st time slot contains signal term and the noise term. From the derivations, it is observed that the signal term sig_{SD} has a value of $N_f b_i E_p \gamma_1$ while the noise term $Z_{noise-SD}$ has a variance of $\sigma^2_{Z_{noise-SD}} = \frac{N_f N_0 E_p \gamma_1}{2} + \frac{N_f N_0 b_i^2 E_p \gamma_1}{2} + \frac{N_f N_0^2 W T_i}{2}$. The SNR at the destination node from S−D link in the 1st time slot is represented as:

$$
\begin{aligned}
\rho_{TR-SD} &= \frac{sig_{SD}^2}{\sigma^2_{Z_{noise-SD}}} \\
&= \frac{(N_f b_i E_p \gamma_1)^2}{\frac{N_f N_0 E_p \gamma_1}{2} + \frac{N_f N_0 b_i^2 E_p \gamma_1}{2} + \frac{N_f N_0^2 W T_i}{2}} \\
&= \frac{(N_f E_p \gamma_1)^2}{N_f N_0 E_p \gamma_1 + \frac{N_f N_0^2 W T_i}{2}} \\
&= \frac{(\frac{E_b \gamma_1}{2})^2}{\frac{N_0 E_b \gamma_1}{2} + \frac{N_f N_0^2 W T_i}{2}} \qquad (4.16)
\end{aligned}
$$

where, energy per bit is given as $E_b = 2N_f T_f$.

In the 1st time slot, UWB TR signal is also transmitted from the source node to the relay node, which is represented by equation 4.2. The signal received at the relay node in 1st time slot is denoted by equation 4.7. The signal received at the relay node in 1st time slot is amplified by an amplifying factor $\sqrt{\beta_{AF}}$, and then forwarded to the destination node in 2nd time slot. The amplified UWB TR signal transmitted from the relay node to the destination node is represented

as:

$$s_{TR-RD}(t) \;=\; r_{TR-SR}(t)\sqrt{\beta_{AF}} \tag{4.17}$$

where, the amplifying gain is defined as $\sqrt{\beta_{AF}} = \sqrt{\left(\frac{E_{SR}}{\mathbb{E}\left\{|h_2^2(t)|\right\}E_{SR}+N_0}\right)}$. Also, $\mathbb{E}$, E_{SR}, $h_2(t)$ and $\sigma^2_{Z_{noise-SR}}$ represent the expectation operator, signal energy, channel response and noise variance of S$-$R link respectively. The signal received at the destination node from R$-$D link in 2$^{\text{nd}}$ time slot is represented as:

$$\begin{aligned} r_{TR-RD}(t) &= \Bigg(\sum_{i=0}^{\infty}\sum_{j=0}^{N_f-1}\Bigg[\sqrt{\beta_{AF}}\sum_{l_2}\alpha_{l_2}p(t-jT_f-(2i+1)T_s-\tau_{l_2})+\sqrt{\beta_{AF}}\sum_{l_2}\alpha_{l_2}b_i \\ &\quad p(t-jT_f-(2i+1)T_s-T_d-\tau_{l_2})+\sqrt{\beta_{AF}}n_{SR}(t)\Bigg]*\sum_{l_3}\alpha_{l_3}\delta(t-\tau_{l_3})\Bigg) \\ &\quad +n_{RD}(t) \\ &= \sum_{i=0}^{\infty}\sum_{j=0}^{N_f-1}\Bigg[\sqrt{\beta_{AF}}\sum_{l_2}\alpha_{l_2}\sum_{l_3}\alpha_{l_3}p(t-jT_f-(2i+1)T_s-\tau_{l_2}-\tau_{l_3})+\sqrt{\beta_{AF}} \\ &\quad b_i\sum_{l_2}\alpha_{l_2}\sum_{l_3}\alpha_{l_3}p(t-jT_f-(2i+1)T_s-T_d-\tau_{l_2}-\tau_{l_3})\Bigg]+\sqrt{\beta_{AF}}n'_{RD}(t) \\ &\quad +n_{RD}(t) \end{aligned} \tag{4.18}$$

where, $n'_{RD}(t) = n_{SR}(t) * h_3(t) = \sum_{l_3}\alpha_{l_3}n_{SR}(t-\tau_{l,3})$ denote the aggregate noise response after convolving the noise response of S$-$R link, with channel response of R$-$D link $h_3(t)$. Also, $n_{RD}(t)$ represent the noise response of R$-$D link.

The received signal $r_{TR-RD}(t)$ obtained at the destination node in the 2$^{\text{nd}}$ time slot is now passed through a TR receiver, whose decision statistics Z_{TR-RD} is expressed as:

$$\begin{aligned} Z_{TR-RD} &= \sum_{j=0}^{N_f-1}\int_{jT_f+(2i+1)T_s+T_d}^{jT_f+(2i+1)T_s+T_d+T_i} r_{TR-RD}(t)r_{TR-RD}(t-T_d)dt \\ &= \underbrace{Z_1(3)}_{signal}+\underbrace{Z_2(3)+Z_3(3)+Z_4(3)+Z_5(3)+Z_6(3)+Z_7(3)+Z_8(3)+Z_9(3)}_{\text{noiseterm}} \end{aligned} \tag{4.19}$$

The signal term $Z_1(3)$ obtained from R$-$D link is expressed as:

$$\begin{aligned} Z_1(3) &= \sum_{j=0}^{N_f-1}\beta_{AF}\Bigg[\int_{jT_f+(2i+1)T_s+T_d}^{jT_f+(2i+1)T_s+T_d+T_i}\Bigg(\sum_{l_2}\alpha_{l_2}\sum_{l_3}\alpha_{l_3}p(t-jT_f-(2i+1)T_s-\tau_{l_2} \\ &\quad -\tau_{l_3})\Bigg)\Bigg(\sum_{m_2}\alpha_{m_2}\sum_{m_3}\alpha_{m_3}b_ip(t-jT_f-(2i+1)T_s-T_d-\tau_{m_2}-\tau_{m_3})\Bigg)dt\Bigg] \end{aligned}$$

$$
\begin{aligned}
&= \beta_{AF} N_f b_i \Bigg[\int_{jT_f+(2i+1)T_s+T_d}^{jT_f+(2i+1)T_s+T_d+T_i} \overbrace{\underbrace{\sum_{l_2} \alpha_{l_2}^2}_{l_2=m_2} \underbrace{\sum_{l_3} \alpha_{l_3}^2}_{l_3=m_3}}^{Value=\gamma_2\gamma_3} p^2(t - jT_f - (2i+1)T_s - \tau_{l_2} \\
&\quad -\tau_{l_3})dt + \overbrace{\underbrace{\sum_{l_2}\sum_{m_2} \alpha_{l_2}\alpha_{m_2}}_{l_2\neq m_2} R(\tau_{l_2} - \tau_{m_2}) \underbrace{\sum_{l_3}\sum_{m_3} \alpha_{l_3}\alpha_{m_3}}_{l_3\neq m_3} R(\tau_{l_3} - \tau_{m_3})}^{Value=0} \Bigg] \\
&= \beta_{AF} N_f b_i E_p \Bigg(\overbrace{\underbrace{\sum_{l_2} \alpha_{l_2}^2}_{l_2=m_2} \underbrace{\sum_{l_3} \alpha_{l_3}^2}_{l_3=m_3}}^{Value=\gamma_2\gamma_3} \Bigg) \\
&= \beta_{AF} N_f b_i E_p \gamma_2 \gamma_3 \qquad (4.20)
\end{aligned}
$$

where, the pulse energy obtained from R−D link is defined as $E_p = \int_{jT_f+(2i+1)T_s+T_d}^{jT_f+(2i+1)T_s+T_d+T_i} p^2(t - jT_f - (2i+1)T_s - \tau_{l_2} - \tau_{l_3})dt$ and autocorrelation function as $R(\tau) = \int_{\infty}^{\infty} p(t)p(t-\tau)dt$. This condition $min\{(\tau_{l_2} - \tau_{m_2})\} > T_p$ for $l_2 \neq m_2$ or $min\{(\tau_{l_3} - \tau_{m_3})\} > T_p$ for $l_3 \neq m_3$ is satisfied to avoid IPI. Hence, $\sum_{l_2\neq m_2}\sum \alpha_{l_2}\alpha_{m_2} R(\tau_{l_2} - \tau_{m_2}) \sum_{l_3\neq m_3}\sum \alpha_{l_3}\alpha_{m_3} R(\tau_{l_3} - \tau_{m_3}) = 0$. As explained earlier in the same section, since a large number of UWB multipath channel gains are considered, the channel gains can be approximated as Gaussian Distributed using the Central Limit Theorem $\sum_{l_2} \alpha_{l_2}^2 = \gamma_2$ and $\sum_{l_3} \alpha_{l_3}^2 = \gamma_3$. As described earlier, since the PSD $\theta_k(f)$ of noise is sufficiently flat, the autocorrelation function of noise can be approximated as $\theta_k(\tau) = \frac{N_0}{2}\delta(\tau)$[175]. To solve the decision variables $Z_2(3)$, $Z_3(3)$, $Z_4(3)$, $Z_5(3)$, $Z_6(3)$, $Z_7(3)$, $Z_8(3)$ and $Z_9(3)$ containing noise terms, variance is evaluated. The variance of noise terms are as solved below.

$$
\begin{aligned}
Var(N_1) &= E[Z_2^2(3)] = \beta_{AF}^2 \sum_{j=0}^{N_f-1} \Bigg[\int_{jT_f+(2i+1)T_s+T_d}^{jT_f+(2i+1)T_s+T_d+T_i} \int_{jT_f+(2i+1)T_s+T_d}^{jT_f+(2i+1)T_s+T_d+T_i} \Bigg(\sum_{l_2} \alpha_{l_2} \sum_{l_3} \\
&\quad \alpha_{l_3} p(t - jT_f - (2i+1)T_s - \tau_{l_2} - \tau_{l_3}) \Bigg) \Bigg(\sum_{m_2} \alpha_{m_2} \sum_{m_3} \alpha_{m_3} p(\tau - jT_f - \\
&\quad (2i+1)T_s - \tau_{m_2} - \tau_{m_3}) \Bigg) \mathbb{E}[n'_{RD}(t - T_d) n'_{RD}(\tau - T_d)] dt d\tau \Bigg] \\
&= \beta_{AF}^2 N_f \Bigg[\int_{jT_f+(2i+1)T_s+T_d}^{jT_f+(2i+1)T_s+T_d+T_i} \int_{jT_f+(2i+1)T_s+T_d}^{jT_f+(2i+1)T_s+T_d+T_i} \Bigg(\sum_{l_2} \alpha_{l_2} \sum_{l_3} \alpha_{l_3} p(t - jT_f \\
&\quad -(2i+1)T_s - \tau_{l_2} - \tau_{l_3}) \Bigg) \Bigg(\sum_{m_2} \alpha_{m_2} \sum_{m_3} \alpha_{m_3} p(\tau - jT_f - (2i+1)T_s - \tau_{m_2} - \\
&\quad \tau_{m_3}) \Bigg) \theta_3'(t - \tau) dt d\tau \Bigg]
\end{aligned}
$$

$$= \beta_{AF}^2 N_f \left(\frac{\gamma_3 N_0}{2}\right) \Bigg[\int_{jT_f+(2i+1)T_s+T_d}^{jT_f+(2i+1)T_s+T_d+T_i} \overbrace{\underbrace{\sum_{l_2} \alpha_{l_2}^2}_{l_2=m_2} \underbrace{\sum_{l_3} \alpha_{l_3}^2}_{l_3=m_3}}^{Value=\gamma_2\gamma_3} p^2(t - jT_f - (2i+1)$$

$$T_s - \tau_{l_2} - \tau_{l_3})dt + \overbrace{\underbrace{\sum_{l_2} \sum_{m_2} \alpha_{l_2}\alpha_{m_2}}_{l_2 \neq m_2} R(\tau_{l_2} - \tau_{m_2}) \underbrace{\sum_{l_3} \sum_{m_3} \alpha_{l_3}\alpha_{m_3}}_{l_3 \neq m_3} R(\tau_{l_3} - \tau_{m_3})}^{Value=0} \Bigg]$$

$$= \beta_{AF}^2 N_f \left(\frac{\gamma_3 N_0}{2}\right) E_p \Bigg(\overbrace{\underbrace{\sum_{l_2} \alpha_{l_2}^2}_{l_2=m_2} \underbrace{\sum_{l_3} \alpha_{l_3}^2}_{l_3=m_3}}^{Value=\gamma_2\gamma_3} \Bigg)$$

$$= \frac{\beta_{AF}^2 N_f N_0 E_p \gamma_2 \gamma_3^2}{2} \tag{4.21}$$

where, the value of $\theta_3^{'}(t-\tau)$ is obtained from Appendix B. Hence, $\int_{jT_f+(2i+1)T_s}^{jT_f+(2i+1)T_s+T_i} \theta_3^{'}(t - \tau)d\tau = \frac{\gamma_3 N_0}{2}$.

$$Var(N_2) = E[Z_3^2(3)] = \beta_{AF}^2 \sum_{j=0}^{N_f-1} \Bigg[\int_{jT_f+(2i+1)T_s+T_d}^{jT_f+(2i+1)T_s+T_d+T_i} \int_{jT_f+(2i+1)T_s+T_d}^{jT_f+(2i+1)T_s+T_d+T_i} \Bigg(\sum_{l_2} \alpha_{l_2} \sum_{l_3}$$

$$\alpha_{l_3} b_i p(t - jT_f - (2i+1)T_s - T_d - \tau_{l_2} - \tau_{l_3}) \Bigg) \Bigg(\sum_{m_2} \alpha_{m_2} \sum_{m_3} \alpha_{m_3} b_i p(\tau - jT_f$$

$$-(2i+1)T_s - T_d - \tau_{m_2} - \tau_{m_3}) \Bigg) \mathbb{E}[n_{RD}^{'}(t) n_{RD}^{'}(\tau)] dt d\tau \Bigg]$$

$$= \beta_{AF}^2 N_f b_i^2 \Bigg[\int_{jT_f+(2i+1)T_s+T_d}^{jT_f+(2i+1)T_s+T_d+T_i} \int_{jT_f+(2i+1)T_s+T_d}^{jT_f+(2i+1)T_s+T_d+T_i} \Bigg(\sum_{l_2} \alpha_{l_2} \sum_{l_3} \alpha_{l_3} p(t - jT_f$$

$$-(2i+1)T_s - T_d - \tau_{l_2} - \tau_{l_3}) \Bigg) \Bigg(\sum_{m_2} \alpha_{m_2} \sum_{m_3} \alpha_{m_3} p(\tau - jT_f - (2i+1)T_s -$$

$$T_d - \tau_{m_2} - \tau_{m_3}) \Bigg) \theta_3^{'}(t-\tau) dt d\tau \Bigg]$$

$$= \beta_{AF}^2 N_f b_i^2 \left(\frac{\gamma_3 N_0}{2}\right) \Bigg[\int_{jT_f+(2i+1)T_s+T_d}^{jT_f+(2i+1)T_s+T_d+T_i} \overbrace{\underbrace{\sum_{l_2} \alpha_{l_2}^2}_{l_2=m_2} \underbrace{\sum_{l_3} \alpha_{l_3}^2}_{l_3=m_3}}^{Value=\gamma_2\gamma_3} p^2(t - jT_f - (2i+1)T_s$$

$$-T_d - \tau_{l_2} - \tau_{l_3})dt + \overbrace{\underbrace{\sum_{l_2} \sum_{m_2} \alpha_{l_2}\alpha_{m_2}}_{l_2 \neq m_2} R(\tau_{l_2} - \tau_{m_2}) \underbrace{\sum_{l_3} \sum_{m_3} \alpha_{l_3}\alpha_{m_3}}_{l_3 \neq m_3} R(\tau_{l_3} - \tau_{m_3})}^{Value=0} \Bigg]$$

$$= \beta_{AF}^2 N_f \left(\frac{\gamma_3 N_0}{2}\right) b_i^2 E_p \Bigg(\overbrace{\underbrace{\sum_{l_2} \alpha_{l_2}^2}_{l_2=m_2} \underbrace{\sum_{l_3} \alpha_{l_3}^2}_{l_3=m_3}}^{Value=\gamma_2\gamma_3} \Bigg)$$

$$= \frac{\beta_{AF}^2 N_f N_0 b_i^2 E_p \gamma_2 \gamma_3^2}{2} \tag{4.22}$$

$$\begin{aligned}
Var(N_3) &= E[Z_4^2(3)] = \beta_{AF} \sum_{j=0}^{N_f-1} \Bigg[\int_{jT_f+(2i+1)T_s+T_d}^{jT_f+(2i+1)T_s+T_d+T_i} \int_{jT_f+(2i+1)T_s+T_d}^{jT_f+(2i+1)T_s+T_d+T_i} \Bigg(\sum_{l_2} \alpha_{l_2} \sum_{l_3} \\
&\alpha_{l_3} p(t - jT_f - (2i+1)T_s - \tau_{l_2} - \tau_{l_3}) \Bigg) \Bigg(\sum_{m_2} \alpha_{m_2} \sum_{m_3} \alpha_{m_3} p(\tau - jT_f - \\
&(2i+1)T_s - \tau_{m_2} - \tau_{m_3}) \Bigg) \mathbb{E}[n_{RD}(t - T_d) n_{RD}(\tau - T_d)] dt d\tau \Bigg] \\
&= \beta_{AF} N_f \Bigg[\int_{jT_f+(2i+1)T_s+T_d}^{jT_f+(2i+1)T_s+T_d+T_i} \int_{jT_f+(2i+1)T_s+T_d}^{jT_f+(2i+1)T_s+T_d+T_i} \Bigg(\sum_{l_2} \alpha_{l_2} \sum_{l_3} \alpha_{l_3} p(t - jT_f \\
&-(2i+1)T_s - \tau_{l_2} - \tau_{l_3}) \Bigg) \Bigg(\sum_{m_2} \alpha_{m_2} \sum_{m_3} \alpha_{m_3} p(\tau - jT_f - (2i+1)T_s - \tau_{m_2} - \\
&\tau_{m_3}) \Bigg) \theta_3(t - \tau) dt d\tau \Bigg] \\
&= \frac{\beta_{AF} N_f N_0}{2} \Bigg[\int_{jT_f+(2i+1)T_s+T_d}^{jT_f+(2i+1)T_s+T_d+T_i} \overbrace{\underbrace{\sum_{l_2} \alpha_{l_2}^2}_{l_2=m_2} \underbrace{\sum_{l_3} \alpha_{l_3}^2}_{l_3=m_3}}^{Value=\gamma_2\gamma_3} p^2(t - jT_f - (2i+1)T_s - \tau_{l_2} \\
&-\tau_{l_3}) dt + \overbrace{\underbrace{\sum_{l_2} \sum_{m_2} \alpha_{l_2} \alpha_{m_2} R(\tau_{l_2} - \tau_{m_2})}_{l_2 \neq m_2} \underbrace{\sum_{l_3} \sum_{m_3} \alpha_{l_3} \alpha_{m_3} R(\tau_{l_3} - \tau_{m_3})}_{l_3 \neq m_3}}^{Value=0} \Bigg] \\
&= \frac{\beta_{AF} N_f N_0 E_p}{2} \Bigg(\overbrace{\underbrace{\sum_{l_2} \alpha_{l_2}^2}_{l_2=m_2} \underbrace{\sum_{l_3} \alpha_{l_3}^2}_{l_3=m_3}}^{Value=\gamma_2\gamma_3} \Bigg) \\
&= \frac{\beta_{AF} N_f N_0 E_p \gamma_2 \gamma_3}{2}
\end{aligned} \tag{4.23}$$

where, $\int_{jT_f+(2i+1)T_s}^{jT_f+(2i+1)T_s+T_i} \theta_3(t-\tau) d\tau = \int_{jT_f+(2i+1)T_s}^{jT_f+(2i+1)T_s+T_i} \frac{N_0}{2} \delta(t-\tau) d\tau = \frac{N_0}{2}$.

$$\begin{aligned}
Var(N_4) &= E[Z_5^2(3)] = \beta_{AF} \sum_{j=0}^{N_f-1} \Bigg[\int_{jT_f+(2i+1)T_s+T_d}^{jT_f+(2i+1)T_s+T_d+T_i} \int_{jT_f+(2i+1)T_s+T_d}^{jT_f+(2i+1)T_s+T_d+T_i} \Bigg(\sum_{l_2} \alpha_{l_2} \\
&\sum_{l_3} \alpha_{l_3} b_i p(t - jT_f - (2i+1)T_s - T_d - \tau_{l_2} - \tau_{l_3}) \Bigg) \Bigg(\sum_{m_2} \alpha_{m_2} \sum_{m_3} \alpha_{m_3} b_i p(\tau - \\
&jT_f - (2i+1)T_s - T_d - \tau_{m_2} - \tau_{m_3}) \Bigg) \mathbb{E}[n_{RD}(t) n_{RD}(\tau)] dt d\tau \Bigg] \\
&= \beta_{AF} N_f b_i^2 \Bigg[\int_{jT_f+(2i+1)T_s+T_d}^{jT_f+(2i+1)T_s+T_d+T_i} \int_{jT_f+(2i+1)T_s+T_d}^{jT_f+(2i+1)T_s+T_d+T_i} \Bigg(\sum_{l_2} \alpha_{l_2} \sum_{l_3} \alpha_{l_3} p(t - \\
&
\end{aligned}$$

$$
\begin{aligned}
& jT_f-(2i+1)T_s-T_d-\tau_{l_2}-\tau_{l_3})\Big)\Big(\sum_{m_2}\alpha_{m_2}\sum_{m_3}\alpha_{m_3}p(\tau-jT_f-(2i+1)T_s \\
& -T_d-\tau_{m_2}-\tau_{m_3})\Big)\theta_3(t-\tau)dtd\tau\Big] \\
= \; & \frac{\beta_{AF}N_fN_0b_i^2}{2}\Big[\int_{jT_f+(2i+1)T_s+T_d}^{jT_f+(2i+1)T_s+T_d+T_i}\overbrace{\underbrace{\sum_{l_2}\alpha_{l_2}^2}_{\mathrm{l_2}=m_2}\underbrace{\sum_{l_3}\alpha_{l_3}^2}_{\mathrm{l_3}=m_3}}^{\mathrm{Value}=\gamma_2\gamma_3}p^2(t-jT_f-(2i+1)T_s- \\
& T_d-\tau_{l_2}-\tau_{l_3})dt+\overbrace{\underbrace{\sum_{l_2}\sum_{m_2}\alpha_{l_2}\alpha_{m_2}}_{\mathrm{l_2}\neq m_2}R(\tau_{l_2}-\tau_{m_2})\underbrace{\sum_{l_3}\sum_{m_3}\alpha_{l_3}\alpha_{m_3}}_{\mathrm{l_3}\neq m_3}R(\tau_{l_3}-\tau_{m_3})}^{\mathrm{Value}=0}\Big] \\
= \; & \frac{\beta_{AF}N_fN_0b_i^2E_p}{2}\Big(\underbrace{\overbrace{\sum_{l_2}\alpha_{l_2}^2\sum_{l_3}\alpha_{l_3}^2}^{\mathrm{Value}=\gamma_2\gamma_3}}_{\mathrm{l_2}=m_2\quad\mathrm{l_3}=m_3}\Big) \\
= \; & \frac{\beta_{AF}N_fN_0b_i^2E_p\gamma_2\gamma_3}{2}
\end{aligned}
\tag{4.24}
$$

$$
\begin{aligned}
Var(N_5) &= E[Z_6^2(3)]=\beta_{AF}^2\sum_{j=0}^{N_f-1}\Big[\int_{jT_f+(2i+1)T_s+T_d}^{jT_f+(2i+1)T_s+T_d+T_i}\int_{jT_f+(2i+1)T_s+T_d}^{jT_f+(2i+1)T_s+T_d+T_i} \\
&\quad \mathbb{E}\Big[\Big\{n_{RD}^{'}(t)n_{RD}^{'}(\tau-T_d)\Big\}^2\Big]dtd\tau\Big] \\
&= \beta_{AF}^2\sum_{j=0}^{N_f-1}\int_{jT_f+(2i+1)T_s+T_d}^{jT_f+(2i+1)T_s+T_d+T_i}\int_{jT_f+(2i+1)T_s+T_d}^{jT_f+(2i+1)T_s+T_d+T_i}\theta_3^{'2}(t-\tau)dtd\tau \\
&= \beta_{AF}^2N_f\int_0^{T_i}\left(\frac{\gamma_3N_0}{2}\right)^2 2Wdt \\
&= \frac{\beta_{AF}^2N_fN_0^2WT_i\gamma_3^2}{2}.
\end{aligned}
\tag{4.25}
$$

$$
\begin{aligned}
Var(N_6) &= E[Z_7^2(3)]=\sum_{j=0}^{N_f-1}\Big[\int_{jT_f+(2i+1)T_s+T_d}^{jT_f+(2i+1)T_s+T_d+T_i}\int_{jT_f+(2i+1)T_s+T_d}^{jT_f+(2i+1)T_s+T_d+T_i} \\
&\quad \mathbb{E}\Big[\{n_{RD}(t)n_{RD}(\tau-T_d)\}^2\Big]dtd\tau\Big] \\
&= \sum_{j=0}^{N_f-1}\Big[\int_{jT_f+(2i+1)T_s+T_d}^{jT_f+(2i+1)T_s+T_d+T_i}\int_{jT_f+(2i+1)T_s+T_d}^{jT_f+(2i+1)T_s+T_d+T_i}\theta_3^2(t-\tau)dtd\tau \\
&= N_f\int_0^{T_i}\frac{N_0^2 2Wdt}{4} \\
&= \frac{N_fN_0^2WT_i}{2}
\end{aligned}
\tag{4.26}
$$

$$
\begin{aligned}
Var(N_7) &= E[Z_8^2(3)] = \beta_{AF} \sum_{j=0}^{N_f-1} \Bigg[\int_{jT_f+(2i+1)T_s+T_d}^{jT_f+(2i+1)T_s+T_d+T_i} \int_{jT_f+(2i+1)T_s+T_d}^{jT_f+(2i+1)T_s+T_d+T_i} \\
&\quad \mathbb{E}\left[n_{RD}^{'}(t) n_{RD}^{'}(\tau) n_{RD}(t-T_d) n_{RD}(\tau-T_d) \right] dt d\tau \\
&= \beta_{AF} N_f \int_{jT_f+(2i+1)T_s+T_d}^{jT_f+(2i+1)T_s+T_d+T_i} \int_{jT_f+(2i+1)T_s+T_d}^{jT_f+(2i+1)T_s+T_d+T_i} \theta_3(t-\tau)\theta_3^{'}(t-\tau) dt d\tau \\
&= \beta_{AF} N_f \int_0^{T_i} \left(\frac{\gamma_3 N_0}{2}\right)\left(\frac{N_0}{2}\right) 2W dt \\
&= \frac{\beta_{AF} N_f N_0^2 W T_i \gamma_3}{2}. \qquad (4.27)
\end{aligned}
$$

$$
\begin{aligned}
Var(N_8) &= E[Z_9^2(3)] = \beta_{AF} \sum_{j=0}^{N_f-1} \Bigg[\int_{jT_f+(2i+1)T_s+T_d}^{jT_f+(2i+1)T_s+T_d+T_i} \int_{jT_f+(2i+1)T_s+T_d}^{jT_f+(2i+1)T_s+T_d+T_i} \\
&\quad \mathbb{E}\left[n_{RD}^{'}(t-T_d) n_{RD}^{'}(\tau-T_d) n_{RD}(t) n_{RD}(\tau) \right] dt d\tau \\
&= \beta_{AF} N_f \int_{jT_f+(2i+1)T_s+T_d}^{jT_f+(2i+1)T_s+T_d+T_i} \int_{jT_f+(2i+1)T_s+T_d}^{jT_f+(2i+1)T_s+T_d+T_i} \theta_3^{'}(t-\tau)\theta_3(t-\tau) dt d\tau \\
&= \beta_{AF} N_f \int_0^{T_i} \left(\frac{\gamma_3 N_0}{2}\right)\left(\frac{N_0}{2}\right) 2W dt \\
&= \frac{\beta_{AF} N_f N_0^2 W T_i \gamma_3}{2}. \qquad (4.28)
\end{aligned}
$$

The decision statistic Z_{TR-RD} obtained at the destination node in 2nd time slot contains signal term sig_{RD} and the noise term $Z_{noise-RD}$. It is observed from the derivations that the signal term sig_{RD} has a value of $\beta_{AF} N_f b_i E_p \gamma_2 \gamma_3$ while the noise term $Z_{noise-RD}$ has a variance of $\sigma^2_{Z_{noise-RD}} = \frac{\beta_{AF} N_f N_0 E_p \gamma_2 \gamma_3 (1+b_i^2+\beta_{AF}\gamma_3+\beta_{AF} b_i^2 \gamma_3)}{2} + \frac{N_f N_0^2 W T_i}{2}(1+\beta_{AF}^2\gamma_3^2+2\beta_{AF}\gamma_3)$. The SNR evaluated at the destination node in 2nd time slot is represented as:

$$
\begin{aligned}
\rho_{TR-RD} &= \frac{sig_{RD}^2}{\sigma^2_{Z_{noise-RD}}} \\
&= \frac{(\beta_{AF} N_f b_i E_p \gamma_2 \gamma_3)^2}{\frac{\beta_{AF} N_f N_0 E_p \gamma_2 \gamma_3 (1+b_i^2+\beta_{AF}\gamma_3+\beta_{AF} b_i^2 \gamma_3)}{2} + \frac{N_f N_0^2 W T_i (1+\beta_{AF}^2\gamma_3^2+2\beta_{AF}\gamma_3)}{2}} \\
&= \frac{(\beta_{AF} N_f b_i E_p \gamma_2 \gamma_3)^2}{\beta_{AF} N_f N_0 E_p \gamma_2 \gamma_3 (1+\beta_{AF}\gamma_3) + \frac{N_f N_0^2 W T_i (1+\beta_{AF}^2\gamma_3^2+2\beta_{AF}\gamma_3)}{2}} \\
&= \frac{(\frac{\beta_{AF} E_b \gamma_2 \gamma_3}{2})^2}{\frac{\beta_{AF} N_0 E_b \gamma_2 \gamma_3 (1+\beta_{AF}\gamma_3)}{2} + \frac{N_f N_0^2 W T_i (1+\beta_{AF}^2\gamma_3^2+2\beta_{AF}\gamma_3)}{2}} \qquad (4.29)
\end{aligned}
$$

where, $b_i^2 = 1$ and $E_b = 2N_f E_p$ for TR$-$PAM system. The decision statistics obtained from the destination node in the two time slots are combined using different combining strategies such as optimum linear combining, linear combining and selective combining, to form the final decision statistic. The derivations of the same are explained in subsequent section.

A. Linear Combining

At the destination node, the decision statistics Z_{TR-SD} and Z_{TR-RD} obtained in 1st and 2nd time slots respectively, are linearly combined to form final decision statistic $Z_{total} = Z_{TR-SD} + Z_{TR-RD} = s_{total-signal} + Z_{noise-total}$. The individual decision statistics obtained from S−D and R−D links are as follows:

$$Z_{TR-SD} = sig_{SD} + Z_{noise-SD} \tag{4.30}$$

$$Z_{TR-RD} = sig_{RD} + Z_{noise-RD} \tag{4.31}$$

The final decision statistic Z_{total} is represented as:

$$\begin{aligned} Z_{total} &= Z_{TR-SD} + Z_{TR-RD} \\ &= \underbrace{sig_{SD} + sig_{RD}}_{\mathrm{s}_{total-signal}} + \underbrace{Z_{noise-SD} + Z_{noise-RD}}_{\mathrm{Z}_{noise-total}} \end{aligned} \tag{4.32}$$

The noise value $Z_{noise-total}$ has a total variance of $\sigma^2_{Z_{noise-total}} = \sigma^2_{Z_{noise-SD}} + \sigma^2_{Z_{noise-RD}}$ as solved in equation 4.33. Here, sig_{SD} and $Z_{noise-SD}$ represents the signal and noise terms obtained from S−D channel link, while sig_{RD} and $Z_{noise-RD}$ denotes the signal and noise terms obtained from R−D channel link. The total noise variance is evaluated as:

$$\begin{aligned} \sigma^2_{Z_{noise-total}} &= \mathbb{E}[Z_{noise-total}]^2 \\ &= \mathbb{E}[(Z_{noise-SD} + Z_{noise-RD})]^2 \\ &= \sigma^2_{Z_{noise-SD}} + \sigma^2_{Z_{noise-RD}} \end{aligned} \tag{4.33}$$

where, $\mathbb{E}[Z^2_{noise-SD}] = \sigma^2_{Z_{noise-SD}}$, $\mathbb{E}[Z^2_{noise-RD}] = \sigma^2_{Z_{noise-RD}}$ and $\mathbb{E}[Z_{noise-SD} Z_{noise-RD}] = 0$, because the noise terms at S−D and R−D link are independent, their cross-correlation is 0. Therefore, the SNR at the destination node due to linear combining is expressed as:

$$\rho_{TR-AF-LC} = \left(\frac{s^2_{total-signal}}{\sigma^2_{Z_{noise-total}}}\right) = \frac{(sig_{SD} + sig_{RD})^2}{(\sigma^2_{Z_{noise-SD}} + \sigma^2_{Z_{noise-RD}})} = \left(\frac{(U)^2}{V+W}\right) \tag{4.34}$$

where, $U = \frac{E_b\gamma_1}{2} + \frac{\beta_{AF}E_b\gamma_2\gamma_3}{2}$, $V = \frac{N_0E_b\gamma_1}{2} + \frac{N_fN_0^2WT_i}{2}$ and
$W = \frac{\beta_{AF}N_0E_b\gamma_2\gamma_3(1+\beta_{AF}\gamma_3)}{2} + \frac{N_fN_0^2WT_i(1+\beta^2_{AF}\gamma^2_3+2\beta_{AF}\gamma_3)}{2}$.

In order to extract the information bit b_i, the final decision statistic Z_{total} is compared to the decision threshold. The decision threshold is decided on the basis of PAM modulation scheme. The final decision criteria $\hat{z}$ for linear combining is represented as:

$$\hat{z} = \begin{cases} 0, & H_0 : Z = Z_{total} = Z_{TR-SD} + Z_{TR-RD} \leq 0 \\ 1, & H_1 : Z = Z_{total} = Z_{TR-SD} + Z_{TR-RD} > 0 \end{cases} \tag{4.35}$$

The individual channel gains for S−D, S−R and R−D channel links may be assumed to be IID Gaussian distributed by applying Central Limit Theorem, since a large number paths are involved. Therefore, the sum of these channel gains will also have a Gaussian distribution with its mean being the sum of individual means and variance being sum of the individual variances. Therefore the joint PDF $f_{\rho_{AF}}(\gamma_1, \gamma_2, \gamma_3)$ of the channel in case of linear combining is represented as:

$$f_{\rho_{TR-AF}}(\gamma_1, \gamma_2, \gamma_3) = \frac{1}{\sqrt{(2\pi(\sigma_{SD}^2))}} \frac{1}{\sqrt{(2\pi(\sigma_{SR}^2))}} \frac{1}{\sqrt{(2\pi(\sigma_{RD}^2))}} \exp\left[\frac{-(\gamma_1 - \mu_{SD})^2}{2\sigma_{SD}^2} + \frac{-(\gamma_2 - \mu_{SR})^2}{2\sigma_{SR}^2} + \frac{-(\gamma_3 - \mu_{RD})^2}{2\sigma_{RD}^2}\right] \tag{4.36}$$

where, μ_k and σ_k^2 represent the mean and variance of channel links, while the index $k \in \{1, 2, 3\}$ refers to S−D, S−R and R−D link respectively, as mentioned in equation 4.5. Since the joint PDF of channel link is IID distributed, it is given by $f_{\rho_{TR-AF}}(\gamma_1, \gamma_2, \gamma_3) = f_{\rho_{TR-AF}}(\gamma_1) f_{\rho_{TR-AF}}(\gamma_2) f_{\rho_{TR-AF}}(\gamma_3)$. Finally, we obtain the BER of UWB TR system using linear combining, which is expressed as:

$$\begin{aligned} BER_{TR-AF-LC} &= \int_0^\infty \int_0^\infty \int_0^\infty Q\left(\sqrt{\rho_{TR-AF-LC}}\right) f_{\rho_{TR-AF}}(\gamma_1, \gamma_2, \gamma_3) d\gamma_1 d\gamma_2 d\gamma_3 \\ &= \int_0^\infty \int_0^\infty \int_0^\infty Q\left(\sqrt{\rho_{TR-AF-LC}}\right) \frac{1}{\sqrt{(2\pi(\sigma_{SD}^2))}} \frac{1}{\sqrt{(2\pi(\sigma_{SR}^2))}} \\ &\quad \frac{1}{\sqrt{(2\pi(\sigma_{RD}^2))}} \exp\left[\frac{-(\gamma_1 - \mu_{SD})^2}{2\sigma_{SD}^2} + \frac{-(\gamma_2 - \mu_{SR})^2}{2\sigma_{SR}^2} + \frac{-(\gamma_3 - \mu_{RD})^2}{2\sigma_{RD}^2}\right] \\ &\quad d\gamma_1 d\gamma_2 d\gamma_3 \end{aligned} \tag{4.37}$$

$$\begin{aligned} &= \int_0^\infty \int_0^\infty \int_0^\infty Q\left(\sqrt{\frac{(U)^2}{V+W}}\right) \frac{1}{\sqrt{(2\pi(\sigma_{SD}^2))}} \frac{1}{\sqrt{(2\pi(\sigma_{SR}^2))}} \frac{1}{\sqrt{(2\pi(\sigma_{RD}^2))}} \\ &\quad \exp\left[\frac{-(\gamma_1 - \mu_{SD})^2}{2\sigma_{SD}^2} + \frac{-(\gamma_2 - \mu_{SR})^2}{2\sigma_{SR}^2} + \frac{-(\gamma_3 - \mu_{RD})^2}{2\sigma_{RD}^2}\right] d\gamma_1 d\gamma_2 d\gamma_3 \end{aligned} \tag{4.38}$$

B. Selective Combining

In selective combining, the SNR corresponding to the decision statistics Z_{TR-SD} and Z_{TR-RD}, are compared and the one with the highest SNR is chosen. ρ_{TR-SD} and ρ_{TR-RD} refers to the SNR mentioned in equation 4.16 and 4.29 respectively. The SNR at destination node due to selective combining is expressed as $\rho_{TR-AF-SC} = Max\{\rho_{TR-SD}, \rho_{TR-RD}\}$. Therefore, the BER of UWB TR system using cooperative dual−hop AF strategy with selective combining is represented as:

$$BER_{TR-AF-SC} = \int_0^\infty \int_0^\infty \int_0^\infty Q\left(\sqrt{\rho_{TR-AF-SC}}\right) f_{\rho_{TR-AF}}(\gamma_1, \gamma_2, \gamma_3) d\gamma_1 d\gamma_2 d\gamma_3$$

$$= \int_0^\infty \int_0^\infty \int_0^\infty Q\left(\sqrt{\rho_{TR-AF-SC}}\right) \frac{1}{\sqrt{(2\pi(\sigma_{SD}^2))}} \frac{1}{\sqrt{(2\pi(\sigma_{SR}^2))}} \frac{1}{\sqrt{(2\pi(\sigma_{RD}^2))}} \exp\left[\frac{-(\gamma_1-\mu_{SD})^2}{2\sigma_{SD}^2} + \frac{-(\gamma_2-\mu_{SR})^2}{2\sigma_{SR}^2} + \frac{-(\gamma_3-\mu_{RD})^2}{2\sigma_{RD}^2}\right] d\gamma_1 d\gamma_2 d\gamma_3 \quad (4.39)$$

Since the joint PDF of channel link is IID distributed, it is given by $f_{\rho_{TR-AF}}(\gamma_1,\gamma_2,\gamma_3) = f_{\rho_{TR-AF}}(\gamma_1) f_{\rho_{TR-AF}}(\gamma_2) f_{\rho_{TR-AF}}(\gamma_3)$.

$$= \int_0^\infty \int_0^\infty \int_0^\infty Q\left(\sqrt{Max\left\{\rho_{TR-SD}, \rho_{TR-RD}\right\}}\right) \frac{1}{\sqrt{(2\pi(\sigma_{SD}^2))}} \frac{1}{\sqrt{(2\pi(\sigma_{SR}^2))}} \frac{1}{\sqrt{(2\pi(\sigma_{RD}^2))}} \exp\left[\frac{-(\gamma_1-\mu_{SD})^2}{2\sigma_{SD}^2} + \frac{-(\gamma_2-\mu_{SR})^2}{2\sigma_{SR}^2} + \frac{-(\gamma_3-\mu_{RD})^2}{2\sigma_{RD}^2}\right] d\gamma_1 d\gamma_2 d\gamma_3 \quad (4.40)$$

C. Optimum Linear Combining

At the destination node, the decision statistics obtained from S−D and R−D links in 1st and 2nd time slots respectively, are optimally combined to form the final decision statistic $Z_{total} = Z_{TR-SD} + \kappa Z_{TR-RD}$. The optimal combining factor $\kappa = \frac{(\sigma^2_{Z_{noise-SD}}) sig_{RD}}{(\sigma^2_{Z_{noise-RD}}) sig_{SD}}$ is solved in equation C.4 of Appendix C. The final decision statistic Z_{total} obtained at the destination node using optimum linear combining scheme is denoted by equation 4.42.

$$\begin{aligned} Z_{total} &= Z_{TR-SD} + \kappa Z_{TR-RD} \\ &= \underbrace{sig_{SD} + \kappa sig_{RD}}_{\mathrm{s}_{total-signal}} + \underbrace{Z_{noise-SD} + \kappa(Z_{noise-RD})}_{\mathrm{Z}_{noise-total}} \end{aligned} \quad (4.41)$$

For solving the noise term, we evaluate its variance.

$$\begin{aligned} \sigma^2_{Z_{noise-total}} &= \mathbb{E}[Z_{noise-total}]^2 \\ &= \mathbb{E}[(Z_{noise-SD} + \kappa Z_{noise-RD})]^2 \\ &= \sigma^2_{Z_{noise-SD}} + \kappa^2 \sigma^2_{Z_{noise-RD}} \end{aligned} \quad (4.42)$$

where, $2\kappa\,\mathbb{E}[Z_{noise-SD} Z_{noise-RD}] = 0$, because the cross correlation of two independent noise terms are 0. Also, $\sigma^2_{Z_{noise-total}}$ and $s_{total-signal}$ represent the total noise variance and total signal term respectively. The SNR at the destination node due to optimum linear combining is duly expressed as:

$$\rho_{TR-AF-LOC} = \left(\frac{s^2_{total-signal}}{\sigma^2_{Z_{noise-total}}}\right) = \frac{(sig_{SD} + \kappa sig_{RD})^2}{(\sigma^2_{Z_{noise-SD}} + \kappa^2 \sigma^2_{Z_{noise-RD}})} = \left(\frac{(U)^2}{V + \kappa^2 W}\right) \quad (4.43)$$

where, $U = \frac{E_b \gamma_1}{2} + \kappa \frac{\beta_{AF} E_b \gamma_2 \gamma_3}{2}$, $V = \frac{N_0 E_b \gamma_1}{2} + \frac{N_f N_0^2 W T_i}{2}$ and
$W = \frac{\beta_{AF} N_0 E_b \gamma_2 \gamma_3 (1+\beta_{AF}\gamma_3)}{2} + \frac{N_f N_0^2 W T_i (1+\beta_{AF}^2 \gamma_3^2 + 2\beta_{AF}\gamma_3)}{2}$.

The final decision statistic Z_{total} is compared to the decision threshold, in order to retrieve the information bit b_i. The decision threshold is determined using PAM modulation scheme. The decision criteria $\hat{z}$ for optimum linear combining is represented as:

$$\hat{z} = \begin{Bmatrix} 0, & H_0 : Z = Z_{total} = Z_{TR-SD} + \kappa Z_{TR-RD} \leq 0 \\ 1, & H_1 : Z = Z_{total} = Z_{TR-SD} + \kappa Z_{TR-RD} > 0 \end{Bmatrix} \tag{4.44}$$

The joint PDF of channel links in case of optimum linear combining is expressed as:

$$\begin{aligned} f_{\rho_{TR-AF}}(\gamma_1, \gamma_2, \gamma_3) &= \frac{1}{\sqrt{(2\pi(\sigma_{SD}^2))}} \frac{1}{\sqrt{(2\pi(\kappa^2\sigma_{SR}^2))}} \frac{1}{\sqrt{(2\pi(\kappa^2\sigma_{RD}^2))}} \exp\left[\frac{-(\gamma_1 - \mu_{SD})^2}{2\sigma_{SD}^2} + \right. \\ &\left. \frac{-(\gamma_2 - \mu_{SR})^2}{2\kappa^2\sigma_{SR}^2} + \frac{-(\gamma_3 - \mu_{RD})^2}{2\kappa^2\sigma_{RD}^2}\right] \end{aligned} \tag{4.45}$$

As the joint PDF of channel link is IID distributed, it is given by $f_{\rho_{TR-AF}}(\gamma_1, \gamma_2, \gamma_3) = f_{\rho_{TR-AF}}(\gamma_1) f_{\rho_{TR-AF}}(\gamma_2) f_{\rho_{TR-AF}}(\gamma_3)$.

Subsequently, the BER of UWB TR system using dual−hop cooperative AF strategy, with optimum linear combining is denoted as:

$$\begin{aligned} BER_{TR-AF-LOC} &= \int_0^\infty \int_0^\infty \int_0^\infty Q\left(\sqrt{\rho_{TR-AF-LOC}}\right) f_{\rho_{TR-AF}}(\gamma_1, \gamma_2, \gamma_3) d\gamma_1 d\gamma_2 d\gamma_3 \\ &= \int_0^\infty \int_0^\infty \int_0^\infty Q\left(\sqrt{\rho_{TR-AF-LOC}} \frac{1}{\sqrt{(2\pi(\sigma_{SD}^2))}} \frac{1}{\sqrt{(2\pi(\kappa^2\sigma_{SR}^2))}} \right. \\ &\frac{1}{\sqrt{(2\pi(\kappa^2\sigma_{RD}^2))}} \exp\left[\frac{-(\gamma_1 - \mu_{SD})^2}{2\sigma_{SD}^2} + \frac{-(\gamma_2 - \mu_{SR})^2}{2\kappa^2\sigma_{SR}^2} + \right. \\ &\left.\left. \frac{-(\gamma_3 - \mu_{RD})^2}{2\kappa^2\sigma_{RD}^2}\right] d\gamma_1 d\gamma_2 d\gamma_3 \end{aligned} \tag{4.46}$$

$$\begin{aligned} &= \int_0^\infty \int_0^\infty \int_0^\infty Q\left(\sqrt{\frac{U^2}{V + \kappa^2 W}}\right) \frac{1}{\sqrt{(2\pi(\sigma_{SD}^2))}} \frac{1}{\sqrt{(2\pi(\kappa^2\sigma_{SR}^2))}} \frac{1}{\sqrt{(2\pi(\kappa^2\sigma_{RD}^2))}} \\ &\exp\left[\frac{-(\gamma_1 - \mu_{SD})^2}{2\sigma_{SD}^2} + \frac{-(\gamma_2 - \mu_{SR})^2}{2\kappa^2\sigma_{SR}^2} + \frac{-(\gamma_3 - \mu_{RD})^2}{2\kappa^2\sigma_{RD}^2}\right] d\gamma_1 d\gamma_2 d\gamma_3 \end{aligned} \tag{4.47}$$

4.3.2 DTR System

In this section, the theoretical BER performance of UWB DTR system is analysed using cooperative AF strategy. The received signal obtained at the destination and relay node in 1st time slot is represented by equation 4.8 and 4.9, respectively. This received signal at the destination node is detected using a DTR receiver, whose decision statistics Z_{DTR-SD} is expressed as:

$$Z_{DTR-SD} = \sum_{j=0}^{N_f - 1} \int_{jT_f + 2iT_s}^{jT_f + 2iT_s + T_i} r_{DTR-SD}(t) r_{DTR-SD}(t - T_s) dt$$

$$= \underbrace{Z_1(k)}_{signal} + \underbrace{Z_2(k) + Z_3(k) + Z_4(k)}_{\text{noise}-term} = \underbrace{Z_1(1)}_{signal} + \underbrace{Z_2(1) + Z_3(1) + Z_4(1)}_{\text{noise}-term} \quad (4.48)$$

where, the index $k \in \{1, 2, 3\}$ represents S$-$D, S$-$R and R$-$D link respectively, as mentioned in equation 4.5 and $T_i = T_p + T_{mds}$ the integration time interval. Here, T_p and T_{mds} denotes pulse duration and multipath delay spread, respectively. Replacing the value of equation 4.8 in equation 4.49, the value of Z_{DTR-SD} is obtained in equation 4.50.

$$= \sum_{j=0}^{N_f-1} \int_{jT_f+2iT_s}^{jT_f+2iT_s+T_i} \left(\left[\sum_{l_1} \alpha_{l_1} b_i p(t - jT_f - 2iT_s - \tau_{l_1}) \right] + n_{SD}(t) \right) \left(\left[\sum_{m_1} \alpha_{m_1} b_{i-1} \right. \right.$$
$$\left. \left. p(t - jT_f - 2iT_s - \tau_{m_1}) \right] + n_{SD}(t - T_s) \right) \quad (4.49)$$

The signal term obtained from S$-$D link is represented as:

$$\begin{aligned} Z_1(1) &= \sum_{j=0}^{N_f-1} \left[\int_{jT_f+2iT_s}^{jT_f+2iT_s+T_i} \left(\sum_{l_1} \alpha_{l_1} b_i p(t - jT_f - 2iT_s - \tau_{l_1}) \right) \left(\sum_{m_1} \alpha_{m_1} b_{i-1} p(t - jT_f - \right. \right. \\ &\quad \left. \left. 2iT_s - \tau_{m_1}) dt \right) \right] \\ &= N_f b_i b_{i-1} \left[\int_{jT_f+2iT_s}^{jT_f+2iT_s+T_i} \sum_{l_1=m_1} \alpha_{l_1}^2 p^2(t - jT_f - 2iT_s - \tau_{l_1}) dt \right. \\ &\quad \left. + \underbrace{\sum_{l_1 \neq m_1} \sum \alpha_{l_1} \alpha_{m_1} R(\tau_{l_1} - \tau_{m_1})}_{value=0} \right] \\ &= N_f b_i b_{i-1} E_p \underbrace{\left(\sum_{l_1} \alpha_{l_1}^2 \right)}_{value=\gamma_1}. \end{aligned} \quad (4.50)$$

where, the pulse energy obtained from S$-$D link is defined as $E_p = \int_{jT_f+2iT_s}^{jT_f+2iT_s+T_i} p^2(t - jT_f - 2iT_s - \tau_{l_1}) dt$ and autocorrelation function as $R(\tau) = \int_{\infty}^{\infty} p(t)p(t - \tau) dt$. To avoid IPI, the assumption used is $min\{(\tau_{l_1} - \tau_{m_1})\} > T_p$ for $l_1 \neq m_1$. Hence, $\sum_{l_1 \neq m_1} \sum \alpha_{l_1} \alpha_{m_1} R(\tau_{l_1} - \tau_{m_1}) = 0$. As explained in Section 4.3.1, since a large number of UWB multipath channel gains are considered, the channel gains may be approximated as Gaussian Distributed using the Central Limit Theorem $\sum_{l_1} \alpha_{l_1}^2 = \gamma_1$. As described in Section 4.3.1, the PSD $\theta_k(f)$ of noise is sufficiently flat, so the autocorrelation function of noise can be approximated as $\theta_k(\tau) = \frac{N_0}{2} \delta(\tau)$ [175]. Since $Z_2(1)$, $Z_3(1)$ and $Z_4(1)$ denote the noise terms, their variances are solved as follows:

$$Var(N_1) = E[Z_2^2(1)] = \sum_{j=0}^{N_f-1} \left[\int_{jT_f+2iT_s}^{jT_f+2iT_s+T_i} \int_{jT_f+2iT_s}^{jT_f+2iT_s+T_i} \left(\sum_{l_1} \alpha_{l_1} b_i p(t - jT_f - 2iT_s - \right. \right.$$

$$
\begin{aligned}
& \tau_{l_1})\Big)\Big(\sum_{m_1}\alpha_{m_1}b_i p(\tau - jT_f - 2iT_s - \tau_{m_1})\Big)\,\mathbb{E}[n_{SD}(t-T_s)n_{SD}(\tau-T_s)]dtd\tau\Big] \\
&= \sum_{j=0}^{N_f-1} b_i^2\Big[\int_{jT_f+2iT_s}^{jT_f+2iT_s+T_i}\int_{jT_f+2iT_s}^{jT_f+2iT_s+T_i}\Big(\sum_{l_1}\alpha_{l_1}p(t-jT_f-2iT_s-\tau_{l_1})\Big)\Big(\sum_{m_1} \\
& \alpha_{m_1}p(\tau-jT_f-2iT_s-\tau_{m_1})\Big)\theta_1(t-\tau)dtd\tau\Big] \\
&= \frac{N_f N_0 b_i^2}{2}\Big[\int_{jT_f+2iT_s}^{jT_f+2iT_s+T_i}\sum_{l_1=m_1}\alpha_{l_1}^2 p^2(t-jT_f-2iT_s-\tau_{l_1})dt \\
& \underbrace{+\sum_{l_1\neq m_1}\sum\alpha_{l_1}\alpha_{m_1}R(\tau_{l_1}-\tau_{m_1})}_{value=0}\Big] \\
&= \frac{N_f N_0 b_i^2 E_p}{2}\underbrace{\Big(\sum_{l_1}\alpha_{l_1}^2\Big)}_{value=\gamma_1} \\
&= \frac{N_f N_0 b_i^2 E_p \gamma_1}{2} \qquad (4.51)
\end{aligned}
$$

where, $\int_{jT_f+2iT_s}^{jT_f+2iT_s+T_i}\theta_1(t-\tau)d\tau = \int_{jT_f+2iT_s}^{jT_f+2iT_s+T_i}\frac{N_0}{2}\delta(t-\tau)d\tau = \frac{N_0}{2}$.

$$
\begin{aligned}
Var(N_2) &= E[Z_3^2(1)] = \sum_{j=0}^{N_f-1}\Big[\int_{jT_f+2iT_s}^{jT_f+2iT_s+T_i}\int_{jT_f+2iT_s}^{jT_f+2iT_s+T_i}\Big(\sum_{l_1}\alpha_{l_1}b_{i-1}p(t-jT_f-2iT_s \\
& -\tau_{l_1})\Big)\Big(\sum_{m_1}\alpha_{m_1}b_{i-1}p(\tau-jT_f-2iT_s-\tau_{m_1})\Big)\,\mathbb{E}[\{n_{SD}(t)n_{SD}(\tau)\}]dtd\tau\Big] \\
&= \sum_{j=0}^{N_f-1} b_{i-1}^2\Big[\int_{jT_f+2iT_s}^{jT_f+2iT_s+T_i}\int_{jT_f+2iT_s}^{jT_f+2iT_s+T_i}\Big(\sum_{l_1}\alpha_{l_1}p(t-jT_f-2iT_s-\tau_{l_1})\Big)\Big(\sum_{m_1} \\
& \alpha_{m_1}p(\tau-jT_f-2iT_s-\tau_{m_1})\Big)\theta_1(t-\tau)dtd\tau\Big] \\
&= \frac{N_f N_0 b_{i-1}^2}{2}\Big[\int_{jT_f+2iT_s}^{jT_f+2iT_s+T_i}\sum_{l_1=m_1}\alpha_{l_1}^2 p^2(t-jT_f-2iT_s-\tau_{l_1})dt \\
& \underbrace{+\sum_{l_1\neq m_1}\sum\alpha_{l_1}\alpha_{m_1}R(\tau_{l_1}-\tau_{m_1})}_{value=0}\Big] \\
&= \frac{N_f N_0 b_{i-1}^2 E_p}{2}\underbrace{\Big(\sum_{l_1}\alpha_{l_1}^2\Big)}_{value=\gamma_1} \\
&= \frac{N_f N_0 b_{i-1}^2 E_p \gamma_1}{2} \qquad (4.52)
\end{aligned}
$$

$$
\begin{aligned}
Var(N_3) &= E[Z_4^2(1)] = \sum_{j=0}^{N_f-1} \Bigg[\int_{jT_f+2iT_s}^{jT_f+2iT_s+T_i} \int_{jT_f+2iT_s}^{jT_f+2iT_s+T_i} \\
&\quad \mathbb{E}\left[\{n_{SD}(t) n_{SD}(\tau - T_s)\}^2 \right] dt d\tau \Bigg] \\
&= \sum_{j=0}^{N_f-1} \left[\int_{jT_f+2iT_s}^{jT_f+2iT_s+T_i} \int_{jT_f+2iT_s}^{jT_f+2iT_s+T_i} \theta_1^2(t-\tau) dt d\tau \right] \\
&= \sum_{j=0}^{N_f-1} \left[\int_{jT_f+2iT_s}^{jT_f+2iT_s+T_i} \int_{jT_f+2iT_s+T_i-t}^{jT_f+2iT_s+T_i} \theta_1^2(u) dt du \right] \\
&= \sum_{j=0}^{N_f-1} \left[\int_0^{T_i} \frac{N_0^2}{4} 2W dt \right] \\
&= \frac{N_f N_0^2 W T_i}{2}. \qquad (4.53)
\end{aligned}
$$

where, $E[n_k^2(t)] = \frac{N_0}{2}$. Hence, the value of $E[\{n_k^2(t)\}^2] = \frac{N_0^2}{4}$.

The decision statistic Z_{DTR-SD} obtained at the destination node in 1st time slot contains signal term and the noise term. It is noted from the above derivations that the signal term sig_{SD} has a value of $N_f b_i b_{i-1} E_p \gamma_1$, while the noise term $Z_{noise-SD}$ has a variance of $\sigma^2_{Z_{noise-SD}} = \frac{N_f N_0 b_i^2 E_p \gamma_1}{2} + \frac{N_f N_0 b_{i-1}^2 E_p \gamma_1}{2} + \frac{N_f N_0^2 W T_i}{2}$. Therefore, the SNR obtained at the destination node from S$-$D link in the 1st time slot is represented as:

$$
\begin{aligned}
\rho_{DTR-SD} &= \frac{sig_{SD}^2}{\sigma^2_{Z_{noise-SD}}} \\
&= \frac{(N_f b_i b_{i-1} E_p \gamma_1)^2}{\frac{N_f N_0 b_i^2 E_p \gamma_1}{2} + \frac{N_f N_0 b_{i-1}^2 E_p \gamma_1}{2} + \frac{N_f N_0^2 W T_i}{2}} \\
&= \frac{(N_f E_p \gamma_1)^2}{N_f N_0 E_p \gamma_1 + \frac{N_f N_0^2 W T_i}{2}} \\
&= \frac{(E_b \gamma_1)^2}{N_0 E_b \gamma_1 + \frac{N_f N_0^2 W T_i}{2}} \qquad (4.54)
\end{aligned}
$$

where, $b_i^2 = b_{i-1}^2 = 1$ and energy per bit for a DTR-PAM system is $E_b = N_f E_p$.

UWB DTR signal transmitted from the source node to the relay node, in 1st time slot is represented by equation 4.4. At relay node, the signal received in 1st time slot, denoted by equation 4.9, is now amplified by an amplifying factor $\sqrt{\beta_{AF}}$, and then forwarded to the destination node in 2nd time slot. This amplified UWB DTR signal transmitted from the relay node to the destination node is represented as:

$$
s_{DTR-RD}(t) = r_{DTR-SR}(t) \sqrt{\beta_{AF}} \qquad (4.55)
$$

The amplifying gain is defined as $\sqrt{\beta_{AF}} = \sqrt{\left(\frac{E_{SR}}{\mathbb{E}\left\{|h_2^2(t)|\right\}E_{SR}+N_0}\right)}$ where, E_{SR}, $h_2(t)$ and $\sigma^2_{Z_{noise-SR}}$ represent the signal energy, channel response and noise variance of S$-$R link respectively. Also, $\mathbb{E}$ denotes the expectation operator. The received signal obtained at the destination node from R$-$D link in 2nd time slot, is represented as:

$$\begin{aligned} r_{DTR-RD}(t) &= \sum_{i=0}^{\infty}\sum_{j=0}^{N_f-1}\left[\left(\sqrt{\beta_{AF}}b_i g_{SR}(t-jT_f-2iT_s)\right)+n_{SR}(t)\right]*\sum_{l_3}\alpha_{l_3}\delta(t-\tau_{l_3})+ \\ &\quad n_{RD}(t) \\ &= \sum_{i=0}^{\infty}\sum_{j=0}^{N_f-1}\left[\sqrt{\beta_{AF}}\left(\sum_{l_2}\alpha_{l_2}b_i p(t-jT_f-2iT_s-\tau_{l_2})+n_{SR}(t)\right)\right] \\ &\quad *\sum_{l_3}\alpha_{l_3}\delta(t-\tau_{l_3})+n_{RD}(t) \\ &= \sum_{i=0}^{\infty}\sum_{j=0}^{N_f-1}\left[\sqrt{\beta_{AF}}\sum_{l_2}\alpha_{l_2}\sum_{l_3}\alpha_{l_3}b_i p(t-jT_f-(2i+1)T_s-\tau_{l_2}-\tau_{l_3})+\right. \\ &\quad \left.\sqrt{\beta_{AF}}n'_{RD}(t)\right]+n_{RD}(t) \end{aligned} \tag{4.56}$$

where, $n'_{RD}(t) = n_{SR}(t) * h_3(t) = \sum_{l_3}\alpha_{l_3}n_{SR}(t-\tau_{l,3})$ denote the aggregate noise response after convolving the noise response of S$-$R link with channel response of R$-$D link $h_3(t)$ and $n_{RD}(t)$ represents the noise response of R$-$D link.

The received signal $r_{DTR-RD}(t)$ obtained at the destination node in the 2nd time slot is passed through a DTR receiver, whose decision statistics Z_{DTR-RD} is expressed as:

$$\begin{aligned} Z_{DTR-RD} &= \sum_{j=0}^{N_f-1}\int_{jT_f+(2i+1)T_s}^{jT_f+(2i+1)T_s+T_i} r_{DTR-RD}(t)r_{DTR-RD}(t-T_s)dt \\ &= \underbrace{Z_1(3)}_{signal}+\underbrace{Z_2(3)+Z_3(3)+Z_4(3)+Z_5(3)+Z_6(3)+Z_7(3)+Z_8(3)+Z_9(3)}_{\mathrm{noise term}} \end{aligned} \tag{4.57}$$

The value of Z_{DTR-RD} is obtained in equation 4.59, by replacing the value of equation 4.57 in equation 4.58.

$$\begin{aligned} &= \sum_{j=0}^{N_f-1}\int_{jT_f+(2i+1)T_s}^{jT_f+(2i+1)T_s+T_i}\left[\left(\sum_{l_2}\alpha_{l_2}\sum_{l_3}\alpha_{l_3}\sqrt{\beta_{AF}}b_i p(t-jT_f-(2i+1)T_s-\tau_{l_2}-\tau_{l_3})+\right.\right. \\ &\quad \sqrt{\beta_{AF}}n'_{RD}(t)+n_{RD}(t)\Big)\Big(\sum_{m_2}\alpha_{m_2}\sum_{m_3}\alpha_{m_3}\sqrt{\beta_{AF}}b_{i-1}p(t-jT_f-(2i+1)T_s-\tau_{m_2} \\ &\quad \left.\left.-\tau_{m_3})+\sqrt{\beta_{AF}}n'_{RD}(t-T_s)+n_{RD}(t-T_s)\right)dt\right] \end{aligned} \tag{4.58}$$

The signal term $Z_1(3)$ obtained from R−D link is expressed as:

$$\begin{aligned}
Z_1(3) &= \sum_{j=0}^{N_f-1} \beta_{AF} \Bigg[\int_{jT_f+(2i+1)T_s}^{jT_f+(2i+1)T_s+T_i} \Bigg(\sum_{l_2} \alpha_{l_2} \sum_{l_3} \alpha_{l_3} b_i p(t - jT_f - (2i+1)T_s - \tau_{l_2} \\
&\quad -\tau_{l_3}) \Bigg) \Bigg(\sum_{m_2} \alpha_{m_2} \sum_{m_3} \alpha_{m_3} b_{i-1} p(t - jT_f - (2i+1)T_s - \tau_{m_2} - \tau_{m_3}) \Bigg) dt \Bigg] \\
&= \beta_{AF} N_f b_i b_{i-1} \Bigg[\int_{jT_f+(2i+1)T_s}^{jT_f+(2i+1)T_s+T_i} \overbrace{\underbrace{\sum_{l_2} \alpha_{l_2}^2}_{l_2=m_2} \underbrace{\sum_{l_3} \alpha_{l_3}^2}_{l_3=m_3}}^{\text{Value}=\gamma_2\gamma_3} p^2(t - jT_f - (2i+1)T_s - \tau_{l_2} \\
&\quad -\tau_{l_3}) dt + \overbrace{\underbrace{\sum_{l_2} \sum_{m_2} \alpha_{l_2}\alpha_{m_2} R(\tau_{l_2} - \tau_{m_2})}_{l_2 \neq m_2} \underbrace{\sum_{l_3} \sum_{m_3} \alpha_{l_3}\alpha_{m_3} R(\tau_{l_3} - \tau_{m_3})}_{l_3 \neq m_3}}^{\text{Value}=0} \Bigg] \\
&= \beta_{AF} N_f b_i b_{i-1} E_p \Bigg(\overbrace{\underbrace{\sum_{l_2} \alpha_{l_2}^2}_{l_2=m_2} \underbrace{\sum_{l_3} \alpha_{l_3}^2}_{l_3=m_3}}^{\text{Value}=\gamma_2\gamma_3} \Bigg) \\
&= \beta_{AF} N_f b_i b_{i-1} E_p \gamma_2 \gamma_3 \qquad (4.59)
\end{aligned}$$

where, the pulse energy obtained from R−D link is represented as $E_p = \int_{jT_f+(2i+1)T_s}^{jT_f+(2i+1)T_s+T_i} p^2(t - jT_f - (2i+1)T_s - \tau_{l_2} - \tau_{l_3})dt$ and autocorrelation function as $R(\tau) = \int_{\infty}^{\infty} p(t)p(t-\tau)dt$. If this condition $min\{(\tau_{l_2} - \tau_{m_2})\} > T_p$ for $l_2 \neq m_2$ or $min\{(\tau_{l_3} - \tau_{m_3})\} > T_p$ for $l_3 \neq m_3$ is satisfied, then IPI becomes negligent. Hence, $\sum_{l_2 \neq m_2} \sum \alpha_{l_2}\alpha_{m_2} R(\tau_{l_2} - \tau_{m_2}) \sum_{l_3 \neq m_3} \sum \alpha_{l_3}\alpha_{m_3} R(\tau_{l_3} - \tau_{m_3}) = 0$. As explained in Section 4.3.1, since a large number of UWB multipath channel gains are considered, the channel gains can be approximated as Gaussian Distributed using the Central Limit Theorem $\sum_{l_2} \alpha_{l_2}^2 = \gamma_2$ and $\sum_{l_3} \alpha_{l_3}^2 = \gamma_3$. It is already described in Section 4.3.1 that, if the PSD $\theta_k(f)$ of noise is sufficiently flat, the autocorrelation function of noise can be approximated as $\theta_k(\tau) = \frac{N_0}{2}\delta(\tau)$[175]. To solve the decision variables $Z_2(3)$, $Z_3(3)$, $Z_4(3)$, $Z_5(3)$, $Z_6(3)$, $Z_7(3)$, $Z_8(3)$ and $Z_9(3)$ containing noise terms, we evaluate its variance, which is solved below.

$$\begin{aligned}
Var(N_1) &= E[Z_2^2(3)] = \beta_{AF}^2 \sum_{j=0}^{N_f-1} \Bigg[\int_{jT_f+(2i+1)T_s}^{jT_f+(2i+1)T_s+T_i} \int_{jT_f+(2i+1)T_s}^{jT_f+(2i+1)T_s+T_i} \Bigg(\sum_{l_2} \alpha_{l_2} \sum_{l_3} \alpha_{l_3} b_i \\
&\quad p(t - jT_f - (2i+1)T_s - \tau_{l_2} - \tau_{l_3}) \Bigg) \Bigg(\sum_{m_2} \alpha_{m_2} \sum_{m_3} \alpha_{m_3} b_i p(\tau - jT_f - \\
&\quad (2i+1)T_s - \tau_{m_2} - \tau_{m_3}) \Bigg) \mathbb{E}[n'_{RD}(t - T_d) n'_{RD}(\tau - T_d)] dt d\tau \Bigg]
\end{aligned}$$

$$
\begin{aligned}
&= \beta_{AF}^2 N_f b_i^2 \Bigg[\int_{jT_f+(2i+1)T_s}^{jT_f+(2i+1)T_s+T_i} \int_{jT_f+(2i+1)T_s}^{jT_f+(2i+1)T_s+T_i} \Bigg(\sum_{l_2} \alpha_{l_2} \sum_{l_3} \alpha_{l_3} p(t - jT_f - \\
&\quad (2i+1)T_s - \tau_{l_2} - \tau_{l_3}) \sum_{m_2} \alpha_{m_2} \sum_{m_3} \alpha_{m_3} p(\tau - jT_f - (2i+1)T_s - \tau_{m_2} - \tau_{m_3}) \\
&\quad \Bigg) \theta_3^{'}(t-\tau) dt d\tau \\
&= \beta_{AF}^2 N_f b_i^2 \left(\frac{\gamma_3 N_0}{2} \right) \Bigg[\int_{jT_f+(2i+1)T_s}^{jT_f+(2i+1)T_s+T_i} \overbrace{\underbrace{\sum_{l_2}}_{l_2=m_2} \alpha_{l_2}^2 \underbrace{\sum_{l_3}}_{l_3=m_3} \alpha_{l_3}^2}^{Value=\gamma_2\gamma_3} p^2(t - jT_f - (2i+1)T_s \\
&\quad - \tau_{l_2} - \tau_{l_3}) dt + \overbrace{\underbrace{\sum_{l_2} \sum_{m_2} \alpha_{l_2}\alpha_{m_2}}_{l_2 \neq m_2} R(\tau_{l_2} - \tau_{m_2}) \underbrace{\sum_{l_3} \sum_{m_3} \alpha_{l_3}\alpha_{m_3}}_{l_3 \neq m_3} R(\tau_{l_3} - \tau_{m_3})}^{Value=0} \Bigg] \\
&= \beta_{AF}^2 N_f \left(\frac{\gamma_3 N_0}{2} \right) b_i^2 E_p \Bigg(\underbrace{\overbrace{\sum_{l_2} \alpha_{l_2}^2 \sum_{l_3} \alpha_{l_3}^2}^{Value=\gamma_2\gamma_3}}_{l_2=m_2 \quad l_3=m_3} \Bigg) \\
&= \frac{\beta_{AF}^2 N_f N_0 b_i^2 E_p \gamma_2 \gamma_3^2}{2}
\end{aligned} \tag{4.60}
$$

where, the value of $\theta_3^{'}(t-\tau)$ is obtained from Appendix B. Hence, $\int_{jT_f+(2i+1)T_s}^{jT_f+(2i+1)T_s+T_i} \theta_3^{'}(t-\tau)d\tau = \frac{\gamma_3 N_0}{2}$.

$$
\begin{aligned}
Var(N_2) &= E[Z_3^2(3)] = \beta_{AF}^2 \sum_{j=0}^{N_f-1} \Bigg[\int_{jT_f+(2i+1)T_s}^{jT_f+(2i+1)T_s+T_i} \int_{jT_f+(2i+1)T_s}^{jT_f+(2i+1)T_s+T_i} \Bigg(\sum_{l_2} \alpha_{l_2} \sum_{l_3} \\
&\quad \alpha_{l_3} b_{i-1} p(t - jT_f - (2i+1)T_s - \tau_{l_2} - \tau_{l_3}) \Bigg) \Bigg(\sum_{m_2} \alpha_{m_2} \sum_{m_3} \alpha_{m_3} b_{i-1} p(\tau - jT_f - \\
&\quad (2i+1)T_s - \tau_{m_2} - \tau_{m_3}) \Bigg) \mathbb{E}[n_{RD}^{'}(t) n_{RD}^{'}(\tau)] dt d\tau \Bigg] \\
&= \beta_{AF}^2 N_f b_{i-1}^2 \Bigg[\int_{jT_f+(2i+1)T_s}^{jT_f+(2i+1)T_s+T_i} \int_{jT_f+(2i+1)T_s}^{jT_f+(2i+1)T_s+T_i} \Bigg(\sum_{l_2} \alpha_{l_2} \sum_{l_3} \alpha_{l_3} p(t - jT_f - \\
&\quad (2i+1)T_s - \tau_{l_2} - \tau_{l_3}) \sum_{m_2} \alpha_{m_2} \sum_{m_3} \alpha_{m_3} p(\tau - jT_f - (2i+1)T_s - \tau_{m_2} - \tau_{m_3}) \\
&\quad \Bigg) \theta_3^{'}(t-\tau) dt d\tau \Bigg] \\
&= \beta_{AF}^2 N_f b_{i-1}^2 \left(\frac{\gamma_3 N_0}{2} \right) \Bigg[\int_{jT_f+(2i+1)T_s}^{jT_f+(2i+1)T_s+T_i} \overbrace{\underbrace{\sum_{l_2}}_{l_2=m_2} \alpha_{l_2}^2 \underbrace{\sum_{l_3}}_{l_3=m_3} \alpha_{l_3}^2}^{Value=\gamma_2\gamma_3} p^2(t - jT_f - (2i+1)T_s
\end{aligned}
$$

$$-\tau_{l_2}-\tau_{l_3})dt+\overbrace{\underbrace{\sum_{l_2}\sum_{m_2}\alpha_{l_2}\alpha_{m_2}}_{\mathrm{l}_2\neq m_2}R(\tau_{l_2}-\tau_{m_2})\underbrace{\sum_{l_3}\sum_{m_3}\alpha_{l_3}\alpha_{m_3}}_{\mathrm{l}_3\neq m_3}R(\tau_{l_3}-\tau_{m_3})}^{\mathrm{V}alue=0}\Bigg]$$

$$= \beta_{AF}^2 N_f\left(\frac{\gamma_3 N_0}{2}\right)b_{i-1}^2E_p\Bigg(\overbrace{\underbrace{\sum_{l_2}\alpha_{l_2}^2}_{\mathrm{l}_2=m_2}\underbrace{\sum_{l_3}\alpha_{l_3}^2}_{\mathrm{l}_3=m_3}}^{\mathrm{V}alue=\gamma_2\gamma_3}\Bigg)$$

$$= \frac{\beta_{AF}^2 N_f N_0 b_{i-1}^2 E_p\gamma_2\gamma_3^2}{2} \tag{4.61}$$

$$\begin{aligned}
Var(N_3) &= E[Z_4^2(3)]=\beta_{AF}\sum_{j=0}^{N_f-1}\Bigg[\int_{jT_f+(2i+1)T_s}^{jT_f+(2i+1)T_s+T_i}\int_{jT_f+(2i+1)T_s}^{jT_f+(2i+1)T_s+T_i}\Bigg(\sum_{l_2}\alpha_{l_2}\sum_{l_3}\\
&\alpha_{l_3}b_i p(t-jT_f-(2i+1)T_s-\tau_{l_2}-\tau_{l_3})\Bigg)\Bigg(\sum_{m_2}\alpha_{m_2}\sum_{m_3}\alpha_{m_3}p(\tau-jT_f-\\
&(2i+1)T_s-\tau_{m_2}-\tau_{m_3})\Bigg)\mathbb{E}[n_{RD}(t-T_d)n_{RD}(\tau-T_d)]dtd\tau\Bigg]\\
&= \beta_{AF}N_f b_i^2\Bigg[\int_{jT_f+(2i+1)T_s}^{jT_f+(2i+1)T_s+T_i}\int_{jT_f+(2i+1)T_s}^{jT_f+(2i+1)T_s+T_i}\Bigg(\sum_{l_2}\alpha_{l_2}\sum_{l_3}\alpha_{l_3}p(t-jT_f\\
&-(2i+1)T_s-\tau_{l_2}-\tau_{l_3})\Bigg)\Bigg(\sum_{m_2}\alpha_{m_2}\sum_{m_3}\alpha_{m_3}p(\tau-jT_f-(2i+1)T_s-\tau_{m_2}\\
&-\tau_{m_3})\Bigg)\theta_3(t-\tau)dtd\tau\Bigg]\\
&= \frac{\beta_{AF}N_f b_i^2 N_0}{2}\Bigg[\int_{jT_f+(2i+1)T_s}^{jT_f+(2i+1)T_s+T_i}\overbrace{\underbrace{\sum_{l_2}\alpha_{l_2}^2}_{\mathrm{l}_2=m_2}\underbrace{\sum_{l_3}\alpha_{l_3}^2}_{\mathrm{l}_3=m_3}}^{\mathrm{V}alue=\gamma_2\gamma_3}p^2(t-jT_f-(2i+1)T_s\\
&-\tau_{l_2}-\tau_{l_3})dt+\overbrace{\underbrace{\sum_{l_2}\sum_{m_2}\alpha_{l_2}\alpha_{m_2}}_{\mathrm{l}_2\neq m_2}R(\tau_{l_2}-\tau_{m_2})\underbrace{\sum_{l_3}\sum_{m_3}\alpha_{l_3}\alpha_{m_3}}_{\mathrm{l}_3\neq m_3}R(\tau_{l_3}-\tau_{m_3})}^{\mathrm{V}alue=0}\Bigg]\\
&= \frac{\beta_{AF}N_f N_0 b_i^2 E_p}{2}\Bigg(\overbrace{\underbrace{\sum_{l_2}\alpha_{l_2}^2}_{\mathrm{l}_2=m_2}\underbrace{\sum_{l_3}\alpha_{l_3}^2}_{\mathrm{l}_3=m_3}}^{\mathrm{V}alue=\gamma_2\gamma_3}\Bigg)\\
&= \frac{\beta_{AF}N_f N_0 b_i^2 E_p\gamma_2\gamma_3}{2}
\end{aligned} \tag{4.62}$$

where, $\int_{jT_f+(2i+1)T_s}^{jT_f+(2i+1)T_s+T_i}\theta_3(t-\tau)d\tau=\int_{jT_f+(2i+1)T_s}^{jT_f+(2i+1)T_s+T_i}\frac{N_0}{2}\delta(t-\tau)d\tau=\frac{N_0}{2}$.

$$Var(N_4) = E[Z_5^2(3)]=\beta_{AF}\sum_{j=0}^{N_f-1}\Bigg[\int_{jT_f+(2i+1)T_s}^{jT_f+(2i+1)T_s+T_i}\int_{jT_f+(2i+1)T_s}^{jT_f+(2i+1)T_s+T_i}\Bigg(\sum_{l_2}\alpha_{l_2}$$

$$
\begin{aligned}
& \sum_{l_3} \alpha_{l_3} b_{i-1} p(t - jT_f - (2i+1)T_s - \tau_{l_2} - \tau_{l_3}) \Big) \Big(\sum_{m_2} \alpha_{m_2} \sum_{m_3} \alpha_{m_3} b_{i-1} p(\tau - jT_f \\
& -(2i+1)T_s - \tau_{m_2} - \tau_{m_3}) \Big) \mathbb{E}[n_{RD}(t) n_{RD}(\tau)] dt d\tau \Big] \\
= \; & \beta_{AF} N_f b_{i-1}^2 \Big[\int_{jT_f+(2i+1)T_s}^{jT_f+(2i+1)T_s+T_i} \int_{jT_f+(2i+1)T_s}^{jT_f+(2i+1)T_s+T_i} \Big(\sum_{l_2} \alpha_{l_2} \sum_{l_3} \alpha_{l_3} p(t - \\
& jT_f - (2i+1)T_s - \tau_{l_2} - \tau_{l_3}) \Big) \Big(\sum_{m_2} \alpha_{m_2} \sum_{m_3} \alpha_{m_3} p(\tau - jT_f - (2i+1)T_s \\
& -\tau_{m_2} - \tau_{m_3}) \Big) \theta_3(t-\tau) dt d\tau \Big] \\
= \; & \frac{\beta_{AF} N_f N_0 b_{i-1}^2}{2} \Big[\int_{jT_f+(2i+1)T_s}^{jT_f+(2i+1)T_s+T_i} \overbrace{\underbrace{\sum_{l_2} \alpha_{l_2}^2}_{l_2=m_2} \underbrace{\sum_{l_3} \alpha_{l_3}^2}_{l_3=m_3}}^{Value=\gamma_2\gamma_3} p^2(t - jT_f - (2i+1)T_s \\
& -\tau_{l_2} - \tau_{l_3}) dt + \overbrace{\underbrace{\sum_{l_2} \sum_{m_2} \alpha_{l_2} \alpha_{m_2}}_{l_2 \neq m_2} R(\tau_{l_2} - \tau_{m_2}) \underbrace{\sum_{l_3} \sum_{m_3} \alpha_{l_3} \alpha_{m_3}}_{l_3 \neq m_3} R(\tau_{l_3} - \tau_{m_3})}^{Value=0} \Big] \\
= \; & \frac{\beta_{AF} N_f N_0 b_{i-1}^2 E_p}{2} \Big(\overbrace{\underbrace{\sum_{l_2} \alpha_{l_2}^2}_{l_2=m_2} \underbrace{\sum_{l_3} \alpha_{l_3}^2}_{l_3=m_3}}^{Value=\gamma_2\gamma_3} \Big) \\
= \; & \frac{\beta_{AF} N_f N_0 b_{i-1}^2 E_p \gamma_2 \gamma_3}{2}
\end{aligned}
\tag{4.63}
$$

$$
\begin{aligned}
Var(N_5) \; = \; & E[Z_6^2(3)] = \beta_{AF}^2 \sum_{j=0}^{N_f-1} \Big[\int_{jT_f+(2i+1)T_s}^{jT_f+(2i+1)T_s+T_i} \int_{jT_f+(2i+1)T_s}^{jT_f+(2i+1)T_s+T_i} \\
& \mathbb{E} \Big[\Big\{ n_{RD}^{'}(t) n_{RD}^{'}(\tau - T_d) \Big\}^2 \Big] dt d\tau \Big] \\
= \; & \beta_{AF}^2 N_f \int_{jT_f+(2i+1)T_s}^{jT_f+(2i+1)T_s+T_i} \int_{jT_f+(2i+1)T_s}^{jT_f+(2i+1)T_s+T_i} \theta_3^{'2}(t-\tau) dt d\tau \\
= \; & \beta_{AF}^2 N_f \int_0^{T_i} \left(\frac{\gamma_3 N_0}{2} \right)^2 2W dt \\
= \; & \frac{\beta_{AF}^2 N_f N_0^2 W T_i \gamma_3^2}{2}.
\end{aligned}
\tag{4.64}
$$

$$
\begin{aligned}
Var(N_6) \; = \; & E[Z_7^2(3)] = \sum_{j=0}^{N_f-1} \Big[\int_{jT_f+(2i+1)T_s}^{jT_f+(2i+1)T_s+T_i} \int_{jT_f+(2i+1)T_s}^{jT_f+(2i+1)T_s+T_i} \\
& \mathbb{E} \Big[\{ n_{RD}(t) n_{RD}(\tau - T_d) \}^2 \Big] dt d\tau \Big]
\end{aligned}
$$

$$\begin{aligned} &= N_f \int_{jT_f+(2i+1)T_s}^{jT_f+(2i+1)T_s+T_i} \int_{jT_f+(2i+1)T_s}^{jT_f+(2i+1)T_s+T_i} \theta_3^2(t-\tau)dtd\tau \\ &= N_f \int_0^{T_i} \frac{N_0^2 2Wdt}{4} \\ &= \frac{N_f N_0^2 W T_i}{2} \end{aligned} \tag{4.65}$$

$$\begin{aligned} Var(N_7) &= E[Z_8^2(3)] = \beta_{AF} \sum_{j=0}^{N_f-1} \Bigg[\int_{jT_f+(2i+1)T_s}^{jT_f+(2i+1)T_s+T_i} \int_{jT_f+(2i+1)T_s}^{jT_f+(2i+1)T_s+T_i} \\ &\quad \mathbb{E}\left[n_{RD}^{'}(t) n_{RD}^{'}(\tau) n_{RD}(t-T_d) n_{RD}(\tau-T_d) \right] dtd\tau \Bigg] \\ &= \beta_{AF} N_f \int_{jT_f+(2i+1)T_s}^{jT_f+(2i+1)T_s+T_i} \int_{jT_f+(2i+1)T_s}^{jT_f+(2i+1)T_s+T_i} \theta_3(t-\tau)\theta_3^{'}(t-\tau)dtd\tau \\ &= \beta_{AF} N_f \int_0^{T_i} \left(\frac{\gamma_3 N_0}{2}\right)\left(\frac{N_0}{2}\right) 2Wdt \\ &= \frac{\beta_{AF} N_f N_0^2 W T_i \gamma_3}{2}. \end{aligned} \tag{4.66}$$

$$\begin{aligned} Var(N_8) &= E[Z_9^2(3)] = \beta_{AF} \sum_{j=0}^{N_f-1} \Bigg[\int_{jT_f+(2i+1)T_s}^{jT_f+(2i+1)T_s+T_i} \int_{jT_f+(2i+1)T_s}^{jT_f+(2i+1)T_s+T_i} \\ &\quad \mathbb{E}\left[n_{RD}^{'}(t-T_d) n_{RD}^{'}(\tau-T_d) n_{RD}(t) n_{RD}(\tau) \right] dtd\tau \Bigg] \\ &= \beta_{AF} N_f \int_{jT_f+(2i+1)T_s}^{jT_f+(2i+1)T_s+T_i} \int_{jT_f+(2i+1)T_s}^{jT_f+(2i+1)T_s+T_i} \theta_3^{'}(t-\tau)\theta_3(t-\tau)dtd\tau \\ &= \beta_{AF} N_f \int_0^{T_i} \left(\frac{\gamma_3 N_0}{2}\right)\left(\frac{N_0}{2}\right) 2Wdt \\ &= \frac{\beta_{AF} N_f N_0^2 W T_i \gamma_3}{2}. \end{aligned} \tag{4.67}$$

The decision statistic Z_{DTR-RD} obtained at the destination node in 2nd time slot contains signal term sig_{RD} and the noise term $Z_{noise-RD}$. From the derivations, it is inferred that the signal term sig_{RD} has a value of $\beta_{AF} N_f b_i b_{i-1} E_p \gamma_2 \gamma_3$ while the noise term $Z_{noise-RD}$ has a variance of $\sigma^2_{Z_{noise-RD}} = \frac{\beta_{AF} N_f N_0 E_p \gamma_2 \gamma_3 (b_i^2 + b_{i-1}^2 + \beta_{AF} b_i^2 \gamma_3 + \beta_{AF} b_{i-1}^2 \gamma_3)}{2} + \frac{N_f N_0^2 W T_i}{2}(1 + \beta_{AF}^2 \gamma_3^2 + 2\beta_{AF}\gamma_3)$. The SNR at the destination node in 2nd time slot due to R$-$D link, is represented as:

$$\begin{aligned} \rho_{DTR-RD} &= \frac{sig_{RD}^2}{\sigma^2_{Z_{noise-RD}}} \\ &= \frac{(\beta_{AF} N_f E_p \gamma_2 \gamma_3)^2}{\frac{\beta_{AF} N_f N_0 E_p \gamma_2 \gamma_3 (b_i^2 + b_{i-1}^2 + \beta_{AF} b_i^2 \gamma_3 + \beta_{AF} b_{i-1}^2 \gamma_3)}{2} + \frac{N_f N_0^2 W T_i}{2}(1 + \beta_{AF}^2 \gamma_3^2 + 2\beta_{AF}\gamma_3)} \\ &= \frac{(\beta_{AF} E_b \gamma_2 \gamma_3)^2}{\frac{\beta_{AF} N_0 E_b \gamma_2 \gamma_3 (b_i^2 + b_{i-1}^2 + \beta_{AF} b_i^2 \gamma_3 + \beta_{AF} b_{i-1}^2 \gamma_3)}{2} + \frac{N_f N_0^2 W T_i}{2}(1 + \beta_{AF}^2 \gamma_3^2 + 2\beta_{AF}\gamma_3)} \end{aligned} \tag{4.68}$$

where, $b_i^2 = b_{i-1}^2 = (b_i b_{i-1})^2 = 1$ and $E_b = N_f E_p$ for DTR$-$PAM system. The decision statistics obtained at the destination node in the two time slots are combined using different combining strategies such as optimum linear combining, linear combining and selective combining, to form the final decision statistic. The derivations of the same are explained in the subsequent section.

A. Linear Combining

At the destination node, the decision statistics Z_{DTR-SD} and Z_{DTR-RD} obtained in 1st and 2nd time slots respectively, are linearly combined to form final decision statistic $Z_{total} = Z_{DTR-SD} + Z_{DTR-RD} = s_{total-signal} + Z_{noise-total}$. The individual decision statistics obtained from S$-$D and R$-$D links are as follows:

$$Z_{DTR-SD} = sig_{SD} + Z_{noise-SD} \tag{4.69}$$

$$Z_{DTR-RD} = sig_{RD} + Z_{noise-RD} \tag{4.70}$$

The final decision statistic Z_{total} is evaluated in equation 4.72.

$$\begin{aligned} Z_{total} &= Z_{DTR-SD} + Z_{DTR-RD} \\ &= \underbrace{sig_{SD} + sig_{RD}}_{s_{total-signal}} + \underbrace{Z_{noise-SD} + Z_{noise-RD}}_{Z_{noise-total}} \end{aligned} \tag{4.71}$$

The total noise variance $\sigma^2_{Z_{noise-total}} = \sigma^2_{Z_{noise-SD}} + \sigma^2_{Z_{noise-RD}}$ corresponding to the noise term $Z_{noise-total}$ is already solved in equation 4.33. Therefore, the SNR evaluated at the destination node due to linear combining is expressed as:

$$\rho_{DTR-AF-LC} = \left(\frac{s^2_{total-signal}}{\sigma^2_{Z_{noise-total}}}\right) = \frac{(sig_{SD} + sig_{RD})^2}{(\sigma^2_{Z_{noise-SD}} + \sigma^2_{Z_{noise-RD}})} = \left(\frac{(U_1)^2}{V_1 + W_1}\right) \tag{4.72}$$

where, $U_1 = E_b\gamma_1 + \beta_{AF} E_b \gamma_2 \gamma_3$, $V_1 = N_0 E_b \gamma_1 + \frac{N_f N_0^2 W T_i}{2}$ and
$W_1 = \beta_{AF} N_0 E_b \gamma_2 \gamma_3 (1 + \beta_{AF}\gamma_3) + \frac{N_f N_0^2 W T_i}{2}(1 + \beta_{AF}^2 \gamma_3^2 + 2\beta_{AF}\gamma_3)$.

In order to extract the information bit, the final decision statistic Z_{total} is compared to the decision threshold. The decision threshold is decided on the basis of PAM modulation scheme. The final decision criteria $\hat{z}$ for linear combining is represented as:

$$\hat{z} = \begin{cases} 0, & H_0 : Z = Z_{total} = Z_{DTR-SD} + Z_{DTR-RD} \leq 0 \\ 1, & H_1 : Z = Z_{total} = Z_{DTR-SD} + Z_{DTR-RD} > 0 \end{cases} \tag{4.73}$$

As explained in the Section 4.3.1, the individual channel gains for S−D, S−R and R−D channel links may be assumed to be IID Gaussian distributed by applying Central Limit Theorem, since a large number paths are involved. Therefore, the sum of these channel gains will also have a Gaussian distribution with its mean being the sum of individual means and variance being sum of the individual variances. The joint PDF $f_{\rho_{AF}}(\gamma_1, \gamma_2, \gamma_3)$ of the channel in case of linear combining is also gaussian and is represented as:

$$f_{\rho_{DTR-AF}}(\gamma_1, \gamma_2, \gamma_3) = \frac{1}{\sqrt{(2\pi(\sigma_{SD}^2))}} \frac{1}{\sqrt{(2\pi(\sigma_{SR}^2))}} \frac{1}{\sqrt{(2\pi(\sigma_{RD}^2))}} \exp\left[\frac{-(\gamma_1 - \mu_{SD})^2}{2\sigma_{SD}^2} + \frac{-(\gamma_2 - \mu_{SR})^2}{2\sigma_{SR}^2} + \frac{-(\gamma_3 - \mu_{RD})^2}{2\sigma_{RD}^2}\right] \tag{4.74}$$

where, μ_k and σ_k^2 represent the mean and variance of channel links while the index $k \in \{1, 2, 3\}$ refers to S−D, S−R and R−D link respectively, as mentioned in equation 4.5. Since the joint PDF of channel link is IID distributed, it is represented as $f_{\rho_{DTR-AF}}(\gamma_1, \gamma_2, \gamma_3) = f_{\rho_{DTR-AF}}(\gamma_1) f_{\rho_{DTR-AF}}(\gamma_2) f_{\rho_{DTR-AF}}(\gamma_3)$. Thus, the BER of UWB DTR system using linear combining is expressed as:

$$\begin{aligned} BER_{DTR-AF-LC} &= \int_0^\infty \int_0^\infty \int_0^\infty Q\left(\sqrt{\rho_{DTR-AF-LC}}\right) f_{\rho_{DTR-AF}}(\gamma_1, \gamma_2, \gamma_3) d\gamma_1 d\gamma_2 d\gamma_3 \\ &= \int_0^\infty \int_0^\infty \int_0^\infty Q\left(\sqrt{\rho_{DTR-AF-LC}}\right) \frac{1}{\sqrt{(2\pi(\sigma_{SD}^2))}} \frac{1}{\sqrt{(2\pi(\sigma_{SR}^2))}} \\ &\quad \frac{1}{\sqrt{(2\pi(\sigma_{RD}^2))}} \exp\left[\frac{-(\gamma_1 - \mu_{SD})^2}{2\sigma_{SD}^2} + \frac{-(\gamma_2 - \mu_{SR})^2}{2\sigma_{SR}^2} + \frac{-(\gamma_3 - \mu_{RD})^2}{2\sigma_{RD}^2}\right] \\ &\quad d\gamma_1 d\gamma_2 d\gamma_3 \end{aligned} \tag{4.75}$$

$$\begin{aligned} &= \int_0^\infty \int_0^\infty \int_0^\infty Q\left(\sqrt{\frac{(U_1)^2}{V_1 + W_1}}\right) \frac{1}{\sqrt{(2\pi(\sigma_{SD}^2))}} \frac{1}{\sqrt{(2\pi(\sigma_{SR}^2))}} \frac{1}{\sqrt{(2\pi(\sigma_{RD}^2))}} \\ &\quad \exp\left[\frac{-(\gamma_1 - \mu_{SD})^2}{2\sigma_{SD}^2} + \frac{-(\gamma_2 - \mu_{SR})^2}{2\sigma_{SR}^2} + \frac{-(\gamma_3 - \mu_{RD})^2}{2\sigma_{RD}^2}\right] d\gamma_1 d\gamma_2 d\gamma_3 \end{aligned} \tag{4.76}$$

B. Selective Combining

In selective combining, the SNR obtained from S−D and R−D links respectively, are compared and the one with the highest SNR is chosen. The SNR at destination node due to selective combining is expressed as $\rho_{DTR-AF-SC} = Max\{\rho_{DTR-SD}, \rho_{DTR-RD}\}$. ρ_{DTR-SD} and ρ_{DTR-RD} refers to the SNR mentioned in equation 4.55 and 4.69 respectively. Therefore, the BER of UWB DTR system using cooperative dual−hop AF strategy with selective combining is represented as:

$$BER_{DTR-AF-SC} = \int_0^\infty \int_0^\infty \int_0^\infty Q\left(\sqrt{\rho_{DTR-AF-SC}}\right) f_{\rho_{DTR-AF}}(\gamma_1, \gamma_2, \gamma_3) d\gamma_1 d\gamma_2 d\gamma_3$$

$$= \int_0^\infty \int_0^\infty \int_0^\infty Q\left(\sqrt{\rho_{TR-SC-AF}}\right) \frac{1}{\sqrt{(2\pi(\sigma_{SD}^2))}} \frac{1}{\sqrt{(2\pi(\sigma_{SR}^2))}} \frac{1}{\sqrt{(2\pi(\sigma_{RD}^2))}} \exp\left[\frac{-(\gamma_1-\mu_{SD})^2}{2\sigma_{SD}^2} + \frac{-(\gamma_2-\mu_{SR})^2}{2\sigma_{SR}^2} + \frac{-(\gamma_3-\mu_{RD})^2}{2\sigma_{RD}^2}\right] d\gamma_1 d\gamma_2 d\gamma_3 \quad (4.77)$$

Since the joint PDF of channel link is IID distributed, it can be denoted as $f_{\rho_{DTR-AF}}(\gamma_1,\gamma_2,\gamma_3) = f_{\rho_{DTR-AF}}(\gamma_1) f_{\rho_{DTR-AF}}(\gamma_2) f_{\rho_{DTR-AF}}(\gamma_3)$.

$$= \int_0^\infty \int_0^\infty \int_0^\infty Q\left(\sqrt{Max\left\{\rho_{DTR-SD}, \rho_{DTR-RD}\right\}}\right) \frac{1}{\sqrt{(2\pi(\sigma_{SD}^2))}} \frac{1}{\sqrt{(2\pi(\sigma_{SR}^2))}} \frac{1}{\sqrt{(2\pi(\sigma_{RD}^2))}} \exp\left[\frac{-(\gamma_1-\mu_{SD})^2}{2\sigma_{SD}^2} + \frac{-(\gamma_2-\mu_{SR})^2}{2\sigma_{SR}^2} + \frac{-(\gamma_3-\mu_{RD})^2}{2\sigma_{RD}^2}\right] d\gamma_1 d\gamma_2 d\gamma_3 \quad (4.78)$$

C. Optimum Linear Combining

The decision statistics at the destination node from S−D and R−D links in 1st and 2nd time slots respectively, are optimally combined to form the final decision statistic $Z_{total} = Z_{DTR-SD} + \kappa Z_{DTR-RD}$. The optimal combining factor $\kappa = \frac{(\sigma^2_{Z_{noise-SD}})sig_{RD}}{(\sigma^2_{Z_{noise-RD}})sig_{SD}}$ is solved in equation C.4 of Appendix C. The final decision statistic Z_{total} obtained at the destination node using optimum linear combining scheme, is denoted by equation 4.81.

$$\begin{aligned} Z_{total} &= Z_{DTR-SD} + \kappa Z_{DTR-RD} \\ &= \underbrace{sig_{SD} + \kappa sig_{RD}}_{s_{total-signal}} + \underbrace{Z_{noise-SD} + \kappa(Z_{noise-RD})}_{Z_{noise-total}} \end{aligned} \quad (4.79)$$

The total noise variance $\sigma^2_{Z_{noise-total}} = \sigma^2_{Z_{noise-SD}} + \kappa^2\sigma^2_{Z_{noise-RD}}$ is solved in equation 4.43. The SNR at the destination node due to optimum linear combining is duly expressed as:

$$\begin{aligned} \rho_{DTR-AF-LOC} &= \left(\frac{s^2_{total-signal}}{\sigma^2_{Z_{noise-total}}}\right) = \frac{(sig_{SD} + \kappa sig_{RD})^2}{(\sigma^2_{Z_{noise-SD}} + \kappa^2\sigma^2_{Z_{noise-RD}})} \\ &= \left(\frac{(U_1)^2}{V_1 + \kappa^2 W_1}\right) \end{aligned} \quad (4.80)$$

where, $U_1 = E_b\gamma_1 + \kappa\beta_{AF}E_b\gamma_2\gamma_3$, $V_1 = N_0E_b\gamma_1 + \frac{N_f N_0^2 WT_i}{2}$ and $W_1 = \beta_{AF}N_0E_b\gamma_2\gamma_3(1+\beta_{AF}\gamma_3) + \frac{N_f N_0^2 WT_i}{2}(1+\beta_{AF}^2\gamma_3^2 + 2\beta_{AF}\gamma_3)$.

In order to extract the transmitted bit, the final decision statistic Z_{total} is compared to the decision threshold. The decision threshold is determined from PAM modulation scheme. The

decision criteria $\hat{z}$ for optimum linear combining is represented as:

$$\hat{z} = \begin{Bmatrix} 0, & H_0 : Z = Z_{total} = Z_{DTR-SD} + \kappa Z_{DTR-RD} \leq 0 \\ 1, & H_1 : Z = Z_{total} = Z_{DTR-SD} + \kappa Z_{DTR-RD} > 0 \end{Bmatrix} \tag{4.81}$$

The joint PDF of channel links for optimum linear combining is expressed as:

$$\begin{aligned} f_{\rho_{DTR-AF}}(\gamma_1, \gamma_2, \gamma_3) &= \frac{1}{\sqrt{(2\pi(\sigma_{SD}^2))}} \frac{1}{\sqrt{(2\pi(\kappa^2\sigma_{SR}^2))}} \frac{1}{\sqrt{(2\pi(\kappa^2\sigma_{RD}^2))}} \exp\left[\frac{-(\gamma_1 - \mu_{SD})^2}{2\sigma_{SD}^2}\right. \\ &\left. + \frac{-(\gamma_2 - \mu_{SR})^2}{2\kappa^2\sigma_{SR}^2} + \frac{-(\gamma_3 - \mu_{RD})^2}{2\kappa^2\sigma_{RD}^2}\right] \end{aligned} \tag{4.82}$$

Since the joint PDF of channel link is IID distributed, it is represented as $f_{\rho_{DTR-AF}}(\gamma_1, \gamma_2, \gamma_3) = f_{\rho_{DTR-AF}}(\gamma_1) f_{\rho_{DTR-AF}}(\gamma_2) f_{\rho_{DTR-AF}}(\gamma_3)$.

Subsequently, the BER of UWB DTR system using dual−hop cooperative AF strategy with optimum linear combining is denoted as:

$$\begin{aligned} BER_{DTR-AF-LOC} &= \int_0^\infty \int_0^\infty \int_0^\infty Q\left(\sqrt{\rho_{DTR-AF-LOC}}\right) f_{\rho_{DTR-AF}}(\gamma_1, \gamma_2, \gamma_3) d\gamma_1 d\gamma_2 d\gamma_3 \\ &= \int_0^\infty \int_0^\infty \int_0^\infty Q\left(\sqrt{\rho_{DTR-AF-LOC}} \frac{1}{\sqrt{(2\pi(\sigma_{SD}^2))}} \frac{1}{\sqrt{(2\pi(\kappa^2\sigma_{SR}^2))}}\right. \\ &\quad \frac{1}{\sqrt{(2\pi(\kappa^2\sigma_{RD}^2))}} \exp\left[\frac{-(\gamma_1 - \mu_{SD})^2}{2\sigma_{SD}^2} + \frac{-(\gamma_2 - \mu_{SR})^2}{2\kappa^2\sigma_{SR}^2} + \right. \\ &\quad \left.\left.\frac{-(\gamma_3 - \mu_{RD})^2}{2\kappa^2\sigma_{RD}^2}\right] d\gamma_1 d\gamma_2 d\gamma_3 \end{aligned} \tag{4.83}$$

$$\begin{aligned} &= \int_0^\infty \int_0^\infty \int_0^\infty Q\left(\sqrt{\frac{U_1^2}{V_1 + \kappa^2 W_1}}\right) \frac{1}{\sqrt{(2\pi(\sigma_{SD}^2))}} \frac{1}{\sqrt{(2\pi(\kappa^2\sigma_{SR}^2))}} \frac{1}{\sqrt{(2\pi(\kappa^2\sigma_{RD}^2))}} \\ &\quad \exp\left[\frac{-(\gamma_1 - \mu_{SD})^2}{2\sigma_{SD}^2} + \frac{-(\gamma_2 - \mu_{SR})^2}{2\kappa^2\sigma_{SR}^2} + \frac{-(\gamma_3 - \mu_{RD})^2}{2\kappa^2\sigma_{RD}^2}\right] d\gamma_1 d\gamma_2 d\gamma_3 \end{aligned} \tag{4.84}$$

4.4 Performance Analysis of a Cooperative DTF AC System

The theoretical BER performance of UWB AC system using cooperative DTF strategy with diversity combining is explained vividly in this section.

4.4.1 TR System

The BER performance analysis of UWB TR system using cooperative DTF strategy is derived analytically in this section. The received signal obtained at the destination node and relay node

in 1st time slot, is represented by equation 4.6 and 4.7, respectively. The received signal at the relay node $r_{TR-SR}(t)$ is passed through a TR receiver, whose decision statistics Z_{SR} is as follows:

$$\begin{aligned} Z_{TR-SR} &= \sum_{j=0}^{N_f-1} \int_{jT_f+2iT_s+T_d}^{jT_f+2iT_s+T_d+T_i} r_{TR-SR}(t) r_{TR-SR}(t-T_d)dt \\ &= \underbrace{Z_1(k)}_{signal} + \underbrace{Z_2(k)+Z_3(k)+Z_4(k)}_{noise-term} = \underbrace{Z_1(2)}_{signal} + \underbrace{Z_2(2)+Z_3(2)+Z_4(2)}_{noise-term} \end{aligned} \quad (4.85)$$

where, the index $k \in \{1,2,3\}$ refers to the S$-$D, S$-$R and R$-$D link respectively, as mentioned in equation 4.5. Here, $T_i = T_{mds}+T_p$ represents the integration time interval, T_{mds} the multipath delay spread and T_p the pulse duration. The signal term obtained from S$-$R link is expressed as:

$$\begin{aligned} Z_1(2) &= \sum_{j=0}^{N_f-1} \Bigg[\int_{jT_f+2iT_s+T_d}^{jT_f+2iT_s+T_d+T_i} \Bigg(\sum_{l_2} \alpha_{l_2} p(t-jT_f-2iT_s-\tau_{l_2}) \sum_{m_2} \alpha_{m_2} b_i p(t-jT_f- \\ &\quad 2iT_s-T_d-\tau_{m_2}) \Bigg) dt \Bigg] \\ &= N_f b_i \Bigg[\int_{jT_f+2iT_s+T_d}^{jT_f+2iT_s+T_d+T_i} \sum_{l_2=m_2} \alpha_{l_2}^2 p^2(t-jT_f-2iT_s-\tau_{l_2})dt \\ &\quad + \underbrace{\sum_{l_2 \neq m_2} \sum \alpha_{l_2}\alpha_{m_2} R(\tau_{l_2}-\tau_{m_2})}_{value=0} \Bigg] \\ &= N_f b_i E_p \underbrace{\left(\sum_{l_2} \alpha_{l_2}^2 \right)}_{value=\gamma_2} \\ &= \underbrace{N_f b_i E_p \gamma_2}_{sig_{SR}} \end{aligned} \quad (4.86)$$

where, the energy of pulse obtained from S$-$D link is represented as $E_p = \int_{jT_f+2iT_s+T_d}^{jT_f+2iT_s+T_d+T_i} p^2(t-jT_f-2iT_s-\tau_{l_2})dt$ and autocorrelation function as $R(\tau) = \int_{\infty}^{\infty} p(t)p(t-\tau)dt$. This condition $min\{(\tau_{l_2}-\tau_{m_2})\} > T_p$for $l_2 \neq m_2$ is satisfied, in order to avoid IPI. Hence, $\sum_{l_2 \neq m_2} \sum \alpha_{l_2}\alpha_{m_2} R(\tau_{l_2}-\tau_{m_2}) = 0$. As explained in section 4.3.1, since a large number of UWB multipath channel gains are considered, channel gains may be approximated as Gaussian Distributed using the Central Limit Theorem $\sum_{l_2} \alpha_{l_2}^2 = \gamma_2$. As described in Section 4.3.1, the PSD of noise $\theta_k(f)$ is sufficiently flat, so its autocorrelation function can be simplified as $\theta_k(\tau) = \frac{N_0}{2}\delta(\tau)$ [175]. The index $k \in \{1,2,3\}$ refers to S$-$D, S$-$R and R$-$D link respectively, as discussed in equation 4.5. The decision variables $Z_2(2)$, $Z_3(2)$ and $Z_4(2)$ denote the noise terms, so their variances

are evaluated as shown below.

$$
\begin{aligned}
Var(N_1) &= E[Z_2^2(2)] = \sum_{j=0}^{N_f-1}\Bigg[\int_{jT_f+2iT_s+T_d}^{jT_f+2iT_s+T_d+T_i}\int_{jT_f+(2i+1)T_s+T_d}^{jT_f+(2i+1)T_s+T_d+T_i}\Bigg(\sum_{l_2}\alpha_{l_2}p(t-jT_f- \\
&\quad 2iT_s-\tau_{l_2})\sum_{m_2}\alpha_{m_2}p(\tau-jT_f-2iT_s-\tau_{m_2})\Bigg)E[n_{SR}(t-T_d)n_{SR}(\tau-T_d)] \\
&\quad dtd\tau\Bigg] \\
&= \sum_{j=0}^{N_f-1}\Bigg[\int_{jT_f+2iT_s+T_d}^{jT_f+2iT_s+T_d+T_i}\Bigg(\sum_{l_2}\alpha_{l_2}p(t-jT_f-2iT_s-\tau_{l_2})\sum_{m_2}\alpha_{m_2}p(\tau-jT_f- \\
&\quad 2iT_s-\tau_{m_2})\Bigg)\theta_2(t-\tau)dtd\tau\Bigg] \\
&= \frac{N_fN_0}{2}\Bigg[\int_{jT_f+2iT_s+T_d}^{jT_f+2iT_s+T_d+T_i}\sum_{l_2=m_2}\alpha_{l_2}^2p^2(t-jT_f-2iT_s-\tau_{l_2})dt+ \\
&\quad \underbrace{\sum_{l_2\neq m_2}\sum\alpha_{l_2}\alpha_{m_2}R(\tau_{l_2}-\tau_{m_2})}_{value=0}\Bigg] \\
&= \frac{N_fN_0E_p}{2}\underbrace{\Bigg(\sum_{l_2}\alpha_{l_2}^2\Bigg)}_{value=\gamma_2} \\
&= \frac{N_fN_0E_p\gamma_2}{2} \qquad (4.87)
\end{aligned}
$$

where, $\mathbb{E}[n_{SR}(t)n_{SR}(\tau)] = \theta_2(t-\tau) = \frac{N_0}{2}\delta(t-\tau)$ and $\int_{2iT_s+jT_f+T_d}^{2iT_s+jT_f+T_d+T_i}\frac{N_0}{2}\delta(t-\tau)d\tau = \frac{N_0}{2}$.

$$
\begin{aligned}
Var(N_2) &= E[Z_3^2(2)] = \sum_{j=0}^{N_f-1}\Bigg[\int_{jT_f+2iT_s+T_d}^{jT_f+2iT_s+T_d+T_i}\int_{jT_f+2iT_s+T_d}^{jT_f+2iT_s+T_d+T_i}\Bigg(\sum_{l_2}\alpha_{l_2}b_ip(t-jT_f- \\
&\quad 2iT_s-T_d-\tau_{l_2})\sum_{m_2}\alpha_{m_2}b_ip(\tau-jT_f-2iT_s-T_d-\tau_{m_2})\Bigg)E[n_{SR}(t)n_{SR}(\tau)] \\
&\quad dtd\tau\Bigg] \\
&= \sum_{j=0}^{N_f-1}b_i^2\Bigg[\int_{jT_f+2iT_s+T_d}^{jT_f+2iT_s+T_d+T_i}\int_{jT_f+2iT_s+T_d}^{jT_f+2iT_s+T_d+T_i}\Bigg(\sum_{l_2}\alpha_{l_2}p(t-jT_f-2iT_s-T_d- \\
&\quad \tau_{l_2})\sum_{m_2}\alpha_{m_2}p(\tau-jT_f-2iT_s-T_d-\tau_{m_2})\Bigg)\theta_2(t-\tau)dtd\tau\Bigg] \\
&= \frac{N_fN_0b_i^2}{2}\Bigg[\int_{jT_f+2iT_s+T_d}^{jT_f+2iT_s+T_d+T_i}\sum_{l_2=m_2}\alpha_{l_2}^2p^2(t-jT_f-2iT_s-\tau_{l_2})dt+ \\
&\quad \underbrace{\sum_{l_2\neq m_2}\sum\alpha_{l_2}\alpha_{m_2}R(\tau_{l_2}-\tau_{m_2})}_{value=0}\Bigg]
\end{aligned}
$$

$$= \frac{N_f N_0 b_i^2 E_p}{2} \underbrace{\left(\sum_{l_2} \alpha_{l_2}^2 \right)}_{value=\gamma_2}$$
$$= \frac{N_f N_0 b_i^2 E_p \gamma_2}{2} \tag{4.88}$$

$$\begin{aligned} Var(N_3) &= E[Z_4^2(2)] = \sum_{j=0}^{N_f-1} \Bigg[\int_{jT_f+2iT_s+T_d}^{jT_f+2iT_s+T_d+T_i} \int_{jT_f+2iT_s+T_d}^{jT_f+2iT_s+T_d+T_i} \\ &\quad \mathbb{E}\left[\{n_{SR}(t) n_{SR}(\tau - T_d)\}^2 \right] dt d\tau \Bigg] \\ &= \sum_{j=0}^{N_f-1} \left[\int_{jT_f+2iT_s+T_d}^{jT_f+2iT_s+T_d+T_i} \int_{jT_f+2iT_s+T_d}^{jT_f+2iT_s+T_d+T_i} \theta_2^2(t-\tau) dt d\tau \right] \\ &= \sum_{j=0}^{N_f-1} \left[\int_{jT_f+2iT_s+T_d}^{jT_f+2iT_s+T_d+T_i} \int_{jT_f+2iT_s+T_d+T_i-t}^{jT_f+2iT_s+T_d+T_i} \theta_2^2(u) dt du \right] \\ &= \sum_{j=0}^{N_f-1} \left[\int_0^{T_i} \frac{N_0^2}{4} 2W dt \right] \\ &= \frac{N_f N_0^2 W T_i}{2}. \end{aligned} \tag{4.89}$$

The value of $E[\{n_k^2(t)\}^2] = E[\{n_{SR}^2(t)\}^2] = \frac{N_0^2}{4}$. The variance of $[n_k^2(t)]$ tends to a Dirac Delta function, where the integral vanishes outside the range $[-t, T_i - t]$. Parsevals theorem is applied to solve equation 4.91.

The decision statistic Z_{TR-SR} obtained at the destination node in the 1st time slot contains signal term and the noise term. From the derivations, it is inferred that the signal term sig_{SR} has a value of $N_f b_i E_p \gamma_2$, while the noise term $Z_{noise-SR}$ has a variance of $\sigma^2_{Z_{noise-SR}} = \frac{N_f N_0 E_p \gamma_2}{2} + \frac{N_f N_0 b_i^2 E_p \gamma_2}{2} + \frac{N_f N_0^2 W T_i}{2}$.

To extract the information bit $b_i^{'}$, the decision statistic Z_{TR-SR} obtained at the relay node is compared to the decision threshold, which is 0 in case of PAM signalling. The decision criteria $\hat{z}$ can be expressed as:

$$b_i^{'} = \hat{z} = \begin{cases} 0, & H_0 : Z = Z_{TR-SR} \leq 0 \\ 1, & H_1 : Z = Z_{TR-SR} > 0 \end{cases} \tag{4.90}$$

Finally the information bit $b_i^{'}$ is extracted. The received signal obtained at the destination node $r_{TR-SD}(t)$ in 1st time slot is detected using a TR receiver, whose decision statistics Z_{TR-SD} is as follows:

$$Z_{TR-SD} = \sum_{j=0}^{N_f-1} \int_{jT_f+2iT_s+T_d}^{jT_f+2iT_s+T_d+T_i} r_{TR-SD}(t) r_{TR-SD}(t - T_d) dt$$

$$= \underbrace{Z_1(k)}_{signal} + \underbrace{Z_2(k) + Z_3(k) + Z_4(k)}_{noise-term} = \underbrace{Z_1(1)}_{signal} + \underbrace{Z_2(1) + Z_3(1) + Z_4(1)}_{noise-term} \quad (4.91)$$

where, the index $k \in \{1, 2, 3\}$ denotes S$-$D, S$-$R and R$-$D link respectively, as mentioned in equation 4.5. The integration time interval is denoted by $T_i = T_p + T_{mds}$ where, T_p and T_{mds} denote pulse duration and multipath delay spread respectively. The signal term obtained from S$-$D link is expressed as:

$$\begin{aligned}
Z_1(1) &= \sum_{j=0}^{N_f-1} \Bigg[\int_{jT_f+2iT_s+T_d}^{jT_f+2iT_s+T_d+T_i} \Bigg(\sum_{l_1} \alpha_{l_1} p(t - jT_f - 2iT_s - \tau_{l_1}) \sum_{m_1} \alpha_{m_1} b_i p(t - jT_f - \\
&\quad 2iT_s - T_d - \tau_{m_1}) \Bigg) dt \Bigg] \\
&= N_f b_i \Bigg[\int_{jT_f+2iT_s+T_d}^{jT_f+2iT_s+T_d+T_i} \sum_{l_1=m_1} \alpha_{l_1}^2 p^2(t - jT_f - 2iT_s - \tau_{l_1}) dt \\
&\quad + \underbrace{\sum_{l_1 \neq m_1} \sum \alpha_{l_1} \alpha_{m_1} R(\tau_{l_1} - \tau_{m_1})}_{value=0} \Bigg] \\
&= N_f b_i E_p \underbrace{\left(\sum_{l_1} \alpha_{l_1}^2 \right)}_{value=\gamma_1} \\
&= \underbrace{N_f b_i E_p \gamma_1}_{sig_{SD}}
\end{aligned} \quad (4.92)$$

where, the pulse energy obtained from S$-$D link is represented as $E_p = \int_{jT_f+2iT_s}^{jT_f+2iT_s+T_i} p^2(t - jT_f - 2iT_s - \tau_{l_1})dt$ and autocorrelation function as $R(\tau) = \int_{\infty}^{\infty} p(t)p(t-\tau)dt$. If the assumption $min\{(\tau_{l_1} - \tau_{m_1})\} > T_p$for $l_1 \neq m_1$ is satisfied, then IPI is avoided. Hence, $\sum_{l_1 \neq m_1} \sum \alpha_{l_1} \alpha_{m_1} R(\tau_{l_1} - \tau_{m_1}) = 0$. As explained in Section 4.3.1, since a large number of UWB multipath channel gains are considered, the channel gains can be approximated as Gaussian Distributed using Central Limit Theorem $\sum_{l_1} \alpha_{l_1}^2 = \gamma_1$. As described in the Section 4.3.1, the autocorrelation function of noise can be approximated as $\theta_k(\tau) = \frac{N_0}{2}\delta(\tau)$ [175]. The index $k \in \{1, 2, 3\}$ refers to S$-$D, S$-$R and R$-$D link respectively, as discussed in equation 4.5. To solve the decision variables $Z_2(1)$, $Z_3(1)$ and $Z_4(1)$ containing noise terms, we evaluate its variances as shown below.

$$\begin{aligned}
Var(N_1) &= E[Z_2^2(1)] = \sum_{j=0}^{N_f-1} \Bigg[\int_{jT_f+2iT_s+T_d}^{jT_f+2iT_s+T_d+T_i} \int_{jT_f+2iT_s+T_d}^{jT_f+2iT_s+T_d+T_i} \Bigg(\sum_{l_1} \alpha_{l_1} p(t - jT_f - \\
&\quad 2iT_s - \tau_{l_1}) \sum_{m_1} \alpha_{m_1} p(\tau - jT_f - 2iT_s - \tau_{m_1}) \Bigg) E[n_{SR}(t - T_d) n_{SR}(\tau - T_d)] \\
&\quad dt d\tau \Bigg]
\end{aligned}$$

$$
\begin{aligned}
&= \sum_{j=0}^{N_f-1}\Bigg[\int_{jT_f+2iT_s+T_d}^{jT_f+2iT_s+T_d+T_i}\Bigg(\sum_{l_1}\alpha_{l_1}p(t-jT_f-2iT_s-\tau_{l_1})\sum_{m_1}\alpha_{m_1}p(\tau- \\
&\quad jT_f-2iT_s-\tau_{m_1})\Bigg)\theta_1(t-\tau)dtd\tau\Bigg] \\
&= \frac{N_fN_0}{2}\Bigg[\int_{jT_f+2iT_s+T_d}^{jT_f+2iT_s+T_d+T_i}\sum_{l_1=m_1}\alpha_{l_1}^2p^2(t-jT_f-2iT_s-\tau_{l_1})dt \\
&\quad \underbrace{+\sum_{l_1\neq m_1}\sum\alpha_{l_1}\alpha_{m_1}R(\tau_{l_1}-\tau_{m_1})}_{value=0}\Bigg] \\
&= \frac{N_fN_0E_p}{2}\underbrace{\Bigg(\sum_{l_1}\alpha_{l_1}^2\Bigg)}_{value=\gamma_1} \\
&= \frac{N_fN_0E_p\gamma_1}{2}
\end{aligned}
\tag{4.93}
$$

where, $\mathbb{E}[n_{SD}(t)n_{SD}(\tau)]=\theta_1(t-\tau)=\frac{N_0}{2}\delta(t-\tau)$ and $\int_{2iT_s+jT_f+T_d}^{2iT_s+jT_f+T_d+T_i}\frac{N_0}{2}\delta(t-\tau)d\tau=\frac{N_0}{2}$.

$$
\begin{aligned}
Var(N_2) &= E[Z_3^2(2)]=\sum_{j=0}^{N_f-1}\Bigg[\int_{jT_f+2iT_s+T_d}^{jT_f+2iT_s+T_d+T_i}\int_{jT_f+2iT_s+T_d}^{jT_f+2iT_s+T_d+T_i}\Bigg(\sum_{l_1}\alpha_{l_1}b_ip(t-jT_f- \\
&\quad 2iT_s-T_d-\tau_{l_1})\sum_{m_1}\alpha_{m_1}b_ip(\tau-jT_f-2iT_s-T_d-\tau_{m_1})\Bigg)E[n_{SD}(t)n_{SD} \\
&\quad (\tau)]dtd\tau\Bigg] \\
&= \sum_{j=0}^{N_f-1}b_i^2\Bigg[\int_{jT_f+2iT_s+T_d}^{jT_f+2iT_s+T_d+T_i}\int_{jT_f+2iT_s+T_d}^{jT_f+2iT_s+T_d+T_i}\Bigg(\sum_{l_1}\alpha_{l_1}p(t-jT_f-2iT_s-T_d- \\
&\quad \tau_{l_1})\sum_{m_1}\alpha_{m_1}p(\tau-jT_f-2iT_s-T_d-\tau_{m_1})\Bigg)\theta_1(t-\tau)dtd\tau\Bigg] \\
&= \frac{N_fN_0b_i^2}{2}\Bigg[\int_{jT_f+2iT_s+T_d}^{jT_f+2iT_s+T_d+T_i}\sum_{l_1=m_1}\alpha_{l_1}^2p^2(t-jT_f-2iT_s-\tau_{l_1})dt \\
&\quad \underbrace{+\sum_{l_1\neq m_1}\sum\alpha_{l_1}\alpha_{m_1}R(\tau_{l_1}-\tau_{m_1})}_{value=0}\Bigg] \\
&= \frac{N_fN_0b_i^2E_p}{2}\underbrace{\Bigg(\sum_{l_1}\alpha_{l_1}^2\Bigg)}_{value=\gamma_1} \\
&= \frac{N_fN_0b_i^2E_p\gamma_1}{2}
\end{aligned}
\tag{4.94}
$$

$$
Var(N_3) = E[Z_4^2(1)]=\sum_{j=0}^{N_f-1}\Bigg[\int_{jT_f+2iT_s+T_d}^{jT_f+2iT_s+T_d+T_i}\int_{jT_f+2iT_s+T_d}^{jT_f+2iT_s+T_d+T_i}
$$

$$
\begin{aligned}
& \mathbb{E}\left[\left\{n_{SD}(t)n_{SD}(\tau - T_d)\right\}^2\right]dtd\tau\Bigg] \\
= & \sum_{j=0}^{N_f-1}\left[\int_{jT_f+2iT_s+T_d}^{jT_f+2iT_s+T_d+T_i}\int_{jT_f+2iT_s+T_d}^{jT_f+2iT_s+T_d+T_i}\theta_1^2(t-\tau)dtd\tau\right] \\
= & \sum_{j=0}^{N_f-1}\left[\int_{jT_f+2iT_s+T_d}^{jT_f+2iT_s+T_d+T_i}\int_{jT_f+2iT_s+T_d+T_i-t}^{jT_f+2iT_s+T_d+T_i}\theta_1^2(u)dtdu\right] \\
= & \sum_{j=0}^{N_f-1}\left[\int_0^{T_i}\frac{N_0^2}{4}2Wdt\right] \\
= & \frac{N_fN_0^2WT_i}{2}.
\end{aligned} \tag{4.95}
$$

The value of $E[\{n_k^2(t)\}^2] = E[\{n_{SD}^2(t)\}^2] = \frac{N_0^2}{4}$. As discussed earlier, the variance of $[n_k^2(t)]$ tends to a Dirac Delta function, where the integral vanishes outside the range $[-t, T_i - t]$. Parsevals theorem is then applied to solve equation 4.97.

The SNR obtained at the relay node is denoted as:

$$
\begin{aligned}
\rho_{TR-SR-DTF} &= \frac{sig_{SR}^2}{\sigma^2_{Z_{noise-SR}}} \\
&= \frac{(N_fb_iE_p\gamma_2)^2}{\frac{N_fN_0E_p\gamma_2}{2} + \frac{N_fN_0b_i^2E_p\gamma_2}{2} + \frac{N_fN_0^2WT_i}{2}} \\
&= \frac{(N_fE_p\gamma_2)^2}{N_fN_0E_p\gamma_2 + \frac{N_fN_0^2WT_i}{2}} \\
&= \frac{(\frac{E_b\gamma_2}{2})^2}{\frac{N_0E_b\gamma_2}{2} + \frac{N_fN_0^2WT_i}{2}}
\end{aligned} \tag{4.96}
$$

where, information bit $b_i = 1$ is transmitted from source node to relay node and energy per bit is denoted as $E_b = 2N_fE_p$. At the relay node, if information bit $b_i^{'} = 0$ is received, then an error is said to occur. Hence, the probability of error obtained at the relay node is expressed as:

$$
P_e = Q\left(\sqrt{\rho_{TR-SR-DTF}}\right)f_{\rho_{DTF}}(\gamma_2)d\gamma_2 \tag{4.97}
$$

where, the PDF of S$-$R link is expressed as $f_{\rho_{DTF}}(\gamma_2)$ = $\frac{1}{\sqrt{(2\pi(\sigma_{SR}^2))}}\exp\left[\frac{-(\gamma_2-\mu_{SR})^2}{2(\sigma_{SR}^2)}\right]$. Furthermore, μ_{SR} and σ_{SR}^2 denotes the mean and variance of S$-$R link of UWB channel respectively.

After extraction of information bit $b_i^{'}$ at the relay node, the UWB signal transmitted from the relay node to the destination node in 2$^{\text{nd}}$ time slot is represented as:

$$
s_{TR-RD}(t) = \sum_{i=0}^{\infty}\sum_{j=0}^{N_f-1}\left[p(t - jT_f - (2i+1)T_s) + b_i^{'}p(t - jT_f - (2i+1)T_s - T_d)\right]
$$

(4.98)

where, $b_i^{'}$ represents the information bit detected at the relay node. The received signal $r_{TR-RD}(t)$ obtained at the destination node in 2nd time slot is represented as:

$$\begin{aligned} r_{TR-RD}(t) &= s_{TR-RD}(t) * h_3(t) \\ &= \sum_{i=0}^{\infty}\sum_{j=0}^{N_f-1}\Big[p(t-jT_f-(2i+1)T_s)+b_i^{'}p(t-jT_f-(2i+1)T_s-T_d)] \\ &\quad *\sum_{l_3}\alpha_{l_3}\delta(t-\tau_{l_3})\Big]+n_{RD}(t) \\ &= \sum_{i=0}^{\infty}\sum_{j=0}^{N_f-1}\sum_{l_3}\Big[\alpha_{l_3}p(t-jT_f-(2i+1)T_s-\tau_{l_3})+\alpha_{l_3}b_i^{'}p(t-jT_f-(2i+1) \\ &\quad T_s-T_d-\tau_{l_3})\Big]+n_{RD}(t) \\ &= \sum_{i=0}^{\infty}\sum_{j=0}^{N_f-1}\Big[g_{RD}(t-jT_f-(2i+1)T_s)+b_i^{'}g_{RD}(t-jT_f-(2i+1)T_s-T_d)\Big] \\ &\quad +n_{RD}(t) \end{aligned} \tag{4.99}$$

The aggregate signal response $g_{RD}(t)$ is expressed as $g_{RD}(t) = \sum_{l_3}\alpha_{l_3}p(t-\tau_{l_3})$. The noise (AWGN) obtained from R$-$D link is denoted by $n_{RD}(t)$. The received signal $r_{TR-RD}(t)$ obtained at the destination node is demodulated using a TR receiver. In case of correct detection at relay node, the decision statistics Z_{TR-RD} at destination node is expressed as:

$$\begin{aligned} Z_{TR-RD} &= \sum_{j=0}^{N_f-1}\int_{(2i+1)T_s+jT_f}^{(2i+1)T_s+jT_f+T_i} r_{TR-RD}(t)r_{TR-RD}(t-T_d)dt \\ &= \underbrace{Z_1(3)}_{signal}+\underbrace{Z_2(3)+Z_3(3)+Z_4(3)}_{\text{noise}-term} \end{aligned} \tag{4.100}$$

Using the same procedure as used for S$-$R link, we obtain the decision statistics for R$-$D link. The signal term sig_{RD} for R$-$D link is represented as:

$$\begin{aligned} Z_1(3) &= \sum_{j=0}^{N_f-1}\Big[\int_{jT_f+(2i+1)T_s+T_d}^{jT_f+(2i+1)T_s+T_d+T_i}\Big(\sum_{l_3}\alpha_{l_3}p(t-jT_f-(2i+1)T_s-\tau_{l_3})\sum_{m_3}\alpha_{m_3}b_i^{'}p(t- \\ &\quad jT_f-(2i+1)T_s-T_d-\tau_{m_3})\Big)dt\Big] \\ &= N_f b_i^{'}\Big[\int_{jT_f+(2i+1)T_s+T_d}^{jT_f+(2i+1)T_s+T_d+T_i}\sum_{l_3=m_3}\alpha_{l_3}^2p^2(t-jT_f-(2i+1)T_s-\tau_{l_3})dt \\ &\quad +\underbrace{\sum_{l_3\neq m_3}\sum\alpha_{l_3}\alpha_{m_3}R(\tau_{l_3}-\tau_{m_3})}_{value=0}\Big] \end{aligned}$$

$$
\begin{aligned}
&= N_f b_i^{'} E_p \underbrace{\left(\sum_{l_3} \alpha_{l_3}^2 \right)}_{value=\gamma_3} \\
&= \underbrace{N_f b_i^{'} E_p \gamma_3}_{sig_{RD}}
\end{aligned} \tag{4.101}
$$

where, $E_p = \int_{jT_f+(2i+1)T_s+T_d}^{jT_f+(2i+1)T_s+T_d+T_i} p^2(t - jT_f - (2i+1)T_s - \tau_{l_3})dt$ represents the pulse energy obtained from S−D link and $R(\tau) = \int_{\infty}^{\infty} p(t)p(t-\tau)dt$ the autocorrelation function of pulse signal. The constraint $min\{(\tau_{l_3} - \tau_{m_3})\} > T_p$ for $l_3 \neq m_3$ is satisfied, to avoid IPI. Hence, $\sum_{l_3 \neq m_3} \sum \alpha_{l_3}\alpha_{m_3} R(\tau_{l_3} - \tau_{m_3}) = 0$. As explained in Section 4.3.1, since a large number of UWB multipath channel gains are considered, channel gains may be approximated as Gaussian Distributed using Central Limit Theorem $\sum_{l_3} \alpha_{l_3}^2 = \gamma_3$. As described in Section 4.3.1, the autocorrelation function of noise can be simplified as $\theta_k(\tau) = \frac{N_0}{2}\delta(\tau)$ [175]. The decision variables $Z_2(3)$, $Z_3(3)$ and $Z_4(3)$ denote the noise terms, so their variances are evaluated as shown below.

$$
\begin{aligned}
Var(N_1) &= E[Z_2^2(3)] = \sum_{j=0}^{N_f-1} \Bigg[\int_{jT_f+(2i+1)T_s+T_d}^{jT_f+(2i+1)T_s+T_d+T_i} \int_{jT_f+(2i+1)T_s+T_d}^{jT_f+(2i+1)T_s+T_d+T_i} \Bigg(\sum_{l_3} \alpha_{l_3} p(t - jT_f \\
&\quad -(2i+1)T_s - \tau_{l_3}) \sum_{m_3} \alpha_{m_3} p(\tau - jT_f - (2i+1)T_s - \tau_{m_3}) \Bigg) E[n_{RD}(t - T_d) \\
&\quad n_{RD}(\tau - T_d)] dt d\tau \Bigg] \\
&= \sum_{j=0}^{N_f-1} \Bigg[\int_{jT_f+(2i+1)T_s+T_d}^{jT_f+(2i+1)T_s+T_d+T_i} \Bigg(\sum_{l_3} \alpha_{l_3} p(t - jT_f - 2iT_s - \tau_{l_3}) \sum_{m_3} \alpha_{m_3} p(\tau - jT_f \\
&\quad -2iT_s - \tau_{m_3}) \Bigg) \theta_3(t-\tau) dt d\tau \Bigg] \\
&= \frac{N_f N_0}{2} \Bigg[\int_{jT_f+(2i+1)T_s+T_d}^{jT_f+(2i+1)T_s+T_d+T_i} \sum_{l_3=m_3} \alpha_{l_3}^2 p^2(t - jT_f - (2i+1)T_s - \tau_{l_3}) dt \\
&\quad + \underbrace{\sum_{l_3 \neq m_3} \sum \alpha_{l_3}\alpha_{m_3} R(\tau_{l_3} - \tau_{m_3})}_{value=0} \Bigg] \\
&= \frac{N_f N_0 E_p}{2} \underbrace{\left(\sum_{l_3} \alpha_{l_3}^2 \right)}_{value=\gamma_3} \\
&= \frac{N_f N_0 E_p \gamma_3}{2}
\end{aligned} \tag{4.102}
$$

where, $\mathbb{E}[n_{RD}(t)n_{RD}(\tau)] = \theta_3(t-\tau) = \frac{N_0}{2}\delta(t-\tau)$ and $\int_{(2i+1)T_s+jT_f+T_d}^{(2i+1)T_s+jT_f+T_d+T_i} \frac{N_0}{2}\delta(t-\tau)d\tau = \frac{N_0}{2}$.

$$\begin{aligned}
Var(N_2) &= E[Z_3^2(2)] = \sum_{j=0}^{N_f-1}\Bigg[\int_{jT_f+(2i+1)T_s+T_d}^{jT_f+(2i+1)T_s+T_d+T_i}\int_{jT_f+(2i+1)T_s+T_d}^{jT_f+(2i+1)T_s+T_d+T_i}\Bigg(\sum_{l_3}\alpha_{l_3}b_i p(t- \\
&\quad jT_f-(2i+1)T_s-T_d-\tau_{l_3})\sum_{m_3}\alpha_{m_3}b_i p(\tau-jT_f-(2i+1)T_s-T_d-\tau_{m_3})\Bigg) \\
&\quad E[n_{RD}(t)n_{RD}(\tau)]dtd\tau\Bigg] \\
&= \sum_{j=0}^{N_f-1} b_i^2\Bigg[\int_{jT_f+(2i+1)T_s+T_d}^{jT_f+(2i+1)T_s+T_d+T_i}\int_{jT_f+(2i+1)T_s+T_d}^{jT_f+(2i+1)T_s+T_d+T_i}\Bigg(\sum_{l_3}\alpha_{l_3}p(t-jT_f-(2i+1) \\
&\quad T_s-T_d-\tau_{l_3})\sum_{m_3}\alpha_{m_3}p(\tau-jT_f-(2i+1)T_s-T_d-\tau_{m_3})\Bigg)\theta_3(t-\tau)dtd\tau\Bigg] \\
&= \frac{N_fN_0b_i^2}{2}\Bigg[\int_{jT_f+(2i+1)T_s+T_d}^{jT_f+(2i+1)T_s+T_d+T_i}\sum_{l_3=m_3}\alpha_{l_3}^2p^2(t-jT_f-2iT_s-\tau_{l_3})dt \\
&\quad \underbrace{+\sum_{l_3\neq m_3}\sum\alpha_{l_3}\alpha_{m_3}R(\tau_{l_3}-\tau_{m_3})}_{value=0}\Bigg] \\
&= \frac{N_fN_0b_i^2E_p}{2}\underbrace{\Bigg(\sum_{l_3}\alpha_{l_3}^2\Bigg)}_{value=\gamma_3} \\
&= \frac{N_fN_0b_i^2E_p\gamma_3}{2} \qquad (4.103)
\end{aligned}$$

$$\begin{aligned}
Var(N_3) &= E[Z_4^2(1)] = \sum_{j=0}^{N_f-1}\Bigg[\int_{jT_f+(2i+1)T_s+T_d}^{jT_f+(2i+1)T_s+T_d+T_i}\int_{jT_f+(2i+1)T_s+T_d}^{jT_f+(2i+1)T_s+T_d+T_i} \\
&\quad \mathbb{E}\Big[\{n_{RD}(t)n_{RD}(\tau-T_d)\}^2\Big]dtd\tau\Bigg] \\
&= \sum_{j=0}^{N_f-1}\Bigg[\int_{jT_f+(2i+1)T_s+T_d}^{jT_f+(2i+1)T_s+T_d+T_i}\int_{jT_f+(2i+1)T_s+T_d}^{jT_f+(2i+1)T_s+T_d+T_i}\theta_3^2(t-\tau)dtd\tau\Bigg] \\
&= \sum_{j=0}^{N_f-1}\Bigg[\int_{jT_f+(2i+1)T_s+T_d}^{jT_f+(2i+1)T_s+T_d+T_i}\int_{jT_f+(2i+1)T_s+T_d+T_i-t}^{jT_f+(2i+1)T_s+T_d+T_i}\theta_3^2(u)dtdu\Bigg] \\
&= \sum_{j=0}^{N_f-1}\Bigg[\int_0^{T_i}\frac{N_0^2}{4}2Wdt\Bigg] \\
&= \frac{N_fN_0^2WT_i}{2}. \qquad (4.104)
\end{aligned}$$

The value of $E[\{n_k^2(t)\}^2] = E[\{n_{RD}^2(t)\}^2] = \frac{N_0^2}{4}$. As discussed earlier, the variance of $[n_k^2(t)]$ tends to a Dirac Delta function, where the integral vanishes outside the range $[-t, T_i - t]$.

Parsevals theorem is applied to solve equation 4.106.

At the destination node, the decision statistic Z_{TR-SD} contains signal term $sig_{SD} = Z_1(1) = N_f E_p b_i^2 \gamma_1$ and noise term $Z_{noise-SD} = Z_2(1) + Z_3(1) + Z_4(1)$ in 1st time slot. The noise term $Z_{noise-SD}$ has a total variance of $\sigma^2_{Z_{noise-SD}} = \sigma^2_{N_1} + \sigma^2_{N_2} + \sigma^2_{N_3} = \frac{N_f N_0 E_p \gamma_1}{2} + \frac{N_f N_0 b_i^2 E_p \gamma_1}{2} + \frac{N_f N_0^2 W T_i}{2}$. Similarly, the decision statistic Z_{TR-RD} obtained from R$-$D link contains signal term $sig_{RD} = Z_1(3) = N_f E_p b_i^{'2} \gamma_3$ and noise term $Z_{noise-RD} = Z_2(3) + Z_3(3) + Z_4(3)$ in 2nd time slot. The noise term $Z_{noise-RD}$ has a total variance of $\sigma^2_{Z_{noise-RD}} = \sigma^2_{N_1} + \sigma^2_{N_2} + \sigma^2_{N_3} = \frac{N_f N_0 E_p \gamma_3}{2} + \frac{N_f N_0 b_i^{'2} E_p \gamma_3}{2} + \frac{N_f N_0^2 W T_i}{2}$.

In case of correct detection, the SNR obtained at the destination node from S$-$D and R$-$D links in 1st and 2nd time slots respectively, are represented as:

$$\begin{aligned} \rho_{SD-DTF} &= \frac{(N_f E_p b_i \gamma_1)^2}{\frac{N_f N_0 E_p \gamma_1}{2} + \frac{N_f N_0 b_i^2 E_p \gamma_1}{2} + \frac{N_f N_0^2 W T_i}{2}} \\ &= \frac{(N_f E_p \gamma_1)^2}{N_f N_0 E_p \gamma_1 + \frac{N_f N_0^2 W T_i}{2}} \\ &= \frac{(\frac{E_b \gamma_1}{2})^2}{\frac{N_0 E_b \gamma_1}{2} + \frac{N_f N_0^2 W T_i}{2}} \end{aligned} \tag{4.105}$$

$$\begin{aligned} \rho_{RD-DTF} &= \frac{(N_f E_p b_i' \gamma_3)^2}{\frac{N_f N_0 E_p \gamma_3}{2} + \frac{N_f N_0 b_i^{'2} E_p \gamma_3}{2} + \frac{N_f N_0^2 W T_i}{2}} \\ &= \frac{(N_f E_p \gamma_3)^2}{N_f N_0 E_p \gamma_3 + \frac{N_f N_0^2 W T_i}{2}} \\ &= \frac{(\frac{E_b \gamma_3}{2})^2}{\frac{N_0 E_b \gamma_3}{2} + \frac{N_f N_0^2 W T_i}{2}} \end{aligned} \tag{4.106}$$

where, $b_i = b_i' = 1$ in case of correct detection. Hence, information bit $b_i' = 1$ is forwarded from the relay to destination node in 2nd time slot. The decision statistics obtained at the destination node in the end of two time slots are combined using linear diversity combining, selective diversity combining and optimum linear diversity combining to form the final decision statistic. The derivatives of the same are explained below in the subsequent sections.

A. Linear Combining

i) *Correct Detection at Relay Node*: At the destination node, the decision statistics Z_{TR-SD} and Z_{TR-RD} obtained from S$-$D and R$-$D links in the 1st and 2nd time slots respectively, are linearly combined to form $Z_{total} = Z_{TR-SD} + Z_{TR-RD} = s_{total-signal} + Z_{noise-total}$,

as mentioned in equation 4.32. The individual decision statistics obtained from S−D and R−D links are mentioned in equation 4.30 and 4.31 respectively. The total noise variance $\sigma^2_{Z_{noise-total}} = \sigma^2_{Z_{noise-SD}} + \sigma^2_{Z_{noise-RD}}$ corresponding to the noise term $Z_{noise-total}$ is solved in equation 4.33.

In case of correct detection, we obtain $b_i^{'} = 1$ at the relay node when information bit 1 ($b_i = 1$) is transmitted from the source node to the relay node. The same detected bit is then forwarded to the destination node. Hence, the SNR obtained at destination node due to correct detection is represented as:

$$\begin{aligned} \rho_{DTF-LC-CD} &= \left(\frac{s^2_{total-signal}}{\sigma^2_{Z_{noise-total}}}\right) = \frac{(sig_{SD} + sig_{RD})^2}{(\sigma^2_{Z_{noise-SD}} + \sigma^2_{Z_{noise-RD}})} \\ &= \frac{(N_f E_p \gamma_1 + N_f E_p \gamma_3)^2}{N_f N_0 E_p \gamma_1 + N_f N_0 E_p \gamma_3 + N_f N_0^2 W T_i} \\ &= \frac{(\frac{E_b \gamma_1}{2} + \frac{E_b \gamma_3}{2})^2}{\frac{N_0 E_b \gamma_1}{2} + \frac{N_0 E_b \gamma_3}{2} + N_f N_0^2 W T_i} \end{aligned} \tag{4.107}$$

In order to extract the information bit, the final decision statistic is compared to a threshold. The threshold is taken to be 0, since PAM modulation scheme is used. Therefore, the final decision criteria $\hat{z}$ can be expressed as:

$$\hat{z} = \begin{Bmatrix} 0, & H_0 : Z = Z_{total} = Z_{TR-SD} + Z_{TR-RD} \leq 0 \\ 1, & H_1 : Z = Z_{total} = Z_{TR-SD} + Z_{TR-RD} > 0 \end{Bmatrix} \tag{4.108}$$

ii) *Incorrect Detection at Relay Node*: In case of incorrect detection, information bit $b_i^{'} = 0$ is detected at relay node when $b_i = 1$ is transmitted from source node to relay node. The incorrect bit $b_i^{'} = 0$ is then forwarded to the destination node. Therefore, the SNR obtained at the destination node due to incorrect detection is represented as:

$$\begin{aligned} \rho_{DTF-LC-ID} &= \frac{(sig_{SD})^2}{(\sigma^2_{Z_{noise-SD}} + \sigma^2_{Z_{noise-RD}})} \\ &= \frac{(N_f E_p \gamma_1)^2}{N_f N_0 E_p \gamma_1 + N_f N_0 E_p \gamma_3 + N_f N_0^2 W T_i} \\ &= \frac{(\frac{E_b \gamma_1}{2})^2}{\frac{N_0 E_b \gamma_1}{2} + \frac{N_0 E_b \gamma_3}{2} + N_f N_0^2 W T_i} \end{aligned} \tag{4.109}$$

Using probability theory, the generalized BER in case of incorrect detection is expressed as:

$$BER = \int_0^\infty \int_0^\infty Q\left(\frac{sig_{SD} - sig_{RD}}{2\sqrt{\sigma^2_{Z_{noise-total}}}}\right) f_{\rho_{DTF}}(\gamma_1, \gamma_3) d\gamma_1 d\gamma_3 \tag{4.110}$$

Due to incorrect detection at relay node, information bit received at destination node (R−D link) is 0 when information bit 1 is transmitted from source node to relay node. Therefore,

$sig_{RD} = 0$.

$$= \int_0^\infty \int_0^\infty Q\left(\frac{sig_{SD}}{2\sqrt{(\sigma^2_{Z_{noise-SD}} + \sigma^2_{Z_{noise-RD}})}}\right) f_{\rho_{DTF}}(\gamma_1, \gamma_3) d\gamma_1 d\gamma_3 \quad (4.111)$$

As explained in Section 4.3.1, the individual channel gains for S−D, S−R and R−D channel links may be assumed to be IID Gaussian distributed by applying Central Limit Theorem, since a large number paths are involved. Therefore, the sum of these channel gains will also have a Gaussian distribution with its mean being the sum of individual means and variance being sum of the individual variances. The joint PDF $f_{\rho_{AF}}(\gamma_1\gamma_3)$ of the channel in case of linear combining is therefore, represented as:

$$f_{\rho_{DTF}}(\gamma_1, \gamma_3) = \frac{1}{\sqrt{(2\pi(\sigma^2_{SD}))}} \frac{1}{\sqrt{(2\pi(\sigma^2_{RD}))}} \exp\left[\frac{-(\gamma_1 - \mu_{SD})^2}{2\sigma^2_{SD}} + \frac{-(\gamma_3 - \mu_{RD})^2}{2\sigma^2_{RD}}\right] d\gamma_1 d\gamma_3 \quad (4.112)$$

Subsequently, the final BER of UWB TR system using linear combining is expressed as:

$$\begin{aligned} BER_{LC-DTF} &= \int_0^\infty \int_0^\infty \left(Q\left(\sqrt{\rho_{DTF-LC-CD}}\right) f_{\rho_{DTF}}(\gamma_1, \gamma_3) d\gamma_1 d\gamma_3\right)(1 - P_e) + \\ &\quad \int_0^\infty \int_0^\infty \left(Q\left(\sqrt{\rho_{DTF-LC-ID}}\right) f_{\rho_{DTF}}(\gamma_1, \gamma_3) d\gamma_1 d\gamma_3\right)(P_e) \\ &= \int_0^\infty \int_0^\infty \left(Q\left(\sqrt{\rho_{DTF-LC-CD}}\right) f_{\rho_{DTF}}(\gamma_1) f_{\rho_{DTF}}(\gamma_3) d\gamma_1 d\gamma_3\right)(1 - P_e) + \\ &\quad \int_0^\infty \int_0^\infty \left(Q\left(\sqrt{\rho_{DTF-LC-ID}}\right) f_{\rho_{DTF}}(\gamma_1) f_{\rho_{DTF}}(\gamma_3) d\gamma_1 d\gamma_3\right)(P_e) \quad (4.113) \end{aligned}$$

Since the joint PDF is IID distributed, it can be represented as $f_{\rho_{DTF}}(\gamma_1, \gamma_3) = f_{\rho_{DTF}}(\gamma_1)$ $f_{\rho_{DTF}}(\gamma_3)$. Replacing the value of equation 4.114 in equation 4.115, we obtain the value of BER in equation 4.116. Therefore, the BER of UWB TR system using cooperative dual−hop DTF strategy with linear combining is expressed as:

$$\begin{aligned} &= \int_0^\infty \int_0^\infty \left(Q\left(\sqrt{\rho_{DTF-LC-CD}}\right) \frac{1}{2\pi\sqrt{(\sigma^2_{SD}\sigma^2_{RD})}} \exp\left[\frac{-(\gamma_1 - \mu_{SD})^2}{2\sigma^2_{SD}} + \frac{-(\gamma_3 - \mu_{RD})^2}{2\sigma^2_{RD}}\right] d\gamma_1 d\gamma_3\right)(1 - P_e) + \int_0^\infty \int_0^\infty \left(Q\left(\sqrt{\rho_{DTF-LC-ID}}\right) \frac{1}{2\pi\sqrt{(\sigma^2_{SD}\sigma^2_{RD})}} \exp\right. \\ &\left.\left[\frac{-(\gamma_1 - \mu_{SD})^2}{2\sigma^2_{SD}} + \frac{-(\gamma_3 - \mu_{RD})^2}{2\sigma^2_{RD}}\right] d\gamma_1 d\gamma_3\right)(P_e) \quad (4.114) \end{aligned}$$

Selective Combining

(i) *Correct Detection at Relay Node*: In selective combining, the SNR obtained from S−D and R−D links in 1st and 2nd time slots respectively are compared, and the one with the highest SNR

is chosen. The probability of selecting the channel link based on the highest SNR is evaluated after integrating the joint PDF of the channel links with proper limits. The joint PDF of channel links S−D and R−D is represented as:

$$f(x,y) = \frac{1}{2\pi\sigma_{SD}\sigma_{RD}} \exp - \left[\frac{(x-\mu_{SD})^2 + (y-\mu_{RD})^2}{2\sigma_{SD}\sigma_{RD}}\right] \tag{4.115}$$

where, x and y represent independent gaussian random variables with means μ_{SD}, μ_{RD} and variances σ^2_{SD}, σ^2_{RD} of S−D and R−D channel links respectively. Hence, the probability that S−D link is selected is represented as:

$$P_1 \;=\; f(x) = \int_{-\infty}^{\infty}\int_{y}^{\infty} f(x,y)dxdy \tag{4.116}$$

Therefore, the probability of selecting R−D link is $P_3 = 1 - P_1$.

ii) *Incorrect Detection at relay node*: In case of incorrect detection, information bit $b_i^{'} = 0$ is detected at the relay node, when information bit $b_i = 1$ is transmitted from source node to relay node. In the next time slot, the incorrectly detected bit $b_i^{'} = 0$ is transmitted from the relay node to the destination node.

Therefore, the final BER of UWB TR system using cooperative dual−hop DTF strategy with selective combining is expressed as:

$$\begin{aligned} BER_{SC-DTF} \;=\; & \left(P_1\int_0^{\infty} Q\left(\sqrt{\rho_{SD-DTF}}\right) f_{\rho_{DTF}}(\gamma_1)d\gamma_1 + P_3\int_0^{\infty} Q\left(\sqrt{\rho_{RD-DTF}}\right)\right. \\ & \left. f_{\rho_{DTF}}(\gamma_3)d\gamma_3\right)(1-P_e) + \left(P_1\int_0^{\infty} Q\left(\sqrt{\rho_{SD-DTF}}\right) f_{\rho_{DTF}}(\gamma_1)d\gamma_1\right. \\ & \left. + P_3\int_0^{\infty}\left(1 - Q\left(\frac{1}{2}\sqrt{\rho_{RD-DTF}}\right)\right) f_{\rho_{DTF}}(\gamma_3)d\gamma_3\right)P_e \end{aligned} \tag{4.117}$$

$$\begin{aligned} = \; & \left(P_1\int_0^{\infty} Q\left(\sqrt{\rho_{SD-DTF}}\right)\frac{1}{\sqrt{(2\pi(\sigma^2_{SD}))}}\exp\left[\frac{-(\gamma_1-\mu_{SD})^2}{2\sigma^2_{SD}}\right]d\gamma_1 + P_3\int_0^{\infty}\right. \\ & \left. Q\left(\sqrt{\rho_{RD-DTF}}\right)\frac{1}{\sqrt{(2\pi(\sigma^2_{RD}))}}\exp\left[\frac{-(\gamma_3-\mu_{RD})^2}{2\sigma^2_{RD}}\right]d\gamma_3\right)(1-P_e) + \left(P_1\int_0^{\infty}\right. \\ & \left. Q\left(\sqrt{\rho_{SD-DTF}}\right)\frac{1}{\sqrt{(2\pi(\sigma^2_{SD}))}}\exp\left[\frac{-(\gamma_1-\mu_{SD})^2}{2\sigma^2_{SD}}\right]d\gamma_1 + P_3\int_0^{\infty}\right. \\ & \left.\left(1 - Q\left(\sqrt{\rho_{RD-DTF}}\right)\right)\frac{1}{\sqrt{(2\pi(\sigma^2_{RD}))}}\exp\left[\frac{-(\gamma_3-\mu_{RD})^2}{2\sigma^2_{RD}}\right]d\gamma_3\right)(P_e) \end{aligned} \tag{4.118}$$

where, $f_{\rho_{DTF}}(\gamma_1) = \frac{1}{\sqrt{(2\pi(\sigma^2_{SD}))}}\exp\left[\frac{-(\gamma_1-\mu_{SD})^2}{2\sigma^2_{SD}}\right]$ and $f_{\rho_{DTF}}(\gamma_3) = \frac{1}{\sqrt{(2\pi(\sigma^2_{RD}))}}\exp\left[\frac{-(\gamma_3-\mu_{RD})^2}{2\sigma^2_{RD}}\right]$ represent the PDF of S−D and R−D channel links respectively.

C. Optimum Linear Combining

(i) *Correct Detection at Relay Node*: The decision statistics obtained at the destination node from S−D and R−D links in 1st and 2nd time slots respectively, are optimally combined to give final decision statistic $Z_{total} = Z_{TR-SD} + \kappa Z_{TR-RD}$. The optimal combining factor κ has a value of $\kappa = \frac{(\sigma^2_{Z_{noise-SD}})s_{RD}}{(\sigma^2_{Z_{noise-RD}})s_{SD}}$ as solved in equation C.4 of Appendix C. The final decision statistic Z_{total} obtained at the destination node using optimum linear combining is represented by equation 4.42. The total noise variance is evaluated in equation 4.43.

The SNR obtained at the destination node due to optimum linear combining is represented as:

$$\begin{aligned}
\rho_{DTF-LOC-CD} &= \left(\frac{s^2_{total-signal}}{\sigma^2_{Z_{noise-total}}}\right) \\
&= \left(\frac{(sig_{SD} + \kappa sig_{RD})^2}{\sigma^2_{Z_{noise-SD}} + \kappa^2\sigma^2_{Z_{noise-RD}}}\right) \\
&= \frac{(N_f E_p \gamma_1 + \kappa N_f E_p \gamma_3)^2}{(N_f N_0 E_p \gamma_1 + \frac{N_f N_0^2 W T_i}{2}) + \kappa^2 (N_f N_0 E_p \gamma_3 + \frac{N_f N_0^2 W T_i}{2})} \\
&= \frac{(\frac{E_b\gamma_1}{2} + \kappa\frac{E_b\gamma_3}{2})^2}{(\frac{N_0 E_b \gamma_1}{2} + \frac{N_f N_0^2 W T_i}{2}) + \kappa^2 (\frac{N_0 E_b \gamma_3}{2} + \frac{N_f N_0^2 W T_i}{2})} \qquad (4.119)
\end{aligned}$$

$$= \frac{(\frac{E_b\gamma_1}{2} + \kappa\frac{E_b\gamma_3}{2})^2}{(X_1 + \kappa^2 Y_1)} \qquad (4.120)$$

where, $X_1 = \frac{N_0 E_b \gamma_1}{2} + \frac{N_f N_0^2 W T_i}{2}$ and $Y_1 = \frac{N_0 E_b \gamma_3}{2} + \frac{N_f N_0^2 W T_i}{2}$. Also, $b_i = b_i^{'} = 1$ in case of correct detection.

The final decision statistic is compared to the decision threshold, in order to extract the information bit. The final decision criteria $\hat{z}$ can be expressed as:

$$\hat{z} = \begin{Bmatrix} 0, & H_0 : Z = Z_{total} = Z_{TR-SD} + \kappa Z_{TR-RD} \leq 0 \\ 1, & H_1 : Z = Z_{total} = Z_{TR-SD} + \kappa Z_{TR-RD} > 0 \end{Bmatrix} \qquad (4.121)$$

ii) *Incorrect Detection at Relay Node*: In case of incorrect detection, $b_i^{'} = 0$ is detected at the relay node, when $b_i = 1$ is transmitted from source to relay node. Further, this erroneously detected bit is forwarded to destination node leading to BER degradation. The SNR at the destination node due to incorrect detection is represented as:

$$\rho_{DTF-LOC-ID} = \frac{(sig_{SD})^2}{(\sigma^2_{Z_{noise-SD}} + \kappa^2\sigma^2_{Z_{noise-RD}})}$$

$$= \frac{(N_f E_p \gamma_1)^2}{(N_f N_0 E_p \gamma_1 + \frac{N_f N_0^2 W T_i}{2}) + \kappa^2 (N_f N_0 E_p \gamma_3 + \frac{N_f N_0^2 W T_i}{2})}$$
$$= \frac{(\frac{E_b \gamma_1}{2})^2}{(\frac{N_0 E_b \gamma_1}{2} + \frac{N_f N_0^2 W T_i}{2}) + \kappa^2 (\frac{N_0 E_b \gamma_3}{2} + \frac{N_f N_0^2 W T_i}{2})} \quad (4.122)$$

Using probability theory, the generalized BER in case of incorrect detection is expressed as:

$$BER = \int_0^\infty \int_0^\infty Q\left(\frac{sig_{SD} - \kappa sig_{RD}}{2\sqrt{\sigma^2_{Z_{noise-total}}}}\right) f_{\rho_{DTF}}(\gamma_1, \gamma_3) d\gamma_1 d\gamma_3 \quad (4.123)$$

When information bit 1 is transmitted from source node to relay node, due to incorrect detection at relay node information bit received at destination node (from R$-$D link) is 0. Therefore, $sig_{RD} = 0$.

$$= \int_0^\infty \int_0^\infty Q\left(\frac{sig_{SD}}{2\sqrt{(\sigma^2_{Z_{noise-SD}} + \kappa^2 \sigma^2_{Z_{noise-RD}})}}\right) f_{\rho_{DTF}}(\gamma_1, \gamma_3) d\gamma_1 d\gamma_3 \quad (4.124)$$

Thus, the BER evaluated at the destination node using optimum linear combining is represented as:

$$\begin{aligned} BER_{LOC-DTF} &= \int_0^\infty \int_0^\infty \left(Q\left(\sqrt{\rho_{DTF-LOC-CD}}\right) f_{\rho_{DTF}}(\gamma_1, \gamma_3) d\gamma_1 d\gamma_3\right)(1 - P_e) + \\ &\quad \int_0^\infty \int_0^\infty \left(Q\left(\sqrt{\rho_{DTF-LOC-ID}}\right) f_{\rho_{DTF}}(\gamma_1, \gamma_3) d\gamma_1 d\gamma_3\right)(P_e) \\ &= \int_0^\infty \int_0^\infty \left(Q\left(\sqrt{\rho_{DTF-LOC-CD}}\right) f_{\rho_{DTF}}(\gamma_1) f_{\rho_{DTF}}(\gamma_3) d\gamma_1 d\gamma_3\right) \\ &\quad (1 - P_e) + \int_0^\infty \int_0^\infty \left(Q\left(\sqrt{\rho_{DTF-LOC-ID}}\right) f_{\rho_{DTF}}(\gamma_1) f_{\rho_{DTF}}(\gamma_3)\right. \\ &\quad \left. d\gamma_1 d\gamma_3\right)(P_e) \end{aligned} \quad (4.125)$$

where, $f_{\rho_{DTF}}(\gamma_1, \gamma_3) = f_{\rho_{DTF}}(\gamma_1) f_{\rho_{DTF}}(\gamma_3)$ because the channel gains are IID and gaussian distributed.

4.4.2 DTR System

In this section, the theoretical BER performance analysis of UWB DTR system using cooperative DTF strategy, is presented. In 1st time slot, the received signal obtained at the destination as well as relay node, is represented by equation 4.8 and 4.9 respectively. This received signal $r_{DTR-SR}(t)$ obtained at the relay node is passed through a DTR receiver, whose decision statistics Z_{DTR-SR} is solved below.

$$Z_{DTR-SR} = \sum_{j=0}^{N_f - 1} \int_{jT_f + 2iT_s}^{jT_f + 2iT_s + T_i} r_{DTR-SR}(t) r_{DTR-SR}(t - T_s) dt$$

$$
\begin{aligned}
&= \underbrace{Z_1(k)}_{signal} + \underbrace{Z_2(k) + Z_3(k) + Z_4(k)}_{\text{noise}-term} \\
&= \underbrace{Z_1(2)}_{signal} + \underbrace{Z_2(2) + Z_3(2) + Z_4(2)}_{\text{noise}-term}
\end{aligned} \tag{4.126}
$$

where, the index $k \in \{1, 2, 3\}$ refers to the S$-$D, S$-$R and R$-$D link respectively, as mentioned in equation 4.5. Here, $T_i = T_{mds} + T_p$ represents the integration time interval. Also, T_{mds} and T_p denote multipath delay spread and pulse duration respectively. Replacing the value of equation 4.9 in equation 4.129, we obtain the value of Z_{DTR-SR} in equation 4.130.

$$
\begin{aligned}
= \sum_{j=0}^{N_f-1} \int_{jT_f+2iT_s}^{jT_f+2iT_s+T_i} &\left(\left[\sum_{l_2} \alpha_{l_2} b_i p(t - jT_f - 2iT_s - \tau_{l_2}) \right] + n_{SR}(t) \right) \left(\left[\sum_{m_2} \alpha_{m_2} b_{i-1} \right. \right. \\
&\left. \left. p(t - jT_f - 2iT_s - \tau_{m_2}) \right] + n_{SR}(t - T_s) \right)
\end{aligned} \tag{4.127}
$$

The signal term obtained from S$-$R link is expressed as:

$$
\begin{aligned}
Z_1(2) &= \sum_{j=0}^{N_f-1} \left[\int_{jT_f+2iT_s}^{jT_f+2iT_s+T_i} \left(\sum_{l_2} \alpha_{l_2} b_i p(t - jT_f - 2iT_s - \tau_{l_2}) \sum_{m_2} \alpha_{m_2} b_{i-1} p(t - jT_f - \right. \right. \\
&\left. \left. 2iT_s - \tau_{m_2}) \right) dt \right] \\
&= N_f b_i b_{i-1} \left[\int_{jT_f+2iT_s}^{jT_f+2iT_s+T_i} \sum_{l_2=m_2} \alpha_{l_2}^2 p^2(t - jT_f - 2iT_s - \tau_{l_2}) dt \right. \\
&\quad \left. + \underbrace{\sum_{l_2 \neq m_2} \sum \alpha_{l_2} \alpha_{m_2} R(\tau_{l_2} - \tau_{m_2})}_{value=0} \right] \\
&= N_f b_i b_{i-1} E_p \underbrace{\left(\sum_{l_2} \alpha_{l_2}^2 \right)}_{value=\gamma_2} \\
&= \underbrace{N_f b_i b_{i-1} E_p \gamma_2}_{sig_{SR}}
\end{aligned} \tag{4.128}
$$

where, $E_p = \int_{jT_f+2iT_s}^{jT_f+2iT_s+T_i} p^2(t - jT_f - 2iT_s - \tau_{l_2}) dt$ represents the pulse energy obtained from S$-$D link and $R(\tau) = \int_{\infty}^{\infty} p(t)p(t - \tau)dt$ as autocorrelation function. Under this assumption, $min\{(\tau_{l_2} - \tau_{m_2})\} > T_p$ for $l_2 \neq m_2$, IPI is avoided. Hence, $\sum_{l_2 \neq m_2} \sum \alpha_{l_2} \alpha_{m_2} R(\tau_{l_2} - \tau_{m_2}) = 0$. As explained in Section 4.3.1, since a large number of UWB multipath channel gains are considered, channel gains can be approximated as Gaussian Distributed using the Central Limit Theorem $\sum_{l_2} \alpha_{l_2}^2 = \gamma_2$. As described in Section 4.3.1, since the PSD $\theta_k(f)$ of noise is sufficiently flat, the autocorrelation function of noise can be approximated as $\theta_k(\tau) = \frac{N_0}{2}\delta(\tau)$[175].

To solve the decision variables $Z_2(2)$, $Z_3(2)$ and $Z_4(2)$ containing noise terms, we evaluate its variances, which is solved below.

$$\begin{aligned}
Var(N_1) &= E[Z_2^2(2)] = \sum_{j=0}^{N_f-1}\Bigg[\int_{jT_f+2iT_s}^{jT_f+2iT_s+T_i}\int_{jT_f+2iT_s}^{jT_f+2iT_s+T_i}\Bigg(\sum_{l_2}\alpha_{l_2}b_i p(t-jT_f-2iT_s \\
&\quad -\tau_{l_2})\sum_{m_2}\alpha_{m_2}b_i p(\tau-jT_f-2iT_s-\tau_{m_2})\Bigg)\mathbb{E}[n_{SR}(t-T_s)n_{SR}(\tau-T_s)]dtd\tau\Bigg] \\
&= \sum_{j=0}^{N_f-1} b_i^2\Bigg[\int_{jT_f+2iT_s}^{jT_f+2iT_s+T_i}\int_{jT_f+2iT_s}^{jT_f+2iT_s+T_i}\sum_{l_2}\alpha_{l_2}p(t-jT_f-2iT_s-\tau_{l_2})\sum_{m_2}\alpha_{m_2} \\
&\quad p(\tau-jT_f-2iT_s-\tau_{m_2})\theta_2(t-\tau)dtd\tau\Bigg] \\
&= \frac{N_f N_0 b_i^2}{2}\Bigg[\int_{jT_f+2iT_s}^{jT_f+2iT_s+T_i}\sum_{l_2=m_2}\alpha_{l_2}^2 p^2(t-jT_f-2iT_s-\tau_{l_2})dt \\
&\quad \underbrace{+\sum_{l_2\neq m_2}\sum\alpha_{l_2}\alpha_{m_2}R(\tau_{l_2}-\tau_{m_2})}_{value=0}\Bigg] \\
&= \frac{N_f N_0 b_i^2 E_p}{2}\underbrace{\Bigg(\sum_{l_2}\alpha_{l_2}^2\Bigg)}_{value=\gamma_2} \\
&= \frac{N_f N_0 b_i^2 E_p\gamma_2}{2} \qquad (4.129)
\end{aligned}$$

where, $\int_{jT_f+2iT_s}^{jT_f+2iT_s+T_i}\theta_2(t-\tau)d\tau = \int_{jT_f+2iT_s}^{jT_f+2iT_s+T_i}\frac{N_0}{2}\delta(t-\tau)d\tau = \frac{N_0}{2}$.

$$\begin{aligned}
Var(N_2) &= E[Z_3^2(2)] = \sum_{j=0}^{N_f-1}\Bigg[\int_{jT_f+2iT_s}^{jT_f+2iT_s+T_i}\int_{jT_f+2iT_s}^{jT_f+2iT_s+T_i}\Bigg(\sum_{l_2}\alpha_{l_2}b_{i-1}p(t-jT_f-2iT_s \\
&\quad -\tau_{l_2})\sum_{m_2}\alpha_{m_2}b_{i-1}p(\tau-jT_f-2iT_s-\tau_{m_2})\Bigg)\mathbb{E}[\{n_{SR}(t)n_{SR}(\tau)\}]dtd\tau\Bigg] \\
&= \sum_{j=0}^{N_f-1} b_{i-1}^2\Bigg[\int_{jT_f+2iT_s}^{jT_f+2iT_s+T_i}\int_{jT_f+2iT_s}^{jT_f+2iT_s+T_i}\Bigg(\sum_{l_2}\alpha_{l_2}p(t-jT_f-2iT_s-\tau_{l_2})\sum_{m_2}\alpha_{m_2} \\
&\quad p(\tau-jT_f-2iT_s-\tau_{m_2})\Bigg)\theta_2(t-\tau)dtd\tau\Bigg] \\
&= \frac{N_f N_0 b_{i-1}^2}{2}\Bigg[\int_{jT_f+2iT_s}^{jT_f+2iT_s+T_i}\sum_{l_2=m_2}\alpha_{l_2}^2 p^2(t-jT_f-2iT_s-\tau_{l_2})dt \\
&\quad \underbrace{+\sum_{l_2\neq m_2}\sum\alpha_{l_2}\alpha_{m_2}R(\tau_{l_2}-\tau_{m_2})}_{value=0}\Bigg]
\end{aligned}$$

$$= \frac{N_f N_0 b_{i-1}^2 E_p}{2} \underbrace{\left(\sum_{l_2} \alpha_{l_2}^2\right)}_{value=\gamma_2}$$
$$= \frac{N_f N_0 b_{i-1}^2 E_p \gamma_2}{2} \tag{4.130}$$

$$\begin{aligned} Var(N_3) &= E[Z_4^2(2)] = \sum_{j=0}^{N_f-1} \Bigg[\int_{jT_f+2iT_s}^{jT_f+2iT_s+T_i} \int_{jT_f+2iT_s}^{jT_f+2iT_s+T_i} \\ &\quad \mathbb{E}\left[\{n_{SR}(t) n_{SR}(\tau - T_s)\}^2 \right] dt d\tau \Bigg] \\ &= \sum_{j=0}^{N_f-1} \left[\int_{jT_f+2iT_s}^{jT_f+2iT_s+T_i} \int_{jT_f+2iT_s}^{jT_f+2iT_s+T_i} \theta_2^2(t-\tau) dt d\tau \right] \\ &= \sum_{j=0}^{N_f-1} \left[\int_{jT_f+2iT_s}^{jT_f+2iT_s+T_i} \int_{jT_f+2iT_s+T_i-t}^{jT_f+2iT_s+T_i} \theta_2^2(u) dt du \right] \\ &= \sum_{j=0}^{N_f-1} \left[\int_0^{T_i} \frac{N_0^2}{4} 2W dt \right] \\ &= \frac{N_f N_0^2 W T_i}{2}. \end{aligned} \tag{4.131}$$

where, $E[n_k^2(t)] = \frac{N_0}{2}$. Hence, the value of $E[\{n_k^2(t)\}^2] = \frac{N_0^2}{4}$.

The decision statistic Z_{DTR-SR} obtained at destination node in the 1st time slot contains signal term and the noise term. From the derivations, it is noted that the signal term sig_{SR} has a value of $N_f b_i b_{i-1} E_p \gamma_2$ while the noise term $Z_{noise-SR}$ has a variance of $\sigma^2_{Z_{noise-SR}} = \frac{N_f N_0 b_i^2 E_p \gamma_2}{2} + \frac{N_f N_0 b_{i-1}^2 E_p \gamma_2}{2} + \frac{N_f N_0^2 W T_i}{2}$.

To extract the information bit $b_i^{'}$, the decision statistic Z_{DTR-SR} obtained at the relay node is compared to the decision threshold. The decision threshold is taken to be 0 because PAM modulation scheme is used. The decision criteria $\hat{z}$ can be expressed as:

$$b_i^{'} = \hat{z} = \begin{cases} 0, & H_0 : Z = Z_{DTR-SR} \leq 0 \\ 1, & H_1 : Z = Z_{DTR-SR} > 0 \end{cases} \tag{4.132}$$

where, $b_i^{'}$ represents the extracted information bit at the relay node. The received signal obtained at the destination node $r_{DTR-SD}(t)$ in 1st time slot is detected using a DTR receiver, whose decision statistics Z_{DTR-SD} is as follows:

$$Z_{DTR-SD} = \sum_{j=0}^{N_f-1} \int_{jT_f+2iT_s}^{jT_f+2iT_s+T_i} r_{DTR-SD}(t) r_{DTR-SD}(t-T_s) dt$$

$$= \underbrace{Z_1(k)}_{signal} + \underbrace{Z_2(k) + Z_3(k) + Z_4(k)}_{noise-term}$$
$$= \underbrace{Z_1(1)}_{signal} + \underbrace{Z_2(1) + Z_3(1) + Z_4(1)}_{noise-term} \quad (4.133)$$

where, the index $k \in \{1, 2, 3\}$ refers to the S−D, S−R and R−D link respectively, as mentioned in equation 4.5. Here, T_i represents the integration time interval. The value of Z_{DTR-SD} is obtained in the equation below, by replacing the value of equation 4.8 in equation 4.136.

$$= \sum_{j=0}^{N_f-1} \int_{jT_f+2iT_s}^{jT_f+2iT_s+T_i} \left(\left[\sum_{l_1} \alpha_{l_1} b_i p(t - jT_f - 2iT_s - \tau_{l_1}) \right] + n_{SD}(t) \right) \left(\left[\sum_{m_1} \alpha_{m_1} b_{i-1} \right. \right.$$
$$\left. \left. p(t - jT_f - 2iT_s - \tau_{m_1}) \right] + n_{SD}(t - T_s) \right) \quad (4.134)$$

The signal term obtained from S−D link is as follows.

$$Z_1(1) = \sum_{j=0}^{N_f-1} \left[\int_{jT_f+2iT_s}^{jT_f+2iT_s+T_i} \left(\sum_{l_1} \alpha_{l_1} b_i p(t - jT_f - 2iT_s - \tau_{l_1}) \sum_{m_1} \alpha_{m_1} b_{i-1} p(t - jT_f - \right. \right.$$
$$\left. \left. 2iT_s - \tau_{m_1}) \right) dt \right]$$
$$= N_f b_i b_{i-1} \left[\int_{jT_f+2iT_s}^{jT_f+2iT_s+T_i} \sum_{l_1=m_1} \alpha_{l_1}^2 p^2(t - jT_f - 2iT_s - \tau_{l_1}) dt + \right.$$
$$\left. \underbrace{\sum_{l_1 \neq m_1} \sum \alpha_{l_1} \alpha_{m_1} R(\tau_{l_1} - \tau_{m_1})}_{value=0} \right]$$
$$= N_f b_i b_{i-1} E_p \underbrace{\left(\sum_{l_1} \alpha_{l_1}^2 \right)}_{value=\gamma_1}$$
$$= \underbrace{N_f b_i b_{i-1} E_p \gamma_1}_{sig_{SD}} \quad (4.135)$$

where, the pulse energy is represented as $E_p = \int_{jT_f+2iT_s}^{jT_f+2iT_s+T_i} p^2(t - jT_f - 2iT_s - \tau_{l_1}) dt$ and autocorrelation function as $R(\tau) = \int_{\infty}^{\infty} p(t)p(t - \tau)dt$. To overcome IPI, the assumption taken is $min\{(\tau_{l_1} - \tau_{m_1})\} > T_p$ for $l_1 \neq m_1$. Hence, $\sum_{l_1 \neq m_1} \sum \alpha_{l_1} \alpha_{m_1}$ $R(\tau_{l_1} - \tau_{m_1}) = 0$. As explained in Section 4.3.1, since a large number of UWB multipath channel gains are considered, the channel gains may be approximated as Gaussian Distributed using the Central Limit Theorem $\sum_{l_1} \alpha_{l_1}^2 = \gamma_1$. As described in Section 4.3.1, since the PSD $\theta_k(f)$ of noise is sufficiently flat, the autocorrelation function of noise can be simplified as $\theta_k(\tau) = \frac{N_0}{2}\delta(\tau)$[175]. Since $Z_2(1)$, $Z_3(1)$ and $Z_4(1)$ denote the noise terms, their variances are

solved as shown below.

$$
\begin{aligned}
Var(N_1) &= E[Z_2^2(1)] = \sum_{j=0}^{N_f-1}\Bigg[\int_{jT_f+2iT_s}^{jT_f+2iT_s+T_i}\int_{jT_f+2iT_s}^{jT_f+2iT_s+T_i}\Bigg(\sum_{l_1}\alpha_{l_1}b_i p(t-jT_f-2iT_s \\
&\quad -\tau_{l_1})\sum_{m_1}\alpha_{m_1}b_i p(\tau-jT_f-2iT_s-\tau_{m_1})\Bigg)\mathbb{E}[n_{SD}(t-T_s)n_{SD}(\tau-T_s)]dtd\tau\Bigg] \\
&= \sum_{j=0}^{N_f-1} b_i^2\Bigg[\int_{jT_f+2iT_s}^{jT_f+2iT_s+T_i}\int_{jT_f+2iT_s}^{jT_f+2iT_s+T_i}\Bigg(\sum_{l_1}\alpha_{l_1}p(t-jT_f-2iT_s-\tau_{l_1})\sum_{m_1}\alpha_{m_1} \\
&\quad p(\tau-jT_f-2iT_s-\tau_{m_1})\Bigg)\theta_1(t-\tau)dtd\tau\Bigg] \\
&= \frac{N_f N_0 b_i^2}{2}\Bigg[\int_{jT_f+2iT_s}^{jT_f+2iT_s+T_i}\sum_{l_1=m_1}\alpha_{l_1}^2 p^2(t-jT_f-2iT_s-\tau_{l_1})dt \\
&\quad \underbrace{+\sum_{l_1\neq m_1}\sum\alpha_{l_1}\alpha_{m_1}R(\tau_{l_1}-\tau_{m_1})\Bigg]}_{value=0} \\
&= \frac{N_f N_0 b_i^2 E_p}{2}\underbrace{\Bigg(\sum_{l_1}\alpha_{l_1}^2\Bigg)}_{value=\gamma_1} \\
&= \frac{N_f N_0 b_i^2 E_p\gamma_1}{2} \qquad (4.136)
\end{aligned}
$$

where, $\int_{jT_f+2iT_s}^{jT_f+2iT_s+T_i}\theta_1(t-\tau)d\tau = \int_{jT_f+2iT_s}^{jT_f+2iT_s+T_i}\frac{N_0}{2}\delta(t-\tau)d\tau = \frac{N_0}{2}$.

$$
\begin{aligned}
Var(N_2) &= E[Z_3^2(1)] = \sum_{j=0}^{N_f-1}\Bigg[\int_{jT_f+2iT_s}^{jT_f+2iT_s+T_i}\int_{jT_f+2iT_s}^{jT_f+2iT_s+T_i}\Bigg(\sum_{l_1}\alpha_{l_1}b_{i-1}p(t-jT_f-2iT_s \\
&\quad -\tau_{l_1})\sum_{m_1}\alpha_{m_1}b_{i-1}p(\tau-jT_f-2iT_s-\tau_{m_1})\Bigg)\mathbb{E}[\{n_{SD}(t)n_{SD}(\tau)\}]dtd\tau\Bigg] \\
&= \sum_{j=0}^{N_f-1} b_{i-1}^2\Bigg[\int_{jT_f+2iT_s}^{jT_f+2iT_s+T_i}\int_{jT_f+2iT_s}^{jT_f+2iT_s+T_i}\Bigg(\sum_{l_1}\alpha_{l_1}p(t-jT_f-2iT_s-\tau_{l_1})\sum_{m_1}\alpha_{m_1} \\
&\quad p(\tau-jT_f-2iT_s-\tau_{m_1})\Bigg)\theta_1(t-\tau)dtd\tau\Bigg] \\
&= \frac{N_f N_0 b_{i-1}^2}{2}\Bigg[\int_{jT_f+2iT_s}^{jT_f+2iT_s+T_i}\sum_{l_1=m_1}\alpha_{l_1}^2 p^2(t-jT_f-2iT_s-\tau_{l_1})dt \\
&\quad \underbrace{+\sum_{l_1\neq m_1}\sum\alpha_{l_1}\alpha_{m_1}R(\tau_{l_1}-\tau_{m_1})\Bigg]}_{value=0} \\
&= \frac{N_f N_0 b_{i-1}^2 E_p}{2}\underbrace{\Bigg(\sum_{l_1}\alpha_{l_1}^2\Bigg)}_{value=\gamma_1}
\end{aligned}
$$

$$= \frac{N_f N_0 b_{i-1}^2 E_p \gamma_1}{2} \tag{4.137}$$

$$\begin{aligned} Var(N_3) &= E[Z_4^2(1)] = \sum_{j=0}^{N_f-1} \Bigg[\int_{jT_f+2iT_s}^{jT_f+2iT_s+T_i} \int_{jT_f+2iT_s}^{jT_f+2iT_s+T_i} \\ &\quad \mathbb{E}\left[\{n_{SD}(t) n_{SD}(\tau - T_s)\}^2 \right] dt d\tau \Bigg] \\ &= \sum_{j=0}^{N_f-1} \Bigg[\int_{jT_f+2iT_s}^{jT_f+2iT_s+T_i} \int_{jT_f+2iT_s}^{jT_f+2iT_s+T_i} \theta_1^2(t-\tau) dt d\tau \Bigg] \\ &= \sum_{j=0}^{N_f-1} \Bigg[\int_{jT_f+2iT_s}^{jT_f+2iT_s+T_i} \int_{jT_f+2iT_s+T_i-t}^{jT_f+2iT_s+T_i} \theta_1^2(u) dt du \Bigg] \\ &= \sum_{j=0}^{N_f-1} \left[\int_0^{T_i} \frac{N_0^2}{4} 2W dt \right] \\ &= \frac{N_f N_0^2 W T_i}{2}. \end{aligned} \tag{4.138}$$

where, $E[n_k^2(t)] = \frac{N_0}{2}$. Hence, the value of $E[\{n_k^2(t)\}^2] = \frac{N_0^2}{4}$. The variance of $[n_k^2(t)]$ tends to a Dirac Delta function, where the integral vanishes outside the range $[-t, T_i - t]$. Parsevals theorem is applied to solve equation 4.141.

The SNR obtained at the relay node in 1st time slot is denoted as:

$$\begin{aligned} \rho_{DTR-SR-DTF} &= \frac{(N_f b_i b_{i-1} E_p \gamma_2)^2}{\frac{N_f N_0 E_p b_i^2 \gamma_2}{2} + \frac{N_f N_0 b_{i-1}^2 E_p \gamma_2}{2} + \frac{N_f N_0^2 W T_i}{2}} \\ &= \frac{(N_f E_p \gamma_2)^2}{N_f N_0 E_p \gamma_2 + \frac{N_f N_0^2 W T_i}{2}} \\ &= \frac{(E_b \gamma_2)^2}{N_0 E_b \gamma_2 + \frac{N_f N_0^2 W T_i}{2}}. \end{aligned} \tag{4.139}$$

where, $b_i^2 = b_{i-1}^2 = (b_i b_{i-1})^2 = 1$ and energy per bit is denoted as $E_b = N_f T_f$. An error occurs at the relay node if it detects an information bit $b_i^{'} = 0$, when information bit $b_i = 1$ is transmitted from source node to relay node. Hence, the probability of error obtained at the relay node is expressed as:

$$P_e = Q\left(\sqrt{\rho_{DTR-SR-DTF}} \right) f_{\rho_{DTF}}(\gamma_2) d\gamma_2 \tag{4.140}$$

where, the PDF of S$-$R link is expressed as $f_{\rho_{DTF}}(\gamma_2) = \frac{1}{\sqrt{(2\pi(\sigma_{SR}^2))}} \exp\left[\frac{-(\gamma_2 - \mu_{SR})^2}{2(\sigma_{SR}^2)} \right]$. Furthermore, μ_{SR} and σ_{SR}^2 denote the mean and variance of S$-$R link of UWB channel respectively.

After extraction of information bit $b_i^{'}$ at the relay node, the signal transmitted from the relay node to the destination node in 2nd time slot is represented as:

$$s_{DTR-RD}(t) = \sum_{i=0}^{\infty}\sum_{j=0}^{N_f-1}\left[b_i^{'}p(t-jT_f-(2i+1)T_s)\right] \tag{4.141}$$

where, $b_i^{'}$ represents the information bit detected at the relay node. The received signal $r_{DTR-RD}(t)$ obtained at the destination node in 2^{nd} time slot is represented as:

$$\begin{aligned} r_{DTR-RD}(t) &= s_{DTR-RD}(t) * h_3(t) \\ &= \sum_{i=0}^{\infty}\sum_{j=0}^{N_f-1}\left[b_i^{'}p(t-jT_f-(2i+1)T_s)] * \sum_{l_3}\alpha_{l_3}\delta(t-\tau_{l_3})\right] + n_{RD}(t) \\ &= \sum_{i=0}^{\infty}\sum_{j=0}^{N_f-1}\sum_{l_3}\left[\alpha_{l_3}b_i^{'}p(t-jT_f-(2i+1)T_s-\tau_{l_3})\right] + n_{RD}(t) \\ &= \sum_{i=0}^{\infty}\sum_{j=0}^{N_f-1}\left[b_i^{'}g_{RD}(t-jT_f-(2i+1)T_s)\right] + n_{RD}(t) \end{aligned} \tag{4.142}$$

The aggregate signal response $g_{RD}(t)$ obtained from R−D link is expressed as $g_{RD}(t) = \sum_{l_3}\alpha_{l_3}p(t-\tau_{l_3})$ whereas, the noise (AWGN) term is denoted by $n_{RD}(t)$. The received signal $r_{DTR-RD}(t)$ obtained at the destination node is demodulated using a DTR receiver, whose decision statistics Z_{DTR-RD} is expressed as:

$$\begin{aligned} Z_{DTR-RD} &= \sum_{j=0}^{N_f-1}\int_{(2i+1)T_s+jT_f}^{(2i+1)T_s+jT_f+T_i} r_{DTR-RD}(t)r_{DTR-RD}(t-T_s)dt \\ &= \underbrace{Z_1(3)}_{signal} + \underbrace{Z_2(3)+Z_3(3)+Z_4(3)}_{\text{noise}-term} \end{aligned} \tag{4.143}$$

where, it is assumed that correct detection has taken place at relay node. Replacing the value of equation 4.145 in equation 4.146, we obtain the value of Z_{DTR-RD} in equation 4.147.

$$\begin{aligned} = \sum_{j=0}^{N_f-1}\int_{jT_f+(2i+1)T_s}^{jT_f+(2i+1)T_s+T_i} &\left(\left[\sum_{l_3}\alpha_{l_3}b_i^{'}p(t-jT_f-(2i+1)T_s-\tau_{l_3})\right]+n_{RD}(t)\right)\left(\left[\sum_{m_3}\right.\right. \\ &\left.\left.\alpha_{m_3}b_{i-1}^{'}p(t-jT_f-(2i+1)T_s-\tau_{m_3})\right]+n_{RD}(t-T_s)\right) \end{aligned} \tag{4.144}$$

The signal term sig_{RD} obtained from R−D link is represented as:

$$\begin{aligned} Z_1(3) = \sum_{j=0}^{N_f-1}\Bigg[\int_{jT_f+(2i+1)T_s}^{jT_f+(2i+1)T_s+T_i} &\left(\sum_{l_3}\alpha_{l_3}b_i^{'}p(t-jT_f-(2i+1)T_s-\tau_{l_3})\sum_{m_3}\alpha_{m_3}b_{i-1}^{'}p(t\right. \\ &\left.-jT_f-(2i+1)T_s-\tau_{m_3})\right)dt\Bigg] \end{aligned}$$

$$
\begin{aligned}
&= N_f b_i^{'} b_{i-1}^{'} \Bigg[\int_{jT_f+(2i+1)T_s}^{jT_f+(2i+1)T_s+T_i} \sum_{l_3=m_3} \alpha_{l_3}^2 p^2(t-jT_f-2iT_s-\tau_{l_3})dt \\
&\quad + \underbrace{\sum_{l_3 \neq m_3} \sum \alpha_{l_3}\alpha_{m_3} R(\tau_{l_3}-\tau_{m_3})}_{value=0} \Bigg] \\
&= N_f b_i^{'} b_{i-1}^{'} E_p \underbrace{\left(\sum_{l_3} \alpha_{l_3}^2 \right)}_{value=\gamma_3} \\
&= \underbrace{N_f b_i^{'} b_{i-1}^{'} E_p \gamma_3}_{sig_{RD}} . \qquad (4.145)
\end{aligned}
$$

where, the energy of pulse is represented as $E_p = \int_{jT_f+2iT_s}^{jT_f+2iT_s+T_i} p^2(t-jT_f-2iT_s-\tau_{l_3})dt$ and autocorrelation function as $R(\tau) = \int_{\infty}^{\infty} p(t)p(t-\tau)dt$. To avoid IPI, this condition $min\{(\tau_{l_3}-\tau_{m_3})\} > T_p$ for $l_3 \neq m_3$, is satisfied. Hence, $\sum_{l_3 \neq m_3} \sum \alpha_{l_3}\alpha_{m_3} R(\tau_{l_3}-\tau_{m_3}) = 0$. As explained in Section 4.3.1, since a large number of UWB multipath channel gains are considered, channel gains can be approximated as Gaussian Distributed using the Central Limit Theorem $\sum_{l_3} \alpha_{l_3}^2 = \gamma_3$. As described in Section 4.3.1, the PSD of noise $\theta_k(f)$ is sufficiently flat so the autocorrelation function can be simplified as $\theta_k(\tau) = \frac{N_0}{2}\delta(\tau)$ [175]. The index $k \in \{1,2,3\}$ represents S−D, S−R and R−D link respectively, as discussed in equation 4.5. To solve the decision variables $Z_2(3)$, $Z_3(3)$ and $Z_4(3)$ containing the noise terms, variances is evaluated as shown below.

$$
\begin{aligned}
Var(N_1) &= E[Z_2^2(3)] = \sum_{j=0}^{N_f-1} \Bigg[\int_{jT_f+(2i+1)T_s}^{jT_f+(2i+1)T_s+T_i} \int_{jT_f+(2i+1)T_s}^{jT_f+(2i+1)T_s+T_i} \Bigg(\sum_{l_3} \alpha_{l_3} b_i^{'} p(t-jT_f- \\
&\quad (2i+1)T_s-\tau_{l_3}) \sum_{m_3} \alpha_{m_3} b_i^{'} p(\tau-jT_f-(2i+1)T_s-\tau_{m_3}) \Bigg) E[n_{RD}(t-T_s) \\
&\quad n_{RD}(\tau-T_s)]dtd\tau \Bigg] \\
&= \sum_{j=0}^{N_f-1} \Bigg[\int_{jT_f+(2i+1)T_s}^{jT_f+(2i+1)T_s+T_i} \Bigg(\sum_{l_3} \alpha_{l_3} b_i^{'} p(t-jT_f-(2i+1)T_s-\tau_{l_3}) \sum_{m_3} \alpha_{m_3} b_i^{'} p(\tau \\
&\quad -jT_f-(2i+1)T_s-\tau_{m_3}) \Bigg) \theta_3(t-\tau)dtd\tau \Bigg] \\
&= \frac{N_f N_0 b_i^{'^2}}{2} \Bigg[\int_{jT_f+(2i+1)T_s}^{jT_f+(2i+1)T_s+T_i} \sum_{l_3=m_3} \alpha_{l_3}^2 p^2(t-jT_f-(2i+1)T_s-\tau_{l_3})dt \\
&\quad + \underbrace{\sum_{l_3 \neq m_3} \sum \alpha_{l_3}\alpha_{m_3} R(\tau_{l_3}-\tau_{m_3})}_{value=0} \Bigg]
\end{aligned}
$$

$$= \frac{N_f N_0 b_i^{'2} E_p}{2} \underbrace{\left(\sum_{l_3} \alpha_{l_3}^2 \right)}_{value=\gamma_3}$$
$$= \frac{N_f N_0 b_i^{'2} E_p \gamma_3}{2} \tag{4.146}$$

where, $\mathbb{E}[n_{RD}(t) n_{RD}(\tau)] = \theta_3(t-\tau) = \frac{N_0}{2}\delta(t-\tau)$ and $\int_{(2i+1)T_s+jT_f}^{(2i+1)T_s+jT_f+T_i} \frac{N_0}{2}\delta(t-\tau)d\tau = \frac{N_0}{2}$.

$$\begin{aligned}
Var(N_2) &= E[Z_3^2(3)] = \sum_{j=0}^{N_f-1} \Bigg[\int_{jT_f+(2i+1)T_s}^{jT_f+(2i+1)T_s+T_i} \int_{jT_f+(2i+1)T_s}^{jT_f+(2i+1)T_s+T_i} \Bigg(\sum_{l_3} \alpha_{l_3} b_{i-1}^{'} p(t - jT_f - \\
&\quad (2i+1)T_s - \tau_{l_3}) \sum_{m_3} \alpha_{m_3} b_{i-1}^{'} p(\tau - jT_f - (2i+1)T_s - \tau_{m_3}) \Bigg) E[n_{RD}(t) n_{RD}(\tau)] \\
&\quad dt d\tau \Bigg] \\
&= \sum_{j=0}^{N_f-1} b_{i-1}^{'2} \Bigg[\int_{jT_f+(2i+1)T_s}^{jT_f+(2i+1)T_s+T_i} \int_{jT_f+(2i+1)T_s}^{jT_f+(2i+1)T_s+T_i} \Bigg(\sum_{l_3} \alpha_{l_3} p(t - jT_f - (2i+1)T_s \\
&\quad - \tau_{l_3}) \sum_{m_3} \alpha_{m_3} p(\tau - jT_f - (2i+1)T_s - \tau_{m_3}) \Bigg) \theta_3(t-\tau) dt d\tau \Bigg] \\
&= \frac{N_f N_0 b_{i-1}^{'2}}{2} \Bigg[\int_{jT_f+(2i+1)T_s}^{jT_f+(2i+1)T_s+T_i} \sum_{l_3=m_3} \alpha_{l_3}^2 p^2(t - jT_f - (2i+1)T_s - \tau_{l_3}) dt \\
&\quad + \underbrace{\sum_{l_3 \neq m_3} \sum \alpha_{l_3} \alpha_{m_3} R(\tau_{l_3} - \tau_{m_3})}_{value=0} \Bigg] \\
&= \frac{N_f N_0 b_{i-1}^{'2} E_p}{2} \underbrace{\left(\sum_{l_3} \alpha_{l_3}^2 \right)}_{value=\gamma_3} \\
&= \frac{N_f N_0 b_{i-1}^{'2} E_p \gamma_3}{2}
\end{aligned} \tag{4.147}$$

$$\begin{aligned}
Var(N_3) &= E[Z_4^2(3)] = \sum_{j=0}^{N_f-1} \Bigg[\int_{jT_f+(2i+1)T_s}^{jT_f+(2i+1)T_s+T_i} \int_{jT_f+(2i+1)T_s}^{jT_f+(2i+1)T_s+T_i} \\
&\quad \mathbb{E}\left[\{n_{RD}(t) n_{RD}(\tau - T_s)\}^2 \right] dt d\tau \Bigg] \\
&= \sum_{j=0}^{N_f-1} \left[\int_{jT_f+(2i+1)T_s}^{jT_f+(2i+1)T_s+T_i} \int_{jT_f+(2i+1)T_s}^{jT_f+(2i+1)T_s+T_i} \theta_3^2(t-\tau) dt d\tau \right] \\
&= \sum_{j=0}^{N_f-1} \left[\int_{jT_f+(2i+1)T_s}^{jT_f+(2i+1)T_s+T_i} \int_{jT_f+(2i+1)T_s+T_i-t}^{jT_f+(2i+1)T_s+T_i} \theta_3^2(u) dt du \right]
\end{aligned}$$

$$
\begin{aligned}
&= \sum_{j=0}^{N_f-1}\left[\int_0^{T_i}\frac{N_0^2}{4}2W\,dt\right] \\
&= \frac{N_f N_0^2 W T_i}{2}.
\end{aligned} \tag{4.148}
$$

The value of $E[\{n_k^2(t)\}^2] = E[\{n_{RD}^2(t)\}^2] = \frac{N_0^2}{4}$. As discussed before in Section 4.3.1, the variance of $[n_k^2(t)]$ tends to a Dirac Delta function, where the integral vanishes outside the range $[-t, T_i - t]$. Parsevals theorem is then applied to solve equation 4.151.

The decision statistic Z_{DTR-SD} obtained from destination node contains signal term $sig_{SD} = Z_1(1) = N_f E_p b_i b_{i-1}\gamma_1$ and noise term $Z_{noise-SD} = Z_2(1) + Z_3(1) + Z_4(1)$ in 1st time slot. The noise term $Z_{noise-SD}$ has a total variance of $\sigma^2_{Z_{noise-SD}} = \sigma^2_{N_1} + \sigma^2_{N_2} + \sigma^2_{N_3} = \frac{N_f N_0 b_i^2 E_p\gamma_1}{2} + \frac{N_f N_0 b_{i-1}^2 E_p\gamma_1}{2} + \frac{N_f N_0^2 W T_i}{2}$. Similarly, the decision statistic Z_{DTR-RD} obtained from destination node contains signal term $sig_{RD} = Z_1(3) = N_f E_p b_i' b_{i-1}'\gamma_3$ and noise term $Z_{noise-RD} = Z_2(3) + Z_3(3) + Z_4(3)$ in 2nd time slot. The noise term $Z_{noise-RD}$ has a total variance of $\sigma^2_{Z_{noise-RD}} = \sigma^2_{N_1} + \sigma^2_{N_2} + \sigma^2_{N_3} = \frac{N_f N_0 b_i'^2 E_p\gamma_3}{2} + \frac{N_f N_0 b_{i-1}'^2 E_p\gamma_3}{2} + \frac{N_f N_0^2 W T_i}{2}$.

In case of correct detection, the SNR obtained at the destination node from S−D and R−D links in 1st and 2nd time slots respectively, are represented as:

$$
\begin{aligned}
\rho_{SD-DTF} &= \frac{sig_{SD}^2}{\sigma^2_{Z_{noise-SD}}} \\
&= \frac{(N_f E_p b_i b_{i-1}\gamma_1)^2}{\frac{N_f N_0 b_i^2 E_p\gamma_1}{2} + \frac{N_f N_0 b_{i-1}^2 E_p\gamma_1}{2} + \frac{N_f N_0^2 W T_i}{2}} \\
&= \frac{(N_f E_p b_i^2\gamma_1)^2}{N_f N_0 E_p b_{i-1}^2\gamma_1 + \frac{N_f N_0^2 W T_i}{2}} \\
&= \frac{(E_b\gamma_1)^2}{N_0 E_b\gamma_1 + \frac{N_f N_0^2 W T_i}{2}}
\end{aligned} \tag{4.149}
$$

$$
\begin{aligned}
\rho_{RD-DTF} &= \frac{sig_{RD}^2}{\sigma^2_{Z_{noise-RD}}} \\
&= \frac{(N_f E_p b_i' b_{i-1}'\gamma_3)^2}{\frac{N_f N_0 E_p b_i'^2\gamma_3}{2} + \frac{N_f N_0 b_{i-1}'^2 E_p\gamma_3}{2} + \frac{N_f N_0^2 W T_i}{2}} \\
&= \frac{(N_f E_p b_i' b_{i-1}'\gamma_3)^2}{N_f N_0 E_p\gamma_3 + \frac{N_f N_0^2 W T_i}{2}} \\
&= \frac{(E_b\gamma_3)^2}{N_0 E_b\gamma_3 + \frac{N_f N_0^2 W T_i}{2}}
\end{aligned} \tag{4.150}
$$

where, $b_i = b_i' = 1$ in case of correct detection. For a DTR−PAM system, $b_i^2 = b_{i-1}^2 = (b_i b_{i-1})^2 = b_i'^2 = b_{i-1}'^2 = (b_i' b_{i-1}')^2 = 1$ and $E_b = N_f E_p$. Hence, information bit $b_i' = 1$ is

forwarded from the relay to destination node in 2nd time slot. The decision statistics obtained at the destination node in the end of two time slots are combined using linear diversity combining, selective diversity combining and optimum linear diversity combining to form the final decision statistic. The derivations of the same are explained in subsequent sections.

A. Linear Combining

i) *Correct Detection at Relay Node*: The decision statistics Z_{DTR-SD} and Z_{DTR-RD} obtained at the destination node in the 1st and 2nd time slots respectively, are linearly combined to give $Z_{total} = Z_{DTR-SD} + Z_{DTR-RD} = s_{total-signal} + Z_{noise-total}$, as mentioned in equation 4.72. The individual decision statistics obtained from S−D and R−D links are mentioned in equation 4.70 and 4.71, respectively. The total noise variance $\sigma^2_{Z_{noise-total}} = \sigma^2_{Z_{noise-SD}} + \sigma^2_{Z_{noise-RD}}$ corresponding to the noise term $Z_{noise-total}$ is solved in equation 4.33.

In case of correct detection, the relay node correctly detects the information bit transmitted from the source node. Thus, $b_i^{'} = 1$ is received at the relay node, when information bit ($b_i = 1$) is transmitted from the source node to the relay node. The correctly detected bit $b_i^{'} = 1$ is then forwarded to the destination node. Subsequently, the SNR at destination node due to correct detection is represented as:

$$\begin{aligned} \rho_{DTF-LC-CD} &= \left(\frac{s^2_{total-signal}}{\sigma^2_{Z_{noise-total}}}\right) = \frac{(sig_{SD} + sig_{RD})^2}{(\sigma^2_{Z_{noise-SD}} + \sigma^2_{Z_{noise-RD}})} \\ &= \frac{(N_f E_p \gamma_1 + N_f E_p \gamma_3)^2}{N_f N_0 E_p \gamma_1 + N_f N_0 E_p \gamma_3 + N_f N_0^2 W T_i} \\ &= \frac{(E_b \gamma_1 + E_b \gamma_3)^2}{N_0 E_b \gamma_1 + N_0 E_b \gamma_3 + N_f N_0^2 W T_i} \end{aligned} \tag{4.151}$$

The final decision statistic is compared to a threshold, to obtain the information bit. The decision threshold is 0, because PAM modulation scheme is used. Hence, the final decision criteria $\hat{z}$ can be expressed as:

$$\hat{z} = \begin{cases} 0, & H_0 : Z = Z_{total} = Z_{DTR-SD} + Z_{DTR-RD} \leq 0 \\ 1, & H_1 : Z = Z_{total} = Z_{DTR-SD} + Z_{DTR-RD} > 0 \end{cases} \tag{4.152}$$

ii) *Incorrect Detection at Relay Node*: In case of incorrect detection, the relay node detects information bit $b_i^{'} = 0$, when information bit ($b_i = 1$) is transmitted from the source node to the relay node. The erroneously detected bit $b_i^{'} = 0$ is forwarded to the destination node. Following the same procedure as mentioned in the previous subsection, the SNR obtained at the

destination node due to incorrect detection is represented as:

$$\begin{aligned}\rho_{DTF-LC-ID} &= \frac{(sig_{SD})^2}{(\sigma^2_{Z_{noise-SD}} + \sigma^2_{Z_{noise-RD}})} \\ &= \frac{(N_f E_p \gamma_1)^2}{N_f N_0 E_p \gamma_1 + N_f N_0 E_p \gamma_3 + N_f N_0^2 W T_i} \\ &= \frac{(E_b \gamma_1)^2}{N_0 E_b \gamma_1 + N_0 E_b \gamma_3 + N_f N_0^2 W T_i} \end{aligned} \tag{4.153}$$

Using probability theory, the generalized BER in case of incorrect detection is calculated as:

$$BER = \int_0^\infty \int_0^\infty Q\left(\frac{sig_{SD} - sig_{RD}}{2\sqrt{\sigma^2_{Z_{noise-total}}}}\right) f_{\rho_{DTF}}(\gamma_1, \gamma_3) d\gamma_1 d\gamma_3 \tag{4.154}$$

Due to incorrect detection at relay node, information bit received at destination node through (R−D) link is 0, when information bit 1 is transmitted from source node to relay node. Therefore, $sig_{RD} = 0$.

$$= \int_0^\infty \int_0^\infty Q\left(\frac{sig_{SD}}{2\sqrt{(\sigma^2_{Z_{noise-SD}} + \sigma^2_{Z_{noise-RD}})}}\right) f_{\rho_{DTF}}(\gamma_1, \gamma_3) d\gamma_1 d\gamma_3 \tag{4.155}$$

As explained in Section 4.3.1, The individual channel gains for S−D, S−R and R−D channel links may be assumed to be IID Gaussian distributed by applying Central Limit Theorem, since a large number paths are involved. Therefore, the sum of these channel gains will also have a Gaussian distribution with its mean being the sum of individual means and variance being sum of the individual variances. The joint PDF $f_{\rho_{AF}}(\gamma_1, \gamma_3)$ of the channel in case of linear combining is represented as:

$$\begin{aligned} f_{\rho_{DTF}}(\gamma_1, \gamma_3) &= \frac{1}{\sqrt{(2\pi(\sigma^2_{SD}))}} \frac{1}{\sqrt{(2\pi(\sigma^2_{RD}))}} \exp\left[\frac{-(\gamma_1 - \mu_{SD})^2}{2\sigma^2_{SD}} + \frac{-(\gamma_3 - \mu_{RD})^2}{2\sigma^2_{RD}}\right] \\ & d\gamma_1 d\gamma_3 \end{aligned} \tag{4.156}$$

Therefore, the final BER of UWB DTR system using linear combining is expressed as:

$$\begin{aligned} BER_{LC-DTF} &= \int_0^\infty \int_0^\infty \left(Q\left(\sqrt{\rho_{DTF-LC-CD}}\right) f_{\rho_{DTF}}(\gamma_1, \gamma_3) d\gamma_1 d\gamma_3\right)(1 - P_e) + \\ & \int_0^\infty \int_0^\infty \left(Q\left(\sqrt{\rho_{DTF-LC-ID}}\right) f_{\rho_{DTF}}(\gamma_1, \gamma_3) d\gamma_1 d\gamma_3\right)(P_e) \\ &= \int_0^\infty \int_0^\infty \left(Q\left(\sqrt{\rho_{DTF-LC-CD}}\right) f_{\rho_{DTF}}(\gamma_1) f_{\rho_{DTF}}(\gamma_3) d\gamma_1 d\gamma_3\right)(1 - P_e) + \\ & \int_0^\infty \int_0^\infty \left(Q\left(\sqrt{\rho_{DTF-LC-ID}}\right) f_{\rho_{DTF}}(\gamma_1) f_{\rho_{DTF}}(\gamma_3) d\gamma_1 d\gamma_3\right)(P_e) \end{aligned} \tag{4.157}$$

Since the joint PDF is IID distributed, it can be represented as $f_{\rho_{DTF}}(\gamma_1, \gamma_3) = f_{\rho_{DTF}}(\gamma_1)$ $f_{\rho_{DTF}}(\gamma_3)$.

Replacing the value of equation 4.159 in equation 4.160, we obtain the BER in equation 4.161. Therefore, the BER of UWB DTR system using cooperative dual−hop DTF strategy with linear combining is represented as:

$$\begin{aligned} = & \int_0^\infty \int_0^\infty \left(Q\left(\sqrt{\rho_{DTF-LC-CD}} \right) \frac{1}{2\pi\sqrt{(\sigma_{SD}^2 \sigma_{RD}^2)}} \exp\left[\frac{-(\gamma_1 - \mu_{SD})^2}{2\sigma_{SD}^2} + \frac{-(\gamma_3 - \mu_{RD})^2}{2\sigma_{RD}^2} \right] \right. \\ & \left. d\gamma_1 d\gamma_3 \right)(1 - P_e) + \int_0^\infty \int_0^\infty \left(Q\left(\sqrt{\rho_{DTF-LC-ID}} \right) \frac{1}{2\pi\sqrt{(\sigma_{SD}^2 \sigma_{RD}^2)}} \exp \right. \\ & \left. \left[\frac{-(\gamma_1 - \mu_{SD})^2}{2\sigma_{SD}^2} + \frac{-(\gamma_3 - \mu_{RD})^2}{2\sigma_{RD}^2} \right] d\gamma_1 d\gamma_3 \right)(P_e) \end{aligned} \tag{4.158}$$

B. Selective Combining

(i) *Correct Detection at Relay Node*: In selective combining, the SNR obtained at the destination node from S−D and R−D links in 1st and 2nd time slots respectively are compared, and the one with the highest SNR is chosen. The probability of selecting the channel link based on the highest SNR is evaluated after integrating the joint PDF of the channel links with proper limits. The joint PDF of channel links S−D and R−D is represented as:

$$f(x, y) = \frac{1}{2\pi\sigma_{SD}\sigma_{RD}} \exp - \left[\frac{(x - \mu_{SD})^2 + (y - \mu_{RD})^2}{2\sigma_{SD}\sigma_{RD}} \right] \tag{4.159}$$

where, x and y represent independent gaussian random variables with means μ_{SD}, μ_{RD} and variances σ_{SD}^2, σ_{RD}^2 of S−D and R−D channel links respectively. Hence, the probability that S−D channel link is selected is represented as:

$$P_1 = f(x) = \int_{-\infty}^{\infty} \int_{y}^{\infty} f(x, y) dx dy \tag{4.160}$$

Therefore, the probability of selecting R−D channel link is $P_3 = 1 - P_1$.

ii)*Incorrect Detection at relay node*: In case of incorrect detection, information bit $b_i' = 0$ is detected at the relay node, when information bit $b_i = 1$ is transmitted from source node to relay node. In the next time slot, this erroneously detected bit $b_i' = 0$ is forwarded to the destination node from the relay node. The final BER of UWB DTR system using cooperative dual−hop DTF strategy with selective combining is represented as:

$$\begin{aligned} BER_{SC-DTF} = & \left(P_1 \int_0^\infty Q\left(\sqrt{\rho_{SD-DTF}} \right) f_{\rho_{DTF}}(\gamma_1) d\gamma_1 + P_3 \int_0^\infty Q\left(\sqrt{\rho_{RD-DTF}} \right) \right. \\ & \left. f_{\rho_{DTF}}(\gamma_3) d\gamma_3 \right)(1 - P_e) + \left(P_1 \int_0^\infty Q\left(\sqrt{\rho_{SD-DTF}} \right) \right) f_{\rho_{DTF}}(\gamma_1) d\gamma_1 \end{aligned}$$

$$+P_3\int_0^{\infty}\left(1-Q\left(\frac{1}{2}\sqrt{\rho_{RD-DTF}}\right)\right)f_{\rho_{DTF}}(\gamma_3)d\gamma_3\Bigg)P_e \tag{4.161}$$

$$\begin{aligned}=\ &\left(P_1\int_0^{\infty}Q\left(\sqrt{\rho_{SD-DTF}}\right)\frac{1}{\sqrt{(2\pi(\sigma_{SD}^2))}}\exp\left[\frac{-(\gamma_1-\mu_{SD})^2}{2\sigma_{SD}^2}\right]d\gamma_1+P_3\int_0^{\infty}\right.\\ &\left.Q\left(\sqrt{\rho_{RD-DTF}}\right)\frac{1}{\sqrt{(2\pi(\sigma_{RD}^2))}}\exp\left[\frac{-(\gamma_3-\mu_{RD})^2}{2\sigma_{RD}^2}\right]d\gamma_3\right)(1-P_e)+\left(P_1\int_0^{\infty}\right.\\ &Q\left(\sqrt{\rho_{SD-DTF}}\right)\frac{1}{\sqrt{(2\pi(\sigma_{SD}^2))}}\exp\left[\frac{-(\gamma_1-\mu_{SD})^2}{2\sigma_{SD}^2}\right]d\gamma_1+P_3\int_0^{\infty}\\ &\left.\left(1-Q\left(\sqrt{\rho_{RD-DTF}}\right)\right)\frac{1}{\sqrt{(2\pi(\sigma_{RD}^2))}}\exp\left[\frac{-(\gamma_3-\mu_{RD})^2}{2\sigma_{RD}^2}\right]d\gamma_3\right)(P_e)\end{aligned} \tag{4.162}$$

where, $f_{\rho_{DTF}}(\gamma_1)=\frac{1}{\sqrt{(2\pi(\sigma_{SD}^2))}}\exp\left[\frac{-(\gamma_1-\mu_{SD})^2}{2\sigma_{SD}^2}\right]$ and $f_{\rho_{DTF}}(\gamma_3)=\frac{1}{\sqrt{(2\pi(\sigma_{RD}^2))}}\exp\left[\frac{-(\gamma_3-\mu_{RD})^2}{2\sigma_{RD}^2}\right]$ represent the PDF of S$-$D and R$-$D channel links respectively.

C. Optimum Linear Combining

(i) *Correct Detection at Relay Node*: The decision statistics obtained at the destination node from S$-$D and R$-$D links in 1st and 2nd time slots respectively, are optimally combined to give final decision statistic $Z_{total}=Z_{DTR-SD}+\kappa Z_{DTR-RD}$. The optimal combining factor κ has a value of $\kappa=\frac{(\sigma^2_{Z_{noise-SD}})s_{RD}}{(\sigma^2_{Z_{noise-RD}})s_{SD}}$ as solved in equation C.4 of Appendix C. The final decision statistic Z_{total} obtained at the destination node using optimum linear combining is represented by equation 4.81.

The SNR evaluated at the destination node due to optimum linear combining is represented as:

$$\begin{aligned}\rho_{DTF-LOC-CD}&=\left(\frac{s^2_{total-signal}}{\sigma^2_{Z_{noise-total}}}\right)\\ &=\left(\frac{(sig_{SD}+\kappa sig_{RD})^2}{\sigma^2_{Z_{noise-SD}}+\kappa^2\sigma^2_{Z_{noise-RD}}}\right)\\ &=\frac{(N_fE_p\gamma_1+\kappa N_fE_p\gamma_3)^2}{(N_fN_0E_p\gamma_1+\frac{N_fN_0^2WT_i}{2})+\kappa^2(N_fN_0E_p\gamma_3+\frac{N_fN_0^2WT_i}{2})}\\ &=\frac{(E_b\gamma_1+\kappa E_b\gamma_3)^2}{(N_0E_b\gamma_1+\frac{N_fN_0^2WT_i}{2})+\kappa^2(N_0E_b\gamma_3+\frac{N_fN_0^2WT_i}{2})}=\frac{(E_b\gamma_1+\kappa E_b\gamma_3)^2}{X_1+\kappa^2Y_1}\end{aligned} \tag{4.163}$$

where, $X_1=N_0E_b\gamma_1+\frac{N_fN_0^2WT_i}{2}$ and $Y_1=N_0E_b\gamma_3+\frac{N_fN_0^2WT_i}{2}$. Also, $b_i=b_i'=1$ in case of correct detection.

The final decision statistic is compared to the decision threshold 0, in order to extract the information bit. The final decision criteria $\hat{z}$ can be expressed as:

$$\hat{z} = \begin{cases} 0, & H_0 : Z = Z_{total} = Z_{DTR-SD} + \kappa Z_{DTR-RD} \leq 0 \\ 1, & H_1 : Z = Z_{total} = Z_{DTR-SD} + \kappa Z_{DTR-RD} > 0 \end{cases} \tag{4.164}$$

ii) *Incorrect Detection at Relay Node*: In case of incorrect detection, the relay node detects information bit $b_i^{'} = 0$ when $b_i = 1$ is transmitted from source to relay node. Further, this incorrectly detected bit is forwarded to destination node, leading to BER degradation. The SNR obtained at the destination node due to incorrect detection is represented as:

$$\begin{aligned} \rho_{DTF-LOC-ID} &= \frac{(sig_{SD})^2}{(\sigma^2_{Z_{noise-SD}} + \kappa^2 \sigma^2_{Z_{noise-RD}})} \\ &= \frac{(N_f E_p \gamma_1)^2}{(N_f N_0 E_p \gamma_1 + \frac{N_f N_0^2 W T_i}{2}) + \kappa^2 (N_f N_0 E_p \gamma_3 + \frac{N_f N_0^2 W T_i}{2})} \\ &= \frac{(E_b \gamma_1)^2}{(N_0 E_b \gamma_1 + \frac{N_f N_0^2 W T_i}{2}) + \kappa^2 (N_0 E_b \gamma_3 + \frac{N_f N_0^2 W T_i}{2})} \end{aligned} \tag{4.165}$$

Using probability theory, the generalized BER in case of incorrect detection is expressed as:

$$BER = \int_0^\infty \int_0^\infty Q\left(\frac{sig_{SD} - \kappa sig_{RD}}{2\sqrt{\sigma^2_{Z_{noise-total}}}}\right) f_{\rho_{DTF}}(\gamma_1, \gamma_3) d\gamma_1 d\gamma_3 \tag{4.166}$$

Due to incorrect detection at relay node, information bit received at destination node (R$-$D link) is 0, when information bit 1 is transmitted from source node to relay node. Therefore, $sig_{RD} = 0$.

$$= \int_0^\infty \int_0^\infty Q\left(\frac{sig_{SD}}{2\sqrt{(\sigma^2_{Z_{noise-SD}} + \kappa^2 \sigma^2_{Z_{noise-RD}})}}\right) f_{\rho_{DTF}}(\gamma_1, \gamma_3) d\gamma_1 d\gamma_3 \tag{4.167}$$

Finally, the BER obtained at the destination node using optimum linear combining is represented as:

$$\begin{aligned} BER_{LOC-DTF} &= \int_0^\infty \int_0^\infty \left(Q\left(\sqrt{\rho_{DTF-LOC-CD}}\right) f_{\rho_{DTF}}(\gamma_1, \gamma_3) d\gamma_1 d\gamma_3\right)(1 - P_e) + \\ &\quad \int_0^\infty \int_0^\infty \left(Q\left(\sqrt{\rho_{DTF-LOC-ID}}\right) f_{\rho_{DTF}}(\gamma_1, \gamma_3) d\gamma_1 d\gamma_3\right)(P_e) \\ &= \int_0^\infty \int_0^\infty \left(Q\left(\sqrt{\rho_{DTF-LOC-CD}}\right) f_{\rho_{DTF}}(\gamma_1) f_{\rho_{DTF}}(\gamma_3) d\gamma_1 d\gamma_3\right) \\ &\quad (1 - P_e) + \int_0^\infty \int_0^\infty \\ &\quad \left(Q\left(\sqrt{\rho_{DTF-LOC-ID}}\right) f_{\rho_{DTF}}(\gamma_1) f_{\rho_{DTF}}(\gamma_3) d\gamma_1 d\gamma_3\right)(P_e) \end{aligned} \tag{4.168}$$

where, $f_{\rho_{DTF}}(\gamma_1, \gamma_3) = f_{\rho_{DTF}}(\gamma_1) f_{\rho_{DTF}}(\gamma_3)$ because the channel gains are IID and gaussian distributed.

4.5 Simulation Results

The BER performance of non−coherent UWB cooperative systems namely TR and DTR, were obtained using regenerative and non−regenerative relay strategies for various diversity combining schemes, over IEEE 802.15.4a UWB CM1 and CM2 channels respectively. The analytical BER expressions for UWB TR and DTR communication system, using cooperative dual-hop relay techniques for various diversity combining schemes, is plotted using numerical integration, and then compared with the simulation results. The main parameters considered for simulations are $N_f = 1, 2$, $N = 200000$, $W = 2\ GHz$, $T_i = 4\ ns$ and $F_{samp} = 10\ GHz$, where N_f represents the number of frames in one symbol, N the number of bits, W the bandwidth of bandpass filter, T_i the integration interval and F_{samp} the sampling frequency. A second order Gaussian derivative pulse $p(t) = 1 \times (1-4\pi((t)/T_k)^2)exp(-2\pi((t)/T_k)^2)$ is used for transmission, where t denotes the time interval and $T_k = 0.15\ ns$ the pulse width control factor. The values of means μ_k, and variances σ_k^2 obtained from UWB CM1 channel are noted to be 12.5 dB and 3.5 dB respectively. Here, the index $k \in \{1, 2, 3\}$ refers to the S−D, S−R and R−D link respectively.

Fig 4.3(a) and (b) represents the BER performance of UWB TR system, using cooperative dual−hop AF strategy, with various diversity combining schemes namely, optimum linear combining, linear combining and selective combining, in IEEE 802.15.4a UWB CM1 environment, for $N_f = 1$ and 2 respectively. It can be observed from both the BER plots in the Figures that using cooperative AF scheme gives a much better BER performance, compared to non−cooperative or single−link. Among the diversity combining schemes, Optimum Linear Combining gives the best BER performance followed by Linear Combining and then Selective Combining, for any SNR. It is also inferred from Fig 4.3(a) and (b) that SNR falls by a margin of $3 - 4\ dB$, as N_f increases from 1 to 2. This leads to degradation in BER performance.

The variation in BER vs SNR plot of UWB TR system using cooperative dual−hop AF strategy with various combining schemes, over IEEE 802.15.4a UWB CM2 environment for $N_f = 1$ and 2, can be inferred from Fig 4.4(a) and (b) respectively. At a BER of 10^{-4}, a NLOS channel (CM2), suffers a SNR loss of $3 - 4\ dB$, compared to LOS environment (CM1), as observed in Fig 4.3(a) and (b). It can also be concluded from both the BER plots in Figures that as far as combining schemes are concerned, Optimum Linear Combining $>$ Linear Combining $>$ Selective Combining $>$ Single−Link. The BER performance degrades, as SNR falls by a margin of $3 - 4\ dB$ for increase in N_f from 1 to 2, as observed in Fig 4.4(a) and (b).

The analytical and simulated BER performance of UWB TR system using dual−hop cooperative AF strategy in UWB CM1 environment, for three diversity combining schemes, (a) optimum linear diversity combining (b) linear diversity combining and (c) selective diversity combining is compared, and the results are as shown in Fig 4.5. The approximate analytical BER expressions for these three diversity combining cases are plotted using numerical integration, and compared with the simulation results for $N_f = 1, 2$. It can be inferred from Fig 4.5(a), (b) and (c) that the simulation plots nearly coincide with the plot of analytical results, at all BER.

The BER performance of UWB DTR system using cooperative dual−hop AF strategy with various diversity combining schemes namely, optimum linear combining, linear combining and selective combining, in IEEE 802.15.4a UWB CM1 environment, for $N_f = 1$ and 2 respectively, is as shown in Fig 4.6(a) and (b). It is observed that the performance of DTR system improves by a SNR margin of $4\ dB$ for $N_f = 1, 2$, at all BER levels. This is because, TR system wastes its energy in transmitting a reference pulse which carries no information whereas, DTR system transmits a differentially modulated signal over the present frame, saving energy. Among the diversity combining schemes, Optimum Linear Combining gives the best BER performance followed by Linear Combining and then Selective Combining, for any SNR. It is also inferred from Fig 4.6(a) and (b) that SNR falls by a margin of $3\ dB$, as N_f increases from 1 to 2. This leads to degradation in BER performance.

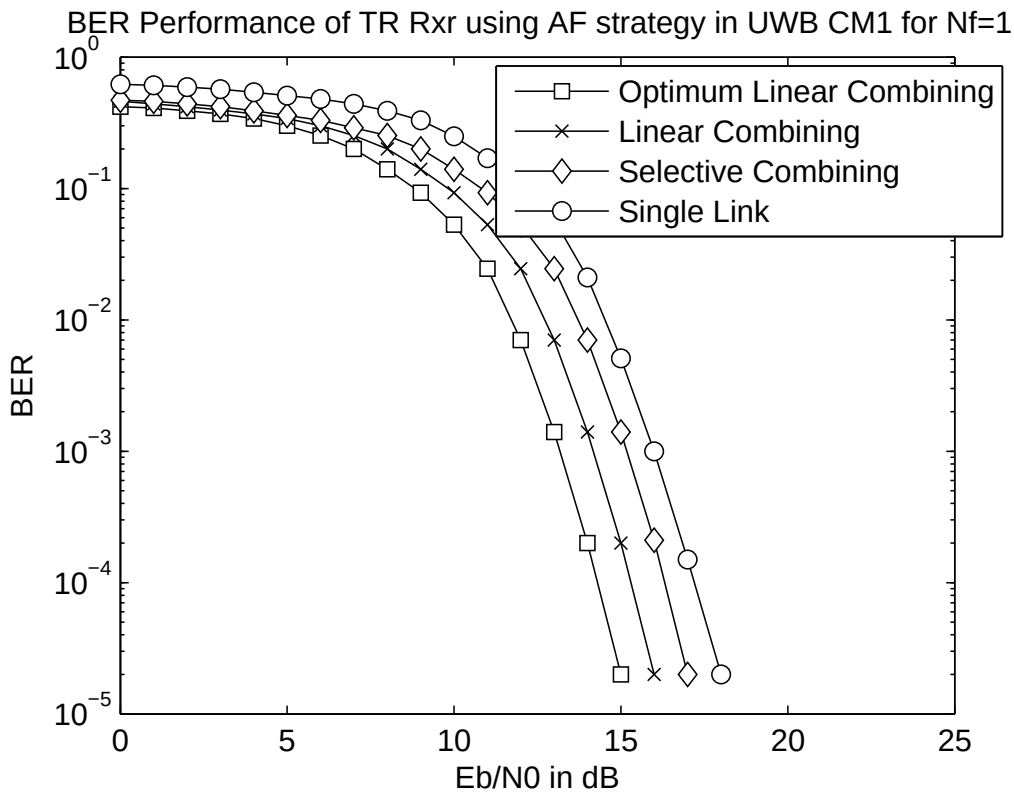

(a)

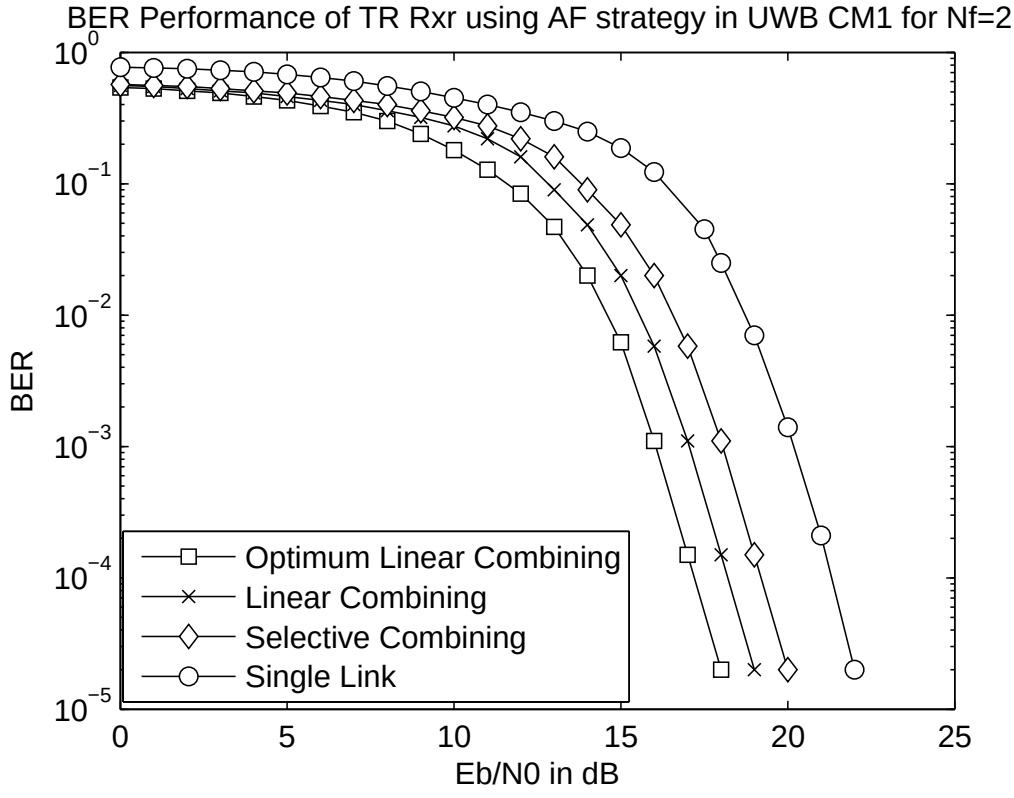

(b)

Figure 4.3: BER performance of UWB TR system using cooperative AF strategy with various combining schemes in CM1 channel for (a) $N_f = 1$ (b) $N_f = 2$

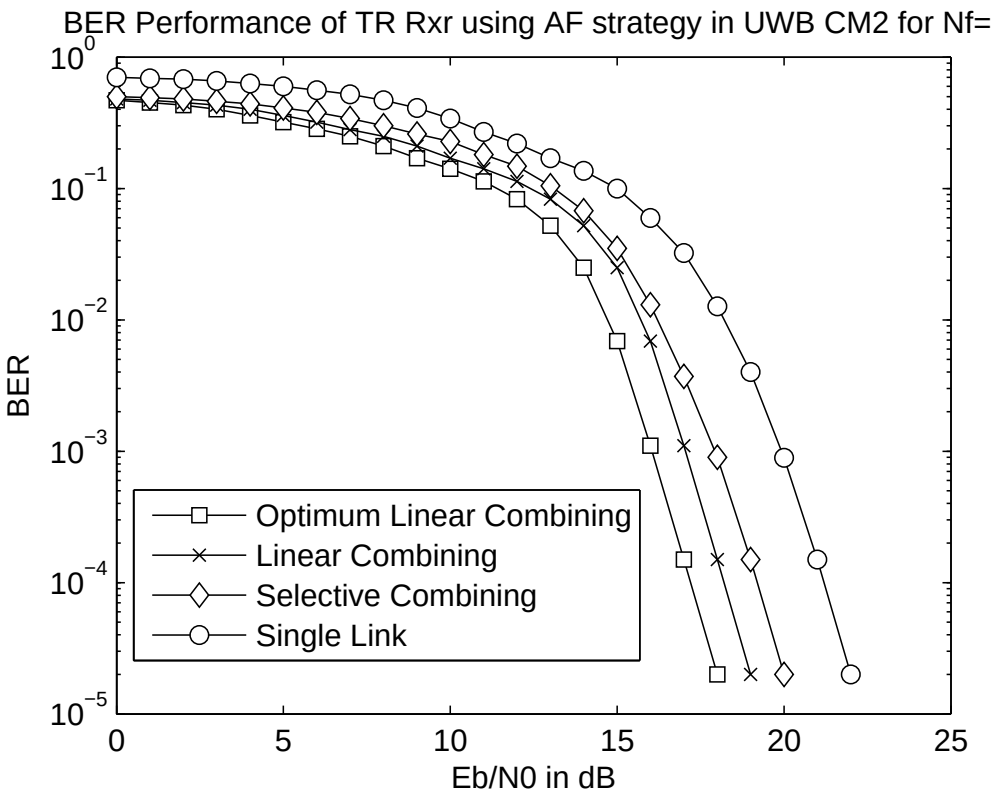

(a)

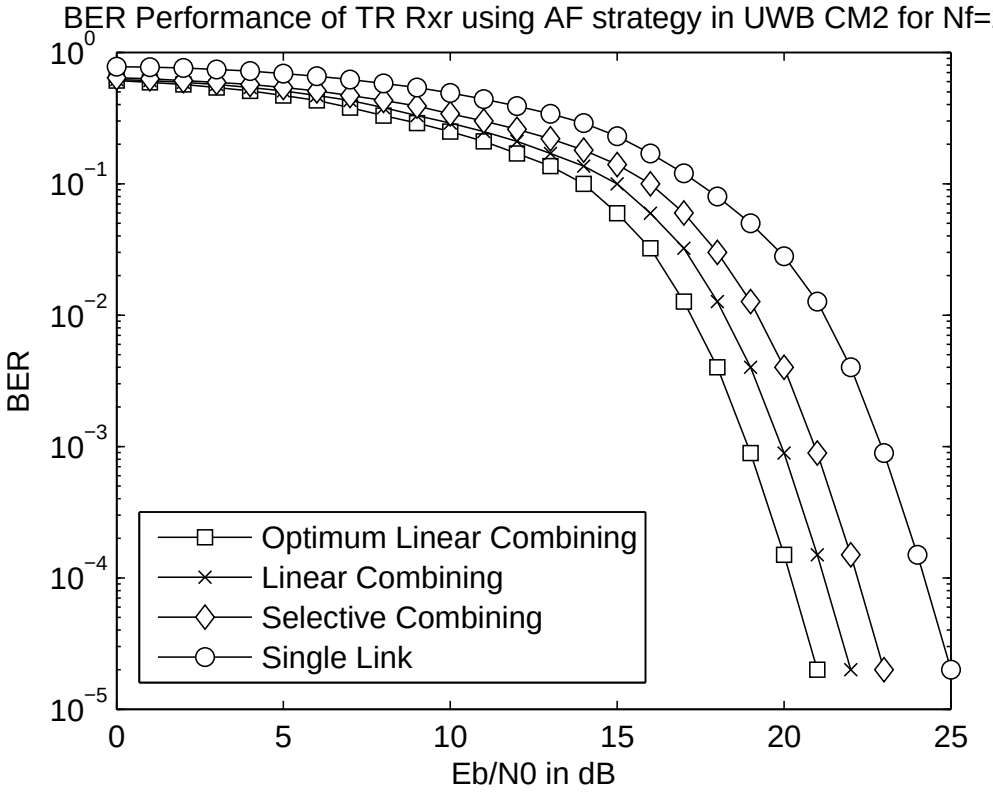

(b)

Figure 4.4: BER performance of UWB TR system using cooperative AF strategy with various combining schemes in CM2 channel for (a) $N_f = 1$ (b) $N_f = 2$

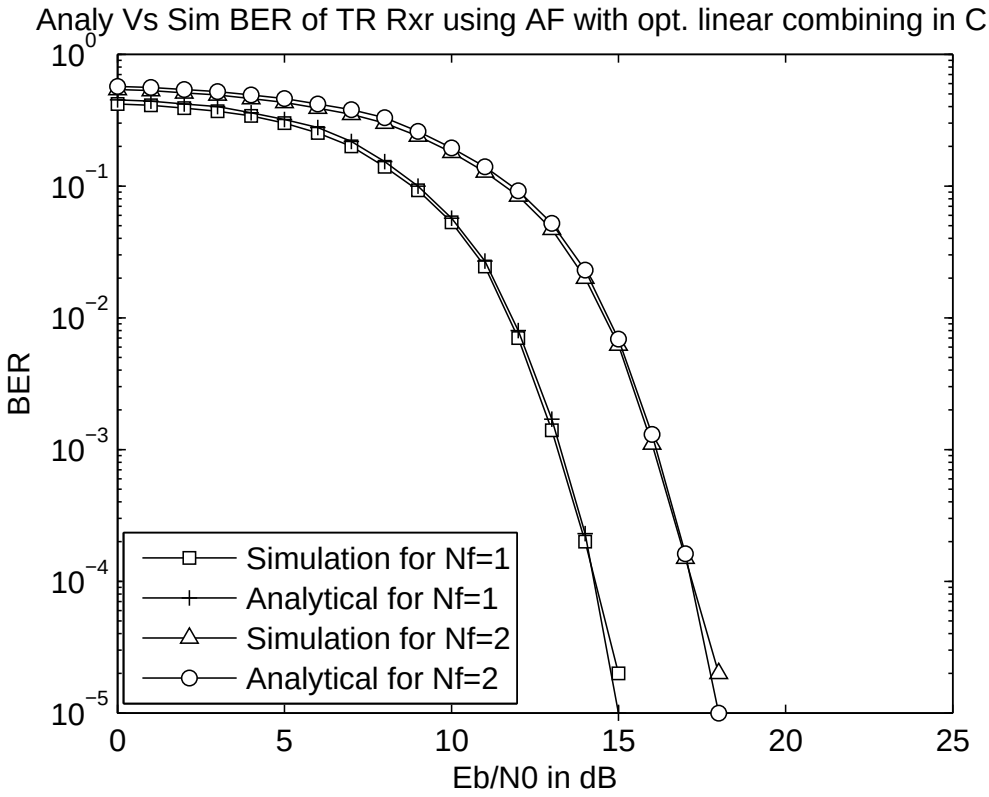
Analy Vs Sim BER of TR Rxr using AF with opt. linear combining in CM1
BER
Eb/N0 in dB
Simulation for Nf=1
Analytical for Nf=1
Simulation for Nf=2
Analytical for Nf=2

(a)

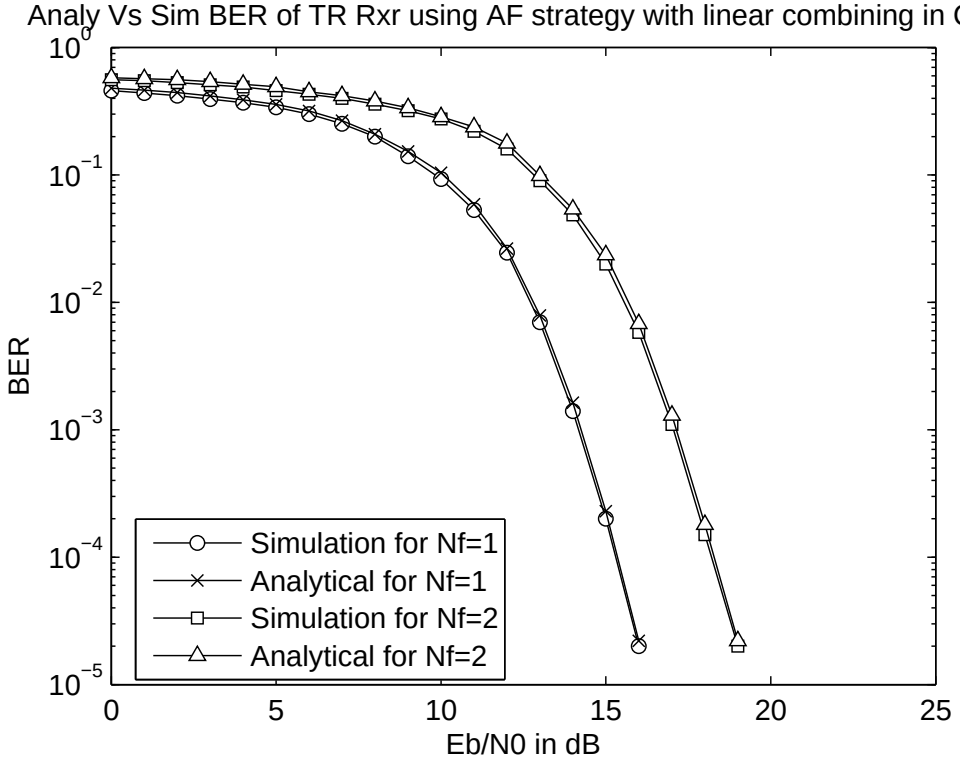
Analy Vs Sim BER of TR Rxr using AF strategy with linear combining in CM1
BER
Eb/N0 in dB
Simulation for Nf=1
Analytical for Nf=1
Simulation for Nf=2
Analytical for Nf=2

(b)

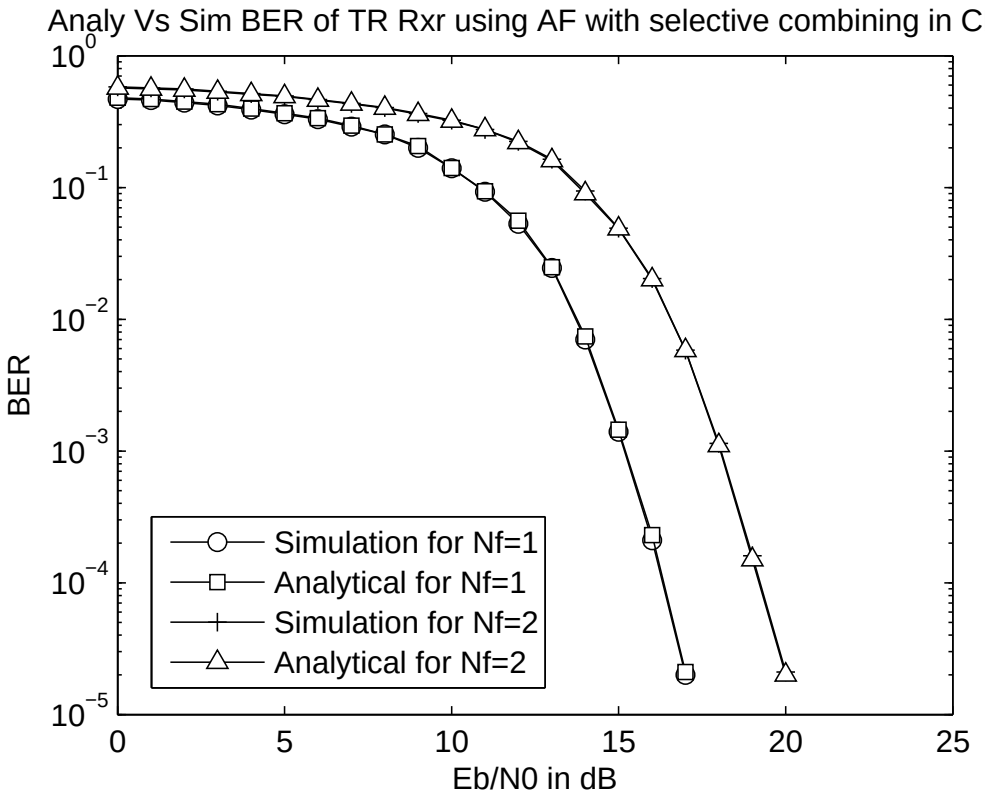

(c)

Figure 4.5: Analytic vs Simulated BER performance comparison of UWB TR system using AF strategy having $N_f = 1, 2$ for various combining schemes namely (a) Optimum Linear Combining (b) Linear Combining and (c) Selective Combining.

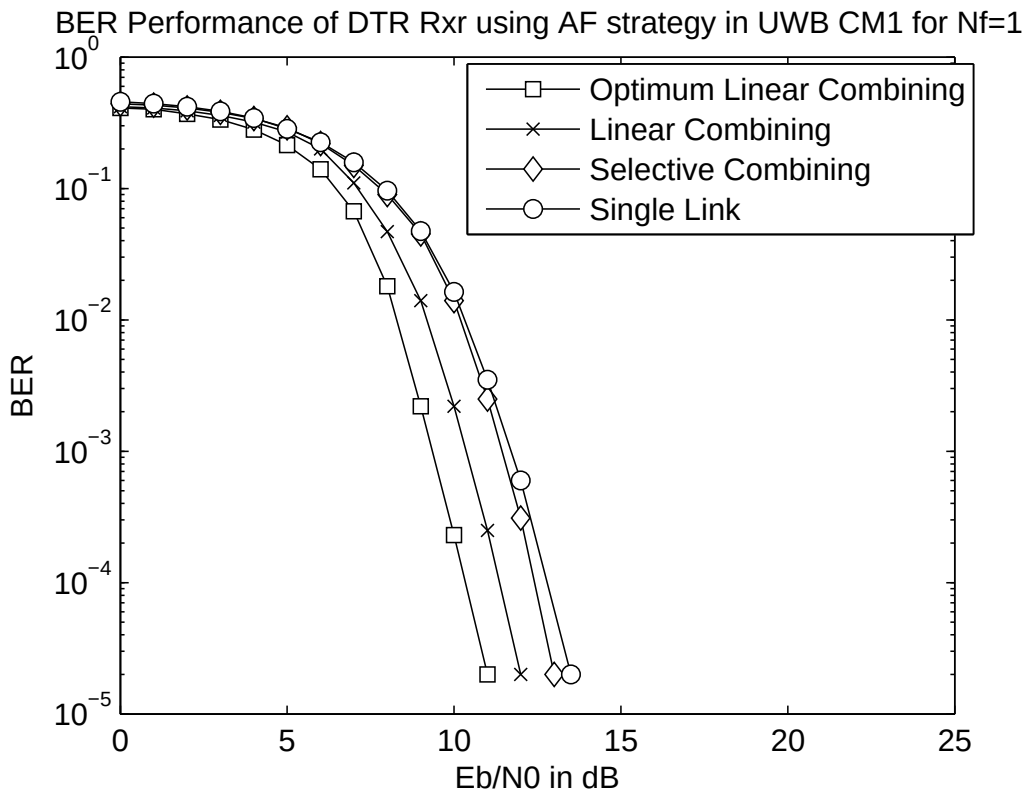

(a)

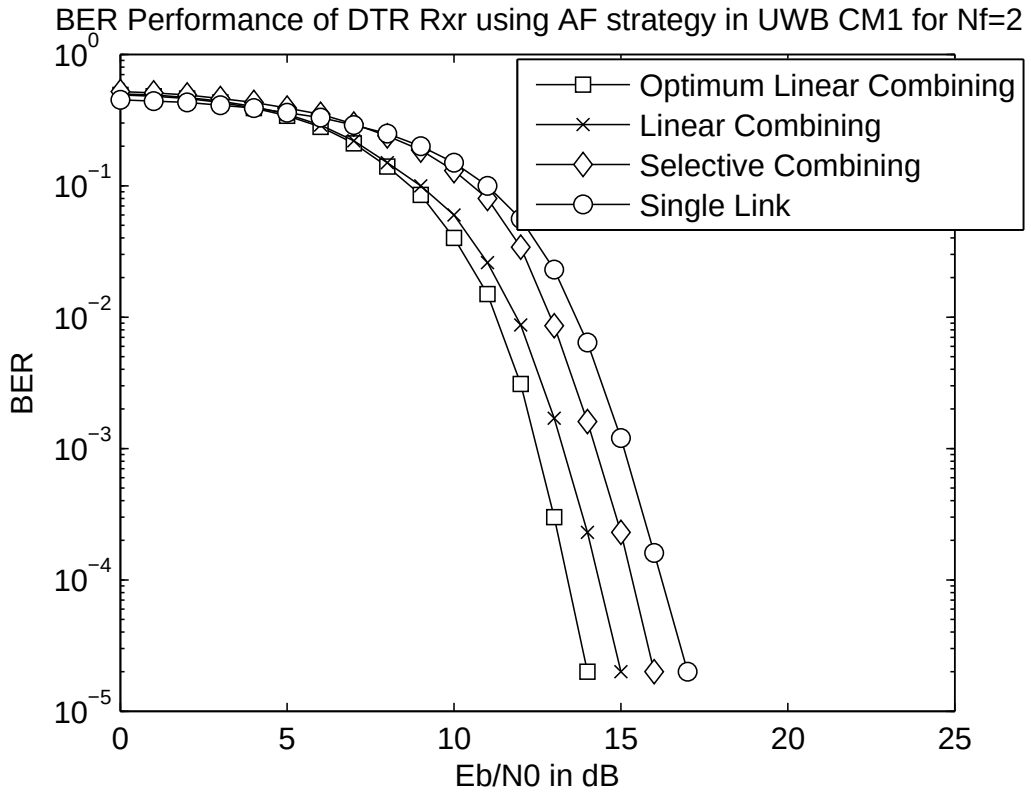

(b)

Figure 4.6: BER performance of UWB DTR system using cooperative AF strategy with various combining schemes in CM1 channel for (a) $N_f = 1$ (b) $N_f = 2$

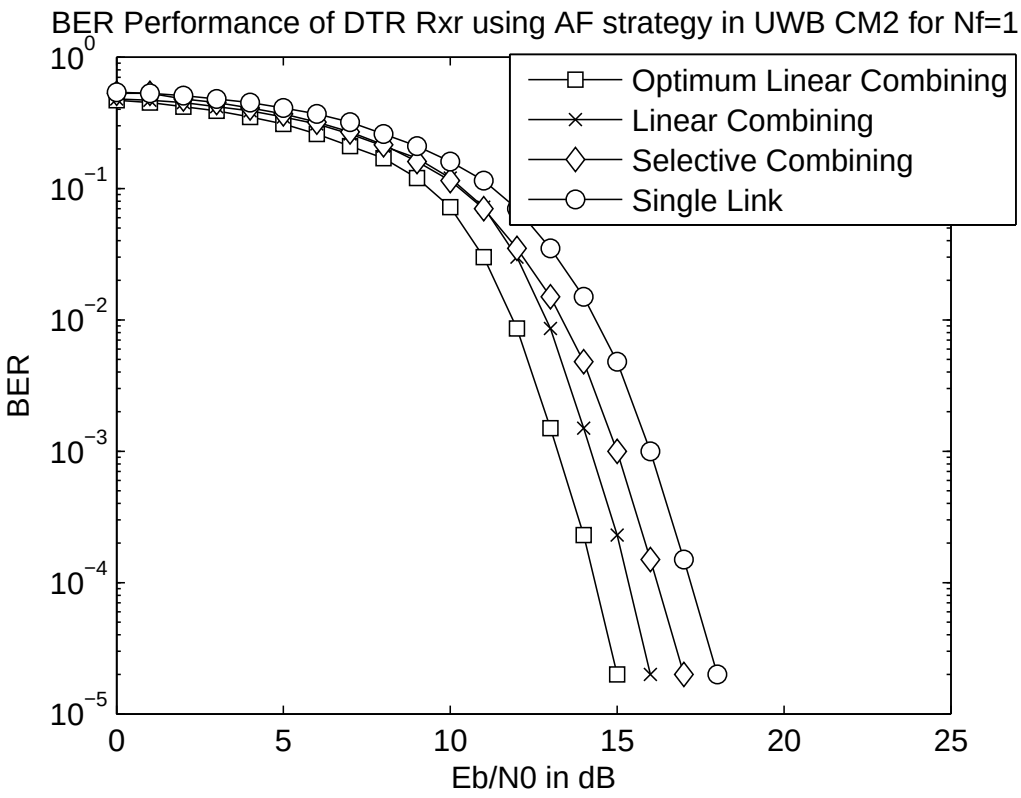

(a)

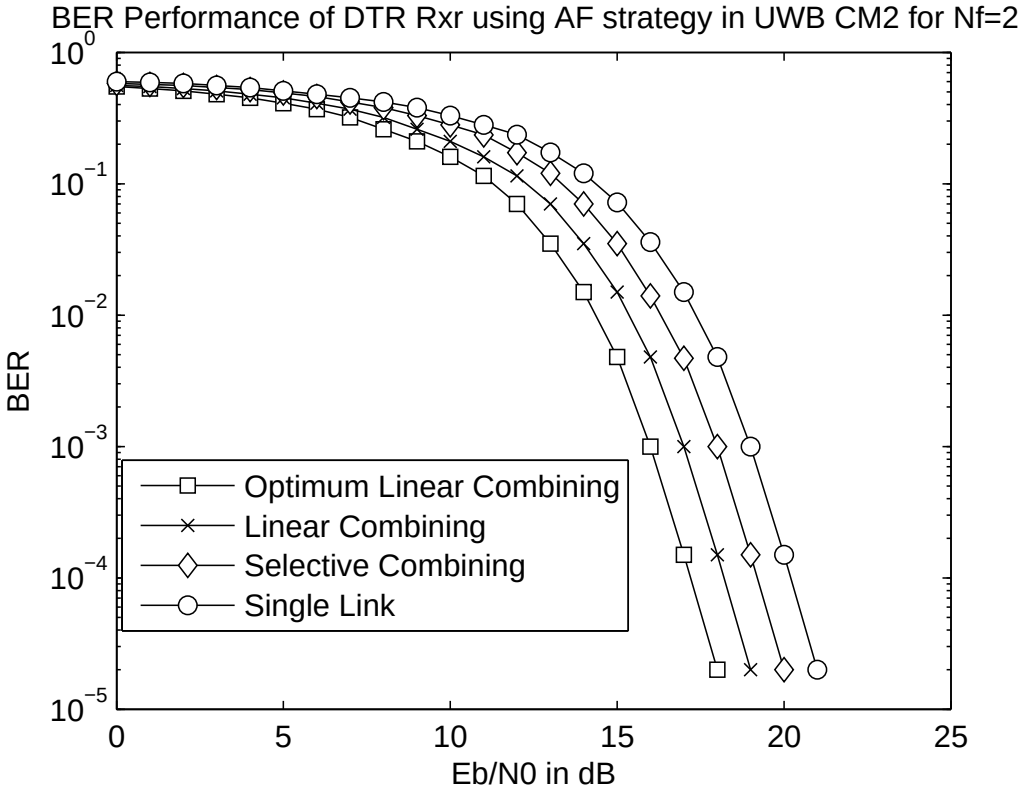

(b)

Figure 4.7: BER performance of UWB DTR system using cooperative AF strategy with various combining schemes in CM2 channel for (a) $N_f = 1$ (b) $N_f = 2$

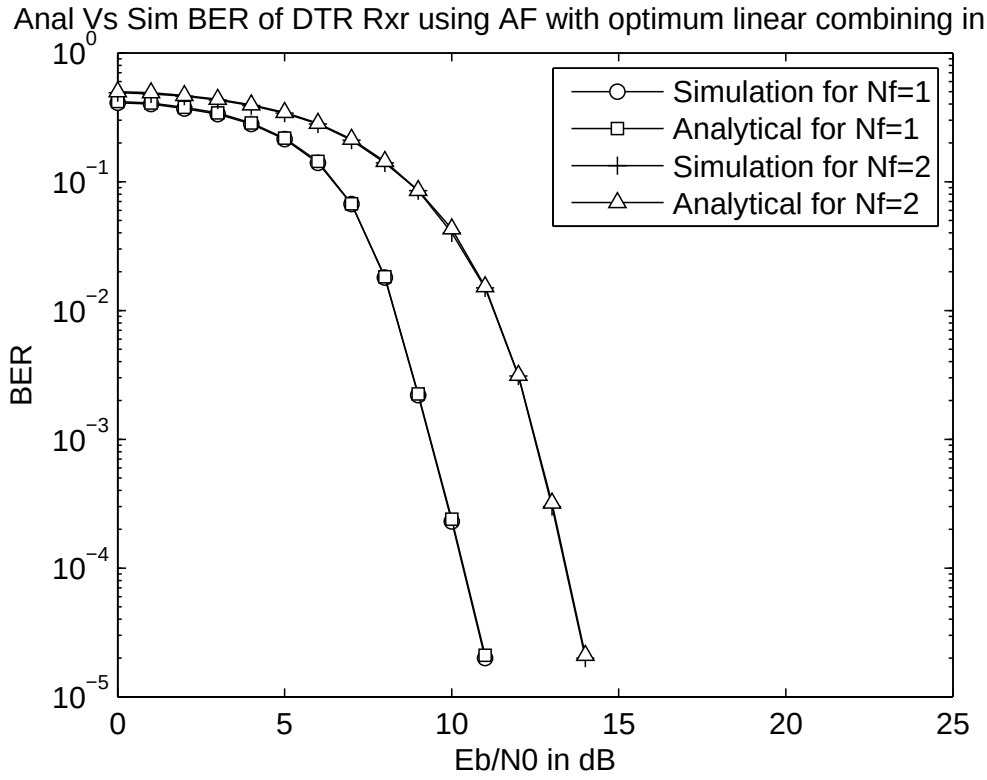
Anal Vs Sim BER of DTR Rxr using AF with optimum linear combining in CM1
Simulation for Nf=1
Analytical for Nf=1
Simulation for Nf=2
Analytical for Nf=2
BER
Eb/N0 in dB

(a)

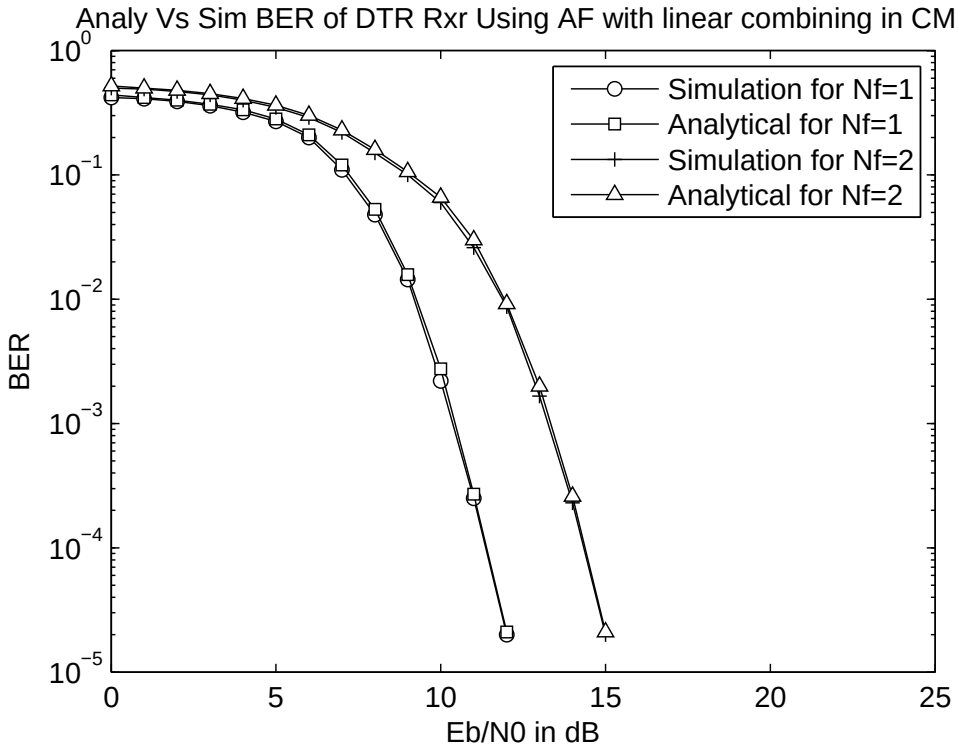
Analy Vs Sim BER of DTR Rxr Using AF with linear combining in CM1
Simulation for Nf=1
Analytical for Nf=1
Simulation for Nf=2
Analytical for Nf=2
BER
Eb/N0 in dB

(b)

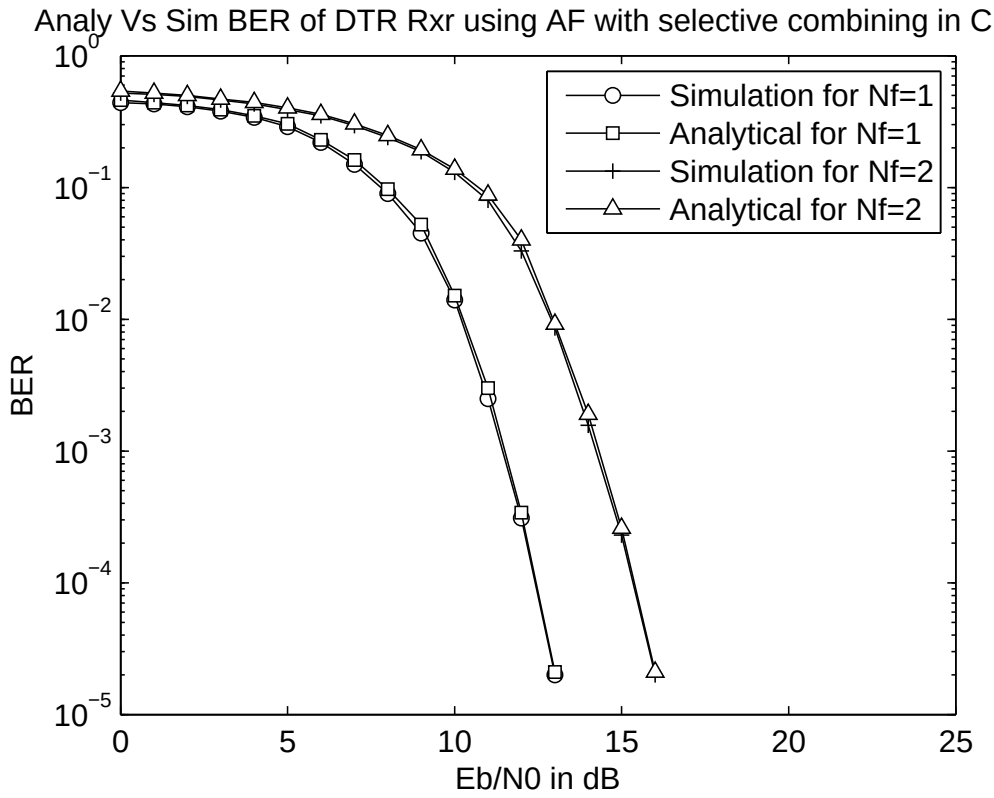

(c)

Figure 4.8: Analytic vs Simulated BER performance comparison of UWB DTR system using AF strategy having $N_f = 1, 2$ for various combining schemes namely (a) Optimum Linear Combining (b) Linear Combining and (c) Selective Combining.

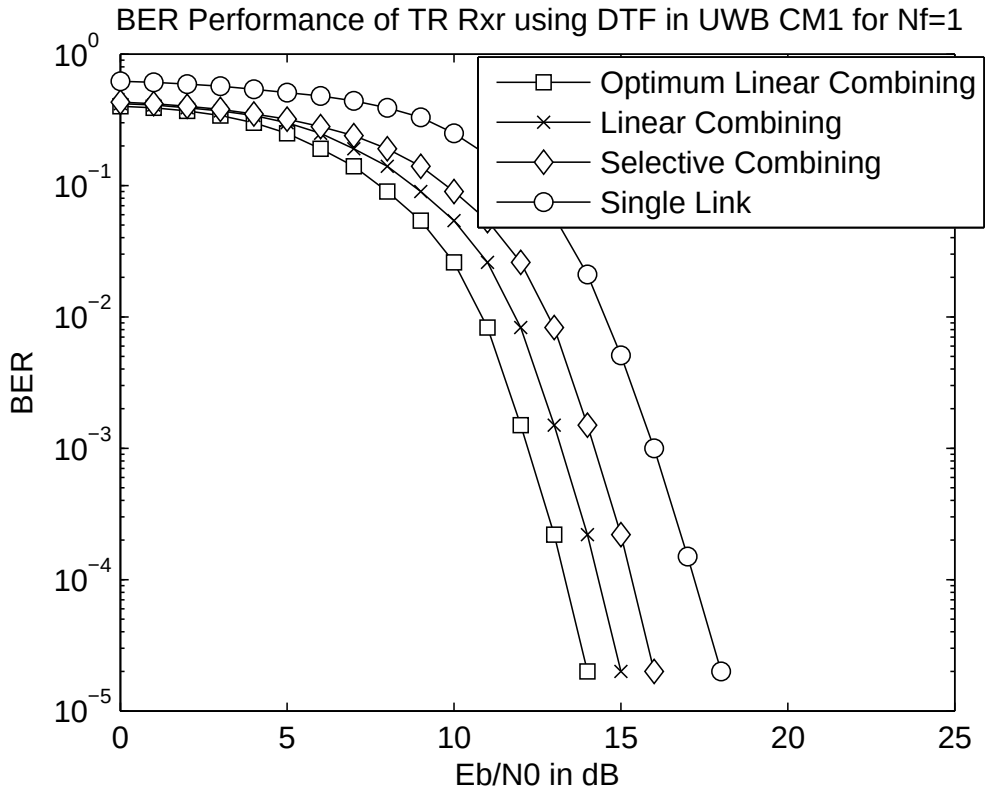

(a)

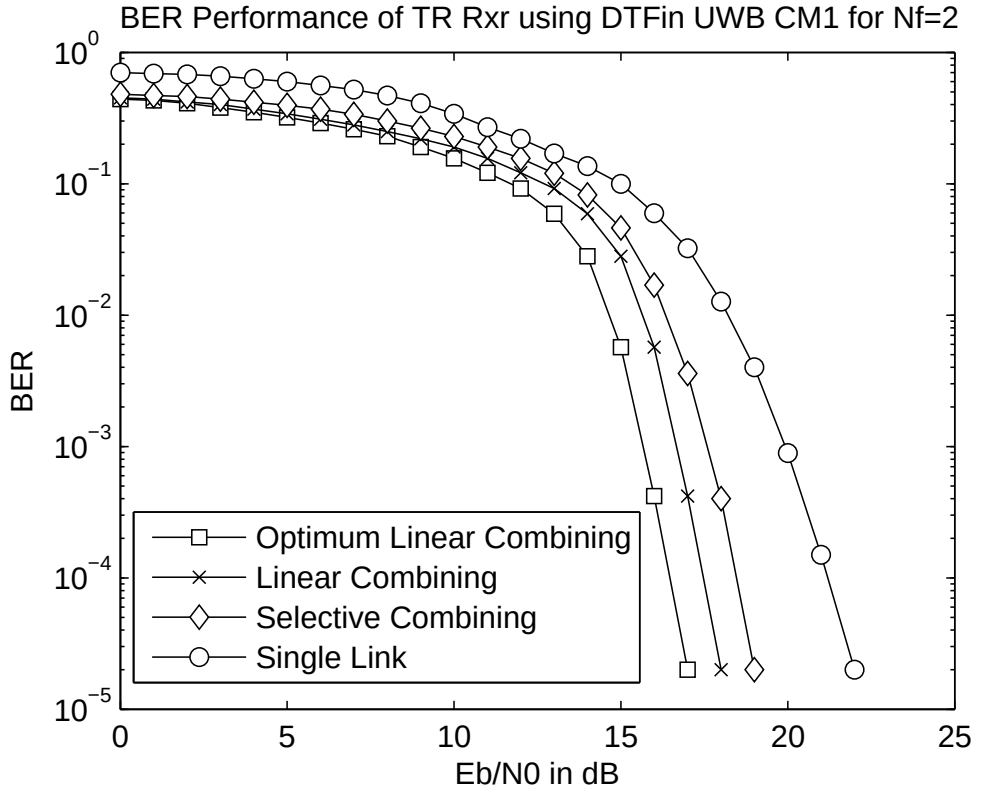

(b)

Figure 4.9: BER performance of UWB TR system using cooperative DTF strategy with various combining schemes in CM1 channel for (a) $N_f = 1$ (b) $N_f = 2$

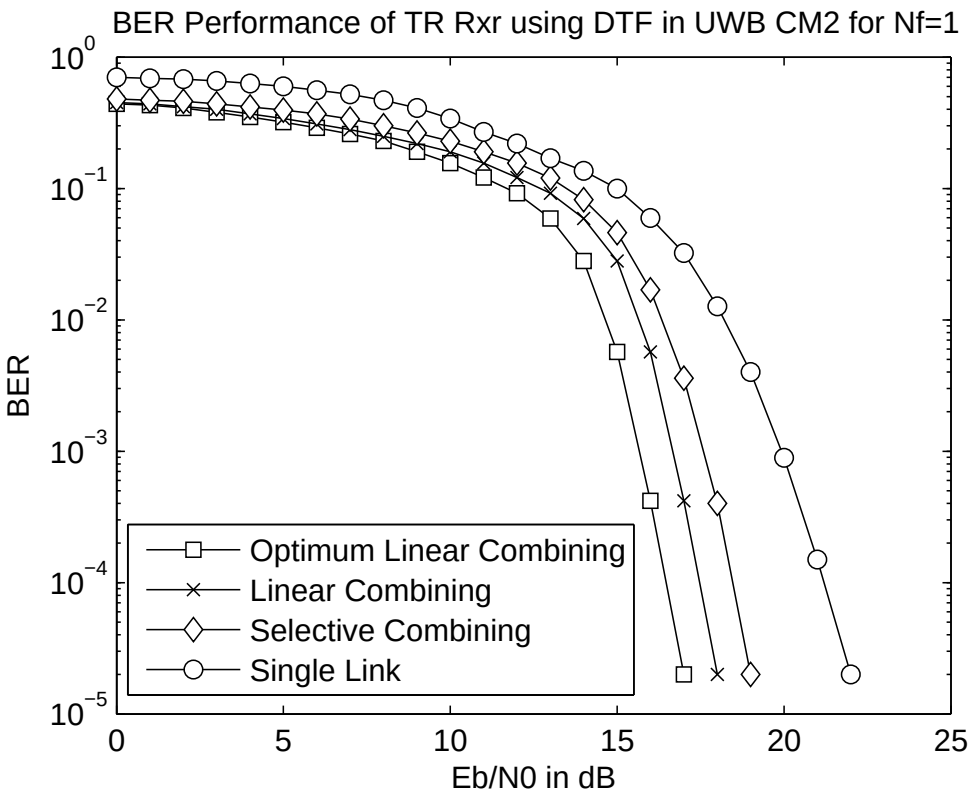

(a)

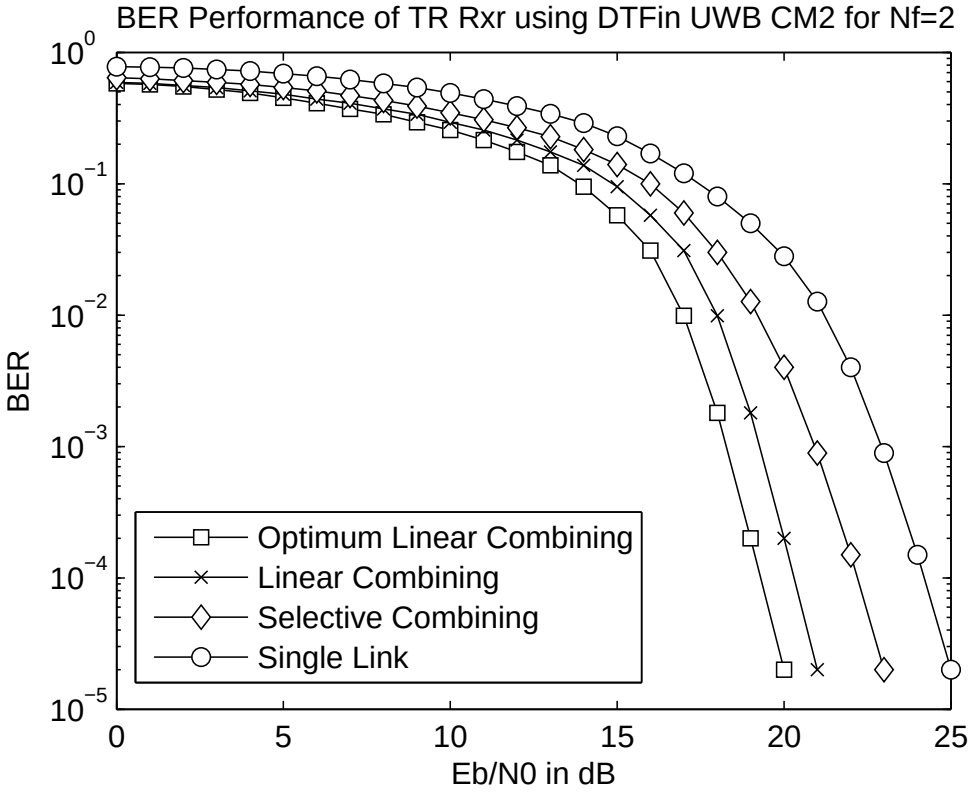

(b)

Figure 4.10: BER performance of UWB TR system using cooperative DTF strategy with various combining schemes in CM2 channel for (a) $N_f = 1$ (b) $N_f = 2$

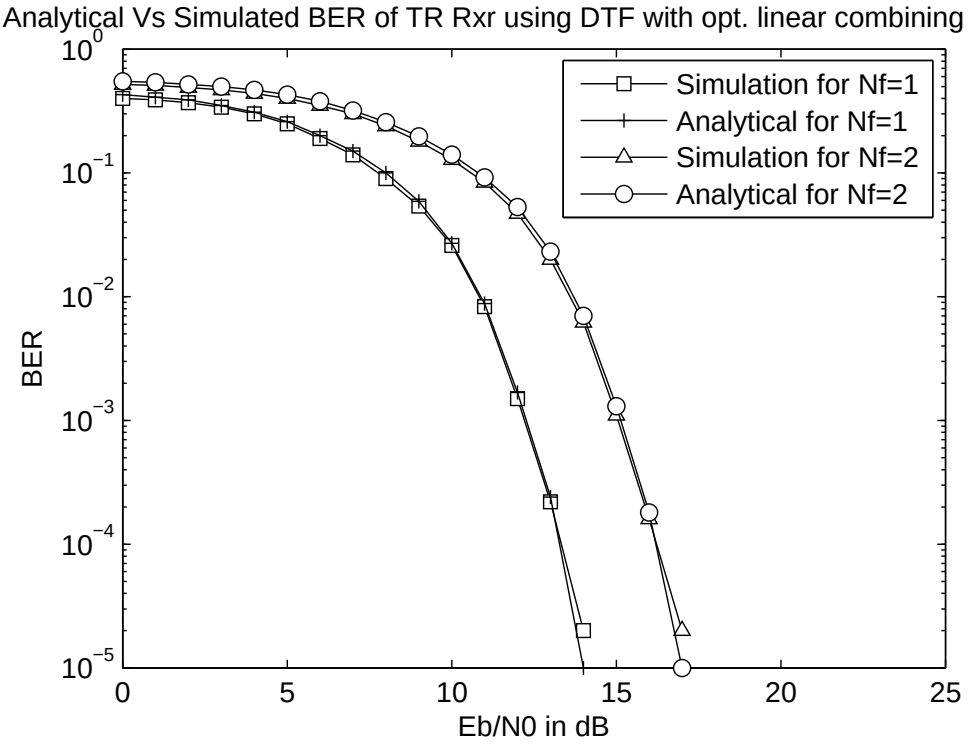
Analytical Vs Simulated BER of TR Rxr using DTF with opt. linear combining in CM1
Simulation for Nf=1
Analytical for Nf=1
Simulation for Nf=2
Analytical for Nf=2
BER
Eb/N0 in dB

(a)

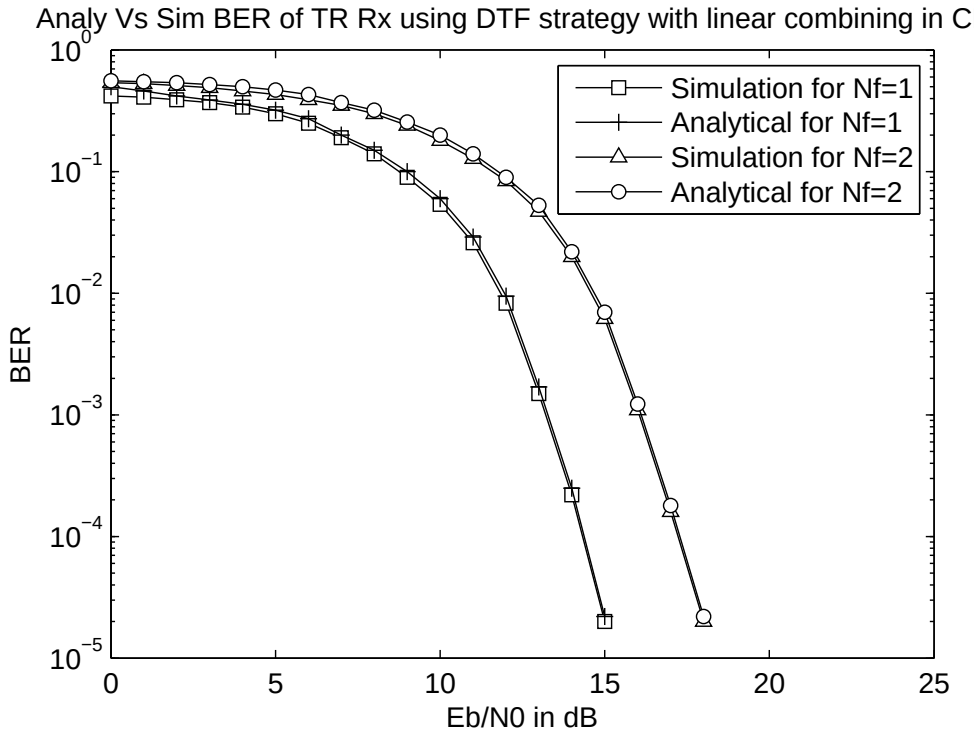
Analy Vs Sim BER of TR Rx using DTF strategy with linear combining in CM1
Simulation for Nf=1
Analytical for Nf=1
Simulation for Nf=2
Analytical for Nf=2
BER
Eb/N0 in dB

(b)

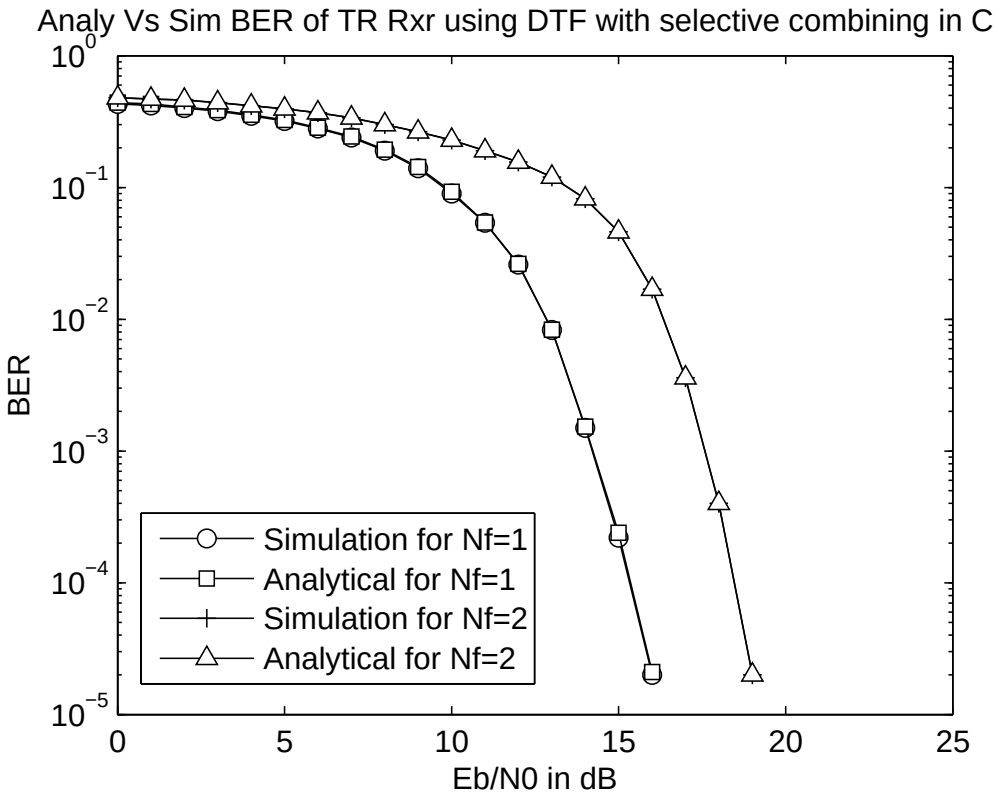

(c)

Figure 4.11: Analytic vs Simulated BER performance comparison of UWB TR system using DTF strategy having $N_f = 1, 2$ for various combining schemes namely (a) Optimum Linear Combining (b) Linear Combining and (c) Selective Combining.

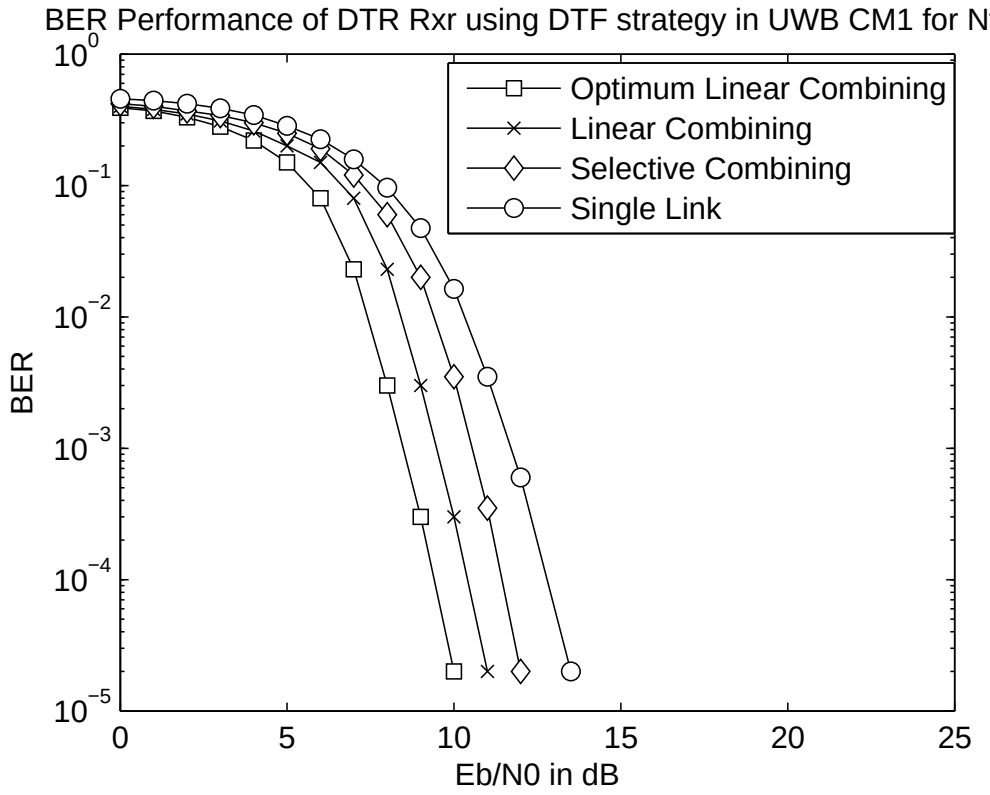

(a)

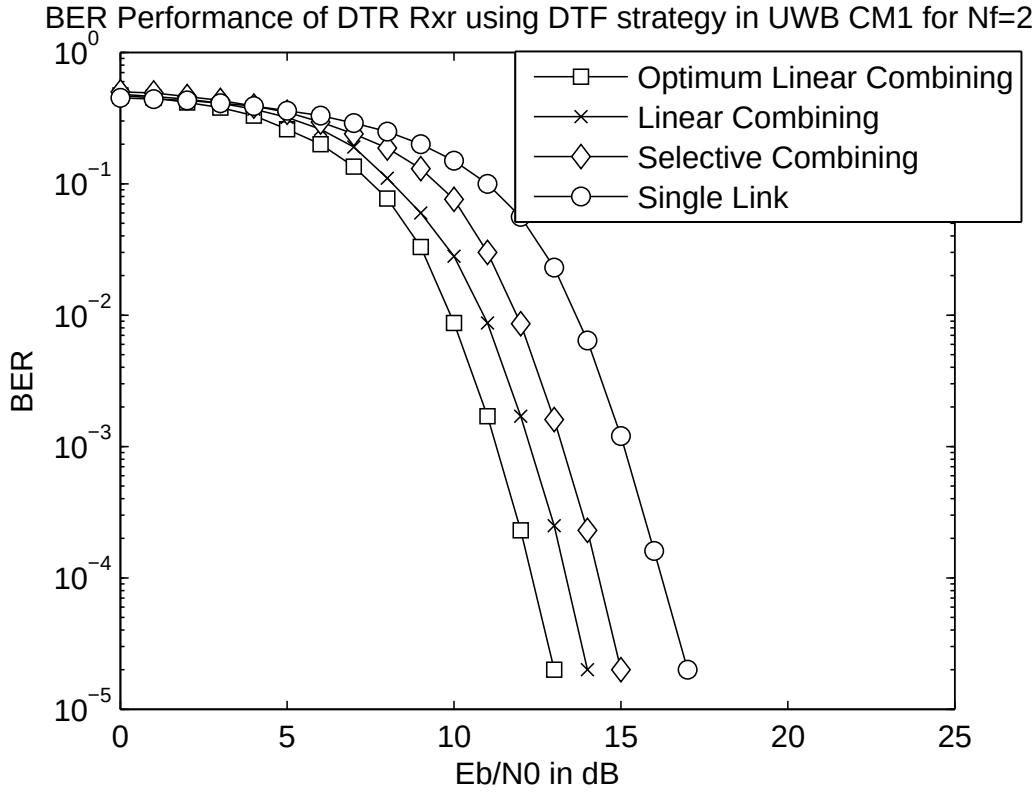

(b)

Figure 4.12: BER performance of UWB DTR system using cooperative DTF strategy with various combining schemes in CM1 channel for (a) $N_f = 1$ (b) $N_f = 2$

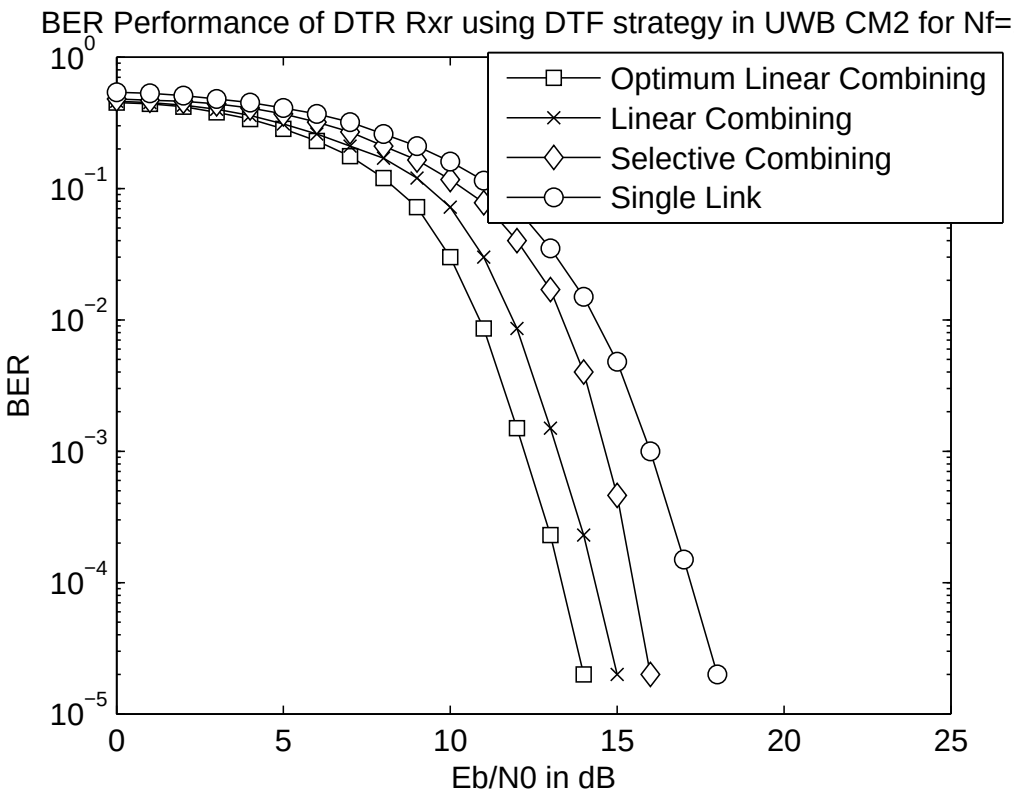

(a)

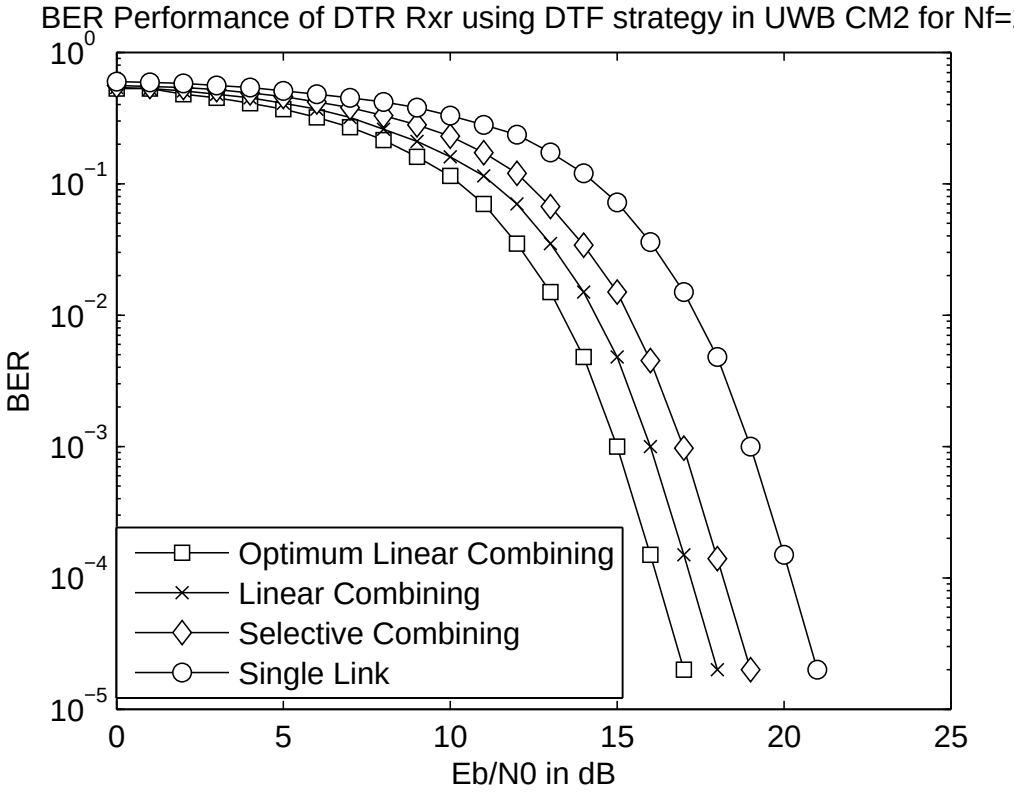

(b)

Figure 4.13: BER performance of UWB DTR system using cooperative DTF strategy with various combining schemes in CM2 channel for (a) $N_f = 1$ (b) $N_f = 2$

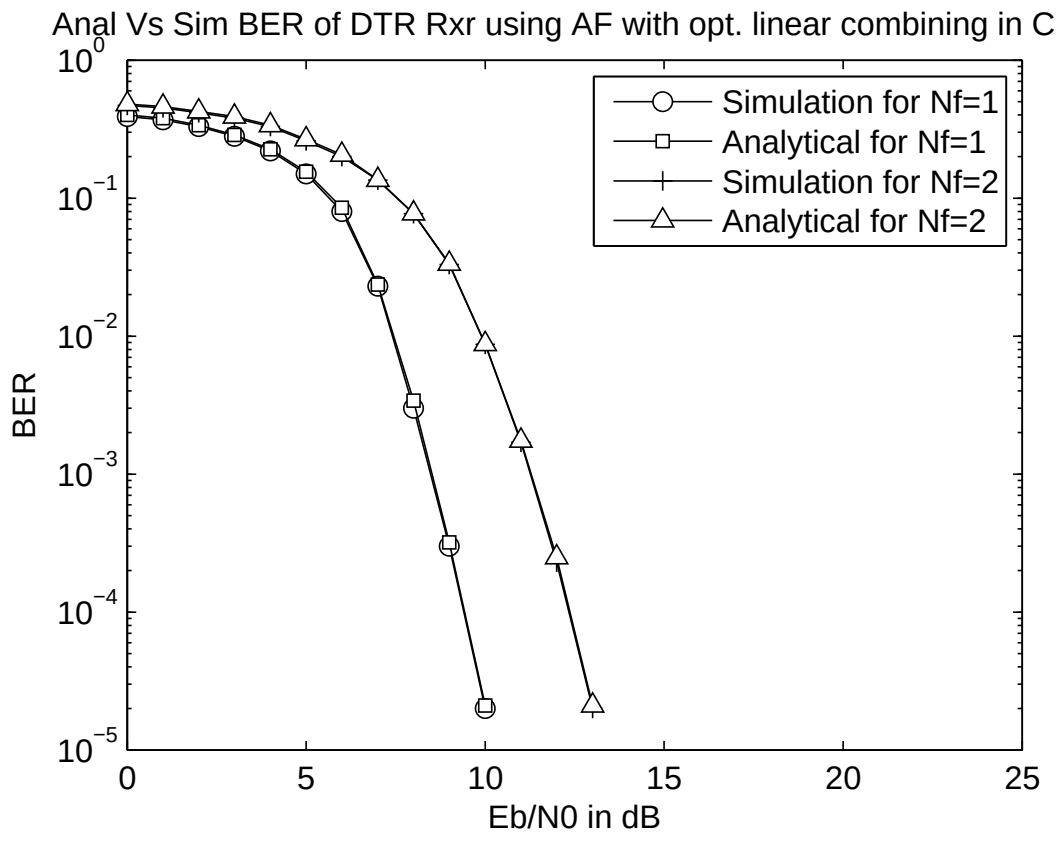
Anal Vs Sim BER of DTR Rxr using AF with opt. linear combining in CM1
Simulation for Nf=1
Analytical for Nf=1
Simulation for Nf=2
Analytical for Nf=2
BER
Eb/N0 in dB

(a)

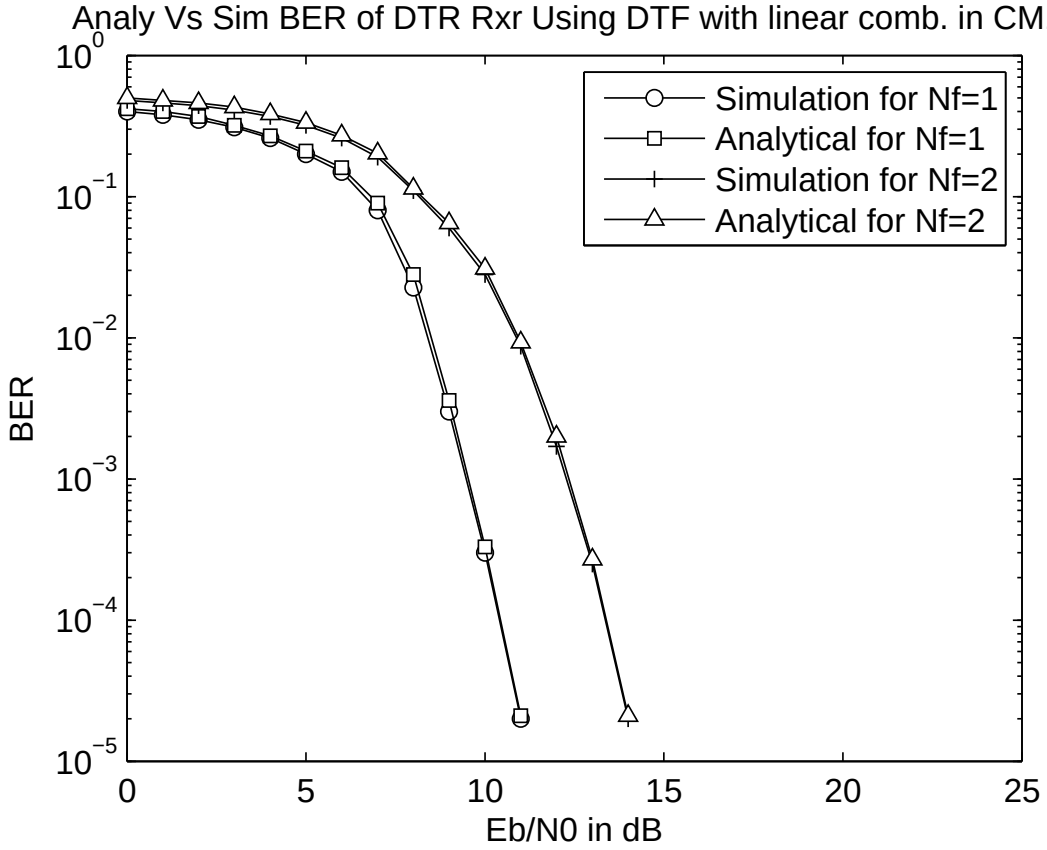
Analy Vs Sim BER of DTR Rxr Using DTF with linear comb. in CM1
Simulation for Nf=1
Analytical for Nf=1
Simulation for Nf=2
Analytical for Nf=2
BER
Eb/N0 in dB

(b)

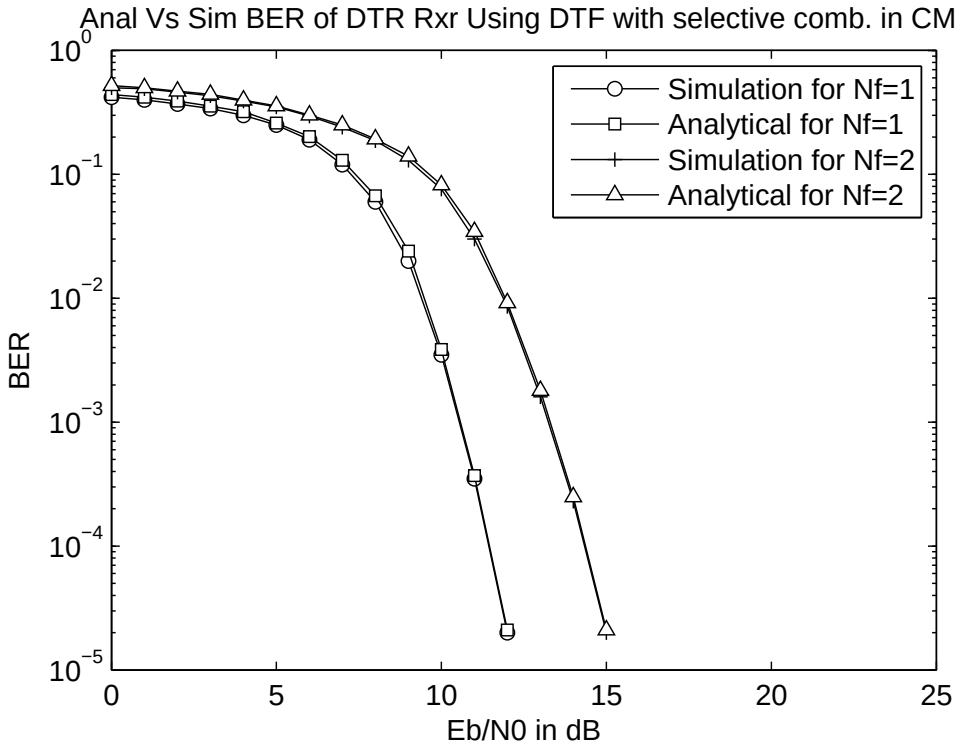

(c)

Figure 4.14: Analytic vs Simulated BER performance comparison of UWB DTR system using DTF strategy having $N_f = 1, 2$ for various combining schemes namely (a) Optimum Linear Combining (b) Linear Combining and (c) Selective Combining.

It is observed from Fig 4.7(a) and (b) that the BER performance of UWB DTR system degrades as we move from CM1 to CM2 environment. This is because, CM2 being a NLOS channel performs worse than CM1, LOS channel. It is also noted that the BER performance falls, as N_f increases from 1 to 2. It is also inferred from the Figures that DTR system gives a SNR gain of $3\ dB$ over TR system in CM2 environment, for $N_f = 1, 2$. In CM2 environment, as far as BER performance of combining schemes are concerned, Optimum Linear Combining $>$ Linear Combining $>$ Selective Combining $>$ Single$-$Link.

Fig 4.8(a), (b) and (c) illustrates the analytical vs simulated BER performance comparison of UWB DTR system using cooperative AF strategy, for optimum diversity combining, linear combining and selective combining respectively, in UWB CM1 environment. It can be inferred from the results that the simulation plots nearly coincide with the plot of analytical results, at all BER for N_f = $1, 2$.

Fig 4.9(a) and (b) illustrates the BER performance of UWB TR system using dual-hop coop-

erative DTF relay strategy for various diversity combining schemes, in UWB CM1 environment having $N_f = 1$ and 2 respectively. It is also observed that increase in number of frames N_f from 1 to 2, leads to degradation in BER performance. At a BER of 10^{-4}, optimum linear diversity combining scheme gives a SNR improvement of 1 dB and 2 dB over linear diversity combining and selective diversity combining, respectively. It is also noted that DTF relay scheme depicts a SNR gain of $1 - 1.5$ dB over AF scheme, at all BER.

The BER performance of UWB TR system using cooperative dual−hop DTF strategy for various diversity combining schemes namely optimum linear diversity combining, linear combining and selective combining, in UWB CM2 environment having $N_f = 1$ and 2 respectively are studied from the results predicted in Fig 4.10(a) and (b). CM2, NLOS channel, suffers a performance loss of 3 dB, compared to LOS, CM1 channel. The BER performance degrades with increase in number of frames N_f. It is also be inferred from the BER plots in all the Figures that DTF relay scheme supersedes AF relay scheme by a margin of $1 - 1.5$ dB, at a BER of 10^{-4}.

The analytical and simulated BER performance of UWB TR system has been compared using dual−hop cooperative DTF relay strategy, for these three diversity combining schemes namely (a) optimum linear diversity combining (b) linear diversity combining and (c) selective diversity combining, and the results are depicted in Fig 4.11. It is also observed that the plot of simulation results for all the diversity combining cases exactly coincide with the analytical results at all BER levels, for N_f=1, 2.

Fig 4.12(a) and (b) shows the variation in BER versus SNR plot of UWB DTR system using dual−hop cooperative DTF relay strategy, for various diversity combining techniques in presence of IEEE 802.15.4a UWB CM1 LOS environment, having $N_f = 1$ and 2 respectively. It is also observed that the increase in number of frames N_f from 1 to 2, leads to degradation in BER performance. At a BER of 10^{-4}, optimum linear diversity combining scheme, gives a SNR improvement of 1 dB and 2 dB over linear diversity combining and selective combining respectively. It is also noted from both the Figures that DTR system using DTF relay strategy with diversity combining gives a SNR gain of 4 dB over TR system, in both cooperative and non−cooperative scenario.

The BER performance of UWB DTR system using dual−hop cooperative DTF relay strategy for various diversity combining schemes, in UWB CM2 environment having $N_f = 1$ and 2 respectively. CM2, being a NLOS channel, gives poor BER performance compared to LOS,

CM1 channel is observed from Fig 4.13(a) and (b). Using CM2 channel, the SNR of UWB DTR system using both cooperative and non−cooperative strategy, falls by a margin of $4\ dB$ when compared to CM1 channel, at a BER of 10^{-4}. The BER performance degrades, as the number of frames N_f increases from 1 to 2, as observed from the BER plots in Figures. Thus, it can be concluded that using cooperative DTF strategy gives a better BER performance than using AF strategy. Among diversity combining techniques, optimum linear diversity combining is found to give the best BER performance followed by linear combining and then selective combining, for UWB CM1 and CM2 channels having $N_f = 1, 2$.

The analytical and simulated BER performance of UWB DTR system has been compared using dual−hop cooperative DTF protocol in UWB CM1 environment for the three diversity combining strategies, and the results are as depicted in Fig 4.14. We have obtained the approximate analytical BER expressions for these three diversity combining cases and compared them with the simulation results, for $N_f = 1, 2$. It is observed that for all the three diversity combining strategies, the plot of simulation results exactly coincide with the plot of analytical results, at all BER levels, for $N_f = 1, 2$.

4.6 Concluding Remarks

In this chapter, we have derived the BER expression for non−coherent UWB TR and DTR (AC) systems using cooperative dual−hop relay strategies for various diversity schemes namely optimum linear combining, linear combining and selective combining over, IEEE 802.15.4a UWB CM1 and CM2 environment. The analytical BER expression derived for TR and DTR systems, based on autocorrelation principle are validated with the simulation results, employing IEEE 802.15.4a UWB standard between the relay nodes and links. The overlapping or the convergence of the simulation results with the analytical results confirm the accuracy and perfectness of approximation used in evaluation of BER. Numerical results depict improvement in BER with increase in number of relay paths L. It is also observed that with increase in number of frames N_f, the BER performance of the UWB system degrades. Also for UWB simulated channels, CM1 being LOS, gives better performance than CM2, NLOS channel. It can also be inferred from the results that among the AC systems discussed, DTR gives a better BER performance compared to TR, in UWB environment for $N_f = 1, 2$. This is because DTR system transmits differentially modulated information and wastes no energy in transmitting a reference

pulse, thereby saving $3 - 4\ dB$ of energy compared to TR system. Furthermore, DTF relay strategy gives a SNR gain of $1\ dB$ over AF relay strategy, at a BER of 10^{-4}.

In this chapter, we present an analytical approach to evaluate the BER performance of non−coherent UWB AC systems namely TR and DTR, using cooperative dual−hop AF and DTF relay strategies with various diversity combining schemes, over IEEE 802.15.4a environment.

Chapter 5

Performance Analysis of Non-Coherent UWB Cooperative ED−OOK System

The BER performance of UWB ED−OOK system using cooperative dual−hop AF and DTF strategy, with various diversity combining schemes over IEEE 802.15.4a environment, is presented in this chapter. Here, the approximate BER expressions derived for various diversity combining cases, namely optimum linear combining, linear combining, and selective combining is based on Energy detection principle. Section 5.1 presents the basic introduction about UWB ED−OOK system, using various cooperative dual−hop relay strategies. Section 5.2 illustrates the system model comprising of signal model, channel model and receiver structure. The detailed theoretical BER performance analysis of UWB ED−OOK system, is derived using cooperative dual−hop AF and DTF strategy for various diversity combining schemes, in Section 5.3 and Section 5.4 respectively. The simulation results are outlined in Section 5.5 while Section 5.6, concludes the paper.

5.1 Introduction

Non−Coherent UWB systems are preferred over its coherent counterpart, because of smaller complexity and non−requirement of channel estimation. The importance of cooperative diversity in UWB systems was outlined in the following literature [43, 96]. The authors [43, 45, 44] have extended the use of AF and DF relay strategies in UWB systems. The previous contributions [157, 155, 48] analysed the BER performance of UWB differential system using cooperative dual−hop relay strategy. Inspite of such contributions, research for cooperative trans-

mission in multipath scenario using non−coherent UWB system, is largely unexplored. The limitation of AC system lies in its hardware complexity because it requires a storage element to store the past samples of the received signal, needed for performing correlation operation [68, 178, 180]. To overcome this problem, low complexity and low cost ED systems are introduced, which works by passing the received signal through a square law detector, followed by integrator and decision device [181, 150]. Furthermore, ED receiver works as an optimal detector in non−coherent detection scenario, as channel estimation is not known. If there is a trade−off between performance and complexity and complexity is preferred, then ED receiver acts as the best choice because of its simplicity and less hardware complexity. Among non−coherent UWB receivers, ED employed with OOK modulation scheme is one of the simplest and least complex detector.

The objective of this chapter is to evaluate the BER performance of UWB ED−OOK system, using dual−hop cooperative AF and DTF protocol with diversity combining schemes, over IEEE 802.15.4a UWB environment. Approximate BER Expressions are analytically evaluated based on energy detection principle for various diversity combining cases, namely optimum linear combining, linear combining and selective combining in UWB ED−OOK system using cooperative dual−hop AF and DTF relay protocol.

5.2 System Model

The cooperative system model has three links S−D, S−R and R−D, as seen in Fig 1.3. In the 1^{st} time slot, information bit modulated by UWB signal is transmitted from the source node to relay as well as destination node. The signal received at relay node in 1^{st} time slot is either amplified by an amplifying factor or detected using a ED−OOK receiver, depending on the relaying protocol used. The amplified or the detected signal is then forwarded to the destination node in the 2^{nd} time slot. The received signal obtained at the destination node using either of the relaying schemes, at the end of 1^{st} and 2^{nd} time slots, are demodulated using an ED−OOK receiver. The decision statistics obtained at the destination node due to energy detection of received signals from S−D and R−D links, are combined using various combining strategies, namely optimum linear combining, linear combining and selective combining, to form the final decision statistic. The final decision statistic is then compared to a threshold to recover the information bit.

5.2.1 Signal Model

This section focuses on UWB ED system using OOK modulation scheme for signalling. The symbol duration T_s consists of N_f frames of T_f duration. A second order Gaussian Derivative UWB pulse $p(t)$ of ultra−short duration T_p modulated by information bit (or symbol) b_i, is transmitted in each frame duration T_f. As illustrated in Fig 1.3, cooperation protocol for dual−hop strategy is such that Source (S) transmits, while Relay (R) and Destination (D) listens in 1^{st} time slot. However, in 2^{nd} time slot, S is silent while R and D communicate with each other. The UWB signal transmitted from the source node to the destination node in 1^{st} time slot is represented as:

$$s_{SD}(t) = \sqrt{E} \sum_{i=-\infty}^{\infty} \sum_{j=0}^{N_f-1} b_i p(t - jT_f - 2iT_s) \tag{5.1}$$

where, $E = \int_{-\infty}^{\infty} p^2(t)dt$ represents the pulse energy at each link. Similarly in the same time slot, the UWB signal transmitted from the source node to relay node is represented as:

$$s_{SR}(t) = \sqrt{E} \sum_{i=-\infty}^{\infty} \sum_{j=0}^{N_f-1} b_i p(t - jT_f - 2iT_s) \tag{5.2}$$

where, $p(t)$ denotes the second order Gaussian derivative pulse, $b_i \in (0, 1)$ the information bit, $T_s = N_f T_f$ the symbol duration, N_f the number of frames in one symbol and T_f the frame duration.

5.2.2 Channel Model

A multipath channel model specified by IEEE 802.15.4a group, is employed for performance evaluation of UWB [30] system. The impulse response of IEEE 802.15.4a UWB channel, based on the modification of SV [34] model is expressed as:

$$h_k(t) = \sum_{l=0}^{L_k-1} \alpha_{l,k} \delta(t - \tau_{l,k}) \tag{5.3}$$

where, the index $k \in (1, 2, 3)$ represents the S−D, S−R and R−D link respectively, $h_k(t)$ the channel model and L the number of multipaths. Also, $\alpha_{l,k}$ and $\tau_{l,k}$ denote the amplitude and delay of the l^{th} path in k^{th} link respectively. IEEE 802.15.4a channel models CM1 and CM2 considered for simulation, have different parameters and correspond to different usage scenario.

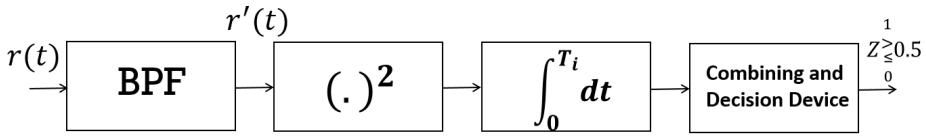

Figure 5.1: UWB ED−OOK Receiver for Cooperative Communication

5.2.3 ED Receiver

ED receiver consists of a BPF, squarer, integrator, and decision device [177], as shown in Fig 5.1. At the destination node, the received signal is first passed through a BPF, where it is filtered. The filtered signal is then squared and the resultant is passed through an integrator. The integrated output obtained from both the time slots is passed through a decision device to obtain a decision statistic, that is compared to a threshold to yield the extracted information bit.

The received signal obtained at the destination node in the 1^{st} time slot is represented as:

$$\begin{aligned} r_{SD}(t) &= \sqrt{E}\sum_{i=-\infty}^{\infty}\sum_{j=0}^{N_f-1} b_i p(t-jT_f-2iT_s) * \sum_{l=0}^{L_1-1}\alpha_{l,1}\delta(t-\tau_{l,1}) + n_{SD}(t) \\ &= \sum_{l=0}^{L_1-1}\alpha_{l,1} g_{SD}(t-jT_f-2iT_s-\tau_{l,1}) + n_{SD}(t) \end{aligned} \tag{5.4}$$

Similarly, the received signal obtained at the relay node in 1^{st} time slot is denoted as:

$$\begin{aligned} r_{SR}(t) &= \sqrt{E}\sum_{i=-\infty}^{\infty}\sum_{j=0}^{N_f-1} b_i p(t-jT_f-2iT_s) * \sum_{l=0}^{L_2-1}\alpha_{l,2}\delta(t-\tau_{l,2}) + n_{SR}(t) \\ &= \sum_{l=0}^{L_2-1}\alpha_{l,2} g_{SR}(t-jT_f-2iT_s-\tau_{l,2}) + n_{SR}(t) \end{aligned} \tag{5.5}$$

where, the aggregate signal response $g_{SD}(t)$ and $g_{SR}(t)$ is represented as $g_{SD}(t-jT_f-2iT_s-\tau_{l,1}) = s_{SD}(t) * \delta(t-\tau_{l,1})$ and $g_{SR}(t-jT_f-2iT_s-\tau_{l,2}) = s_{SR}(t) * \delta(t-\tau_{l,2})$ respectively. Here, $*$ denotes the convolution operator. The noise (AWGN) terms at S−D and S−R link are expressed as $n_{SD}(t)$ and $n_{SR}(t)$ respectively. It may also be noted that the multipath delay spread $T_{mds} > T_p$, to avoid any interference among the symbols at the receiver end.

5.3 Performance Analysis of a Cooperative AF ED-OOK system

The theoretical BER performance analysis of UWB ED−OOK system, using cooperative dual−hop AF strategy is explained vividly in this section. The received signal obtained at the destination and relay node at the end of 1st slot, is represented by equation 5.4 and 5.5 respectively. In the 1st time slot, the signal received at the destination node is detected using an ED−OOK receiver, whose decision statistics Z_{SD} is expressed as:

$$\begin{aligned} Z_{SD} &= \sum_{j=0}^{N_f-1} \int_{2iT_s+jT_f}^{2iT_s+jT_f+T_i} r_{SD}^2(t)dt \\ &= \underbrace{Z_1(k)}_{signal} + \underbrace{Z_2(k) + Z_3(k)}_{\text{noise}-term} = \underbrace{Z_1(1)}_{signal} + \underbrace{Z_2(1) + Z_3(1)}_{\text{noise}-term} \end{aligned} \tag{5.6}$$

where, the index $k \in \{1, 2, 3\}$ refers to S−D, S−R and R−D link respectively, as mentioned in equation 5.3. Also, $T_i = T_p + T_{mds}$ represents the integration time interval. Here, T_p and T_{mds} denotes pulse duration and multipath delay spread, respectively. Replacing the value of equation 5.4 in equation 5.6, we obtain the value of Z_{SD} in equation 5.7. The equation 5.7 holds true only under the constraint, that there is no IPI at the receiver end.

$$\begin{aligned} Z_{SD} &= \sum_{j=0}^{N_f-1} \int_{2iT_s+jT_f}^{2iT_s+jT_f+T_i} \left(\sum_{l=0}^{L_1-1} \alpha_{l,1} g_{SD}(t - jT_f - 2iT_s - \tau_{l,1}) + n_{SD}(t) \right)^2 \\ &= \sum_{j=0}^{N_f-1} \sum_{l=0}^{L_1-1} \alpha_{l,1}^2 \int_{2iT_s+jT_f}^{2iT_s+jT_f+T_i} g_{SD}^2(t - jT_f - 2iT_s - \tau_{l,1})dt + 2 \sum_{j=0}^{N_f-1} \sum_{l=0}^{L_1-1} \alpha_{l,1} \\ &\quad \int_{2iT_s+jT_f}^{2iT_s+jT_f+T_i} g_{SD}(t - jT_f - 2iT_s - \tau_{l,1}) n_{SD}(t)dt + \sum_{j=0}^{N_f-1} \int_{2iT_s+jT_f}^{2iT_s+jT_f+T_i} \\ &\quad n_{SD}^2(t)dt \end{aligned} \tag{5.7}$$

The signal term obtained from S−D link is represented as:

$$\begin{aligned} Z_1(1) &= \sum_{j=0}^{N_f-1} \sum_{l=0}^{L_1-1} \alpha_{l,1}^2 \int_{2iT_s+jT_f}^{2iT_s+jT_f+T_i} g_{SD}^2(t - jT_f - 2iT_s - \tau_{l,1})dt \\ &= sig_{SD} = Z_1(1) = N_f E_{SD} \gamma_1 \end{aligned} \tag{5.8}$$

where, $E_{SD} = \int_{2iT_s+jT_f}^{2iT_s+jT_f+T_i} g_{SD}^2(t - jT_f - 2iT_s - \tau_{l,1})dt$ denotes the received signal energy obtained from S−D link, due to transmission of information bit $b_i \in \{0, 1\}$ in 1st time slot. The channel gains $\alpha_{l,k}$ for IEEE 802.15.4a UWB multipath channels are assumed to be IID Nakagami. Consequently, their squares will be IID Gamma distributed [179]. Hence, by invoking

the Central Limit Theorem $\sum_{l_k} \alpha_{l_k}^2 = \gamma_k$ may be approximated as Gaussian distributed. The decision variables $Z_2(1)$ and $Z_3(1)$ denote the noise terms, so their variances are evaluated as shown below.

The filtering of AWGN process having PSD $\frac{N_0}{2}$ with a BPF W, results in noise terms $n_k(t)$. Here, the index $k \in \{1, 2, 3\}$ refers to S$-$D, S$-$R and R$-$D link respectively, as discussed in equation 5.3. The autocorrelation function of noise $\theta_k(\tau)$ is given by [175]:-

$$\theta_k(\tau) = \mathbb{E}[n_k(t)n_k(t-\tau)] = \frac{N_0}{2}\frac{Sin(\pi W\tau)}{\pi W\tau}cos(2\pi f_c\tau) \tag{5.9}$$

where, $\mathbb{E}[.]$ denotes the statistical expectation operator and f_c carrier frequency of BPF. Since the Bandwidth is assumed to be sufficiently large, the frequency response of the received signal $g_k(t)$ at destination node falls inside the PSD $\theta_k(f)$ of $n_k(t)$. As PSD of noise $\theta_k(f)$ is sufficiently flat, its autocorrelation function can be simplified as $\theta_k(\tau) = \frac{N_0}{2}\delta(\tau)$ [175]. The noise variances calculated for S$-$D link is as follows.

$$\begin{aligned}
\sigma_{N_1}^2 &= \mathbb{E}[Z_2^2(1)] = 2\sum_{j=0}^{N_f-1}\sum_{l=0}^{L_2-1}\alpha_{l,1}^2\int_{2iT_s+jT_f}^{2iT_s+jT_f+T_i}\int_{2iT_s+jT_f}^{2iT_s+jT_f+T_i} g_{SD}(t-jT_f-2iT_s-\tau_{l,1}) \\
&\quad g_{SD}(\tau-jT_f-2iT_s-\tau_{l,1})\,\mathbb{E}[n_{SD}(t)n_{SD}(\tau)]dtd\tau \\
&= 2N_f\gamma_1\int_{2iT_s+jT_f}^{2iT_s+jT_f+T_i} g_{SD}(t-jT_f-2iT_s-\tau_{l,1})g_{SD}(\tau-jT_f-2iT_s-\tau_{l,1}) \\
&\quad \theta_1(t-\tau)dtd\tau \\
&= 2N_f\gamma_1\frac{N_0}{2}\int_{2iT_s+jT_f}^{2iT_s+jT_f+T_i} g_{SD}^2(t-jT_f-2iT_s-\tau_{l,1})dt \\
&= N_fN_0E_{SD}\gamma_1
\end{aligned} \tag{5.10}$$

where, $\mathbb{E}[n_{SD}(t)n_{SD}(\tau)] = \theta_1(t-\tau) = \frac{N_0}{2}\delta(t-\tau)$ and $\int_{2iT_s+jT_f}^{2iT_s+jT_f+T_i}\frac{N_0}{2}\delta(t-\tau)d\tau = \frac{N_0}{2}$.

$$\begin{aligned}
\sigma_{N_2}^2 &= \mathbb{E}[Z_3^2(1)] = \sum_{j=0}^{N_f-1}\int_{2iT_s+jT_f}^{2iT_s+jT_f+T_i}\int_{2iT_s+jT_f}^{2iT_s+jT_f+T_i}\mathbb{E}\left[\left\{n_{SD}^2(t)\right\}^2\right]dtd\tau \\
&= N_f\int_0^{T_i}\int_{T_i-t}^{T_i}\frac{N_0^2}{2}d\tau dt = N_f\int_0^{T_i}\frac{N_0^2}{2}2Wdt = N_fN_0^2WT_i
\end{aligned} \tag{5.11}$$

where, the value of $\mathbb{E}\left[\left\{n_{SD}^2(t)\right\}^2\right] = \frac{N_0^2}{2}$ is solved in equation A.2 of Appendix A. As the variance of $[n_k^2(t)]$ tends to Dirac-Delta function, the integral vanishes outside the range $[-t, T_i - t]$. Parsevals Theorem is applied to solve equation 5.11.

The signal received at the relay node in 1st time slot, is amplified by an amplifying factor $\sqrt{\beta_{AF}}$ and forwarded to the destination node in 2nd time slot. The amplified signal transmitted

from the relay node to the destination node is represented as:

$$s_{RD}(t) = r_{SR}(t)\sqrt{\beta_{AF}} \tag{5.12}$$

where, the amplifying gain is defined as $\sqrt{\beta_{AF}} = \sqrt{\left(\frac{E_{SR}}{\mathbb{E}\left\{|h_2^2(t)|\right\}E_{SR}+N_0}\right)}$ and $\mathbb{E}$ denotes the expectation operator. Here, E_{SR}, $h_2(t)$ and $\sigma^2_{Z_{noise-SR}} = N_f N_0 E_{SR}\gamma_2 + N_f N_0^2 W T_i$ represent signal energy, channel response and noise variance of S−R link respectively. The signal received at the destination node from R−D link in 2nd time slot is represented as:

$$\begin{aligned} r_{RD}(t) &= \left(\sqrt{\beta_{AF}}\sum_{l=0}^{L_2-1}\alpha_{l,2}g_{SR}(t-jT_f-(2i+1)T_s-\tau_{l,2})+n_{SR}(t)\right) * \sum_{l=0}^{L_3-1}\alpha_{l,3}\delta(t- \\ &\quad \tau_{l,3})+n_{RD}(t) \\ &= \sqrt{\beta_{AF}}\sum_{l=0}^{L_2-1}\alpha_{l,2}\sum_{l=0}^{L_3-1}\alpha_{l,3}g_{SR}(t-jT_f-(2i+1)T_s-\tau_{l,2}-\tau_{l,3})+\sqrt{\beta_{AF}}n_{RD}^{'}(t) \\ &\quad +n_{RD}(t) \end{aligned} \tag{5.13}$$

where, $n_{RD}^{'}(t) = n_{SR}(t) * h_3(t) = \sum_{l=0}^{L_3-1}\alpha_{l,3}n_{SR}(t-\tau_{l,3})$ represents the aggregate noise response after convolving the noise response of S−R link with channel response of R−D link $h_3(t)$ and $n_{RD}(t)$ denotes the noise response of R−D link.

The received signal $r_{RD}(t)$ obtained at the destination node in the 2nd time slot, is passed through a ED−OOK receiver, whose decision statistics Z_{RD} is expressed as:

$$\begin{aligned} Z_{RD} &= \sum_{j=0}^{N_f-1}\int_{(2i+1)T_s+jT_f}^{(2i+1)T_s+jT_f+T_i} r_{RD}^2(t)dt \\ &= \underbrace{Z_1(3)}_{signal} + \underbrace{Z_2(3)+Z_3(3)+Z_4(3)+Z_5(3)+Z_6(3)}_{\text{noiseterm}} \end{aligned} \tag{5.14}$$

Replacing the value of equation 5.13 in equation 5.14, we obtain the value of Z_{RD} in equation 5.15.

$$\begin{aligned} &= \sum_{j=0}^{N_f-1}\int_{(2i+1)T_s+jT_f}^{(2i+1)T_s+jT_f+T_i}\left(\sqrt{\beta_{AF}}\sum_{l=0}^{L_2-1}\sum_{l=0}^{L_3-1}\alpha_{l,2}\alpha_{l,3}g_{SR}(t-jT_f-(2i+1)T_s-\tau_{l,2}-\tau_{l,3})\right. \\ &\quad \left.+\sqrt{\beta_{AF}}n_{RD}^{'}(t)+n_{RD}(t)\right)^2 dt \end{aligned} \tag{5.15}$$

The signal term obtained from R−D link is represented as:

$$\begin{aligned} Z_1(3) &= \beta_{AF}\sum_{j=0}^{N_f-1}\sum_{l=0}^{L_2-1}\alpha_{l,2}^2\sum_{l=0}^{L_3-1}\alpha_{l,3}^2\int_{(2i+1)T_s+jT_f}^{(2i+1)T_s+jT_f+T_i} g_{SR}^2(t-jT_f-(2i+1)T_s-\tau_{l,2} \\ &\quad -\tau_{l,3})dt \end{aligned}$$

$$= \quad Z_1(3) = \beta_{AF} N_f E_{RD} \gamma_2 \gamma_3 \tag{5.16}$$

where, $E_{RD} = \int_{(2i+1)T_s+jT_f}^{(2i+1)T_s+jT_f+T_i} g_{SR}^2(t - jT_f - (2i+1)T_s - \tau_{l,2} - \tau_{l,3})dt$ represents the received signal energy obtained from R$-$D link. As explained earlier, since a large number of UWB multipath channel gains are considered, the channel gains can be approximated as Gaussian Distributed using the Central Limit Theorem $\sum_{l_2} \alpha_{l_2}^2 = \gamma_2$ and $\sum_{l_3} \alpha_{l_3}^2 = \gamma_3$. As described earlier, since the PSD $\theta_k(f)$ of noise is sufficiently flat, the autocorrelation function of noise can be approximated as $\theta_k(\tau) = \frac{N_0}{2}\delta(\tau)$[175]. As the decision variables $Z_2(3)$, $Z_3(3)$, $Z_4(3)$, $Z_5(3)$ and $Z_6(3)$ contain noise terms, their variances are evaluated as shown below.

$$\begin{aligned}
\sigma_{N_1}^2 &= E[Z_2^2(3)] = 2\beta_{AF}^2 \sum_{j=0}^{N_f-1} \sum_{l=0}^{L_2-1} \alpha_{l,2}^2 \sum_{l=0}^{L_3-1} \alpha_{l,3}^2 \int_{(2i+1)T_s+jT_f}^{(2i+1)T_s+jT_f+T_i} g_{SR}(t - jT_f - (2i+1)T_s \\
&\quad -\tau_{l,2} - \tau_{l,3}) g_{SR}(\tau - jT_f - (2i+1)T_s - \tau_{l,2} - \tau_{l,3}) E[n_{RD}^{'}(t) n_{RD}^{'}(\tau)] dt d\tau] \\
&= 2\beta_{AF}^2 N_f \gamma_2 \gamma_3 \left(\gamma_3 \frac{N_0}{2}\right) \int_{(2i+1)T_s+jT_f}^{(2i+1)T_s+jT_f+T_i} g_{SR}^2(t - jT_f - (2i+1)T_s - \tau_{l,2} \\
&\quad -\tau_{l,3}) dt \\
&= \beta_{AF}^2 N_f N_0 E_{RD} \gamma_2 \gamma_3^2
\end{aligned} \tag{5.17}$$

where, $\int_{(2i+1)T_s+jT_f}^{(2i+1)T_s+jT_f+T_i} \theta_2(t-\tau)d\tau = \int_{(2i+1)T_s+jT_f}^{(2i+1)T_s+jT_f+T_i} \frac{N_0}{2}\delta(t-\tau)d\tau = \frac{N_0}{2}$. The value of $\mathbb{E}[n_{RD}^{'}(t) n_{RD}^{'}(\tau)]$ is solved in Appendix B.

$$\begin{aligned}
\sigma_{N_2}^2 &= E[Z_3^2(3)] = 2\sqrt{\beta_{AF}}^2 \sum_{j=0}^{N_f-1} \sum_{l=0}^{L_2-1} \alpha_{l,2}^2 \sum_{l=0}^{L_3-1} \alpha_{l,3}^2 \int_{(2i+1)T_s+jT_f}^{(2i+1)T_s+jT_f+T_i} \int_{(2i+1)T_s+jT_f}^{(2i+1)T_s+jT_f+T_i} \\
&\quad g_{SR}(t - jT_f - (2i+1)T_s - \tau_{l,2} - \tau_{l,3}) g_{SR}(\tau - jT_f - (2i+1)T_s - \tau_{l,2} - \tau_{l,3}) \\
&\quad \mathbb{E}[n_{RD}(t) n_{RD}(\tau)] dt d\tau \\
&= 2\beta_{AF} N_f \gamma_2 \gamma_3 \frac{N_0}{2} \int_{(2i+1)T_s+jT_f}^{(2i+1)T_s+jT_f+T_i} g_{SR}^2(t - jT_f - (2i+1)T_s - \tau_{l,2} - \tau_{l,3}) dt \\
&= \beta_{AF} N_f N_0 E_{RD} \gamma_2 \gamma_3
\end{aligned} \tag{5.18}$$

where, $\theta_3(t-\tau) = \mathbb{E}[n_{RD}(t) n_{RD}(\tau)] = \frac{N_0}{2}(t-\tau)$ and $\int_{(2i+1)T_s+jT_f}^{(2i+1)T_s+jT_f+T_i} \frac{N_0}{2}\delta(t-\tau) = \frac{N_0}{2}$.

$$\begin{aligned}
\sigma_{N_3}^2 &= E[Z_4^2(3)] = \beta_{AF}^2 \sum_{j=0}^{N_f-1} \int_{(2i+1)T_s+jT_f}^{(2i+1)T_s+jT_f+T_i} \int_{(2i+1)T_s+jT_f}^{(2i+1)T_s+jT_f+T_i} \mathbb{E}\left[\left\{ n_{RD}^{'2}(t) \right\}^2 \right] \\
&\quad dt d\tau \\
&= \beta_{AF}^2 N_f \int_0^{T_i} 2\left(\gamma_3 \frac{N_0}{2}\right)^2 2W dt \\
&= \beta_{AF}^2 N_f N_0^2 W T_i \gamma_3^2
\end{aligned} \tag{5.19}$$

where, $\mathbb{E}\left[\left\{ n_{RD}^{'2}(t) \right\}^2 \right] = 3\left(\gamma_3 \frac{N_0}{2}\right)^2 - \left(\gamma_3 \frac{N_0}{2}\right)^2 = 2\left(\gamma_3 \frac{N_0}{2}\right)^2$

$$\begin{aligned}\sigma_{N_4}^2 &= E[Z_5^2(3)] = \sum_{j=0}^{N_f-1} \int_{(2i+1)T_s+jT_f}^{(2i+1)T_s+jT_f+T_i} \int_{(2i+1)T_s+jT_f}^{(2i+1)T_s+jT_f+T_i} \mathbb{E}\left[\left\{n_{RD}^2(t)\right\}^2\right] dtd\tau \\ &= N_f \int_0^{T_i} \frac{{N_0}^2}{2} 2W dt \\ &= N_f N_0^2 W T_i \end{aligned} \tag{5.20}$$

where, the value of $\mathbb{E}\left[\left\{n_{RD}^2(t)\right\}^2\right] = \frac{{N_0}^2}{2}$ is obtained from equation A.2 of Appendix A.

$$\begin{aligned}\sigma_{N_5}^2 &= E[Z_6^2(3)] = 2\sum_{j=0}^{N_f-1} \beta_{AF} \int_{(2i+1)T_s+jT_f}^{(2i+1)T_s+jT_f+T_i} \int_{(2i+1)T_s+jT_f}^{(2i+1)T_s+jT_f+T_i} \\ &\quad \mathbb{E}[n_{RD}(t)n_{RD}^{'}(t)n_{RD}(\tau)n_{RD}^{'}(\tau)]dtd\tau \\ &= 2\sum_{j=0}^{N_f-1} \beta_{AF} \int_{(2i+1)T_s+jT_f}^{(2i+1)T_s+jT_f+T_i} \int_{(2i+1)T_s+jT_f}^{(2i+1)T_s+jT_f+T_i} \\ &\quad \mathbb{E}[n_{RD}(t)n_{RD}(\tau)]\,\mathbb{E}[n_{RD}^{'}(t)n_{RD}^{'}(\tau)]dtd\tau \\ &= 2\beta_{AF}N_f \int_{(2i+1)T_s+jT_f}^{(2i+1)T_s+jT_f+T_i} \int_{(2i+1)T_s+jT_f}^{(2i+1)T_s+jT_f+T_i} \theta_3(t-\tau)\theta_3^{'}(t-\tau)dtd\tau \\ &= 2\beta_{AF}N_f \int_0^{T_i} \left(\frac{N_0}{2}\right)\left(\gamma_3\frac{N_0}{2}\right) 2W dt \\ &= \beta_{AF}N_f N_0^2 W T_i \gamma_3 \end{aligned} \tag{5.21}$$

where, $\mathbb{E}[n_{RD}(t)n_{RD}^{'}(t)n_{RD}(\tau)n_{RD}^{'}(\tau)] = \mathbb{E}[n_{RD}(t)n_{RD}(\tau)]\,\mathbb{E}[n_{RD}^{'}(t)n_{RD}^{'}(\tau)]$ since the noise terms corresponding to different links are independent in nature.

The decision statistic Z_{SD} contains signal term $sig_{SD} = Z_1(1) = N_f E_{SD}\gamma_1$ and noise term $Z_{noise-SD} = Z_2(1) + Z_3(1)$. The noise term $Z_{noise-SD}$ has a total variance of $\sigma^2_{Z_{noise-SD}} = N_f N_0 E_{SD}\gamma_1 + N_f N_0^2 W T_i$. Similarly, the decision statistic Z_{RD} contains signal term $sig_{RD} = Z_1(3) = \beta_{AF}N_f E_{RD}\gamma_2\gamma_3$ and noise term $Z_{noise-RD} = Z_2(3) + Z_3(3) + Z_4(3) + Z_5(3) + Z_6(3)$. The noise term $Z_{noise-RD}$ has a total variance of $\sigma^2_{Z_{noise-RD}} = \beta_{AF}^2 N_f N_0 E_{RD}\gamma_2\gamma_3^2 + \beta_{AF}N_f N_0 E_{RD}\gamma_2\gamma_3 + \beta_{AF}N_f N_0^2 W T_i\gamma_3^2 + N_f N_0^2 W T_i + \beta_{AF}N_f N_0^2 W T_i\gamma_3$.

The SNR obtained at the destination node from S−D and R−D links in 1st and 2nd time slot respectively, is represented as follows:

$$\rho_{SD-AF} = \frac{\left(N_f E_{SD}\gamma_1\right)^2}{N_f N_0 E_{SD}\gamma_1 + N_f N_0^2 W T_i} \tag{5.22}$$

$$\rho_{RD-AF} = \left(\frac{(D)^2}{E+F}\right) \tag{5.23}$$

where, $D = \beta_{AF} N_f E_{RD} \gamma_2 \gamma_3$, $E = \beta_{AF} N_f N_0 E_{RD} \gamma_2 \gamma_3 [1 + \beta_{AF} \gamma_3]$ and $F = N_f N_0^2 W T_i [1 + \beta_{AF}^2 \gamma_3^2 + \beta_{AF} \gamma_3]$. The decision statistics obtained at the destination node in the two time slots, are combined using different combining strategies such as optimum linear combining, linear combining and selective combining, to form the final decision statistic, as explained below in the subsequent sections.

5.3.1 Linear Combining

The decision statistics Z_{SD} and Z_{RD} obtained at the destination node in 1^{st} and 2^{nd} time slots respectively, are linearly combined to form final decision statistic $Z_{total} = Z_{SD} + Z_{RD} = s_{total-signal} + Z_{noise-total}$. The individual decision statistics obtained from S$-$D and R$-$D links are as follows:

$$Z_{SD} = sig_{SD} + Z_{noise-SD} \tag{5.24}$$

$$Z_{RD} = sig_{RD} + Z_{noise-RD} \tag{5.25}$$

The final decision statistic Z_{total} is represented as:

$$\begin{aligned} Z_{total} &= Z_{SD} + Z_{RD} \\ &= \underbrace{sig_{SD} + sig_{RD}}_{\text{s}_{total-signal}} + \underbrace{Z_{noise-SD} + Z_{noise-RD}}_{\text{Z}_{noise-total}} \end{aligned} \tag{5.26}$$

The noise term $Z_{noise-total}$ has a total variance of $\sigma^2_{Z_{noise-total}} = \sigma^2_{Z_{noise-SD}} + \sigma^2_{Z_{noise-RD}}$ as solved in equation 5.27. Here, sig_{SD} and $Z_{noise-SD}$ represents the signal and noise terms obtained from S$-$D channel link while, sig_{RD} and $Z_{noise-RD}$ denotes the signal and noise terms obtained from R$-$D channel link. The total noise variance is evaluated as:

$$\begin{aligned} \sigma^2_{Z_{noise-total}} &= \mathbb{E}[Z_{noise-total}]^2 \\ &= \mathbb{E}[(Z_{noise-SD} + Z_{noise-RD})]^2 \\ &= \sigma^2_{Z_{noise-SD}} + \sigma^2_{Z_{noise-RD}} \end{aligned} \tag{5.27}$$

where, $\mathbb{E}[Z^2_{noise-SD}] = \sigma^2_{Z_{noise-SD}}$, $\mathbb{E}[Z^2_{noise-RD}] = \sigma^2_{Z_{noise-RD}}$ and $\mathbb{E}[Z_{noise-SD} Z_{noise-RD}] = 0$ as the noise terms from S$-$D and R$-$D link are independent, their cross$-$correlation is 0. Subsequently, the SNR at the destination node due to linear combining is expressed as:

$$\rho_{AF-LC} = \left(\frac{s^2_{total-signal}}{\sigma^2_{Z_{noise-total}}} \right) = \frac{(sig_{SD} + sig_{RD})^2}{(\sigma^2_{Z_{noise-SD}} + \sigma^2_{Z_{noise-RD}})} = \left(\frac{(C)^2}{A + B} \right) \tag{5.28}$$

where, $A = N_f N_0(E_{SD}\gamma_1 + WT_i N_0)$, $B = \beta_{AF} N_f N_0 E_{RD}\gamma_2\gamma_3[1 + \beta_{AF}\gamma_3] + N_f N_0^2 WT_i[1 + \beta_{AF}^2\gamma_3^2 + \beta_{AF}\gamma_3]$ and $C = N_f E_{SD}\gamma_1 + \beta_{AF} N_f E_{RD}\gamma_2\gamma_3$.

The information bit is extracted by comparing the final decision statistic Z_{total} to a decision threshold, which is calculated using OOK modulation scheme. The final decision criteria $\hat{z}$ for linear combining is represented as:

$$\hat{z} = \begin{cases} 0, & H_0 : Z = Z_{total} \leq \frac{\eta_1^\zeta N_f E_{SD} + \eta_{23}^\zeta \beta_{AF} N_f E_{RD}}{2} \\ 1, & H_1 : Z = Z_{total} > \frac{\eta_1^\zeta N_f E_{SD} + \eta_{23}^\zeta \beta_{AF} N_f E_{RD}}{2} \end{cases} \tag{5.29}$$

where, $\eta_1^\zeta = \mathbb{E}[\gamma_1]$ and $\eta_{23}^\zeta = \mathbb{E}[\gamma_2\gamma_3]$. Also, $\zeta \in \{CM1\}$ represents UWB CM1 channel.

By applying the Central Limit Theorem, the individual channel gains for S−D, S−R and R−D channel links may be assumed to be IID Gaussian distributed since a large number paths are involved. Therefore, the sum of these channel gains will also have a Gaussian distribution with its mean being the sum of individual means and variance being sum of the individual variances. The joint PDF $f_{\rho_{AF}}(\gamma_1, \gamma_2, \gamma_3)$ of the channel in case of linear combining is also gaussian and is represented as:

$$\begin{aligned} f_{\rho_{AF}}(\gamma_1, \gamma_2, \gamma_3) &= \frac{1}{\sqrt{(2\pi(\sigma_{SD}^2))}} \frac{1}{\sqrt{(2\pi(\sigma_{SR}^2))}} \frac{1}{\sqrt{(2\pi(\sigma_{RD}^2))}} \exp\left[\frac{-(\gamma_1 - \mu_{SD})^2}{2\sigma_{SD}^2} + \right. \\ &\left. \frac{-(\gamma_2 - \mu_{SR})^2}{2\sigma_{SR}^2} + \frac{-(\gamma_3 - \mu_{RD})^2}{2\sigma_{RD}^2}\right] \end{aligned} \tag{5.30}$$

where, μ_k and σ_k^2 represent the mean and variance of channel links. The index $k \in \{1, 2, 3\}$ refers to S−D, S−R and R−D link respectively, as mentioned in equation 5.3. Since the joint PDF of channel link is IID distributed, it is given by $f_{\rho_{AF}}(\gamma_1, \gamma_2, \gamma_3) = f_{\rho_{AF}}(\gamma_1) f_{\rho_{AF}}(\gamma_2) f_{\rho_{AF}}(\gamma_3)$. Finally, the BER of UWB ED−OOK system using linear combining is expressed as:

$$\begin{aligned} BER_{LC-AF} &= \int_0^\infty \int_0^\infty \int_0^\infty Q\left(\frac{1}{2}\sqrt{\rho_{AF-LC}}\right) f_{\rho_{AF}}(\gamma_1, \gamma_2, \gamma_3) d\gamma_1 d\gamma_2 d\gamma_3 \\ &= \int_0^\infty \int_0^\infty \int_0^\infty Q\left(\frac{1}{2}\sqrt{\rho_{AF-LC}}\right) \frac{1}{\sqrt{(2\pi(\sigma_{SD}^2))}} \frac{1}{\sqrt{(2\pi(\sigma_{SR}^2))}} \frac{1}{\sqrt{(2\pi(\sigma_{RD}^2))}} \\ &\quad \exp\left[\frac{-(\gamma_1 - \mu_{SD})^2}{2\sigma_{SD}^2} + \frac{-(\gamma_2 - \mu_{SR})^2}{2\sigma_{SR}^2} + \frac{-(\gamma_3 - \mu_{RD})^2}{2\sigma_{RD}^2}\right] d\gamma_1 d\gamma_2 d\gamma_3 \end{aligned} \tag{5.31}$$

$$\begin{aligned} &= \int_0^\infty \int_0^\infty \int_0^\infty Q\left(\frac{1}{2}\sqrt{\frac{(C)^2}{A+B}}\right) \frac{1}{\sqrt{(2\pi(\sigma_{SD}^2))}} \frac{1}{\sqrt{(2\pi(\sigma_{SR}^2))}} \frac{1}{\sqrt{(2\pi(\sigma_{RD}^2))}} \\ &\quad \exp\left[\frac{-(\gamma_1 - \mu_{SD})^2}{2\sigma_{SD}^2} + \frac{-(\gamma_2 - \mu_{SR})^2}{2\sigma_{SR}^2} + \frac{-(\gamma_3 - \mu_{RD})^2}{2\sigma_{RD}^2}\right] d\gamma_1 d\gamma_2 d\gamma_3 \end{aligned} \tag{5.32}$$

5.3.2 Selective Combining

In selective combining, the SNR corresponding to the decision variables Z_{SD} and Z_{RD} obtained from S−D and R−D link respectively are compared, and the one with the highest SNR is chosen. ρ_{SD-AF} and ρ_{RD-AF} denotes the SNR obtained from S−D and R−D links respectively, as mentioned in equation 5.22 and 5.23 respectively.

The SNR at destination node due to selective combining is expressed as $\rho_{AF-SC} = Max\left\{\rho_{SD-AF}, \rho_{RD-AF}\right\}$. Therefore, the BER of UWB ED−OOK system using cooperative dual−hop AF strategy with selective combining is represented as:

$$\begin{aligned} BER_{SC-AF} &= \int_0^\infty \int_0^\infty \int_0^\infty Q\left(\frac{1}{2}\sqrt{\rho_{AF-SC}}\right) f_{\rho_{AF}}(\gamma_1,\gamma_2,\gamma_3) d\gamma_1 d\gamma_2 d\gamma_3 \\ &= \int_0^\infty \int_0^\infty \int_0^\infty Q\left(\frac{1}{2}\sqrt{\rho_{AF-SC}}\right) \frac{1}{\sqrt{(2\pi(\sigma_{SD}^2))}} \frac{1}{\sqrt{(2\pi(\sigma_{SR}^2))}} \frac{1}{\sqrt{(2\pi(\sigma_{RD}^2))}} \\ &\quad \exp\left[\frac{-(\gamma_1-\mu_{SD})^2}{2\sigma_{SD}^2} + \frac{-(\gamma_2-\mu_{SR})^2}{2\sigma_{SR}^2} + \frac{-(\gamma_3-\mu_{RD})^2}{2\sigma_{RD}^2}\right] d\gamma_1 d\gamma_2 d\gamma_3 \end{aligned} \quad (5.33)$$

The joint PDF of channel link is IID distributed, hence it can be represented as $f_{\rho_{AF}}(\gamma_1,\gamma_2,\gamma_3) = f_{\rho_{AF}}(\gamma_1) f_{\rho_{AF}}(\gamma_2) f_{\rho_{AF}}(\gamma_3)$. Replacing the value of ρ_{AF-SC} in equation 5.34, we obtain the final BER expression of UWB ED−OOK system using selective combining, in equation 5.35.

$$\begin{aligned} &= \int_0^\infty \int_0^\infty \int_0^\infty Q\left(\frac{1}{2}\sqrt{Max\left\{\rho_{SD-AF}, \rho_{RD-AF}\right\}}\right) \frac{1}{\sqrt{(2\pi(\sigma_{SD}^2))}} \frac{1}{\sqrt{(2\pi(\sigma_{SR}^2))}} \frac{1}{\sqrt{(2\pi(\sigma_{RD}^2))}} \\ &\quad \exp\left[\frac{-(\gamma_1-\mu_{SD})^2}{2\sigma_{SD}^2} + \frac{-(\gamma_2-\mu_{SR})^2}{2\sigma_{SR}^2} + \frac{-(\gamma_3-\mu_{RD})^2}{2\sigma_{RD}^2}\right] d\gamma_1 d\gamma_2 d\gamma_3 \end{aligned} \quad (5.34)$$

5.3.3 Optimum Linear Combining

The decision statistics obtained at the destination node from S−D and R−D links in 1st and 2nd time slots respectively, are optimally combined to form the final decision statistic $Z_{total} = Z_{SD} + \kappa Z_{RD}$. The optimal combining factor $\kappa = \frac{(\sigma^2_{Z_{noise-SD}})sig_{RD}}{(\sigma^2_{Z_{noise-RD}})sig_{SD}}$ is solved in equation C.4 of Appendix C. The final decision statistic Z_{total} obtained at the destination node using optimum linear combining scheme, is denoted by equation 5.36.

$$\begin{aligned} Z_{total} &= Z_{SD} + \kappa Z_{RD} \\ &= \underbrace{sig_{SD} + \kappa sig_{RD}}_{\mathrm{s}_{total-signal}} + \underbrace{Z_{noise-SD} + \kappa(Z_{noise-RD})}_{\mathrm{Z}_{noise-total}} \end{aligned} \quad (5.35)$$

For solving the noise term, we evaluate its variance which is solved below.

$$\sigma^2_{Z_{noise-total}} = \mathbb{E}[Z_{noise-total}]^2$$

$$= \mathbb{E}[(Z_{noise-SD} + \kappa Z_{noise-RD})]^2$$
$$= \sigma^2_{Z_{noise-SD}} + \kappa^2 \sigma^2_{Z_{noise-RD}} \quad (5.36)$$

where, $2\kappa\,\mathbb{E}[Z_{noise-SD}Z_{noise-RD}] = 0$, because the cross correlation of two independent noise terms are 0. Also, $\sigma^2_{Z_{noise-total}}$ and $s_{total-signal}$ represent the total noise variance and total signal term respectively. Therefore, the SNR at the destination node due to optimum linear combining is duly expressed as:

$$\rho_{AF-LOC} = \left(\frac{s^2_{total-signal}}{\sigma^2_{Z_{noise-total}}}\right) = \frac{(sig_{SD} + \kappa sig_{RD})^2}{(\sigma^2_{Z_{noise-SD}} + \kappa^2\sigma^2_{Z_{noise-RD}})} = \left(\frac{(X)^2}{A + \kappa^2 B}\right) \quad (5.37)$$

where, $X = N_f E_{SD}\gamma_1 + \kappa\beta_{AF}N_f E_{RD}\gamma_2\gamma_3$, $A = N_f N_0(E_{SD}\gamma_1 + WT_i N_0)$ and $B = \beta_{AF}N_f N_0 E_{RD}\gamma_2\gamma_3[1 + \beta_{AF}\gamma_3] + N_f N_0^2 WT_i[1 + \beta^2_{AF}\gamma^2_3 + \beta_{AF}\gamma_3]$.

In order to recover the transmitted bit, the final decision statistic Z_{total} is compared to the decision threshold, which depends on OOK signalling. The decision criteria $\hat{z}$ for optimum linear combining is represented as:

$$\hat{z} = \begin{cases} 0, & H_0 : Z = Z_{total} \leq \frac{\eta_1^\zeta N_f E_{SD} + \kappa\eta_{23}^\zeta \beta_{AF} N_f E_{RD}}{2} \\ 1, & H_1 : Z = Z_{total} > \frac{\eta_1^\zeta N_f E_{SD} + \kappa\eta_{23}^\zeta \beta_{AF} N_f E_{RD}}{2} \end{cases} \quad (5.38)$$

where, $\eta_1^\zeta = \mathbb{E}[\gamma_1]$ and $\eta_{23}^\zeta = \mathbb{E}[\gamma_2\gamma_3]$. Also, $\zeta \in \{CM1\}$ represents UWB CM1 channel. The joint PDF of channel links in case of optimum linear combining is expressed as:

$$f_{\rho_{AF}}(\gamma_1,\gamma_2,\gamma_3) = \frac{1}{\sqrt{(2\pi(\sigma^2_{SD}))}}\frac{1}{\sqrt{(2\pi(\kappa^2\sigma^2_{SR}))}}\frac{1}{\sqrt{(2\pi(\kappa^2\sigma^2_{RD}))}}\exp\left[\frac{-(\gamma_1-\mu_{SD})^2}{2\sigma^2_{SD}} + \frac{-(\gamma_2-\mu_{SR})^2}{2\kappa^2\sigma^2_{SR}} + \frac{-(\gamma_3-\mu_{RD})^2}{2\kappa^2\sigma^2_{RD}}\right] \quad (5.39)$$

Since the joint PDF of channel link is IID distributed, it is represented as $f_{\rho_{AF}}(\gamma_1,\gamma_2,\gamma_3) = f_{\rho_{AF}}(\gamma_1)f_{\rho_{AF}}(\gamma_2)f_{\rho_{AF}}(\gamma_3)$.

Finally, the BER of UWB ED−OOK system using dual−hop cooperative AF strategy with optimum linear combining is denoted as:

$$BER_{LOC-AF} = \int_0^\infty\int_0^\infty\int_0^\infty Q\left(\frac{1}{2}\sqrt{\rho_{AF-LOC}}\right) f_{\rho_{AF}}(\gamma_1,\gamma_2,\gamma_3)d\gamma_1 d\gamma_2 d\gamma_3$$
$$= \int_0^\infty\int_0^\infty\int_0^\infty Q\left(\frac{1}{2}\sqrt{\rho_{AF-LOC}}\frac{1}{\sqrt{(2\pi(\sigma^2_{SD}))}}\frac{1}{\sqrt{(2\pi(\kappa^2\sigma^2_{SR}))}}\right.$$
$$\left.\frac{1}{\sqrt{(2\pi(\kappa^2\sigma^2_{RD}))}}\exp\left[\frac{-(\gamma_1-\mu_{SD})^2}{2\sigma^2_{SD}} + \frac{-(\gamma_2-\mu_{SR})^2}{2\kappa^2\sigma^2_{SR}} + \frac{-(\gamma_3-\mu_{RD})^2}{2\kappa^2\sigma^2_{RD}}\right]\right.$$
$$d\gamma_1 d\gamma_2 d\gamma_3 \quad (5.40)$$

$$= \int_0^\infty \int_0^\infty \int_0^\infty Q\left(\frac{1}{2}\sqrt{\frac{X^2}{A+\kappa^2 B}}\right) \frac{1}{\sqrt{(2\pi(\sigma_{SD}^2))}} \frac{1}{\sqrt{(2\pi(\kappa^2\sigma_{SR}^2))}} \frac{1}{\sqrt{(2\pi(\kappa^2\sigma_{RD}^2))}}$$
$$\exp\left[\frac{-(\gamma_1-\mu_{SD})^2}{2\sigma_{SD}^2} + \frac{-(\gamma_2-\mu_{SR})^2}{2\kappa^2\sigma_{SR}^2} + \frac{-(\gamma_3-\mu_{RD})^2}{2\kappa^2\sigma_{RD}^2}\right] d\gamma_1 d\gamma_2 d\gamma_3 \quad (5.41)$$

5.4 Performance Analysis of a Cooperative DTF ED-OOK System

The theoretical BER performance analysis of UWB ED−OOK system, using dual−hop cooperative DTF relay strategy is presented in this section [182]. At the end of 1st time slot, the signal received at the destination node and relay node is represented by equation 5.4 and 5.5 respectively. It can be simplified as:

$$r_{SD}(t) = \sum_{l=0}^{L_1-1} \alpha_{l,1} b_i g_{SD}(t - jT_f - 2iT_s - \tau_{l,1}) + n_{SD}(t) \quad (5.42)$$

$$r_{SR}(t) = \sum_{l=0}^{L_2-1} \alpha_{l,2} b_i g_{SR}(t - jT_f - 2iT_s - \tau_{l,2}) + n_{SR}(t) \quad (5.43)$$

where, the aggregate signal response $g_{SD}(t)$ and $g_{SR}(t)$ at S−D link and S−R link respectively are expressed as $g_{SD}(t-jT_f-2iT_s-\tau_{l,1}) = \sqrt{E}\sum_{i=-\infty}^{\infty}\sum_{j=0}^{N_f-1} p(t-jT_f-2iT_s) * \delta(t-\tau_{l,1})$ and $g_{SR}(t-jT_f-2iT_s-\tau_{l,2}) = \sqrt{E}\sum_{i=-\infty}^{\infty}\sum_{j=0}^{N_f-1} p(t-jT_f-2iT_s) * \delta(t-\tau_{l,2})$.

The received signal obtained at the relay node $r_{SR}(t)$ is passed through a ED−OOK receiver, whose decision statistics Z_{SR} is as follows:

$$\begin{aligned} Z_{SR} &= \sum_{j=0}^{N_f-1} \int_{2iT_s+jT_f}^{2iT_s+jT_f+T_i} r_{SR}^2(t)dt \\ &= \underbrace{Z_1(k)}_{signal} + \underbrace{Z_2(k) + Z_3(k)}_{noise-term} \\ &= \underbrace{Z_1(2)}_{signal} + \underbrace{Z_2(2) + Z_3(2)}_{noise-term} \end{aligned} \quad (5.44)$$

where, the index $k \in \{1,2,3\}$ denotes S−D, S−R and R−D link respectively, as mentioned in equation 5.3. Here, $T_i = T_p + T_{mds}$ represents the integration time interval, T_p the pulse duration and T_{mds} the multipath delay spread. Further, multipath delay spread should be $T_{mds} > T_p$ to avoid any interference among the symbols. Replacing the value of equation 5.44 in equation 5.45, we obtain the value of Z_{SR} in equation 5.46. The equation 5.46 holds true only when there

is no IPI at the receiver end.

$$
\begin{aligned}
&= \sum_{j=0}^{N_f-1} \int_{2iT_s+jT_f}^{2iT_s+jT_f+T_i} \left(\sum_{l=0}^{L_2-1} \alpha_{l,2} b_i g_{SR}(t - jT_f - 2iT_s - \tau_{l,2}) + n_{SR}(t) \right)^2 \\
&= \sum_{j=0}^{N_f-1} \int_{2iT_s+jT_f}^{2iT_s+jT_f+T_i} \sum_{l=0}^{L_2-1} \alpha_{l,2}^2 b_i^2 g_{SR}^2(t - jT_f - 2iT_s - \tau_{l,2}) dt + 2 \sum_{j=0}^{N_f-1} \int_{2iT_s+jT_f}^{2iT_s+jT_f+T_i} \\
&\quad \sum_{l=0}^{L_2-1} \alpha_{l,2} b_i g_{SR}(t - jT_f - 2iT_s - \tau_{l,2}) n_{SR}(t) dt + \sum_{j=0}^{N_f-1} \int_{2iT_s+jT_f}^{2iT_s+jT_f+T_i} n_{SR}^2(t) dt \quad (5.45)
\end{aligned}
$$

Therefore, the signal component sig_{SR} is represented as:

$$
\begin{aligned}
Z_1(2) &= \sum_{j=0}^{N_f-1} \sum_{l=0}^{L_2-1} \alpha_{l,2}^2 b_i^2 \int_{2iT_s+jT_f}^{2iT_s+jT_f+T_i} g_{SR}^2(t - jT_f - 2iT_s - \tau_{l,2}) dt \\
&= sig_{SR} = N_f E_{SR} b_i^2 \gamma_2 \quad (5.46)
\end{aligned}
$$

where, $E_{SR} = \int_{-\infty}^{\infty} g_{SR}^2(t - jT_f - 2iT_s - \tau_{l,2}) dt$ denotes the received signal energy obtained from S−R link. As explained in Section 5.3, since a large number of UWB multipath channel gains are considered, the channel gains can be approximated as Gaussian Distributed using the Central Limit Theorem.

As described in Section 5.3, since the PSD $\theta_k(f)$ of noise is sufficiently flat, the autocorrelation function can be approximated as $\theta_k(\tau) = \frac{N_0}{2}\delta(\tau)$ [175]: The noise variances $\sigma_{N_1}^2$ and $\sigma_{N_2}^2$ are obtained by solving the decision variables $Z_2(k)$ and $Z_3(k)$, containing the noise terms.

$$
\begin{aligned}
\sigma_{N_1}^2 &= \mathbb{E}[Z_2^2(k)] = \mathbb{E}[Z_2^2(2)] \\
&= 2 \sum_{j=0}^{N_f-1} \sum_{l=0}^{L_2-1} \alpha_{l,2}^2 b_i^2 \int_{2iT_s+jT_f}^{2iT_s+jT_f+T_i} \int_{2iT_s+jT_f}^{2iT_s+jT_f+T_i} g_{SR}^2(t - jT_f - 2iT_s - \tau_{l,2}) \\
&\quad \mathbb{E}[n_{SR}(t) n_{SR}(\tau)] dt d\tau \\
&= 2N_f \gamma_2 b_i^2 \int_{2iT_s+jT_f}^{2iT_s+jT_f+T_i} \int_{2iT_s+jT_f}^{2iT_s+jT_f+T_i} g_{SR}(t - jT_f - 2iT_s - \tau_{l,2}) g_{SR}(\tau - jT_f \\
&\quad -2iT_s - \tau_{l,2}) \theta_2(t - \tau) dt d\tau \\
&= 2N_f \gamma_2 \frac{N_0}{2} b_i^2 \int_{2iT_s+jT_f}^{2iT_s+jT_f+T_i} g_{SR}^2(t - jT_f - 2iT_s - \tau_{l,2}) dt \\
&= N_f N_0 E_{SR} b_i^2 \gamma_2 \quad (5.47)
\end{aligned}
$$

where, $\mathbb{E}[n_{SR}(t) n_{SR}(\tau)] = \theta_2(t - \tau) = \frac{N_0}{2}\delta(t - \tau)$ and $\int_{2iT_s+jT_f}^{2iT_s+jT_f+T_i} \frac{N_0}{2}\delta(t - \tau) d\tau = \frac{N_0}{2}$.

$$
\sigma_{N_2}^2 = \mathbb{E}[Z_3^2(k)] = \mathbb{E}[Z_3^2(2)]
$$

$$
\begin{aligned}
&= \sum_{j=0}^{N_f-1} \int_{2iT_s+jT_f}^{2iT_s+jT_f+T_i} \int_{2iT_s+jT_f}^{2iT_s+jT_f+T_i} \mathbb{E}[\left\{n_{SR}^2(t)\right\}^2] dt d\tau \\
&= N_f \int_0^{T_i} \int_{T_i-t}^{T_i} \frac{N_0^2}{2} d\tau dt = N_f \int_0^{T_i} \frac{N_0^2}{2} 2W dt \\
&= N_f N_0^2 W T_i
\end{aligned} \tag{5.48}
$$

As discussed in Section 5.3, the variance of $[n_k^2(t)]$ tends to a Dirac Delta function, where the integral vanishes outside the range $[-t, T_i - t]$. Further, we apply Parsevals theorem to solve Equation 5.49. The value of $\mathbb{E}[\{n_{SR}^2(t)\}^2]$ is evaluated in Appendix A. Similarly, the value of $\mathbb{E}[\{n_{SD}^2(t)\}^2]$ and $\mathbb{E}[\{n_{RD}^2(t)\}^2]$ are also obtained from Appendix A.

In order to extract the information bit $b_i^{'}$, the decision statistic Z_{SR} obtained at the relay node is compared to the decision threshold. The decision threshold is taken to be $\frac{\eta_k^{\zeta} N_f E_{SR}}{2}$, for OOK modulation scheme. The decision criteria $\hat{z}$ can be expressed as:

$$
b_i^{'} = \hat{z} = \begin{Bmatrix} 0, & H_0 : Z = Z_{SR} \leq \frac{\eta_k^{\zeta} N_f E_{SR}}{2} \\ 1, & H_1 : Z = Z_{SR} > \frac{\eta_k^{\zeta} N_f E_{SR}}{2} \end{Bmatrix} \tag{5.49}
$$

where, $\eta_k^{\zeta} = \mathbb{E}\{\gamma_k\} = \mathbb{E}\{\gamma_2\}$ for S$-$R link. Here, $\zeta \in \{CM1\}$ denotes UWB CM1 channel.

The received signal obtained at the destination node $r_{SD}(t)$ at the end of 1$^{\text{st}}$ time slot, is detected using a ED$-$OOK receiver, whose decision statistics Z_{SD} is as follows:

$$
\begin{aligned}
Z_{SD} &= \sum_{j=0}^{N_f-1} \int_{2iT_s+jT_f}^{2iT_s+jT_f+T_i} r_{SD}^2(t) dt \\
&= \underbrace{Z_1(1)}_{signal} + \underbrace{Z_2(1) + Z_3(1)}_{\text{noise}-term}
\end{aligned} \tag{5.50}
$$

The value of Z_{SD} is obtained in equation 5.52, by replacing the value of equation 5.43 in equation 5.51. The equation 5.52 holds true only if IPI is avoided.

$$
\begin{aligned}
&= \sum_{j=0}^{N_f-1} \int_{2iT_s+jT_f}^{2iT_s+jT_f+T_i} \left(\sum_{l=0}^{L_1-1} \alpha_{l,1} \sum_{j=0}^{N_f-1} b_i g_{SD}(t - jT_f - 2iT_s - \tau_{l,1}) + n_{SD}(t) \right)^2 \\
&= \sum_{j=0}^{N_f-1} \int_{2iT_s+jT_f}^{2iT_s+jT_f+T_i} \sum_{l=0}^{L_1-1} \alpha_{l,1}^2 b_i^2 g_{SD}^2(t - jT_f - 2iT_s - \tau_{l,1}) dt + 2 \sum_{j=0}^{N_f-1} \int_{2iT_s+jT_f}^{2iT_s+jT_f+T_i} \\
&\quad \sum_{l=0}^{L_1-1} \alpha_{l,1} b_i g_{SD}(t - jT_f - 2iT_s - \tau_{l,2}) n_{SD}(t) dt + \sum_{j=0}^{N_f-1} \int_{2iT_s+jT_f}^{2iT_s+jT_f+T_i} n_{SD}^2(t) dt
\end{aligned} \tag{5.51}
$$

Using the same procedure as used for S$-$R link, we obtain the decision statistics for S$-$D link.

The signal term sig_{SD} for S−D link is represented as:

$$\begin{aligned} Z_1(1) &= \sum_{j=0}^{N_f-1}\sum_{l=0}^{L_1-1}\alpha_{l,1}^2 b_i^2 \int_{2iT_s+jT_f}^{2iT_s+jT_f+T_i} g_{SD}^2(t-jT_f-2iT_s-\tau_{l,1})dt \\ &= sig_{SD} = N_f E_{SD} b_i^2 \gamma_1 \end{aligned} \tag{5.52}$$

where, $E_{SD} = \int_{-\infty}^{\infty} g_{SD}^2(t-jT_f-2iT_s-\tau_{l,1})dt$ represents the received signal energy obtained from S−D link. As explained in Section 5.3, since a large number of UWB multipath channel gains are considered, the channel gains can be approximated as Gaussian Distributed using the Central Limit Theorem $\sum_{l_1}\alpha_{l_1}^2 = \gamma_1$. As described in Section 5.3, since the PSD $\theta_k(f)$ of noise is sufficiently flat, the autocorrelation function of noise can be approximated as $\theta_k(\tau) = \frac{N_0}{2}\delta(\tau)$[175].

The variances are evaluated for noise terms $Z_2(1)$ and $Z_3(1)$ as solved below.

$$\begin{aligned} \sigma_{N_1}^2 &= \mathbb{E}[Z_2^2(k)] = \mathbb{E}[Z_2^2(1)] \\ &= 2\sum_{j=0}^{N_f-1}\sum_{l=0}^{L_1-1}\alpha_{l,1}^2 b_i^2 \int_{2iT_s+jT_f}^{2iT_s+jT_f+T_i}\int_{2iT_s+jT_f}^{2iT_s+jT_f+T_i} g_{SD}^2(t-jT_f-2iT_s-\tau_{l,1}) \\ &\quad \mathbb{E}[n_{SD}(t)n_{SD}(\tau)]dtd\tau \\ &= 2N_f\gamma_2 b_i^2 \int_{2iT_s+jT_f}^{2iT_s+jT_f+T_i}\int_{2iT_s+jT_f}^{2iT_s+jT_f+T_i} g_{SD}(t-jT_f-2iT_s-\tau_{l,1})g_{SD}(\tau-jT_f \\ &\quad -2iT_s-\tau_{l,1})\theta_1(t-\tau)dtd\tau \\ &= 2N_f\gamma_1\frac{N_0}{2}b_i^2\int_{2iT_s+jT_f}^{2iT_s+jT_f+T_i} g_{SD}^2(t-jT_f-2iT_s-\tau_{l,1})dt \\ &= N_f N_0 E_{SD} b_i^2 \gamma_1 \end{aligned} \tag{5.53}$$

$$\begin{aligned} \sigma_{N_2}^2 &= \mathbb{E}[Z_3^2(k)] = \mathbb{E}[Z_3^2(1)] \\ &= \sum_{j=0}^{N_f-1}\int_{2iT_s+jT_f}^{2iT_s+jT_f+T_i}\int_{2iT_s+jT_f}^{2iT_s+jT_f+T_i}\mathbb{E}[\{n_{SR}^2(t)\}^2]dtd\tau \\ &= N_f\int_0^{T_i}\int_{T_i-t}^{T_i}\frac{N_0^2}{2}d\tau dt = N_f\int_0^{T_i}\frac{N_0^2}{2}2Wdt \\ &= N_f N_0^2 W T_i \end{aligned} \tag{5.54}$$

The SNR obtained at the relay node at the end of 1st time slot is denoted as:

$$\begin{aligned} \rho_{SR-DTF} &= \frac{sig_{SR}^2}{\sigma_{Z_{noise-SR}}^2} \\ &= \frac{(N_f E_{SR} b_i^2\gamma_2)^2}{N_f N_0 E_{SR} b_i^2\gamma_2 + N_f N_0^2 W T_i} \end{aligned}$$

$$= \frac{(N_f E_{SR}\gamma_2)^2}{N_f N_0 E_{SR}\gamma_2 + N_f N_0^2 W T_i} \tag{5.55}$$

where, information bit $b_i = 1$ is transmitted from source node to relay node. At the relay node, error occurs if information bit $b_i^{'} = 0$ is received. Therefore, the probability of error obtained at the relay node is expressed as:

$$P_e = \int_0^{\infty} Q\left(\frac{1}{2}\sqrt{\rho_{SR-DTF}}\right) f_{\rho_{DTF}}(\gamma_2) d\gamma_2 \tag{5.56}$$

where, the PDF of S$-$R link is expressed as $f_{\rho_{DTF}}(\gamma_2) = \frac{1}{\sqrt{(2\pi(\sigma_{SR}^2))}} \exp\left[\frac{-(\gamma_2-\mu_{SR})^2}{2(\sigma_{SR}^2)}\right]$. Furthermore, μ_{SR} and σ_{SR}^2 denote the mean and variance of S$-$R link of UWB channel respectively.

After extraction of information bit $b_i^{'}$ at the relay node, the signal transmitted from the relay node to the destination node in 2nd time slot is represented as:

$$s_{RD}(t) = \sqrt{E} \sum_{i=-\infty}^{\infty} \sum_{j=0}^{N_f-1} b_i^{'} p(t - jT_f - (2i+1)T_s) \tag{5.57}$$

where, $E = \int_{-\infty}^{\infty} p^2(t)dt$ represents the pulse energy at each link and $b_i^{'}$ the detected bit at relay node. The received signal $r_{RD}(t)$ obtained at the destination node in 2nd time slot is represented as:

$$\begin{aligned} r_{RD}(t) &= \sqrt{E} \sum_{i=-\infty}^{\infty} \sum_{j=0}^{N_f-1} b_i^{'} p(t - jT_f - (2i+1)T_s) * \sum_{l=0}^{L_3-1} \alpha_{l,3}\delta(t - \tau_{l,3}) + \\ &\quad n_{RD}(t) \\ &= \sum_{l=0}^{L_3-1} \alpha_{l,3} b_i^{'} g_{RD}(t - jT_f - (2i+1)T_s - \tau_{l,3}) + n_{RD}(t) \end{aligned} \tag{5.58}$$

The aggregate signal response $g_{RD}(t)$ at R$-$D link is expressed as $g_{RD}(t - jT_f - (2i+1)T_s - \tau_{l,3}) = \sqrt{E}\sum_{i=-\infty}^{\infty}\sum_{j=0}^{N_f-1} p(t - jT_f - (2i+1)T_s) * \delta(t - \tau_{l,3})$. The noise (AWGN) obtained at R$-$D link is denoted by $n_{RD}(t)$. The received signal $r_{RD}(t)$ obtained at the destination node in 2nd time slot, is demodulated using a ED$-$OOK receiver. The decision statistics Z_{RD} in case of correct detection is expressed as:

$$\begin{aligned} Z_{RD} &= \sum_{j=0}^{N_f-1} \int_{(2i+1)T_s + jT_f}^{(2i+1)T_s + jT_f + T_i} r_{RD}^2(t)dt \\ &= \underbrace{Z_1(3)}_{signal} + \underbrace{Z_2(3) + Z_3(3)}_{\text{noise}-term} \end{aligned} \tag{5.59}$$

The value of Z_{RD} is obtained in equation 5.61 by replacing the value of equation 5.59 in equation 5.60. For the condition of no IPI, equation 5.61 holds true.

$$= \sum_{j=0}^{N_f-1} \int_{(2i+1)T_s + jT_f}^{(2i+1)T_s + jT_f + T_i} \left(\sum_{l=0}^{L_3-1} \alpha_{l,3} b_i^{'} g_{RD}(t - jT_f - (2i+1)T_s - \tau_{l,3}) + \right.$$

$$
\begin{aligned}
& n_{RD}(t)\Big)^2 \\
= & \sum_{j=0}^{N_f-1} \int_{(2i+1)T_s+jT_f}^{(2i+1)T_s+jT_f+T_i} \sum_{l=0}^{L_3-1} \alpha_{l,3}^2 b_i^{'2} g_{RD}^2(t-jT_f-(2i+1)T_s-\tau_{l,3})dt \\
& +2\sum_{j=0}^{N_f-1} \int_{(2i+1)T_s+jT_f}^{(2i+1)iT_s+jT_f+T_i} \sum_{l=0}^{L_3-1} \alpha_{l,3} b_i^{'} g_{RD}(t-jT_f-(2i+1)T_s-\tau_{l,3}) \\
& n_{RD}(t)dt + \sum_{j=0}^{N_f-1} \int_{(2i+1)T_s+jT_f}^{(2i+1)T_s+jT_f+T_i} n_{RD}^2(t)dt
\end{aligned} \tag{5.60}
$$

Using the same procedure as used for S−R link, we obtain the decision statistics for R−D link. The signal term sig_{RD} for R−D link is represented as:

$$
\begin{aligned}
Z_1(3) &= \sum_{j=0}^{N_f-1} \sum_{l=0}^{L_3-1} \alpha_{l,3}^2 b_i^{'2} \int_{(2i+1)T_s+jT_f}^{(2i+1)T_s+jT_f+T_i} g_{RD}^2(t-jT_f-(2i+1)T_s- \\
& \tau_{l,3})dt \\
&= sig_{RD} = N_f E_{RD} b_i^{'2} \gamma_3
\end{aligned} \tag{5.61}
$$

where, $E_{RD} = \int_{-\infty}^{\infty} g_{RD}^2(t-jT_f-(2i+1)T_s-\tau_{l,3})dt$ represents the received signal energy obtained from the R−D link. As explained in Section 5.3, since a large number of UWB multipath channel gains are considered, the channel gains can be approximated as Gaussian Distributed using the Central Limit Theorem $\sum_{l_2} \alpha_{l_2}^2 = \gamma_2$ and $\sum_{l_3} \alpha_{l_3}^2 = \gamma_3$. As described in Section 5.3, since the PSD $\theta_k(f)$ of noise is sufficiently flat, the autocorrelation function of noise can be approximated as $\theta_k(\tau) = \frac{N_0}{2}\delta(\tau)$[175].As the decision variables $Z_2(3)$ and $Z_3(3)$ denote the noise terms, their variances are evaluated as:

$$
\begin{aligned}
\sigma_{N_1}^2 &= \mathbb{E}[Z_2^2(k)] = \mathbb{E}[Z_2^2(3)] \\
&= 2\sum_{j=0}^{N_f-1} \sum_{l=0}^{L_3-1} \alpha_{l,3}^2 b_i^{'2} \int_{(2i+1)T_s+jT_f}^{(2i+1)T_s+jT_f+T_i} \int_{(2i+1)T_s+jT_f}^{(2i+1)T_s+jT_f+T_i} g_{RD}^2(t-jT_f \\
& -(2i+1)T_s-\tau_{l,3})\,\mathbb{E}[n_{RD}(t)n_{RD}(\tau)]dtd\tau \\
&= N_f N_0 E_{RD} b_i^{'2} \gamma_3
\end{aligned} \tag{5.62}
$$

$$
\begin{aligned}
\sigma_{N_2}^2 &= \mathbb{E}[Z_3^2(k)] = \mathbb{E}[Z_3^2(3)] \\
&= \sum_{j=0}^{N_f-1} \int_{2iT_s+jT_f}^{2iT_s+jT_f+T_i} \int_{2iT_s+jT_f}^{2iT_s+jT_f+T_i} \mathbb{E}[\{n_{RD}^2(t)\}^2]dtd\tau \\
&= N_f N_0^2 W T_i
\end{aligned} \tag{5.63}
$$

Parsevals theorem is applied to solve equation 5.64.

The decision statistic Z_{SD} obtained at destination node contains signal term $sig_{SD} = Z_1(1) = N_f E_{SD} b_i^2 \gamma_1$ and noise term $Z_{noise-SD} = Z_2(1)+Z_3(1)$ at the end of 1st time slot. The noise term $Z_{noise-SD}$ has a total variance of $\sigma^2_{Z_{noise-SD}} = \sigma^2_{N_1} + \sigma^2_{N_2} = N_f N_0 E_{SD} b_i^2 \gamma_1 + N_f N_0^2 W T_i$. Similarly, the decision statistic Z_{RD} obtained at destination node at the end of 2nd time contains signal term $sig_{RD} = Z_1(3) = N_f E_{RD} b_i^{'2} \gamma_3$ and noise term $Z_{noise-RD} = Z_2(3) + Z_3(3)$. The noise term $Z_{noise-RD}$ has a total variance of $\sigma^2_{Z_{noise-RD}} = \sigma^2_{N_1} + \sigma^2_{N_2} = N_f N_0 E_{RD} b_i^{'2} \gamma_3 + N_f N_0^2 W T_i$.

In case of correct detection, the individual SNR obtained at the destination node from S−D and R−D links in 1st and 2nd time slots respectively, are represented as:

$$\begin{aligned} \rho_{SD-DTF} &= \frac{sig^2_{SD}}{\sigma^2_{Z_{noise-SD}}} \\ &= \frac{\left(N_f E_{SD} b_i^2 \gamma_1\right)^2}{N_f N_0 E_{SD} b_i^2 \gamma_1 + N_f N_0^2 W T_i} \\ &= \frac{\left(N_f E_{SD} \gamma_1\right)^2}{N_f N_0 E_{SD} \gamma_1 + N_f N_0^2 W T_i} \end{aligned} \tag{5.64}$$

$$\begin{aligned} \rho_{RD-DTF} &= \frac{sig^2_{RD}}{\sigma^2_{Z_{noise-RD}}} \\ &= \frac{\left(N_f E_{RD} b_i^{'2} \gamma_3\right)^2}{N_f N_0 E_{RD} b_i^{'2} \gamma_3 + N_f N_0^2 W T_i} \\ &= \frac{\left(N_f E_{RD} \gamma_3\right)^2}{N_f N_0 E_{RD} \gamma_3 + N_f N_0^2 W T_i} \end{aligned} \tag{5.65}$$

where, $b_i = b_i^{'} = 1$ in case of correct detection. Therefore, information bit $b_i^{'} = 1$ is forwarded from the relay to destination node in 2nd time slot. The decision statistics obtained at the destination node in two time slots are combined using linear diversity combining, selective diversity combining and optimum linear diversity combining to form the final decision statistic, are subsequently described in the following section.

5.4.1 Linear Combining

i) *Correct Detection at Relay Node*: The decision statistics Z_{SD} and Z_{RD} obtained at the destination node in the 1st and 2nd time slots from S−D and R−D link respectively, are linearly combined to give $Z_{total} = Z_{SD} + Z_{RD} = s_{total-signal} + Z_{noise-total}$, as mentioned in equation 5.26. The individual decision statistics obtained from S−D and R−D links respectively, are mentioned in equation 5.24 and 5.25 respectively. The total noise variance

$\sigma^2_{Z_{noise-total}} = \sigma^2_{Z_{noise-SD}} + \sigma^2_{Z_{noise-RD}}$ corresponding to the noise term $Z_{noise-total}$ is evaluated in equation 5.27.

When information bit 1 ($b_i = 1$) is transmitted from the source node to the relay node, $b_i^{'} = 1$ is obtained at the relay node in case of correct detection. The same detected bit $b_i^{'}$ is then transmitted from the relay node to the destination node. Subsequently, the SNR obtained at destination node due to correct detection is represented as:

$$\begin{aligned} \rho_{DTF-LC-CD} &= \left(\frac{s^2_{total-signal}}{\sigma^2_{Z_{noise-total}}}\right) = \frac{(sig_{SD} + sig_{RD})^2}{(\sigma^2_{Z_{noise-SD}} + \sigma^2_{Z_{noise-RD}})} \\ &= \frac{(N_f E_{SD} b_i^2 \gamma_1 + N_f E_{RD} b_i^{'2} \gamma_3)^2}{N_f N_0 E_{SD} b_i^2 \gamma_1 + N_f N_0 E_{RD} b_i^{'2} \gamma_3 + 2 N_f N_0^2 W T_i} \\ &= \frac{(N_f E_{SD} \gamma_1 + N_f E_{RD} \gamma_3)^2}{N_f N_0 E_{SD} \gamma_1 + N_f N_0 E_{RD} \gamma_3 + 2 N_f N_0^2 W T_i} \end{aligned} \tag{5.66}$$

where, $b_i = b_i^{'} = 1$ in case of correct detection.

In order to extract the information bit, the final decision statistic is compared to a threshold. OOK modulation scheme is used to determine the decision threshold. Thus, the final decision criteria $\hat{z}$ can be expressed as:

$$\hat{z} = \begin{cases} 0, & H_0 : Z = Z_{total} \leq \frac{\eta_1^{\zeta} N_f E_{SD} + \eta_3^{\zeta} N_f E_{RD}}{2} \\ 1, & H_1 : Z = Z_{total} > \frac{\eta_1^{\zeta} N_f E_{SD} + \eta_3^{\zeta} N_f E_{RD}}{2} \end{cases} \tag{5.67}$$

where, $\eta_1^{\zeta} = \mathbb{E}[\gamma_1]$ and $\eta_3^{\zeta} = \mathbb{E}[\gamma_3]$. Also, $\zeta \in \{CM1\}$ reprents UWB CM1 channel.

ii) *Incorrect Detection at Relay Node*: In case of incorrect detection, when $b_i = 1$ is transmitted from source node to relay node, the detected bit at relay node is $b_i^{'} = 0$. This erroneously detected bit $b_i^{'} = 0$ is forwarded to the destination node. Subsequently, the SNR obtained at the destination node due to incorrect detection is represented as:

$$\begin{aligned} \rho_{DTF-LC-ID} &= \frac{(sig_{SD})^2}{(\sigma^2_{Z_{noise-SD}} + \sigma^2_{Z_{noise-RD}})} \\ &= \frac{(N_f E_{SD} \gamma_1)^2}{N_f N_0 (E_{SD} \gamma_1 + E_{RD} \gamma_3 + 2 N_0 W T_i)} \end{aligned} \tag{5.68}$$

Using probability theory, the generalized BER evaluated in case of incorrect detection is expressed as:

$$BER = \int_0^{\infty} \int_0^{\infty} Q\left(\frac{sig_{SD} - sig_{RD}}{2\sqrt{\sigma^2_{Z_{noise-total}}}}\right) f_{\rho_{DTF}}(\gamma_1, \gamma_3) d\gamma_1 d\gamma_3 \tag{5.69}$$

Due to incorrect detection at relay node, information bit $b_i^{'}$ received at destination node through R$-$D link is 0, when information bit 1 is transmitted from source node to relay node. Therefore, $sig_{RD} = 0$.

$$= \int_0^\infty \int_0^\infty Q\left(\frac{sig_{SD}}{2\sqrt{(\sigma^2_{Z_{noise-SD}} + \sigma^2_{Z_{noise-RD}})}}\right) f_{\rho_{DTF}}(\gamma_1, \gamma_3) d\gamma_1 d\gamma_3 \tag{5.70}$$

As described in Section 5.3, the individual channel gains for S$-$D, S$-$R and R$-$D channel links may be assumed to be IID Gaussian distributed by applying Central Limit Theorem, since a large number paths are involved. Therefore, the sum of these channel gains will also have a Gaussian distribution with its mean being the sum of individual means and variance being sum of the individual variances. Here, μ_k and σ_k^2 represent the individual mean and variance of channel links respectively. The joint PDF in case of linear combining is represented as:

$$f_{\rho_{DTF}}(\gamma_1, \gamma_3) = \frac{1}{\sqrt{(2\pi(\sigma^2_{SD}))}} \frac{1}{\sqrt{(2\pi(\sigma^2_{RD}))}} \exp\left[\frac{-(\gamma_1 - \mu_{SD})^2}{2\sigma^2_{SD}} + \frac{-(\gamma_3 - \mu_{RD})^2}{2\sigma^2_{RD}}\right] d\gamma_1 d\gamma_3 \tag{5.71}$$

The final BER of UWB ED$-$OOK system using linear combining is expressed as:

$$\begin{aligned} BER_{LC-DTF} &= \int_0^\infty \int_0^\infty \left(Q\left(\frac{1}{2}\sqrt{\rho_{DTF-LC-CD}}\right) f_{\rho_{DTF}}(\gamma_1, \gamma_3) d\gamma_1 d\gamma_3\right)(1 - P_e) + \\ &\quad \int_0^\infty \int_0^\infty \left(Q\left(\frac{1}{2}\sqrt{\rho_{DTF-LC-ID}}\right) f_{\rho_{DTF}}(\gamma_1, \gamma_3) d\gamma_1 d\gamma_3\right)(P_e) \\ &= \int_0^\infty \int_0^\infty \left(Q\left(\frac{1}{2}\sqrt{\rho_{DTF-LC-CD}}\right) f_{\rho_{DTF}}(\gamma_1) f_{\rho_{DTF}}(\gamma_3) d\gamma_1 d\gamma_3\right)(1 - P_e) + \\ &\quad \int_0^\infty \int_0^\infty \left(Q\left(\frac{1}{2}\sqrt{\rho_{DTF-LC-ID}}\right) f_{\rho_{DTF}}(\gamma_1) f_{\rho_{DTF}}(\gamma_3) d\gamma_1 d\gamma_3\right)(P_e) \end{aligned} \tag{5.72}$$

where, the value of P_e is solved in equation 5.57. Since the joint PDF is IID distributed, it can be represented as $f_{\rho_{DTF}}(\gamma_1, \gamma_3) = f_{\rho_{DTF}}(\gamma_1)$
$f_{\rho_{DTF}}(\gamma_3)$.

Finally, the BER of UWB ED$-$OOK system using cooperative dual$-$hop DTF strategy with linear combining is obtained in equation 5.74 by replacing the value of equation 5.72 in equation 5.73, which is given by:

$$\begin{aligned} &= \int_0^\infty \int_0^\infty \left(Q\left(\frac{1}{2}\sqrt{\rho_{DTF-LC-CD}}\right) \frac{1}{2\pi\sqrt{(\sigma^2_{SD}\sigma^2_{RD})}} \exp\left[\frac{-(\gamma_1 - \mu_{SD})^2}{2\sigma^2_{SD}} + \frac{-(\gamma_3 - \mu_{RD})^2}{2\sigma^2_{RD}}\right] \right. \\ &\quad \left. d\gamma_1 d\gamma_3\right)(1 - P_e) + \int_0^\infty \int_0^\infty \left(Q\left(\frac{1}{2}\sqrt{\rho_{DTF-LC-ID}}\right) \frac{1}{2\pi\sqrt{(\sigma^2_{SD}\sigma^2_{RD})}} \exp \right. \\ &\quad \left. \left[\frac{-(\gamma_1 - \mu_{SD})^2}{2\sigma^2_{SD}} + \frac{-(\gamma_3 - \mu_{RD})^2}{2\sigma^2_{RD}}\right] d\gamma_1 d\gamma_3\right)(P_e) \end{aligned} \tag{5.73}$$

5.4.2 Selective Combining

(i) *Correct Detection at Relay Node*: In selective combining, the SNR obtained from S−D and R−D links in 1st and 2nd time slots respectively are compared, and the one with the highest SNR is chosen. The probability of selecting the channel link based on the highest SNR is evaluated after integrating the joint PDF of the channel links with proper limits. The joint PDF of channel links S−D and R−D is represented as:

$$f(x,y) = \frac{1}{2\pi\sigma_{SD}\sigma_{RD}} \exp - \left[\frac{(x-\mu_{SD})^2 + (y-\mu_{RD})^2}{2\sigma_{SD}\sigma_{RD}}\right] \tag{5.74}$$

where, x and y denote independent Gaussian random variables with means μ_{SD}, μ_{RD} and variances σ^2_{SD}, σ^2_{RD} of S−D and R−D channel links respectively. The probability that S−D channel link is selected is represented as:

$$P_1 \;=\; f(x) = \int_{-\infty}^{\infty}\int_{y}^{\infty} f(x,y)dxdy \tag{5.75}$$

Therefore, the probability of selecting R−D channel link is $P_3 = 1 - P_1$.

ii) *Incorrect Detection at relay node*: If information bit $b_i = 1$ is transmitted from source node to relay node, $b_i^{'} = 0$ is detected at the relay node, then an incorrect detection takes place. This incorrectly detected bit $b_i^{'} = 0$ is transmitted from the relay node to the destination node. Therefore, the final BER of UWB ED−OOK system, using cooperative dual−hop DTF strategy with selective combining is represented as:

$$\begin{aligned} BER_{SC-DTF} \;=\; & \left(P_1\int_0^{\infty} Q\left(\frac{1}{2}\sqrt{\rho_{SD-DTF}}\right) f_{\rho_{DTF}}(\gamma_1)d\gamma_1 + P_3\int_0^{\infty} Q\left(\frac{1}{2}\sqrt{\rho_{RD-DTF}}\right)\right. \\ & \left. f_{\rho_{DTF}}(\gamma_3)d\gamma_3\right)(1-P_e) + \left(P_1\int_0^{\infty} Q\left(\frac{1}{2}\sqrt{\rho_{SD-DTF}})\right) f_{\rho_{DTF}}(\gamma_1)d\gamma_1\right. \\ & \left. + P_3\int_0^{\infty}\left(1 - Q\left(\frac{1}{2}\sqrt{\rho_{RD-DTF}}\right)\right) f_{\rho_{DTF}}(\gamma_3)d\gamma_3\right)P_e \end{aligned} \tag{5.76}$$

$$\begin{aligned} = \; & \left(P_1\int_0^{\infty} Q\left(\frac{1}{2}\sqrt{\rho_{SD-DTF}}\right)\frac{1}{\sqrt{(2\pi(\sigma^2_{SD}))}}\exp\left[\frac{-(\gamma_1-\mu_{SD})^2}{2\sigma^2_{SD}}\right]d\gamma_1 + P_3\int_0^{\infty}\right. \\ & \left. Q\left(\frac{1}{2}\sqrt{\rho_{RD-DTF}}\right)\frac{1}{\sqrt{(2\pi(\sigma^2_{RD}))}}\exp\left[\frac{-(\gamma_3-\mu_{RD})^2}{2\sigma^2_{RD}}\right]d\gamma_3\right)(1-P_e) + \left(P_1\int_0^{\infty}\right. \\ & \left. Q\left(\frac{1}{2}\sqrt{\rho_{SD-DTF}}\right)\frac{1}{\sqrt{(2\pi(\sigma^2_{SD}))}}\exp\left[\frac{-(\gamma_1-\mu_{SD})^2}{2\sigma^2_{SD}}\right]d\gamma_1 + P_3\int_0^{\infty}\right. \\ & \left.\left(1 - Q\left(\frac{1}{2}\sqrt{\rho_{RD-DTF}}\right)\right)\frac{1}{\sqrt{(2\pi(\sigma^2_{RD}))}}\exp\left[\frac{-(\gamma_3-\mu_{RD})^2}{2\sigma^2_{RD}}\right]d\gamma_3\right)(P_e) \end{aligned} \tag{5.77}$$

where, $f_{\rho_{DTF}}(\gamma_1) = \frac{1}{\sqrt{(2\pi(\sigma^2_{SD}))}}\exp\left[\frac{-(\gamma_1-\mu_{SD})^2}{2\sigma^2_{SD}}\right]$ and $f_{\rho_{DTF}}(\gamma_3) = \frac{1}{\sqrt{(2\pi(\sigma^2_{RD}))}}\exp\left[\frac{-(\gamma_3-\mu_{RD})^2}{2\sigma^2_{RD}}\right]$ represent the PDF of S−D and R−D channel links respectively.

5.4.3 Optimum Linear Combining

(i) *Correct Detection at Relay Node*: The decision statistics obtained at the destination node in 1st and 2nd time slots respectively, are optimally combined to give final decision statistic $Z_{total} = Z_{SD} + \kappa Z_{RD}$. The optimal combining factor κ has a value of $\kappa = \frac{(\sigma^2_{Z_{noise-SD}})s_{RD}}{(\sigma^2_{Z_{noise-RD}})s_{SD}}$, as solved in equation C.4 of Appendix C. The final decision statistic Z_{total} obtained at the destination node using optimum linear combining is represented by equation 5.36. For solving the noise term, the variance of the noise terms, are evaluated as shown in equation 5.37.

Thus, the SNR obtained at the destination node due to optimum linear combining is represented as:

$$\begin{aligned} \rho_{DTF-LOC-CD} &= \left(\frac{s^2_{total-signal}}{\sigma^2_{Z_{noise-total}}}\right) \\ &= \left(\frac{(sig_{SD} + \kappa sig_{RD})^2}{\sigma^2_{Z_{noise-SD}} + \kappa^2\sigma^2_{Z_{noise-RD}}}\right) \\ &= = \frac{(N_f E_{SD}\gamma_1 + \kappa N_f E_{RD}\gamma_3)^2}{X_1 + \kappa^2 Y_1} \end{aligned} \tag{5.78}$$

where, $X_1 = N_f N_0 E_{SD}\gamma_1 + N_f N_0^2 W T_i$ and $Y_1 = N_f N_0 E_{RD}\gamma_3 + N_f N_0^2 W T_i$. Also, $b_i = b_i^{'} = 1$ in case of correct detection.

The final decision statistic is compared to the decision threshold, to recover the transmitted bit. The decision threshold is decided on the basis of OOK modulation scheme. The final decision criteria $\hat{z}$ can be expressed as:

$$\hat{z} = \begin{Bmatrix} 0, & H_0 : Z = Z_{total} \leq \frac{\eta_1^{\zeta} N_f E_{SD} + \kappa \eta_3^{\zeta} N_f E_{RD}}{2} \\ 1, & H_1 : Z = Z_{total} > \frac{\eta_1^{\zeta} N_f E_{SD} + \kappa \eta_3^{\zeta} N_F E_{RD}}{2} \end{Bmatrix} \tag{5.79}$$

ii) *Incorrect Detection at Relay Node*:- In case of incorrect detection, $b_i^{'} = 0$ is detected at the relay node, when $b_i = 1$ is transmitted from source to relay node. Further, this incorrectly detected bit is forwarded to the destination node, leading to BER degradation. The SNR obtained at the destination node due to incorrect detection is represented as:

$$\begin{aligned} \rho_{DTF-LOC-ID} &= \frac{(sig_{SD})^2}{(\sigma^2_{Z_{noise-SD}} + \kappa^2\sigma^2_{Z_{noise-RD}})} \\ &= \frac{(N_f E_{SD}\gamma_1)^2}{X_1 + \kappa^2 Y_1} \end{aligned} \tag{5.80}$$

In case of incorrect detection, the generalized BER is represented as:

$$BER = \int_0^{\infty}\int_0^{\infty} Q\left(\frac{sig_{SD} - \kappa sig_{RD}}{2\sqrt{\sigma^2_{Z_{noise-total}}}}\right) f_{\rho_{DTF}}(\gamma_1, \gamma_3) d\gamma_1 d\gamma_3 \tag{5.81}$$

Due to incorrect detection at relay node, information bit received at destination node through R−D link is 0, when bit 1 is transmitted from source node to relay node. Thus, $sig_{RD} = 0$.

$$= \int_0^\infty \int_0^\infty Q\left(\frac{sig_{SD}}{2\sqrt{(\sigma^2_{Z_{noise-SD}} + \kappa^2\sigma^2_{Z_{noise-RD}})}}\right) f_{\rho_{DTF}}(\gamma_1, \gamma_3) d\gamma_1 d\gamma_3 \quad (5.82)$$

Subsequently, the BER obtained at the destination node using optimum linear combining is represented as:

$$\begin{aligned} BER_{LOC-DTF} &= \int_0^\infty \int_0^\infty \left(Q\left(\frac{1}{2}\sqrt{\rho_{DTF-LOC-CD}}\right) f_{\rho_{DTF}}(\gamma_1, \gamma_3) d\gamma_1 d\gamma_3\right)(1 - P_e) + \\ &\quad \int_0^\infty \int_0^\infty \left(Q\left(\frac{1}{2}\sqrt{\rho_{DTF-LOC-ID}}\right) f_{\rho_{DTF}}(\gamma_1, \gamma_3) d\gamma_1 d\gamma_3\right)(P_e) \\ &= \int_0^\infty \int_0^\infty \left(Q\left(\frac{1}{2}\sqrt{\rho_{DTF-LOC-CD}}\right) f_{\rho_{DTF}}(\gamma_1) f_{\rho_{DTF}}(\gamma_3) d\gamma_1 d\gamma_3\right) \\ &\quad (1 - P_e) + \int_0^\infty \int_0^\infty \left(Q\left(\frac{1}{2}\sqrt{\rho_{DTF-LOC-ID}}\right) f_{\rho_{DTF}}(\gamma_1) f_{\rho_{DTF}}(\gamma_3)\right. \\ &\quad \left. d\gamma_1 d\gamma_3\right)(P_e) \end{aligned} \quad (5.83)$$

where, $f_{\rho_{DTF}}(\gamma_1, \gamma_3) = f_{\rho_{DTF}}(\gamma_1) f_{\rho_{DTF}}(\gamma_3)$ because the channel gains are IID and Gaussian distributed. The value of P_e is evaluated as given in equation 5.57. The joint PDF in case of optimum linear combining is expressed as:

$$\begin{aligned} f_{\rho_{DTF}}(\gamma_1, \gamma_3) &= \frac{1}{\sqrt{(2\pi\sigma^2_{SD})}} \frac{1}{\sqrt{(2\pi\kappa^2\sigma^2_{RD})}} \exp\left[\frac{-(\gamma_1 - \mu_{SD})^2}{2\sigma^2_{SD}} + \frac{-(\gamma_3 - \mu_{RD})^2}{2\kappa^2\sigma^2_{RD}}\right] \\ &\quad d\gamma_1 d\gamma_3 \end{aligned} \quad (5.84)$$

Finally, the BER of UWB ED−OOK system using cooperative dual−hop DTF strategy with optimum linear diversity combining is obtained by replacing the value of equation 5.86 in equation 5.85.

$$\begin{aligned} BER_{LOC-DTF} &= \int_0^\infty \int_0^\infty \left(Q\left(\frac{1}{2}\sqrt{\rho_{DTF-LOC-CD}}\right) \frac{1}{2\pi\sqrt{\sigma^2_{SD}\kappa^2\sigma^2_{RD}}} \exp\left[\frac{-(\gamma_1 - \mu_{SD})^2}{2\sigma^2_{SD}} + \right.\right. \\ &\quad \left.\left. \frac{-(\gamma_3 - \mu_{RD})^2}{2\kappa^2\sigma^2_{RD}}\right] d\gamma_1 d\gamma_3\right)(1 - P_e) + \int_0^\infty \int_0^\infty \left(Q\left(\frac{1}{2}\sqrt{\rho_{DTF-LOC-ID}}\right)\right. \\ &\quad \left. \frac{1}{2\pi\sqrt{\sigma^2_{SD}\kappa^2\sigma^2_{RD}}} \exp\left[\frac{-(\gamma_1 - \mu_{SD})^2}{2\sigma^2_{SD}} + \frac{-(\gamma_3 - \mu_{RD})^2}{2\kappa^2\sigma^2_{RD}}\right] d\gamma_1 d\gamma_3\right)(P_e) \end{aligned} \quad (5.85)$$

5.5 Simulation Results

In this section, we present the Matlab simulations for the BER performance of ED−OOK system using various diversity combining schemes namely optimum linear combining, linear com-

bining and selective combining, over IEEE 802.15.4a UWB CM1 and CM2 channels respectively. Also, the analytical BER expressions derived in Section 5.4 are plotted using numerical integration, and then compared with the simulation results. The main parameters considered for simulations are $N_f = 1, 2$, $N = 200000$, $W = 2$ GHz, $T_i = 4\ ns$ and $F_{samp} = 10\ GHz$, where N_f represents the number of frames in one symbol, N the number of bits, W the bandwidth of bandpass filter, T_i the integration interval and F_{samp} the sampling frequency. A second order Gaussian derivative pulse $p(t) = (1 - 4\pi((t)/T_k).^2)exp(-2\pi((t)/T_k)^2)$ is used for transmission, where t denotes the time interval and $T_k = 0.15\ ns$ the pulse width control factor. The values of means μ_k and variances σ_k^2 obtained from UWB CM1 channel is noted to be $12.5\ dB$ and $3.5\ dB$ respectively. The index $k \in \{1, 2, 3\}$ refers to S$-$D, S$-$R and R$-$D link respectively, as mentioned in equation 5.3.

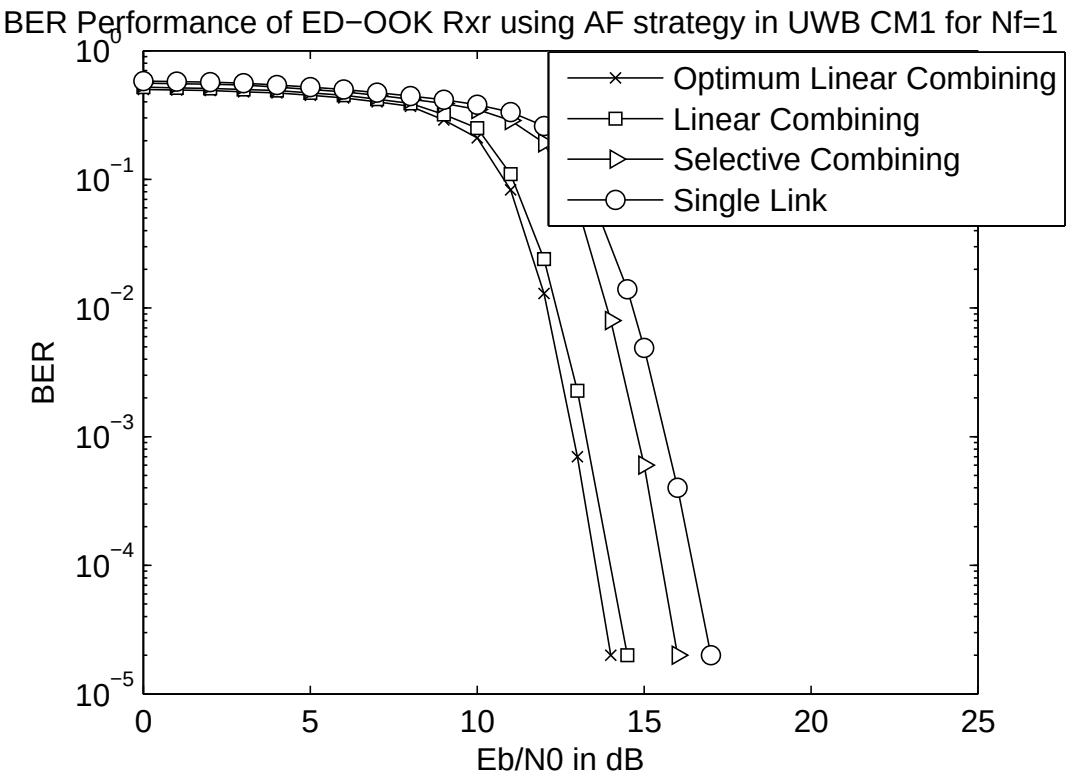

(a)

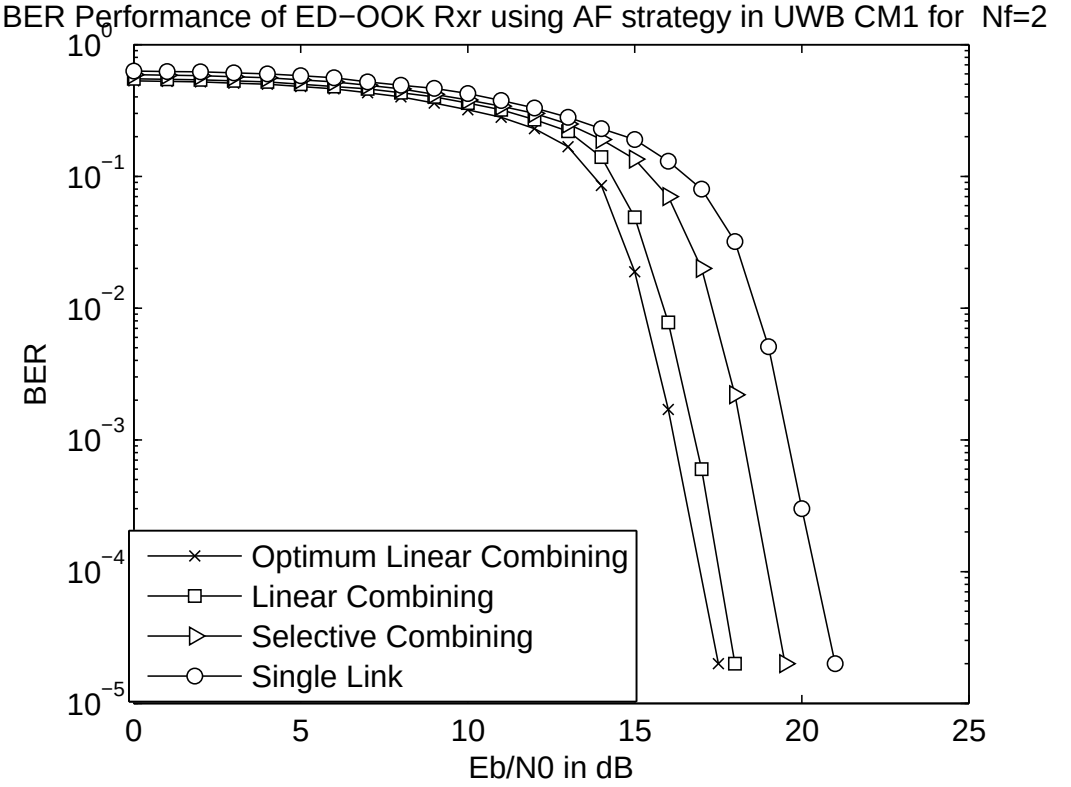

(b)

Figure 5.2: BER performance of UWB ED−OOK system using cooperative AF strategy with various combining schemes in UWB CM1 channel for (a) $N_f = 1$ (b) $N_f = 2$

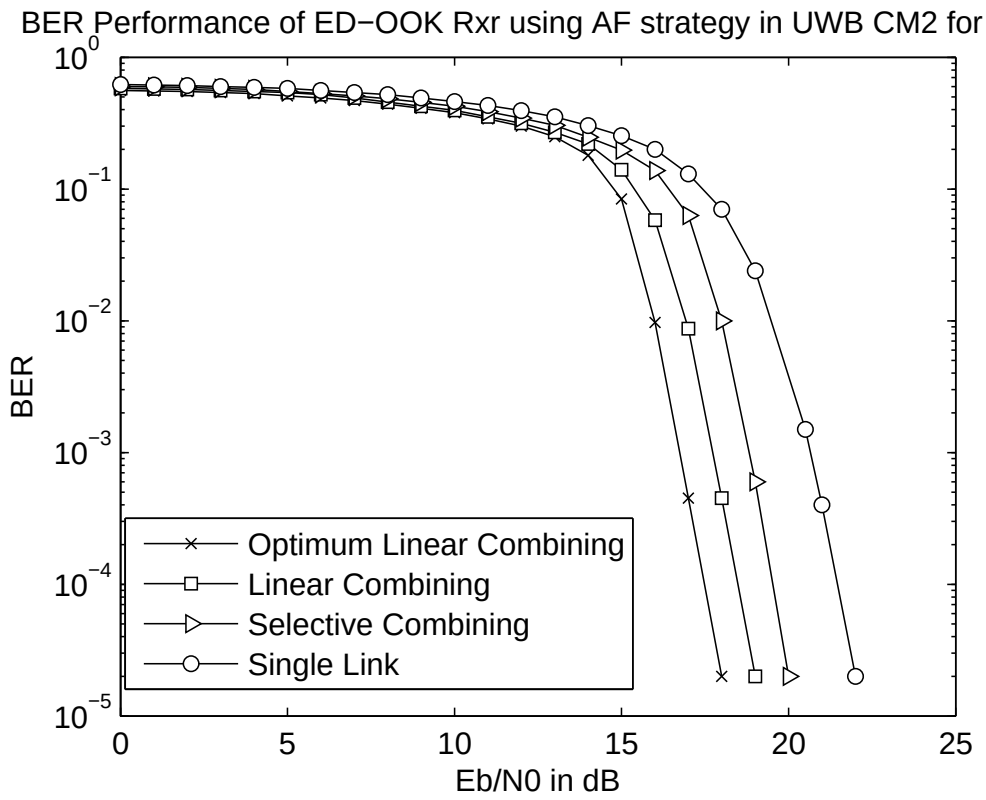

(a)

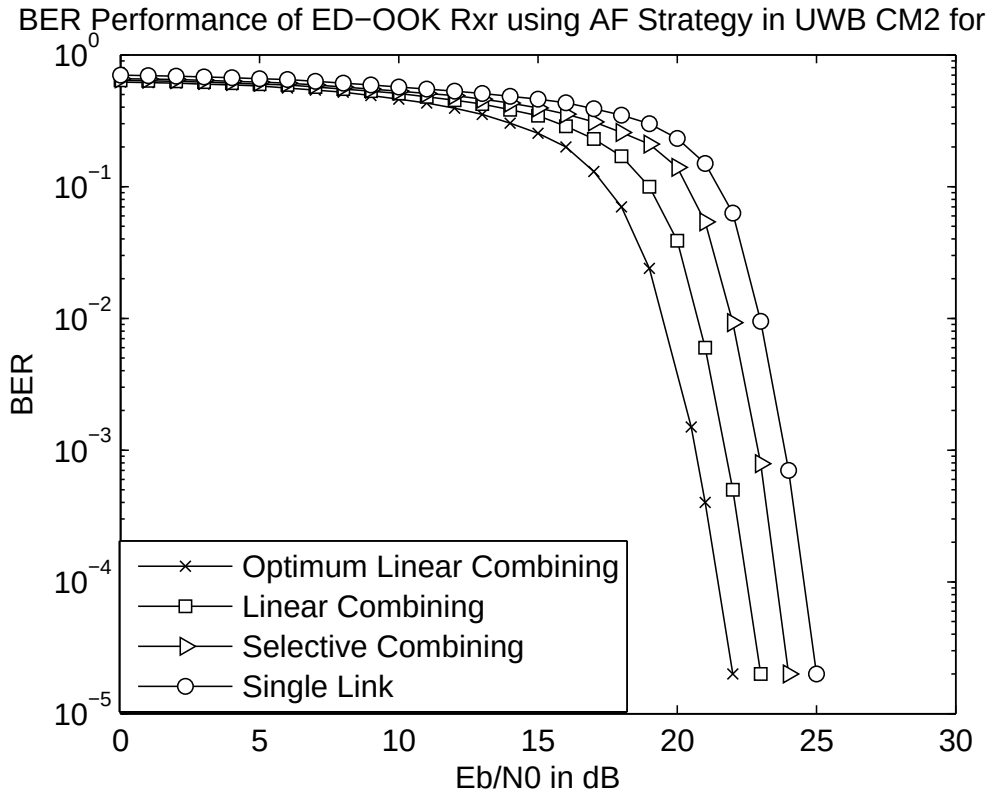

(b)

Figure 5.3: BER performance of UWB ED−OOK system using cooperative AF strategy with various combining schemes in UWB CM2 channel for (a) $N_f = 1$ (b) $N_f = 2$

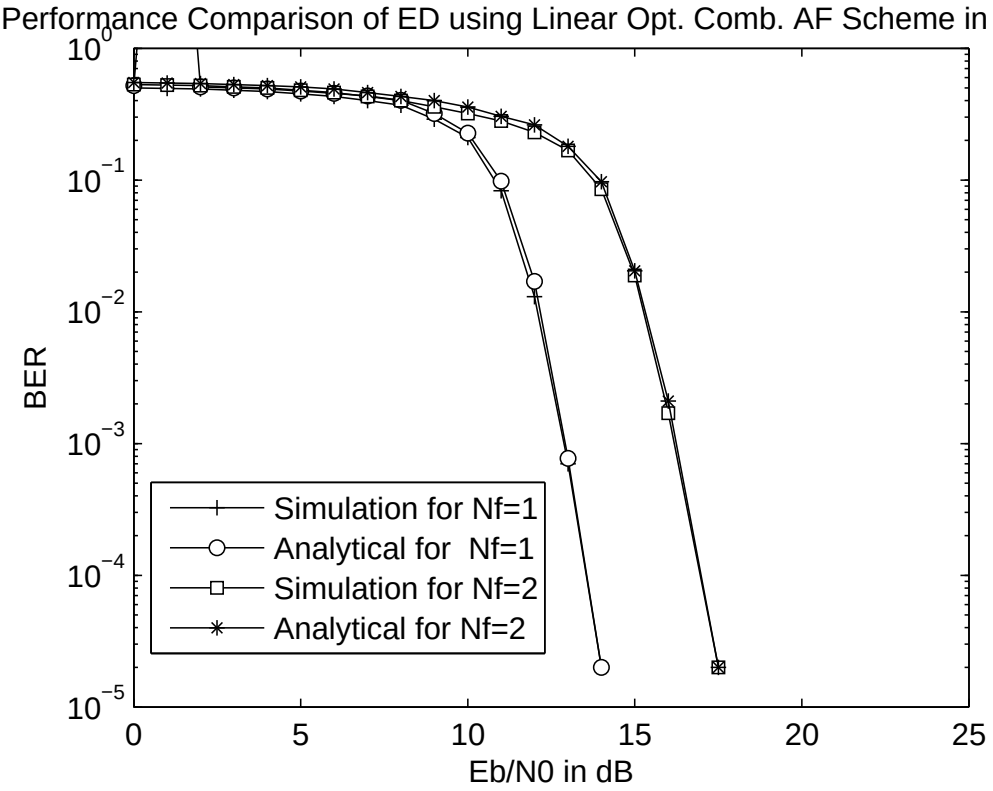
Performance Comparison of ED using Linear Opt. Comb. AF Scheme in CM1
BER
Eb/N0 in dB
Simulation for Nf=1
Analytical for Nf=1
Simulation for Nf=2
Analytical for Nf=2

(a)

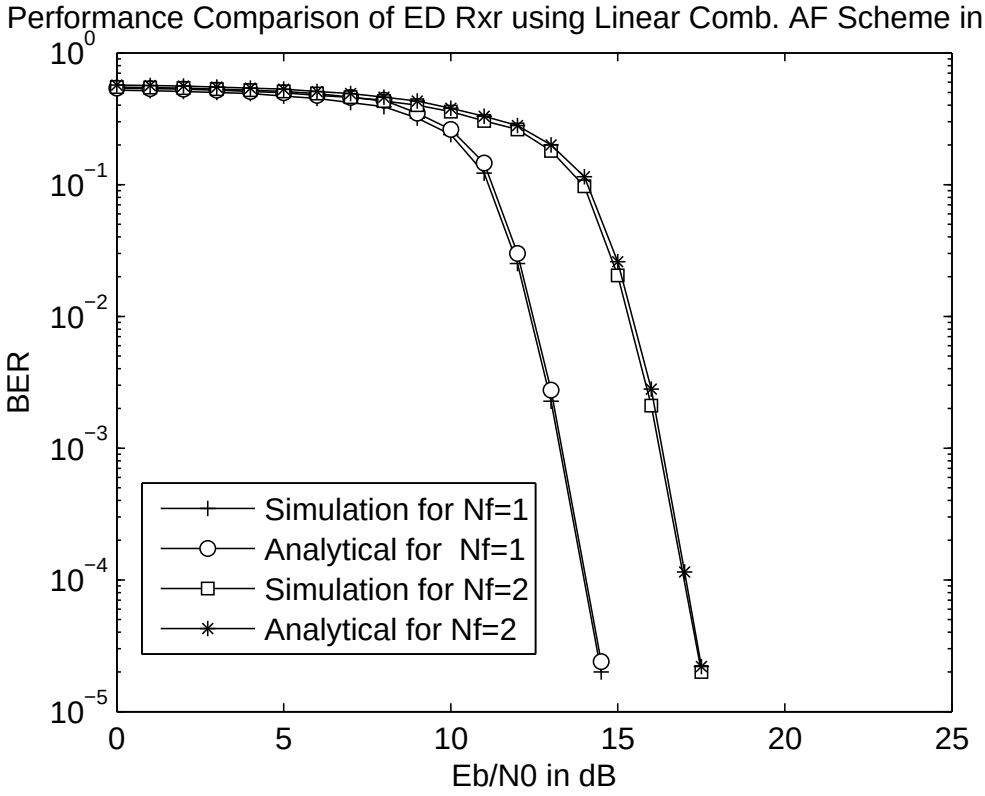
Performance Comparison of ED Rxr using Linear Comb. AF Scheme in CM1
BER
Eb/N0 in dB
Simulation for Nf=1
Analytical for Nf=1
Simulation for Nf=2
Analytical for Nf=2

(b)

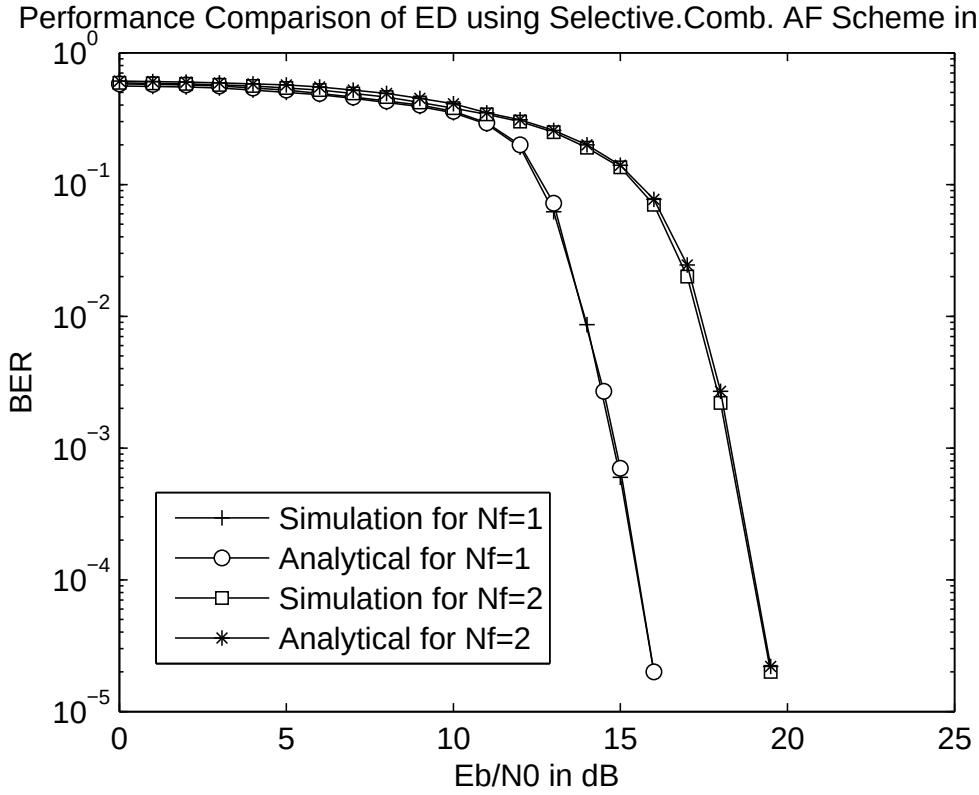

(c)

Figure 5.4: Analytic vs Simulated BER performance comparison of UWB ED−OOK system using AF strategy having $N_f = 1, 2$ for various combining schemes namely (a) Optimum Linear Combining (b) Linear Combining and (c) Selective Combining.

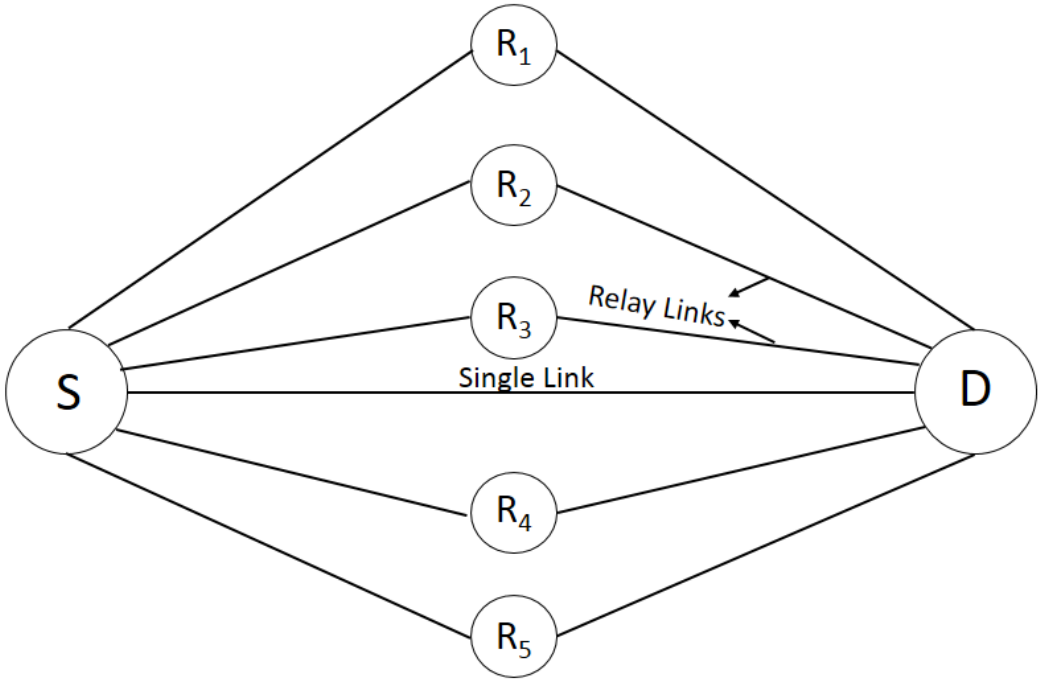

(a)

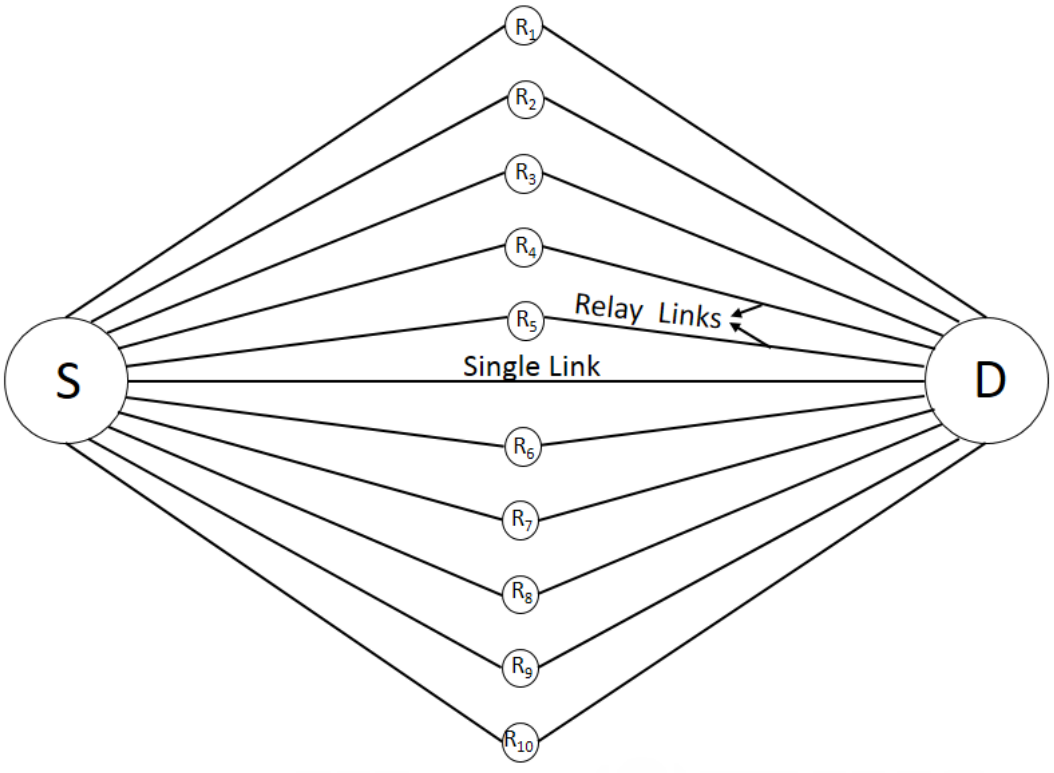

(b)

Figure 5.5: Dual−Hop Cooperative System Model with single−link and (a) $L = 5$ relay paths (b) $L = 10$ relay paths

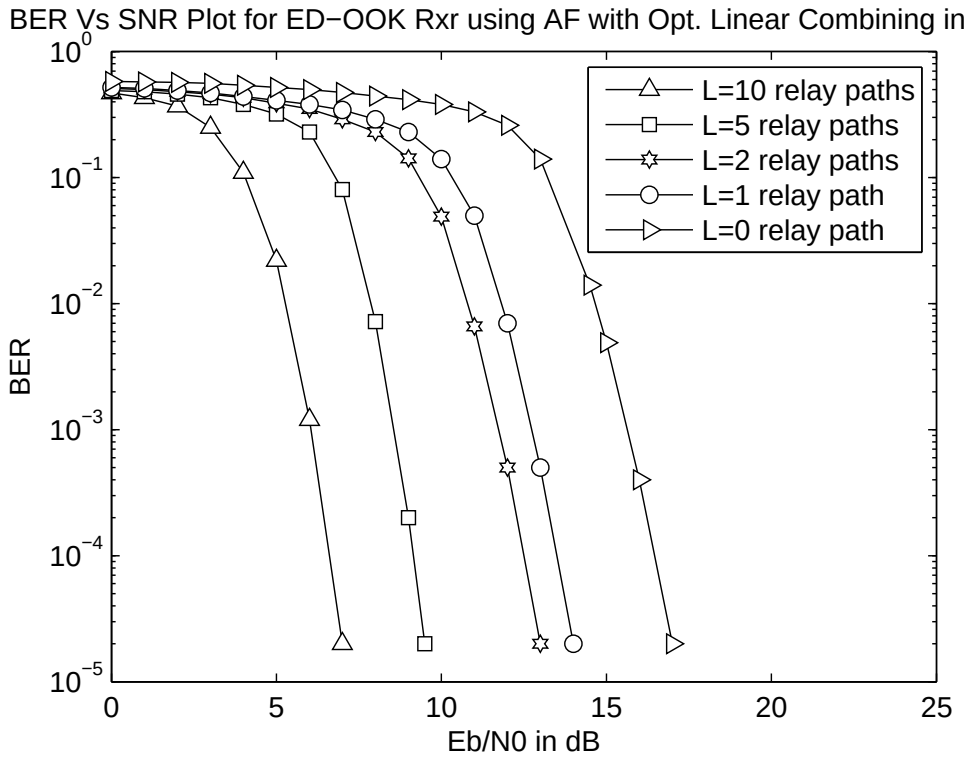
BER Vs SNR Plot for ED−OOK Rxr using AF with Opt. Linear Combining in CM1
BER
Eb/N0 in dB
L=10 relay paths
L=5 relay paths
L=2 relay paths
L=1 relay path
L=0 relay path

(a)

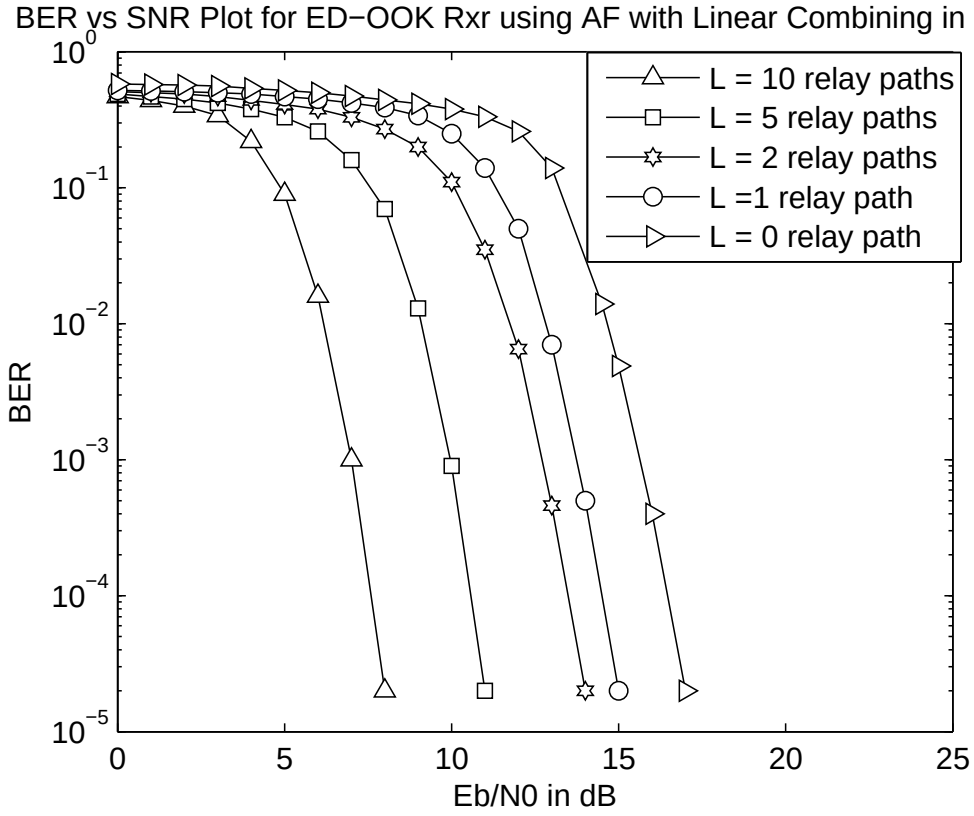
BER vs SNR Plot for ED−OOK Rxr using AF with Linear Combining in CM1
BER
Eb/N0 in dB
L = 10 relay paths
L = 5 relay paths
L = 2 relay paths
L =1 relay path
L = 0 relay path

(b)

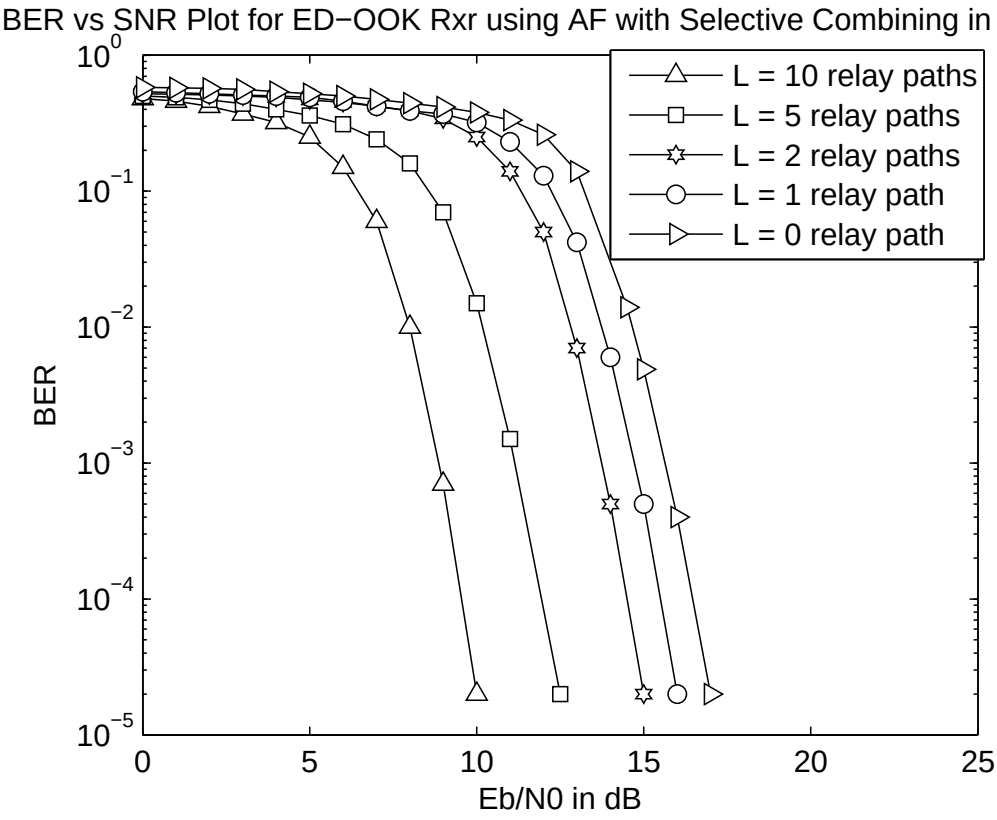

(c)

Figure 5.6: BER performance of UWB ED−OOK system using dual−hop cooperative AF strategy in UWB CM1 channel with (a) Optimum Linear Diversity Combining for $L = 0, 1, 2, 5, 10$ relay paths (b) Linear Diversity Combining for $L = 0, 1, 2, 5, 10$ relay paths and (c) Selective Diversity Combining for $L = 0, 1, 2, 5, 10$ relay paths.

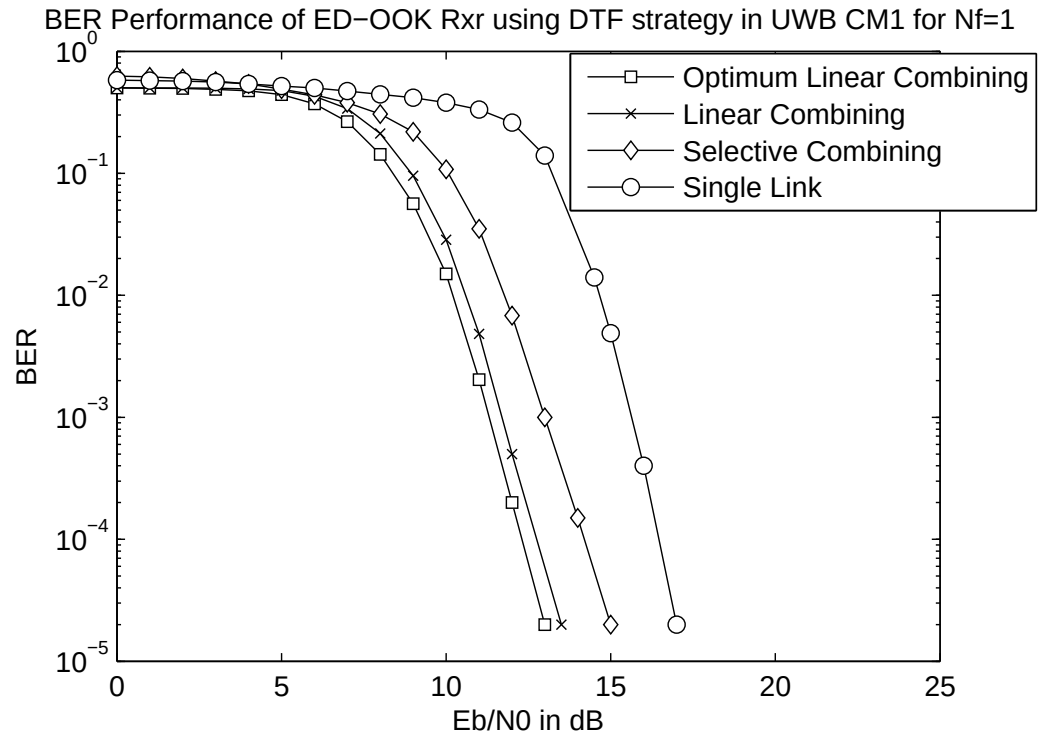

(a)

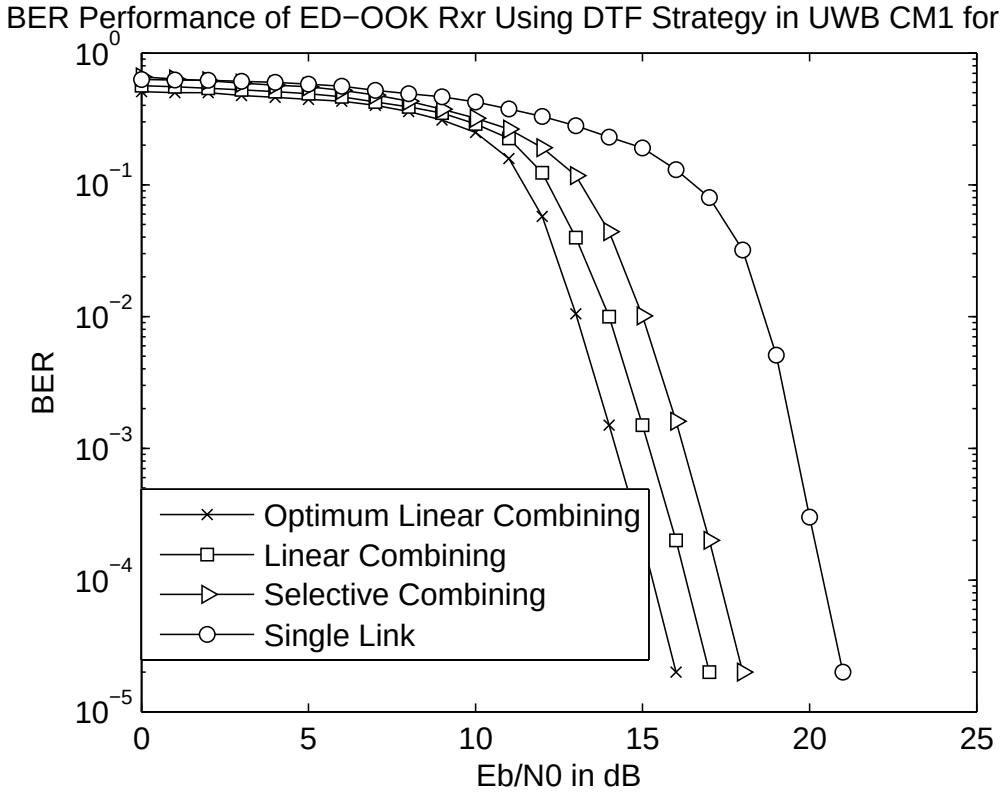

(b)

Figure 5.7: BER performance of UWB ED−OOK system using cooperative DTF strategy with various combining schemes in UWB CM1 channel for (a) $N_f = 1$ (b) $N_f = 2$

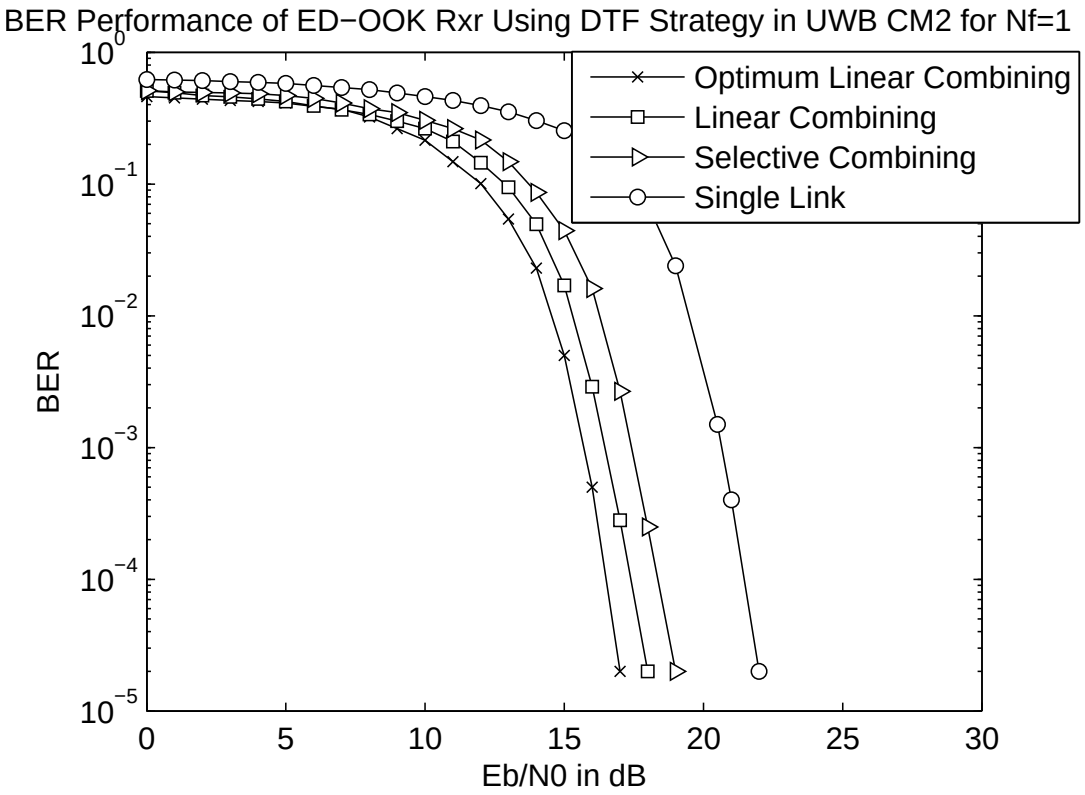

(a)

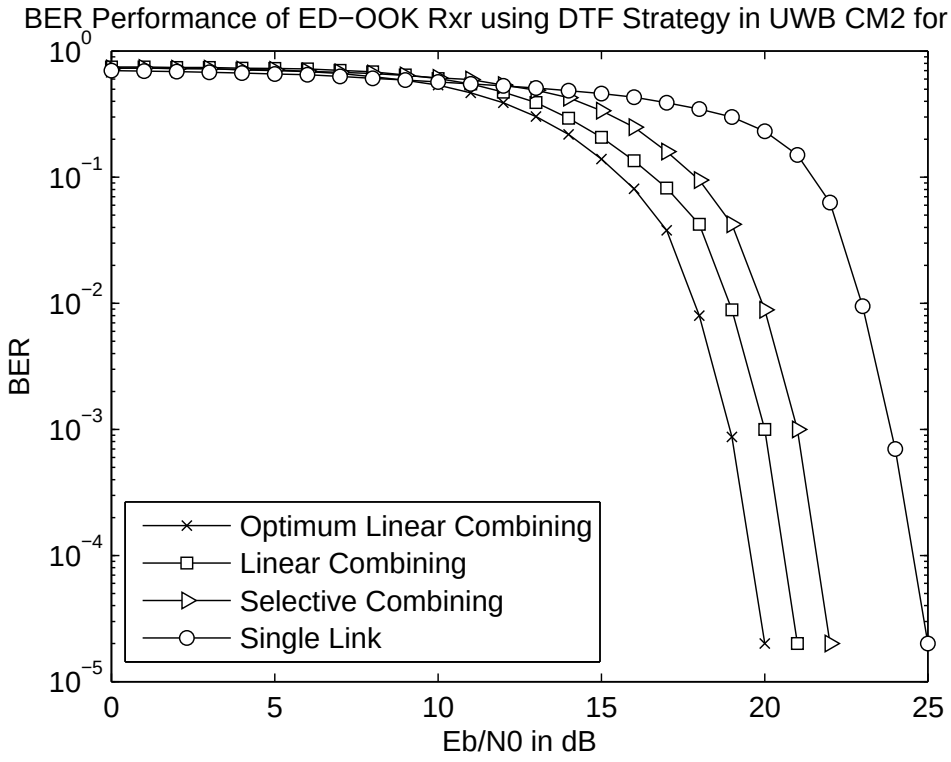

(b)

Figure 5.8: BER performance of UWB ED−OOK system using cooperative DTF strategy with various combining schemes in UWB CM2 channel for (a) $N_f = 1$ (b) $N_f = 2$

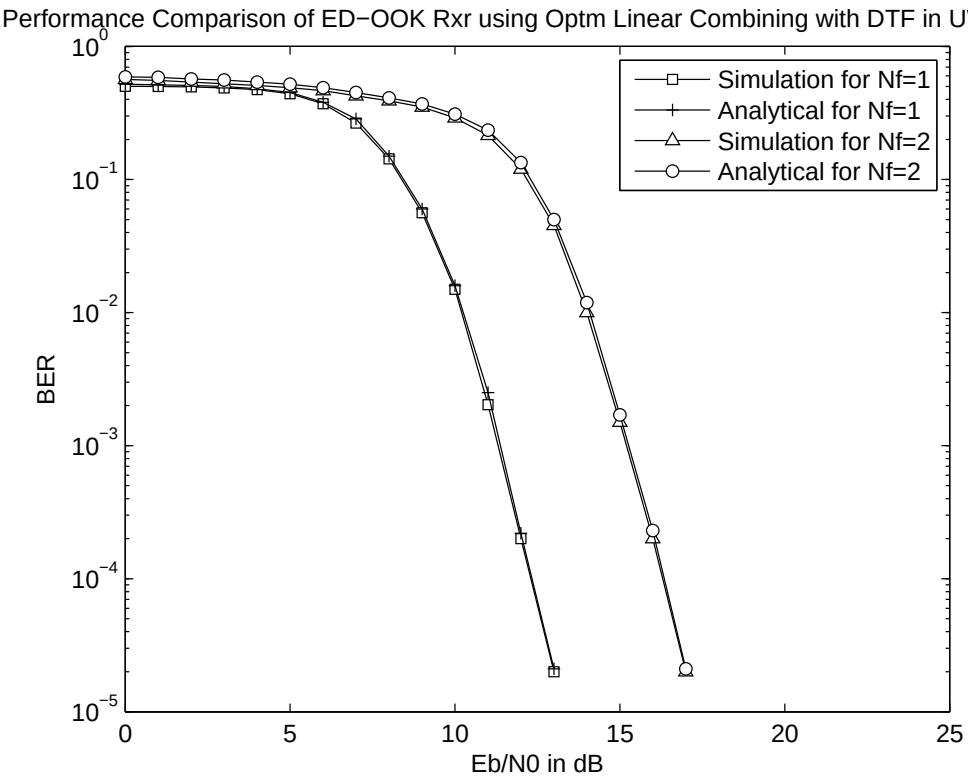
Performance Comparison of ED−OOK Rxr using Optm Linear Combining with DTF in UWB CM1
Simulation for Nf=1
Analytical for Nf=1
Simulation for Nf=2
Analytical for Nf=2
BER
Eb/N0 in dB

(a)

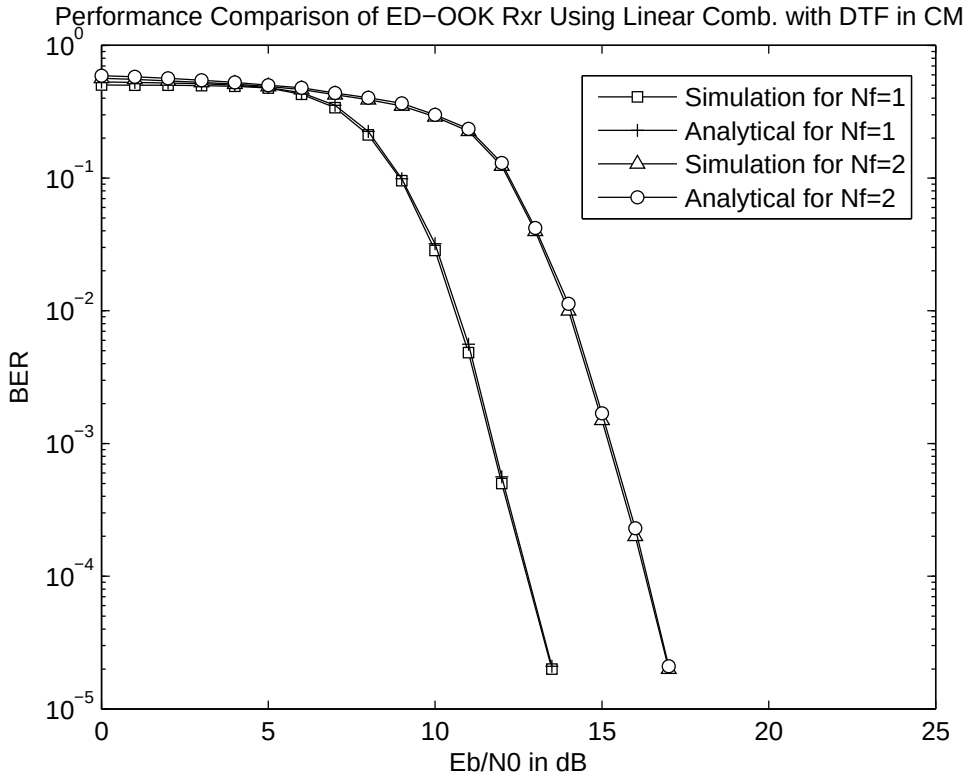
Performance Comparison of ED−OOK Rxr Using Linear Comb. with DTF in CM1
Simulation for Nf=1
Analytical for Nf=1
Simulation for Nf=2
Analytical for Nf=2
BER
Eb/N0 in dB

(b)

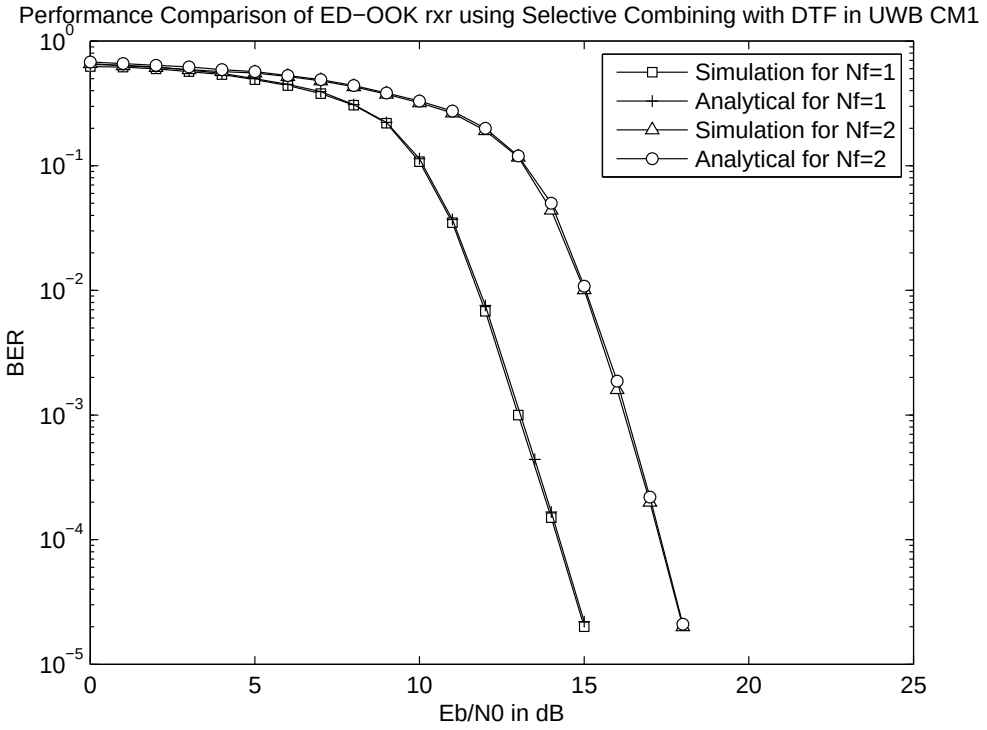

(c)

Figure 5.9: Analytic vs Simulated BER performance comparison of UWB ED−OOK system using DTF strategy in UWB CM1 channel having $N_f = 1, 2$ for (a) Optimum Linear Diversity Combining scheme (b) Linear Diversity Combining scheme and (c) Selective Diversity Combining scheme.

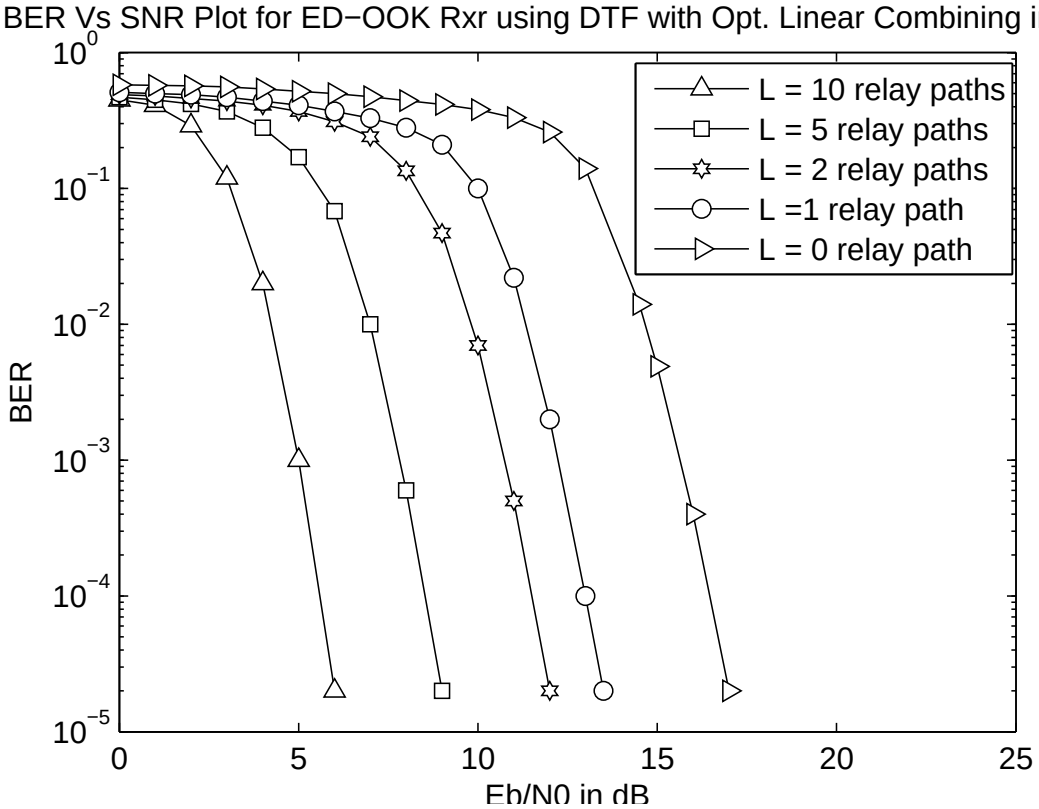
BER Vs SNR Plot for ED−OOK Rxr using DTF with Opt. Linear Combining in CM1
BER
Eb/N0 in dB
L = 10 relay paths
L = 5 relay paths
L = 2 relay paths
L =1 relay path
L = 0 relay path

(a)

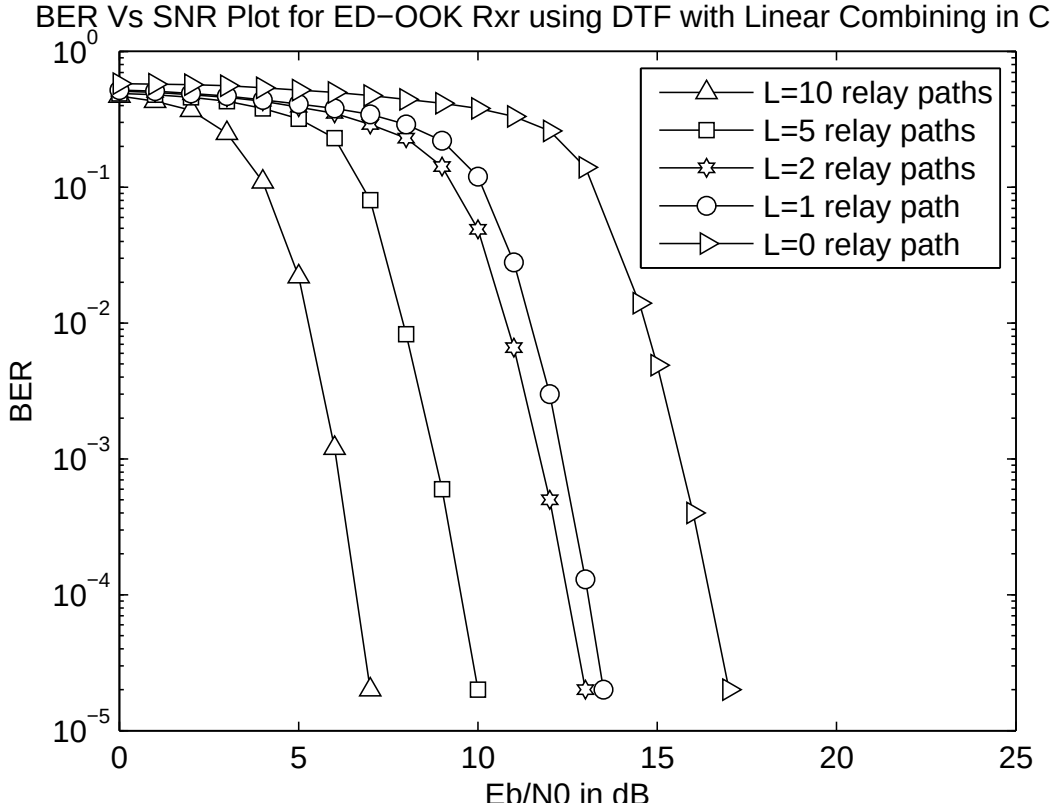
BER Vs SNR Plot for ED−OOK Rxr using DTF with Linear Combining in CM1
BER
Eb/N0 in dB
L=10 relay paths
L=5 relay paths
L=2 relay paths
L=1 relay path
L=0 relay path

(b)

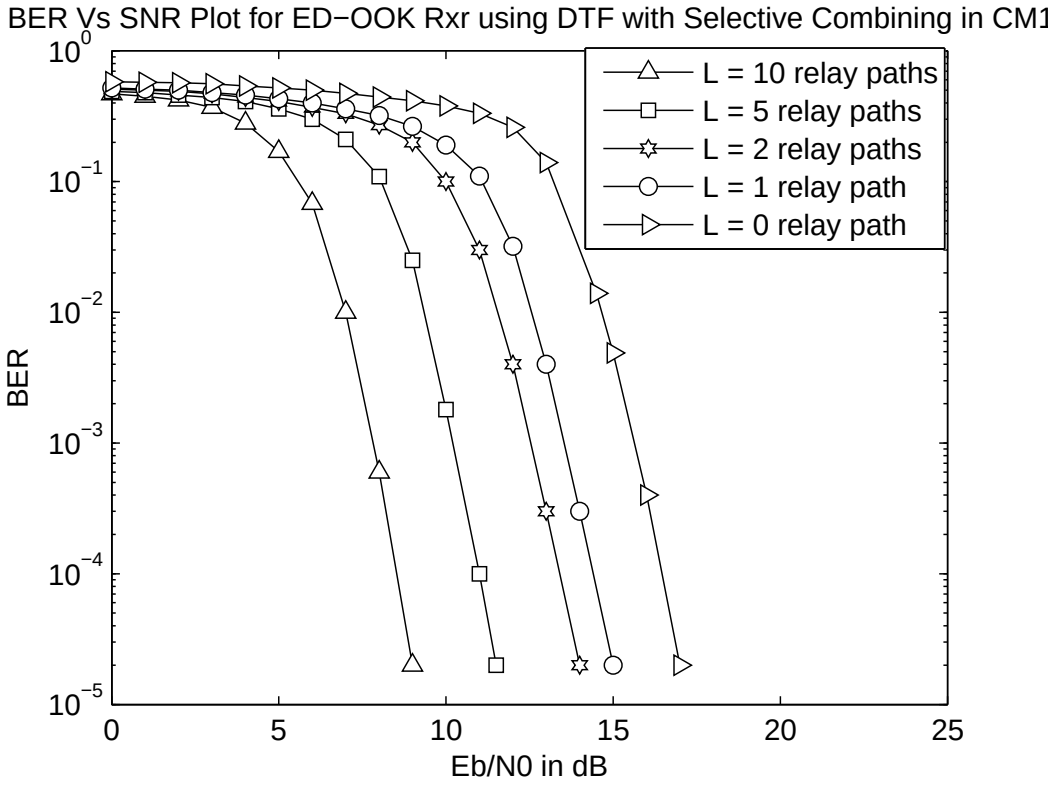

(c)

Figure 5.10: BER performance of UWB ED−OOK system using dual−hop cooperative DTF strategy in UWB CM1 channel with (a) Optimum Linear Diversity Combining for $L = 0, 1, 2, 5, 10$ relay paths (b) Linear Diversity Combining for $L = 0, 1, 2, 5, 10$ relay paths and (c) Selective Diversity Combining for $L = 0, 1, 2, 5, 10$ relay paths.

Fig 5.2(a) and (b) represents the BER performance of UWB ED−OOK system, using cooperative dual−hop AF strategy with various diversity combining schemes, over IEEE 802.15.4a UWB CM1 environment, for $N_f = 1$ and 2 respectively. It can be observed from both the Figures (a and b) that using cooperative AF scheme gives a much better BER performance, compared to non−cooperative or single−link. Among the diversity combining schemes, Optimum Linear Combining gives the best BER performance followed by Linear Combining and then Selective Combining, for any SNR. It is also inferred from Fig 5.2(a) and (b) that BER performance degrades as SNR falls by a margin of $3 - 4\ dB$, with increase in N_f from 1 to 2.

The variation in BER vs SNR plot of UWB ED−OOK system, using cooperative dual−hop AF strategy with various combining schemes in IEEE 802.15.4a UWB CM2 environment for $N_f = 1$ and 2, can be inferred from Fig 5.3(a) and (b) respectively. At a BER of 10^{-4}, CM2, NLOS channel suffers a SNR loss of $4 - 5\ dB$, compared to CM1, LOS environment, as observed in Fig 5.2(a) and (b). It can be concluded from both the Figures that as far as combining schemes are concerned, Optimum Linear Combining $>$ Linear Combining $>$ Selective Combining $>$ Single−Link. The SNR falls by a margin of $3 - 4\ dB$, when N_f changes from 1 to 2, as observed from the BER plots in the Figures. The inference drawn from the BER plots in the Figures reveal that, using dual−hop cooperative AF strategy gives a better BER performance, compared to non−cooperative scheme.

Fig 5.4 illustrates the analytical and simulated BER performance comparison of UWB ED−OOK system, using dual−hop cooperative AF strategy in UWB CM1 environment for all the three diversity combining cases. The approximate analytical BER expressions for these three diversity combining cases are plotted using numerical integration, and compared with the simulation results for $N_f = 1, 2$. The Fig 5.4(a), (b) and (c) confirms the convergence of analytical accuracy of the evaluated BER with that of the simulation BER plot.

The dual−hop cooperative system model having single path and $L = 5$ and 10 relay paths is represented in Fig 5.5(a) and (b), respectively. The BER performance of UWB ED−OOK system, using dual−hop cooperative AF strategy for various diversity combining schemes having $L = 0, 1, 2, 5, 10$ relay paths, is investigated in Fig 5.6 (a), (b) and (c). It can be concluded from the Figures that increase in relay paths ($L = 10$), gives better BER performance compared to using less number of relay paths ($L = 0, 1, 2, 5$), for any diversity combining scheme. The reason being, more the number of multipaths, more is the multipath energy extracted. Therefore, greater the diversity more is the improvement in BER performance. It can also be inferred from

the simulation results that UWB ED−OOK system, using cooperative AF strategy with various diversity combining schemes and ($L = 1, 2, 5, 10$) relay paths (diversity), gives a much better BER performance compared to single−link or non−cooperative case $L = 0$.

Fig 5.7(a) and (b) shows the variation in BER versus SNR of UWB ED−OOK system, using dual−hop cooperative DTF relay strategy, for various diversity combining techniques, in presence of IEEE 802.15.4a UWB CM1 LOS environment, having $N_f = 1$ and 2 respectively. It is also observed that increasing the number of frames N_f from 1 to 2, degrades the BER performance. At a BER of 10^{-4}, optimum linear diversity combining scheme, gives a SNR improvement of $0.5\ dB$ and $1.5\ dB$ over linear diversity combining and selective combining respectively. It is also noted from both the Figures that ED−OOK system suffers a SNR loss of $1.5 - 3\ dB$, using non−cooperative or single−link strategy, as compared to when using cooperative DTF strategy with diversity combining.

The BER performance of UWB ED−OOK system, using dual−hop cooperative DTF relay strategy with various diversity combining schemes, in UWB CM2 environment is as shown in Fig 5.8(a) and (b)for $N_f = 1$ and 2, respectively. CM2, being a NLOS channel, gives poor BER performance compared to LOS, CM1 channel. Using CM2 channel, the SNR of UWB ED−OOK system using both cooperative and non−cooperative strategy falls by a margin of $3.5 - 4.5\ dB$, when compared to CM1 channel, at a BER of 10^{-4}. The BER performance degrades as the number of frames N_f increases from 1 to 2, as observed from the BER plots in the Figures. As noted from the results, Optimum linear diversity combining gives the best BER performance compared to linear diversity combining and selective diversity combining. It can be concluded that using cooperative DTF strategy, gives a better BER performance than using non−cooperative strategy. Among diversity combining techniques, optimum linear diversity combining is found to give the best BER performance, followed by linear combining and then selective combining, for UWB CM2 channels having $N_f = 1, 2$.

The analytical and simulated BER performance of UWB ED−OOK system has been compared using dual−hop cooperative DTF protocol in UWB CM1 environment, for all the three diversity combining schemes and the results are as depicted in Fig 5.9. The obtained approximate analytical BER expressions for all these three diversity combining schemes is compared with the simulation results for $N_f = 1, 2$. From the Fig 5.9(a), (b) and (c), represented for optimum linear combining, linear combining and selective combining, it is observed that the plot of simulation results exactly coincide with the plot of analytical results at all BER levels

for $N_f = 1, 2$.

The dual−hop cooperative system model having single path and $L = 5$ and 10 relay paths respectively, is as shown in Fig 5.5(a) and (b). The BER performance of UWB ED−OOK system, using dual−hop cooperative DTF strategy for various diversity combining schemes having $L = 0, 1, 2, 5, 10$ relay paths, are represented in Fig 5.10(a), (b) and (c). It can be concluded from the Figures that BER performance of UWB ED−OOK system, for a cooperative system model having $L = 10$ relay paths and using any diversity combining scheme, is the best compared to $L = 0, 1, 2, 5$ relay paths. This is because, as the number of multipaths increases, the multipath energy extracted also increases. Thus, improvement in BER performance is noted, leading to greater diversity. It can also be inferred from the simulation results that UWB ED−OOK system, using cooperative DTF strategy with various diversity combining schemes and ($L = 1, 2, 5, 10$) relay paths (diversity) gives a much better BER performance compared to single−link or non−cooperative case $L = 0$.

5.6 Concluding Remarks

The analytical BER expression for UWB ED−OOK system using cooperative dual−hop AF and DTF relay protocol for various diversity combining scenarios namely, optimum linear diversity combining, linear diversity combining and selective diversity combining, was derived. The expressions were validated with the simulation results, employing IEEE 802.15.4a UWB standard between the relay nodes and links. The convergence of the simulation results with the analytical results, confirm the accuracy and perfectness of approximation used in evaluation of BER. Numerical results clearly indicate an improvement in BER, with increase in number of relay paths, L. This is because, more the number of relay paths, more is the diversity combining hence, better is the BER performance. Also, CM1, being LOS in nature, gives a better BER performance than CM2, which is NLOS in nature. It is also observed that, increase in number of frames N_f, leads to degradation in BER performance for UWB CM1 and CM2 environment. It can be inferred from the simulation results that, cooperative DTF strategy gives a SNR gain of $1\ dB$ when compared to AF strategy, at a BER of 10^{-4}. Furthermore, it can be concluded from the simulation results that using dual−hop cooperative AF and DTF strategy with diversity combining, gives a SNR gain of $2 - 4\ dB$ at a BER of 10^{-4}, compared to non−cooperative or single−link scheme. Also, among the diversity combining schemes, Optimum Linear Diversity

Combining gives the best BER performance when compared to the other combining schemes.

In this chapter, we present a novel analytical approach to evaluate the BER performance of non−coherent UWB ED-OOK system, based on energy detection, using cooperative dual−hop AF and DTF relay strategies with various diversity combining schemes, over IEEE 802.15.4a environment. Further, the analytical results are also validated with the simulation results.

Chapter 6

Performance Analysis of Non-Coherent UWB Cooperative ED−PPM System

In this chapter, the BER performance analysis of UWB ED−PPM system, using cooperative dual−hop AF and DTF strategy for various diversity combining schemes, over IEEE 802.15.4a environment is presented. The approximate BER expressions are derived based on energy detection principle, for various diversity combining cases, namely optimum linear combining, linear combining, and selective combining. Section 6.1 introduces UWB ED−PPM system using various cooperative dual−hop relay strategies. Section 6.2 presents the system model comprising of cooperative signal model, channel model and receiver structure. The detailed theoretical BER performance analysis of UWB ED−PPM system is evaluated using cooperative dual−hop AF and DTF strategy for various diversity combining schemes, in Section 6.3 and Section 6.4 respectively. The simulation results are outlined in Section 6.5 while Section 6.6, concludes the chapter.

6.1 Introduction

Non−Coherent UWB systems are preferred over its coherent counterpart, because of smaller complexity and non−requirement of channel estimation. The contributions mentioned in the literature are confined to the BER performance of non−coherent AC receivers, which include TR and DTR, using cooperative dual−hop and multi−hop relay technologies [157, 93, 101, 68]. Maichalernnukul [93] discussed the BER performance of UWB system using multi−antenna relay technology in dual−hop system while, Yazdi [101] investigated the BER performance of

UWB system using DF relay protocol. The problems faced by AC systems led to the advent of ED systems. ED systems, work by squaring the received signal followed by integration and detection through decision device [66, 67], that requires less hardware complexity and simpler implementation. In case of ED−OOK system, if information bit 1 is transmitted, significant pulse energy is captured during integration interval whereas, no energy is captured during integration interval during transmission of bit 0. The disadvantage of using ED system based on OOK scheme is that it does not transmit a Gaussian second order pulse when information bit 0 is transmitted, as a result inducing more noise during detection. This leads to degradation in BER performance. To rectify this problem, ED−PPM system is introduced. For a ED−PPM system, when information bit 0 is transmitted, there is no shift in Gaussian second order pulse, while a PPM shift of Δ takes place, in case of information bit 1.

The objective of this chapter is to analyse and evaluate the BER performance of UWB ED−PPM system using dual−hop cooperative AF and DTF strategy for various diversity combining schemes, over IEEE 802.15.4a UWB environment. Approximate BER expressions are analytically evaluated based on Energy Detection principle, for various diversity combining cases, namely optimum linear combining, linear combining and selective combining in UWB ED−PPM system using cooperative dual−hop AF and DTF relay protocol.

6.2 System Model

The system model comprises of a dual−hop UWB cooperative system, with one source, relay and destination node each, as shown in Fig 1.3. UWB signal modulated by the information bit (or symbol), is transmitted from source node to relay node as well as destination node, in 1^{st} time slot. The relay node amplifies or detects the signal received from the source node, and then forwards it to the destination node in the 2^{nd} time slot, depending on the relay strategy. At the destination node, the signals obtained from S−D and R−D links using AF or DTF relaying scheme are demodulated using ED−PPM receiver. The decision statistics obtained at the destination node from S−D and R−D links are then combined using different combining strategies to form final decision statistic, which is then compared to a threshold to decide the information bit.

6.2.1 Channel Model

Throughout the chapter, we employ a multipath channel model specified by IEEE 802.15.4a group, for performance evaluation of UWB [30] system. The impulse response of IEEE 802.15.4a UWB channel, based on the modification of SV model [34] is expressed as:

$$h_k(t) = \sum_{l=0}^{L_k-1} \alpha_{l,k}\delta(t - \tau_{l,k}) \tag{6.1}$$

where, $\alpha_{l,k}$ and $\tau_{l,k}$ represents the amplitude response and delay response of l^{th} multipath in k^{th} link respectively. The indices $k \in \{1, 2, 3\}$ are used to denote S−D link, S−R link and R−D link respectively. The channel gains $\alpha_{l,k}$ follow Nakagami distribution, while δ denotes Delta−Dirac function. The UWB channel models chosen for simulation are CM1−CM2, which represent different UWB environments.

6.2.2 Signal Model

The cooperation strategy has been extended to an UWB ED system, employing PPM modulation scheme for signalling. The symbol duration or signalling interval $T_s = N_f T_f$ is composed of N_f frames, each of duration T_f. In each frame duration T_f, a second order Gaussian derivative pulse $p(t) = (1 - 4\pi((t)/T_k)^2)exp(-2\pi((t)/T_k)^2)$ of duration T_p, modulated by information bit b_i, is transmitted. The term t denotes time interval and T_k the pulse width factor. When $b_i = 1$, the transmitted Gaussian second order pulse $p(t)$ is shifted by Δ units, while there is no shift in pulse position, when $b_i = 0$. The multipath delay spread of the channel T_{mds} satisfies the condition $T_{mds} >> T_p$, to avoid any interference among the symbols. We also assume that PPM shift Δ and frame duration T_f, satisfies the relation $\Delta > T_p + T_{mds} + T_g$ and $T_f = 2\Delta$, such that there is no ISI at the receiver side. Here, T_g represents the guard band duration.

The UWB signal transmitted from the source node to relay node in 1^{st} time slot is represented as:

$$s_{SD}(t) \;=\; \sqrt{E} \sum_{i=-\infty}^{\infty} \sum_{j=0}^{N_f-1} p(t - jT_f - 2iT_s - \Delta b_i) \tag{6.2}$$

where, the pulse energy at each link is expressed as $E = \int_{-\infty}^{\infty} p^2(t)dt$. Similarly, UWB signal transmitted from the source node to destination node in 1^{st} time slot is represented as:

$$s_{SR}(t) \;=\; \sqrt{E} \sum_{i=-\infty}^{\infty} \sum_{j=0}^{N_f-1} p(t - jT_f - 2iT_s - \Delta b_i) \tag{6.3}$$

where, $b_i \in (0,1)$ represents the information bit and Δ the PPM shift. When $b_i = 1$, the transmitted Gaussian second order pulse $p(t)$ is shifted by Δ units, while there is no shift in pulse position $p(t)$, when $b_i = 0$. The multipath delay spread of the channel satisfies the condition $T_{mds} >> T_p$ [30], to avoid IPI at the receiver end. We also assume that PPM shift Δ and frame duration T_f, satisfies the condition $\Delta > T_p + T_{mds} + T_g$ and $T_f = 2\Delta$, such that there is no interference at the receiver side. Here, T_g represents the guard band duration.

The signal received at the destination node in 1st time slot is denoted as:

$$\begin{aligned} r_{SD}(t) &= \sqrt{E}\sum_{i=-\infty}^{\infty}\sum_{j=0}^{N_f-1} p(t - jT_f - 2iT_s - \Delta b_i) * \sum_{l=0}^{L_1-1}\alpha_{l,1}\delta(t-\tau_{l,1}) + n_{SD}(t) \\ &= \sum_{l=0}^{L_1-1}\alpha_{l,1} g_{SD}(t - jT_f - 2iT_s - \Delta b_i - \tau_{l,1}) + n_{SD}(t) \end{aligned} \tag{6.4}$$

Similarly, the signal received at the relay node in 1st time slot is denoted as:

$$\begin{aligned} r_{SR}(t) &= \sqrt{E}\sum_{i=-\infty}^{\infty}\sum_{j=0}^{N_f-1} p(t - jT_f - 2iT_s - \Delta b_i) * \sum_{l=0}^{L_2-1}\alpha_{l,2}\delta(t-\tau_{l,2}) + n_{SR}(t) \\ &= \sum_{l=0}^{L_2-1}\alpha_{l,2} g_{SR}(t - jT_f - 2iT_s - \Delta b_i - \tau_{l,2}) + n_{SR}(t) \end{aligned} \tag{6.5}$$

where, $*$ denotes the convolution operator. The aggregate signal response $g_{SD}(t)$ and $g_{SR}(t)$ from S$-$D and S$-$R links are represented as $g_{SD}(t-jT_f-2iT_s-\Delta b_i-\tau_{l,1}) = s_{SD}(t)*\delta(t-\tau_{l,1})$ and $g_{SR}(t - jT_f - 2iT_s - \Delta b_i - \tau_{l,2}) = s_{SR}(t) * \delta(t - \tau_{l,2})$ respectively. The noise (AWGN) terms at S$-$D and S$-$R link are expressed as $n_{SD}(t)$ and $n_{SR}(t)$ respectively.

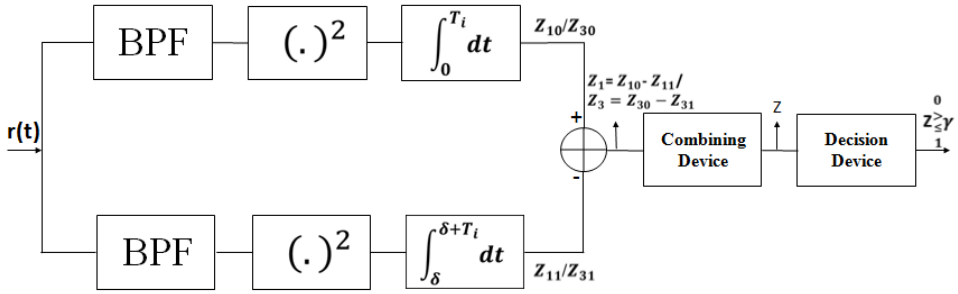

Figure 6.1: ED$-$PPM Receiver for Cooperative Communication

6.2.3 Receiver Structure

A non$-$coherent UWB ED$-$PPM receiver comprising of BPF, squarer, integrator, subtracter, combining and decision device, is used to recover the information bit. As illustrated in Fig 6.1,

the upper division works when information bit 0 is transmitted, else the lower division works, in case of information bit 1. The individual decision statistics Z_{10} and Z_{11} obtained from S−D link in 1^{st} time slot due to information bit 0 and 1 respectively, are passed through a subtracter to generate the decision statistic $Z_{SD} = Z_1 = Z_{10} - Z_{11}$. Similarly, decision statistics Z_{30} and Z_{31} obtained from R−D link in 2^{nd} time slot due to information bit 0 and 1 respectively, are passed through a subtracter to generate the decision statistic $Z_{RD} = Z_3 = Z_{30} - Z_{31}$. The decision statistics Z_{SD} and Z_{RD} obtained from S−D and R−D links in both the time slots, are combined using various combining strategies to give the final decision statistic Z_{total}, which is then compared to a threshold, to decide on the transmitted bit.

6.3 Performance Analysis of a Cooperative AF ED-PPM System

This section discusses the theoretical BER performance of UWB ED−PPM system using cooperative AF relay strategy, with various combining strategies [183]. The received signal $r_{SD}(t)$ obtained at the destination node in 1^{st} time slot, is passed through a ED−PPM receiver. The decision statistics Z_{SD} obtained from S−D link, is represented as $Z_{SD} = Z_1 = Z_{10} - Z_{11}$ where, Z_{10} and Z_{11} denote the decision statistics obtained from S−D link due to transmission of information bit 0 and 1 respectively.

$$Z_{lm} = \sum_{j=0}^{N_f-1} \int_{2iT_s+jT_f+m\Delta}^{2iT_s+jT_f+m\Delta+T_i} r_l^2(t)dt \tag{6.6}$$

where, the subscripts $l \in \{1,2,3\}$ denote S−D, S−R and R−D link respectively and $m \in \{0,1\}$ the transmitted information bit.

$$\begin{aligned} Z_{10} &= \sum_{j=0}^{N_f-1} \int_{2iT_s+jT_f}^{2iT_s+jT_f+T_i} r_{SD}^2(t)dt \\ &= \underbrace{A_1}_{signal} + \underbrace{A_2 + A_3}_{\text{noise}-term} = \underbrace{s_{10}}_{signal} + \underbrace{Z_{noise-10}}_{\text{noise}-term} \end{aligned} \tag{6.7}$$

$$\begin{aligned} Z_{11} &= \sum_{j=0}^{N_f-1} \int_{2iT_s+jT_f+\Delta}^{2iT_s+jT_f+\Delta+T_i} r_{SD}^2(t)dt \\ &= \underbrace{B_1}_{signal} + \underbrace{B_2 + B_3}_{\text{noise}-term} = \underbrace{s_{11}}_{signal} + \underbrace{Z_{noise-11}}_{\text{noise}-term} \end{aligned} \tag{6.8}$$

where, $T_i = T_{mds} + T_p$ represents the integration time interval. Here, T_p and T_{mds} denote pulse duration and multipath delay spread respectively. The value of decision statistic Z_{10} is obtained in equation 6.9, by replacing the value of equation 6.4 in equation 6.7, as shown below.

$$\begin{aligned} Z_{10} &= \sum_{j=0}^{N_f-1} \int_{2iT_s+jT_f}^{2iT_s+jT_f+T_i} \left(\sum_{l=0}^{L_1-1} \alpha_{l,1} g_{SD}(t - jT_f - 2iT_s - \Delta b_i - \tau_{l,1}) + n_{SD}(t) \right)^2 \\ &= \sum_{j=0}^{N_f-1} \sum_{l=0}^{L_1-1} \alpha_{l,1}^2 \int_{2iT_s+jT_f}^{2iT_s+jT_f+T_i} g_{SD}^2(t - jT_f - 2iT_s - \Delta b_i - \tau_{l,1}) dt + 2 \sum_{j=0}^{N_f-1} \sum_{l=0}^{L_1-1} \\ &\quad \alpha_{l,1} \int_{2iT_s+jT_f}^{2iT_s+jT_f+T_i} g_{SD}(t - jT_f - 2iT_s - \Delta b_i - \tau_{l,1}) n_{SD}(t) dt + \sum_{j=0}^{N_f-1} \int_{2iT_s+jT_f}^{2iT_s+jT_f+T_i} \\ &\quad n_{SD}^2(t) dt \end{aligned} \tag{6.9}$$

The equation 6.9 holds true only for the condition, that there is no IPI at the receiver end. The signal component A_1 is obtained from decision variable Z_{10}.

$$\begin{aligned} A_1 &= \sum_{j=0}^{N_f-1} \sum_{l=0}^{L_1-1} \alpha_{l,1}^2 \int_{2iT_s+jT_f}^{2iT_s+jT_f+T_i} g_{SD}^2(t - jT_f - 2iT_s - \Delta b_i - \tau_{l,1}) dt \\ &= s_{10} = N_f E_{10} \gamma_1 \end{aligned} \tag{6.10}$$

where, $E_{10} = \int_{2iT_s+jT_f}^{2iT_s+jT_f+T_i} g_{SD}^2(t - jT_f - 2iT_s - \Delta b_i - \tau_{l,1}) dt$ denotes the received signal energy component in Z_{10}. The channel gains $\alpha_{l,k}$ for IEEE 802.15.4a UWB multipath channels are assumed to be IID Nakagami. Consequently, their squares will be IID Gamma distributed [179]. Hence, by the Central Limit Theorem, the channel gains can be approximated as Gaussian distributed $\sum_{l_1} \alpha_{l_1}^2 = \gamma_1$. As the decision variables A_2 and A_3 denote the noise terms, their variances are evaluated.

The noise terms $n_k(t)$ are obtained by filtering AWGN process, having a single$-$sided PSD of $\frac{N_0}{2}$ with a BPF, having one-sided Bandwidth of W. The autocorrelation function of noise $\theta_k(\tau)$ is given by [175]:

$$\theta_k(\tau) = \mathbb{E}[n_k(t) n_k(t - \tau)] = \frac{N_0}{2} \frac{Sin(\pi W \tau)}{\pi W \tau} cos(2\pi f_c \tau) \tag{6.11}$$

where, $\mathbb{E}[.]$ denotes the statistical expectation operator and f_c carrier frequency of BPF. Since the Bandwidth is assumed to be sufficiently large, the frequency response of the received signal $g_k(t)$ at destination node falls inside the PSD $\theta_k(f)$ of $n_k(t)$. As PSD $\theta_k(f)$ is sufficiently flat, the autocorrelation function of noise can be simplified as $\theta_k(\tau) = \frac{N_0}{2} \delta(\tau)$ [175].

The noise variances are assumed to be independent of the channel under consideration.

Hence, the noise variances A_2 and A_3 obtained from Z_{10} are as follows:

$$\begin{aligned}\sigma^2_{N_1} &= \mathbb{E}[A2^2] = 2\sum_{j=0}^{N_f-1}\sum_{l=0}^{L_1-1}\alpha^2_{l,1}\int_{2iT_s+jT_f}^{2iT_s+jT_f+T_i}\int_{2iT_s+jT_f}^{2iT_s+jT_f+T_i} g_{SD}(t-jT_f-2iT_s-\Delta b_i- \\ &\quad \tau_{l,1})g_{SD}(\tau-jT_f-2iT_s-\Delta b_i-\tau_{l,1})\,\mathbb{E}[n_{SD}(t)n_{SD}(\tau)]dtd\tau \\ &= 2N_f\gamma_1\int_{2iT_s+jT_f}^{2iT_s+jT_f+T_i}\int_{2iT_s+jT_f}^{2iT_s+jT_f+T_i} g_{SD}(t-jT_f-2iT_s-\Delta b_i-\tau_{l,1})g_{SD}(\tau-jT_f \\ &\quad -2iT_s-\Delta b_i-\tau_{l,1})\theta_1(t-\tau)dtd\tau \\ &= 2N_f\gamma_1\frac{N_0}{2}\int_{2iT_s+jT_f}^{2iT_s+jT_f+T_i} g^2_{SD}(t-jT_f-2iT_s-\Delta b_i-\tau_{l,1})dt = N_fN_0E_{10}\gamma_1. \quad (6.12)\end{aligned}$$

where, $\mathbb{E}[n_{SD}(t)n_{SD}\tau] = \theta_1(t-\tau) = \frac{N_0}{2}\Delta(t-\tau)$ and $\int_{2iT_s+jT_f}^{2iT_s+jT_f+T_i}\frac{N_0}{2}\Delta(t-\tau)d\tau = \frac{N_0}{2}$.

$$\begin{aligned}\sigma^2_{N_2} &= \mathbb{E}[A_3^2] = \sum_{j=0}^{N_f-1}\int_{2iT_s+jT_f}^{2iT_s+jT_f+T_i}\int_{2iT_s+jT_f}^{2iT_s+jT_f+T_i}\mathbb{E}\left[\left\{n^2_{SD}(t)\right\}^2\right]dtd\tau \\ &= N_f\int_0^{T_i}\int_{T_i-t}^{T_i}\frac{N_0^2}{2}dtd\tau = N_f\int_0^{T_i}\frac{N_0^2}{2}2Wdt = N_fN_0^2WT_i \quad (6.13)\end{aligned}$$

where, the value of $\mathbb{E}\left[\left\{n^2_{SD}(t)\right\}^2\right] = \frac{N_0^2}{2}$ as solved in Appendix A. The total noise term $Z_{noise-10}$ has a total variance of $\sigma^2_{Z_{noise-10}} = \sigma^2_{N_1} + \sigma^2_{N_2} = N_fN_0E_{10}\gamma_1 + N_fN_0^2WT_i$. The variance of $n^2_k(t)$ tends to Dirac-Delta function, where the integral vanishes outside the range $[-t, T_i - t]$. This is solved using Parsevals theorem, as observed in equation 6.13.

Similarly, the decision statistics Z_{11} is obtained by replacing the value of equation 6.4 in equation 6.8. In case of no IPI, equation 6.14 holds good.

$$\begin{aligned}Z_{11} &= \sum_{j=0}^{N_f-1}\int_{2iT_s+jT_f+\Delta}^{2iT_s+jT_f+\Delta+T_i}\left(\sum_{l=0}^{L_1-1}\alpha_{l,1}g_{SD}(t-jT_f-2iT_s-\Delta b_i-\tau_{l,1})+n_{SD}(t)\right)^2 \\ &= \sum_{j=0}^{N_f-1}\sum_{l=0}^{L_1-1}\alpha^2_{l,1}\int_{2iT_s+jT_f+\Delta}^{2iT_s+jT_f+\Delta+T_i} g^2_{SD}(t-jT_f-2iT_s-\Delta b_i-\tau_{l,1})dt + 2\sum_{j=0}^{N_f-1}\sum_{l=0}^{L_1-1} \\ &\quad \alpha_{l,1}\int_{2iT_s+jT_f+\Delta}^{2iT_s+jT_f+\Delta+T_i} g_{SD}(t-jT_f-2iT_s-\Delta b_i-\tau_{l,1})n_{SD}(t)dt + \sum_{j=0}^{N_f-1} \\ &\quad \int_{2iT_s+jT_f+\Delta}^{2iT_s+jT_f+\Delta+T_i} n^2_{SD}(t)dt \quad (6.14)\end{aligned}$$

The signal component B_1 is obtained from decision variable Z_{11}.

$$\begin{aligned}B_1 &= \sum_{j=0}^{N_f-1}\sum_{l=0}^{L_1-1}\alpha^2_{l,1}\int_{2iT_s+jT_f+\Delta}^{2iT_s+jT_f+\Delta+T_i} g^2_{SD}(t-jT_f-2iT_s-\Delta b_i-\tau_{l,1})dt \\ &= s_{11} = N_fE_{11}\gamma_1 \quad (6.15)\end{aligned}$$

where, $E_{11} = \int_{2iT_s+jT_f+\Delta}^{2iT_s+jT_f+\Delta+T_i} g_{SD}^2(t - jT_f - 2iT_s - \Delta b_i - \tau_{l,1})dt$ denotes the received signal energy component in Z_{11}.

Similarly, the noise variances B_2 and B_3 obtained from Z_{11} are as follows.

$$\begin{aligned}
\sigma_{N_1}^2 &= \mathbb{E}[B_2^2] = 2\sum_{j=0}^{N_f-1}\sum_{l=0}^{L_1-1}\alpha_{l,1}^2 \int_{2iT_s+jT_f+\Delta}^{2iT_s+jT_f+\Delta+T_i}\int_{2iT_s+jT_f+\Delta}^{2iT_s+jT_f+\Delta+T_i} g_{SD}(t - jT_f - 2iT_s - \Delta b_i \\
&\quad -\tau_{l,1})g_{SD}(\tau - jT_f - 2iT_s - \Delta b_i - \tau_{l,1})\,\mathbb{E}[n_{SD}(t)n_{SD}(\tau)]dtd\tau \\
&= 2N_f\gamma_1 \int_{2iT_s+jT_f+\Delta}^{2iT_s+jT_f+\Delta+T_i}\int_{2iT_s+jT_f+\Delta}^{2iT_s+jT_f+\Delta+T_i} g_{SD}(t - jT_f - 2iT_s - \Delta b_i - \tau_{l,1})g_{SD}(\tau - \\
&\quad jT_f - 2iT_s - \Delta b_i - \tau_{l,1})\theta_1(t-\tau)dtd\tau \\
&= 2N_f\gamma_1\frac{N_0}{2}\int_{2iT_s+jT_f+\Delta}^{2iT_s+jT_f+\Delta+T_i} g_{SD}^2(t - jT_f - 2iT_s - \Delta b_i - \tau_{l,1})dt \\
&= N_f N_0 E_{11}\gamma_1 \qquad (6.16)
\end{aligned}$$

where, $\mathbb{E}[n_{SD}(t)n_{SD}\tau] = \theta_1(t-\tau) = \frac{N_0}{2}\Delta(t-\tau)$ and $\int_{2iT_s+jT_f+\Delta}^{2iT_s+jT_f+\Delta+T_i}\frac{N_0}{2}\Delta(t-\tau)d\tau = \frac{N_0}{2}$.

$$\begin{aligned}
\sigma_{N_2}^2 &= \mathbb{E}[B_3^2] = \sum_{j=0}^{N_f-1}\int_{2iT_s+jT_f+\Delta}^{2iT_s+jT_f+\Delta+T_i}\int_{2iT_s+jT_f+\Delta}^{2iT_s+jT_f+\Delta+T_i}\mathbb{E}\left[\left\{n_{SD}^2(t)\right\}^2\right]dtd\tau \\
&= N_f\int_0^{T_i}\int_{T_i-t}^{T_i}\frac{N_0^2}{2}d\tau dt = N_f\int_0^{T_i}\frac{N_0^2}{2}2Wdt = N_f N_0^2 W T_i \qquad (6.17)
\end{aligned}$$

where, the value of $\mathbb{E}\left[\left\{n_{SD}^2(t)\right\}^2\right] = \frac{N_0^2}{2}$ is solved in Appendix A. The noise term $Z_{noise-11}$ has a total variance of $\sigma_{Z_{noise-11}}^2 = \sigma_{N_1}^2 + \sigma_{N_2}^2 = N_f N_0 E_{11}\gamma_1 + N_f N_0^2 W T_i$. Parseval's theorem has been used to solve equation 6.17.

The signal received at the relay node in 1st time slot, is amplified by an amplifying factor $\sqrt{\beta_{AF}}$ and then forwarded to the destination node in the 2nd time slot. The amplified signal transmitted from the relay node to the destination node is represented as:

$$s_3(t) = r_2(t)\sqrt{\beta_{AF}} = s_{RD}(t) = r_{SR}(t)\sqrt{\beta_{AF}} \qquad (6.18)$$

where, index $k \in \{2,3\}$ represents S$-$R and R$-$D link respectively. The amplifying gain is defined as $\sqrt{\beta_{AF}} = \sqrt{\left(\frac{E_{SR}}{\mathbb{E}\left\{|h_2^2(t)|\right\}E_{SR}+N_0}\right)}$. Also, E_{SR}, $h_2(t)$ and $\sigma_{Z_{noise-SR}}^2 = N_f N_0(E_{20} + E_{21}\gamma_2 + 2N_f N_0^2 W T_i)$ represent the signal energy, channel response and noise variance of S$-$R link respectively. The signal received at the destination node from R$-$D link in 2nd time slot is represented as:

$$r_{RD}(t) = \left(\sqrt{\beta_{AF}}\sum_{l=0}^{L_2-1}\alpha_{l,2}g_{SR}(t - jT_f - (2i+1)T_s - \Delta b_i - \tau_{l,2}) + n_{SR}(t)\right) * \sum_{l=0}^{L_3-1}\alpha_{l,3}$$

$$\begin{aligned} & \delta(t-\tau_{l,3}) + n_{RD}(t) \\ = \; & \sqrt{\beta_{AF}} \sum_{l=0}^{L_2-1} \alpha_{l,2} \sum_{l=0}^{L_3-1} \alpha_{l,3} g_{SR}(t - jT_f - (2i+1)T_s - \Delta b_i - \tau_{l,2} - \tau_{l,3}) + \\ & \sqrt{\beta_{AF}} n_{RD}^{'}(t) + n_{RD}(t) \end{aligned} \tag{6.19}$$

where, $n_{RD}^{'}(t) = n_{SR}(t) * h_3(t) = \sum_{l=0}^{L_3-1} \alpha_{l,3} n_{SR}(t-\tau_{l,3})$ denotes the aggregate noise response after convolving the noise response of S−R link with channel response of R−D link $h_3(t)$. Also, $n_{RD}(t)$ represents the noise response of R−D link.

The received signal $r_{RD}(t)$ obtained at the destination node in 2nd time slot, is passed through a ED−PPM receiver. The decision statistics Z_{30} obtained from R−D link is simplified as:

$$\begin{aligned} Z_{30} &= \sum_{j=0}^{N_f-1} \int_{(2i+1)T_s+jT_f}^{(2i+1)T_s+jT_f+T_i} r_{RD}^2(t)dt \\ &= \underbrace{C_1}_{signal} + \underbrace{C_2 + C_3 + C_4 + C_5 + C_6}_{\text{noise}-term} \\ &= \underbrace{s_{30}}_{signal} + \underbrace{Z_{noise-30}}_{\text{noise}-term} \end{aligned} \tag{6.20}$$

The value of Z_{30} is obtained in equation 6.21, by replacing the value of equation 6.19 in equation 6.20. It is assumed that there is no IPI, so equation 6.20 holds true.

$$\begin{aligned} = \; & \sum_{j=0}^{N_f-1} \int_{(2i+1)T_s+jT_f}^{(2i+1)T_s+jT_f+T_i} \left(\sqrt{\beta_{AF}} \sum_{l=0}^{L_2-1} \alpha_{l,2} \sum_{l=0}^{L_3-1} \alpha_{l,3} g_{SR}(t - jT_f - (2i+1)T_s - \Delta b_i - \tau_{l,2} \right. \\ & \left. -\tau_{l,3}) + \sqrt{\beta_{AF}} n_{RD}^{'}(t) + n_{RD}(t) \right)^2 \end{aligned} \tag{6.21}$$

The signal component obtained from Z_{30} is as follows.

$$\begin{aligned} C_1 &= \beta_{AF} \sum_{j=0}^{N_f-1} \sum_{l=0}^{L_2-1} \alpha_{l,2} \sum_{l=0}^{L_3-1} \alpha_{l,3} \int_{(2i+1)T_s+jT_f}^{(2i+1)T_s+jT_f+T_i} g_{SR}^2(t - jT_f - (2i+1)T_s - \Delta b_i - \tau_{l,2} - \\ & \tau_{l,3})dt \\ &= s_{30} = \beta_{AF} N_f E_{30} \gamma_2 \gamma_3 \end{aligned} \tag{6.22}$$

where, $E_{30} = \int_{(2i+1)T_s+jT_f}^{(2i+1)T_s+jT_f+T_i} g_{SR}^2(t - jT_f - 2iT_s - \Delta b_i - \tau_{l,2} - \tau_{l,3})dt$ denotes the received signal energy component in Z_{30}. As explained earlier, since a large number of UWB multipath channel gains are considered, the channel gains can be approximated as Gaussian Distributed using the Central Limit Theorem $\sum_{l_2} \alpha_{l_2}^2 = \gamma_2$ and $\sum_{l_3} \alpha_{l_3}^2 = \gamma_3$. As described earlier, since the PSD $\theta_k(f)$ of noise is sufficiently flat, the autocorrelation function of noise can be approximated

as $\theta_k(\tau) = \frac{N_0}{2}\delta(\tau)$[175]. The noise variances obtained from Z_{30} are as follows:

$$\begin{aligned}\sigma^2_{N_1} &= \mathbb{E}[C_2^2] = 2\beta_{AF}^2 \sum_{j=0}^{N_f-1}\sum_{l=0}^{L_2-1}\alpha_{l,2}^2\sum_{l=0}^{L_3-1}\alpha_{l,3}^2\int_{(2i+1)T_s+jT_f}^{(2i+1)T_s+jT_f+T_i}\int_{(2i+1)T_s+jT_f}^{(2i+1)T_s+jT_f+T_i} g_{SR}(t-jT_f \\ &\quad -(2i+1)T_s-\Delta b_i-\tau_{l,2}-\tau_{l,3})g_{SR}(\tau-jT_f-(2i+1)T_s-\Delta b_i-\tau_{l,2}-\tau_{l,3}) \\ &\quad \mathbb{E}[n_{RD}^{'}(t)n_{RD}^{'}(\tau)]dtd\tau \\ &= \beta_{AF}^2 N_f N_0 E_{30}\gamma_2\gamma_3^2 \end{aligned} \tag{6.23}$$

where, $\int_{(2i+1)T_s+jT_f}^{(2i+1)T_s+jT_f+T_i}\theta_2(t-\tau)d\tau = \int_{(2i+1)T_s+jT_f}^{(2i+1)T_s+jT_f+T_i}\frac{N_0}{2}\delta(t-\tau)d\tau = \frac{N_0}{2}$. The value of $\mathbb{E}[n_{RD}^{'}(t)$ $n_{RD}^{'}(\tau)]$ is solved in Appendix B.

$$\begin{aligned}\sigma^2_{N_2} &= \mathbb{E}[C_3^2] = 2\beta_{AF} \sum_{j=0}^{N_f-1}\sum_{l=0}^{L_2-1}\alpha_{l,2}^2\sum_{l=0}^{L_3-1}\alpha_{l,3}^2\int_{(2i+1)T_s+jT_f}^{(2i+1)T_s+jT_f+T_i}\int_{(2i+1)T_s+jT_f}^{(2i+1)T_s+jT_f+T_i} g_{SR}(t \\ &\quad -jT_f-(2i+1)T_s-\Delta b_i-\tau_{l,2}-\tau_{l,3})g_{SR}(\tau-jT_f-(2i+1)T_s-\Delta b_i-\tau_{l,2}-\tau_{l,3}) \\ &\quad \mathbb{E}[n_{RD}(t)n_{RD}(\tau)]dtd\tau \\ &= \beta_{AF} N_f N_0 E_{30}\gamma_2\gamma_3 \end{aligned} \tag{6.24}$$

where, $\theta_3(t-\tau) = \mathbb{E}[n_{RD}(t)n_{RD}(\tau)] = \frac{N_0}{2}\delta(t-\tau)$ and $\int_{2iT_s+jT_f}^{2iT_s+jT_f+T_i}\frac{N_0}{2}\delta(t-\tau)d\tau = \frac{N_0}{2}$.

$$\begin{aligned}\sigma^2_{N_3} &= \mathbb{E}[C_4^2] = \sum_{j=0}^{N_f-1}\beta_{AF}^2\int_{(2i+1)T_s+jT_f}^{(2i+1)T_s+jT_f+T_i}\int_{(2i+1)T_s+jT_f}^{(2i+1)T_s+jT_f+T_i}\mathbb{E}\left[\left\{n_{RD}^{'2}(t)\right\}^2\right] \\ &\quad dtd\tau \\ &= \beta_{AF}^2 N_f\int_0^{T_i} 2\left(\gamma_3\frac{N_0}{2}\right)^2 2Wdt \\ &= \beta_{AF}^2 N_f N_0^2 W T_i\gamma_3^2 \end{aligned} \tag{6.25}$$

where, the value of $\mathbb{E}\left[\left\{n_{RD}^{'2}(t)\right\}^2\right] = 3\left(\gamma_3\frac{N_0}{2}\right)^2 - \left(\gamma_3\frac{N_0}{2}\right)^2 = 2\left(\gamma_3\frac{N_0}{2}\right)^2$ is obtained from Appendix A and Appendix B.

$$\begin{aligned}\sigma^2_{N_4} &= \mathbb{E}[C_5^2] = \sum_{j=0}^{N_f-1}\int_{(2i+1)T_s+jT_f}^{(2i+1)T_s+jT_f+T_i}\int_{(2i+1)T_s+jT_f}^{(2i+1)T_s+jT_f+T_i}\mathbb{E}\left[\left\{n_{RD}^{2}(t)\right\}^2\right]dtd\tau \\ &= N_f\int_0^{T_i}\int_{T_i-t}^{T_i}\frac{N_0^2}{2}2Wd\tau dt = N_f\int_0^{T_i}\frac{N_0^2}{2}2Wdt \\ &= N_f N_0^2 W T_i \end{aligned} \tag{6.26}$$

where, the value of $\mathbb{E}\left[\left\{n_{RD}^{2}(t)\right\}^2\right] = \frac{N_0^2}{2}$ is as derived in Appendix A.

$$\begin{aligned}\sigma^2_{N_5} &= \mathbb{E}[C_6^2] = 2\sum_{j=0}^{N_f-1}\beta_{AF}\int_{(2i+1)T_s+jT_f}^{(2i+1)T_s+jT_f+T_i}\int_{(2i+1)T_s+jT_f}^{(2i+1)T_s+jT_f+T_i}\mathbb{E}[n_{RD}(t)n'_{RD}(t)n_{RD}(\tau)\\ &\quad n'_{RD}(\tau)]dtd\tau\\ &= 2\beta_{AF}N_f\int_0^{T_i}\left(\frac{N_0}{2}\right)\left(\gamma_3\frac{N_0}{2}\right)2Wdt\\ &= \beta_{AF}N_fN_0^2WT_i\gamma_3 \end{aligned} \tag{6.27}$$

where, $\mathbb{E}[n_{RD}(t)n'_{RD}(t)n_{RD}(\tau)n'_{RD}(\tau)] = \mathbb{E}[n_{RD}(t)n_{RD}(\tau)]\,\mathbb{E}[n'_{RD}(t)n'_{RD}(\tau)]$. Since the noise terms correspond to different links, they are independent in nature. The noise−term $Z_{noise-30}$ has a total variance of $\sigma^2_{Z_{noise-30}} = \sigma^2_{N_1} + \sigma^2_{N_2} + \sigma^2_{N_3} + \sigma^2_{N_4} + \sigma^2_{N_5} = \beta^2_{AF}N_fN_0E_{30}\gamma_2\gamma_3^2 + \beta_{AF}N_fN_0E_{30}\gamma_2\gamma_3 + \beta_{AF}N_fN_0^2WT_i\gamma_3^2 + N_fN_0^2WT_i + \beta_{AF}N_fN_0^2WT_i\gamma_3$.

Similarly, the decision statistics Z_{31} obtained from R−D link is as follows.

$$\begin{aligned}Z_{31} &= \sum_{j=0}^{N_f-1}\int_{(2i+1)T_s+jT_f+\Delta}^{(2i+1)T_s+jT_f+\Delta+T_i} r^2_{RD}(t)dt\\ &= \underbrace{D_1}_{signal} + \underbrace{D_2+D_3+D_4+D_5+D_6}_{\text{noise}-term}\\ &= \underbrace{s_{31}}_{signal} + \underbrace{Z_{noise-31}}_{\text{noise}-term}\end{aligned} \tag{6.28}$$

The value of Z_{31} in equation 6.29 is obtained by replacing the value of equation 6.19 in equation 6.28. The condition that there is no IPI is satisfied, for equation 6.29 to hold true.

$$\begin{aligned}&= \sum_{j=0}^{N_f-1}\int_{(2i+1)T_s+jT_f+\Delta}^{(2i+1)T_s+jT_f+\Delta+T_i}\Bigg(\sqrt{\beta_{AF}}\sum_{l=0}^{L_2-1}\alpha_{l,2}\sum_{l=0}^{L_3-1}\alpha_{l,3}g_{SR}(t-jT_f\\ &\quad -(2i+1)T_s-\Delta b_i-\tau_{l,2}-\tau_{l,3})+\sqrt{\beta_{AF}}n'_{RD}(t)+n_{RD}(t)\Bigg)^2\end{aligned} \tag{6.29}$$

The signal term D_1 obtained from Z_{31} is solved below.

$$\begin{aligned}D_1 &= \beta_{AF}\sum_{j=0}^{N_f-1}\sum_{l=0}^{L_2-1}\alpha_{l,2}\sum_{l=0}^{L_3-1}\alpha_{l,3}\int_{(2i+1)T_s+jT_f+\Delta}^{(2i+1)T_s+jT_f+\Delta+T_i} g^2_{SR}(t-jT_f-(2i+1)T_s-\Delta b_i-\\ &\quad \tau_{l,2}-\tau_{l,3})dt\\ &= s_{31} = \beta_{AF}N_fE_{31}\gamma_2\gamma_3\end{aligned} \tag{6.30}$$

where, $E_{31} = \int_{(2i+1)T_s+jT_f+\Delta}^{(2i+1)T_s+jT_f+\Delta+T_i} g^2_{SR}(t-jT_f-(2i+1)T_s-\Delta b_i-\tau_{l,2}-\tau_{l,3})dt$ denotes the received signal energy component in Z_{31}. The noise variances obtained from Z_{31} are as follows:

$$\sigma^2_{N_1} = \mathbb{E}[D_2^2] = 2\beta^2_{AF}\sum_{j=0}^{N_f-1}\sum_{l=0}^{L_2-1}\alpha^2_{l,2}\sum_{l=0}^{L_3-1}\alpha^2_{l,3}\int_{(2i+1)T_s+jT_f}^{(2i+1)T_s+jT_f+T_i}\int_{(2i+1)T_s+jT_f}^{(2i+1)T_s+jT_f+T_i} g_{SR}(t-jT_f$$

$$
\begin{aligned}
& -(2i+1)T_s - \Delta b_i - \tau_{l,2} - \tau_{l,3}) g_{SR}(\tau - jT_f - (2i+1)T_s - \Delta b_i - \tau_{l,2} - \tau_{l,3}) \\
& \mathbb{E}[n'_{RD}(t) n'_{RD}(\tau)] dt d\tau \\
= \;& \beta_{AF}^2 N_f N_0 E_{31} \gamma_2 \gamma_3^2 \qquad (6.31)
\end{aligned}
$$

where, $\int_{(2i+1)T_s+jT_f+\Delta}^{(2i+1)T_s+jT_f+\Delta+T_i} \theta_2(t-\tau)d\tau = \int_{(2i+1)T_s+jT_f+\Delta}^{(2i+1)T_s+jT_f+\Delta+T_i} \frac{N_0}{2}\delta(t-\tau)d\tau = \frac{N_0}{2}$. The value of $\mathbb{E}[n'_{RD}(t)n'_{RD}(\tau)]$ is solved in Appendix B.

$$
\begin{aligned}
\sigma_{N_2}^2 = \;& \mathbb{E}[D_3^2] = 2\beta_{AF} \sum_{j=0}^{N_f-1} \sum_{l=0}^{L_2-1} \alpha_{l,2}^2 \sum_{l=0}^{L_3-1} \alpha_{l,3}^2 \int_{(2i+1)T_s+jT_f+\Delta}^{(2i+1)T_s+jT_f+\Delta+T_i} \int_{(2i+1)T_s+jT_f+\delta}^{(2i+1)T_s+jT_f+\Delta+T_i} g_{SR}(t \\
& -jT_f - (2i+1)T_s - \Delta b_i - \tau_{l,2} - \tau_{l,3}) g_{SR}(\tau - jT_f - (2i+1)T_s - \Delta b_i - \tau_{l,2} - \tau_{l,3}) \\
& \mathbb{E}[n_{RD}(t) n_{RD}(\tau)] dt d\tau \\
= \;& \beta_{AF} N_f N_0 E_{31} \gamma_2 \gamma_3 \qquad (6.32)
\end{aligned}
$$

where, $\theta_3(t-\tau) = \mathbb{E}[n_{RD}(t)n_{RD}(\tau)] = \frac{N_0}{2}\delta(t-\tau)$ and $\int_{(2i+1)T_s+jT_f}^{(2i+1)T_s+jT_f+T_i} \frac{N_0}{2}\delta(t-\tau)d\tau = \frac{N_0}{2}$.

$$
\begin{aligned}
\sigma_{N_3}^2 = \;& \mathbb{E}[D_4^2] = \sum_{j=0}^{N_f-1} \beta_{AF}^2 \int_{(2i+1)T_s+jT_f+\Delta}^{(2i+1)T_s+jT_f+\Delta+T_i} \int_{(2i+1)T_s+jT_f+\Delta}^{(2i+1)T_s+jT_f+\Delta+T_i} \mathbb{E}\left[\left\{ n'^2_{RD}(t) \right\}^2 \right] \\
& dt d\tau \\
= \;& \beta_{AF}^2 N_f \int_0^{T_i} 2\left(\gamma_3 \frac{N_0}{2}\right)^2 2W dt \\
= \;& \beta_{AF}^2 N_f N_0^2 W T_i \gamma_3^2 \qquad (6.33)
\end{aligned}
$$

Here, the value of $\mathbb{E}\left[\left\{ n'^2_{RD}(t) \right\}^2 \right] = 3\left(\gamma_3 \frac{N_0}{2}\right)^2 - \left(\gamma_3 \frac{N_0}{2}\right)^2 = 2\left(\gamma_3 \frac{N_0}{2}\right)^2$ is obtained from Appendix A and Appendix B.

$$
\begin{aligned}
\sigma_{N_4}^2 = \;& \mathbb{E}[D_5^2] = \sum_{j=0}^{N_f-1} \int_{(2i+1)T_s+jT_f+\Delta}^{(2i+1)T_s+jT_f+\Delta+T_i} \int_{(2i+1)T_s+jT_f+\Delta}^{(2i+1)T_s+jT_f+\Delta+T_i} \mathbb{E}\left[\left\{ n^2_{RD}(t) \right\}^2 \right] \\
& dt d\tau \\
= \;& N_f \int_0^{T_i} \int_{T_i-t}^{T_i} \frac{N_0^2}{2} 2W d\tau dt = N_f \int_0^{T_i} \frac{N_0^2}{2} 2W dt \\
= \;& N_f N_0^2 W T_i \qquad (6.34)
\end{aligned}
$$

Here, the value of $\mathbb{E}\left[\left\{ n^2_{RD}(t) \right\}^2 \right] = \frac{N_0^2}{2}$ is derived in Appendix A.

$$
\sigma_{N_5}^2 = \mathbb{E}[D_6^2] = 2 \sum_{j=0}^{N_f-1} \beta_{AF} \int_{(2i+1)T_s+jT_f+\Delta}^{(2i+1)T_s+jT_f+\Delta+T_i} \int_{(2i+1)T_s+jT_f+\Delta}^{(2i+1)T_s+jT_f+\Delta+T_i} \mathbb{E}[n_{RD}(t) n'_{RD}(t) n_{RD}(\tau)
$$

$$
\begin{aligned}
& n_{RD}^{'}(\tau)]dtd\tau \\
= \; & 2\beta_{AF}N_f \int_0^{T_i} \left(\frac{N_0}{2}\right)\left(\gamma_3\frac{N_0}{2}\right)2Wdt \\
= \; & \beta_{AF}N_f N_0^2 W T_i \gamma_3
\end{aligned} \tag{6.35}
$$

where, $\mathbb{E}[n_{RD}(t)n_{RD}^{'}(t)n_{RD}(\tau)n_{RD}^{'}(\tau)] = \mathbb{E}[n_{RD}(t)n_{RD}(\tau)]\,\mathbb{E}[n_{RD}^{'}(t)n_{RD}^{'}(\tau)]$. Since the noise terms correspond to different links they are independent in nature. The noise-term $Z_{noise-31}$ has a total variance of $\sigma^2_{Z_{noise-31}} = \sigma^2_{N_1} + \sigma^2_{N_2} + \sigma^2_{N_3} + \sigma^2_{N_4} + \sigma^2_{N_5} = \beta^2_{AF}N_f N_0 E_{31}\gamma_2\gamma_3^2 + \beta_{AF}N_f N_0 E_{31}\gamma_2\gamma_3 + \beta_{AF}N_f N_0^2 W T_i \gamma_3^2 + N_f N_0^2 W T_i + \beta_{AF}N_f N_0^2 W T_i \gamma_3$.

The decision statistics Z_{SD} and Z_{RD} obtained from S−D and R−D links in 1st and 2nd time slots respectively, are represented as:

$$
\begin{aligned}
Z_{SD} &= Z_{10} - Z_{11} = \overbrace{(\underbrace{s_{10}}_{signal} + \underbrace{Z_{noise-10}}_{noise-term})}^{Bit0} - \overbrace{(\underbrace{s_{11}}_{signal} + \underbrace{Z_{noise-11}}_{noise-term})}^{Bit1} \\
&= \overbrace{(\underbrace{s_{10} - s_{11}}_{sig_{SD}})}^{TotalSignal} + \overbrace{(\underbrace{Z_{noise-10} - Z_{noise-11}}_{Z_{noise-SD}})}^{TotalNoise}
\end{aligned} \tag{6.36}
$$

$$
\begin{aligned}
Z_{RD} &= Z_{30} - Z_{31} = \overbrace{(\underbrace{s_{30}}_{signal} + \underbrace{Z_{noise-30}}_{noise-term})}^{Bit0} - \overbrace{(\underbrace{s_{31}}_{signal} + \underbrace{Z_{noise-31}}_{noise-term})}^{Bit1} \\
&= \overbrace{(\underbrace{s_{30} - s_{31}}_{sig_{RD}})}^{TotalSignal} + \overbrace{(\underbrace{Z_{noise-30} - Z_{noise-31}}_{Z_{noise-RD}})}^{TotalNoise}
\end{aligned} \tag{6.37}
$$

where, Z_{10} and Z_{11} denote the decision statistics obtained from S−D link, when information bit 0 and 1 are transmitted respectively. Similarly, Z_{30} and Z_{31} represent the decision statistics obtained from R−D link, for bit 0 and 1 are transmitted respectively.

6.3.1 Linear Combining

The decision statistics Z_{SD} and Z_{RD} obtained from S−D and R−D links in 1st and 2nd time slots respectively, are linearly combined to form final decision statistic Z_{total}. Also, s_{SD} and $Z_{noise-SD}$ represent signal and noise terms obtained from S−D link respectively whereas, s_{RD} and $Z_{noise-RD}$ denote signal and noise terms obtained from R−D link respectively.

$$
\begin{aligned}
Z_{total} &= Z_{SD} + Z_{RD} = (sig_{SD} + Z_{noise-SD}) + (sig_{RD} + Z_{noise-RD}) \\
&= \underbrace{(sig_{SD} + sig_{RD})}_{s_{total-signal}} + \underbrace{(Z_{noise-SD} + Z_{noise-RD})}_{Z_{total-noise}}
\end{aligned} \tag{6.38}
$$

The total noise variance $\sigma^2_{Z_{total-noise}}$ for the noise-term $Z_{total-noise}$ is evaluated as shown below.

$$\begin{aligned}\sigma^2_{Z_{total-noise}} &= \mathbb{E}[(Z_{noise-total})^2] = \mathbb{E}[(Z_{noise-SD} + Z_{noise-RD})^2] \\ &= \mathbb{E}[Z^2_{noise-SD}] + \mathbb{E}[Z^2_{noise-RD}] + 2\,\mathbb{E}[Z_{noise-SD}Z_{noise-RD}] \\ &= \sigma^2_{Z_{noise-SD}} + \sigma^2_{Z_{noise-RD}} \end{aligned} \tag{6.39}$$

where, $\mathbb{E}[Z^2_{noise-SD}] = \sigma^2_{Z_{noise-SD}}$, $\mathbb{E}[Z^2_{noise-RD}] = \sigma^2_{Z_{noise-RD}}$ and $\mathbb{E}[Z_{noise-SD}Z_{noise-RD}] = 0$. As the noise terms from S$-$D and R$-$D link are independent, their cross-correlation is 0. The noise variances $\sigma^2_{Z_{noise-SD}}$ and $\sigma^2_{Z_{noise-RD}}$ are derived in Appendix D.

Therefore, the SNR evaluated at the destination node due to linear combining is expressed as:

$$\begin{aligned}\rho_{AF-LC} &= \left(\frac{s^2_{total-signal}}{\sigma^2_{Z_{noise-total}}}\right) = \frac{(sig_{SD} + sig_{RD})^2}{(\sigma^2_{Z_{noise-SD}} + \sigma^2_{Z_{noise-RD}})} \\ &= \left(\frac{(E_1)^2}{F_1 + G_1}\right) \end{aligned} \tag{6.40}$$

where, $F_1 = N_f N_0 \{\gamma_1(E_{10} + E_{11}) + 2N_0 WT_i\}$, $G_1 = \beta_{AF} N_f N_0 \gamma_2\gamma_3(E_{30}+E_{31}) \{1 + \beta_{AF}\gamma_3\}$ $+ 2N_f N_0^2 WT_i \{1 + \beta_{AF}\gamma_3^2 + \beta_{AF}\gamma_3\}$ and $E_1 = N_f\gamma_1(E_{10} - E_{11}) + \beta_{AF} N_f \gamma_2\gamma_3(E_{30} - E_{31})$.

The final decision statistic Z_{total} is compared to a decision threshold 0 to give the extracted information bit. PPM modulation scheme is adapted to determine this decision threshold 0. The final decision criteria $\hat{z}$ in case of linear combining is represented as:

$$\hat{z} = \begin{cases} 0, & H_0 : Z = Z_{total} = (Z_{10} - Z_{11}) + (Z_{30} - Z_{31}) > 0 \\ 1, & H_1 : Z = Z_{total} = (Z_{10} - Z_{11}) + (Z_{30} - Z_{31}) \leq 0 \end{cases} \tag{6.41}$$

The individual channel gains for S$-$D, S$-$R and R$-$D channel links may be assumed to be IID Gaussian distributed by applying Central Limit Theorem, since a large number paths are involved. Therefore, the sum of these channel gains will also have a Gaussian distribution with its mean being the sum of individual means and variance being sum of the individual variances. The joint PDF in case of linear combining is represented as:

$$\begin{aligned} f_{\rho_{AF}}(\gamma_1, \gamma_2, \gamma_3) &= \frac{1}{\sqrt{(2\pi(\sigma^2_{SD}))}} \frac{1}{\sqrt{(2\pi(\sigma^2_{SR}))}} \frac{1}{\sqrt{(2\pi(\sigma^2_{RD}))}} \exp\left[\frac{-(\gamma_1 - \mu_{SD})^2}{2\sigma^2_{SD}} + \right. \\ &\quad \left. \frac{-(\gamma_2 - \mu_{SR})^2}{2\sigma^2_{SR}} + \frac{-(\gamma_3 - \mu_{RD})^2}{2\sigma^2_{RD}}\right] \end{aligned} \tag{6.42}$$

where, μ_k and σ^2_k represent the mean and variance of channel links, while the index $k \in \{1, 2, 3\}$ refers to S$-$D, S$-$R and R$-$D link respectively, as mentioned in equation 6.1. Since the joint

PDF of channel link is IID distributed, it is given by $f_{\rho_{AF}}(\gamma_1,\gamma_2,\gamma_3) = f_{\rho_{AF}}(\gamma_1)f_{\rho_{AF}}(\gamma_2)f_{\rho_{AF}}(\gamma_3)$. Finally, the BER of UWB ED−PPM system using linear combining is expressed as:

$$\begin{aligned} BER_{LC-AF} &= \int_0^\infty\int_0^\infty\int_0^\infty Q\left(\sqrt{\frac{\rho_{AF-LC}}{2}}\right) f_{\rho_{AF}}(\gamma_1,\gamma_2,\gamma_3)d\gamma_1 d\gamma_2 d\gamma_3 \\ &= \int_0^\infty\int_0^\infty\int_0^\infty Q\left(\sqrt{\frac{\rho_{AF-LC}}{2}}\right) \frac{1}{\sqrt{(2\pi(\sigma_{SD}^2))}}\frac{1}{\sqrt{(2\pi(\sigma_{SR}^2))}}\frac{1}{\sqrt{(2\pi(\sigma_{RD}^2))}} \\ &\quad \exp\left[\frac{-(\gamma_1-\mu_{SD})^2}{2\sigma_{SD}^2}+\frac{-(\gamma_2-\mu_{SR})^2}{2\sigma_{SR}^2}+\frac{-(\gamma_3-\mu_{RD})^2}{2\sigma_{RD}^2}\right]d\gamma_1 d\gamma_2 d\gamma_3 \quad (6.43) \end{aligned}$$

$$\begin{aligned} &= \int_0^\infty\int_0^\infty\int_0^\infty Q\left(\sqrt{\frac{(E_1)^2}{2(F_1+G_1)}}\right) \frac{1}{\sqrt{(2\pi(\sigma_{SD}^2))}}\frac{1}{\sqrt{(2\pi(\sigma_{SR}^2))}}\frac{1}{\sqrt{(2\pi(\sigma_{RD}^2))}} \\ &\quad \exp\left[\frac{-(\gamma_1-\mu_{SD})^2}{2\sigma_{SD}^2}+\frac{-(\gamma_2-\mu_{SR})^2}{2\sigma_{SR}^2}+\frac{-(\gamma_3-\mu_{RD})^2}{2\sigma_{RD}^2}\right]d\gamma_1 d\gamma_2 d\gamma_3 \quad (6.44) \end{aligned}$$

6.3.2 Selective Combining

In selective combining, the SNR obtained from S−D and R−D links respectively in 1^{st} and 2^{nd} time slots, are compared and the one with the highest SNR is chosen.

The SNR obtained at the destination node from S−D and R−D links in 1st and 2nd time slot respectively, are represented as:

$$\rho_{SD-AF} = \frac{(N_f\gamma_1(E_{10}-E_{11}))^2}{N_fN_0\gamma_1(E_{10}+E_{11})+2N_fN_0^2WT_i} \quad (6.45)$$

$$\rho_{RD-AF} = \frac{M^2}{N} \quad (6.46)$$

where, $M = \beta_{AF}N_f\gamma_2\gamma_3(E_{30}-E_{31})$, $N = \beta_{AF}N_fN_0\gamma_2\gamma_3(E_{30}+E_{31})\{1+\beta_{AF}\gamma_3\}+2N_fN_0^2WT_i\{1+\beta_{AF}\gamma_3^2+\beta_{AF}\gamma_3\}$ and $E_1 = N_f\gamma_1(E_{10}-E_{11})+\beta_{AF}N_f\gamma_2\gamma_3(E_{30}-E_{31})$. The SNR obtained at destination node due to selective combining is expressed as $\rho_{AF-SC} = Max\{\rho_{SD-AF},\rho_{RD-AF}\}$. ρ_{SD-AF} and ρ_{RD-AF} refers to the SNR mentioned in equation 6.45 and 6.46, respectively. Subsequently, the BER of UWB ED−PPM system using cooperative dual−hop AF strategy with selective combining is represented as:

$$\begin{aligned} BER_{SC-AF} &= \int_0^\infty\int_0^\infty\int_0^\infty Q\left(\sqrt{\frac{\rho_{AF-SC}}{2}}\right) f_{\rho_{AF}}(\gamma_1,\gamma_2,\gamma_3)d\gamma_1 d\gamma_2 d\gamma_3 \\ &= \int_0^\infty\int_0^\infty\int_0^\infty Q\left(\sqrt{\frac{\rho_{AF-SC}}{2}}\right) \frac{1}{\sqrt{(2\pi(\sigma_{SD}^2))}}\frac{1}{\sqrt{(2\pi(\sigma_{SR}^2))}}\frac{1}{\sqrt{(2\pi(\sigma_{RD}^2))}} \\ &\quad \exp\left[\frac{-(\gamma_1-\mu_{SD})^2}{2\sigma_{SD}^2}+\frac{-(\gamma_2-\mu_{SR})^2}{2\sigma_{SR}^2}+\frac{-(\gamma_3-\mu_{RD})^2}{2\sigma_{RD}^2}\right]d\gamma_1 d\gamma_2 d\gamma_3 \quad (6.47) \end{aligned}$$

Since the joint PDF of channel link is IID distributed, it is given by $f_{\rho_{AF}}(\gamma_1, \gamma_2, \gamma_3) = f_{\rho_{AF}}(\gamma_1)$ $f_{\rho_{AF}}(\gamma_2) f_{\rho_{AF}}(\gamma_3)$. Finally, the BER of UWB ED$-$PPM system can be represented as:

$$\begin{aligned} = & \int_0^\infty \int_0^\infty \int_0^\infty Q\left(\sqrt{\frac{Max\left\{\rho_{SD}, \rho_{RD}\right\}}{2}}\right) \frac{1}{\sqrt{(2\pi(\sigma_{SD}^2))}} \frac{1}{\sqrt{(2\pi(\sigma_{SR}^2))}} \frac{1}{\sqrt{(2\pi(\sigma_{RD}^2))}} \\ & \exp\left[\frac{-(\gamma_1 - \mu_{SD})^2}{2\sigma_{SD}^2} + \frac{-(\gamma_2 - \mu_{SR})^2}{2\sigma_{SR}^2} + \frac{-(\gamma_3 - \mu_{RD})^2}{2\sigma_{RD}^2}\right] d\gamma_1 d\gamma_2 d\gamma_3 \end{aligned} \tag{6.48}$$

6.3.3 Optimum Linear Combining

The decision statistics obtained at the destination node in the 1st and 2nd time slots respectively, are optimally combined by a combining factor κ, solved in equation C.4 of Appendix C, to give a final decision statistic Z_{total}.

$$\begin{aligned} Z_{total} &= Z_{SD} + \kappa Z_{RD} = (sig_{SD} + Z_{noise-SD}) + \kappa(sig_{RD} + Z_{noise-RD}) \\ &= \underbrace{(sig_{SD} + \kappa sig_{RD})}_{s_{total-signal}} + \underbrace{(Z_{noise-SD} + \kappa Z_{noise-RD})}_{Z_{total-noise}} \end{aligned} \tag{6.49}$$

where, $s_{total-signal}$ and $Z_{total-noise}$ represent the total signal and noise component, respectively. The total noise variance $\sigma^2_{Z_{total-noise}}$ corresponding to the noise term $\sigma^2_{Z_{total-noise}}$ is evaluated as shown below.

$$\begin{aligned} \sigma^2_{Z_{total-noise}} &= \mathbb{E}[(Z_{noise-total})^2] = \mathbb{E}[(Z_{noise-SD} + \kappa Z_{noise-RD})^2] \\ &= \mathbb{E}[Z^2_{noise-SD}] + \kappa^2\, \mathbb{E}[Z^2_{noise-RD}] + 2\kappa\, \mathbb{E}[Z_{noise-SD} Z_{noise-RD}] \\ &= \sigma^2_{Z_{noise-SD}} + \kappa^2 \sigma^2_{Z_{noise-RD}} \end{aligned} \tag{6.50}$$

where, $\mathbb{E}[Z^2_{noise-SD}] = \sigma^2_{Z_{noise-SD}}$, $\mathbb{E}[Z^2_{noise-RD}] = \sigma^2_{Z_{noise-RD}}$ and $\mathbb{E}[Z_{noise-SD} Z_{noise-RD}] = 0$ because the noise terms from S$-$D and R$-$D links are independent, their cross-correlation is 0. The noise variances $\sigma^2_{Z_{noise-SD}}$ and $\sigma^2_{Z_{noise-RD}}$ are derived in Appendix D.

Therefore, the SNR calculated at the destination node due to optimum linear combining is expressed as:

$$\begin{aligned} \rho_{AF-LOC} &= \left(\frac{s^2_{total-signal}}{\sigma^2_{Z_{noise-total}}}\right) = \frac{(sig_{SD} + \kappa sig_{RD})^2}{(\sigma^2_{Z_{noise-SD}} + \kappa^2 \sigma^2_{Z_{noise-RD}})} \\ &= \left(\frac{(S)^2}{F_1 + \kappa^2 G_1}\right) \end{aligned} \tag{6.51}$$

where, $F_1 = N_f N_0 \left\{\gamma_1(E_{10} + E_{11}) + 2N_0 W T_i\right\}$, $G_1 = \beta_{AF} N_f N_0 \gamma_2 \gamma_3 (E_{30} + E_{31}) \left\{1 + \beta_{AF}\gamma_3\right\}$ $+ 2N_f N_0^2 W T_i \left\{1 + \beta_{AF}\gamma_3^2 + \beta_{AF}\gamma_3\right\}$ and $S = N_f \gamma_1 (E_{10} - E_{11}) + \kappa \beta_{AF} N_f \gamma_2 \gamma_3 (E_{30} - E_{31})$.

The final decision statistic Z_{total} is compared to a decision threshold, to obtain the information bit. PPM modulation scheme is employed to determine the decision threshold. The final decision criteria $hatz$ in case of optimum linear combining is expressed as:

$$\hat{z} = \begin{Bmatrix} 0, & H_0 : Z = Z_{total} = (Z_{10} - Z_{11}) + \kappa(Z_{30} - Z_{31}) > 0 \\ 1, & H_1 : Z = Z_{total} > (Z_{10} - Z_{11}) + \kappa(Z_{30} - Z_{31}) \leq 0 \end{Bmatrix} \tag{6.52}$$

The joint PDF in case of optimal linear combining is represented as:

$$\begin{aligned} f_{\rho_{AF}}(\gamma_1, \gamma_2, \gamma_3) &= \frac{1}{\sqrt{(2\pi(\sigma_{SD}^2))}} \frac{1}{\sqrt{(2\pi\kappa^2(\sigma_{SR}^2))}} \frac{1}{\sqrt{(2\pi\kappa^2(\sigma_{RD}^2))}} \exp\left[\frac{-(\gamma_1 - \mu_{SD})^2}{2\sigma_{SD}^2} + \right. \\ &\left. \frac{-(\gamma_2 - \mu_{SR})^2}{2\kappa^2\sigma_{SR}^2} + \frac{-(\gamma_3 - \mu_{RD})^2}{2\kappa^2\sigma_{RD}^2}\right] \end{aligned} \tag{6.53}$$

where, μ_k and σ_k^2 represent the mean and variance of channel links while the index $k \in \{1, 2, 3\}$ refers to S−D, S−R and R−D links respectively, as mentioned in equation 6.1. Since the joint PDF of channel link is IID distributed, it is represented as $f_{\rho_{AF}}(\gamma_1, \gamma_2, \gamma_3) = f_{\rho_{AF}}(\gamma_1) f_{\rho_{AF}}(\gamma_2)$ $f_{\rho_{AF}}(\gamma_3)$. Therefore, the BER of UWB ED−PPM system using optimum linear combining is expressed as:

$$\begin{aligned} BER_{LOC-AF} &= \int_0^\infty \int_0^\infty \int_0^\infty Q\left(\sqrt{\frac{\rho_{AF-LOC}}{2}}\right) f_{\rho_{AF}}(\gamma_1, \gamma_2, \gamma_3) d\gamma_1 d\gamma_2 d\gamma_3 \\ &= \int_0^\infty \int_0^\infty \int_0^\infty Q\left(\sqrt{\frac{\rho_{AF-LOC}}{2}}\right) \frac{1}{\sqrt{(2\pi(\sigma_{SD}^2))}} \frac{1}{\sqrt{(2\pi\kappa^2(\sigma_{SR}^2))}} \\ &\quad \frac{1}{\sqrt{(2\pi\kappa^2(\sigma_{RD}^2))}} \exp\left[\frac{-(\gamma_1 - \mu_{SD})^2}{2\sigma_{SD}^2} + \frac{-(\gamma_2 - \mu_{SR})^2}{2\kappa^2\sigma_{SR}^2} + \frac{-(\gamma_3 - \mu_{RD})^2}{2\kappa^2\sigma_{RD}^2}\right] \\ &\quad d\gamma_1 d\gamma_2 d\gamma_3 \end{aligned} \tag{6.54}$$

$$\begin{aligned} &= \int_0^\infty \int_0^\infty \int_0^\infty Q\left(\sqrt{\frac{(S)^2}{2(F_1 + \kappa^2 G_1)}}\right) \frac{1}{\sqrt{(2\pi(\sigma_{SD}^2))}} \frac{1}{\sqrt{(2\pi\kappa^2(\sigma_{SR}^2))}} \frac{1}{\sqrt{(2\pi\kappa^2(\sigma_{RD}^2))}} \\ &\quad \exp\left[\frac{-(\gamma_1 - \mu_{SD})^2}{2\sigma_{SD}^2} + \frac{-(\gamma_2 - \mu_{SR})^2}{2\kappa^2\sigma_{SR}^2} + \frac{-(\gamma_3 - \mu_{RD})^2}{2\kappa^2\sigma_{RD}^2}\right] d\gamma_1 d\gamma_2 d\gamma_3 \end{aligned} \tag{6.55}$$

6.4 Performance Analysis of a Cooperative DTF ED-PPM System

This section discusses the theoretical BER performance of UWB ED−PPM system, using cooperative DTF relay strategy for various diversity combining schemes. In the end of 1st time slot, the signal received at the destination as well as relay node is represented by Equation

6.4 and 6.5 respectively. The received signal $r_{SR}(t)$ obtained at the relay node, is passed through a ED$-$PPM receiver. The decision statistics Z_{SR} obtained at S$-$R link is represented as $Z_{SR} = Z_2 = Z_{20} - Z_{21}$ where, Z_{20} and Z_{21} denote the decision statistics obtained from S$-$R link due to transmission of information bit 0 and 1 respectively.

$$Z_{lm} = \sum_{j=0}^{N_f-1} \int_{2iT_s+jT_f+m\delta}^{2iT_s+jT_f+m\delta+T_i} r_l^2(t)dt \tag{6.56}$$

where, the subscripts $l \in \{1,2,3\}$ denote S$-$D, S$-$R and R$-$D link respectively and $m \in \{0,1\}$ the transmitted information bit. It is assumed that information bit $b_i = 1$ is transmitted from source node to relay as well as destination node. Therefore, the decision statistics obtained from S$-$R link is $Z_{SR} = Z_2 = Z_{21}$, since $Z_{20} = 0$.

$$\begin{aligned} Z_{21} &= \sum_{j=0}^{N_f-1} \int_{2iT_s+jT_f+\Delta}^{2iT_s+jT_f+\Delta+T_i} r_{SR}^2(t)dt \\ &= \underbrace{P_1}_{signal} + \underbrace{P_2+P_3}_{noise-term} = \underbrace{s_{21}}_{signal} + \underbrace{Z_{noise-21}}_{noise-term} \end{aligned} \tag{6.57}$$

where, $T_i = T_{mds} + T_p$ represents the integration time interval. Here, T_p and T_{mds} denotes pulse duration and multipath delay spread, respectively. The decision statistics Z_{21} may be simplified as shown below. In case of no IPI, equation 6.65 holds true.

$$\begin{aligned} Z_{21} &= \sum_{j=0}^{N_f-1} \int_{2iT_s+jT_f+\Delta}^{2iT_s+jT_f+\Delta+T_i} \left(\sum_{l=0}^{L_2-1} \alpha_{l,2} g_{SR}(t - jT_f - 2iT_s - \Delta b_i - \tau_{l,2}) + n_{SR}(t) \right)^2 \\ &= \sum_{j=0}^{N_f-1} \sum_{l=0}^{L_2-1} \alpha_{l,2}^2 \int_{2iT_s+jT_f+\delta}^{2iT_s+jT_f+\Delta+T_i} g_{SR}^2(t - jT_f - 2iT_s - \Delta b_i - \tau_{l,1})dt + 2 \sum_{j=0}^{N_f-1} \sum_{l=0}^{L_2-1} \\ &\quad \alpha_{l,2} \int_{2iT_s+jT_f+\Delta}^{2iT_s+jT_f+\Delta+T_i} g_{SR}(t - jT_f - 2iT_s - \Delta b_i - \tau_{l,2}) n_{SR}(t)dt + \sum_{j=0}^{N_f-1} \\ &\quad \int_{2iT_s+jT_f+\Delta}^{2iT_s+jT_f+\Delta+T_i} n_{SR}^2(t)dt \end{aligned} \tag{6.58}$$

where, information bit $b_i = 1$ is transmitted from the source node to relay node in 1^{st} time slot. The signal term obtained from Z_{21} is evaluated below.

$$\begin{aligned} P_1 &= \sum_{j=0}^{N_f-1} \sum_{l=0}^{L_2-1} \alpha_{l,2}^2 \int_{2iT_s+jT_f+\Delta}^{2iT_s+jT_f+\Delta+T_i} g_{SR}^2(t - jT_f - 2iT_s - \Delta - \tau_{l,2})dt \\ &= s_{11} = N_f E_{21} \gamma_2 \end{aligned} \tag{6.59}$$

where, $E_{21} = \int_{2iT_s+jT_f+\Delta}^{2iT_s+jT_f+\Delta+T_i} g_{SR}^2(t - jT_f - 2iT_s - \Delta - \tau_{l,2})dt$ denotes the received signal energy component in Z_{21}. As explained earlier in Section 6.3, since a large number of UWB multipath

channel gains are considered, channel gains can be approximated as Gaussian distributed using the Central Limit Theorem.

The noise variances are assumed to be independent of the channel under consideration and are represented as:

$$\begin{aligned}\sigma^2_{N_1} &= \mathbb{E}[P_2^2] = 2\sum_{j=0}^{N_f-1}\sum_{l=0}^{L_2-1}\alpha^2_{l,2}\int_{2iT_s+jT_f+\Delta}^{2iT_s+jT_f+\Delta+T_i}\int_{2iT_s+jT_f+\Delta}^{2iT_s+jT_f+\Delta+T_i} g_{SR}(t-jT_f-2iT_s-\Delta \\ &\quad -\tau_{l,2})g_{SR}(\tau-jT_f-2iT_s-\Delta-\tau_{l,2})\,\mathbb{E}[n_{SR}(t)n_{SR}(\tau)]dtd\tau \\ &= 2N_f\gamma_2\int_{2iT_s+jT_f+\Delta}^{2iT_s+jT_f+\Delta+T_i}\int_{2iT_s+jT_f+\Delta}^{2iT_s+jT_f+\Delta+T_i} g_{SR}(t-jT_f-2iT_s-\Delta-\tau_{l,2})g_{SR}(\tau-jT_f \\ &\quad -2iT_s-\Delta-\tau_{l,2})\theta_2(t-\tau)dtd\tau \\ &= 2N_f\gamma_2\frac{N_0}{2}\int_{2iT_s+jT_f+\Delta}^{2iT_s+jT_f+\Delta+T_i} g^2_{SR}(t-jT_f-2iT_s-\Delta-\tau_{l,2})dt \\ &= N_fN_0E_{21}\gamma_2 \end{aligned} \tag{6.60}$$

where, $\mathbb{E}[n_{SR}(t)n_{SR}(\tau)] = \theta_2(t-\tau) = \frac{N_0}{2}\delta(t-\tau)$ and $\int_{2iT_s+jT_f+\Delta}^{2iT_s+jT_f+\Delta+T_i}\frac{N_0}{2}\delta(t-\tau)d\tau = \frac{N_0}{2}$.

$$\begin{aligned}\sigma^2_{N_2} &= \mathbb{E}[P_3^2] = \sum_{j=0}^{N_f-1}\int_{2iT_s+jT_f+\Delta}^{2iT_s+jT_f+\Delta+T_i}\int_{2iT_s+jT_f+\Delta}^{2iT_s+jT_f+\Delta+T_i}\mathbb{E}\left[\left\{n^2_{SR}(t)\right\}^2\right]dtd\tau \\ &= N_f\int_0^{T_i}\int_{T_i-t}^{T_i}\frac{N_0^2}{2}dtd\tau = N_f\int_0^{T_i}\frac{N_0^2}{2}2Wdt \\ &= N_fN_0^2WT_i \end{aligned} \tag{6.61}$$

where, the value of $\mathbb{E}\left[\left\{n^2_{SR}(t)\right\}^2\right] = \frac{N_0^2}{2}$ as solved in Appendix A. The variance of $n^2_k(t)$ tends to Dirac−Delta function, where the integral vanishes outside the range $[-t, T_i - t]$. Parsevals theorem is used to solve equation 6.62. The noise term has a total variance of $\sigma^2_{Z_{noise-21}} = \sigma^2_{N_1} + \sigma^2_{N_2} = N_fN_0E_{21}\gamma_2 + N_fN_0^2WT_i$.

To extract the information bit $b_i^{'}$ at the relay node, the decision statistic Z_{SR} is compared to a decision threshold. As we have used PPM scheme, the decision threshold is taken to be 0. The decision criteria $\hat{z}$ can be expressed as:

$$b_i^{'} = \hat{z} = \begin{Bmatrix} 0, & H_0 : Z = Z_{SR} = Z_{21} > 0 \\ 1, & H_1 : Z = Z_{SR} = Z_{21} \leq 0 \end{Bmatrix} \tag{6.62}$$

The received signal $r_{SD}(t)$ obtained at the destination node in 1^{st} time slot, is detected using a ED−PPM receiver, whose decision statistics Z_{SD} obtained from S−D link is given as $Z_{SD} = Z_1 = Z_{10} - Z_{11}$ where, Z_{10} and Z_{11} represent the decision statistics obtained from

S−D link due to transmission of information bit 0 and 1 respectively. Since it is assumed that information bit $b_i = 1$ is transmitted from source node to destination node, the decision statistics obtained from S−D link is $Z_{SD} = Z_1 = Z_{11}$, as $Z_{10} = 0$.

$$\begin{aligned} Z_{11} &= \sum_{j=0}^{N_f-1} \int_{2iT_s+jT_f+\Delta}^{2iT_s+jT_f+\Delta+T_i} r_{SD}^2(t)dt \\ &= \underbrace{Q_1}_{signal} + \underbrace{Q_2 + Q_3}_{noise-term} = \underbrace{s_{11}}_{signal} + \underbrace{Z_{noise-11}}_{noise-term} \end{aligned} \tag{6.63}$$

The decision statistics Z_{11} is simplified as shown below, taking into consideration that there is no IPI.

$$\begin{aligned} Z_{11} &= \sum_{j=0}^{N_f-1} \int_{2iT_s+jT_f+\Delta}^{2iT_s+jT_f+\Delta+T_i} \left(\sum_{l=0}^{L_1-1} \alpha_{l,1} g_{SD}(t - jT_f - 2iT_s - \Delta b_i - \tau_{l,1}) + n_{SD}(t) \right)^2 \\ &= \sum_{j=0}^{N_f-1} \sum_{l=0}^{L_1-1} \alpha_{l,1}^2 \int_{2iT_s+jT_f+\Delta}^{2iT_s+jT_f+\Delta+T_i} g_{SD}^2(t - jT_f - 2iT_s - \Delta - \tau_{l,1})dt + 2 \sum_{j=0}^{N_f-1} \sum_{l=0}^{L_1-1} \alpha_{l,1} \\ &\quad \int_{2iT_s+jT_f+\Delta}^{2iT_s+jT_f+\Delta+T_i} g_{SD}(t - jT_f - 2iT_s - \Delta - \tau_{l,1}) n_{SD}(t)dt + \sum_{j=0}^{N_f-1} \int_{2iT_s+jT_f+\Delta}^{2iT_s+jT_f+\Delta+T_i} \\ &\quad n_{SD}^2(t)dt \end{aligned} \tag{6.64}$$

The signal term obtained from Z_{11} is given below.

$$\begin{aligned} Q_1 &= \sum_{j=0}^{N_f-1} \sum_{l=0}^{L_1-1} \alpha_{l,1}^2 \int_{2iT_s+jT_f+\Delta}^{2iT_s+jT_f+\Delta+T_i} g_{SD}^2(t - jT_f - 2iT_s - \Delta - \tau_{l,1})dt \\ &= s_{11} = N_f E_{11} \gamma_1 \end{aligned} \tag{6.65}$$

where, $E_{11} = \int_{2iT_s+jT_f+\Delta}^{2iT_s+jT_f+\Delta+T_i} g_{SD}^2(t - jT_f - 2iT_s - \Delta b_i - \tau_{l,1})dt$ denotes the received signal energy component in Z_{11}. As explained in Section 6.3, since a large number of UWB multipath channel gains are considered, the channel gains can be approximated as Gaussian Distributed using the Central Limit Theorem $\sum_{l_1} \alpha_{l_1}^2 = \gamma_1$. As described in Section 6.3, since the PSD $\theta_k(f)$ of noise is sufficiently flat, the autocorrelation function of noise can be approximated as $\theta_k(\tau) = \frac{N_0}{2}\delta(\tau)$[175].

As the noise variances are assumed to be independent of the channel under consideration, the variances Q_2 and Q_3 obtained from Z_{11} are as follows:

$$\begin{aligned} \sigma_{N_1}^2 &= \mathbb{E}[Q_2^2] = 2 \sum_{j=0}^{N_f-1} \sum_{l=0}^{L_1-1} \alpha_{l,1}^2 \int_{2iT_s+jT_f+\Delta}^{2iT_s+jT_f+\Delta+T_i} \int_{2iT_s+jT_f+\Delta}^{2iT_s+jT_f+\Delta+T_i} g_{SD}(t - jT_f - 2iT_s - \Delta \\ &\quad - \tau_{l,1}) g_{SD}(\tau - jT_f - 2iT_s - \Delta - \tau_{l,1}) \, \mathbb{E}[n_{SD}(t) n_{SD}(\tau)] dt d\tau \end{aligned}$$

$$
\begin{aligned}
&= 2N_f\gamma_1 \int_{2iT_s+jT_f+\Delta}^{2iT_s+jT_f+\Delta+T_i} \int_{2iT_s+jT_f+\Delta}^{2iT_s+jT_f+\Delta+T_i} g_{SD}(t-jT_f-2iT_s-\Delta-\tau_{l,1})g_{SD}(\tau-jT_f \\
&\quad -2iT_s-\Delta-\tau_{l,1})\theta_1(t-\tau)dtd\tau \\
&= 2N_f\gamma_1\frac{N_0}{2}\int_{2iT_s+jT_f+\Delta}^{2iT_s+jT_f+\Delta+T_i} g_{SD}^2(t-jT_f-2iT_s-\Delta-\tau_{l,1})dt \\
&= N_fN_0E_{10}\gamma_1 \qquad (6.66)
\end{aligned}
$$

where, $\mathbb{E}[n_{SD}(t)n_{SD}(\tau)] = \theta_1(t-\tau) = \frac{N_0}{2}\delta(t-\tau)$ and $\int_{2iT_s+jT_f+\Delta}^{2iT_s+jT_f+\Delta+T_i}\frac{N_0}{2}\delta(t-\tau)d\tau = \frac{N_0}{2}$.

$$
\begin{aligned}
\sigma_{N_2}^2 &= \mathbb{E}[Q_3^2] = \sum_{j=0}^{N_f-1}\int_{2iT_s+jT_f+\Delta}^{2iT_s+jT_f+\Delta+T_i}\int_{2iT_s+jT_f+\Delta}^{2iT_s+jT_f+\Delta+T_i}\mathbb{E}\left[\left\{n_{SD}^2(t)\right\}^2\right]dtd\tau \\
&= N_f\int_0^{T_i}\int_{T_i-t}^{T_i}\frac{N_0^2}{2}dtd\tau = N_f\int_0^{T_i}\frac{N_0^2}{2}2Wdt = N_fN_0^2WT_i \qquad (6.67)
\end{aligned}
$$

where, the value of $\mathbb{E}\left[\left\{n_{SD}^2(t)\right\}^2\right] = \frac{N_0^2}{2}$ is evaluated in Appendix A. As the variance of $n_k^2(t)$ tends to Dirac-Delta function, the integral vanishes outside the range $[-t, T_i - t]$. Parsevals theorem is applied to solve equation 6.68. The total noise variance $\sigma_{Z_{noise-11}}^2$ corresponding to noise term $Z_{noise-11}$ has a value of = $\sigma_{N_1}^2 + \sigma_{N_2}^2 = N_fN_0E_{11}\gamma_1 + N_fN_0^2WT_i$.

The SNR obtained at the relay node in 1st time slot is denoted as:

$$
\rho_{SR-DTF} = \frac{N_fE_{21}\gamma_2}{N_fN_0E_{21}\gamma_2 + N_fN_0^2WT_i} \qquad (6.68)
$$

where, information bit $b_i = 1$ is transmitted from source node to relay node. At the relay node, an error occurs if information bit $b_i^{'} = 0$ is received. Therefore, the probability of error P_e obtained at the relay node is expressed as:

$$
P_e = Q\left(\frac{\sqrt{\rho_{SR-DTF}}}{2}\right)f_{\rho_{DTF}}(\gamma_2)d\gamma_2 \qquad (6.69)
$$

where, the PDF of S−R link is expressed as $f_{\rho_{DTF}}(\gamma_2)$ = $\frac{1}{\sqrt{(2\pi(\sigma_{SR}^2))}}\exp\left[\frac{-(\gamma_2-\mu_{SR})^2}{2(\sigma_{SR}^2)}\right]$. Furthermore, μ_{SR} and σ_{SR}^2 denotes the mean and variance of S−R link of 802.15.4a UWB channel respectively.

After extraction of information bit at the relay node, signal transmitted from the relay node to the destination node in 2nd time slot is represented as:

$$
s_{RD}(t) = \sqrt{E}\sum_{i=-\infty}^{\infty}\sum_{j=0}^{N_f-1}p(t-jT_f-(2i+1)T_s-\Delta b_i^{'}) \qquad (6.70)
$$

where, the pulse signal energy is represented as $E = \int_{-\infty}^{\infty}p^2(t)dt$. The detected information bit at the relay node is denoted as $b_i^{'}$. The received signal $r_{RD}(t)$ obtained at the destination node

in 2nd time slot is represented as:

$$\begin{aligned} r_{RD}(t) &= \sqrt{E}\sum_{i=-\infty}^{\infty}\sum_{j=0}^{N_f-1} p(t-jT_f-(2i+1)T_s-\Delta b_i^{'}) * \sum_{l=0}^{L_3-1}\alpha_{l,3}\delta(t-\tau_{l,3}) + \\ & n_{RD}(t) \\ &= \sum_{l=0}^{L_3-1}\alpha_{l,3}g_{RD}(t-jT_f-(2i+1)T_s-\Delta b_i^{'}-\tau_{l,3}) + n_{RD}(t) \end{aligned} \tag{6.71}$$

The aggregate signal response $g_{RD}(t)$ at R$-$D link is expressed as $g_{RD}(t-jT_f-(2i+1)T_s-\Delta b_i^{'}-\tau_{l,3}) = \sqrt{E}\sum_{i=-\infty}^{\infty}\sum_{j=0}^{N_f-1} p(t-jT_f-(2i+1)T_s-\Delta b_i^{'}) * \delta(t-\tau_{l,3})$. The noise (AWGN) obtained from R$-$D link is given by $n_{RD}(t)$. The received signal $r_{RD}(t)$ obtained at destination node is then demodulated using a ED$-$PPM receiver, whose decision statistics Z_{RD} is represented as $Z_{RD} = Z_3 = Z_{30} - Z_{31}$ where, Z_{30} and Z_{31} denote the decision statistics obtained from R$-$D link, due to transmission of information bit 0 and 1 respectively. In case of correct detection at destination node, information bit 1 is received, when information bit 1 is forwarded from relay to destination node. Therefore, the decision statistics obtained at destination node from R$-$D link is expressed as $Z_{RD} = Z_3 = Z_{31}$, since $Z_{30} = 0$.

$$\begin{aligned} Z_{31} &= \sum_{j=0}^{N_f-1}\int_{(2i+1)T_s+jT_f+\Delta}^{(2i+1)T_s+jT_f+\Delta+T_i} r_{RD}^2(t)dt \\ &= \underbrace{R_1}_{signal} + \underbrace{R_2+R_3}_{\text{noise}-term} = \underbrace{s_{31}}_{signal} + \underbrace{Z_{noise-31}}_{\text{noise}-term} \end{aligned} \tag{6.72}$$

The decision statistics Z_{31} may be simplified as shown below. In case of no IPI, equation 6.74 holds good.

$$\begin{aligned} Z_{31} &= \sum_{j=0}^{N_f-1}\int_{(2i+1)T_s+jT_f+\Delta}^{(2i+1)T_s+jT_f+\Delta+T_i}\Bigg(\sum_{l=0}^{L_3-1}\alpha_{l,3}g_{RD}(t-jT_f-(2i+1)T_s-\Delta b_i^{'}-\tau_{l,3}) + \\ & n_{RD}(t)\Bigg)^2 \\ &= \sum_{j=0}^{N_f-1}\sum_{l=0}^{L_3-1}\alpha_{l,3}^2\int_{(2i+1)T_s+jT_f+\Delta}^{(2i+1)T_s+jT_f+\Delta+T_i} g_{RD}^2(t-jT_f-(2i+1)T_s-\Delta-\tau_{l,3})dt + 2\sum_{j=0}^{N_f-1} \\ & \sum_{l=0}^{L_3-1}\alpha_{l,3}\int_{(2i+1)T_s+jT_f+\Delta}^{(2i+1)T_s+jT_f+\Delta+T_i} g_{RD}(t-jT_f-(2i+1)T_s-\Delta-\tau_{l,3})n_{RD}(t)dt + \sum_{j=0}^{N_f-1} \\ & \int_{(2i+1)T_s+jT_f+\Delta}^{(2i+1)T_s+jT_f+\Delta+T_i} n_{RD}^2(t)dt \end{aligned} \tag{6.73}$$

where, $b_i^{'} = 1$ is the correctly detected bit transmitted from relay to destination node. The signal

component R_1 obtained from R−D link is as follows.

$$\begin{aligned} R_1 &= \sum_{j=0}^{N_f-1}\sum_{l=0}^{L_3-1}\alpha_{l,3}^2\int_{(2i+1)T_s+jT_f+\Delta}^{(2i+1)T_s+jT_f+\Delta+T_i} g_{RD}^2(t-jT_f-(2i+1)T_s-\Delta-\tau_{l,3}) \\ &\quad dt \\ &= s_{31} = N_f E_{31}\gamma_3 \end{aligned} \tag{6.74}$$

where, $E_{31} = \int_{(2i+1)T_s+jT_f+\Delta}^{(2i+1)T_s+jT_f+\Delta+T_i} g_{RD}^2(t-jT_f-(2i+1)T_s-\Delta-\tau_{l,3})dt$ denotes the received signal energy component in Z_{31}. As explained in Section 6.3, since a large number of UWB multipath channel gains are considered, the channel gains can be approximated as Gaussian Distributed using the Central Limit Theorem $\sum_{l_3}\alpha_{l_3}^2 = \gamma_3$. As described in Section 6.3, since the PSD $\theta_k(f)$ of noise is sufficiently flat, the autocorrelation function of noise can be approximated as $\theta_k(\tau) = \frac{N_0}{2}\delta(\tau)$[175].

The noise variances are assumed to be independent of the channel under consideration. Hence, the noise variances R_2 and R_3 obtained from Z_{31} are as follows:

$$\begin{aligned} \sigma_{N_1}^2 &= \mathbb{E}[R_2^2] = 2\sum_{j=0}^{N_f-1}\sum_{l=0}^{L_3-1}\alpha_{l,3}^2\int_{(2i+1)T_s+jT_f+\Delta}^{(2i+1)T_s+jT_f+\Delta+T_i}\int_{(2i+1)T_s+jT_f+\Delta}^{(2i+1)T_s+jT_f+\Delta+T_i} g_{RD}(t-jT_f \\ &\quad -(2i+1)T_s-\Delta-\tau_{l,3})g_{RD}(\tau-jT_f-(2i+1)T_s-\Delta-\tau_{l,3})\,\mathbb{E}[n_{RD}(t)n_{RD}(\tau)] \\ &\quad dtd\tau \\ &= 2N_f\gamma_3\int_{(2i+1)T_s+jT_f+\Delta}^{(2i+1)T_s+jT_f+\Delta+T_i}\int_{(2i+1)T_s+jT_f+\Delta}^{(2i+1)T_s+jT_f+\Delta+T_i} g_{RD}(t-jT_f-(2i+1)T_s-\Delta-\tau_{l,3}) \\ &\quad g_{RD}(\tau-jT_f-(2i+1)T_s-\Delta-\tau_{l,3})\theta_3(t-\tau)dtd\tau \\ &= 2N_f\gamma_3\frac{N_0}{2}\int_{(2i+1)T_s+jT_f+\Delta}^{(2i+1)T_s+jT_f+\Delta+T_i} g_{RD}^2(t-jT_f-(2i+1)T_s-\Delta-\tau_{l,3})dt \\ &= N_f N_0 E_{31}\gamma_3 \end{aligned} \tag{6.75}$$

where, $\mathbb{E}[n_{RD}(t)n_{RD}(\tau)] = \theta_3(t-\tau) = \frac{N_0}{2}\delta(t-\tau)$ and $\int_{2iT_s+jT_f+\Delta}^{2iT_s+jT_f+\Delta+T_i}\frac{N_0}{2}\delta(t-\tau)d\tau = \frac{N_0}{2}$.

$$\begin{aligned} \sigma_{N_2}^2 &= \mathbb{E}[R_3^2] = \sum_{j=0}^{N_f-1}\int_{(2i+1)T_s+jT_f+\Delta}^{(2i+1)T_s+jT_f+\Delta+T_i}\int_{(2i+1)T_s+jT_f+\Delta}^{(2i+1)T_s+jT_f+\Delta+T_i}\mathbb{E}\left[\left\{n_{RD}^2(t)\right\}^2\right] \\ &\quad dtd\tau \\ &= N_f\int_0^{T_i}\int_{T_i-t}^{T_i}\frac{N_0^2}{2}dtd\tau = N_f\int_0^{T_i}\frac{N_0^2}{2}2Wdt = N_f N_0^2 W T_i \end{aligned} \tag{6.76}$$

where, the value of $\mathbb{E}\left[\left\{n_{RD}^2(t)\right\}^2\right] = \frac{N_0^2}{2}$ is evaluated as given in equation A.2 of Appendix A. The variance of $n_k^2(t)$ tends to Dirac-Delta function, where the integral vanishes outside the range $[-t, T_i - t]$. This is solved using Parsevals theorem, as observed in equation 6.77. The

decision statistic Z_{RD} obtained at the destination node contains signal term $sig_{RD} = s_{31} = N_f E_{31}\gamma_3$ and noise term $Z_{noise-RD}$. The noise term has a total variance of $\sigma^2_{Z_{noise-RD}} = N_f N_0 E_{31}\gamma_3 + N_f N_0^2 W T_i$.

The SNR obtained at the destination node from S−D and R−D links in 1st and 2nd time slots respectively, are represented as:

$$\rho_{SD-DTF} = \frac{(N_f E_{11}\gamma_1)^2}{N_f N_0 E_{11}\gamma_1 + N_f N_0^2 W T_i} \tag{6.77}$$

$$\rho_{RD-DTF} = \frac{(N_f E_{31}\gamma_3)^2}{N_f N_0 E_{31}\gamma_3 + N_f N_0^2 W T_i} \tag{6.78}$$

where, $b_i = b_i^{'} = 1$ in case of correct detection. Thus, correctly detected information bit $b_i^{'} = 1$ is forwarded from the relay node to destination node in 2nd time slot. At destination node, the decision statistics obtained from the two time slots are combined using linear diversity combining, selective diversity combining and optimum linear diversity combining to form a final decision statistic, which is subsequently evaluated in the following section.

6.4.1 Linear Combining

i) *Correct Detection at Relay Node*: At the destination node, the decision statistics Z_{SD} and Z_{RD} obtained from S−D and R−D links in 1st and 2nd time slots respectively, are linearly combined to form $Z_{total} = Z_{SD} + Z_{RD} = s_{total-signal} + Z_{noise-total}$, as mentioned in equation 6.38. The individual decision statistics obtained from S−D and R−D links are mentioned in equation 6.36 and 6.37 respectively. The total noise variance $\sigma^2_{Z_{noise-total}} = \sigma^2_{Z_{noise-SD}} + \sigma^2_{Z_{noise-RD}}$ corresponding to the noise term $Z_{noise-total}$ is evaluated in equation 6.39.

When information bit ($b_i = 1$) is transmitted from the source node to the relay node, $b_i^{'} = 1$ is obtained at the relay node, in case of correct detection. The correctly detected bit is then forwarded to the destination node. Subsequently, the SNR obtained at destination node due to correct detection is represented as:

$$\begin{aligned}\rho_{DTF-LC-CD} &= \left(\frac{s^2_{total-signal}}{\sigma^2_{Z_{noise-total}}}\right) = \frac{(sig_{SD} + sig_{RD})^2}{(\sigma^2_{Z_{noise-SD}} + \sigma^2_{Z_{noise-RD}})} \\ &= \frac{(s_{11} + s_{31})^2}{\sigma^2_{Z_{noise-11}} + \sigma^2_{Z_{noise-31}}} \\ &= \frac{(N_f E_{11}\gamma_1 + N_f E_{31}\gamma_3)^2}{N_f N_0 E_{11}\gamma_1 + N_f N_0 E_{31}\gamma_3 + 2N_f N_0^2 W T_i}\end{aligned} \tag{6.79}$$

where, $b_i = b_i^{'} = 1$ in case of correct detection.

In order to extract the information bit, the final decision statistic Z_{total} is compared to a decision threshold 0. PPM signalling is employed to determine the decision threshold. The final decision criteria $\hat{z}$ can be expressed as:

$$\hat{z} = \begin{cases} 0, & H_0 : Z = Z_{total} = (Z_{10} - Z_{11}) + (Z_{30} - Z_{31}) > 0 \\ 1, & H_1 : Z = Z_{total} = (Z_{10} - Z_{11}) + (Z_{30} - Z_{31}) \leq 0 \end{cases} \tag{6.80}$$

ii) *Incorrect Detection at Relay Node*: In case of incorrect detection, when $b_i = 1$ is transmitted from source node to relay node, the detected bit at relay node is $b_i^{'} = 0$. The incorrectly detected bit is forwarded to the destination node in the next time slot. Thus, the SNR at the destination node due to incorrect detection is represented as:

$$\begin{aligned} \rho_{DTF-LC-ID} &= \frac{(sig_{SD})^2}{(\sigma^2_{Z_{noise-SD}} + \sigma^2_{Z_{noise-RD}})} \\ &= \frac{(s_{10})^2}{\sigma^2_{Z_{noise-10}} + \sigma^2_{Z_{noise-31}}} \\ &= \frac{(N_f E_{10}\gamma_1)^2}{N_f N_0(E_{10}\gamma_1 + E_{31}\gamma_3 + 2N_0 W T_i)} \end{aligned} \tag{6.81}$$

Using probability theory, the generalized BER in case of incorrect detection is expressed as:

$$BER = \int_0^\infty \int_0^\infty Q\left(\frac{sig_{SD} - sig_{RD}}{2\sqrt{\sigma^2_{Z_{noise-total}}}}\right) f_{\rho_{DTF}}(\gamma_1, \gamma_3) d\gamma_1 d\gamma_3 \tag{6.82}$$

When information bit 1 is transmitted from source node to relay node, due to erroneous detection at relay node, the information bit received at destination node through R−D link is 0. Therefore, $sig_{RD} = 0$.

$$= \int_0^\infty \int_0^\infty Q\left(\frac{sig_{SD}}{2\sqrt{(\sigma^2_{Z_{noise-SD}} + \sigma^2_{Z_{noise-RD}})}}\right) f_{\rho_{DTF}}(\gamma_1, \gamma_3) d\gamma_1 d\gamma_3 \tag{6.83}$$

As described earlier in Section 6.3, the individual channel gains for S−D, S−R and R−D channel links may be assumed to be IID Gaussian distributed by applying Central Limit Theorem, since a large number paths are involved. Therefore, the sum of these channel gains will also have a Gaussian distribution with its mean being the sum of individual means and variance being sum of the individual variances. The joint PDF in case of linear combining is represented as:

$$f_{\rho_{DTF}}(\gamma_1, \gamma_3) = \frac{1}{\sqrt{(2\pi(\sigma^2_{SD}))}} \frac{1}{\sqrt{(2\pi(\sigma^2_{RD}))}} \exp\left[\frac{-(\gamma_1 - \mu_{SD})^2}{2\sigma^2_{SD}} + \frac{-(\gamma_3 - \mu_{RD})^2}{2\sigma^2_{RD}}\right]$$

$$d\gamma_1 d\gamma_3 \tag{6.84}$$

The final BER of UWB ED−PPM system using linear combining is expressed as:

$$\begin{aligned} BER_{LC-DTF} &= \int_0^\infty \int_0^\infty Q\left(\sqrt{\frac{\rho_{DTF-LC-CD}}{2}}\right) f_{\rho_{DTF}}(\gamma_1,\gamma_3) d\gamma_1 d\gamma_3 \Bigg)(1-P_e) + \\ &\quad \int_0^\infty \int_0^\infty Q\left(\sqrt{\frac{\rho_{DTF-LC-ID}}{2}}\right) f_{\rho_{DTF}}(\gamma_1,\gamma_3) d\gamma_1 d\gamma_3 \Bigg)(P_e) \\ &= \int_0^\infty \int_0^\infty Q\left(\sqrt{\frac{\rho_{DTF-LC-CD}}{2}}\right) f_{\rho_{DTF}}(\gamma_1) f_{\rho_{DTF}}(\gamma_3) d\gamma_1 d\gamma_3 \Bigg)(1-P_e) + \\ &\quad \int_0^\infty \int_0^\infty Q\left(\sqrt{\frac{\rho_{DTF-LC-ID}}{2}}\right) f_{\rho_{DTF}}(\gamma_1) f_{\rho_{DTF}}(\gamma_3) d\gamma_1 d\gamma_3 \Bigg)(P_e) \end{aligned} \tag{6.85}$$

where, the value of P_e is solved in equation 6.70. Since the joint PDF is IID distributed, it can be given by $f_{\rho_{DTF}}(\gamma_1,\gamma_3) = f_{\rho_{DTF}}(\gamma_1) f_{\rho_{DTF}}(\gamma_3)$. Therefore, the BER of UWB ED−PPM system using cooperative dual−hop DTF strategy with linear combining is obtained below by replacing the value of equation 6.86 in equation 6.85.

$$\begin{aligned} &= \int_0^\infty \int_0^\infty Q\left(\sqrt{\frac{\rho_{DTF-LC-CD}}{2}}\right) \frac{1}{2\pi\sqrt{(\sigma_{SD}^2\sigma_{RD}^2)}} \exp\left[\frac{-(\gamma_1-\mu_{SD})^2}{2\sigma_{SD}^2} + \frac{-(\gamma_3-\mu_{RD})^2}{2\sigma_{RD}^2}\right] \\ &\quad d\gamma_1 d\gamma_3 \Bigg)(1-P_e) + \int_0^\infty \int_0^\infty Q\left(\sqrt{\frac{\rho_{DTF-LC-ID}}{2}}\right) \frac{1}{2\pi\sqrt{(\sigma_{SD}^2\sigma_{RD}^2)}} \exp \\ &\quad \left[\frac{-(\gamma_1-\mu_{SD})^2}{2\sigma_{SD}^2} + \frac{-(\gamma_3-\mu_{RD})^2}{2\sigma_{RD}^2}\right] d\gamma_1 d\gamma_3 \Bigg)(P_e) \end{aligned} \tag{6.86}$$

6.4.2 Selective Combining

(i) *Correct Detection at Relay Node*: In selective combining, the SNR obtained at the destination node from S−D and R−D links in 1st and 2nd time slots respectively are compared, and the one with the highest SNR is chosen. The probability of selecting the channel link based on the highest SNR is evaluated after integrating the joint PDF of the channel links with proper limits. The joint PDF of channel links S−D and R−D is represented as:

$$f(x,y) = \frac{1}{2\pi\sigma_{SD}\sigma_{RD}} \exp - \left[\frac{(x-\mu_1)^2 + (y-\mu_3)^2}{2\sigma_{SD}\sigma_{RD}}\right] \tag{6.87}$$

where, x and y represent independent gaussian random variables with means μ_{SD}, μ_{RD} and variances σ_{SD}^2, σ_{RD}^2 of S−D and R−D channel links respectively. Hence, the probability that S−D channel link is selected is represented as:

$$P_1 = f(x) = \int_{-\infty}^{\infty} \int_y^\infty f(x,y) dx dy \tag{6.88}$$

Therefore, the probability of selecting R−D channel link is $P_3 = 1 - P_1$.

ii) *Incorrect Detection at relay node*: When information bit $b_i = 1$ is transmitted from source node to relay node, due to erroneous detection at relay node, information bit $b_i^{'} = 0$ is obtained. In the next time slot, the incorrectly detected bit $b_i^{'} = 0$ is transmitted from the relay node to the destination node.

The final BER of UWB ED−PPM system using cooperative dual−hop DTF strategy with selective combining is expressed as:

$$\begin{aligned} BER_{SC-DTF} &= \left(P_1 \int_0^{\infty} Q\left(\sqrt{\frac{\rho_{SD-DTF}}{2}}\right) f_{\rho_{DTF}}(\gamma_1) d\gamma_1 + P_3 \int_0^{\infty} Q\left(\sqrt{\frac{\rho_{RD-DTF}}{2}}\right) \right. \\ &\left. f_{\rho_{DTF}}(\gamma_3) d\gamma_3\right)(1 - P_e) + \left(P_1 \int_0^{\infty} Q\left(\sqrt{\frac{\rho_{SD-DTF}}{2}}\right) f_{\rho_{DTF}}(\gamma_1) d\gamma_1 \right. \\ &\left. + P_3 \int_0^{\infty} \left(1 - Q\left(\sqrt{\frac{\rho_{RD-DTF}}{2}}\right) f_{\rho_{DTF}}(\gamma_3) d\gamma_3\right) P_e \right. \end{aligned} \tag{6.89}$$

$$\begin{aligned} &= \left(P_1 \int_0^{\infty} Q\left(\sqrt{\frac{\rho_{SD-DTF}}{2}}\right) \frac{1}{\sqrt{(2\pi(\sigma_{SD}^2))}} \exp\left[\frac{-(\gamma_1 - \mu_{SD})^2}{2\sigma_{SD}^2}\right] d\gamma_1 + P_3 \int_0^{\infty} \right. \\ &\left. Q\left(\sqrt{\frac{\rho_{RD-DTF}}{2}}\right) \frac{1}{\sqrt{(2\pi(\sigma_{RD}^2))}} \exp\left[\frac{-(\gamma_3 - \mu_{RD})^2}{2\sigma_{RD}^2}\right] d\gamma_3\right)(1 - P_e) + \left(P_1 \int_0^{\infty} \right. \\ &\left. Q\left(\sqrt{\frac{\rho_{SD-DTF}}{2}}\right) \frac{1}{\sqrt{(2\pi(\sigma_{SD}^2))}} \exp\left[\frac{-(\gamma_1 - \mu_{SD})^2}{2\sigma_{SD}^2}\right] d\gamma_1 + P_3 \int_0^{\infty} \right. \\ &\left. \left(1 - Q\left(\sqrt{\frac{\rho_{RD-DTF}}{2}}\right) \frac{1}{\sqrt{(2\pi(\sigma_{RD}^2))}} \exp\left[\frac{-(\gamma_3 - \mu_{RD})^2}{2\sigma_{RD}^2}\right] d\gamma_3\right)(P_e) \right. \end{aligned} \tag{6.90}$$

where, $f_{\rho_{DTF}}(\gamma_1) = \frac{1}{\sqrt{(2\pi(\sigma_{SD}^2))}} \exp\left[\frac{-(\gamma_1 - \mu_{SD})^2}{2\sigma_{SD}^2}\right]$ and $f_{\rho_{DTF}}(\gamma_3) = \frac{1}{\sqrt{(2\pi(\sigma_{RD}^2))}} \exp\left[\frac{-(\gamma_3 - \mu_{RD})^2}{2\sigma_{RD}^2}\right]$ represent the PDF of S−D and R−D channel links respectively.

6.4.3 Optimum Linear Combining

(i) *Correct Detection at Relay Node*: At the destination node, the decision statistics obtained from the destination node in 1st and 2nd time slots respectively, are optimally combined to give final decision statistic $Z_{total} = Z_{SD} + \kappa Z_{RD}$. The optimal combining factor κ has a value of $\kappa = \frac{(\sigma^2_{Z_{noise-SD}})s_{RD}}{(\sigma^2_{Z_{noise-RD}})s_{SD}}$, as solved in equation C.4 of Appendix C. The final decision statistic Z_{total} obtained at the destination node using optimum linear combining is represented by equation 6.50. To solving the noise term $Z_{noise-total}$, we evaluate its variance, which is already obtained in equation 6.51.

The SNR at the destination node due to optimum linear combining is expressed as:

$$\begin{aligned}\rho_{DTF-LOC-CD} &= \left(\frac{s^2_{total-signal}}{\sigma^2_{Z_{noise-total}}}\right) \\ &= \left(\frac{(sig_{SD}+\kappa sig_{RD})^2}{\sigma^2_{Z_{noise-SD}}+\kappa^2\sigma^2_{Z_{noise-RD}}}\right) \\ &= \frac{(s_{11}+\kappa s_{31})^2}{\sigma^2_{Z_{noise-11}}+\kappa^2\sigma^2_{Z_{noise-31}}} \\ &= \frac{(N_f E_{11}\gamma_1+\kappa N_f E_{31}\gamma_3)^2}{N_f N_0(E_{11}\gamma_1+N_0WT_i)+\kappa^2 N_f N_0(E_{31}\gamma_3+N_0WT_i)}\end{aligned} \tag{6.91}$$

Also, $b_i = b_i^{'} = 1$ in case of correct detection.

In order to extract the information bit, the final decision statistic is compared to a decision threshold, which is decided on the basis of PPM modulation scheme. The final decision criteria $\hat{z}$ can be expressed as:

$$\hat{z} = \begin{Bmatrix} 0, & H_0 : Z = Z_{total} = (Z_{10}-Z_{11})+\kappa(Z_{30}-Z_{31}) \leq 0 \\ 1, & H_1 : Z = Z_{total} = (Z_{10}-Z_{11})+\kappa(Z_{30}-Z_{31}) > 0 \end{Bmatrix} \tag{6.92}$$

ii) *Incorrect Detection at Relay Node*: In case of erroneous detection, $b_i^{'} = 0$ is detected at the relay node, when $b_i = 1$ is transmitted from source to relay node. Further, this incorrectly detected bit is forwarded from the relay node to destination node, leading to BER degradation. Therefore, the SNR at the destination node due to incorrect detection is represented as:

$$\begin{aligned}\rho_{DTF-LOC-ID} &= \frac{(sig_{SD})^2}{(\sigma^2_{Z_{noise-SD}}+\kappa^2\sigma^2_{Z_{noise-RD}})} \\ &= \frac{(s_{10})^2}{\sigma^2_{Z_{noise-10}}+\kappa^2\sigma^2_{Z_{noise-31}}} \\ &= \frac{(N_f E_{10}\gamma_1)^2}{N_f N_0(E_{10}\gamma_1+N_0WT_i)+\kappa^2 N_f N_0(E_{31}\gamma_3+N_0WT_i)}\end{aligned} \tag{6.93}$$

The BER in case of incorrect detection can be expressed as:

$$BER = \int_0^\infty \int_0^\infty Q\left(\frac{sig_{SD}-\kappa sig_{RD}}{2\sqrt{\sigma^2_{Z_{noise-total}}}}\right) f_{\rho_{DTF}}(\gamma_1,\gamma_3)d\gamma_1 d\gamma_3 \tag{6.94}$$

Due to incorrect detection at relay node, the information bit received at destination node from R$-$D link is 0, when information bit 1 is transmitted from source node to relay node. Thus, $sig_{RD} = 0$.

$$= \int_0^\infty \int_0^\infty Q\left(\frac{sig_{SD}}{2\sqrt{(\sigma^2_{Z_{noise-SD}}+\kappa^2\sigma^2_{Z_{noise-RD}})}}\right) f_{\rho_{DTF}}(\gamma_1,\gamma_3)d\gamma_1 d\gamma_3 \tag{6.95}$$

The BER at the destination node using optimum linear combining can be expressed as:

$$\begin{aligned} BER_{LOC-DTF} &= \int_0^\infty \int_0^\infty Q\left(\sqrt{\frac{\rho_{DTF-LOC-CD}}{2}}\right) f_{\rho_{DTF}}(\gamma_1,\gamma_3) d\gamma_1 d\gamma_3 \Bigg)(1-P_e) + \\ &\quad \int_0^\infty \int_0^\infty Q\left(\sqrt{\frac{\rho_{DTF-LOC-ID}}{2}}\right) f_{\rho_{DTF}}(\gamma_1,\gamma_3) d\gamma_1 d\gamma_3 \Bigg)(P_e) \\ &= \int_0^\infty \int_0^\infty Q\left(\sqrt{\frac{\rho_{DTF-LOC-CD}}{2}}\right) f_{\rho_{DTF}}(\gamma_1) f_{\rho_{DTF}}(\gamma_3) d\gamma_1 d\gamma_3 \Bigg) \\ &\quad (1-P_e) + \int_0^\infty \int_0^\infty Q\left(\sqrt{\frac{\rho_{DTF-LOC-ID}}{2}}\right) f_{\rho_{DTF}}(\gamma_1) f_{\rho_{DTF}}(\gamma_3) \\ &\quad d\gamma_1 d\gamma_3 \Bigg)(P_e) \end{aligned} \tag{6.96}$$

where, $f_{\rho_{DTF}}(\gamma_1,\gamma_3) = f_{\rho_{DTF}}(\gamma_1) f_{\rho_{DTF}}(\gamma_3)$ because the channel gains are IID Gaussian distributed. Also, P_e is obtained from equation 6.70. The joint PDF in case of optimum linear combining is expressed as:

$$\begin{aligned} f_{\rho_{DTF}}(\gamma_1,\gamma_3) &= \frac{1}{\sqrt{(2\pi\sigma_{SD}^2)}} \frac{1}{\sqrt{(2\pi\kappa^2\sigma_{RD}^2)}} \exp\left[\frac{-(\gamma_1-\mu_{SD})^2}{2\sigma_{SD}^2} + \frac{-(\gamma_3-\mu_{RD})^2}{2\kappa^2\sigma_{RD}^2}\right] \\ &\quad d\gamma_1 d\gamma_3 \end{aligned} \tag{6.97}$$

Replacing the value of equation 6.99 in equation 6.98, we obtain the final BER, as observed in equation 6.100. Finally, the BER of UWB ED−PPM system using cooperative dual−hop DTF strategy with optimum linear diversity combining is expressed as:

$$\begin{aligned} BER_{LOC-DTF} &= \int_0^\infty \int_0^\infty Q\left(\sqrt{\frac{\rho_{DTF-LOC-CD}}{2}}\right) \frac{1}{2\pi\sqrt{\sigma_{SD}^2\kappa^2\sigma_{RD}^2}} \exp\left[\frac{-(\gamma_1-\mu_{SD})^2}{2\sigma_{SD}^2} + \right. \\ &\quad \left. \frac{-(\gamma_3-\mu_{RD})^2}{2\kappa^2\sigma_{RD}^2}\right] d\gamma_1 d\gamma_3 \Bigg)(1-P_e) + \int_0^\infty \int_0^\infty Q\left(\sqrt{\frac{\rho_{DTF-LOC-ID}}{2}}\right) \\ &\quad \frac{1}{2\pi\sqrt{\sigma_{SD}^2\kappa^2\sigma_{RD}^2}} \exp\left[\frac{-(\gamma_1-\mu_{SD})^2}{2\sigma_{SD}^2} + \frac{-(\gamma_3-\mu_{RD})^2}{2\kappa^2\sigma_{RD}^2}\right] d\gamma_1 d\gamma_3 \Bigg) \\ &\quad (P_e) \end{aligned} \tag{6.98}$$

6.5 Simulation Results

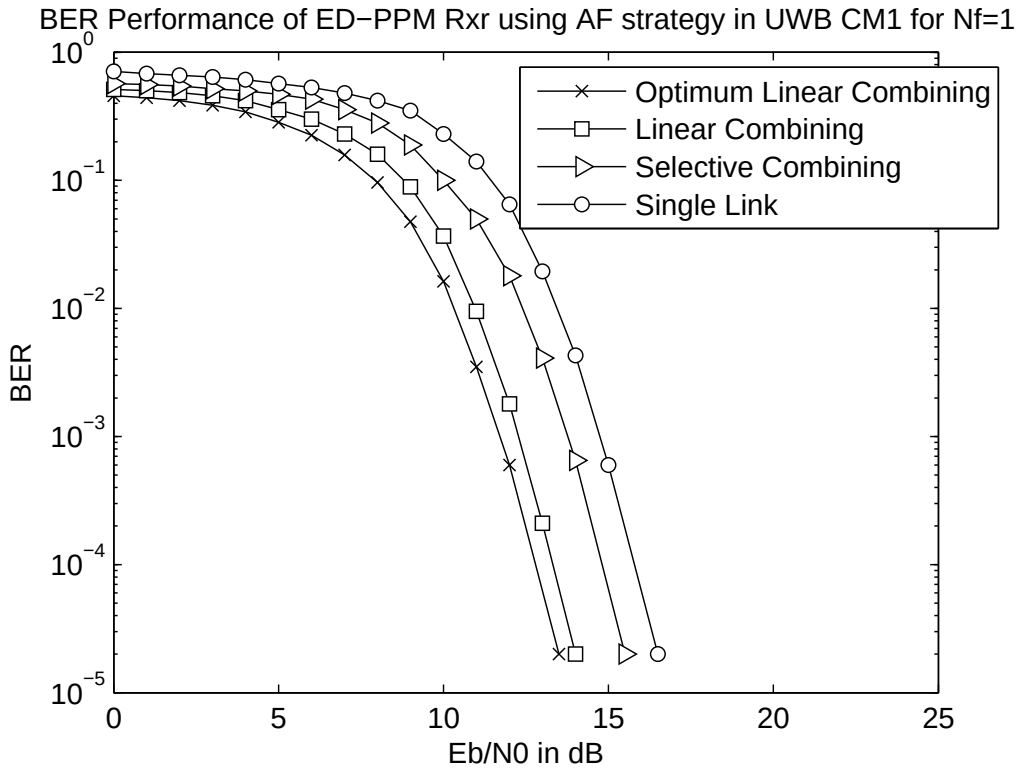

(a)

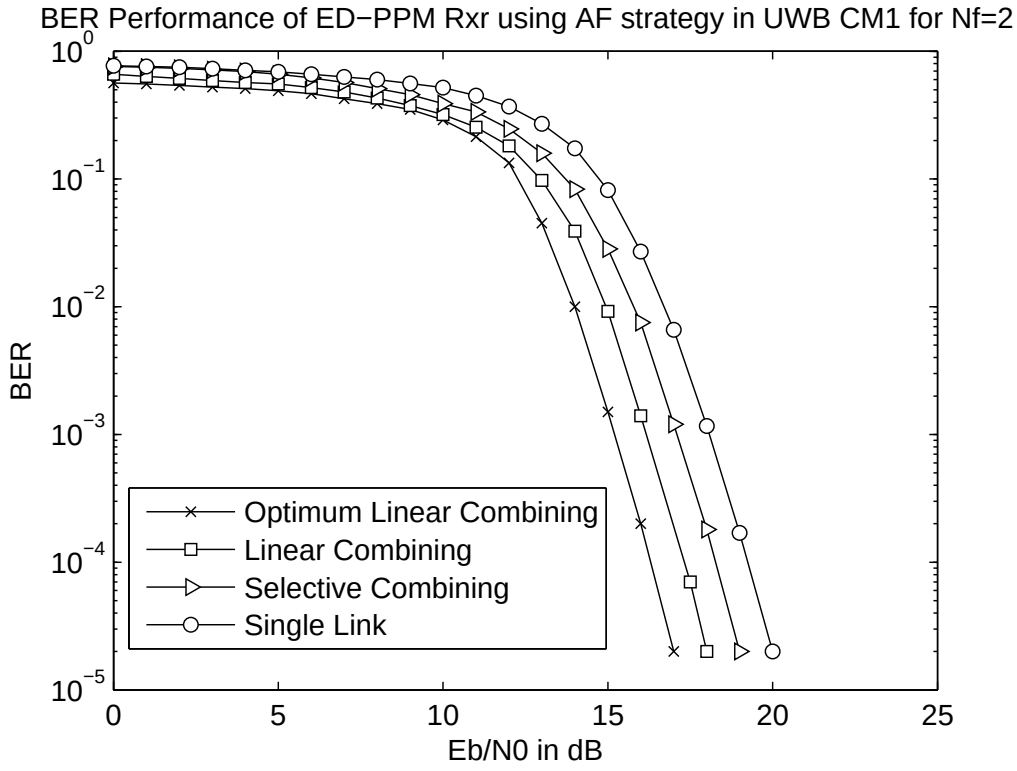

(b)

Figure 6.2: BER performance of UWB ED−PPM system using cooperative AF strategy with various combining schemes in CM1 channel for (a) $N_f = 1$ (b) $N_f = 2$

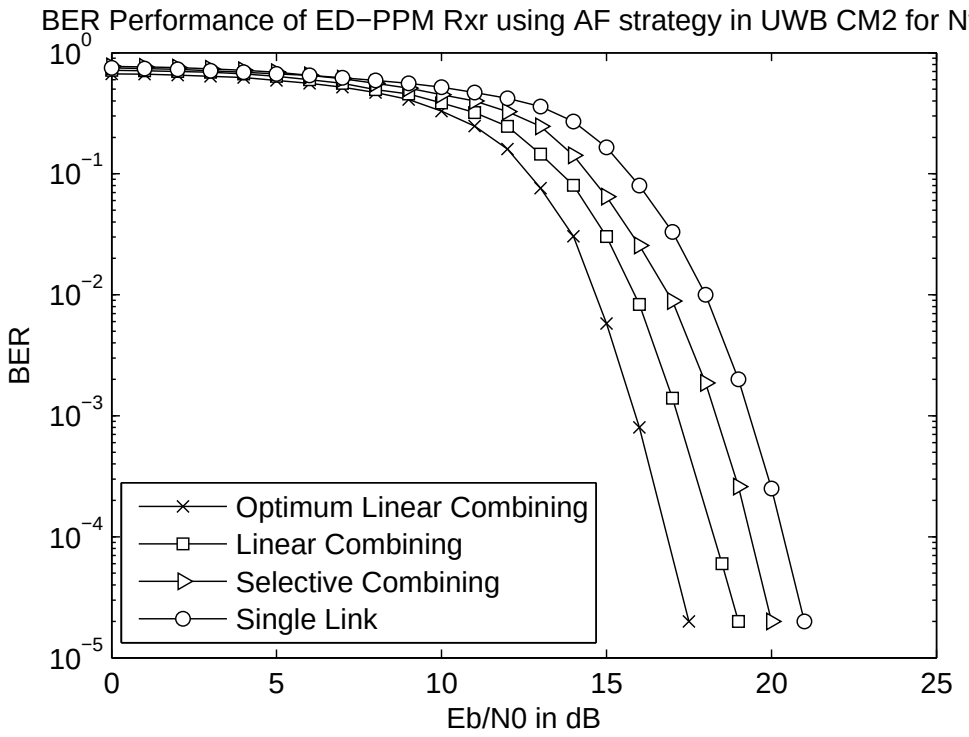

(a)

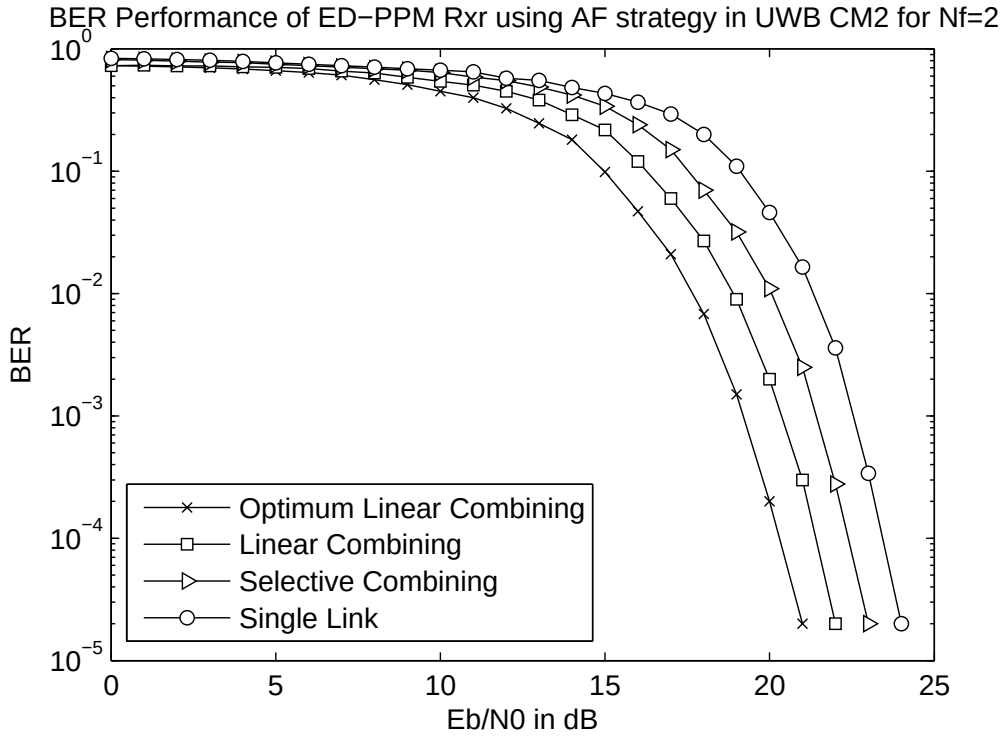

(b)

Figure 6.3: BER performance of UWB ED−PPM system using cooperative AF strategy with various combining schemes in CM2 channel for (a) $N_f = 1$ (b) $N_f = 2$

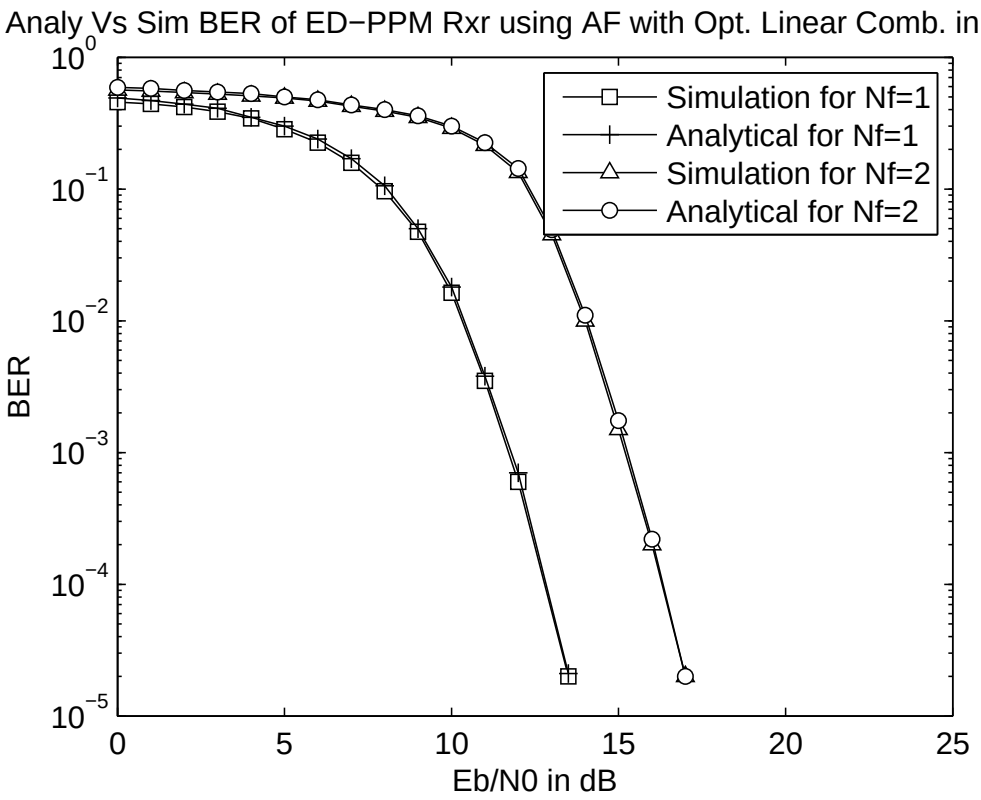
Analy Vs Sim BER of ED−PPM Rxr using AF with Opt. Linear Comb. in CM1
Simulation for Nf=1
Analytical for Nf=1
Simulation for Nf=2
Analytical for Nf=2
BER
Eb/N0 in dB

(a)

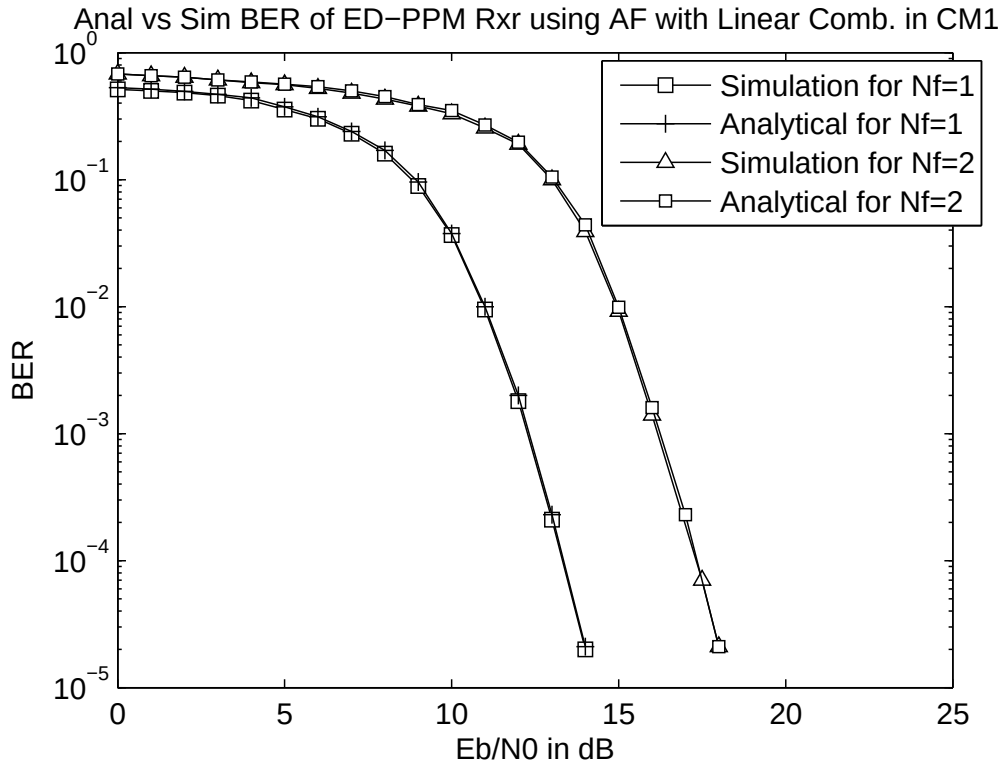
Anal vs Sim BER of ED−PPM Rxr using AF with Linear Comb. in CM1
Simulation for Nf=1
Analytical for Nf=1
Simulation for Nf=2
Analytical for Nf=2
BER
Eb/N0 in dB

(b)

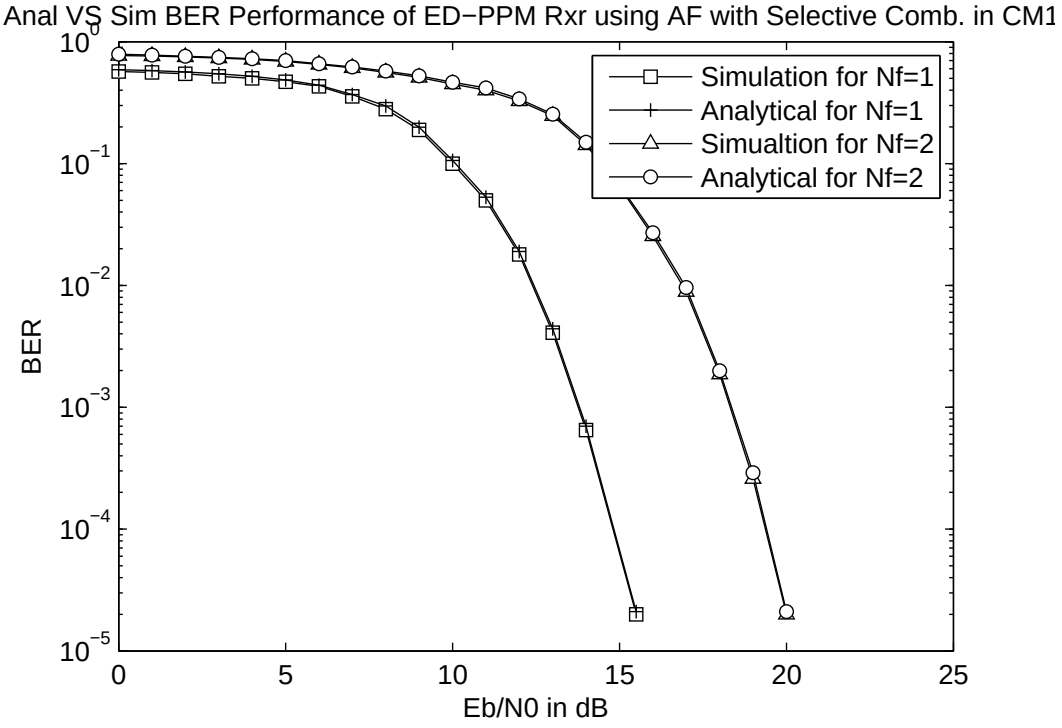

(c)

Figure 6.4: Analytic vs Simulated BER performance comparison of UWB ED−PPM system using AF strategy in CM1 channel having $N_f = 1, 2$ for various combining schemes namely (a) Optimum Linear Combining (b) Linear Combining (c) Selective Combining

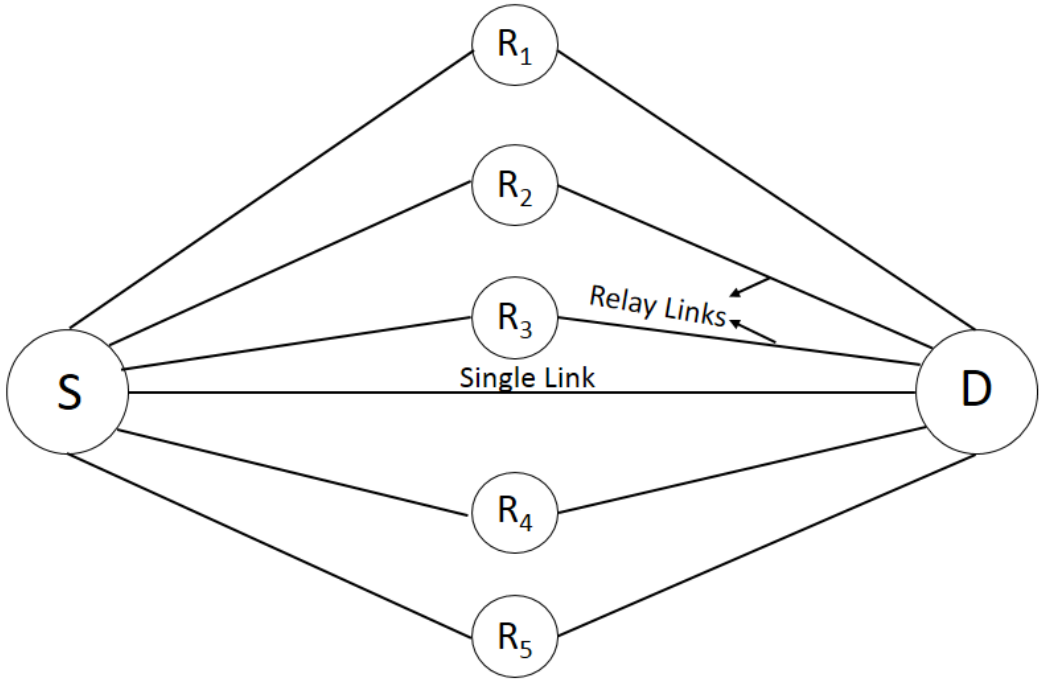

(a)

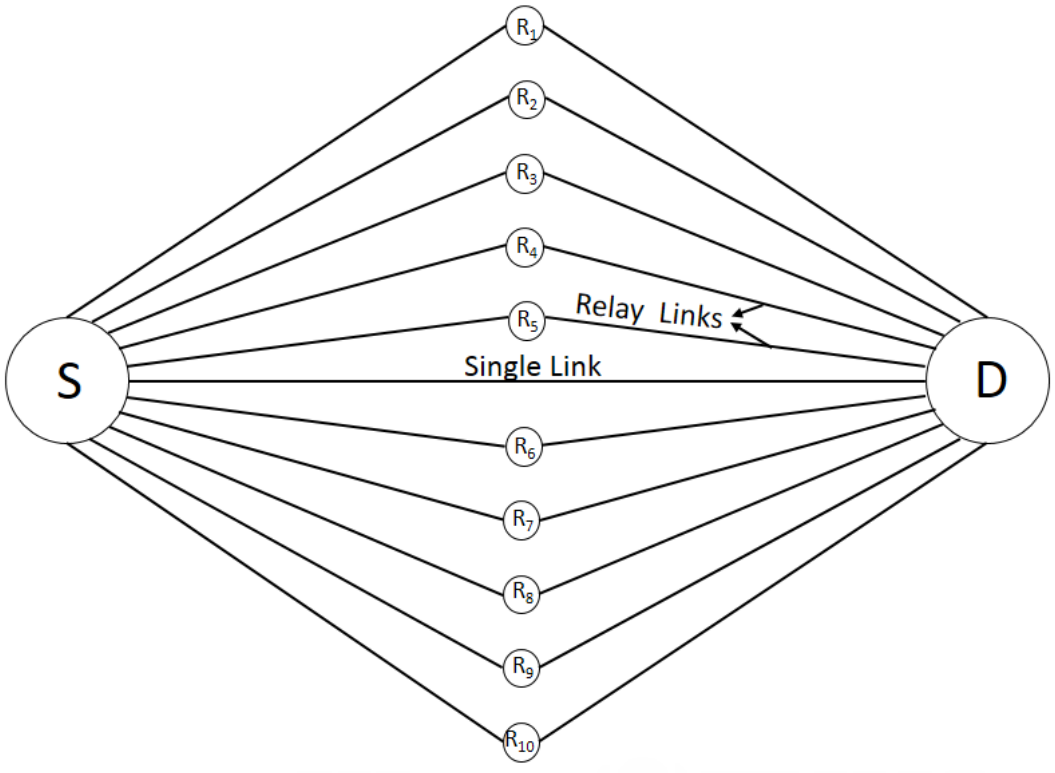

(b)

Figure 6.5: Dual−Hop Cooperative System Model with single−link and (a) L=5 relay paths (b) L=10 relay paths

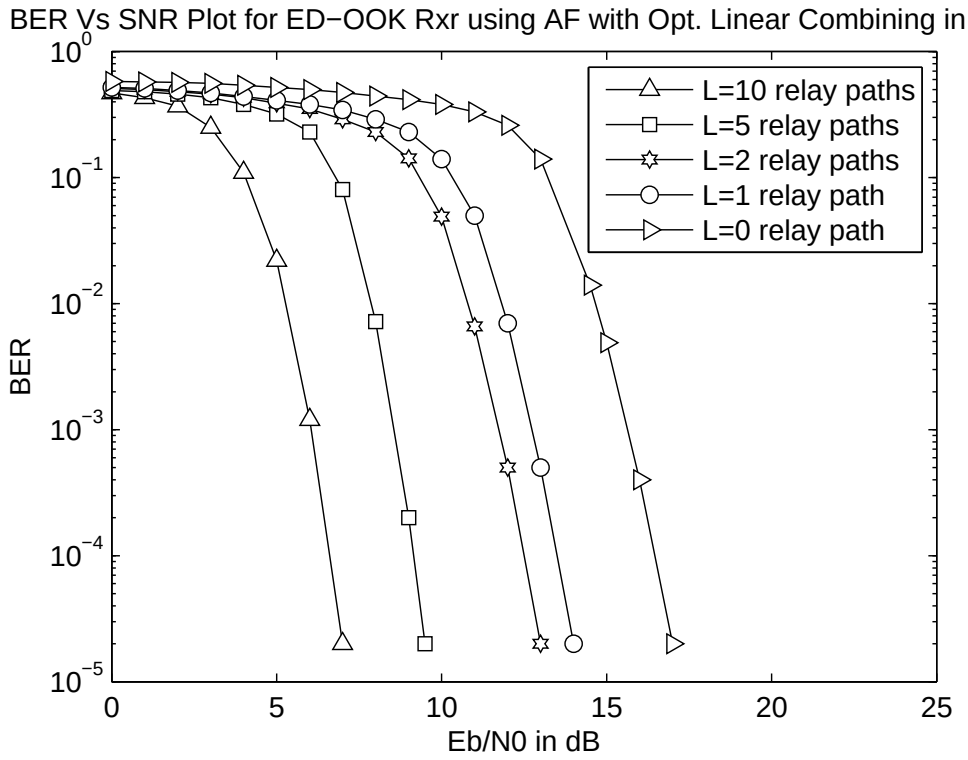
BER Vs SNR Plot for ED−OOK Rxr using AF with Opt. Linear Combining in CM1
BER
Eb/N0 in dB
L=10 relay paths
L=5 relay paths
L=2 relay paths
L=1 relay path
L=0 relay path

(a)

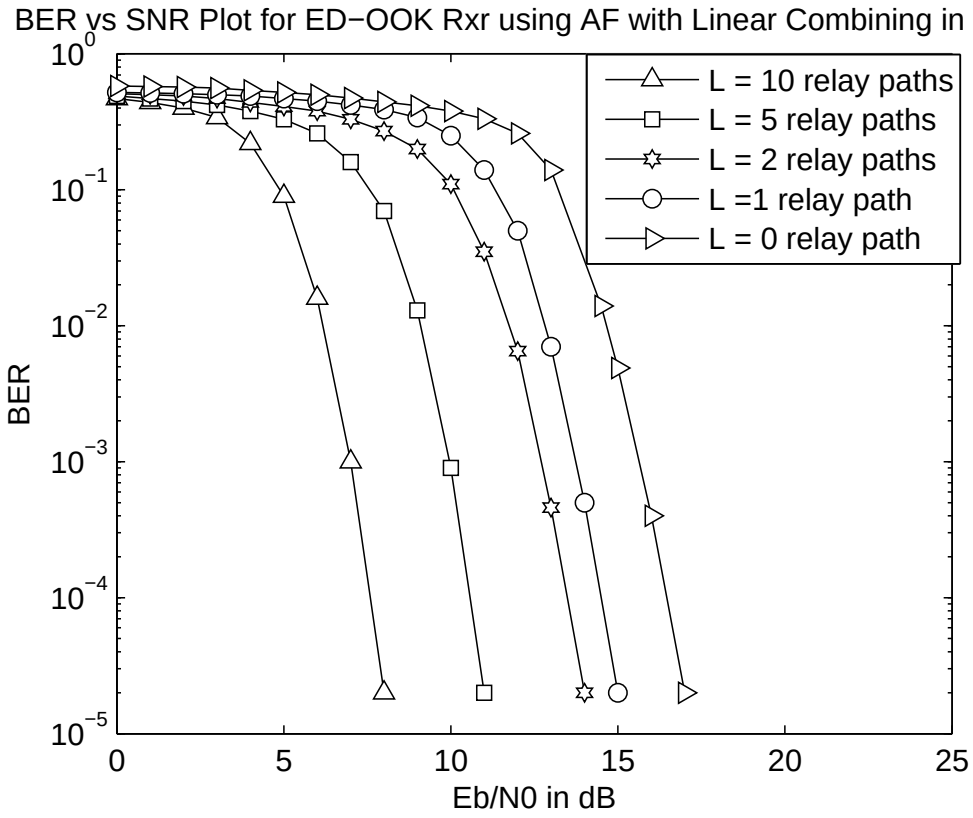
BER vs SNR Plot for ED−OOK Rxr using AF with Linear Combining in CM1
BER
Eb/N0 in dB
L = 10 relay paths
L = 5 relay paths
L = 2 relay paths
L =1 relay path
L = 0 relay path

(b)

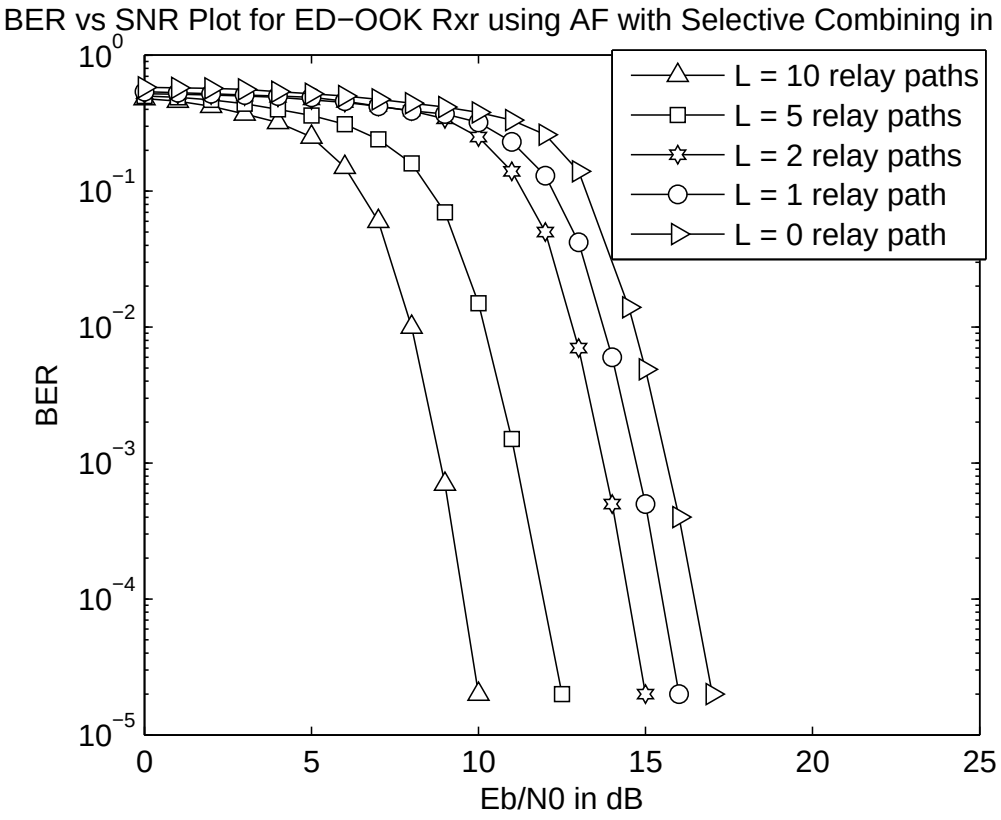

(c)

Figure 6.6: BER performance of UWB ED−PPM system using dual-hop cooperative AF strategy in CM1 channel with (a) Optimum Linear Diversity Combining for $L = 0, 1, 2, 5, 10$ relay paths (b) Linear Diversity Combining for $L = 0, 1, 2, 5, 10$ relay paths and (c) Selective Diversity Combining for $L = 0, 1, 2, 5, 10$ relay paths

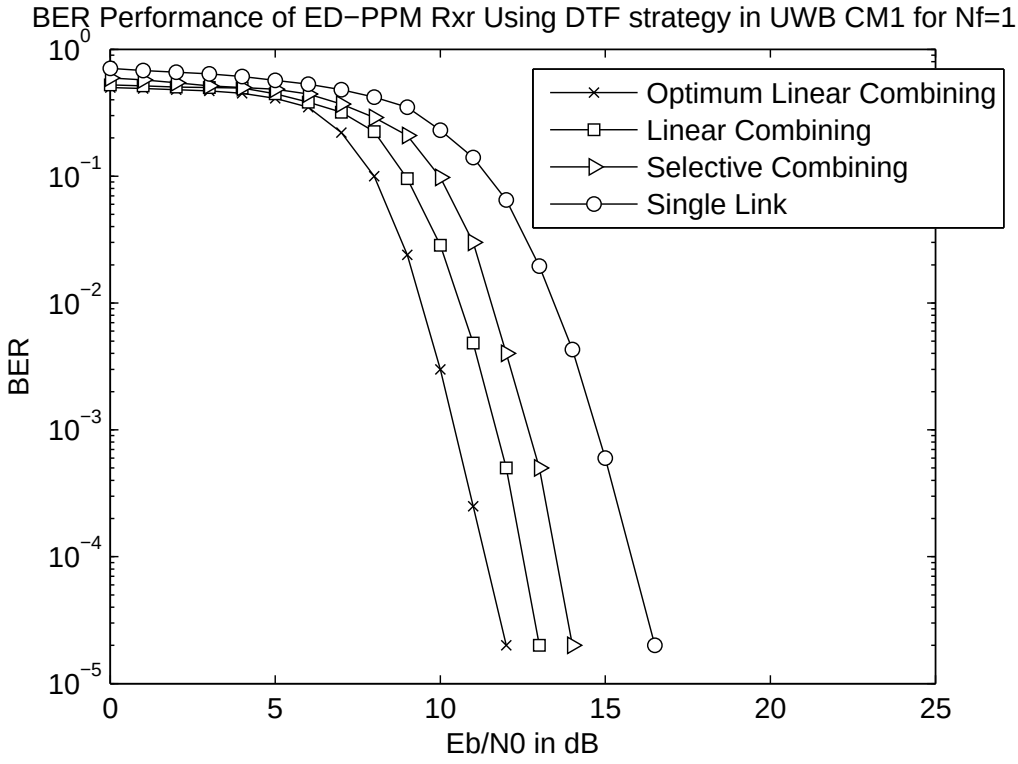

(a)

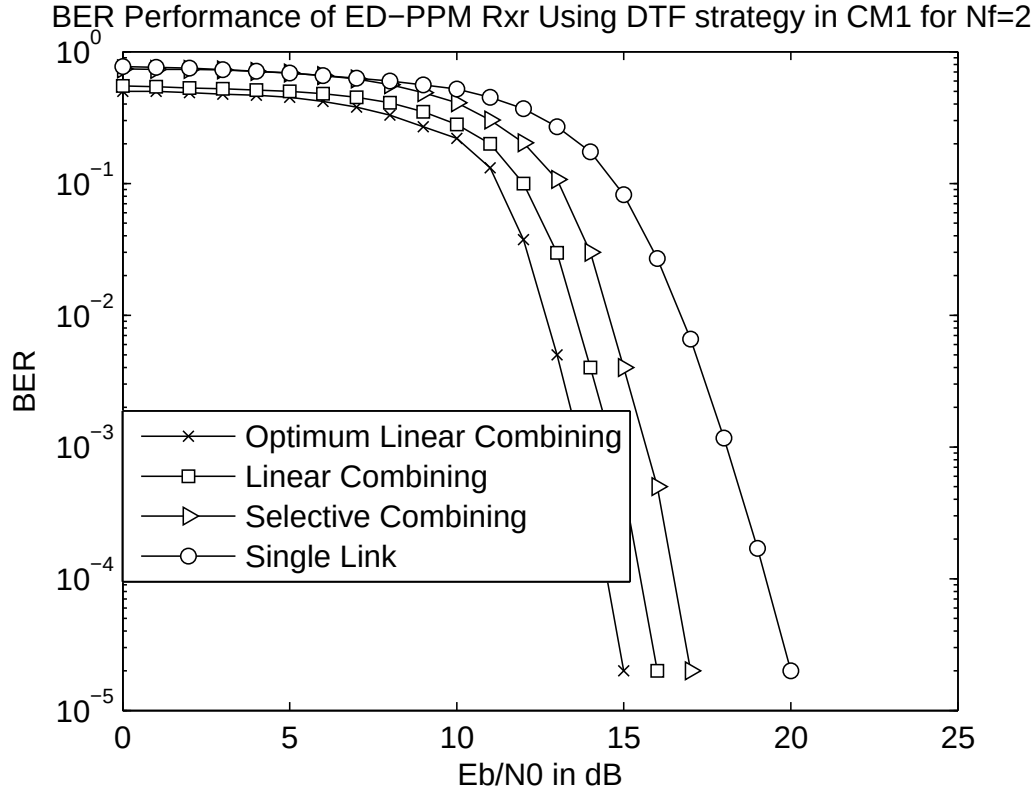

(b)

Figure 6.7: BER performance of UWB ED−PPM system using cooperative DTF strategy with various combining schemes in CM1 channel for (a) $N_f = 1$ (b) $N_f = 2$

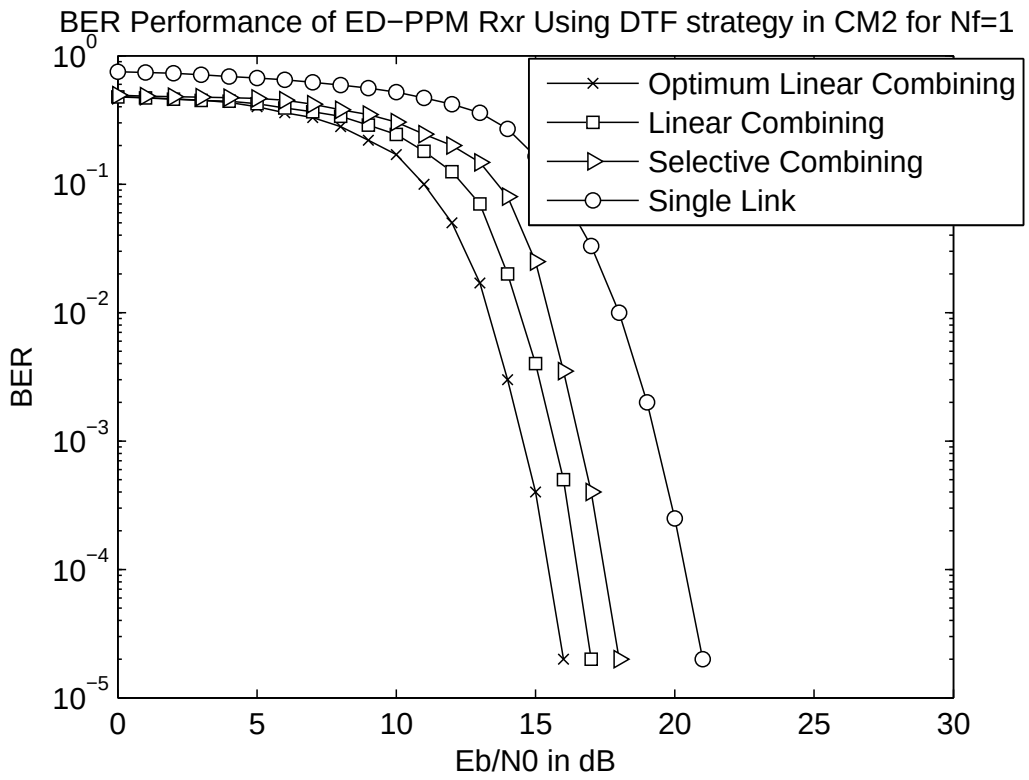

(a)

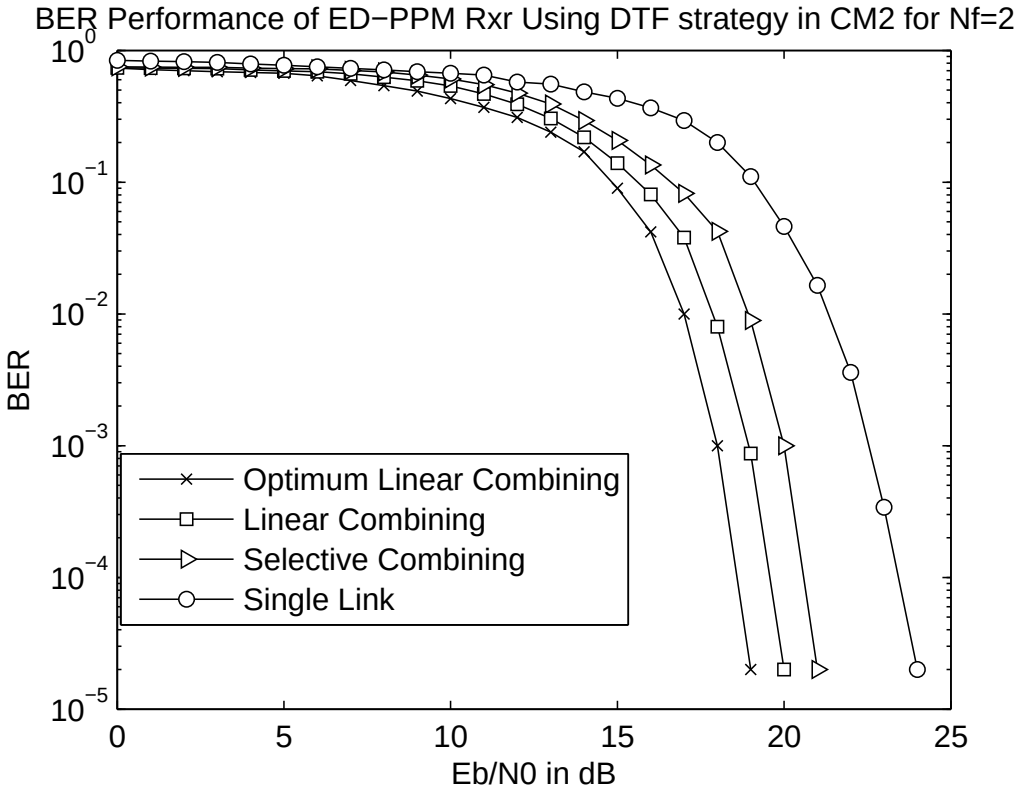

(b)

Figure 6.8: BER performance of UWB ED−PPM system using cooperative DTF strategy with various combining schemes in CM2 channel for (a) $N_f = 1$ (b) $N_f = 2$

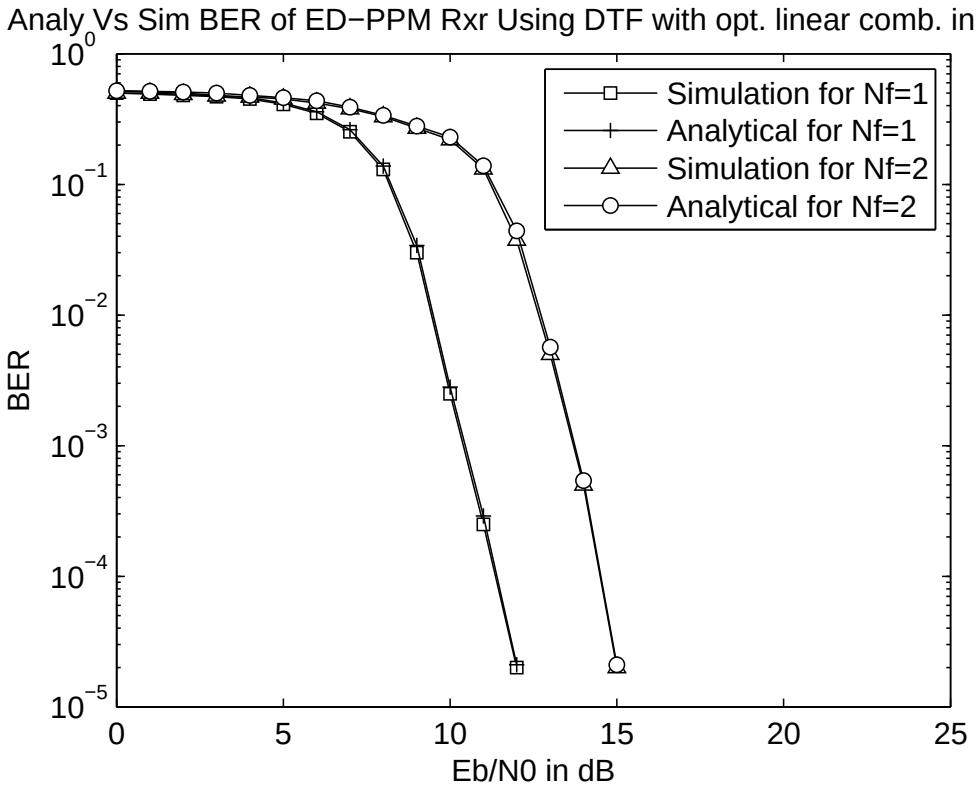
Analy Vs Sim BER of ED−PPM Rxr Using DTF with opt. linear comb. in CM1
BER
Eb/N0 in dB
Simulation for Nf=1
Analytical for Nf=1
Simulation for Nf=2
Analytical for Nf=2

(a)

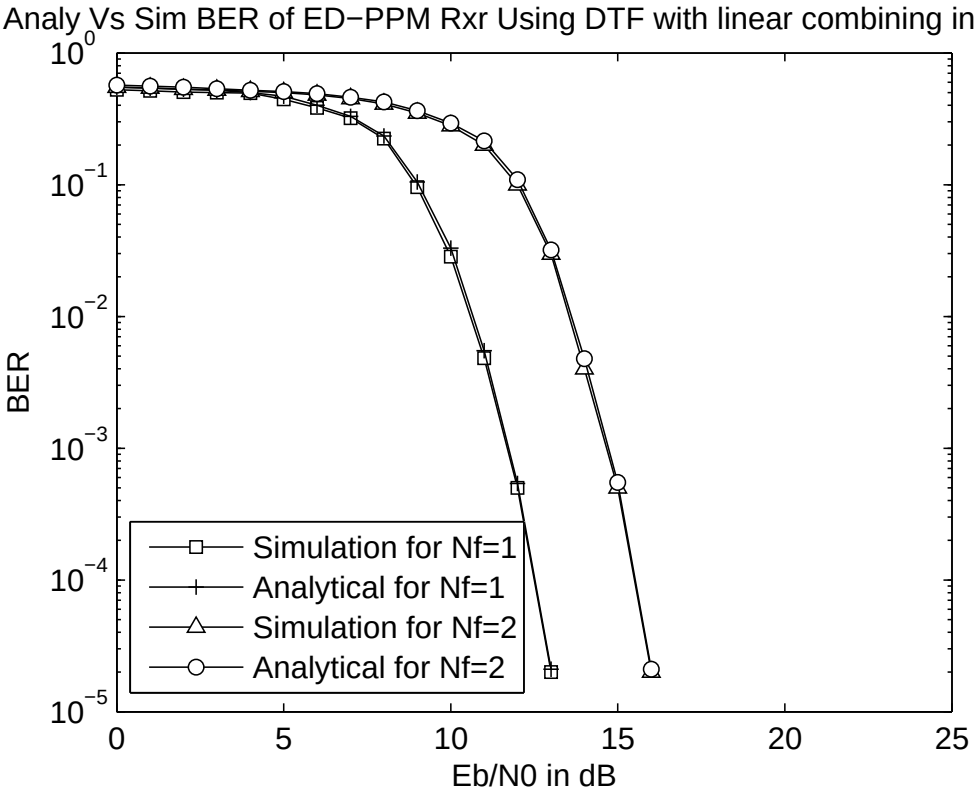
Analy Vs Sim BER of ED−PPM Rxr Using DTF with linear combining in CM1
BER
Eb/N0 in dB
Simulation for Nf=1
Analytical for Nf=1
Simulation for Nf=2
Analytical for Nf=2

(b)

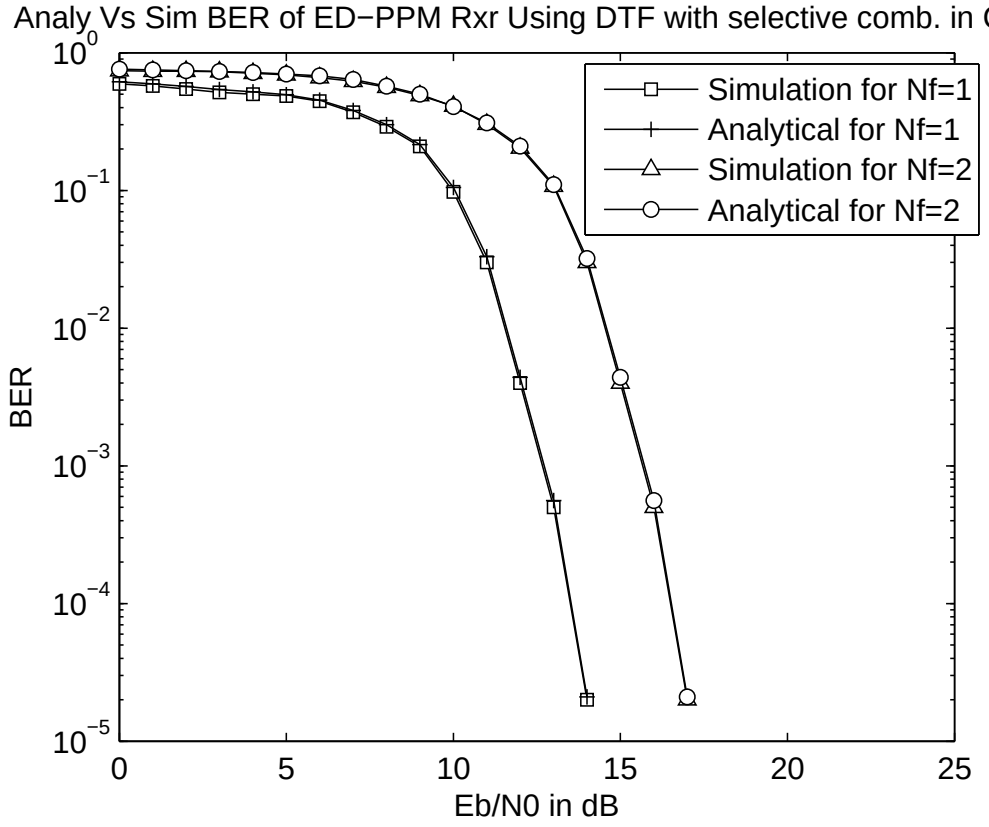

(c)

Figure 6.9: Analytic vs Simulated BER performance comparison of UWB ED−PPM system using DTF strategy in CM1 channel having $N_f = 1, 2$ for various combining schemes namely (a) Optimum Linear Combining (b) Linear Combining (c) Selective Combining

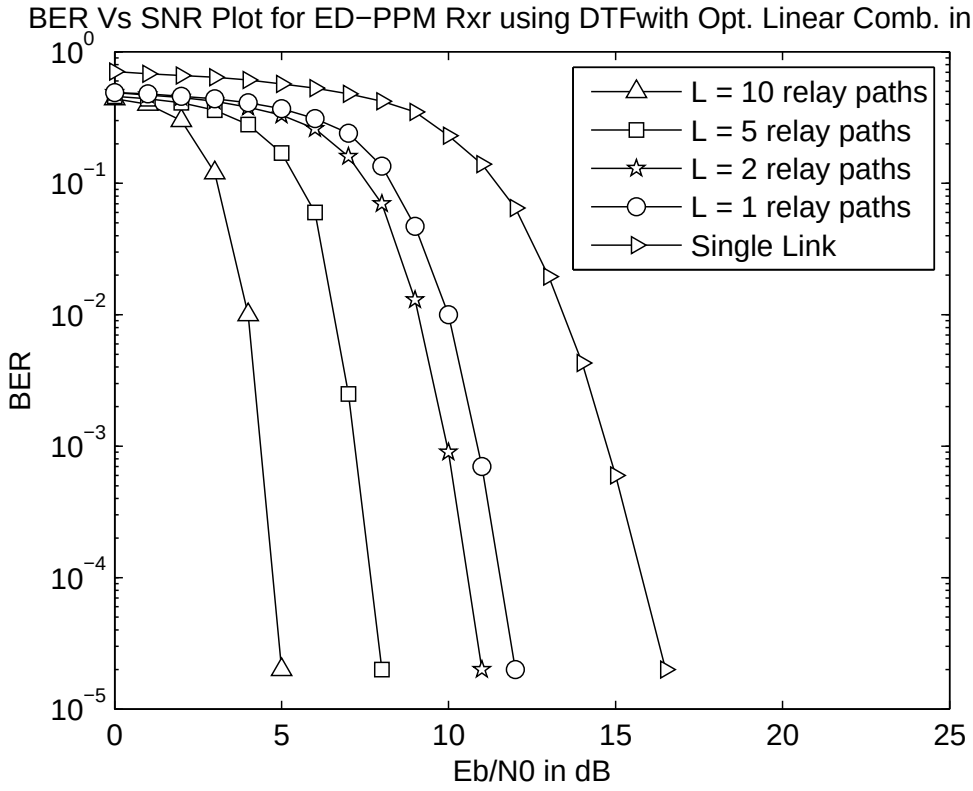
BER Vs SNR Plot for ED−PPM Rxr using DTFwith Opt. Linear Comb. in CM1
BER
Eb/N0 in dB
L = 10 relay paths
L = 5 relay paths
L = 2 relay paths
L = 1 relay paths
Single Link

(a)

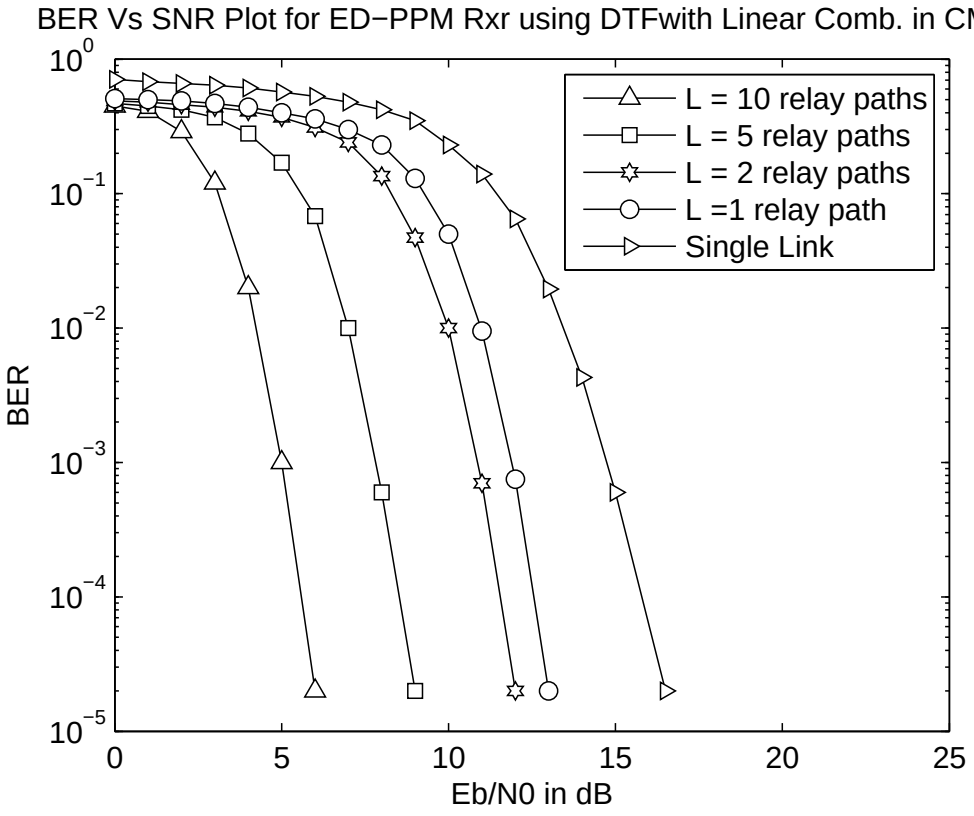
BER Vs SNR Plot for ED−PPM Rxr using DTFwith Linear Comb. in CM1
BER
Eb/N0 in dB
L = 10 relay paths
L = 5 relay paths
L = 2 relay paths
L =1 relay path
Single Link

(b)

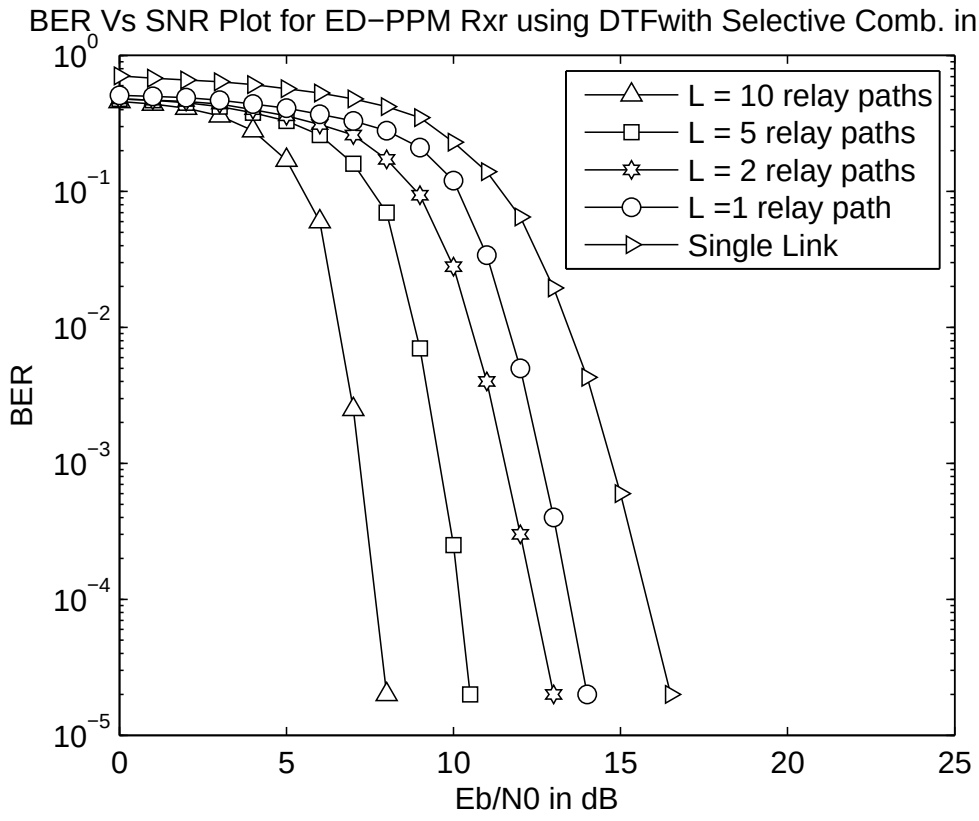

(c)

Figure 6.10: BER performance of UWB ED−PPM system using dual−hop Cooperative DTF strategy in CM1 channel with (a) Optimum Linear Diversity Combining for $L = 0, 1, 2, 5, 10$ relay paths (b) Linear Diversity Combining for $L = 0, 1, 2, 5, 10$ relay paths and (c) Selective Diversity Combining for $L = 0, 1, 2, 5, 10$ relay paths

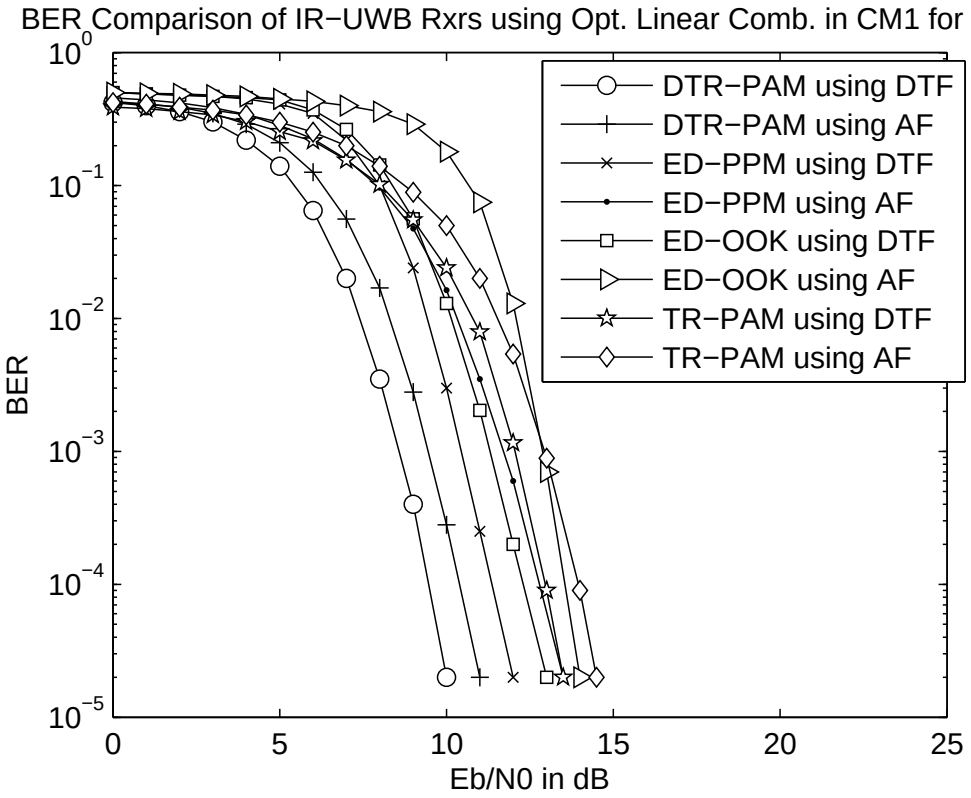
BER Comparison of IR−UWB Rxrs using Opt. Linear Comb. in CM1 for Nf=1
BER
Eb/N0 in dB
DTR−PAM using DTF
DTR−PAM using AF
ED−PPM using DTF
ED−PPM using AF
ED−OOK using DTF
ED−OOK using AF
TR−PAM using DTF
TR−PAM using AF

(a)

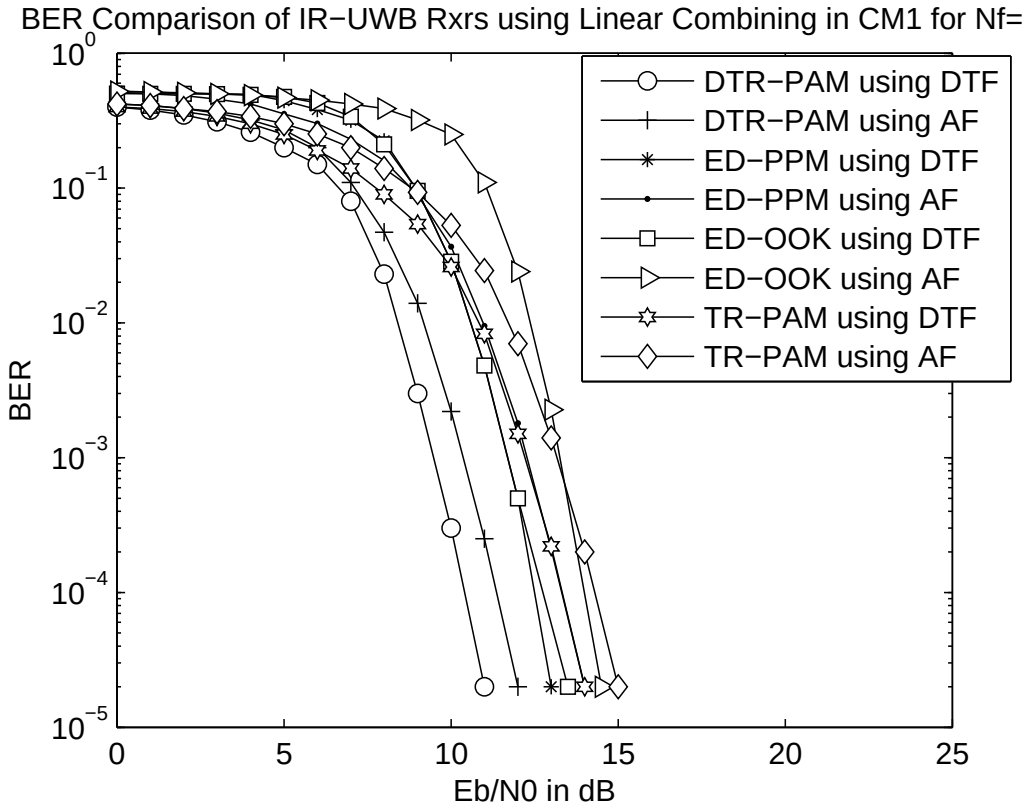
BER Comparison of IR−UWB Rxrs using Linear Combining in CM1 for Nf=1
BER
Eb/N0 in dB
DTR−PAM using DTF
DTR−PAM using AF
ED−PPM using DTF
ED−PPM using AF
ED−OOK using DTF
ED−OOK using AF
TR−PAM using DTF
TR−PAM using AF

(b)

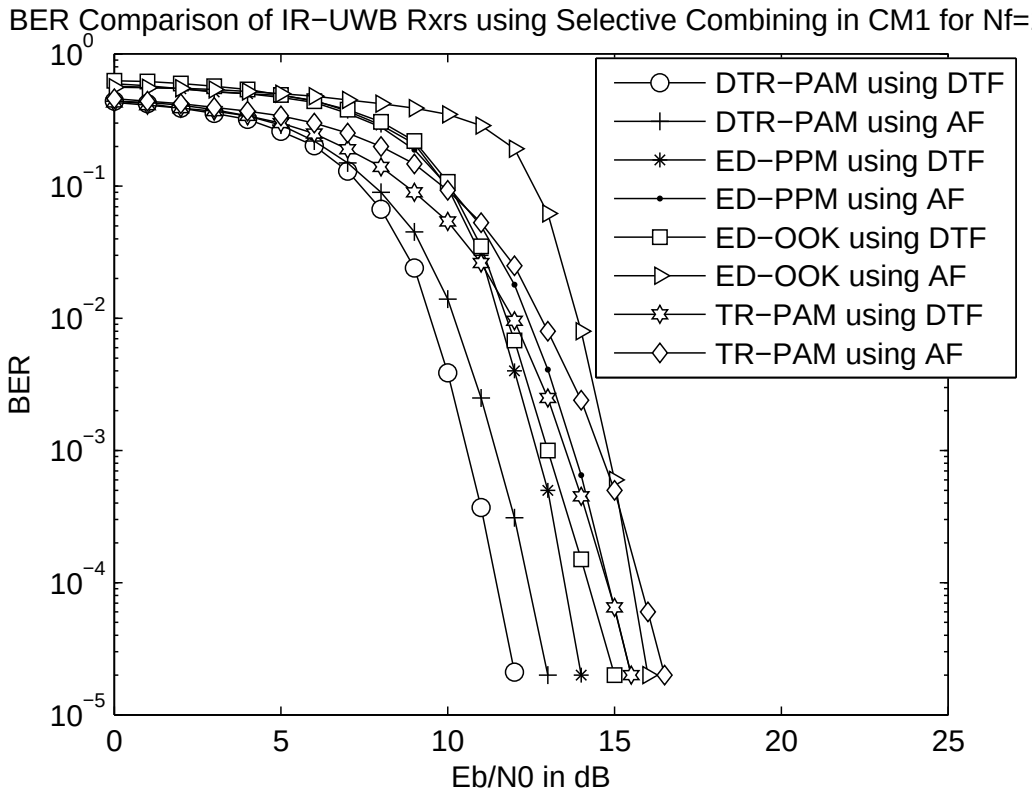

(c)

Figure 6.11: BER performance comparison of non−coherent UWB receivers using dual−hop Cooperative DTF strategy over CM1 environment with (a) Optimum Linear Diversity Combining (b) Linear Diversity Combining and (c) Selective Diversity Combining

This section gives the computer simulation results for the BER performance of ED−PPM system, using cooperative dual−hop relay strategies with various diversity combining schemes, namely optimum linear combining, linear combining and selective combining, over UWB CM1 and CM2 channels respectively. Matlab tool was used to obtain the computer simulations. The analytical BER expressions obtained for the performance analysis of cooperative dual−hop UWB ED−PPM system, using cooperative AF and DTF relay strategies with various combining schemes, are plotted using numerical integration, and then compared with the simulation results. The main parameters considered for simulations are $N_f = 1, 2$, $N = 200000$, $W = 2\ GHz$, $T_i = 4\ ns$ and $F_{samp} = 10\ GHz$, where N_f represents the number of frames in one symbol, N the number of bits, W the bandwidth of bandpass filter, T_i the integration interval and F_{samp} the sampling frequency. A second order Gaussian derivative pulse $p(t) = 1 - 4\pi((t)/T_k)^2)exp(-2 \times pi. \times ((t)/T_k).^2)$ is used for transmission, where t denotes the time interval and $T_k = 0.15\ ns$ the pulse width control factor. The values of means μ_k and variances σ_k^2 obtained from UWB CM1 channel, are noted to be 12.5 dB and 3.5 dB respectively. The index $k \in \{1, 2, 3\}$ here refers to S−D, S−R and R−D link respectively, as discussed in equation 5.3.

Fig 6.2(a) and (b) illustrates the BER performance of UWB ED−PPM system using cooperative dual−hop AF strategy with various diversity combining, over IEEE 802.15.4a UWB CM1 environment, for $N_f = 1$ and 2 respectively. It is inferred from the BER plots in the Figures that using cooperative AF scheme gives a much better BER performance, compared to non−cooperative or single−link. Among the diversity combining schemes, Optimum Linear Combining gives the best BER performance followed by Linear Combining and then Selective Combining for any SNR. It is also concluded that SNR gain degrades by a margin of $3 - 4\ dB$, as N_f increases from 1 to 2. This leads to BER degradation.

The variation in BER vs SNR of UWB ED−PPM system using cooperative dual−hop AF strategy with various combining schemes in IEEE 802.15.4a UWB CM2 environment for $N_f = 1$ and 2, can be inferred from Fig 6.3(a) and (b) respectively. At a BER of 10^{-4}, NLOS channel i.e. CM2, suffers a SNR loss of $4\ dB$, compared to LOS environment i.e. CM1, as observed in Fig 6.3(a) and (b). It can also be concluded from both the Figures that as far as combining schemes are concerned, Optimum Linear Combining $>$ Linear Combining $>$ Selective Combining $>$ Single−Link. It is observed from the Figures that as N_f changes from 1 to 2, SNR degrades by a margin of $3 - 4\ dB$, leading to degradation in BER performance.

Fig 6.4(a), (b) and (c) compares the analytical vs simulated BER performance of UWB ED−PPM receiver using cooperative AF strategy, with various diversity combining schemes, in UWB CM1 channel. It can be inferred from the results that the simulation plots nearly coincide with the plot of analytical results at all BER for N_f = $1, 2$.

The dual−hop cooperative system model having single path and $L = 5$ and 10 relay paths are as shown in Fig 6.5(a) and (b). respectively. Fig 6.6(a), (b) and (c) presents the BER performance of UWB ED−PPM system using dual−hop cooperative AF strategy for various diversity combining schemes having $L = 0, 1, 2, 5, 10$ relay paths. It can be concluded from the Figures that increase in relay paths ($L = 10$) gives better performance, compared to using less number of relay paths ($L = 0, 1, 2, 5$), using any of the diversity combining schemes. This is because more the number of multipaths, more is the multipath energy extracted. Therefore, greater the diversity more is the improvement in BER performance. It can also be inferred from the simulation results that UWB ED−PPM system, using cooperative AF strategy with various diversity combining schemes and ($L = 1, 2, 5, 10$) relay paths (diversity) gives a much better BER performance compared to single−link or non−cooperative case $L = 0$.

Fig 6.7(a) and (b) illustrates the BER performance of UWB ED−PPM system using dual−hop cooperative DTF relay strategy for various diversity combining schemes, in UWB CM1 environment having $N_f = 1$ and 2 respectively. It is observed that increase in number of frames N_f from 1 to 2, leads to degradation in BER performance. At a BER of 10^{-4}, optimum linear diversity combining scheme gives a SNR improvement of $1\ dB$ and $2\ dB$ over linear diversity combining and selective diversity combining, respectively. It is also observed that DTF relay scheme gives a SNR gain of $1\ dB$ over AF scheme, at all BER.

The BER performance of UWB ED−PPM system using cooperative dual−hop DTF strategy for various diversity combining schemes, in UWB CM2 environment having $N_f = 1$ and 2 respectively, is presented in Fig 6.8(a) and (b). It is inferred that CM2, NLOS channel suffers a performance loss of $3\ dB$, compared to LOS, CM1 channel. Also, the BER performance degrades with increase in number of frames N_f. It can also be observed from the Figures that DTF relay scheme supersedes AF relay scheme, by a margin of $1\ dB$ at a BER of 10^{-4}.

The analytical and simulated BER performance of UWB ED−PPM system, has been compared using dual−hop cooperative DTF relay strategy, for all these three diversity combining schemes and the results are as depicted in Fig 6.9. Fig 6.9 (a), (b) and (c) confirms the convergence of analytical accuracy of the evaluated BER with the simulated BER plots for all these

three diversity combining schemes namely optimum combining, linear combining and selective combining respectively, for $N_f = 1, 2$.

Fig 6.5(a) and (b) represents a dual−hop cooperative system model having $L = 5$ and 10 relay paths respectively. Fig 6.10(a), (b) and (c) presents the BER performance of UWB ED−PPM system using dual−hop cooperative DTF strategy, for various diversity combining schemes having $L = 0, 1, 2, 5, 10$ relay paths. It can be concluded from the Figures that BER performance of UWB ED−PPM system using cooperative DTF strategy with various diversity combining schemes and ($L = 1, 2, 5, 10$) relay diversity paths, gives a much better BER performance compared to single−link $L = 0$. The reason being, more the number of multipaths, more is the multipath energy extracted. Therefore, greater the diversity more is the improvement in BER performance.

The BER performance of non−coherent UWB receivers namely AC (TR and DTR) and ED (OOK and PPM) using cooperative dual-hop AF and DTF relay strategies with various diversity combining schemes, over UWB CM1 channel, for N_f = 1, is compared as shown in Fig 6.11(a), (b) and (c). It can be inferred from the simulation results that DTF relay scheme enjoys a SNR gain of $1\ dB$ over AF relay scheme, for any BER. DTR outperforms ED−PPM, ED−OOK, TR by a SNR margin of $2\ dB$, $2.5 - 3\ dB$, $3 - 3.5\ dB$ respectively, at a BER of 2×10^{-5}. It can be concluded from all the Figures that as far as BER performance of non−coherent UWB systems are concerned, DTR $>$ ED−PPM $>$ ED−OOK $>$ TR. This is because, in case of ED, all the useful received signal energy is recovered, despite having a higher noise contribution due to squaring operation whereas, TR wastes $3\ dB$ of energy transmitting a reference pulse. DTR system sends differentially modulated data, thereby requiring less energy in transmitting the same information as TR system, since it does not waste energy in transmitting a reference pulse. Furthermore, DTR system transmits differentially modulated data, thereby giving the best BER performance among all the non−coherent UWB receivers. Among the low complexity ED systems, ED−PPM supersedes ED−OOK by a SNR margin of $1\ dB$, at a BER of 10^{-4}. This is because ED−OOK system does not transmit a Gaussian second order pulse when information bit 0 is transmitted, as a result inducing more noise during detection. This leads to degradation in BER performance.

6.6 Concluding Remarks

The approximate BER expression for UWB ED−PPM system using dual−hop cooperative AF and DTF relay network, is derived in the chapter. The analytical BER expressions are obtained for three cases namely optimum linear diversity combining, linear diversity combining and selective diversity combining. The expressions are validated with the simulation results employing IEEE 802.15.4a UWB standard between the relay nodes and links. The overlapping or the convergence of the simulation results with the analytical results, confirm the accuracy and perfectness of approximation used in evaluation of BER. Numerical results depict improvement in BER with increase in number of relay paths L. CM1, LOS in nature gives a better BER performance than CM2, NLOS in nature. It is also observed that with increase in number of frames N_f, leads to degradation in BER performance for UWB CM1 and CM2 environment. It can be inferred from the simulation results that, using dual−hop cooperative relay schemes give a performance gain of $2 - 3\ dB$, compared to non−cooperative scheme. Furthermore, DTF relay strategy gives a SNR gain of 1 dB over AF relay strategy, at a BER of 10^{-4}. The simulation results clearly depict that despite the slight superiority of AC systems namely DTR over ED systems in BER performance, ED systems are preferred because of its low hardware complexity, low cost and simpler implementation. Among the low complexity ED systems, ED−PPM supersedes ED−OOK by a SNR margin of $1\ dB$, at a BER of 10^{-4}. This is because ED−OOK system does not transmit a Gaussian second order pulse when information bit 0 is transmitted, as a result inducing more noise during detection. This leads to degradation in BER performance. Thus it can be concluded that ED−PPM system acts a perfect alternative..

In this chapter we present an analytical approach based on energy detection, to evaluate the BER performance of UWB ED−PPM system using cooperative dual−hop AF and DTF relay strategies with various diversity combining schemes, over IEEE 802.15.4a environment. Furthermore, the analytical approach is validated with the computer simulations. The conclusion of the research work carried out in this thesis is presented in the next chapter.

Chapter 7

Conclusions and Future Work

The work presented in this thesis, evaluates the BER performance of non−coherent UWB systems namely AC and ED, using various diversity combining schemes in cooperative and non−cooperative scenario from both analytical as well as simulation perspective. The issues pertaining to single−link scenario is studied, which leads to cooperative scheme, that overcomes the various issues of UWB such as wide coverage area, high data rate and good BER performance. The performance improvement in using the cooperative scheme is demonstrated using a cooperative dual−hop system model, with AF and DTF relay strategies. This chapter summarises the various findings from the work done in this thesis, giving suggestions for further investigations.

7.1 Concluding Remarks

UWB is advantageous over other wireless counterpart due to large bandwidth, ability to transmit extremely short duration pulses, superior penetration property, low cost, low power consumption, high precision ranging and simple implementation. The huge bandwidth occupancy of UWB signal, makes it robust to multipath fading and ISI effects. UWB finds its applications in military, medical applications, WSN and vehicle to vehicle communication. The detectors used for UWB signals include coherent RAKE receiver and non−coherent receivers. Coherent RAKE receivers are complex due to its requirement for accurate CSI and synchronization for extracting multipath energy from multipath components. So, non−coherent receivers are preferred, that are simple and less complex, even though the BER performance of non−coherent receivers are poor compared to the coherent receivers. Thus, we restrict our study to UWB

non−coherent AC (TR and DTR) and ED systems. It is observed from the various study in literature that AC systems suffer from hardware complexity issue as they require long analog DL's for performing correlation during detection. To overcome this issue, ED is the preferred choice. The strict guidelines of FCC restrict UWB from achieving wide coverage range due to its low PSD. Hence, cooperative technology was introduced to relay the transmitted signal. The thesis aims to study the BER performance of non−coherent cooperative scheme.

The BER performance of single−link non−coherent UWB systems namely TR, DTR, ED−OOK and ED−PPM is analysed in this thesis work. The analytical BER expression for various non−coherent UWB systems has been derived over IEEE 802.15.4a UWB environment, using single−link approach and compared with the simulation results. It is observed that the analytical results exactly coincide with the simulation results for $N_f = 1, 2$ and hence, proves our accuracy and precision in evaluation of BER.

A novel analytical approach is presented to analyse the BER performance of non−coherent UWB AC system namely TR and DTR, using cooperative dual−hop AF and DTF relay protocol for various diversity combining schemes, over IEEE 802.15.4a environment. The various diversity combining schemes used are optimum combining, linear combining and selective combining. The analytical BER expression derived for TR and DTR system is based on autocorrelation principle and is validated with simulation results for $N_f = 1, 2$.

The BER performance of non−coherent UWB ED−OOK system using cooperative dual−hop AF and DTF relay strategy for various combining schemes namely optimum combining, linear combining and selective combining is evaluated using a novel analytical approach, based on approximation. The expressions were validated with the simulation results, employing IEEE 802.15.4a UWB standard between the relay nodes and links. The convergence of the simulation results with the analytical results, confirms the accuracy and perfectness of approximation used in evaluation of BER.

The disadvantage of using ED system based on OOK modulation scheme is that it does not transmit a gaussian second order pulse, when information symbol 0 is transmitted, as a result inducing more noise during detection. This leads to degradation in BER performance. So, to overcome this problem, we present a novel analytical approach based on energy detection principle to evaluate the BER performance of UWB ED−PPM system, using cooperative dual−hop AF and DTF strategy for various diversity combining schemes. The analytical results derived for BER performance of UWB ED−OOK system, were found to coincide with the simulation

results for $N_f = 1, 2$ employing, IEEE 802.15.4a UWB standard between the S−D, S−R and R−D links.

Numerical results depict that among all the non−coherent UWB systems discussed, DTR gives the best BER performance, followed by ED−PPM which in turn performs better than ED−OOK whereas, TR gives the worst performance among all. This is because TR wastes $3\ dB$ of energy in transmitting a reference pulse. This is overcome using a DTR system which transmits differentially modulated information and wastes no energy in transmitting a reference pulse, thereby saving energy as compared to TR system. It is also observed that despite the slight superiority of AC systems namely DTR over ED systems in BER performance, ED systems are preferred because of its low hardware complexity, low cost and simpler implementation. Among the low complexity ED systems, ED−PPM supersedes ED−OOK, by a SNR margin of $1\ dB$ at a BER of 10^{-4}. This is because ED−OOK system does not transmit a gaussian second order pulse, when information symbol 0 is transmitted, as a result inducing more noise during detection, leading to BER degradation.

Simulation results clearly illustrate an improvement in BER performance with increase in number of relay paths L in cooperative scenario. This is due to the increase in multipaths, which leads to increase in extracted multipath energy. Therefore, greater the diversity, more is the improvement in BER performance. CM1, LOS in nature gives a better BER performance than CM2, NLOS in nature for both single−link and cooperative scenario. Under similar conditions, the BER performance of a non−coherent UWB system, degrades with increase in N_f from 1 to 2. It can be inferred from the simulation results that cooperative DTF strategy gives a SNR gain of $1\ dB$, when compared to AF strategy, at a BER of 10^{-4}. Furthermore, it can be concluded from the simulation results that using dual−hop cooperative AF and DTF strategy with diversity combining, gives a SNR gain of $2 - 4\ dB$ at a BER of 10^{-4}, compared to non−cooperative or single−link scheme. The overlapping or the convergence of the simulation results with the analytical results, confirms the accuracy and perfectness of approximation used in evaluation of BER. Among the diversity combining schemes, optimum combining performs much better than linear combining, which in turn performs better than selective combining.

7.2 Future Work

The following aspects may suitably be explored for the future scope of this work to give more insight into the performance analysis of non−coherent IR−UWB cooperative communication system.

The BER performance of non−coherent UWB ED system using cooperative relay technology is still unexplored till date. In this thesis, we have a presented a novel cooperative approach, based on energy detection to evaluate the BER performance of UWB ED system using cooperative dual−hop relay technology with diversity combining, over IEEE 802.15.4a environment. Using the same consideration and constraints, the work can be extended using multi−hop relay strategy. This will lead to more diversity gain and hence will improve the BER performance of UWB ED system.

The focus of the thesis work is to evaluate the BER performance of non−coherent UWB ED system using cooperative AF and DTF relay strategy with diversity combining. The same work can be further explored using cooperative DF technology which uses error correcting codes such as Reed Solomon, Convolution, LDPC etc. to improve the BER performance.

Till now we have evaluated the BER performance of non−coherent UWB system using cooperative dual−hop relay strategies for various diversity combining schemes, in presence of a single user. The same work can be extended using cooperative dual−hop or multi−hop relay strategies in presence of multiple users. Using multiple users will further lead to multiple access interference. Some special receivers namely Quasi−Decorrelator, Quasi−MMSE, Linear MMSE Combining, Pulse Discarding, Iterative Detectors, Sub−Optimal and Optimal Frame Combining receivers can be used to mitigate MAI in non−coherent cooperative UWB systems.

The BER performance of non−coherent UWB ED and AC systems using cooperative relay strategies with diversity combining are based on autocorrelation and energy detection principle respectively. The novel approach followed by us in our thesis is based on BER approximation. Performance bounds can be applied based on some direct approach for eg. Gil Palaez Theorem, CF etc. to improve the BER performance.

The BER performance of a non−coherent cooperative UWB system can be further enhanced, if ED is replaced with Weighted Energy Detector (WED). Using WED, a perfect trade−off can be achieved i.e. low complexity with improved BER performance, in comparison to ED. The received signal can be first squared and then passed through a group of parallel integrators, where each of the integrators uses a different integration time window to perform

integration within the symbol period. The evaluation of the energy obtained from the corresponding integrators can be used to determine the weights, which help in improving the SNR ratio. If the SNR is high the weights will be large, otherwise if the signal strength is weak, then the weighting factor will also be less.

Appendix A

Evaluation of Noise Variance

Determination of noise variance $n_k^2(t)$

Let $x = n_{SD}(t), n_{SR}(t), n_{RD}(t)$ and $y = x^2$. Therefore the variance of y can be simplified as:

$$\sigma_y^2 = \mathbb{E}[y^2] - \{\mathbb{E}[y]\}^2 = \mathbb{E}[x^4] - \left\{\mathbb{E}[x^2]\right\}^2 \tag{A.1}$$

$$= 3\left\{\sigma_x^2\right\}^2 - \left\{\sigma_x^2\right\}^2 = 2\left\{\sigma_x^2\right\}^2 = \frac{N_0^2}{2} \tag{A.2}$$

where, $\mathbb{E}[x] = 0$ and $\sigma_x^2 = \frac{N_0}{2}$. The term $k \in \{1, 2, 3\}$ represents S$-$D, S$-$R and R$-$D link respectively.

Appendix B

Evaluation of Expectation of Noise

Determination of $\mathbb{E}[n^{'}_{RD}(t)n^{'}_{RD}(\tau)]$

The aggregate noise response $n^{'}_{RD}(t)$ of R-D link is expressed as $n^{'}_{RD}(t) = \sum_{l=0}^{L_3-1} \alpha_{l,3}$ $n_{SR}(t-\tau_{l,3})$

$$\mathbb{E}[n^{'}_{RD}(t)n^{'}_{RD}(\tau)] = \underbrace{\sum_{l=0}^{L_3-1}\sum_{k=0}^{K_3-1} \alpha_{l,3}\alpha_{k,3}\,\mathbb{E}[n_{SR}(t-\tau_{l,3})n_{SR}(\tau-\tau_{k,3})]}_{\mathrm{V}alue=0} + \sum_{l=0}^{L_3-1} \alpha_{l,3}^2\,\mathbb{E}[n_{SR}(t-\tau_{l,3})n_{SR}(\tau-\tau_{l,3})] \quad \text{(B.1)}$$

$$= \gamma_3\theta_2(t-\tau) \quad \text{(B.2)}$$

$$= \frac{\gamma_3 N_0\delta(t-\tau)}{2} \quad \text{(B.3)}$$

where, $\sum_{l=0}^{L_k-1} \alpha_{l,k}^2 = \gamma_k$ and $\mathbb{E}[n_{SR}(t)n_{SR}(\tau)]$ = $\mathbb{E}[n_2(t)n_2(\tau)]$=$\theta_2(t-\tau)$.

The term $\sum_{l=0}^{L_3-1}\sum_{k=0}^{K_3-1} \alpha_{l,3}\alpha_{k,3}\,\mathbb{E}[n_{SR}(t-\tau_{l,3})n_{SR}(\tau-\tau_{k,3})]$ has a value of 0 because the expectation of noise component with different delays is always 0.

Appendix C

Linear Optimal Combining Factor

Determination of Linear Optimal Combining Factor κ

In order to evaluate the value of κ, we differentiate the SNR expression given by equations (4.44,4.82,4,122,4.167,5.38,5.80,6.52 and 6.93) w.r.t. κ and equate the result to 0.

$$\frac{d\gamma_{AF-LOC}}{d\kappa} = \frac{d\gamma_{DTF-LOC-CD}}{d\kappa} = \frac{(A1 - B1)}{C1} = 0 \tag{C.1}$$

where, $A1 = 2(sig_{SD} + \kappa sig_{RD})sig_{RD}(\sigma^2_{Z_{noise-SD}} + \kappa^2\sigma^2_{Z_{noise-RD}})$,
$B1 = (sig_{SD} + \kappa sig_{RD})^2 2\kappa(\sigma^2_{Z_{noise-RD}})$ and $C1 = (\sigma^2_{Z_{noise-SD}} + \kappa^2\sigma^2_{Z_{noise-RD}})^2$.

$$\begin{aligned}\frac{d\gamma_{DTF}}{d\kappa} &= 2[(sig_{SD} + \kappa sig_{RD})sig_{RD}(\sigma^2_{Z_{noise-SD}} + \kappa^2\sigma^2_{Z_{noise-RD}})] - [(sig_{SD} + \kappa s_{RD})^2 \\ &\quad 2\kappa\sigma^2_{Z_{noise-RD}}] = 0\end{aligned} \tag{C.2}$$

Solving we get,

$$\begin{aligned}&= -\kappa^2(2sig_{SD}sig_{RD}\sigma^2_{Z_{noise-RD}}) + 2\kappa(\sigma^2_{Z_{noise-SD}}sig^2_{RD} - \sigma^2_{Z_{noise-RD}}sig^2_{SD}) \\ &\quad +(2sig_{SD}sig_{RD}\sigma^2_{Z_{noise-SD}}) = 0\end{aligned} \tag{C.3}$$

Using quadratic rule, we find the roots for κ.

$$\kappa = \frac{-4(\sigma^2_{Z_{noise-SD}})sig^2_{RD}}{-4sig_{SD}sig_{RD}\sigma^2_{Z_{noise-RD}}} = \frac{(\sigma^2_{Z_{noise-SD}})sig_{RD}}{(\sigma^2_{Z_{noise-RD}})sig_{SD}} \tag{C.4}$$

The optimum value of κ is given by Equation C.4 as it gives proper roots.

Appendix D

Evaluation of Variance Terms

Determination of Variance Terms for S−D and R−D Link

The noise variance of S−D link is evaluated as follows:

$$\sigma^2_{Z_{noise-SD}} = \mathbb{E}[(Z_{noise-SD})^2] = \mathbb{E}[(Z_{noise-1})^2] \tag{D.1}$$

Replacing the value of $Z_{noise-SD}$ given in equation 6.36, we obtain:

$$\begin{aligned}\mathbb{E}[(Z_{noise-10} - Z_{noise-11})^2] &= \mathbb{E}[(Z_{noise-10})^2] + \mathbb{E}[(Z_{noise-11})^2] \\ &\quad -2\,\mathbb{E}[Z_{noise-10}Z_{noise-11}] \\ &= \sigma^2_{Z_{noise-10}} + \sigma^2_{Z_{noise-11}}\end{aligned} \tag{D.2}$$

where, $\mathbb{E}[Z^2_{noise-10}] = \sigma^2_{Z_{noise-11}}$, $\mathbb{E}[Z^2_{noise-11}] = \sigma^2_{Z_{noise-11}}$ and $\mathbb{E}[Z_{noise-10}Z_{noise-11}] = 0$ because the noise terms at S−D and R−D link are independent hence their cross-correlation is 0. In the noise term $Z_{noise-lm}$, the subscripts $l \in \{1, 2, 3\}$ denote S−D, S−R and R−D link respectively and $m \in \{0, 1\}$ the transmitted information bit. Therefore, the total variance of S−D link is as follows:

$$\sigma^2_{Z_{noise-SD}} = \sigma^2_{Z_{noise-1}} = \sigma^2_{Z_{noise-10}} + \sigma^2_{Z_{noise-11}} \tag{D.3}$$

Similarly, the noise variance of R−D link is evaluated as follows:

$$\sigma^2_{Z_{noise-RD}} = \mathbb{E}[(Z_{noise-RD})^2] = \mathbb{E}[(Z_{noise-3})^2] \tag{D.4}$$

Replacing the value of $Z_{noise-RD}$ given in equation 6.37, we obtain:

$$\mathbb{E}[(Z_{noise-30} - Z_{noise-31})^2] = \mathbb{E}[(Z_{noise-30})^2] + \mathbb{E}[(Z_{noise-31})^2]$$

$$
\begin{aligned}
& -2\,\mathbb{E}[Z_{noise-30}Z_{noise-31}] \\
= \;& \sigma^2_{Z_{noise-30}} + \sigma^2_{Z_{noise-31}} \qquad \text{(D.5)}
\end{aligned}
$$

where, $\mathbb{E}[Z^2_{noise-30}] = \sigma^2_{Z_{noise-30}}$, $\mathbb{E}[Z^2_{noise-31}] = \sigma^2_{Z_{noise-31}}$ and $\mathbb{E}[Z_{noise-30}Z_{noise-31}] = 0$ because the noise terms at S$-$D and R$-$D link are independent hence their cross$-$correlation is 0. Therefore, the total variance of S$-$D link is as follows:

$$
\sigma^2_{Z_{noise-RD}} = \sigma^2_{Z_{noise-3}} = \sigma^2_{Z_{noise-30}} + \sigma^2_{Z_{noise-31}} \qquad \text{(D.6)}
$$

Bibliography

[1] M. Z. Win and R. A. Scholtz, "Impulse radio: How it works," *IEEE Communication Letters*, vol. 2, no. 2, pp. 36-38, 1998.

[2] R. Hazra and A. Tyagi, "A Survey on Various Coherent and Non-Coherent IR-UWB Receivers," *Wireless Personal Communications, Springer*, vol. 79, no. 3, pp. 2339-2369, 2014.

[3] M. Z. Win and R. A. Scholtz, "Ultra-wide bandwidth time-hopping spread-spectrum impulse radio for wireless multiple-access communications," *IEEE Transactions on Communications*, vol. 48, pp. 679-691, 2000.

[4] R. S. Kshetrimayum, "An introduction to UWB Communication systems," *IEEE Potentials*, vol. 28. no. 2, pp. 9-13, 2009.

[5] Federal Communications Commission (FCC), Revision of part 15 of the commissions rules against regarding Ultra-Wideband Transmission Systems. First Report and Order, ET Docket 98- 153, FCC 02-48, Adopted: Feb 2002, Release Apr 2002. http://www.ntia.doc.gov/fcc-filing/2000/ ntia-comments-revision-part-15-commissions-regarding-ultrawideband-transmission-syst.

[6] D. Porcino and W. Hirt, "Ultra-wideband radio technology: Potential and challenges ahead," *IEEE Communications Magazine*, vol. 41, no. 7, pp. 66-74, 2003.

[7] Maria-Gabriella Di Benedetto and B. R. Vojic, "Ultra wide band wireless communications: A tutorial," *Journal Of Communications and Networks*, vol. 5, no. 4, pp. 290-302, 2003.

[8] M. Di Benedetto and G. Giancola, *Understanding ultra wide band radio fundamentals*, 1st Edition , Prentice Hall PTR, 2004.

[9] G. R. Aiello and G. D. Rogerson, "Ultra-wideband wireless systems," *IEEE Microwave Magazine*, vol. 4, no. 2, pp. 36-47, 2003.

[10] D. Wentzloff, R. Blazquez, F. S. Lee, P. Ginsburg, J. Powell and A. P. Chandrakeshan, "System design considerations for ultra-wideband communication," *IEEE Communications Magazine*, vol. 43, no. 8, pp. 114-121, 2005.

[11] M. Di Benedetto, T. Kaiser, A. F. Molisch, I. Oppermann, C. Politano and D. Porcino, *UWB Communication Systems A Comprehensive Overview*, Eurasip Book Series on Signal Processing and Communications and Hindawi Publishing Corporation, 2006.

[12] F. Nekoogar,*Ultra-Wideband Communications: Fundamentals and Applications*, Englewood Cliffs, NJ: Prentice-Hall, 2005.

[13] X. Shen, M. Guizani, R. C. Qiu and T. Le-Ngoc, *Ultra-Wideband Wireless Communications and Networks*, Wiley and Sons Pvt. Ltd, 2006.

[14] A. R. Forouzan, M. Nasiri−Kenari, and J. A. Salehi, "Performance analysis of time-hopping spread-spectrum multiple-access systems: Uncoded and coded schemes," *IEEE Transactions on Wireless Communication*, vol. 1, no. 4, pp. 671-681, 2002.

[15] G. Ross, *The transient analysis of multiple beam feed networks for array systems*, Ph.D Dissertation, Dept. Elec. Eng., Polytech. Inst. Brooklyn, NY, USA, 1963.

[16] H. F. Harmauth, *Transmission of Information by Orthogonal Functions*, First Edition, Springer, New York, 1969.

[17] T. W. Barrett, "History of Ultra Wideband (UWB) Radar and Communications: Pioneers and Innovators," *in Proceedings of Progress in Electromagnetics Symposium 2000 (PIERS 2000)*, Cambridge, MA, July 2000.

[18] M. Ghavami, L. B. Michael and R. Kohno, *Ultra Wideband Signals and Systems in Communication Engineering*, First Edition, John Wiley and Sons, Ltd, 2004.

[19] R. A. Scholtz, "Multiple access with time-hopping impulse modulation," *in Proceedings of IEEE Military Communications (Milcom)*, vol. 2, pp. 447-450, Boston, USA, 1993.

[20] S. Mohammad and S. Sadough, *A tutorial on ultra wideband modulation and detection schemes*. http://www.faculties.sbu.ac.in/sadough/pdf/uwbtutorial.pdf. Accessed Apr 2009.

[21] K. Maichalernnukul, F. Zheng, and T. Kaiser, "Design and performance of dual−hop MIMO UWB transmissions," *IEEE Transactions on Vehicular Technology*, vol. 59, no. 6, pp. 2906-2920, 2010.

[22] J. R. Fernandes and D. Wentzloff, "Recent advances in IR-UWB transceivers: An overview," *in Proceedings of IEEE International Symposium on Circuits and Systems (ISCAS)*, pp. 3284-3287, Paris, 2010.

[23] *Universal Serial Bus Specification*, Revision 2.0, 2000.

[24] J. Zhang, P. V. Orlik, Z. Sahinoglu, A. F. Molisch, and P. Kinney, "UWB Systems for Wireless Sensor Networks," *Proceedings of the IEEE*, vol. 97, no. 2, pp. 313-331, 2009.

[25] Z. Zou, D. S. Mendoza, P. Wang, Q. Zhou, J. Mao, F. Jonsson, H. Tenhuen and L. R. Zheng, "A low-power and flexible energy detection IR-UWB receiver for RFID and wireless sensor networks," *IEEE Transactions on Circuits and Systems I*, vol. 58, no. 7, pp. 1470-1482, 2011.

[26] R. Cardinali, L. De Nardis, M. Di Benedetto, and P. Lombarde, "UWB ranging accuracy in high-and low-data-rate applications," *IEEE Transactions on Microwave Theory Technology*, vol. 54, no. 4, pp. 1865-1875, 2006.

[27] Z. Hasan, U. Phuyal, V. Yadav, A. K. Chaturvedi and V. K. Bhargava, "ISI-free pulses for high data-rate ultra-wideband wireless systems," *Canadian Journal of Electrical and Computer Engineering*, vol. 32, no. 4, pp. 187-192, 2007.

[28] L. Stoica, *Non coherent energy detection transceivers for ultra wideband impulse radio systems*, Ph.D Dissertation, University of Oulu, 2008.

[29] D. Cassioli, M. Z. Win, F. Vatalaro and A. F. Molisch, "Performance of low complexity rake reception in a realistic UWB channel," *in Proceedings of IEEE International Conference on Communications (ICC)*, vol. 2, pp. 763-767, New-York, USA, 2002.

[30] A. F. Molisch et al, "IEEE 802.15.4a channel model-final report," 2004.

[31] R. Bose, "Ultra wideband indoor channel modelling for personal area networking," *First European Conference on Antennas and Propagation, EuCAP*, pp. 1-4, Nice, France, 2006.

[32] M. Z. Win and R. A. Scholtz, "On the Robustness of Ultra-Wide Bandwidth Signals in Dense Multipath Environments," *IEEE Communication Letters*, vol. 2, no. 2, pp. 51-53, 1998.

[33] R. C. Qiu, "A study of the ultra-wideband wireless propagation channel and optimum UWB receiver design," *IEEE Journal on Selected Areas in Communication*, vol. 20, no. 9, pp. 1628-1637, 2002.

[34] A. Saleh and R. Valenzuela "A statistical model for indoor multipath propagation," *IEEE Journal on Selected Areas in Communications*, vol. 47, no. 9, pp. 128-137, 1987.

[35] A. F. Molisch, D. Cassioli, C. Chong, S. Emami, A. Fort, B. Kannan, J. Karedal, J. Kunisch, H. G. Schantz, K. Siwiak, and M. Z. Win, "A comprehensive standardized model for ultrawideband propagation channels," *IEEE Transactions on Antennas and Propagation* , vol. 54, no. 11, pp. 3151-3166, 2006.

[36] Z. Ahmadian and L. Lampe, "Performance Analysis of the IEEE 802.15.4a UWB System," *IEEE Transactions on Communications*, vol. 57, no. 5, pp. 1474-1485, 2009.

[37] J. M. Cramer and R. A. Scholtz, "Evaluation of an Ultra-Wideband Propagation Channel," *IEEE Transactions On Antennas and Propagation*, vol. 50, no. 5, pp. 560-570, 2002.

[38] G. Bacci, M. Luise, and H. V. Poor, "Performance of rake receivers in IR-UWB networks using energy-efficient power control," *IEEE Transactions on Wireless Communication*, vol. 7, no. 6, pp. 2289-2299, 2008.

[39] C. Carbonelli and U. Mengali, "Synchronization algorithms for UWB signals," *IEEE Transactions on Communications*, vol. 54, no. 2, pp. 329-338, 2006.

[40] A. Gerosa, M. D. Costa, A. Bevilacqua, D. Vogrig, and A. Neviani, "An Energy-Detector for Non-Coherent Impulse-Radio UWB Receivers," *IEEE Transactions On Circuits and Systems I:Regular Papers*, vol. 56, no. 5, pp. 1030-1040, 2009.

[41] L. Cai, L. Huang, Z. Fu, J. Yang, and W. Wang, "An energy detection receiver for non-coherent IR-UWB," *Journal of Semiconductors*, vol. 32, no. 6, pp. 1-8, 2011.

[42] H. Katiyar, A. Rastogi and R. Agarwal, "Cooperative communication: A review," *IETE Technical Review*, vol. 28, no. 5, pp. 409-417, 2011.

[43] C. Abou-Rjeily, "A symbol-by-symbol cooperative diversity scheme for relay-assisted UWB communications with PPM," *IEEE Journal on Selected Areas in Communication*, vol. 31, no. 8, pp. 1436-1445, 2013.

[44] C. Abou-Rjeily, N. Daniele, and J. Belfiore, "On the Amplify-and-Forward Cooperative Diversity with Time-hopping Ultra-wideband Communications," *IEEE Transactions on Communications*, vol. 56, no. 4, pp. 630-641, 2008.

[45] C. Abou-Rjeily, N. Daniele and J. C. Belfiore, "On the decode-and-forward cooperative diversity with coherent and non-coherent UWB systems," *in Proceedings of IEEE International Conference on Ultra−Wideband (ICUWB)*, pp. 435-440, Waltham, MA, 2006.

[46] C. Abou-Rjeily, "A novel selective-relaying protocol for cooperative IR-UWB communications with PPM," *in Proceedings of IEEE International Conference on Wireless Communications and Mobile Computing Conference (IWCMC)*, pp. 216-221, Cyprus, 2012.

[47] S. Berger, M. Kuhn, A. Wittneben, T. Unger, and A. Klein, "Recent advances in amplify-and-forward two-hop relaying [Accepted from Open Call]," *IEEE Communications Magazine*, vol. 47, no. 7, pp. 50-56, 2009.

[48] Z. Bai and Y. Xu, "MGF based performance analysis of dual-hop regenerative relaying IR-UWB systems," *International Journal of Electronics and Communication (AEU), Elsevier*, vol. 66, no. 8, pp. 641-646, 2012.

[49] J. Yuan, Y. Li and L. Chu, "Differential modulation and relay selection with detect-and-forward cooperative relaying," *IEEE Transactions on Vehicular Technology*, vol. 59, no. 1, pp. 261-268, 2010.

[50] A. A. Aziz, Y. Iwanami and E. Okamato, "Efficient combining technique with a low complexity detect-and-forward relay for cooperative diversity scheme," *in Proceedings of IEEE Region 10 Conference, TENCON*, vol. 9, pp. 1-6, Singapore, 2009.

[51] A. Jain, G. V. V. Sharma, U. B. Desai, and S. N. Merchant, "Exact analysis of the piecewise linear combiner for decode and forward cooperation with three relays," *IEEE Transactions on Wireless Communication*, vol. 10, no. 8, pp. 2461-2467, 2011.

[52] A. Jain, G. V. V. Sharma, U. B. Desai, and S. N. Merchant, "Exact error analysis for the piecewise linear combiner for decode and forward cooperation with two relays," *in Proceedings of National Conference on Communication (NCC)*, pp. 1-5, Bangalore, India, 2011.

[53] G. V. V. Sharma, Vijay Ganwani, U. B. Desai and S. N. Merchant, "Performance Analysis of Maximum Likelihood Detection for Decode and Forward MIMO Relay Channels in Rayleigh Fading," *IEEE Transactions on Wireless Communications*, vol. 9, no. 9, pp. 2880-2889, 2010.

[54] Y. Lee and M. H. Tsai, "Performance of decode-and-forward cooperative communications over Nakagami-m fading channels," *IEEE Transactions on Vehicular Technology*, vol. 58, no. 3, pp. 1218-1228, 2009.

[55] M. M. Fareed and M. Uysal, "On relay selection for decode-and-forward relaying," *IEEE Transactions on Wireless Communication*, vol. 8, no. 7, pp. 3341-3346, 2009.

[56] J. Romme, and K. Witrisal, "Transmitted-reference UWB systems using weighted autocorrelation receivers," *IEEE Transactions on Microwave Theory and Technology*, vol. 54, no. 4, pp. 1754-1761, 2006.

[57] Y. L. Chao and R. A. Scholtz, "Ultra-wideband transmitted reference systems," *IEEE Transactions on Vehicular Technology*, vol. 54, no. 5, pp. 1556-1569, 2005.

[58] A. A. D Amico, U. Mengali, and L. Taponecco, "Synchronization for differential transmitted reference UWB receivers," *IEEE Transactions on Wireless Communications*, vol. 6, no. 11, pp. 4154-4163, 2007.

[59] Z. Liang, X. Dong, A. Gulliver and X. Liao, "Performance of transmitted reference pulse cluster ultra-wideband systems with forward error correction," *International Journal of Communication Systems, John Wiley & Sons, Ltd*, vol. 27, no. 2, pp. 265-276, 2014.

[60] Z. Liang, X. Dong and T. A. Gulliver, "Performance of coded transmitted reference pulse cluster UWB systems," *in Proceedings of Asilomar Conference on Signals, Systems and Computers*, pp. 1990-1995, USA, 2008.

[61] Z. Liang, X. Dong, T. A. Gulliver and X. Liao, "Performance of transmitted reference pulse cluster ultra-wideband systems with forward error correction," *International Journal of Communication Systems, Wiley,* vol. 27, no. 2, pp. 265-276, 2012.

[62] X. Dong, L. Jin, and P. Orlik, "A new transmitted reference pulse cluster system for UWB communications," *IEEE Transactions on Vehicular Technology*, vol. 57, no. 5, pp. 3217-3224, 2008.

[63] X. Dong and X. Dong, "Bi-directional cooperative relays for transmitted reference pulse cluster UWB systems," *in Proceedings of IEEE Global Telecommunications Conference (Globecom)*, pp. 1-5, Florida, USA, 2010.

[64] S. He and X. Dong, "Implementation of a low complexity UWB transmitted reference pulse cluster system," *in Proceedings of IEEE Vehicular Technology Conference Fall, (VTC-Fall)*, pp. 1-5, Ottawa, 2010.

[65] A. Rabbachin and I. Oppermann, "Synchronization analysis for UWB systems with a low-complexity energy collection receiver," *in Proceedings of IEEE Joint UWBST and IWUWBS*, pp. 288-292, Kyoto, Japan, 2004.

[66] S. Y. Jong, "Design of a preamble signal for synchronization in ultra-wideband non-coherent energy detection receivers," *International Journal of Communication Systems, John Wiley & Sons, Ltd*, vol. 26, no. 4, pp. 465-480, 2013.

[67] S. A. Ji, S. J. Lee and J. S. Kim, "Simplified structure of weighted energy detector for UWB-IR systems," *IEEE Electronic Letters*, vol. 48, no. 1, pp. 48-50, 2012.

[68] R. Hazra and A. Tyagi, "Cooperative Impulse Radio Ultra-Wideband Communication Using Coherent and Non-Coherent Detectors: A Review," *Wireless Personal Communications, Springer*, vol. 77, no. 1, pp. 719-748, 2014.

[69] W. P. Siriwongpairat, W. Su, Z. Han and K.-J.-R. Liu, "Employing cooperative diversity for performance enhancement in UWB communication systems," *in Proceedings*

IEEE Wireless Communication and Networking Conference (WCNC), vol. 4, pp. 1854-1859, 2006.

[70] J. N. Lanemann, D. N. C. Tse and G. W. Wornell, "Cooperative Diversity in wireless networks: Efficient protocols and outage behavior," *IEEE Transactions on Information Theory*, vol. 51, no. 12, pp. 3062-3080, 2004.

[71] J. N. Lanemann,*Cooperative diversity in wireless networks:Algorithm and architectures*, Ph.D dissertation, MIT, Cambridge, MA, 2002. http://citeseerx.ist.psu.edu/viewdoc/download?

[72] A. Sendoris, E. Erkip and B. Aazhang, "User cooperative diversity part I: system description," *IEEE Transactions on Communications*, vol. 51, no. 11, pp. 1927-1938, 2003.

[73] A. Sendonaris, E. Erkip, and B. Aazhang, "User cooperation diversity part II: implementation aspects and performance analysis," *IEEE Transactions on Communications*, vol. 51, no. 11, pp. 1939-1948, 2003.

[74] A. Jamshidi, and M. Nasiri-Kenari, "Performance analysis of transmitter-side cooperation-receiver side-relaying schemes for heterogeneous sensor networks," *IEEE Transactions on Vehicular Technology*, vol. 57, no. 3, pp. 1548-1563, 2008.

[75] G. Kramer, M. Gastpar, and P. Gupta, "Cooperative strategies and capacity theorems for relay networks," *IEEE Transactions on Information Theory*, vol. 51, no. 9, pp. 3037-3063, 2005.

[76] E. C. Van Der Meulen, "Three-terminal communication channels," *Advances in Applied Probability*, vol. 3, no. 1, pp. 120-154, 1971.

[77] T. M. Cover and A. A. El Gamal, "Capacity theorems for the relay channel," *IEEE Transactions on Information Theory*, vol. 25, no. 5, pp. 572-584, 1979.

[78] M. Kulkarni, L. Choudhary, B. Kumbhani and R. S. Kshetrimayum, "Performance analysis comparison of transmit antenna selection with maximal ratio combining and orthogonal space time block codes in equicorrelated Rayleigh fading multiple input multiple output channels," *IET Communications*, vol. 8, no. 10, pp. 1850-1858, 2014.

[79] B. Kumbhani, L. N. B. Reddy and R. S, Kshetrimayum, "Approximate SER of cooperative communication over generalized eta-mu and kappa-mu fading channels," *The Journal of Engineering, IET*, vol. 1, no. 1, 2014.

[80] H. A. Suraweera, H. K. Garg, and A. Nallanathan, "Performance analysis of two hop amplify-and-forward systems with interference at the relay," *IEEE Communication Letters*, vol. 14, no. 8, pp. 692-694, 2010.

[81] A. Bin Sediq and H. Yanikomeroglu, "Performance Analysis of Selection Combining of Signals With Different Modulation Levels in Cooperative Communications," *IEEE Transactions on Vehicular Technology*, vol. 60, no. 4, pp. 1880-1887, 2011.

[82] A. Bin Sediq and H. Yanikomeroglu, "Performance Analysis of SNR-based Selection Combining and BER-based Selection Combining of Signals With Different Modulation Levels in Cooperative Communications," *in Proceedings of IEEE International Conference on Vehicular Technology Conference (VTC-Fall)*, pp. 1-5, Alaska, USA, 2009.

[83] P. R. Sahu and A. K. Chaturvedi, "Performance Analysis of Predetection EGC in exponentially correlated Nakagami-m fading channel," *IEEE Transactions on Communications*, vol. 53, no. 8, pp. 1252-1256, 2005.

[84] P. R. Sahu and A. K. Chaturvedi, "Performance Analysis of a Predetection EGC receiver in exponentially correlated Nakagami-m fading channel for noncoherent binary modulations," *IEEE Transactions on Wireless Communications*, vol. 5, no. 7, pp. 1634-1638, 2006.

[85] M. Z. Win and R. A. Scholtz, "Characterization of ultra-wide bandwidth wireless indoor channels: A communication-theoretic view," *IEEE Journal on Selected Areas in Communication*, vol. 20, no. 9, pp. 1613-1627, 2002.

[86] J. D. Choi and W. E. Stark, "Performance analysis of RAKE receivers for ultra-wideband communications with PPM and OOK in multipath channels," *in Proceedings of IEEE International Conference on Communications (ICC)*, vol. 3, pp. 1969-1973, New York, USA, 2002.

[87] J. Zhang, R. A. Kennedy and T. D. Abhayapala, "Performance of RAKE reception for ultra wideband signals in a lognormal-fading channel," *in Proceedings of IEEE International Workshop on Ultra wideband systems (IWUWBS)*, Oulo, Finland, 2003.

[88] C. Kundu and R. Bose, "An alternate method for calculating average probability of error in log-normal channel for UWB," *in Proceedings of National Conference on Communications (NCC)*, pp. 1-5, New-Delhi, India, 2013.

[89] A. A. D' Amico, U. Mengali and L. Taponecco, "Performance comparisons between two signalling formats for UWB communications," *in Proceedings of IEEE International Conference on Communications (ICC)*, vol. 6, pp. 3404-3408, Paris, France, 2004.

[90] B. Mielczarek, M. O. Wessman and A. Svensson, "Performance of coherent UWB rake receivers with channel estimators," *in Proceedings of IEEE Vehicular Technology Conference, (VTC-Fall)*, vol. 3, pp. 1880-1884, USA, 2003.

[91] M. Di Renzo, F. Tempesta, L. A. Annoni, F. Santucci, F. Graziosi, R. Minutolo, and M. Montanari, "Performance Evaluation of IRUWB DRake Receivers over IEEE 802.15.4a Multipath Fading Channels with NarrowBand Interference," *in Proceedings of IEEE International Conference on Ultrawideband (ICUWB)*, pp. 71-76, Vancouver, Canada, 2009.

[92] M. Di Renzo, F. Graziosi, and F. Santucci, "An exact framework for performance analysis of IR-UWB systems: The need for approximations," *IEEE Communication Letters*, vol. 11, no. 10, pp. 769-771, 2007.

[93] K. Maichalernnukul, T. Kaiser and F. Zheng, "On the performance of coherent and non-coherent UWB detection systems using a relay with multiple antennas," *IEEE Transactions on Wireless Communications*, vol. 8, no. 7, pp. 3407-3414, 2009.

[94] K. Maichalernnukul, T. Kaiser and F. Zheng, "Performance investigation of a UWB relay system using multiple relays with multiple antennas in IEEE 802.15.3a channel," *in Proceedings of IEEE Vehicular Technology Conference (VTC)*, pp. 1-6, Barcelona, 2009.

[95] G. N. Shirazi, P. Y. Kong and C. K. Tham, "A low-overhead cooperative retransmission scheme for IR-UWB networks," *Research Letters in Communication, Journal of Electrical and Computer Engineering*, vol. 2008, Article ID 291858, 2008.

[96] G. N. Shirazi, P. Y. Kong and C. K. Tham, "Optimal cooperative relaying schemes in IR-UWB networks," *IEEE Transactions on Mobile Computing*, vol. 9, no. 7, pp. 969-981, 2010.

[97] Z. Zeinalpour-Yazdi, M. Nasiri-Kenari, and B. Aazhang, "Performance of UWB linked relay network with time-reversed transmission in the presence of channel estimation error," *IEEE Transactions on Wireless Communications*, vol. 11, no. 8, pp. 2958-2969.

[98] Z. Bai, Y. Xu, B. Shen and K. S. Kwak, "Performance analysis of dual−hop UWB system with non−regenerative relaying scheme," *in Proceedings of IEEE International Conference on Advanced Communication Technology (ICACT)*, pp. 1221-1225, Seoul, 2011.

[99] Y. Xu, Z. Bai, and K. S. Kwak, "On the performance of dual−hop regenerative cooperative relaying of IR−UWB System," *in Proceedings of IEEE International Symposium on Communications and Information Technologies (ISCIT)*, pp. 323-327, Hangzhou, 2011.

[100] Y. Xu, Z. Bai, X. Yang, A. L. Wang and K. S. Kwak, "Closed−form BER analysis of dual−hop non−regenerative IR−UWB system over multipath channels," *in Proceedings of IEEE International Conference on Communication Technology (ICCT)*, pp. 126-130, Jinan, 2011.

[101] Z. Zeinalpour Yazdi, M. Nasiri-Kenari and B. Aazhang, "Bit Error Probability Analysis of UWB Communications with a Relay Node," *IEEE Transactions on Wireless Communications*, vol. 9, no. 2, pp. 802-813, 2010.

[102] K. Maichalernnukul, Z. Feng, and T. Kaiser, "Dual-hop UWB transmissions using a multiple antenna relay with antenna selection versus single-antenna relay selection," *in Proceedings of IEEE International ITG Conference on Source and Channel Coding (SCC)*, pp. 1-6, Germany, 2010.

[103] K. Maichalernnukul, "Outage performance of dual-hop UWB transmissions using a multiple-antenna relay with antenna selection versus single-antenna relay selection," *Journal of Communications*, vol. 7, no. 4, pp. 329-348, 2012.

[104] Y. Yang, D. Wang, M. Li, and Y. Song, "A relay selection scheme for IR-UWB networks based on distance information," *in Proceedings of IEEE International Conference on Information Theory and Information Security (ICITIS)*, pp. 1046-1049, Beijing, 2010.

[105] G. Pan, E. Ekici and Q. Feng, "Performance analysis of cooperative time hopping UWB systems with multi-user interference," *IEEE Transactions on Wireless Communications*, vol. 11, no. , pp. 1969-1975, 2012.

[106] K. Maichalernnukul, Z. Feng, and T. Kaiser, "Performance of ultrawideband cooperative relay systems in the presence of narrowband interference," *in Proceedings of IEEE International Conference on ultra-wideband (ICUWB)*, pp. 405-409, 2011.

[107] K. Witrisal, G. Leus, G. J. M. Janssen, M. Pausini, F. Troesch, T. Zasowski, and J. Romme, "Noncoherent ultra-wideband systems," *IEEE Signal Processing Magazine*, vol. 26, no. 4, pp. 48-66, 2009.

[108] G. Leus and A. J. Van-Der Veen, "A weighted autocorrelation receiver for transmitted reference ultra wideband communications," *in Proceedings of IEEE Workshop on Signal Processing Advances for Wireless Communications, SPAWC*, pp. 965-969, USA, 2005.

[109] L. Yang, G. B. Giannakis and A. Swami, "Noncoherent ultra−wideband radios," *in Proceedings of IEEE Military Communications Conference (MILCOM)*, vol. 2, pp. 786-791, Monterey, USA, 2004.

[110] L. Yang, G. B. Giannakis, and A. Swami, "Noncoherent Ultra-Wideband (De) Modulation," *IEEE Transactions on Communications*, vol. 55, no. 4, pp. 810-819, 2007.

[111] R. A. Scholtz, "Optimal and suboptimal receivers for ultra-wideband transmitted reference systems," *in Proceedings of IEEE International Conference on Global Telecommunications Conference (GLOBECOM)* , vol. 2, pp. 759-763, USA, 2003.

[112] J. A. Salehi and M. Farhang, "Optimum Receiver Design for Transmitted-Reference Signaling," *IEEE Transactions on Communications*, vol. 58, no. 5, pp. 1589-1598, 2010.

[113] S. Franz, and U. Mitra, "Generalized UWB transmitted reference systems," *IEEE Journal on Selected Areas in Communication*, vol. 24, no. 4, pp. 780-786, 2003.

[114] S. Franz, and U. Mitra, "On optimal data detection schemes for UWB transmitted reference systems," *in Proceedings of IEEE Global Telecommunications Conference (Globecom)*, vol. 2, pp. 744-748, USA, 2006.

[115] A. A. D' Amico and U. Mengali, "GLRT receivers for UWB systems," *IEEE Communication Letters*, vol. 9, no. 6, pp. 487-489, 2005.

[116] J. D. Choi and W. E. Stark, "Performance of ultra-wideband communications with suboptimal receivers in multipath channels," *IEEE Journal on Selected Areas in Communications*, vol. 20, no. 9, pp. 1754-1766, 2002.

[117] T. Jia and D. I. Kim, "Multiple access performance of balanced UWB transmitted-reference systems in multipath," *IEEE Transactions on Wireless Communications*, vol. 7, no. 3, pp. 1084-1094, 2008.

[118] T. Q. S. Quek and M. Z. Win, "Analysis of UWB transmitted-reference communication systems in dense multipath channels," *IEEE Journal on Selected Areas in Communication*, vol. 23, no. 9, pp. 1863-1874, 2005.

[119] T. Q. S. Quek, M. Z. Win, and D. Dardari, "Unified analysis of UWB transmitted-reference schemes in the presence of narrowband interference," *IEEE Transactions on Wireless Communication*, vol. 6, no. 6, pp. 2126-2138, 2007.

[120] T. Q. S. Quek, M. Z. Win, and D. Dardari, "UWB transmitted reference signaling schemes-part II: narrowband interference analysis," *in Proceedings of IEEE International Conference on Ultra-Wideband (ICUWB)*, pp. 593-598, Zurich, Switzerland, 2005.

[121] X. Luo and G. B. Giannakis, "Achievable rates of transmitted−reference ultra−wideband radio with PPM," *IEEE Transactions on Communications*, vol. 54, no. 9, pp. 1536-1541, 2006.

[122] Niranjayan and N. Beaulieu, "Accurate performance analysis of TR UWB systems with arbitrary front-end filters," *in Proceedings of IEEE International Conference on Communication*, pp. 4122-4127, Glasgow, United Kingdom, Jan 2007.

[123] Niranjayan and N. Beaulieu, "General performance analysis of TR UWB systems," *IEEE Transactions on Wireless Communication*, pp. 4122-4127, Glasgow, United Kingdom, Jan 2007.

[124] T. Su, Y. Wang, F. Huang and M. J. Lancaster, "Wide-band super-conducting microstrip delay line," *IEEE Transactions on Microwave Theory and Techniques*, vol. 52, no. 11, pp. 2482-2487, Dec. 2008.

[125] Kuylenstierna, A. Vorobiev, P. Linne'r and S. Gevorgian, "Ultrawide-Band Tunable True-time Delay Lines Using Ferroelectric Varactors," *IEEE Transactions on Microwave Theory and Techniques*, vol. 53, no. 6, pp. 2164-2170, Jun. 2005.

[126] Zhang, S. W. Cheung and T. I. Yuk, "A compact and UWB time-delay line inspired by CRLH TL unit cell," *in Proceedings IEEE Region 10 Conference*, pp. 868-872, Fukuoka, Japan, Nov. 2010.

[127] Azizzadeh and L. Mohammadi, "Degradation of BER by group delay in digital phase modulation," *in Proceedings of IEEE AICT*, pp. 350-354, 2011.

[128] Y. Jin and K. S. Kwak, "A Robust Non-coherent Receiver for TR UWB with the Impact of Group Delay Ripple," *IEICE Transactions on Communication*, vol. E95B, no. 6, pp. 1983-1989, Jun. 2012.

[129] J. Romme and K. Witrisal, "Oversampled Weighted Autocorrelation Receivers for Transmitted-Reference UWB Systems," *in Proceedings of IEEE Vehicular Technology Conference Proceedings (VTC Spring)*, vol. 2, pp. 1375-1380, 2005.

[130] K. Witrisal, G. Leus, G. J. M. Janssen, M. Pausini, F. Troesch, T. Zasowski, and J. Romme, "Noncoherent ultra-wideband systems," *IEEE Signal Processing Magazine*, vol. 26, no. 4, pp. 48-66, 2009.

[131] W. Gifford and M. Win, "On transmitted-reference UWB communications," *in Proceedings of Asilomar Conference Signals, Systems and Computing*, pp. 1526-1531, Pacific Grove, CA, Nov. 2004.

[132] D. L. Goeckel and Q. Durisi, "Slightly frequency-shifted reference ultra-wideband (UWB) radio," *IEEE Transactions on Communications*, vol. 55, no. 3, pp. 508-519, 2007.

[133] X. Dong, A. C. Y. Lee and L. Xiao, "A new UWB dual pulse transmission and detection technique," *in Proceedings of IEEE International Conference*, pp. 2835-2839, Seoul, Korea, 2005.

[134] X. Dong, L. Xiao and A. C. Y. Lee, "Performance analysis of dual pulse transmission in UWB channels," *IEEE Communication Letters*, vol. 10, no. 8, pp. 626-628, Aug. 2006.

[135] Z. Xu and B. M. Sadler, "Multiuser transmitted reference ultra-wideband communication systems," *IEEE Journal on Selected Areas in Communication*, vol. 24, no. 4, pp. 766-772, 2006.

[136] X. Dong, L. Xin and P. Orlik, "A new transmitted reference pulse cluster system for UWB communications," *IEEE Transactions on Vehicular Technology*, vol. 57, no. 5, pp. 3217-3224, Sep. 2008.

[137] L. Xin, X. Dong and Z. Liang, "Integration interval determination algorithms for BER minimization in UWB transmitted reference pulse cluster systems," *IEEE Transactions on Wireless Communications*, vol. 9, no. 8, pp. 2408-2414, Aug. 2010.

[138] M. Casu and G. Durisi, "Implementation aspects of a transmitted-reference UWB receiver," *Wireless Communication and Mobile Computing*, vol. 5,no. 5,pp. 537-549, Aug 2005.

[139] W. Namgoong, "A channelized digital ultra-wideband receiver," *IEEE Transactions on Wireless Communications*, vol. 3,no. 5, pp. 502-510, May 2003.

[140] J. Tang, Z. Xu and B. M. Sadler, "Performance analysis of b-bit digital receivers for TR-UWB systems with inter-pulse interference," *IEEE Transactions on Wireless Communication*, vol. 6, no. 2, pp. 494-505, Feb. 2007.

[141] Y. Jin, H. Liu, K. J. Kim and K. S. Kwak, "Receiver for Transmitted Reference Pulse Cluster UWB Communications," *IEEE Transactions on Vehicular Technology*, vol. 63, no. 9, pp. 4734-4738, Nov. 2014.

[142] M. Ho, V. S. Somayazulu, J. Foerster, and S. Roy, "A differential detector for an ultra-wideband communications system," *in Proceedings of IEEE Vehicular Technology Conference (VTC Spring)*, vol. 4, pp. 1896-1900, 2002.

[143] M. Di Renzo, L. A. Annoni, F. Graziosi, and F. Santucci, "A novel class of algorithms for timing acquisition of differential transmitted reference UWB receivers: Architecture, performance analysis and system design," *IEEE Transactions on Wireless Communications*, vol. 7, no. 6, pp. 2368-2387, 2008.

[144] M. Paussini, and G. J. M. Janssen, "Analysis and comparison of autocorrelation receivers for IR-UWB signals based on differential detection," *in Proceedings of IEEE International Conference on Acoustics, Speech and Signal Processing (ICASSP)*, vol. 4, pp. 513-516, Japan, 2004.

[145] M. Paussini, G. J. M. Janssen, and K. Witrisal, "Performance enhancement of differential UWB autocorrelation receivers under ISI," *IEEE Journal on Selected Areas in Communications*, vol. 24, no. 4, pp. 815-821, 2006.

[146] A. A. D Amico, and L. Taponecco, "A differential receiver for UWB systems," *IEEE Transactions on Wireless Communications*, vol. 5, no. 7, pp. 1601-1605, 2006.

[147] V. Lottici and Z. Tian, "Multiple Symbol Differential Detection for UWB Communications," *IEEE Transactions on Wireless Communications*, vol. 7, no. 5, pp. 1656-1666, 2008.

[148] X. Cheng, and Y. L. Guan, "Mitigation of cross-modulation interference in UWB energy detector receivers," *IEEE Communication Letters*, vol. 13, no. 6, pp. 375-377, 2009.

[149] S. Cui, *Modulation and multiple access techniques for ultra-wideband communication systems*, Ph.D dissertation, Cleveland State University.

[150] A. A. D Amico, U. Mengali, and E. Arias-de-Reyna, "Energy-detection UWB receivers with multiple energy measurements," *IEEE Transactions on Wireless Communications*, vol. 6, no. 7, pp. 2652-2659, 2007.

[151] C. Kundu and R. Bose, "Performance of a Multi-Hop UWB Transmitted Reference System using Decode and Forward Relays," *Wireless Personal Communications, Springer*, vol. 77, no. 3, pp. 1801-1814, 2014.

[152] S. Qing-Hua, X. Xuan-li, L. Di, and Q. Xin, "Performance analysis of cooperative ultra-wideband communication system," *in Proceedings of IEEE International Conference on communications and mobile computing (CMC)*, vol. 2, pp. 217-220, Shenzen, 2010.

[153] W. Feng, X. Chengqi, and Z. Yan, "The TR-UWB receiver based on spatial diversity," *Journal of Electronics (China)*, vol. 26, no. 5, pp. 623-630, 2009.

[154] M. Mondelli, Q. Zhou, X. Ma, and V. Lottici, "A cooperative approach for amplify-and-forward differential transmitted reference IR-UWB relay systems," *in Proceedings of IEEE International Conference on Acoustics, Speech and Signal Processing (ICASSP)*, pp. 2905-2908, Japan, 2012.

[155] T. M. Wu and Y. F. Hou, "Performance analysis of cooperative communication in the UWB differential transmitted reference system," *in Proceedings of IEEE Vehicular Technology Conference (VTC Spring)*, pp. 1-5, Budapest, 2011.

[156] M. Hamdi, J. Mietzner and R. Schober, "Double-differential encoding for dual-hop amplify-and forward relaying in IR UWB systems," *in Proceedings of IEEE Vehicular Technology Conference (VTC Spring)*, pp. 1-5, Taiwan, 2010.

[157] M. Hamdi, J. Mietzner and R. Schober, "Multiple-differential encoding for multi-hop amplify-and forward relaying in IR-UWB systems," *IEEE Transactions on Wireless Communications*, vol. 10, no. 8, pp. 2577-2591, 2011.

[158] Z. Wang, T. Lv, H. Gao, and Y. Li, "A novel two-way relay UWB network with joint non-coherent detection in multipath," *in Proceedings of IEEE Vehicular Technology Conference (VTC Spring)*, pp. 1-5, Budapest, 2011.

[159] N. He and C. Tepedelenlioglu, "Performance Analysis of Non-Coherent UWB Receivers at Different Synchronization Levels," *IEEE Transactions on Wireless Communications*, vol. 5, no. 6, pp. 1266-1273, 2006.

[160] V. Lottici, A. N. D' Andrea and U. Mengali, "Channel estimation for ultra-wideband communications," *IEEE Journal on Selected Areas in Communication*, vol. 20, no. 9, pp. 1638-1645, Dec. 2002.

[161] C. Carbonelli, U. Mengali, and U. Mitra, "Synchronisation and channel estimation for UWB signals," *in Proceedings of IEEE International Conference on Global Telecommunications (Globecom)*, San-Francisco, US, Dec 2003.

[162] G. Durisi, and S. Benedetto, "Comparison between Coherent and Noncoherent Receivers for UWB Communications," *Eurasip Journal on Advances in Signal Processing*, vol. 3, pp. 359-368, 2005.

[163] R. Zhang and X. Dong, "Synchronization and Integration Region Optimization for UWB Signals with Non-coherent Detection and Auto-correlation Detection," *IEEE Transactions on Communications*, vol. 56, no. 5, pp. 790-798, 2008.

[164] R. Hoctor and H. Tomilson, "Delay hopped Transmitted Reference RF Communications," *in Proceedings of IEEE International Conference on Ultra Wideband Systems and Technologies (UWBST)*, pp. 265-269, Baltimore, 2002.

[165] R. Hazra and A. Tyagi, "Performance Comparison of Non-Coherent IR-UWB Receivers ," *In Proceedings of IEEE International Conference on Signal Processing and Communication, ICSC*, pp. 143-148, Noida, India, 2013.

[166] Mohammad G. Khan, *On Coherent and Non-Coherent Receiver Structure for Impulse Radio UWB Systems*, Thesis, Blekinge Institute of Technology, Sweden.

[167] Eva A. Arias-de-Reyna, A. A. D' Amico and U. Mengali, "UWB energy detection receivers with partial channel knowledge," *in Proceedings of IEEE International Conference on Communications, (ICC)*, pp. 4688-4693, Istanbul, 2006.

[168] T. Ali, P. Siddiqua and M. A. Matin, "Performance Evaluation of Different Modulation Schemes for Ultra Wide Band Systems," *J. Electr. Eng.*, vol. 65, no. 3, pp. 184-188, 2014.

[169] L. Li and J. K. Townsend, "M-ary PPM for transmitted reference ultra-wideband communications," *IEEE Transactions on Communications*, vol. 58, no. 7, pp. 1912-1917, 2010.

[170] C. Liang, L. Wang, and F. Zhang, "A modified transmitted reference UWB receiver," *in Proceedings of IEEE International Conference on Wireless Communications, Networking and Mobile Computing, WiCOM*, pp. 1-4, China, 2008.

[171] H. Khani and P. Azmi, "Performance analysis of a high data rate UWB-DTR system in dense multipath channels," *Progress in Electromagnetics Research B*, vol. 5, pp. 119-131, 2008.

[172] M. E. Sahin, I. Guvenc and H. Arsalan, "Optimization of Energy Detector Receivers for UWB systems," *in Proceedings of IEEE Vehicular Technology Conference (VTC)*, vol. 2, pp. 1386-1390, 2005.

[173] R. Hazra and A. Tyagi, "Performance Analysis of TR, ATR and DTR Receivers in IR-UWB Communication System," *In Proceedings of IEEE International Conference on Signal Processing, Communication and Computing, ICSPCC*, Kunming, China, 2013.

[174] R. Hazra and A. Tyagi, "Performance Analysis of Non-Coherent IR-UWB Receivers ," *In Proceedings of IEEE International Conference on Signal Processing, Computing and Control, ISPCC*, Solan, India, 2013.

[175] John G. Proakis, *Digital Communications*, 4^{th} Edition, New York: McGrawHill, 2001.

[176] D. Chen and J. N. Laneman, "Modulation and demodulation for cooperative diversity in wireless systems," *IEEE Transactions on Wireless Communications*, vol. 5, no. 7, pp. 1785-1794, 2006.

[177] H. A. Shaban and M. Abou El-Nasir, "Performance Comparison Of ED, TR and DTR IR UWB Receivers For Combined PAM-PPM Modulation In Realistic UWB Channels," *Progress In Electromagnetics Research Letters*, vol. 30, pp. 91-103, 2012.

[178] R. Hazra and A. Tyagi, "Performance Analysis of IR-UWB TR receiver using cooperative dual hop AF strategy," *in Proceedings of Advances in Computing, Communications and Informatics, ICACCI*, pp. 2537-2543, New-Delhi, 2014.

[179] G. K. Karagiannidis, N. C. Sagias, T. A. Tsiftsis, "Closed-Form Statistics for the sum of Squared Nakagami-m Variates and its Applications," *IEEE Transactions on Communications*, vol. 54, no. 8, pp. 1353-1359, 2006.

[180] R. Hazra and A. Tyagi, "Performance analysis of impulse-radio ultra-wideband energy detector system using cooperative dual-hop amplify and forward strategy," *International Journal of Communication Systems, Wiley*, Accepted, In Publishing House, (To appear online in August, 2015).

[181] S. Gishkori and G. Leus, "Compressive Sampling based energy detection of Ultra-Wideband Pulse Position Modulation," *IEEE Transactions on Signal Processing*, vol. 61, no. 15, pp. 3866-3879, 2013.

[182] R. Hazra and A. Tyagi, "Performance Analysis of IR-UWB ED-OOK system using Cooperative Dual-Hop DTF Strategy with Diversity Combining," *IEEE Systems Journal*, Communicated.

[183] R. Hazra and A. Tyagi, "Bit error rate performance of IR-UWB ED-PPM system using cooperative dual-hop AF strategy," *IET Communications*, vol. 10, no. 1, pp. 34-43, Jan 2016.

List of Publications

International Journals

1. **R. Hazra** and A. Tyagi, "Cooperative Impulse Radio Ultra-Wideband Communication Using Coherent and Non-Coherent Detectors: A Review," *Wireless Personal Communications, Springer*, vol. 77, no. 1, pp. 719-748, July 2014.

2. **R. Hazra** and A. Tyagi, "A Survey on Various Coherent and Non-Coherent IR-UWB Receivers," *Wireless Personal Communications, Springer*, vol. 79, no. 3, pp. 2339-2369, Dec 2014.

3. **R. Hazra** and A. Tyagi, "Performance analysis of impulse-radio ultra-wideband energy detector system using cooperative dual-hop amplify and forward strategy," *International Journal of Communication Systems, Wiley*, Accepted, Published Online, (August 2015), DOI: 10.1002/dac.3018.

4. **R. Hazra** and A. Tyagi, "Bit error rate performance of IR-UWB ED-PPM system using cooperative dual-hop AF strategy," *IET Communications*, vol. 10, no. 1, pp. 34-43, Jan 2016.

5. **R. Hazra** and A. Tyagi, "Performance Analysis of IR-UWB ED-OOK system using Cooperative Dual-Hop DTF Strategy with Diversity Combining," *IEEE Systems Journal*, Communicated.

6. **R. Hazra** and A. Tyagi, "BER Analysis of IR-UWB DTR System using Cooperative Dual-Hop AF and DTF Strategy," *AEU, Elsevier*, To be Communicated Shortly.

International Conferences

1. **R. Hazra** and A. Tyagi, "Performance Analysis of TR, ATR and DTR Receivers in IR-UWB Communication System," *In Proceedings of IEEE International Conference on Signal Processing, Communication and Computing, ICSPCC*, Kunming, China, 2013.

2. **R. Hazra** and A. Tyagi, "Performance Analysis of Non-Coherent IR-UWB Receivers ," *In Proceedings of IEEE International Conference on Signal Processing, Computing and Control, ISPCC*, Solan, India, 2013.

3. **R. Hazra** and A. Tyagi, "Performance Comparison of Non-Coherent IR-UWB Receivers ," *In Proceedings of IEEE International Conference on Signal Processing and Communication, ICSC*, pp. 143-148, Noida, India, 2013.

4. **R. Hazra** and A. Tyagi, "Performance analysis of IR-UWB TR receiver using cooperative dual hop AF strategy," *In Proceedings of International Conference on Advances in Computing, Communications and Informatics, ICACCI*, pp. 2537-2543, New-Delhi, India, 2014.